

Contract NAS-12803
DRL No. T760
Item No. 5
DRD No. MA-129T
BAC Report 8693-950001
NASA CR-

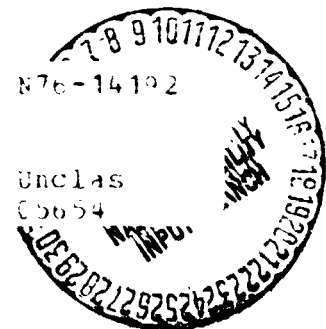
144632

FINAL REPORT for SPACE SHUTTLE ORBIT MANEUVERING ENGINE REUSABLE THRUST CHAMBER PROGRAM

DATE: MAY 1975

(NASA-CR-144632) SPACE SHUTTLE ORBIT
MANEUVERING ENGINE REUSABLE THRUST CH. 5B
PROGRAM Final Report (Textron, Inc.,
Buffalo, N.Y.) 354 p HC \$17.75 CSCL 21a

G3/2.



Bell Aerospace Company

Contract NAS 9-12803
DRL No. T760
Item No. 5
DRD No. MA-129T
BAC Report 8693-950001

FINAL REPORT
FOR
SPACE SHUTTLE ORBIT MANEUVERING ENGINE
REUSABLE THRUST CHAMBER PROGRAM
DATE: MAY 1975

PREPARED BY:



John M. Senneff, Project Manager/Technical Director
Textron - Bell Aerospace

APPROVED BY:



Merl Lausten, Program Monitor
National Aeronautics and Space Administration
Lyndon B. Johnson Space Center
Houston, Texas

Bell Aerospace Company

NOTICE

This report was prepared as an account of Government-sponsored work. Neither the United States, nor the National Aeronautics and Space Administration (NASA), nor any person acting on behalf of NASA:

- A.) Makes any warranty or representation, expressed or implied, with respect to the accuracy, completeness, or usefulness of the information contained in this report, or that the use of any information, apparatus, method, or process disclosed in this report may not infringe privately-owned rights; or
- B.) Assumes any liabilities with respect to the use of, or for damages resulting from the use of, any information, apparatus, method or process disclosed in this report.

As used above, "person acting on behalf of NASA" includes any employee or contractor of NASA, or employee of such contractor, to the extent that such employee or contractor of NASA or employee of such contractor prepares, disseminates, or provides access to any information pursuant to his employment or contract NASA, or his employment with such contractor.

Bell Aerospace Company

ABSTRACT

The objective of the contract was the evaluation of potential reusable thrust chamber and injector concepts for the Space Shuttle Orbit Maneuvering Engine. The effort started with parametric engine calculations which were carried out by computer program for N_2O_4 /Amine, LOX/Amine and LOX/Hydrocarbon propellant combinations for engines incorporating regenerative cooled and insulated columbium thrust chambers. The calculation methods are described including the fuel vortex film cooling method of combustion gas temperature control, and performance prediction. A method of acceptance of a regeneratively cooled heat rejection reduction using a silicone oil additive was also demonstrated by heated tube heat transfer testing. Technical and cost rating of the individual engines were carried out. Six thousand pound thrust columbium thrust chamber assemblies were designed, fabricated and tested. Test results, using the columbium thrust chamber, verified that the predicted performance could be obtained with a modest margin at the design operating temperature. Regeneratively cooled thrust chamber operation was also demonstrated where the injector was characterized for the OME application with a channel wall regenerative thrust chamber furnished to the program from a company sponsored effort. MMH regenerative cooled chamber tests exhibited an Isp of 317 seconds with low heat rejection and low nozzle extension temperatures. Bomb stability testing of the demonstration chambers/injectors demonstrated recovery for the nominal design of acoustic cavities. Cavity geometry changes were also evaluated to assess their damping margin. The final task of the program was to demonstrate that the originally developed 10 inch diameter combustion pattern could be compressed to operate in an 8 inch diameter thrust chamber. This task was completed with both performance and combustion stability demonstrated.

Bell Aerospace Company

FOREWORD

The purpose of this contract was to furnish information which would assist in the selection of a cooling scheme for the Orbit Maneuvering Engine for the Space Shuttle. In the course of the contract, the emphasis shifted from analytical techniques to design data assembly to the proof of concept of the insulated columbium thrust chamber and finally to a definition of combustion chamber operation.

From the program results, each of the changing goals was accomplished with data supporting the varied design concepts. Altitude thrust chamber data supported the contention that a non-actively cooled columbium thrust chamber of the OME size could be operated to the program requirements. Additional simulated altitude data at the Bell Aerospace Company's Test Center and at the NASA's White Sands Test Facility showed that a high performance regeneratively cooled thrust chamber was available and that facility bias was insignificant. The significant contributions of the program were the evidence that a reusable thrust chamber with 317 seconds specific impulse was feasible and the concept of reusability could also be applied to an insulated columbium thrust chamber that would exceed a performance of 310 seconds specific impulse.

To accomplish these tasks, substantial personal effort was required in various specialties including efforts in computer assembling and programming for the study efforts, data collection and dissemination, thrust chamber design and test operations. The successful completion of these major tasks was made possible by the cooperation and significant contributions of Messrs. John Burr, Willard Sanscrainte, Jerauld Panosian and Joseph Martino respectively. Mr. Sanscrainte's assembly and coordination of the original program tasks into this document is also gratefully acknowledged.

Bell Aerospace Company

TABLE OF CONTENTS

<u>SECTION</u>		<u>PAGE</u>
	ABSTRACT	
	FOREWORD	
	SUMMARY	
I	INTRODUCTION	I-1
II	PROGRAM SCHEDULE	II-1
III	INITIAL ENGINE EVALUATIONS - TASKS I AND II	III-1
	A. Parametric Study Definitions	III-1
	B. Basic Engine Descriptions	III-2
	C. Off-Limits Operation	III-14
	D. Engine Computer Program, General	III-20
	E. Calculation Definitions	III-22
	1) Thrust Coefficients	III-22
	2) Fuel Vortex Gas Film Temperature	III-24
	3) C*, Characteristic Velocity	III-31
	4) Chamber Geometry	III-31
	5) Thermal Calculations; Regenerative Cooled Chamber	III-32
	6) Injector Cooling	III-37
	7) Feed Pressures	III-42
	8) Weights	III-45
	F. Predicted Engine Data	III-48
	G. Engine Ratings and Recommendations	III-49
	1) General	III-49
	2) Technical Ratings	III-50
	3) Cost Comparisons	III-58
	4) Recommendations	III-63
IV	6000 LBF COLUMBIUM CHAMBER DESIGN, FABRICATION AND DEMONSTRATION TEST	IV-1
	A. Columbiu Thrust Chamber Design (Task III)	IV-1
	B. Columbiu Thrust Chamber Fabrication (Tasks IV and VI)	IV-3
	C. Demonstration Testing (Task V)	IV-7
	1) General	IV-7
	2) Test Injector Descriptions	IV-8
	3) Injector Checkout Firings	IV-14
	4) Chamber Demonstration Tests	IV-25

Bell Aerospace Company

TABLE OF CONTENTS (CONT'D)

<u>SECTION</u>		<u>PAGE</u>
	(a) Test Facility	IV-25
	(b) Instrumentation and Data Acquisition	IV-28
	(c) Test Results, Stainless Steel Injector	IV-30
	(d) Test Results, Aluminum Injector #1	IV-33
D.	Demonstration Testing (Task VIII)	IV-53
1.	Chamber Demonstration Tests - Aluminum Injector #2	IV-53
	(a) Test Results - Effect of L* and A50 Fuel	IV-53
	(b) The Effect of Varying L* Using MMH Fuel	IV-53
	(c) The Effect on Performance of Varying P	IV-57
	(d) Effect of P on Nozzle Temperatures	IV-57
	(e) Conclusions From Testing	IV-61
V	TASK VII - HEAT TRANSFER TESTING	V- 1
	A. Test Plan	V- 2
	B. Test Specimen	V- 2
	C. Test Applications	V- 3
	D. Propellant Supply System	V- 6
	E. Test Instrumentation	V- 9
	F. Test Procedure	V-12
	G. Data Reduction	V-13
	H. Results of Test Program	V-16
	J. Conclusions	V-23
VI	TASK IX - INJECTOR CHARACTERISTICS AND STABILITY TESTING	VI-1
	A. Injector Tests at Elevated Propellant Temperatures	IV-1
	B. Test Hardware	VI-2
	C. Test Results	VI-5
	D. Conclusions from Injector Characteristics with Heated Propellant	VI-5
	E. Bomb Chamber Checkout Tests	VI-5
	F. Acoustic Temperature Stability Testing	VI-14
	G. Conclusions from Bomb Tests	VI-18

Bell Aerospace Company

TABLE OF CONTENTS (CONT'D)

<u>SECTION</u>		<u>PAGE</u>
VII	TASK X - REGENERATIVELY COOLED THRUST CHAMBER DEMONSTRATION	VII-1
	A. Test Hardware	VII-1
	B. Regeneratively Cooled Thrust Chamber Test Results	VII-10
	1) Performance	VII-15
	2) Heat Rejection	VII-15
	3) Shell and Nozzle Temperature	VII-15
	4) Start Transients	VII-23
VIII	TASK XI - OME MODEL INJECTOR	VIII-1
IX	TASK XII - HEATED PROPELLANT INJECTOR STABILITY TESTING	IX-1
	A. Preliminary Test Results	IX-2
	1) Hardware Changes for Preliminary Testing	IX-5
	2) Test Setup	IX-7
	3) Test Results	IX-7
	4) Preliminary Test Conclusions	IX-21
	a) Bomb Injector	IX-21
	B. Heated Propellant Stability Test Results-Test Hardware	IX-21
	1) Test Results - Series 1	IX-29
	2) Test Results - Series 2	IX-29
	3) Test Results - Series 3	IX-35
	4) Test Results - Series 4	IX-39
	5) Test Results - Series 5	IX-44
	6) Test Results - Test Series 6	IX-44
	C. Acoustic Cavity Gas Temperatures	IX-44
	D. Conclusions Resulting from Tests	IX-46
X	TASK XIII - WSTF TEST AND ANALYSIS SUPPORT	X-1
	A. Test Hardware	X-2
	B. Test Facility	X-12
	1) WSTF Facility	X-12
	C. Test Program	X-23
	D. Test Results	X-25

Bell Aerospace Company

TABLE OF CONTENTS (CONT'D)

<u>SECTION</u>		<u>PAGE</u>
	1) Transient Characteristics	X-27
	2) Stability Characteristics	X-27
	E. Normalization of Test Data	X-36
	1) General	X-36
	2) WSTF Test Data Normalized	X-37
	3) WSTF and BAC Data Comparison	X-44
	4) Thermal Data	X-48
	5) Regenerative Chamber Coolant Temperature Rise and Heat Load	X-48
	6) Regenerative Chamber Back Wall Temp	X-54
	7) Regenerative Chamber Coolant Jacket ΔP	X-54
	F. Conclusions	X-54
	1) Safety	X-54
	2) Performance	X-54
	3) Heat Transfer	X-55
	4) Stability	X-55
XI	TASK XIV - TRIPLET INJECTOR DYNAMIC STABILITY VERIFICATION	XI-1
	A. Design Definition	XI-1
	B. Stability Bomb Configuration Evaluation	XI-6
	C. Stability Test Results	XI-10
	1) Fuel Vortex vs Fuel Film Coolant	XI-14
	2) Effect of Chamber Overlap	XI-19
	3) Flush and Full Fin Damper	XI-19
	4) Reduced Entrance Size	XI-22
	5) Comparison of Stable Configurations	XI-22
	D. Conclusions Resulting From Task XIV Testing	XI-25
XII	TASK XV - OME - 8 INCH TRIPLET INJECTOR OPTIMIZATION	XII-1
	A. Design Definition	XII-1
	1) Core Pattern	XII-1
	B. Film Coolant Orifices	XII-7
	C. Acoustic Cavity	XII-7
	D. Test Chamber	XII-11

Bell Aerospace Company

TABLE OF CONTENTS (CONT'D)

<u>SECTION</u>		<u>PAGE</u>
	1) Test Results	XII-11
	2) Performance	XII-11
	3) Stability Results	XII-13
XIII	RECOMMENDATIONS AND CONCLUSIONS	XIII-1

Bell Aerospace Company

ILLUSTRATIONS

<u>FIGURE NO.</u>		<u>PAGE</u>
II-1	Schedule of Program Tasks	II-2
III-2	Gimbal Mount Configurations	III-9
III-3	N ₂ O ₄ /Amine Stainless Steel Channel Wall Chamber	III-10
III-4	N ₂ O ₄ /Amine Drilled Aluminum Chamber.....	III-11
III-5	Insulated Columbiu Thrust Chamber Assy.....	III-12
III-6	LOX/Amine Injector Typical.....	III-13
III-7	Off Limits Operation.....	III-17
III-8	MMH Ultimate Heat Flux	III-19
III-9	Engine Computer Program-General-Regenerative Cooling.....	III-26
III-10	Parametric Calculations - Insulated Columbiu.....	III-27
III-11	T _{Film} Versus P^*	III-28
III-12	T _{Film} Versus P^*	III-29
III-13	3500 Lb. Thrust Chamber Test Data.....	III-30
III-14	Calculation Definition Chamber Geometry.....	III-33
III-15	3500 Lb Thrust Chamber Temperature Gradient.....	III-35
III-16	Percent Q/A Reduction Versus P_c	III-39
	N ₂ O ₄ /MMH + 1% Si Oil	
III-17	Fixed Engine Pressure Drops.....	III-41
III-18	Regenerative Engine Flow Circuits.....	III-43
III-19	Insulated Columbiu Engine Flow Circuits.....	III-44
III-20	Thrust and P_c Versus Specific Impulse.....	III-54
III-21	Thrust and P_c Versus Maximum Diameter.....	III-55
III-22	Specific Impulse Versus Mixture Ratio.....	III-56
IV-1	Contract Thrust Chamber.....	IV-2
IV-2	OME Columbiu Thrust Chamber.....	IV-4
IV-3	Coated Columbiu Thrust Chamber.....	IV-6
IV-4	Stainless Steel Injector Assembly.....	IV-9
IV-5	Stainless Steel Injector.....	IV-10
IV-6	Aluminum Injector #1.....	IV-11
IV-7	Aluminum Injector Assembly-Design Data.....	IV-12
IV-8	10 Inch Diameter Aluminum Injector No. 2.....	IV-13
IV-9	Start Chamber Assembly.....	IV-15
IV-10	Test Stand Installation.....	IV-17
IV-11	OME Program - Start Hardware.....	IV-18
IV-12	C* Versus Test Cell D-4.....	IV-19
IV-13	Q _{Nozzle} Versus P - Test Cell D-4.....	IV-21
IV-14	Polar Plot Injector 001-1 S/N-1 Q/A Versus Flow Passage.....	IV-22
IV-15	Aluminum Injector #1 With Columbiu Nozzle Section for Sea Level Checkout.....	IV-23
IV-16	Altitude Facility Schematic Design.....	IV-27
IV-17	1BN Altitude Chamber.....	IV-27
IV-18	Pyroscanner Data S/N 03 - Run Number 799.....	IV-34
IV-19	Pyroscanner Data S/N 12 - Run Number 799.....	IV-35
IV-20	Pyroscanner Data S/N 12 - Run Number 804.....	IV-36

Bell Aerospace Company

ILLUSTRATIONS (CONT'D)

<u>FIGURE NO.</u>		<u>PAGE</u>
IV-21	Columbium Thrust Chamber Assembly.....	IV-38
IV-22	Aluminum Injector Assembly - Design Data.....	IV-41
IV-23	Thermocouple Temperature Time History Insulated-Test Number 828 - Aluminum Injector Number 1 MOD A.....	IV-42
IV-24	Thermocouple Temperature Time History Insulated - Test Number 828-Aluminum Injector Number 1 MOD A.....	IV-43
IV-25	Specific Impulse-Aluminum Injector MOD A Runs 816 Thru 839.....	IV-45
IV-26	Maximum Temperature Aluminum Injector MOD A Runs 816 Thru 839 (Fixed Vortex Flow Orifice).	IV-46
IV-27	Longitudinal Temperature Distribution Insulated Test Number 828, 60 Second Data.....	IV-47
IV-28	Data Regression Analysis - Aluminum Injector MOD A.....	IV-48
IV-29	Maximum Wall Temperature Radiation Cooled and Insulated.....	IV-49
IV-30	Columbium Thrust Chamber Performance - Temp Map Aluminum Injector, Runs 829-839.....	IV-50
IV-31	Predicted T_{max} and Cold Test Data.....	IV-51
IV-32	Demonstration Test Data Summary.....	IV-52
IV-33	Specific Impulse Versus Mixture Ratio Aluminum Injector No. 2-26L*, 30L*, 34L*.....	IV-55
IV-34	Maximum Pyroscanner Temperature Versus Mixture Ratio-Aluminum Injector Number 2-30L*.	IV-56
IV-35	Specific Impulse Versus Mixture Ratio-Aluminum Injector Number 2-26L* Chamber.....	IV-58
IV-36	Maximum Pyroscanner Temperature Versus Percent Vortex Flow.....	IV-59
IV-37	Maximum Pyroscanner Temperature Versus Percent Vortex Flow.....	IV- 60
IV-38	Specific Impulse Versus Mixture Ratio-Aluminum Injector Number 2-30L*, 34L* Chamber.....	IV-62
IV-39	Maximum Pyroscanner Temperature Versus Percent Vortex Flow.....	IV-63
V-1	Thermocouple Pattern.....	V- 4
V-2	Aluminum Oxide Thermocouples.....	V- 5
V-3	0.125 Diameter Tubes, 0.015 Inch Wall.....	V- 7
V-4	Propellant Supply System Schematic.....	V- 8
V-5	Flow Control Panel.....	V-10
V-6	Heat Transfer Test Panel.....	V-11
V-7	Heat Transfer Test Panel.....	V-11
V-8	Curve-Average Inside Wall Temperature - Heat Flux-BTU/Sec in ²	V-20
V-9	Q/A Versus Inside Wall Temperature.....	V-21
V-10	Q/A Versus Inside Wall Temperature.....	V-22
VI-1	Test Hardware-Heated Propellant Tests.....	VI-4
VI-2	Heated Propellant Tests-Data Time Histories...	VI-6

Bell Aerospace Company

ILLUSTRATIONS (CONT'D)

<u>FIGURE NO.</u>		<u>PAGE</u>
VI-3	C* Versus Total O/F Ambient Propellants- 10 Inch Aluminum Injector MOD A	VI-7
VI-4	C* Versus Total O/F Heated Fuel, Ambient Oxidizer % P (Nominal P_c , O/F) = 2.9.....	VI-8
VI-5	C* Versus Total O/F Heated Fuel, Ambient Oxidizer and Heated Fuel. Heated Oxidizer.....	VI-9
VI-6	10 Inch Aluminum Number 1 MOD A Heat Rejected Versus Vortex Flow-10 Sec Data.....	VI-10
VI-7	Data Analysis Heated Propellant Testing Aluminum Injector Number 1 MOD A.....	VI-11
VI-8	Insulated Columbiu Engine Projected Operation.	VI-12
VI-9	Stainless Steel Injector Number 1 Bomb Test....	VI-13
VI-10	Aluminum Injector Assembly - Design Data.....	VI-15
VI-11	Bomb Test Assembly.....	VI-16
VII-1	Injector/Vortex Ring Test Assembly-10 Inch OME Regen Chamber.....	VII-2
VII-2	10 Inch Diameter Aluminum Injector Number 2....	VII-3
VII-3	Aluminum Injector Assembly - Design Data.....	VII-4
VII-4	Demonstration Chamber Assembly.....	VII-5
VII-5	Demonstration Chamber Columbiu No. Extension.....	VII-7
VII-6	Schematic of Solenoid Installation.....	VII-8
VII-7	Inlet Pressure Versus Spring Cavity Pressure...	VII-9
VII-8	Regeneratively Cooled Chamber Propellant Flow Schematic.....	VII-14
VII-9	OME Performance - I_{sp} ∞ Versus O/F.....	VII-16
VII-10	OME Performance C* Versus O/F.....	VII-17
VII-11	OME Performance Versus Time-Run Number 1BN-887.	VII-18
VII-12	OME Performance - Jacket Fuel Temperature Rise Versus O/F.....	VII-19
VII-13	OME Regenerative Chamber-Fuel Jacket Tempera- ture Rise Versus Time	VII-20
VII-14	Total Heat Load vs Chamber Pressure.....	VII-21
VII-15	Regenerative Chamber Thermocouple Locations...	VII-22
VII-16	OME Performance-Maximum Chamber Skin Temper- ature (at injector end) Versus O/F.....	VII-24
VII-17	OME Regen Chamber - Temperature Profile Run Number 1BN-887.....	VII-25
VII-18	OME 6K Regeneratively Cooled Chamber-Cell 1BN Run 887.....	VII-26
VII-19	OME 6K Regenerative Cooled Chamber-Temperature Versus Time Plot.....	VII-27
VII-20	OME 6K Regenerative Cooled Chamber-Temperature Versus Time Plot.....	VII-28
VII-21	OME 6K Regenerative Cooled Chamber-Temperature Versus Time Plot.....	VII-29

Bell Aerospace Company

ILLUSTRATIONS (CONT'D)

<u>FIGURE NO.</u>		<u>PAGE</u>
VII-22	OME 6K Regenerative Cooled Chamber-Temperature Versus Time Plot.....	VII-30
VII-23	OME 6K Regenerative Cooled Chamber-Temperature Versus Time Plot.....	VII-31
VIII-1	Aluminum Injector Number 2.....	VIII-2
VIII-2	10 Inch Diameter Aluminum Injector No. 2.....	VIII-5
VIII-3	Vortex Ring.....	VIII-6
IX-1	Acoustic Damper Installation.....	IX-6
IX-2A	Vortex Ring Instrumentation-8693-473140-19.....	IX-8
IX-2B	Vortex Ring Instrumentation-8693-473140-3A.....	IX-8
IX-3	Thermocouple Installation Fuel Vortex Ring.....	IX-9
IX-4	Uncooled Chamber Assembly.....	IX-10
IX-5	Water Cooled Nozzle Assembly.....	IX-11
IX-6	Acoustic Cavity Gas Temperature Versus Time Cavity Number 1.....	IX-15
IX-7	Acoustic Cavity Gas Temperature Versus Time Cavity Number 2.....	IX-16
IX-8	Acoustic Cavity Gas Temperature Versus Time Cavity Number 3.....	IX-17
IX-9	Acoustic Cavity Gas Temperature Versus Time Cavity Number 4.....	IX-18
IX-10	Acoustic Cavity Gas Temperature Versus Time Cavity Numbers 1-4.....	IX-20
IX-11	Bomb Inserter Assembly.....	IX-22
IX-12	Thrust Chamber Assembly - Bomb Test.....	IX-23
IX-13	Adapter Bomb Installation.....	IX-24
IX-14	Cavity Temperature Test Thermocouple Locations.....	IX-25
IX-15	Injector and Damper Ring.....	IX-26
IX-16	Acoustic Ring.....	IX-27
IX-17	Bomb Inserter.....	IX-28
IX-18	Acoustic Cavity Arrangements.....	IX-30
IX-19	Acoustic Damper Detail.....	IX-31
IX-20	Oscillograph Run.....	IX-32
IX-21	OME Injector S/N 2 - Cavity Temperature Versus Time, Test 4567 D-4.....	IX-33
IX-22	OME Injector S/N 2 - Cavity Temperature Versus Time, Test 4571 D-4.....	IX-34
IX-23	Bomb Damp Time - Oscillograph Run, Test 4571...	IX-36
IX-24	Unstable Test No. 4572 D-4, Oscillograph Record (0.5 Second Bomb-12:3T Cavity).....	IX-37

Bell Aerospace Company

ILLUSTRATIONS (CONT'D)

<u>FIGURE NO.</u>		<u>PAGE</u>
IX-25	Injector Damage After Unstable Fire Test.....	IX-38
IX-26	Unstable Test No. 4573 D-4 Oscillograph Record.	IX-40
IX-27	OME Injector S/N-2 Cavity Temperature Versus Time, Test No. 4573 D-4.....	IX-41
IX-28	Unstable Test No. 4574 D-4, Oscillograph Record.	IX-42
IX-29	Cavity Temperatures Unstable and Stable Tests..	IX-43
IX-30	OME Injector S/N -2, Cavity Temperature Versus Time, Test No. 4576 D-4.....	IX-45
IX-31	Task XII - Stability Test Results (Fuel Vortex Cooling).....	IX-47
X-1	Thrust Chamber Assembly.....	X-3
X-2	Thrust Chamber Assembly-Exploded View.....	X-4
X-3	Triplet Element Injector.....	X-5
X-4	Acoustic Ring.....	X-6
X-5	Film Coolant Ring.....	X-7
X-6	Liner-Channel Wall OME Chamber.....	X-8
X-7	Regenerative Thrust Chamber.....	X-9
X-8	Interface, Assy Of Regen Test Hardware.....	X-10
X-9	Calculated Chamber Temperatures.....	X-11
X-10	Thrust Chamber Mounted in WSTF Altitude Test Cell Area 401.....	X-17
X-11	Regenerative Chamber Instrumentation Location..	X-18
X-12	Start Transient-Test 1-4-1, 29 October 1973.....	X-28
X-13	Shutdown Transient Test 1-4-1, 29 October 1973.	X-29
X-14	Isp ($\epsilon=76.7$) vs R_o/f -6K OME Regen Comparison of 30L* and 34L*-Al Injector S/N 2.....	X-30
X-15	Isp _{oo} ($\epsilon=76.7$) vs R_o/f -6K OME Regen Comparison of Unsat. and Sat. Propellant at 30L*.....	X-31
X-16	Isp _{oo} ($\epsilon=76.7$) vs R_o/f -6K OME Regen Comparison of Unsat. and Sat. Propellants at 30L*.....	X-32
X-17	Isp _{oo} ($\epsilon=76.7$) vs R_o/f - 6K OME Regen Comparison of Ambient and Heated Propellant.....	X-33
X-18	WSTF Data-Comparison of Performance with Chamber Pressure.....	X-34
X-19	WSTF Data, Isp _{oo} ($\epsilon=76.7$) Versus R_o/f _{o-a}	X-35
X-20	Specific Impulse Versus Mixture Ratio 6K OME Regenerative Chamber-30L*, 34L*	X-39
X-21	Specific Impulse Versus Mixture Ratio 6K OME Regenerative Chamber-30L* Aluminum Injector Number 2.....	X-40
X-22	Specific Impulse Versus Mixture Ratio 6K OME Regenerative Chamber-30L*, 34L*, Aluminum Injector Number 2.....	X-41

Bell Aerospace Company

ILLUSTRATIONS (CONT'D)

<u>FIGURE NO.</u>		<u>PAGE</u>
X-23	Specific Impulse Versus Mixture Ratio 6K OME Regenerative Chamber-34L* Aluminum Injector Number 2.....	X-42
X-24	Specific Impulse Versus Mixture Ratio 6K OME Regenerative Chamber-30L*, 34L*, Aluminum Injector Number 2, WSTF Test DATA.....	X-43
X-25	Specific Impulse Versus Mixture Ratio 6K OME Regenerative Chamber-Aluminum Injector Number 2, Combined WSTF/BAC DATA.....	X-45
X-26	Specific Impulse Versus Mixture Ratio- 6K OME Regenerative Chamber Aluminum Injector No. 2 Combined WSTF/BAC Data.....	X-47
X-27	Test: WSTF, Series 1, Seq. 4, Test 1.....	X-49
X-28	Heat Load Versus Chamber Pressure, 6K OME Regenerative Chamber.....	X-50
X-29	Chamber Backwall Temperature Characteristics 6K OME Regenerative Chamber.....	X-51
X-30	Jacket Pressure Drop Versus Coolant Flowrate...	X-52
XI-1	Injector S/N A1-2 Rework (Add Fuel Barrier Orifices).....	XI-2
XI-2	Acoustic Ring (Building Block).....	XI-4
XI-3	Insert, Entrance, Acoustic Slot (Bell Type -.580 Opening).....	XI-5
XI-4	Bomb Installations.....	XI-7
XI-5	Bomb Shrapnel Evaluation.....	XI-8
XI-6	Insul. Cork Bomb (6.9 Grain).....	XI-9
XI-7	Bomb Holder Assembly.....	XI-11
XI-8	Bomb Overpressure Comparison.....	XI-12
XI-9	Acoustic Damper Configurations.....	XI-13
XI-10	Task XIV - Test Results.....	XI-16
XI-11	Task XIV - Test Results.....	XI-17
XI-12	Cavity Temperatures Film Cooling and Vortex Cooling Tests.....	XI-18
XI-13	Task XIV - Test Results.....	XI-20
XI-14	Task XIV - Test Results.....	XI-21
XI-15	Task XIV - Test Results.....	XI-23
XI-16	Task XIV - Test Results.....	XI-24
XII-1	8 Inch Diameter Injector Element Comparison....	XII-4
XII-2	Water Flow Model, Assy of 8 Inch OME Fuel Orifices.....	XII-5
XII-3	Orifice Plate-Water Flow Model.....	XII-6
XII-4	Pressure Map Comparison.....	XII-8
XII-5	Test Hardware Assembly (8 Inch Diameter Injector)	XII-10
XII-6	Acoustic Cavity Test Configuration.....	XII-14
XII 7	Task XV Stability Test Results.....	XII-15

Bell Aerospace Company

TABLES

<u>TABLE NO.</u>		<u>PAGE</u>
<u>Section III</u>		
I	Chamber Cooling Concepts and Propellants.....	III-3
II	Nominal and Parametric Design Definitions.....	III-4
III	Parametric Data Plots.....	III-5
IV	Additional Data - Printout.....	III-6
V	Fuel Vortex Gas Film Temperature, T_{Film}	III-25
VI	Q/A Burnout Equations.....	III-38
VII	Dimension Constraints.....	III-38
VIII	Task I-Nominal Engine Data, $P_c=125$ psia, DEX= 50, 30% Bell.....	III-51
IX	Task II-Nominal Engine Data $P_c=100$ psia, DEX= 50, 80% Bell.....	III-52
X	Computer Printout Sample.....	III-53
XI	Technical Rating Factors Task I and Task II....	III-59
		III-60
XII	Engine Rates	III-61
XIII	Cost Comparisons $\times 10^6$	III-62
<u>Section IV</u>		
I	OME Thrust Program-Sea Level Test Data.....	IV-16
II	Aluminum Injector Number 2 - Sea Level Test Data Checkout Firings Injector A1 #1 MOD A.....	IV-24
III	Check Tests - Injector A1 #2.....	IV-26
IV	Instrumentation Accuracy-Frequency Response..	IV-31
V	OME Data Summary of Altitude Tests.....	IV-32
VI	Test Data Summary-Aluminum No. 1 MOD A Inj.....	IV-39 & 40
VII	Test Data Summary-Aluminum No. 2 Injector.....	IV-54
<u>Section V</u>		
I	Results of Test Program.....	V-17
		V-18
		V-19
<u>Section VI</u>		
I	Test Data Summary - Heated Propellant Testing... Aluminum Injector Number 1 MOD A.....	VI-3
II	Flat Face Injector Bomb Tests.....	VI-17
<u>Section VII</u>		
I	Regenerative Chamber Testing.....	VII-11
II	6K OME Regenerative Chamber Test Summary at Altitude.....	VII-12
<u>Section VIII</u>		
I	Injector Core Design.....	VIII-3
II	Aluminum Injector S/N 2	VIII-4

Bell Aerospace Company

TABLES (CONT'D)

<u>TABLE NO.</u>		<u>PAGE</u>
<u>Section IX</u>		
I	Test Summary.....	IX-3
II	Test Summary of Bomb Tests-Bomb Stability Program - Task XII	IX-4
III	Test Summary of Checkout Runs-Bomb Stability Program.....	IX-12
IV	Hardware Configuration.....	IX-13
V	Hardware Configuration.....	IX-29
<u>Section X</u>		
I	Demonstrator Thrust Chamber Design Characteris- tics.....	X-13
II	Injector Characteristics.....	X-14
III	Test Hardware For Test Series 1.....	X-15
IV	Hardware Configuration for Test Series 2.....	X-16
V	General Instrumentation List.....	X-17
		X-20
VI	BAC 6K OMS Engine Technology Support Program Facility and Engine Instrumentation List.....	X-21 & 22
VII	Test Program Summary.....	X-24
VIII	Altitude Test Summary at WSTF-10/27/73 to 11/2/73.....	X-26
IX	Regeneratively Cooled Thrust Chamber Thermal Data.....	X-53
<u>Section XI</u>		
I	Test Summary of Bomb Tests-Bomb Stability Program, Task XIV.....	XI-15
<u>Section XII</u>		
I	8 Inch Diameter Injector Design	XII-3
II	Injector Comparison.....	XII-9
III	Model 8693 OME - 8 Inch Diameter Injector S/N - 1 - Stability Test Summary.....	XII-12
IV	Data of Runs 4610-4614-4604.....	XII-13

Bell Aerospace Company

SUMMARY

The requirement for longevity of the Orbit Maneuvering Engine for the Space Shuttle precipitated the requirement for a "reusable" thrust chamber concept. The term "reusable" was further defined to be an engine which could accomplish 1000 starts and 15 hours of accumulated run time. These duration requirements far exceeded current hardware capabilities, and subsequently directly this program into a preliminary study design and fabricate for proof sequence of tasks. The initial study entailed propellant trade-off studies where the optimum propellant appeared to be LOX-MMH, with the N_2O_4 /Amine propellants closely following. Subsequent decisions directed demonstrations to be made with the N_2O_4 -MMH propellant combination.

The thrust chamber design study recommended in favor of two thrust chamber concepts including the high performance, but expensive, regeneratively cooled thrust chamber and a lower performance, less expensive, design called an insulated columbium thrust chamber. The final recommendation of the study emphasized costs and favored the insulated columbium concept.

The insulated columbium thrust chamber concept, being mildly unconventional, was considered to require proof testing, which was accomplished in the next phase of the contract. These proof tests included operation of a full size 10 inch diameter columbium thrust chamber at simulated altitude conditions. The testing was performed to prove both the capability of fabrication and the cooling, which would allow the proper limit of $2400^{\circ}F$ wall temperatures. Several lengths of chambers were tested and a final performance of slightly over 310 seconds Isp was accomplished.

Subsequent interest in the columbium chamber concept was reduced as further studies of the regeneratively cooled chamber indicated that cyclic requirements could be achieved and the higher performance of the regeneratively cooled chamber utilized. Subsequent program efforts emphasized the use of conventional injector designs with the regeneratively cooled chamber, combustion stability testing was a major portion of the effort. The concern in accomplishing adequate performance with the regeneratively cooled chamber came about when competing designs were found to be performance sensitive to fuel temperature. This sensitivity was not found using the Bell triplet injector design and led to the further testing for combustion stability at Bell and altitude performance tests at WSTF as proof of concept demonstrations. Subsequent testing showed the acoustic damper combustion stability devices to be very effective, performance tests demonstrated 317

Bell Aerospace Company

seconds specific impulse with a properly shaped OME sized nozzle. These altitude tests were performed with a channel wall regeneratively cooled company furnished thrust chamber in combination with a NASA furnished nozzle skirt.

The final task of this program was the design, fabrication, and demonstration of an 8.2 inch diameter triplet element injector which was compatible with the size of competing thrust chambers. All previous testing at Bell was accomplished using a 10 inch diameter injector. Originally, the 10 inch injector design was based on extensive empirical data where the spacing and arrangement of the individual elements could be predicted from previous designs. The design of the 8.2 inch injector was a compromise where the primary injector parameters maintained were the number and arrangement of injection elements and the type of element used. The testing conducted with the 8.2 inch injector confirmed this selection of parameters and the sea level combustion efficiency was measured at a value which would produce 316 seconds Isp on an OME engine. The limited stability testing conducted was also positive, producing a design with substantial stability margin and fulfilling all of the OME requirements. A summary of the demonstration tests performed within the program is as follows:

PROGRAM TEST SUMMARY (Number of Tests Conducted)				
Injector	SS 1 Stainless Steel With Baffle (10" Dia.)	Al 1 Aluminum Flat Face With Damper (10" Dia.)	Al 2 Aluminum Flat Face With Damper (10" Dia.)	Al 3 Aluminum Flat Face With Damper (8" Dia.)
Type of Testing				
Injector Testing Performance and Heat Rejection	18	42	18	11
Injector Stability (Bomb) Tests	5		60	
Columbium Chamber Demonstration and Evaluation (Altitude)	21	23	26	
Regenerative Chamber Demonstration and Evaluation (Altitude)			65*	
*Includes 47 tests at the NASA, WSTF				

Bell Aerospace Company

I. INTRODUCTION

This document is submitted in compliance with the Final Report documentation requirements of Contract NAS 9-12803, Space Shuttle Orbit Maneuvering Engine Reusable Thrust Chamber Program. The overall objective of the contract was the determination of the feasibility of potential reusable thrust chamber concepts for the OME by analyses followed by test evaluation of the principal candidates. The information and data developed supported the NASA-JSC and shuttle vehicle contractor Orbit Maneuvering System (OMS) studies and provided a firm technical foundation for the final definition of the OME engine.

The program effort requirements were divided into the following tasks:

Task I - Reusable OME Thrust Chamber Evaluation: Definition of and parametric study of pressure fed engine assembly utilizing N₂O₄ oxidizer with MMH and 50/50 blend fuels. The baseline engine was defined as 6000 lbs thrust, 125 psia chamber pressure with a nozzle exit diameter of 50 inches. Three types of regeneratively cooled and one non-regenerative cooled thrust chambers were to be studied; channel wall, drilled aluminum and tubular regenerative cooled and insulated columbium non-regenerative cooled. The engine assembly definitions included a stainless steel injector with appropriate thrust chamber attachment, radiation cooled nozzle extension, gas actuated series - parallel redundant engine propellant valves, and engine gimbal mount. The required parametric output data included specific impulse, engine assembly weight, envelope and feed pressures for the range of design variables:

Thrust	- 4000 to 10,000 lbf
Chamber Pressure	- 100 to 200 psia
Nozzle Exit Diameter	- 40 to 60 inches
Mixture Ratio	- Optimum $\pm 20\%$
Nozzle % Bell	- Approximately 72 to 100

The thermal margin definitions for the regenerative cooled engines and the nominal operating temperature of the columbium thrust chamber were established.

The task also required a comparative assessment of the engine concepts based on technical and cost factors and the recommendation of the preferred engine concept.

Task II - Alternate OME Propellant Combinations: Effort similar to task I except that the oxidizer was LOX with MMH, N₂H₄, propane and RP-1 fuels. The engine assembly definitions included an

Bell Aerospace Company

ignition system. The preferred engine concept was to be established against the same technical and cost ratings as Task I. A final recommendation was also to be made considering both Task I and Task II propellants and engine definitions.

Task III - Columbiu Thrust Chamber Design: Establish design based on the nominal engine definition of Tasks I and II with an exit area ratio of 15:1 and a characteristic length L^* of 30 inches when assembled with the test injector.

Task IV - Columbiu Thrust Chamber Fabrication: Fabrication of Task III thrust chamber.

Task V - Columbiu Thrust Chamber Testing: Injector checkout firings followed by tests of the chamber at altitude. Testing with and without external insulation was required.

Task VI - Alternate Cb Chamber Fabrication: This task was originally defined as "Reusable OME Thrust Chamber Update", an update of the Task I and II studies based on program demonstration tests. The redefinition to "Alternate Cb Chamber Fabrication" was made to enable additional Cb chamber demonstration at reduced and increased L^* , 26 and 34 inches respectively.

Task VII - Heat Transfer Testing: The effort was added shortly after program go-ahead to evaluate silicone oil (SO) additive to MMH fuel. The SO additive was originally proposed for inclusion in the Task I and II studies for the regeneratively cooled chambers to reduce the average heat rejection to the fuel coolant.

Task VIII - Alternate Thrust Chamber and Testing: The effort required test firings of the 6000 lbf columbiu chambers at altitude, with 26, 30 and 34 inch L^* 's with N_2O_4 /MMH propellants. Tests with N_2O_4 /50-50 blend were also required. The tests were made at various values of P , the ratio of fuel vortex film cooling flow rate to total propellant flow rate.

Task IX - Injector Characterization and Stability Testing: The task required characterization of injector operation for regenerative chamber operation. Heated propellant tests were required in water cooled hardware followed by short duration firing, bomb testing in an uncooled chamber with vortex film cooling flow rate set for regen operation.

Task X - Regenerative Cooled Thrust Chamber Demonstration: Required testing at BAC of a 6000 lbf regenerative cooled chamber with N_2O_4 /MMH propellants.

Bell Aerospace Company

Task XI - OME Model Injector: Required delivery to NASA of an injector employed for chamber demonstration tests.

Task XII - Heated Propellant Injector Stability Testing: Extended the range of injector bomb test conditions and included tests to define the steady state operating temperatures of the injector acoustic cavities.

Task XIII - WSTF Test and Analysis Support: Called for delivery of the Task X hardware to the NASA White Sands Test Facility and engineering support at WSTF to conduct a series of regenerative cooled chamber firings with a full nozzle extension, area ratio equal to 76.7:1. Post test data analyses and comparison with the Task X data was also required.

Task XIV - Triplet Injector Dynamic Stability Testing: Called for bomb stability margin demonstration by reducing the acoustic cavity area and depths. Testing of a range of oxidizer temperatures with fuel fed temperature simulating regeneratively cooled chamber operation was also required.

Task XV - OME 8 Inch Triplet Injector Optimization: Design, fabrication and test of an 8 inch triplet injector. The hydraulic characteristics were required to be consistent with OME operation and the test demonstrations were to include performance, heat flux and dynamic stability.

The initial contract included Tasks I through VI. Tasks VII through XV were negotiated as contract changes and extended the contract completion date from 6/73 to 3/75. Task XVI, Injector Heat Flux Uniformity was deleted.

Bell Aerospace Company

II. PROGRAM SCHEDULE

The program tasks were carried out as shown in Figure II-1. Task VII heated tube heat transfer testing was conducted to support the parametric engine studies and ratings of Tasks I and II. By agreement with NASA-MSD, the columbium demonstration thrust chamber design was started in the second program month in advance of the recommendations from the Task I and II effort. The fabrication of that chamber (Task IV) was complete in January.

Initial columbium chamber testing under Task V was carried out with a 10 inch diameter injector incorporating baffles for dynamic stability. Task V was interrupted in May and June to permit testing with higher performance injectors which were made available from company sponsored programs. Those injectors incorporated acoustic cavities for dynamic stability.

Task VI consisted of the fabrication of a reduced L^* columbium chamber which was evaluated by firing tests under Task VIII. Task IX included test firings to characterize a 10 inch diameter triplet injector with acoustic cavities for operation with a regeneratively cooled chamber and to conduct initial evaluation of the bomb stability provided by the acoustic cavities. Task X consisted of test firings with an MMH cooled regenerative thrust chamber at BAC under simulated altitude test conditions. The chamber was then test fired at the NASA White Sands Test Facility (Task XIII) to confirm its projected performance with a full nozzle extension.

The additional stability characterization of the flat face triplet injector with acoustic cavities was conducted under Task XII with heated propellants simulating regeneratively cooled thrust chamber operation. Stability testing of the 10 inch diameter injectors was completed under Task XIV which included additional geometric modification of the acoustic cavities and modified chamber film cooling. The program concluded with the evaluation of an 8 inch diameter injector constructed and evaluated for performance, heat rejection and stability under Task XV.

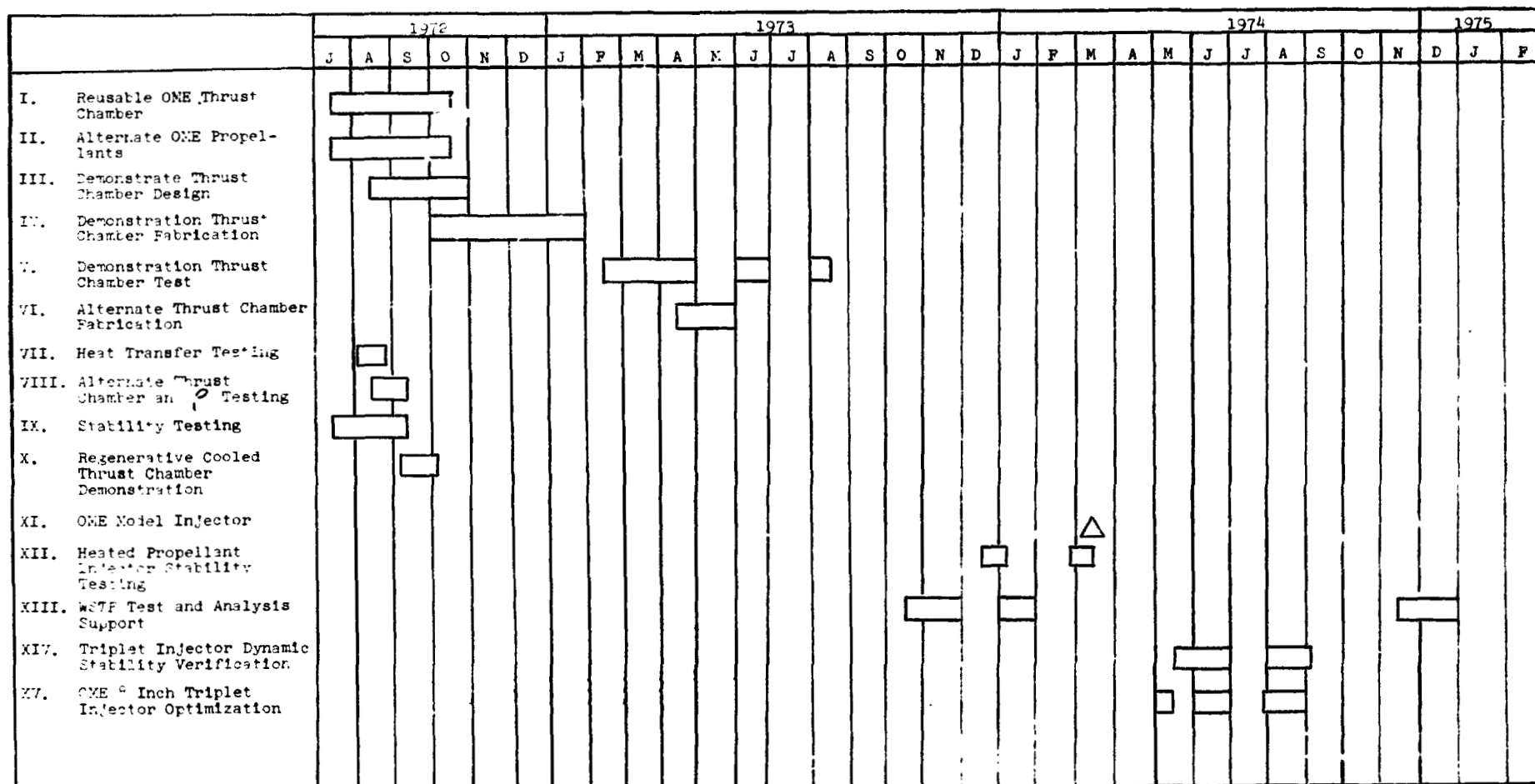
The initial input of Task I and II effort was made shortly after program go-ahead by "OME Parametric Data Two Week Data Dump", BAC Report No. 8693-953003, July 1972. A limited number of cases were considered with emphasis placed on Isp as a function of regenerative cooling margin and Ido design throat temperature, and Isp versus O/F and P_c for the nominal engine definitions. Engine feed pressures were given as a function of mixture ratio chamber

ORIGINAL PAGE IS
OF POOR QUALITY

BELL AEROSPACE COMPANY

FIGURE II-1

SCHEDULE OF PROGRAM TASKS



II-2

Bell Aerospace Company

pressure; preliminary engine weights were presented. The additional effort to complete the ADEPT computer program was outlined. Agreements were reached with the program monitor at the two week data dump meeting for the definition of regenerative cooled engine margin and several other definitions for the ADEPT program.

Bell Aerospace Company

III. TASKS I AND II - INITIAL ENGINE EVALUATION

A. Parametric Study Definitions

The Task I propellant combinations were limited by the contract work statement to N_2O_4/MMH and $N_2O_4/A-50$. The logic for the selection of the alternate propellants of Task II included the potential performance improvement relative to the Task I N_2O_4 /Amine propellants, handling characteristics and vehicle tankage requirements. Performance improvement and handling reduced the alternate oxidizer to liquid oxygen. Fluorine and oxidizers containing fluorine were considered unacceptable based on handling. Other oxidizers, HNO_3 , H_2O_2 , offered no performance improvement. The selection of fuels for use with LOX included regenerative cooling potential, sensitivity of performance with mixture ratio, potential ignition problems and cost. The review of fuels lead to the selection of MMH , $A-50$, N_2H_4 , C_3H_8 and $RP-1$ with N_2H_4 and C_3H_8 limited to non-regenerative cooled thrust chambers.

The thrust chamber concepts were limited first by the reusability and long accumulated operating life required for the Space Shuttle. Those requirements excluded ablative and heat sink concepts. Non-regenerative cooled thrust chambers were included because of their potential simplicity relative to regenerative cooled approaches where simplicity includes the elimination of the regen fuel heating circuit and the possible malfunction problems associated with that circuit for off-limits operation and to pressurizing gas entrainment in the fuel feed to the engine. Non-regenerative cooled designs were narrowed to a single approach, insulated coated columbium, based on the vehicle installation constraints (which eliminated a radiation cooled design) and the large technology base for columbium alloys and coatings. A beryllium inter-regen chamber is limited to lower thrust levels than required for the OME Reference 1. A graphite composite chamber presents excessive durability problems. Other non-regen approaches, heat pipe, transpiration cooling, were considered advanced state-of-the-art approaches with many unresolved problems with respect to the propellants and thrust levels of interest.

The list of regenerative cooled approaches was reduced to drilled aluminum, "channel wall" and tube wall designs. Drilled aluminum thrust chambers are supported by the many years of operational experience with the 16,000 lb. thrust BAC Agena engine. Relative to drilled aluminum, a drilled stainless steel chamber would offer the advantage of improved compatibility with atmospheric moisture

Bell Aerospace Company

and HNO_3 where HNO_3 formation requires the malfunction of an N_2O_4 leak into the chamber together with atmospheric moisture. The improved compatibility of drilled stainless steel would be at the expense of reduced thermal margin and increased fabrication costs. The "channel wall" regen chamber, stainless steel liner with longitudinal cooling slots and an electro-deposited nickel closeout is considered state-of-the-art based on several technology programs (Reference 2 and 3), and the similarity to O_2/H_2 chambers (including the SSME) employing a copper alloy liner with an E.D. nickel jacket. A single case of the tube wall chamber was included in the studies for comparative purposes. The tube wall approach has the largest operational usage data base but also the potential problems of tube fabrication for the OME size engines and the reduced reliability associated with the large number of tube-to-tube joints.

Tables I and II present a summary of the chamber cooling concepts and propellants studied and the nominal parametric range of the engine design characteristics. The concepts, propellants and design characteristics of the tables were based on the proposed effort as modified by contract negotiation with NASA-JSC. The inclusion of MMH + SO, MMH with 1% silicone oil was based on BAC tests which showed an average heat rejection reduction with the SO additive with negligible change in performance. Several Agena stage launches have been made with SO additive to UDMH. Other tests have demonstrated the feasibility of MMH + SO as described in sub-section E. The definition of off-limits operating capability to be included in the engine point designs is discussed in sub-section C.

Table III gives the definition of data plots required to summarize the parametric calculations. Additional data to be generated for each point design is listed in Table IV.

B. Basic Engine Description

The common features of all engines studied were the definition of a stainless steel injector, a flexure type gimbal mount located near the thrust chamber throat, and a series parallel redundant propellant valve assembly. The selection of a stainless steel injector was based on the long life and minimum servicing required for the space shuttle. An aluminum injector definition would reduce engine weight but add the complexity of aluminum salt formation and corrosion in the presence of N_2O_4 plus moisture and atmospheric moisture alone. The specific selection of 304 stainless steel was based on tests which showed that material to be least susceptible to potential hydrogen embrittlement from H_2

TABLE I

CHAMBER COOLING CONCEPTS AND PROPELLANTS

OME

TASK	PROPELLANTS		CONCEPTS				CALCULATED DATA	
	OXIDIZER	FUEL	CWR	DAR	TWR ^①	Icb	NOMINAL	PARAMETRIC
I	N ₂ O ₄	MMH	✓	✓	✓	✓	✓	✓
		MMH + Si	✓	✓		—	✓	
		50-50	✓	✓		✓	✓ ^②	
II	LOX	MMH	✓	✓		✓	✓	✓
		MMH + Si	✓	✓		—	✓	
		50-50	✓	✓		✓	✓	
		N ₂ H ₄	—	—		✓	✓	
		C ₃ H ₈	—	—		✓	✓	
		RPI	✓	✓		—	✓	✓

① NOMINAL ONLY

② PLUS 10K, P_c 125, DEX 40 - 60, CWR AND Icb

CWR - STAINLESS STEEL CHANNEL WALL REGEN

DAR - DRILLED ALUMINUM REGEN

TWR - TUBE WALL REGEN

Icb - INSULATED COLUMBIUM

TABLE II
NOMINAL AND PARAMETRIC DESIGN DEFINITIONS

	NOMINAL		PARAMETRIC	
	TASK I	II	I	II
THRUST, LBF	6K →		4K - 10K →	
P _C , PSIA	125	100	100 - 200	75 - 200
O/F	OPT ^① →		OPT ± 20% →	
EXIT I.D., INCHES	50 →		40 - 60 →	
% BELL	80		^② - 110 →	

① N₂O₄/AMINE EQUAL VOLUME TANKAGE

② MINIMUM LENGTH RAO OPTIMUM

OFF LIMITS DEFINITION:

+12% O/F

-10% P_C

90°F Propellant Feed Temperature

TABLE III
PARAMETRIC DATA PLOTS

		O/F	OFF LIMITS	% BELL	DEX
A. NOMINAL F, P _C					
I _{SP}					
WT		X		X	X
LT		X	-	X	X
FFP		X	X		
T _{MAX} (ICB)		X		-	-
D _{MAX}		X	X	X	X
B.	I _{SP}	[@ NOMINAL O/F, OFF LIMITS % BELL, 80 AND 100 DEX, 40, 50, 60 INCHES			
	WT				
	LT				
	D _{MAX}				
	FFP				

I_{SP} = ∞ ALTITUDE, 70°F PROPELLANT FEED
 WT = TOTAL ENGINE ASSEMBLY WEIGHT
 LT = TOTAL ENGINE LENGTH
 FFP = ENGINE FUEL FEED PRESSURE
 T_{MAX} = MAXIMUM WALL TEMPERATURE INSULATED COLUMBIUM
 D_{MAX} = ENGINE EXIT ENVELOPE FOR ±7% GIMBAL
 DEX = NOZZLE EXIT INSIDE DIAMETER

TABLE IV
ADDITIONAL DATA - PRINTOUT

(ALL DESIGNS)

AREA RATIO

c^* , C_F , c^* AND C_F EFFICIENCIES

TOTAL FLOWRATE

BARRIER FLOW FRACTION

SUBASSEMBLY WEIGHTS

THICKNESSES; DENSITIES, WEIGHT BREAKDOWN

CHAMBER DIMENSIONS, D_t , D_c AND OTHERS

BAFFLE WIDTH

AREA RATIO OF COLUMBIUM TO TITANIUM EXTENSION JOINT

COOLING MARGINS AT NOMINAL

(REGEN)

TEMPERATURE OUT OF JACKET

NUMBER OF COOLING PASSAGES

PASSAGE DIMENSIONS

Q/A , H_g , T_{WALL} GAS

AREA RATIO REGEN TO COLUMBIUM EXTENSION JOINT

COOLANT VELOCITIES

Bell Aerospace Company

and H+ generated by the combustion process (Reference 4). The common injector assembly definition included a 5 leg baffle to eliminate combustion stability sensitivity through the fourth tangential mode and acoustic slots at its outer periphery to dampen for the first radial mode of high frequency instability. Regenerative cooling of the baffle was selected to minimize the loss of combustion efficiency (compared to "flow through" cooling schemes with propellant injection from the baffle tips) and to insure low operating temperatures consistent with the OME thermal cycle life requirement. The baffle and injector face coolant slots were defined to eliminate all injector face welds to add to the thermal cycle life capability. The injector concept included fuel-ox-fuel triplet injection elements except for the outermost elements which were ox-fuel doublets with the ox orifice closest to the wall. The triplet elements were taken for maximum combustion efficiency; the doublet elements provided maximum tolerance to orifice contamination plugging. Finally, the injector was characterized as providing fuel "vortex" film cooling. Vortex film cooling consists of injection of fuel through orifices drilled tangential to the chamber wall and perpendicular to the chamber centerline. The vortex fuel injection occurs in a recess in the wall reducing the number of injection orifices required. The film cooling approach also provides circumferentially uniform film injection in the event of malfunction due to plugging of one or two of the injection orifices, a capability demonstrated with a 600 lbf, fuel vortex film cooled chamber at BAC (Reference 5).

The definition of the series - parallel redundant engine valve was made to maximize engine propellant valve reliability. The design characteristics of the LM Ascent engine valve assembly were followed. The valve was scaled to each engine point design to maintain a nominal pressure drop of 1.4 psi maximum across both parallel legs, matching the LM Ascent engine.

A sketch of the flexure type gimbal mount for the regeneratively cooled and insulated columbium engines is shown in Figure III-2. The insulated columbium engines required a cylindrical structure to tie the gimbal ring to the injector. The relatively high columbium chamber wall temperature precluded a direct structural mounting of the gimbal ring to the chamber.

The channel wall regen thrust chamber (CWR) was characterized as a 304 stainless steel liner with electrical discharge machined cooling passages parallel to the chamber centerline. The cooling passage closeout and outer shell consisted of electro-formed nickel. The attachment of the injector to chamber was defined as

Bell Aerospace Company

as a welded joint (Figure III-3). The thrust chamber was completed with a radiation cooled, columbium/titanium nozzle extension bolted to the fuel coolant inlet manifold. The fuel coolant inlet manifold was located at a chamber divergent area ratio of approximately 10:1, the location being far enough out such that the uncooled nozzle extension would not exceed 2400°F at the design operating conditions. The attachment flange and higher temperature area of the extension was designed to use coated columbium. A titanium section completed the nozzle extension, with this section welded to the columbium portion at an area ratio compatible with titanium operation. The specific extension alloys selected were C103 columbium and 6Al-4V titanium based on the demonstrated formability and welding of these alloys for the LM Service Module engine.

The drilled aluminum regen chamber consisted of a 6061 aluminum alloy chamber with drilled fuel cooling passages (Figure III-4). The injector to chamber attachment required a flange joint with redundant seals. The nozzle extension definition was the same as the CWR assembly. The tube wall chamber consisted of brazed stainless steel tubes, weld-on-injector and bolt-on nozzle extension.

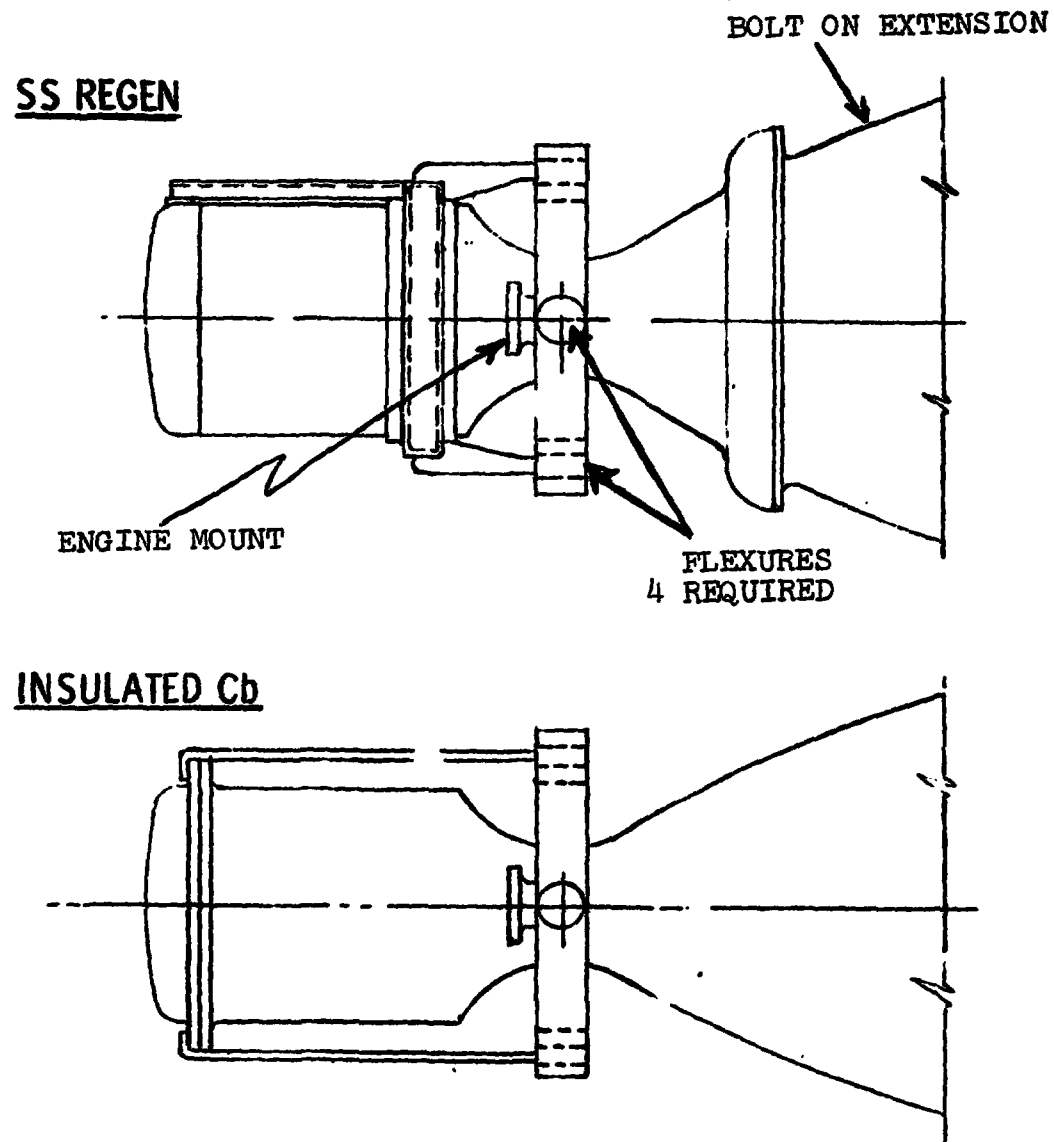
The insulated columbium chamber included a bolt-on injector, a seamless C103 chamber and weld-on C103 nozzle extension terminating in a weld-on titanium extension section, Figure III-5. The chamber insulation was established as 12 lb/ft³ dynaflex based on the test results of Reference 6. The dynaflex insulation was terminated at an area ratio of 10:1 and included a thin titanium outer shell to hold the insulation in place against the coated columbium wall. The insulation thickness was to be defined to limit the outer surface temperature to 300°F.

The Task II LOX engines' ignition subsystem is shown in Figure III-6. The torch ignitor fuel and oxidizer feed systems included series parallel redundant valving and a capacitive exciter. The subsystem also included redundant pressure sensors and a power supply/timer to provide the following engine start sequence:

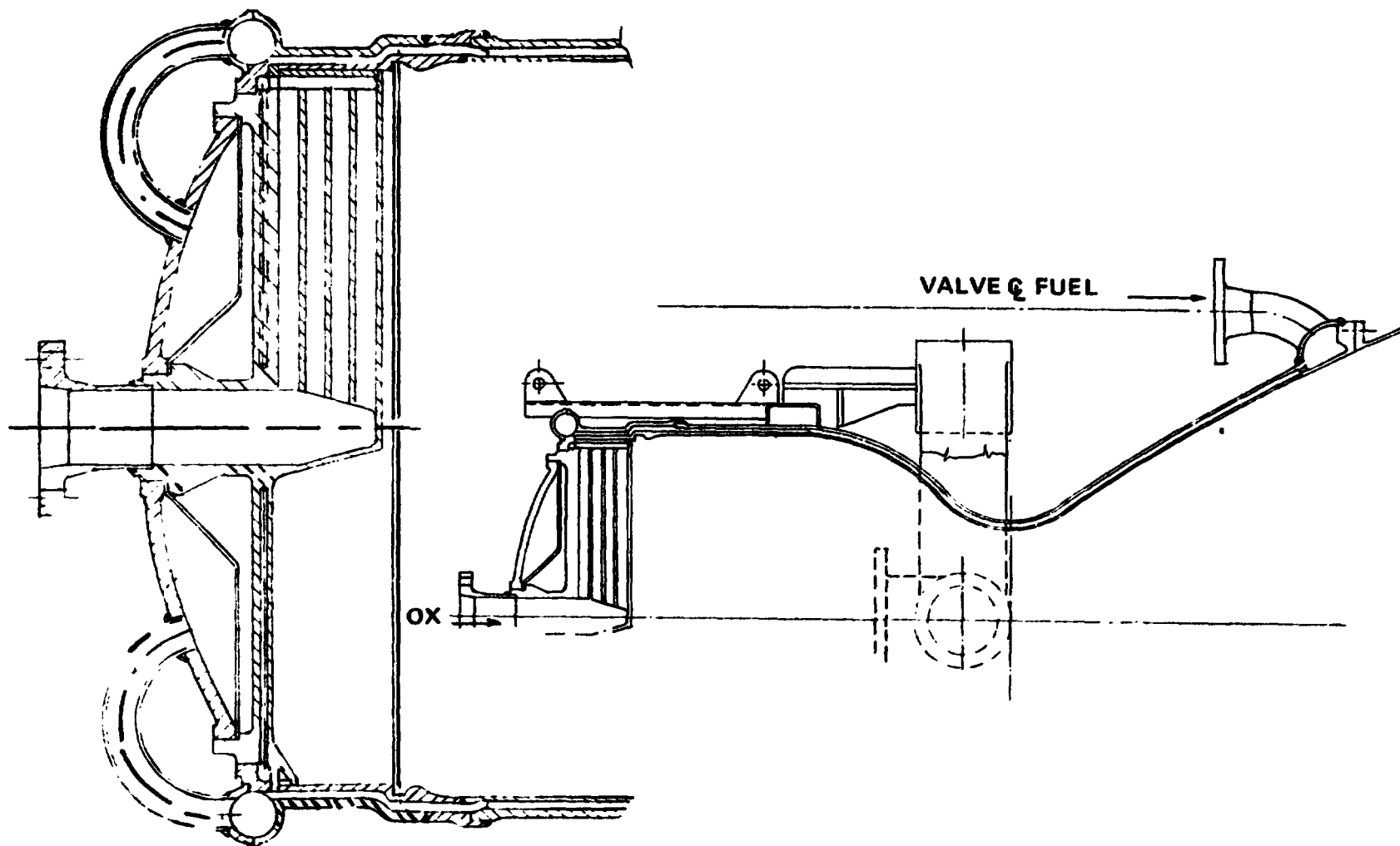
- Spark on
- Ignitor ox valves open
- Ignitor fuel valves
- Pressure transducer confirmation of ignitor operation
- Main propellant valves open
- Engine P_c confirmation
- Ignitor Subsystem off

FIGURE III-2

GIMBAL MOUNT CONFIGURATIONS



N₂O₄/AMINE STAINLESS STEEL CHANNEL WALL CHAMBER



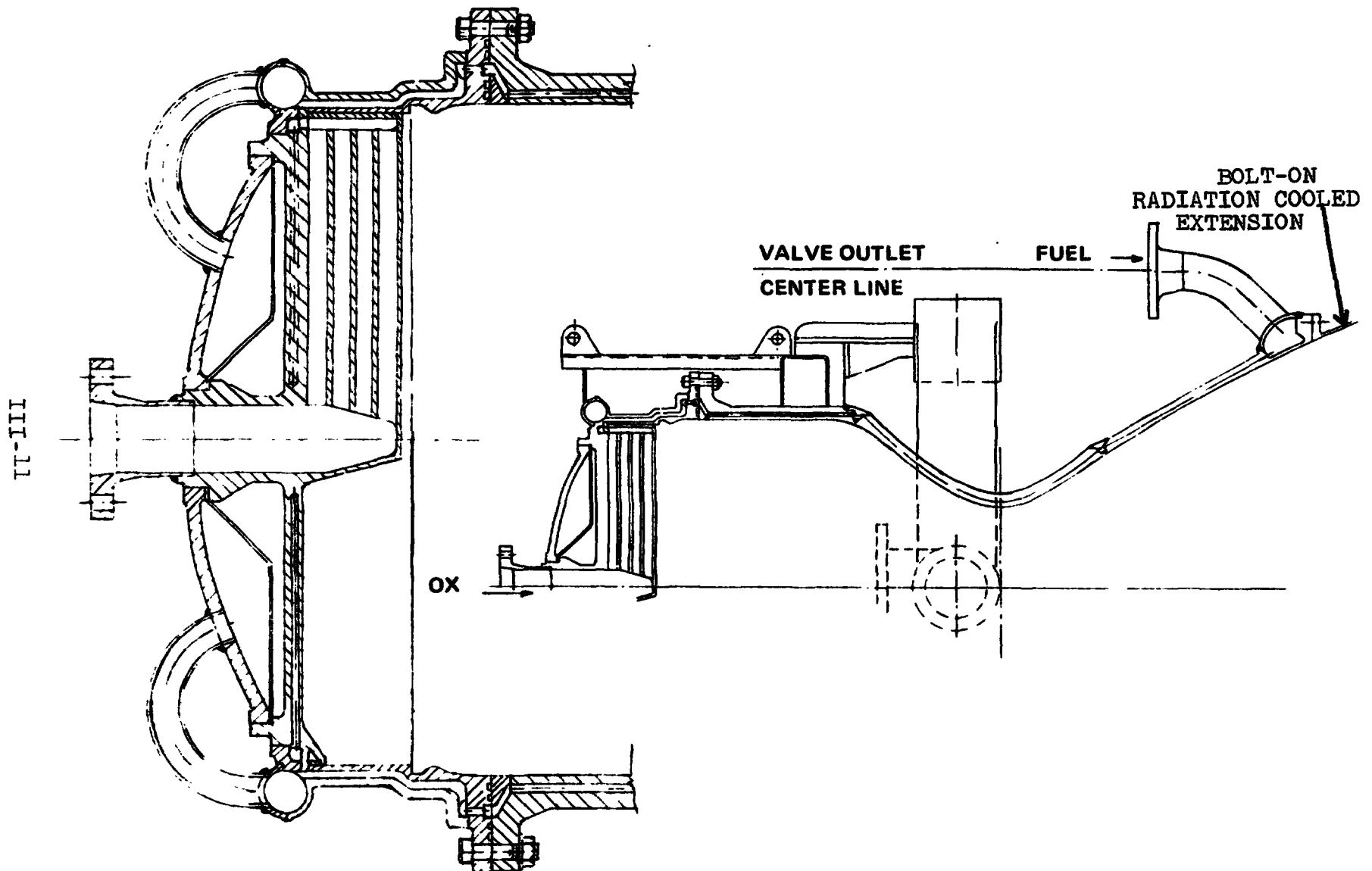
Bell Aerospace Company

ORIGINAL PAGE IS
OF POOR QUALITY

FIGURE III-3

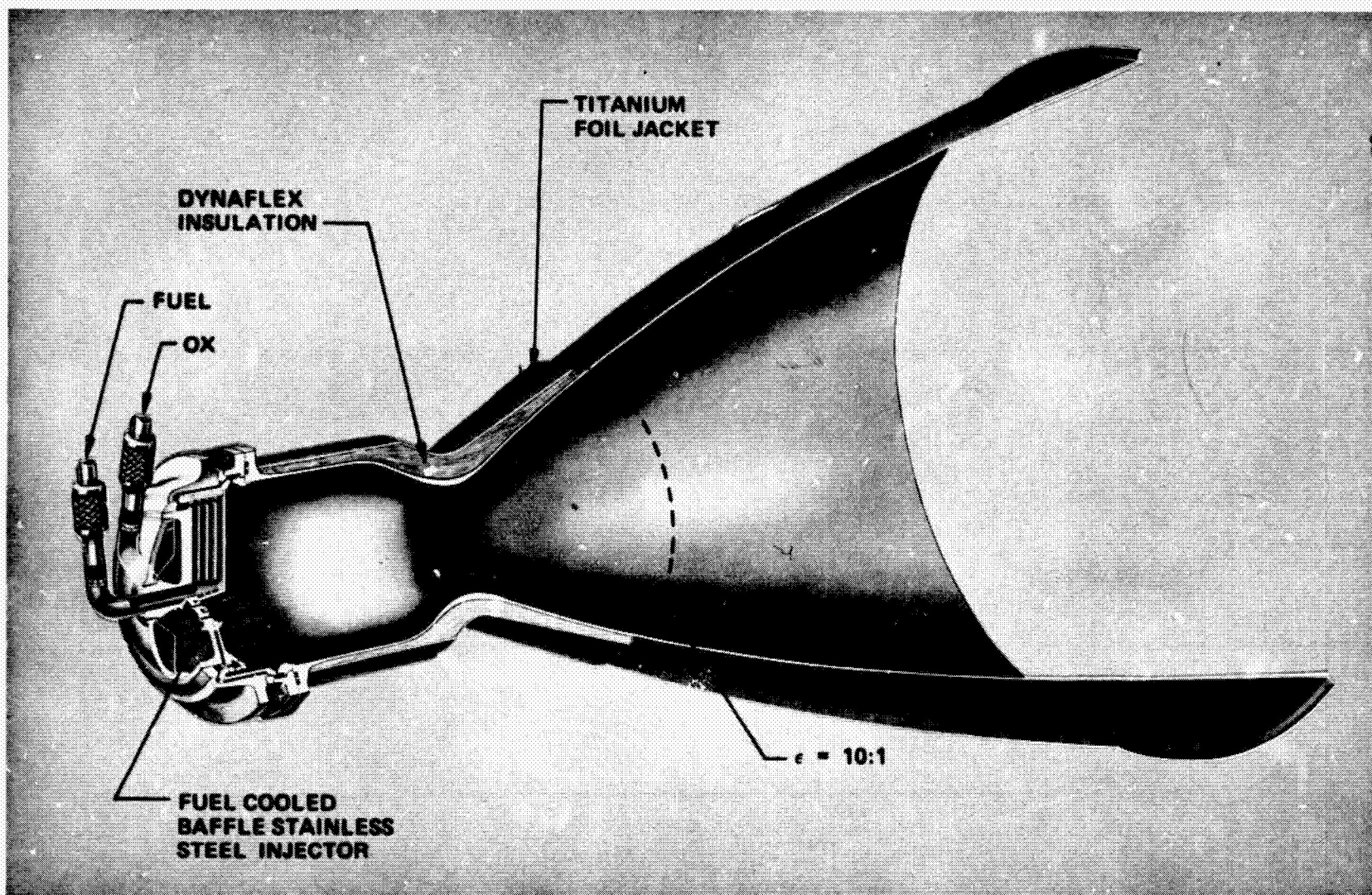
III-10

N_2O_4 /AMINE DRILLED ALUMINUM CHAMBER



Bell Aerospace Company

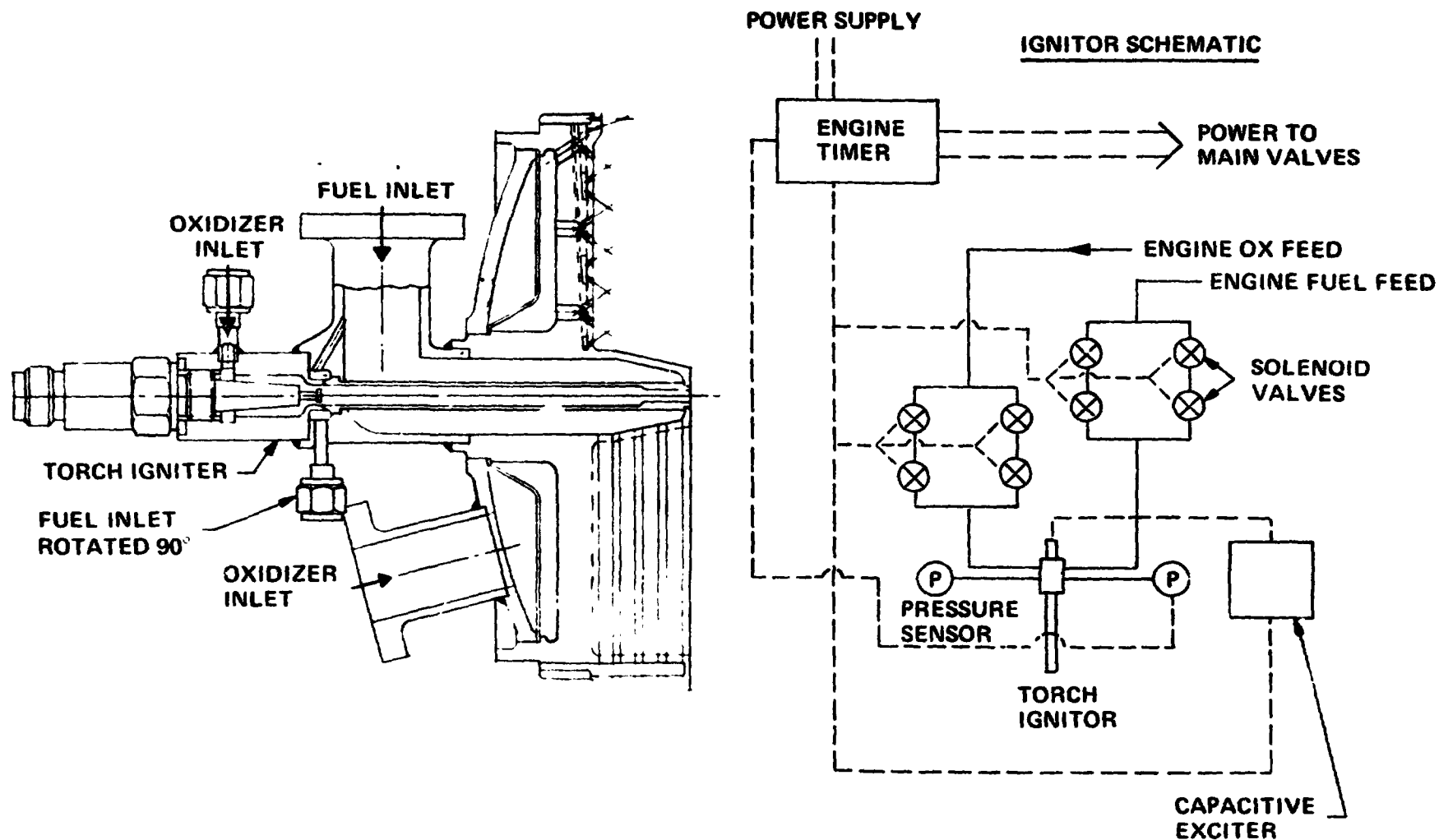
FIGURE III-4



ORIGINAL PAGE IS
OF POOR QUALITY

FIGURE III-5. INSULATED COLUMBIUM THRUST CHAMBER ASSEMBLY

III-12



LOX/AMINE INJECTOR - TYPICAL

FIGURE III-6

Bell Aerospace Company

C. Off-Limits Operation

By agreement with NASA-MSC, off-limits operating conditions were defined as -10% P_c , +12% O/F with a 90°F propellant feed temperature and that each regenerative cooled point design calculated would reflect an 80% utilization of the available fuel heat sink at those off-limits conditions or a margin of 0.20. Each regenerative cooled point design calculated would reflect an 80% utilization of the available fuel heat sink at those off-limits conditions or a margin of 0.20. Each regenerative cooled point design, therefore, exhibited a higher margin at the design point conditions:

$$\begin{array}{l} \text{Operating margin} \\ \text{regen chambers at} \\ \text{design point} \end{array} = \frac{T_{\text{sat}} - T_{\text{out}}}{T_{\text{sat}} - T_{\text{in}}} \quad 0.20$$

where

- T_{sat} = the fuel saturation temperature at chamber pressure
- T_{out} = calculated fuel coolant temperature to the injected orifices; $T_{\text{out}} = T_{\text{in}} + \Delta T$ where ΔT is the calculated regen passage temperature rise and T_{in} = the engine fuel feed temperature.

The off-limits operation represent 12% low fuel feed pressure combined with an 8% low oxidizer feed pressure.

The off-limits definitions were intended to cover only those propellant feed system malfunctions that would change the engine fuel and oxidizer feed pressures. The additional malfunction of pressurizing gas injection or gas bubbles in the CME propellant supply and engine injector malfunctions which could cause loss of circumferentially uniform heat rejection were not included in the off-limits definitions. The additional potential malfunctions were included in the engine technical ratings as described in sub-section G.

The off-limits conditions of high O/F and low P_c with high propellant feed temperatures represent the worst case off-limits condition; the high O/F and low P_c reduced the fuel coolant flow rate increasing its temperature rise while the heat rejected to the coolant increases. The heat flux increases because the reduction of the gas side heat transfer coefficient at reduced P_c is more than offset by the increased gas driving temperature. As will be discussed later, the driving temperature is a function of the vortex film coolant flow and that film coolant flow is a fixed percentage of the fuel flow to the injector. Thus, the reduced fuel flow at high O/F and low P_c resulted in a driving

Bell Aerospace Company

gas temperature increase greater than the decrease in the gas side heat transfer coefficient.

The utilization of 80% of the available heat sink at the off-limits conditions as a regen chamber design constraint recognizes the need for essentially 100% OME reliability and safety. If the fuel temperature were to reach saturation downstream of the regeneratively cooled passages the boiling fuel would cause a loss of fuel flow control; the fuel flow would drop rapidly causing burnout of the chamber and, potentially, damage to the shuttle itself. The preceding conditions would argue for conservatism in the selection of the utilization of available heat sink, 80% utilization would appear to be too high. On the other hand, the possibility of departure from the design conditions by $-10\% P_c$, $+12\% O/F$ together with a $90^\circ F$ propellant feed temperature is undoubtedly remote given the reliability that will be incorporated in the OME propellant feed system through redundancy of pressure regulators etc., and incorporation of pressure and temperature sensors to guard against operation in a degraded mode. In addition, the thermal control of N_2O_4 /Amine propellant which has been demonstrated by the Apollo program suggests that the occurrence of propellant feed temperatures above $+90^\circ F$ is remote. The Task II oxidizer would require LOX tank insulation and proper isolation of LOX and fuel in the OME propellant valve to prevent freezing of the fuel. The Task II propellants would require greater care of engine and tankage design but no insurmountable problems would be anticipated. Thus, there is a low probability of OME operation at the worst case off-limits conditions which argues for reduced regenerative engine thermal design margin.

Another factor associated with utilization of a large percentage of available heat sink is the anticipated run-to-run and engine-to-engine tolerance for the regen cooling passage temperature rise. Low temperature rise tolerance has been achieved by the Agena engine, $\pm 10^\circ F$. That tolerance should be achievable with the OME engine.

The selection of the off-limits definitions was judged to recognize both the need for high reliability and safety together with the low probability of wide departure from the nominal operating conditions.

The off-limits design margin definition of the insulated columbium engine was taken as follows:

$$\text{Margin} = \frac{T_{SL} - T_{off}}{T_{SL} - T_{nom}}$$

Bell Aerospace Company

where

- T_{SL} = the structural limit temperature the coated columbium.
- T_{off} = the calculated maximum columbium temperature at the off-limits conditions.
- T_{nom} = the calculated maximum columbium temperature at the design conditions.

The logic for the establishment of the I_{cb} chamber margin definition included the following:

-The regenerative margin definition includes a relatively short duration condition; wide departure of engine operation from nominal and approaching the off-limits definition could be sensed in flight, and corrective action taken. At worst, the limits encompass one mission or approximately 1000 seconds of firing.

-In the context of relatively short duration off limits operation, the columbium coating temperature limit is approximately 3000°F and the loss of coating would not immediately compromise the engine operation. An uncoated chamber operating in a vacuum would probably survive 1000 seconds of firing. The coating acts primarily as a barrier to hydrogen embrittlement given the reducing atmosphere at the wall from the film coolant. Uncoated columbium sections were embrittled to a depth of 0.010 inches after 2400 seconds of exposure to N_2H_4 decomposition gases.

-The stress rupture life of columbium alloys at various temperatures is shown in Figure III-7. The figure also gives short term thickness requirements as a function of temperature. (Thermocouple data with vortex film cooling shows that the maximum chamber temperature is at least 600°F less than at the throat station.) SCb 291 columbium would provide a high stress rupture life and short term yield strength with a throat thickness of less than 0.10 inches. More easily fabricated C103 columbium could provide adequate life and short term strength at 0.19 inch wall thickness at the throat. With a C103 chamber, the short term structural temperature limit is 3000°F.

-The maximum operating temperature tolerance for vortex film cooled chambers is approximately +50°F.

-With T_{nom} defined as 2400°F, the predicted operating temperature for minus 10% T_c , +12% O/F and 90° propellant feed temperature is approximately 2600°F, including a +50°F tolerance.

OFF-LIMITS OPERATION

REQUIRED COLUMBIUM THICKNESS VERSUS STRESS RUPTURE LIFE

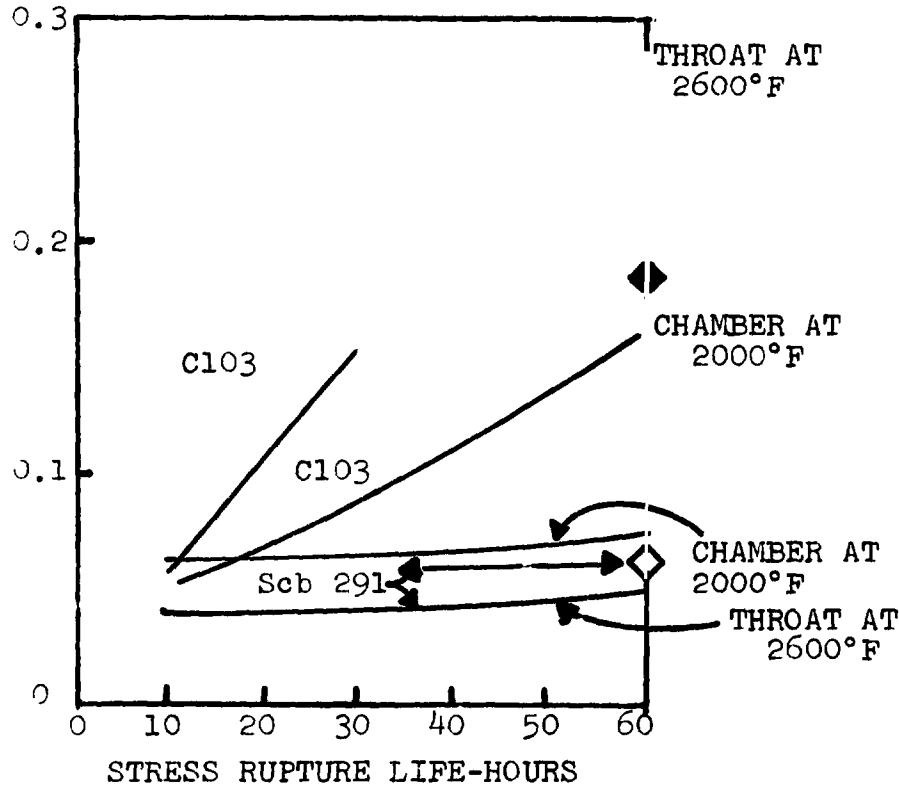
$P_c = 125 \text{ PSIA}$
 $D_c = 10 \text{ IN.}$
 $D_t = 6 \text{ IN.}$

◆ THROAT AT
 2400°F
 ◇ CHAMBER AT
 1800°F MAX

SHORT TERM Cb THICKNESS VERSUS TEMPERATURE

$P_c = 125$
 $D_t = 6 \text{ IN.}$

REQUIRED THICKNESS-INCHES



REQUIRED THICKNESS-INCHES

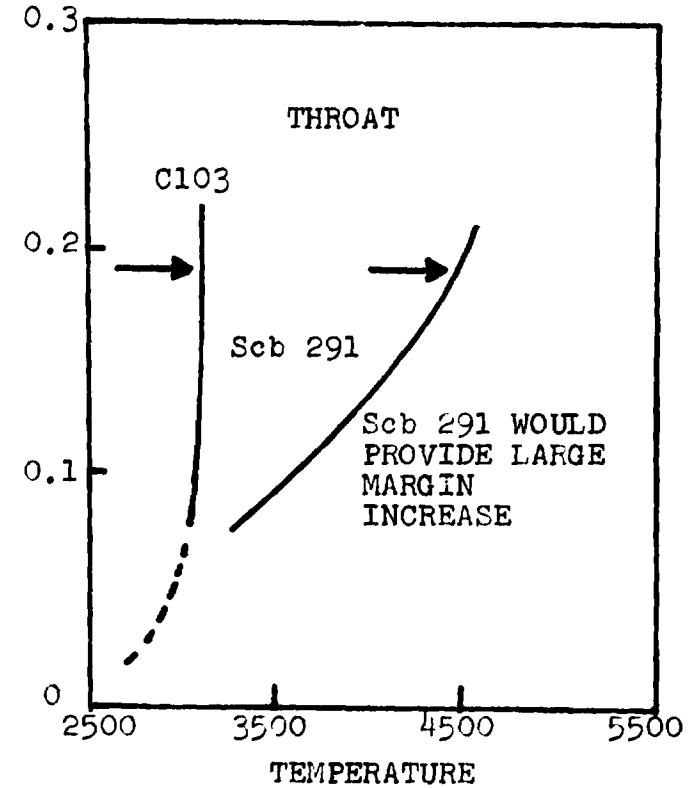


FIGURE III-7

Bell Aerospace Company

The Icb margin with the above definitions and calculated values at the off-limits conditions would be:

$$\frac{3000-2600}{3000-2400} = 0.67$$

or considerably greater than the regenerative cooled margin of 0.20 at the off limits condition. The problem with the definition of the Icb margin relative to that of the regen chambers is the difficulty in selecting a nominal temperature, T_{nom} , comparable to the regen T_{in} , the fuel feed temperature. The definition of T_{nom} of 2400°F may be somewhat optimistic for the purposes of margin definition. If T_{nom} were redefined as a minimum temperature of 1000°F representing essentially unlimited life, Icb margin would be:

$$\frac{3000-2600}{3000-1000} = 0.20 = \text{regen margin definition}$$

Therefore, the selection of a nominal operating temperature 2400°F against an upper limit of 3000° appears to provide an off-limits operating margin at least comparable to the regen definition.

The second element of regen chamber cooling margin, the ratio of maximum calculated heat flux to burnout heat flux was defined as 0.67 at the off limits conditions. The burnout mechanism addressed here is that associated with film cooling in the regenerative cooled passages at sufficiently high heat flux or Q/A and/or low coolant velocity. Q/A burnout limits were established empirically by flow testing various propellants through electrically heated tube sections by several investigators, (Reference 7). Q/A data for MMH is shown in Figure III-8 plotted against VAT sub, the velocity in the heated tube section times the temperature difference between the propellant saturation temperature in the tube section and the recorded fluid temperature. The burnout equation employed in the regen engine calculations is superimposed on the data. Also included is data from Task VII of the contract effort, comparative testing of MMH and MMH with silicone oil additive. The equation selected should be conservative, most of the data shown was recorded for test conditions which did not result in burnout of the test section.

The final topic under off-limits operation is injector baffle and face cooling. Fuel cooling of the Icb engine injector was readily accomplished with high thermal margins. Oxidizer cooling was assumed for the regenerative cooled N_2O_4 oxidizer engines to increase the predicted I_{sp} . If fuel cooling of both the regen chamber and injector were assumed the increased amount of gas side fuel film coolant required to meet the thermal margins would reduce I_{sp} . Fuel cooling of both the chamber and

Bell Aerospace Company

MMH ULTIMATE HEAT FLUX

- BELL DATA MMH
- BELL DATA MMH + 1% Si
- △ ROCKETDYNE DATA (BURNOUT)
- × ROCKETDYNE

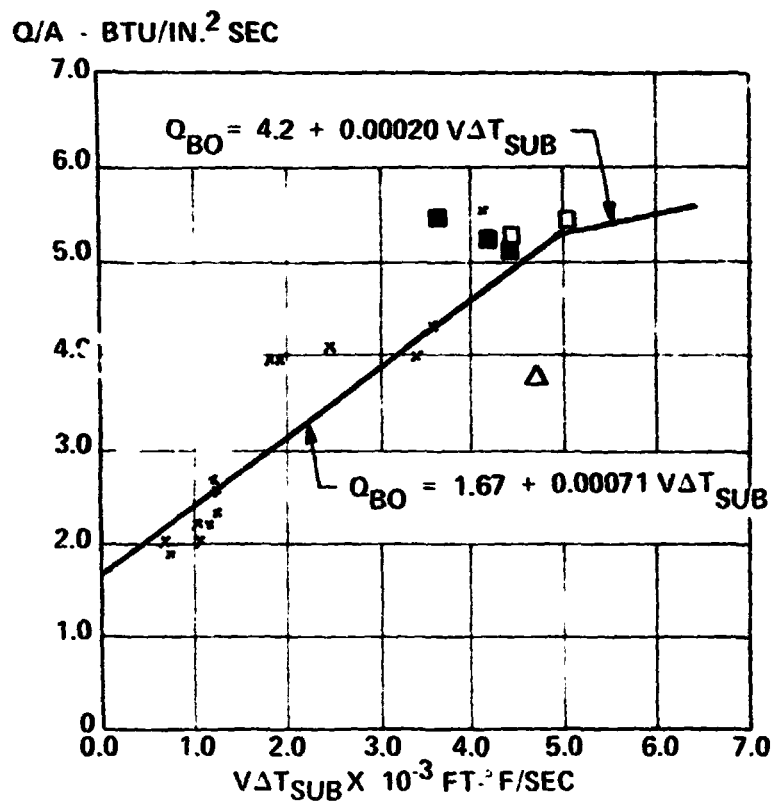


FIGURE III-8

Bell Aerospace Company

injector was required for the Task II LOX engines due to the small temperature difference between LOX feed temperature and its saturation temperature at chamber pressure.

D. Engine Computer Program, General

With the exception of the tube wall regen engine, all nominal and parametric engine data was calculated using an engine design computer program designated ADEPT (Advanced Design Engine Parametric Technology). Each point design was a separate, complete series of calculations with a print out of approximately 110 items of performance, temperature, weight and physical dimensions to define the point design. Selected output data required for the parametric cases was also punched on cards for machine plotting. The large number of calculations required for the cases and data defined by Tables I through III, suggested that the most cost effective and accurate way to carry out the work would be by defining a complete engine computer program. The Task I and II effort centered around the ADEPT program definition. This section will briefly describe the general features of the OME engine computer program. The following section will describe the detail inputs, defining equations and subroutines which were incorporated.

Figure III-9 gives the basic flow of the machine calculations for the regenerative cooled engines. The program input includes type of chamber (CWR or DAR), the propellant combination, engine nominal F , P_c , O/F , nozzle exit diameter, nozzle % bell and chamber L^* . The off-limits conditions of P_c , O/F and feed temperature and the required thermal margin at those conditions complete the input. As discussed above, the off limits conditions were set at +12% O/F , -10% P_c and +90°F.

The first step in the calculations is a trial fuel vortex film temperature from which a fuel vortex flow rate is calculated. Iterative cooling calculations are started with initial values of nominal propellant flow rates, \dot{w}_{nom} , and by off limits definition, \dot{w}_{off} limits, calculated therefrom. The iteration includes calculation of C_f for the propellant combination, mixture ratio, % bell and exit diameter, throat area from $F = P_c A_t C_f$, chamber diameter from a defined functional relationship for the thrust level and P_c together with equations for c^* which predict the combustion efficiency as a function of the amount of film cooling, propellant combination and mixture ratio. A subroutine calculates the chamber divergent nozzle area ratio based on the operating conditions and the upper temperature limit for the radiation cooled nozzle extension. The iteration continues with cooling passage definitions from a heat transfer routine initially for the off limits definitions. Initial throat cooling passage sizes are assumed and the thermal calculations iterate the passage sizes against the burnout heat flux margin. The fuel

Bell Aerospace Company

temperature rise for the N_2O_4 propellant cases is then compared against that margin definition. The LOX cases include the calculation of the additional fuel heat input for injector cooling. The N_2O_4 injector cooling subroutine outputs the thermal margin for that heat transfer process. The comparison of fuel temperature rise against the off limits margin of ≥ 0.2 results in a reset of the barrier flow if that criteria is not met and calculations are repeated until it is met. (In some cases, the fuel cooling margin which can be achieved is outputted.) Those cases were encountered in the parametric calculations and will be discussed in the following sections. After the off-limits margin is met, (or calculated), the program continues with a calculation of the heat transfer to the fuel at the input nominal conditions of P_c , O/F and propellant feed temperature using the chamber geometry definition from the preceding iterative off-limits calculations. The calculation of the chamber coolant velocity at each station allows an integration for total jacket pressure drop.

The chamber coolant passage definition and thermal calculations are then compared against the minimum fabrication dimensions for the cooling passages and the gas side wall temperature limits. The wall temperature (Twg) limits for the operation at the point design are based on preliminary thermal cycle life calculations. Upper temperature limits were defined for each regen chamber in order that the chamber be capable of 4000 thermal cycles of operation. If the coolant passages were smaller than the defined minimum passage size and/or the Twg exceeded the upper temperature limit for cycle life, the case was recalculated at an increased fuel film coolant flow. When those conditions were met the engine fuel and oxidizer feed pressures are calculated from the appropriate definition of fixed pressure drops together with the calculated chamber cooling passage, injector cooling passage and combustion zone pressure drops.

The area ratio for the nozzle extension junction between columbium and titanium is calculated based on an upper structural temperature limit of the titanium. The chamber outer shell thickness definitions are based on pressure and inner wall thermal loads. The injector thicknesses were defined as a function of chamber pressure and chamber diameter for adequate structural strength. The auxiliary weights, valve assembly, gimbal ring and gimbal ring mount are calculated by equations based on preliminary design of those subassemblies. The combustion chamber and nozzle extension thickness definitions are checked against or set by minimum gage definitions for fabrication. The weight calculation of the thrust chamber follows, completing the engine weight definition as the final step of the regenerative cooled engine calculations.

Bell Aerospace Company

The portion of the ADEPT program for the insulated columbium chamber and engine is less complex than the regenerative cases (Figure III-10). The input includes a trial value of the fuel vortex film cooling flow rate. Calculation of the area ratio, ϵ , and C_f "actual" (predicted) is followed by determination of c^* based on a functional relationship between the combustion efficiency, the chamber L^* and the fuel vortex film coolant flow rate, ρ . The complete chamber geometry is established including the chamber insulation thickness for an external temperature of 300°F. (The insulation is assumed to terminate at divergent nozzle area ratio of 10:1.) The calculation of the maximum columbium wall temperature from $T_{\max} = f(\rho, c^*, P_c, A_t)$ for nominal and off limits conditions results in iteration of ρ until $T_{\max} = 2400^\circ\text{F}$ for nominal operation. Injector fuel cooling margin calculations are followed by definition of engine fuel pressures, and weights similar to the regenerative cooled engines. The Icb engine includes the definition of titanium for the nozzle extension downstream of the area ratio at which the calculated extension temperature equals the structural temperature limit for titanium.

E. Calculation Definitions

1) Thrust Coefficient

The thrust coefficient at infinite altitude C_{f_∞} was calculated as follows:

$$C_{f_\infty} = \eta_{BL} \eta_{DIV} \eta_{KINETIC} C_{f_\infty \text{ S.E.}}$$

Where:

η_{BL} = boundary layer efficiency

η_{DIV} = divergence efficiency

$\eta_{KINETIC}$ = kinetic efficiency

$C_{f_\infty \text{ S.E.}}$ = shifting equilibrium thrust coefficient at infinite altitude

The three efficiencies recognize the divergent nozzle losses given homogeneous, 100% shifting equilibrium product of combustion at the physical throat plane. The departure of the real case from homogeneous, 100% shifting equilibrium gases at the physical throat plane were considered to be self-compensating based on test results with various thrust chambers at BAC which are described in the following paragraph. The lack of 100% shifting equilibrium gas products, the combustion process is not 100% efficient relative to that criteria, and the curvature of the sonic velocity

Bell Aerospace Company

location relative to a geometric throat diameter tend to reduce C_f . The lack of gas radial homogeneity, "core" gases with an O/F above the O/F of the engine feed is surrounded by a heat fuel film at the wall with zero O/F, increases C_f in the range of film coolant flows under consideration.

Regression analysis of altitude test data for a 600 lb thrust unit operating with zero to 13% vortex film coolant flow (film coolant total propellant flow = .13) shows that recorded P_c , and vortex flow values are not statistically significant relative to the C_f determined by recorded thrust and P_c , $C_F = F/P_c A_t$. The value of throat area is based on throat measurement corrected to the operating temperature. The lack of correlation of C_f with P_c and vortex flow also indicates a lack of dependence of C_f on the actual combustion efficiency. Therefore, the average C_f value for the tests, 1.7367, is the best estimate of C_f . The calculated value of $C_f = \eta_{BL} \eta_{DIV}$ for the nominal P_c and thruster O/F is 1.7322.

$\eta_{KINETIC} C_{f_{\infty}}$ S.E.

The test data and analyses support the selection of the method of $C_{f_{\infty}}$ calculation employed in the ADEPT program.

The thrust coefficient efficiencies employed for the machine calculations were incorporated into the program as follows:

η_{BL} : 15 sample $C_{f_{\infty}}$ calculations were made with the JANNAF TBL, turbulent boundary layer, program and those results were compared with one dimensional inviscid $C_{f_{\infty}}$ for the same nozzles. The nozzles were representative of the total range of nozzle sizes. The ratio of the TBL and inviscid values provided η_{BL} . The 15 values of η_{BL} were inputted as a table with provision for linear interpolation.

η_{DIV} : defined by equation as a function of area ratio and nozzle length for optimum RAO nozzles. The equation was established by curve fitting data points from JANNAF TDK computer program data spanning the range of nozzle geometries. The two dimensional values were compared with one dimensional calculations to define an efficiency.

$\eta_{KINETIC}$: calculated by curve fit equation of selected points of the ratio of one dimensional kinetic computer output to one dimensional equilibrium data. Standard JANNAF ODK and ODE programs were employed. Twelve to 25 ODK values were calculated for each propellant combination depending on the parametric range to be calculated by the engine program.

Bell Aerospace Company

$C_{f\infty}$ S.E.: the shifting equilibrium values of the thrust coefficient at infinite altitude were inputted in tabular form for each propellant combination as a function of P_c , O/F and area ratio. Linear interpolation of the tabular data was included.

2) Fuel Vortex Gas Film Temperature, T_{Film}

T_{film} is employed as the driving gas temperature for the regenerative cooling calculations at relatively low values of fuel film cooling ratio, ρ , w fuel film/w total flow. Values for the regenerative cooled engines were generally less than 4%. T_{film} was also taken as the wall temperature of the insulated columbium thrust chambers with values of ρ in the range of 10% to provide columbium temperatures at a maximum of 2400°F.

Table V shows the functional relationship between T_{film} and ρ^* where ρ^* is defined in terms of ρ , the vortex film cooling length L , the chamber diameter D_c , the characteristic velocity c^* , chamber pressure P_c and the area of the throat, A_t . The derivation of the vortex cooling parameter, ρ^* , is described in Reference 5. Fuel vortex film cooling is accomplished by tangential injection of liquid fuel on the wall just downstream of the injector as described earlier.

The values of the constants in the T_{film} , ρ^* equation of Table V were based on test data, the theoretical combustion temperature of the propellant combination at normal P_c and O/F, and the fuel decomposition temperature or normal boiling point at chamber pressure. Figure III-11 shows the T_{film} ρ^* relationships for N_2O_4 with MMH and $N_2O_4/50-50$ blend propellants. At $\rho^* = 0$ T_{film} approaches the theoretical combustion temperature of the propellants adjusted downward by an assumed combustion efficiency. At high values of fuel vortex film cooling ρ and ρ^* T_{film} approaches the decomposition temperature of the amine fuels. The figure includes firing data which was available at the time of the Task I and II effort which defined the shape of the curve between the limits of high values of ρ^* and $\rho^* = 0$.

The T_{max} , ρ^* equation constants of Table V for the LOX/Amine propellant combinations were estimated based on the N_2O_4 /Amine test data with adjustment of the curves to reflect the combustion temperature at optimum I_{sp} mixture ratios. The values for LOX/ C_3H_8 and LOX/RP-1 reflect the decrease of T_{max} to the boiling point of the fuel at high values of ρ and ρ^* , Figure III-12. Two data points were obtained with a 600 lbf chamber with $N_2O_4/50-50$ blend propellants injector feed and separately fed C_3H_8 and RP-1 vortex cooling. The T_{max} , ρ^* curves were adjusted linearly upward at those points for the combustion temperature ratios of LOX and the fuels to that of $N_2O_4/50-50$.

TABLE V

FUEL VORTEX GAS FILM TEMPERATURE, T_{FILM}

$$T_{\text{FILM}} = C_1 + C_2 e^{-(C_3 \rho^* + C_4 \rho^{*2})}$$

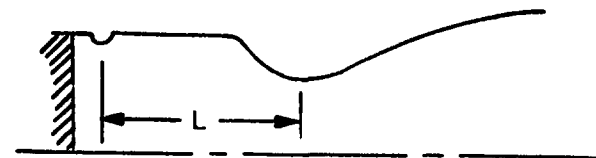
$$\text{WHERE } \rho^* = \frac{\rho}{\frac{L}{D_C^{0.8}} \left(\frac{c^*}{P_C A_t} \right)^{0.2}}$$

$$e = 2.7187$$

$$T_{\text{FILM}} = T_{\text{MAX. INSULATED WALL}}$$

$$\rho = \frac{\text{VORTEX FLOWRATE}}{\text{TOTAL ENGINE FLOWRATE}}$$

L = VORTEX LENGTH



	$\frac{C_1}{1833}$	$\frac{C_2}{3003}$	$\frac{C_3}{15.2}$	$\frac{C_4}{590}$	BASIS
$\text{N}_2\text{O}_4/\text{MMH}$	1833	3003	15.2	590	DATA CURVE FIT AND EXTRAPOLATION TO THEORETICAL T_c AT $\rho^* = \rho = 0$ AND ESTIMATED FUEL DECOMP. TEMPERATURE AT HIGH ρ^*
$\text{N}_2\text{O}_4/50-50$	1833	3349	15.0	470	
LOX/MMH	1833	3593	28.5	360	
LOX/50-50	1833	3658	26.3	230	ESTIMATED ON BASIS OF ABOVE THEORETICAL T_c AT OPT. I_{sp} O/F
$\text{LOX/N}_2\text{H}_4$	1833	3658	26.3	230	
$\text{LOX/C}_3\text{H}_8$	90	5152	20.4	220	ABOVE PLUS ONE DATA POINT EACH WITH 600 LB - HDW, FUEL SAT. TEMPERATURE AT HIGH ρ^*
LOX/RPI	625	4864	9.0	410	

ENGINE COMPUTER PROGRAM - GENERAL - REGENERATIVE COOLING

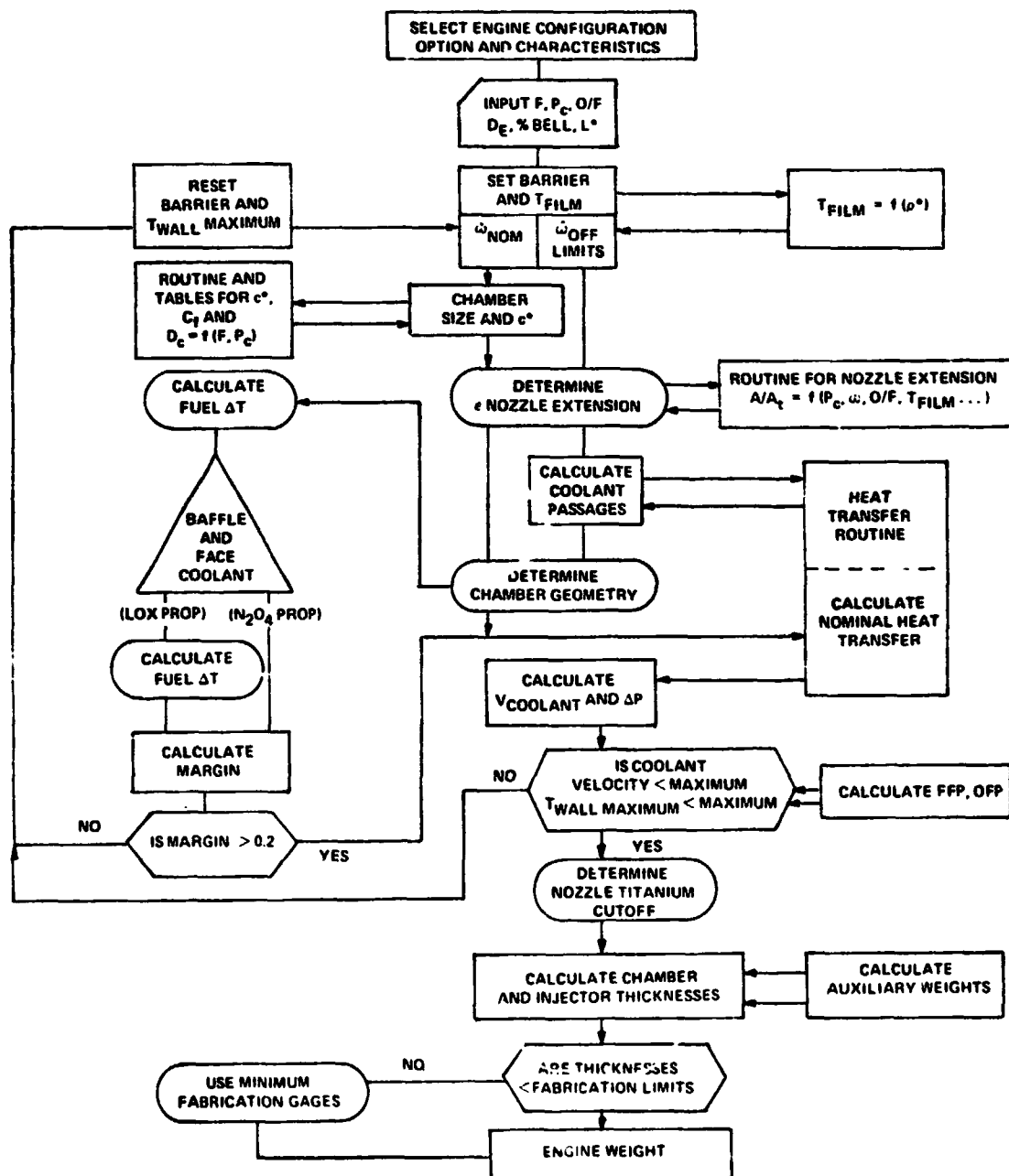
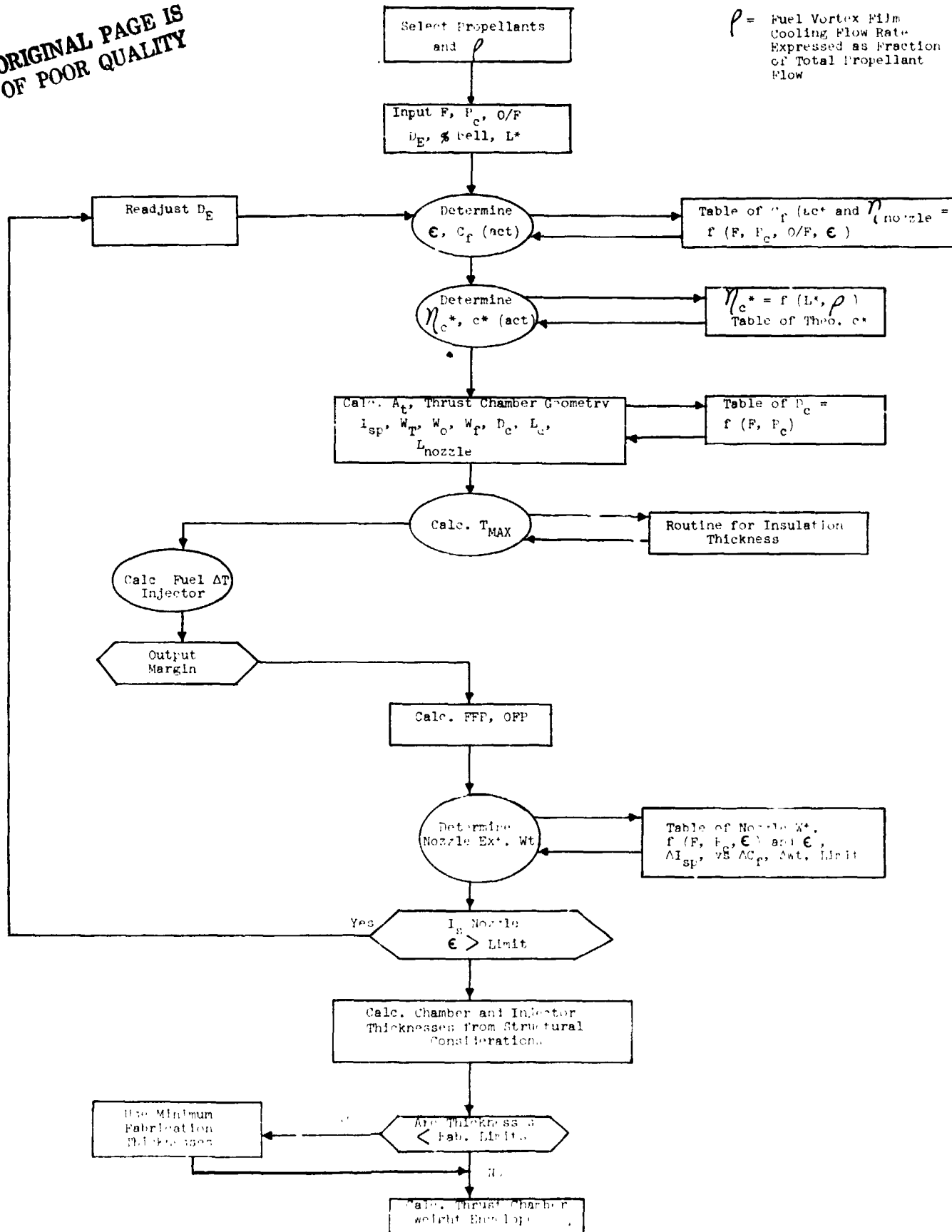


FIGURE V-

ORIGINAL PAGE IS
OF POOR QUALITY

ρ = Fuel Vortex Film
Cooling Flow Rate
Expressed as Fraction
of Total Propellant
Flow



ONE PARAMETRIC INPUT PROGRAM

FIGURE V-1

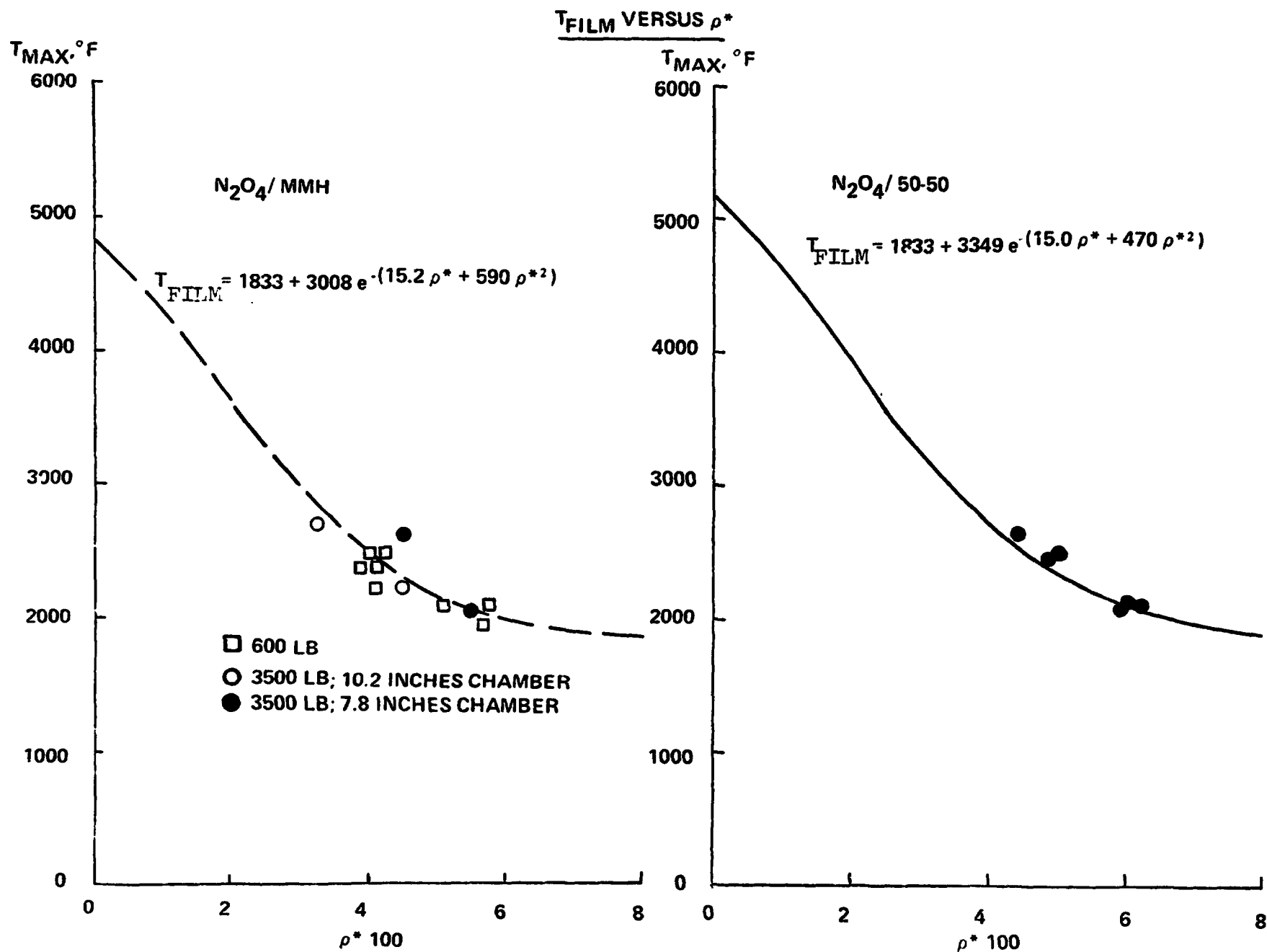


FIGURE III-11

T_{FILM} VERSUS ρ^*

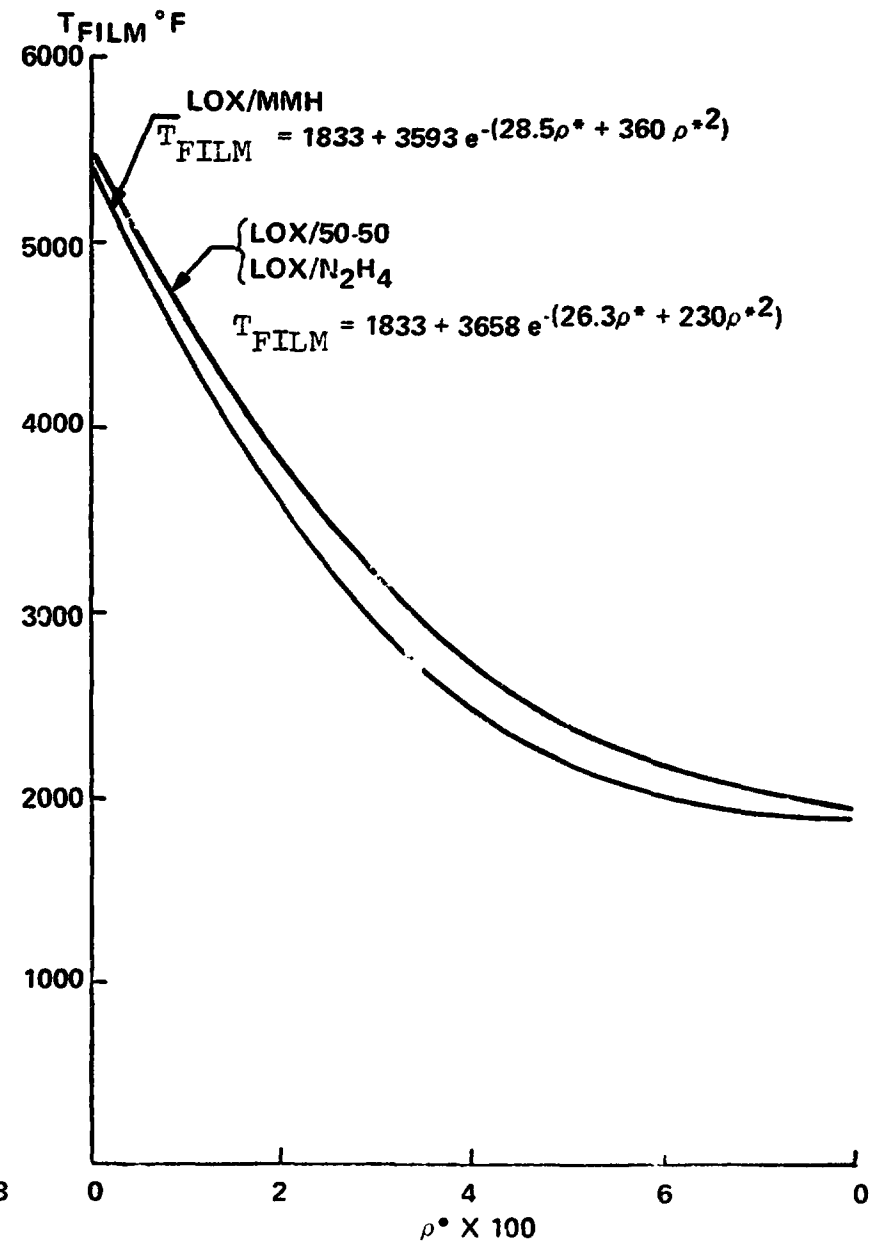
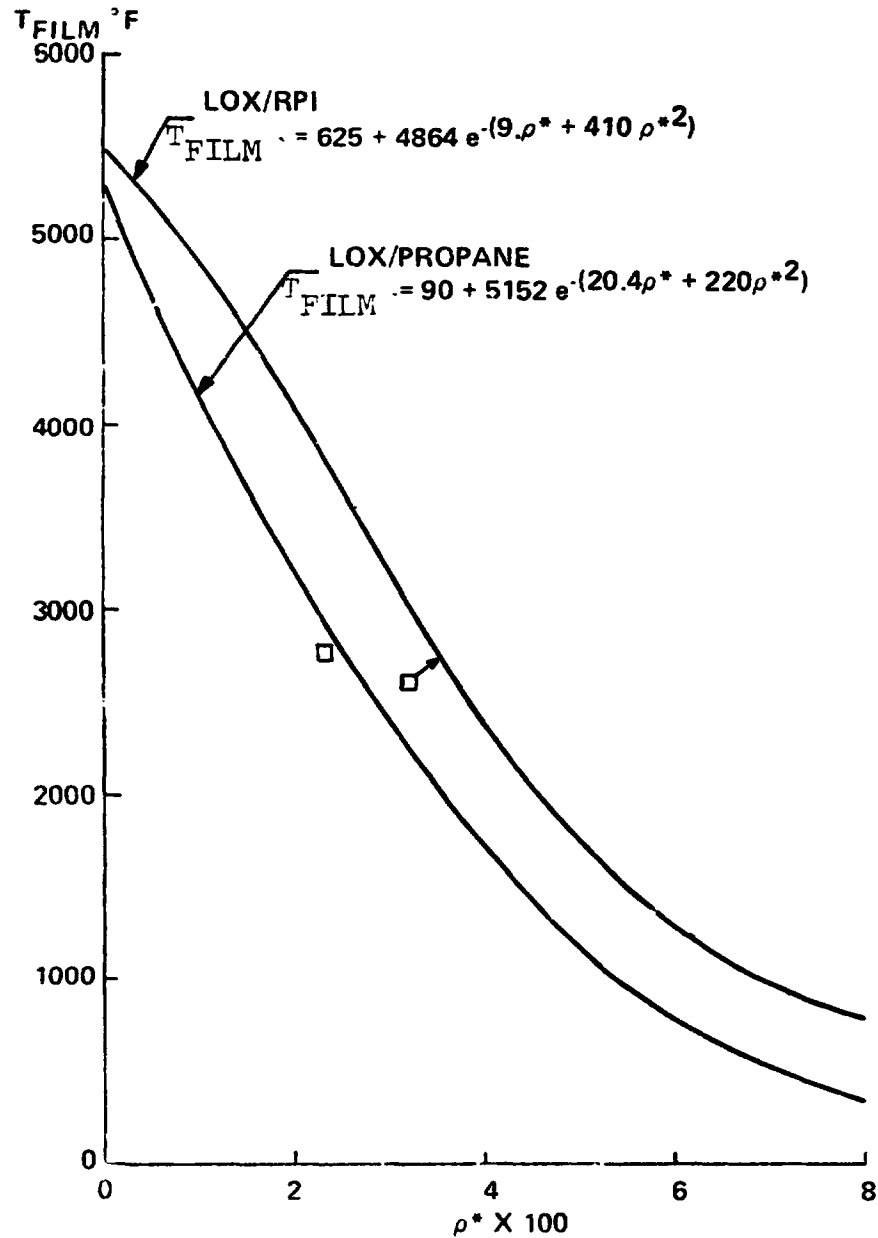


FIGURE III-12

3500 LB THRUST CHAMBER TEST DATA

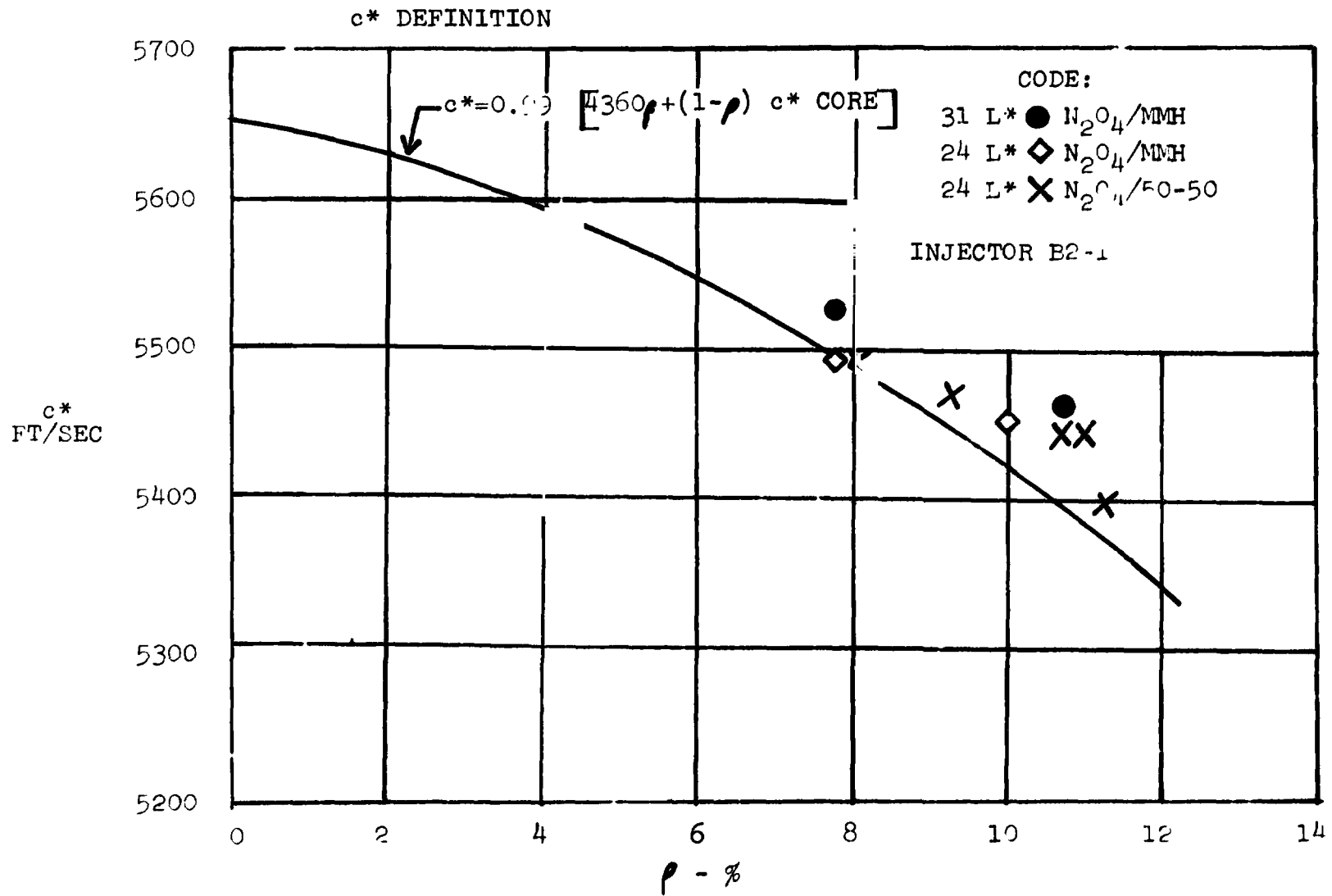


FIGURE III-13

Bell Aerospace Company

3) C*, Characteristic Velocity Equations

The most applicable c^* data available for thrust chamber operation with fuel vortex film cooling consisted of a series of tests conducted with an unbaflled LM ascent engine injector. The firings were made at a nominal P_c of 120 psia and an O/F of approximately 1.60. The data is shown in Figure III-13 together with the c^* equation included in the ADEPT program for N_2O_4 /amine combinations. The equation selected was approximately 1% lower than the data for an L^* of 31 inches based on an anticipated reduction of combustion efficiency for the defined OME injectors which included five leg baffles as described in sub-section B. The projection of the c^* equation to the lower values of ρ , applicable to the regenerative cooled chamber operation, was based on previous experience that a reasonable upper limit of c^* for operation with no film coolant is approximately 99% of theoretical characteristic velocity.

The N_2O_4 /Amine c^* equation was assumed to be applicable to the LOX/Amine combinations. The contribution of the vortex coolant flow, 4320 ρ ft/sec, to the total c^* was assumed to be constant with LOX oxidizer. The c^* equations for LOX/RP-1 and LOX/ C_3H_8 were based on the limited firing data at 600 lb_f described in the preceding section. The tests indicated a reduced c^* contribution with RP-1 and C_3H_8 equivalent to 1600 ρ and 1500 ρ respectively. Thus the c^* equation for LOX/RP-1 became:

$$c^* = 1,600 \rho - 0.99 (1 - \rho) c^*_{core}$$

where

c^*_{core} = the theoretical value at the injector O/F

$$O/F_{core} = \frac{(O/F)_T}{1 - \rho (O/F)_T}$$

and

$(O/F)_T$ = the engine total or overall mixture ratio

4) Chamber Geometry

Combustion chamber inside diameter was defined (Figure III-14) by considerations of combustion efficiency, vortex film cooling effectiveness total heat rejected to the regenerative coolant, pressure drop across the combustion zone, engine length, and injector plus combustion chamber weight. With the exception

Bell Aerospace Company

of weight, the considerations favor larger diameter units. The relatively high performance, pressure fed, $N_2O_4/50-50$ blend, LM Ascent and Service Module Engines were characterized by thrust to combustor area ratios of 72 and approximately 86 lbf/in^2 respectively. Those thrust to area ratios translate to 10.0 and 9.4 inch D_c respectively for the normal 6K OME engine. Contraction ratios above 3.0 reduce the pressure drop across the combustion zone to less than 2 psi, favoring the larger of the two nominal thrust engines. The functional relationship of T_{max} and P^* and the definition of P^* favors lower ratios of chamber length (injector face to throat) to chamber diameter ratios or chamber diameters approaching chamber lengths. For the case of equal combustion volumes and using classical heat transfer equations at a chamber pressure of 125 psia, an 8 inch diameter chamber would reject over 30% more heat to the fuel regenerative coolant than a 10 inch diameter chamber. With minimum length engines, and a fixed diameter exit of 50 inches, the length difference for 6K engines with an L^* of 30 inches represents approximately 0.4 seconds I_{sp} advantage for a 10 inch diameter unit relative to an 8 inch diameter assembly. The weight penalty for equal combustion volumes is approximately 10 lbs for the case of the nominal OME engine for a 10 inch diameter chamber versus an 8 inch diameter unit.

In general, the comparisons of the effects of chamber diameter suggested that the shorter length, lower pressure drop larger diameter chambers designed for a thrust area ratio combustor of approximately 70 lbf/in^2 at nominal chamber pressures would offset the increased weight of those engines relative to smaller diameter designs. The net advantage of the larger diameter units defined by Figure III-14 would be reduced coolant heat flux, increased film coolant effectiveness and potentially higher combustion efficiency.

The characteristic chamber lengths were selected on the basis of the test firings with vortex film cooling at 3400 lbf , the L^* 's of the LM Ascent and SM Engines and literature data for LOX/Amine and LOX/Hydrocarbon units. The selected L^* was 30 inches for all propellant combinations with the exception of LOX/RP-1 which was taken as 40 inches.

5) Thermal Calculations; Regenerative Cooled Chambers

The machine calculations for the heat input to the regenerative fuel coolant involved an iterative process as described earlier.

Bell Aerospace Company

CALCULATION DEFINITIONS CHAMBER GEOMETRY

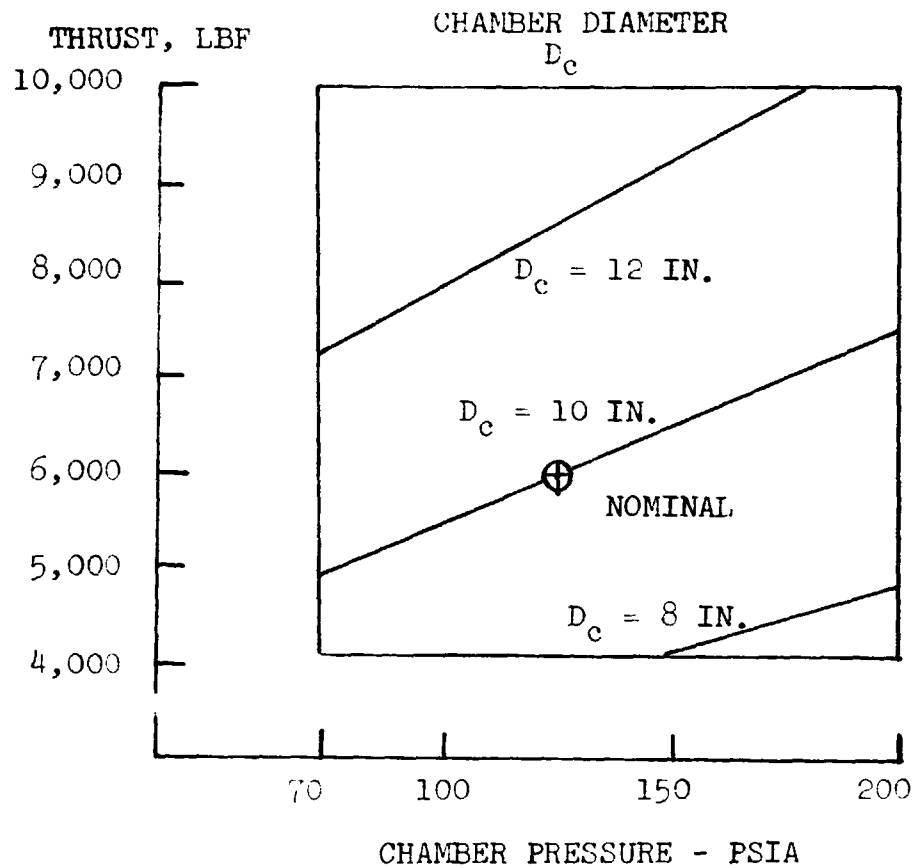


FIGURE III-14

Bell Aerospace Company

The basic regenerative cooling equation

$$Q/A = \int_{L_l}^{L_T} h_g (T_{\text{film}} - T_{wg}) = \frac{k}{x} (T_{wg} - T_l) = h_l (T_{wL} - T_{\text{bulk}})$$

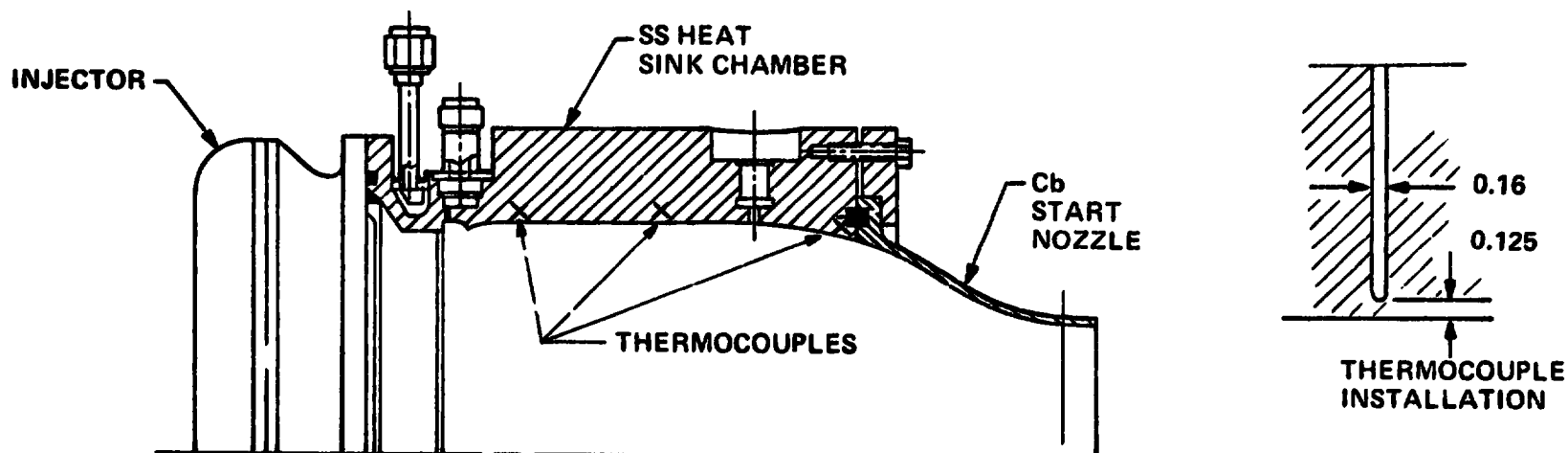
required subroutines to establish the total chamber length L_T , the fuel vortex liquid length L_l , and h_g and h_l the gas side and liquid side film coefficients, respectively. Maximum Q/A at the throat was adjusted to provide the defined margin relative to the burnout heat flux. The subroutines and the definition of burnout heat flux are described in the following paragraphs.

The chamber length from the injector face to the throat was established by the chamber diameter definition of section d) together with the appropriate L^* value and calculated area of the throat. The divergent nozzle area ratio for the regenerative chamber was established by a subroutine for the radiation cooled nozzle extension.

The calculated T_{film} and the gas side heat transfer coefficient at the throat were extrapolated to divergent nozzle stations and a heat balance sought for the radiation cooling process which provided a maximum nozzle extension temperature of 2400°F at nominal operating conditions. The station providing the 2400°F extension defined the required divergent nozzle area ratio of the regen chamber. The 2400°F temperature was selected based on the use of coated columbium for the nozzle extension from the attachment flange to an area ratio consistent with the structural limitations of titanium, as discussed in sub-section C.

The definition of the fuel vortex liquid length, L_l , was included to account for the region of low heat input to the regenerative coolant. The injected fuel vortex film coolant persists as a liquid film for a distance along the chamber wall until heated by the combustion to vaporization and decomposition. The low temperatures at the head end of the chamber were verified during the 3500 lbf firing, Figure III-15. The L_l was calculated using an equation from reference 1 for a similar process of liquid film hot gas interaction. The reference also provides an expression of heat flux to the wall for the region of the liquid film. Thus the total heat input to the chamber coolant included that calculated for the total chamber length from injector face to the nozzle extension flange minus the liquid length, $L_T - L_l$, plus the low heat input for the liquid length region. The possibility of an optimistic total heat flux reduction by accounting for the liquid length was off set by the assumption that the driving gas temperature for the remainder of the chamber barrel section and convergent nozzle was equal to that calculated for the throat station as shown in Figure III-15.

3500 LB THRUST CHAMBER TEMPERATURE GRADIENT



T_{GAS} ASSUMED BY CALCULATIONS

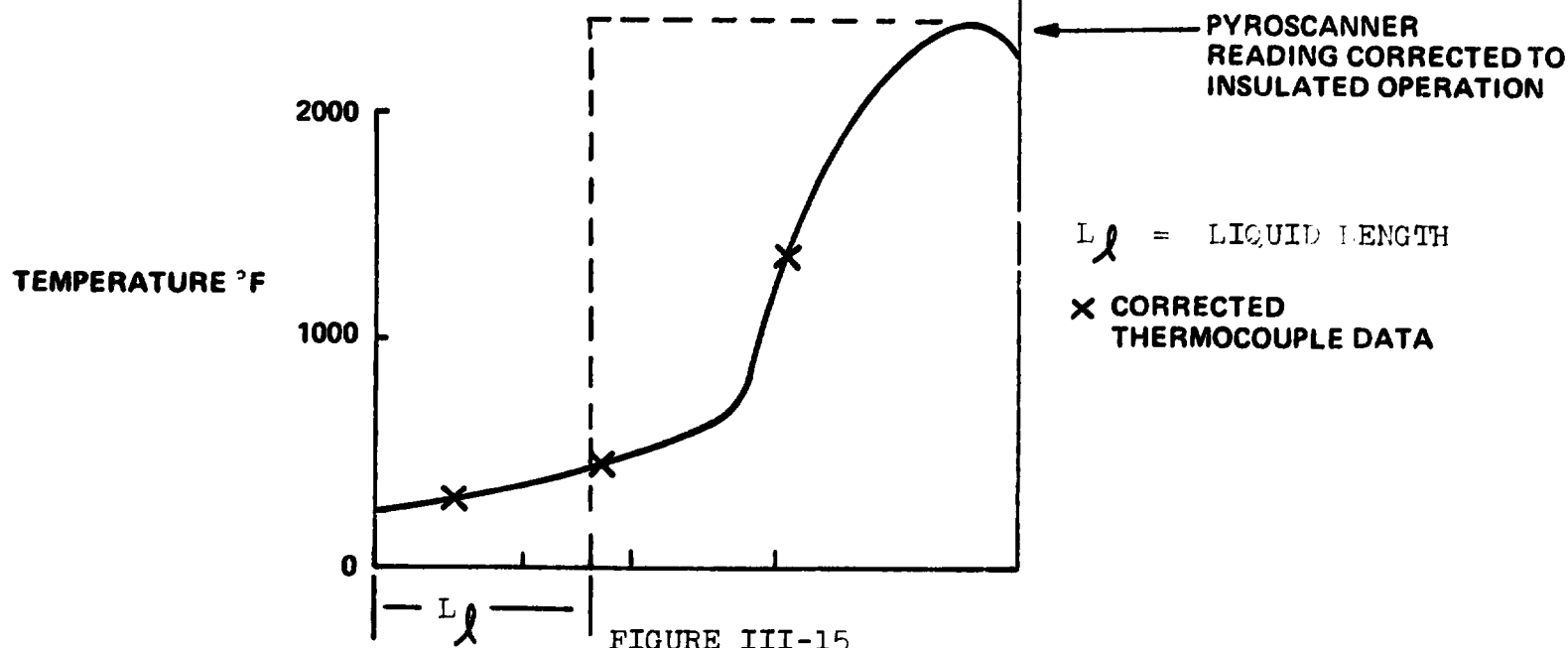


FIGURE III-15

Bell Aerospace Company

The gas side and liquid side film coefficients, h_g and h_l , were calculated using industry accepted methods. For example, the throat station h_g was calculated:

$$h_g = 0.026 \left(\frac{w}{AT} \right)^{0.8} \left(\frac{K PR^{0.4}}{\mu^{0.8}} \right) \frac{1}{DT^{0.2}}$$

where w = combustion gas flow rate, lb/sec
 A = throat area, in²
 D = throat diameter, inches
 K, PR, μ = ratio of specific heats, Prandtl number and viscosity for the combustion gases at the reference enthalpy (Reference 8) temperature.

The h_g for other stations was ratioed from the throat station value:

$$\begin{aligned} h_{g, \text{ chamber}} &= h_{g, \text{ throat}} (A/AT)^{0.8} \\ h_{g, \text{ divergent nozzle}} &= h_{g, \text{ throat}} (A/AT)^{1.2} \\ &\quad \text{for } A/A < 4:1 \\ &= h_{g, \text{ throat}} (A/AT)^{0.9} \\ &\quad \text{for } A/AT > 4:1 \end{aligned}$$

The calculations of L_T , L_l , h_g , h_l and that of T_{film} plus inputs of k (thermal conductivity) and values of x (thickness) for the chamber material under consideration and the defined fuel inlet temperature, allowed integration of the basic regen cooling equation to establish the fuel temperature at the chamber outlet.

The calculated maximum heat flux at the throat, was compared against heat flux burnout relationships established by heated tube testing at various facilities. The equations employed in the ADEPT program are given by Table VI. Insufficient margin, Q/A calculated + $Q/\text{Burnout} < 1.5$, lead to iteration of the throat cooling passage dimensions to increase the coolant velocity and the value of $Q/\text{Burnout}$ that iteration was constrained. The minimum passage sizes were based on reasonable manufacturing limits and two dimensional heat transfer calculations. The heat

Bell Aerospace Company

transfer analyses indicated maximum land width (channel wall) or hole spacing (drilled aluminum) to preclude excessively high values of T_{wg} for the material between the cooling passages. Failure to reach the Q/A margin definition of 1.5 lead to a complete recalculation with a higher value of fuel film coolant.

Table VII also shows the gas side wall thicknesses assumed on the basis of fabrication limits and the limits of the gas side wall temperature. As mentioned earlier, the gas side wall temperature limits were set based on structural calculations. The calculations showed that the maximum temperature was dictated by the required thermal cycle life of 4000 firings. The thermal cycle calculations were based on the cumulative damage criteria of Robinson-Taira, Reference 9 with stresses calculated by the methods of Reference 10. The temperatures corresponding to the neat amine fuels were determined by the structural calculations. The temperatures for MMH with silicone oil additive and the hydrocarbon fuels were degraded from the values for the neat fuels because the silica and carbon deposits result in a fluctuating T_{wg} as the deposits build up and flake off. The process of carbon deposition is described in the literature (Reference 11). The silica depositions were noted in tests at Bell with the silicone oil additive.

The total heat flux reductions for the carbon and silica deposits were taken from the literature and Bell test results. The total chamber Q/A was reduced by 70% for RP-1 and 52% for C_2H_8 . An average of 30% reduction was assumed for silicone oil additive to the amine fuels based on the test results presented in Figure III-16.

6) Injector Cooling

The injector cooling subroutine assumed a gas driving temperature equal to the theoretical combustion temperature and an h_g equal to $1/2$ of that calculated for the chamber barrel section. Those assumptions were consistent with baffle test data from the IM Ascent engine program. A baffle length of 1.5 inches was taken as representative for the range of chamber diameters included in the parametric studies. The stainless steel baffle cooling passages were defined as four rectangular parallel flow passages with a minimum wall thickness of 0.030 inches. The baffle was a variable to allow cooling passage change for coolant velocity adjustment to meet the burnout heat flux margin of 1.5.

The heat input to the injector face coolant was raticed on the basis of injector diameter chamber pressure and combustion temperature from a baseline 10 inch diameter injector at the nominal design point with N_2O_4 /MMH propellants.

The Q/A burnout equation for N_2O_4 injector baffle cooling was taken as:

TABLE VI

Q/A BURNOUT EQUATIONS

$$Q/A \text{ cal.} = Q/A \text{ Burnout} \times 1.5$$

$$Q/A \text{ burnout} = C_1 + C_2 V \Delta T_{\text{sub}}$$

where

V = coolant velocity

$$\Delta T_{\text{sub}} = T_{\text{saturation}} - T_{\text{bulk}}$$

	C_1	$C_2 \times 10^4$	$V \Delta T_{\text{sub}} \times 10^{-3}$
MMH	1.67	7.1	5
	4.20	2.0	5
50/50	1.67	7.1	3.1
	2.75	3.6	3.1

TABLE VII

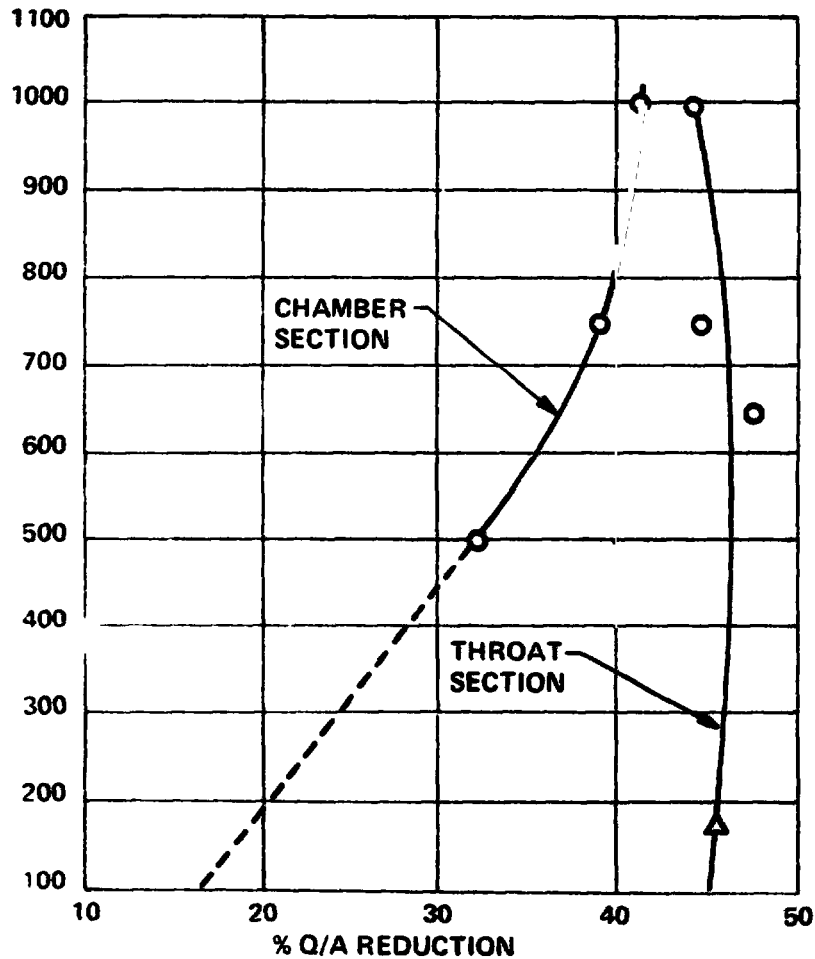
DIMENSION CONSTRAINTS

		Min (in.)	Max (in.)	Thickness Gas Side Wall
Channel Wall	Channel Width	0.075	0.300	0.030
	Channel Depth	0.050	0.075	
	Land Width	0.075	--	
Drilled Aluminum	Hole Diameter	0.095	0.110	0.060
	Hole Spacing	0.170	--	

PERCENT Q/A REDUCTION VERSUS P_c

$N_2O_4/MEH + 1\%$ SI OIL

CHAMBER PRESSURE -
PSIA



○ BAC 2000 LBF NICKLE WALL CHAMBER
AFRPL-TR-72-78
SEPTEMBER 1972

△ 5000 LBF ALUMINUM NOZZLE
BAC REPORT D8693-953001
FEBRUARY 1972 WITH 4% FUEL
VORTEX COOLING

% REDUCTION BASED ON Q/A'S
OF 2K AND 5K FIRED WITHOUT
THEN WITH SI OIL ADDITIVE

FIGURE III-16

Bell Aerospace Company

$$Q/A_{B.O.} = 1.00 + 0.00135 V \Delta T_{SUB}$$

The selection of 35 psi also allows off limits operation to the defined conditions of -10% P_c and +12% O/F without sustained low frequency oscillations.

The definition of 35 psi for the injectors fuel orifices defines the ΔP of the oxidizer orifices. High combustion efficiency over a range of mixture ratios requires equal ox and fuel injector pressure drops at nominal mixture ratio based on Bell experience with the triplet injector element selected.

The variable pressure drops identified in Figure III-17 were calculated for each case. The chamber cooling passage pressure drops were calculated by summing the average ΔP for 13 increments of cooling passage length:

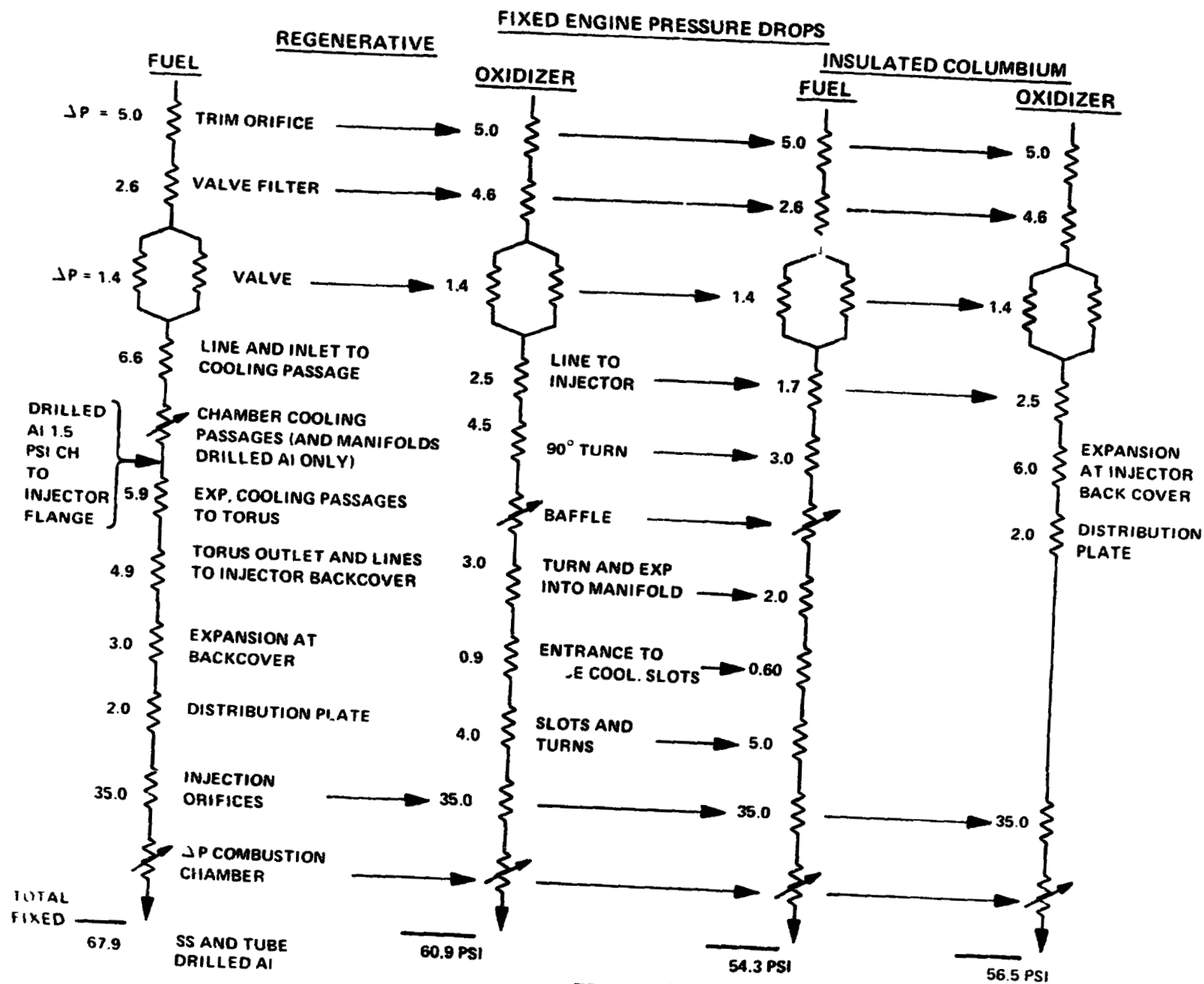
$$\sum \Delta P = \left[\frac{f_L \rho V^2}{2g D_H} \right]_1^{13}$$

$$\text{where } f = 0.00140 + \frac{0.125}{R_e^{0.32}}$$

$$\left. \begin{array}{l} l = \text{section length} \\ \rho = \text{fuel density} \\ V = \text{fuel velocity} \\ D_H = \text{hydraulic diameter} \end{array} \right\} \begin{array}{l} \text{section average} \\ \text{values} \end{array}$$

The pressure drop of the drilled aluminum chamber was reduced, based on sample calculations, for EDM tapering of the drilled holes to larger diameters in the convergent and divergent sections of the nozzle.

The injector baffle ΔP was calculated as above except that one length was required; the cooling passages were defined with constant cross-section by the thermal calculations.



Bell Aerospace Company

The combustion zone ΔP was calculated by:

ORIGINAL PAGE IS
OF POOR QUALITY

$$\frac{P_{c1}}{P_c} = \frac{1 + \gamma M^2}{\left(1 + \frac{\gamma - 1}{2}\right)^{\gamma/\gamma - 1}}$$
$$\Delta P = P_{c1} - P_c$$

where: M = calculated Mach number at the entrance to the throat
 γ = ratio of specific heats
 P_{c1} = pressure at the injector face
 P_c = design chamber pressure at throat entrance

7) Feed Pressure

Engine flow schematics for feed pressure determination are shown in Figures III-18 and III-19 which resulted in the fixed pressure drops of Figure III-17.

The valve ΔP is the same as incorporated in the LM Ascent engine and assures a negligible change in engine thrust, approximately 1%, for failure of one of the parallel legs to open or to stay open for or during engine firing. The valve and filter weights were adjusted as a function of flow rates and flow passage cross-sectional area over the parametric range to account for the constant pressure drops. The definition constant line and manifold drops also assumed variable flow passage cross-sectional area as a function of propellant flow rates.

The injector orifice pressure drop, 35 psi, is based on in part on test results from the development of the LM Ascent engine. Operation with helium saturated propellants at 190 psia tank pressure resulted in low frequency chamber pressure oscillations during the engine starting transient for fuel injector orifice pressure drops below approximately 27 psi. The duration of the oscillations increased with decreasing fuel orifice pressure drop to approximately 21 psi. Below 21 psi the oscillations were sustained for the firing duration. The concern with even a short period of low frequency oscillation on start is the potential of those oscillations to initiate high frequency instability. A fuel orifice design ΔP of 35 psi provides margin for the low frequency oscillations during the engine start transient at the nominal design point.

REGENERATIVE ENGINE FLOW CIRCUITS

FUEL REGENERATIVE COOLED CHAMBER OXIDIZER COOLED BAFFLES AND INJECTOR FACE

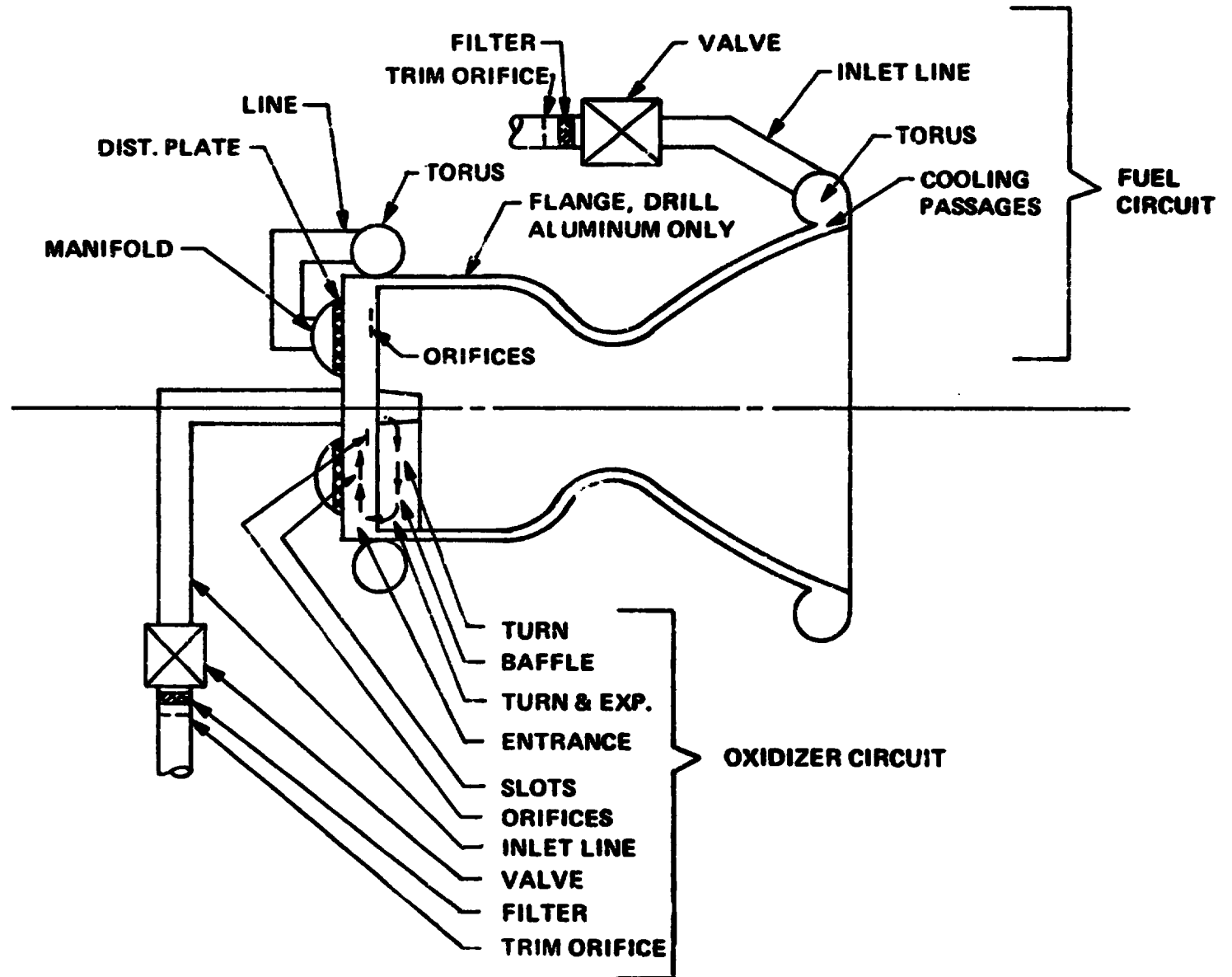


FIGURE III-18

INSULATED COLUMBIUM ENGINE FLOW CIRCUITS

FUEL COOLED BAFFLE AND INJECTOR FACE

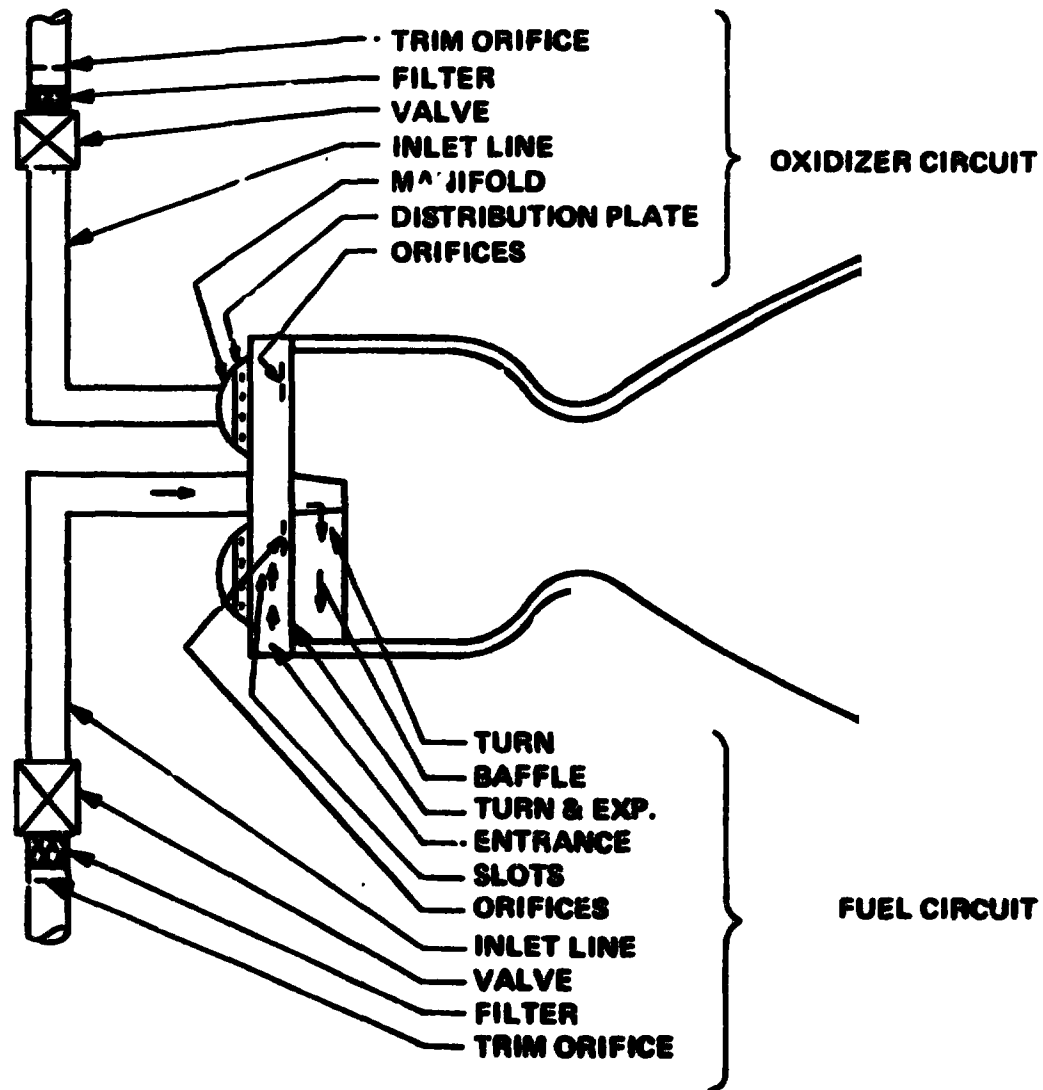


FIGURE III-19

Bell Aerospace Company

8) Weights

a. Structural Criteria

The requirement of design for 4000 thermal cycles was established as the limiting structural criteria for the regenerative cooled thrust chamber. The gas side wall temperatures limits imposed by that requirement were discussed earlier.

The insulated columbium thrust chamber and its integral nozzle extension and the nozzle extension of the regenerative cooled chambers were sized on the basis of creep life. The creep life design requirement was 60 hours at the nominal operating temperature. The nozzle extension operating definitions included the throat load and an assumed 12g gimbal load. A value of 2.5 times the throat load was assumed for non-operating vibration. Minimum gage for fabrication was taken as 0.020 inches. The assumed loads set the upper temperature limit for the titanium nozzle extension at 1400°F. With the exception of the columbium in the vicinity of the mounting flange, the controlling definition of the extension thickness was the 0.020 inch minimum gage.

The engine elements designed on the basis of pressure and thrust included factors of safety of 1.5 and 2.0 on yield strength and ultimate strengths, respectively.

b. Thrust Chamber Assembly

Injector weights were developed from 7 equations for the various sections as a function of injector diameter with appropriate thickness changes as a function of diameter and design chamber pressure. The injector mounting flange weight for the insulated columbium and drilled aluminum chambers was a separate equation.

The thrust chamber was divided into 5 sections longitudinally with each section capable of being defined by 5 layers of materials or, in the case of the regen chamber, partial voids. The five sections were the barrel, convergent nozzle and 3 sections of divergent nozzle. The contoured sections were defined by curve fit equations checked at several chamber sizes. The 3 to 5 layers were defined by material, material density and thickness. The thicknesses were set by thermal/structural requirements. For example, the insulated columbium chamber barrel section weight calculations included inside silicide coating thickness of .005 inches, the columbium wall of thickness, t , based on pressure and diameter, an outside silicide coating of .005 inches, a layer of 12 lb/ft³ dynaflex insulation of calculated thickness t_1 and a 0.005" thick titanium outer jacket. The electro deposited nickel closeout of the channel wall

Bell Aerospace Company

chamber was set at 0.090 inches based on structural checks. The drilled aluminum chamber thicknesses from the cooling holes to the outside surface was taken as 0.250 inches at the throat and 0.120 inches in the barrel section and divergent nozzle. Chamber and nozzle extension flange weights were added when appropriate. The regenerative inlet manifold was a separate equation based on a constant cross section torus. The nozzle extension weight included a 1/2 by 1/2 x 0.20 thick titanium stiffening ring at the nozzle exit and 0.005 inch silicide on the inside and outside surfaces.

c. Propellant Valve Assembly

A study to define the series/parallel redundant OME propellant valve weight was carried out in some detail. The baseline of the valve calculations was a modified version of the LM Ascent engine series-parallel redundant valve. The baseline weight include all stainless steel main valve and actuator bodies and stainless steel gas operated solenoids. The valve body and filter weights were scaled on the basis of the propellant volumetric flow rates to the OME thrust levels. Bell set torque requirements were defined as a function of set diameter to size the valve actuators and to establish an actuator and solenoid weight correction for changes in operating pressure. The sizing included the assumption that the gas actuation pressure was equal to the engine feed pressure. Valve assembly weight calculations were then carried out at nominal and at the extremes of propellant volumetric flow rates and feed pressure. The more detailed valve equation weights were found to be essentially equal to a simplified form of the valve scaling equation. Therefore, the simplified equations were employed in the ADEPT program. Those equations are as follows:

$$\text{N}_2\text{O}_4/\text{AMINES-VALVE ASSEMBLY WEIGHT} = 32.1$$

$$\sqrt{\frac{F}{3500}}$$

$$\text{LOX/FUELS-VALVE ASSEMBLY WEIGHT} = 33.6$$

$$\left[\sqrt{\frac{F}{3500}} \right] 1.1$$

The 32.1 and 33.6 values reduce the difference between the simplified and more detailed weight calculations to ± 0.5 pounds over the complete parametric ranges. The 1.1 factor applied to the LOX valves attempted to account for greater fuel-LOX isolation and/or insulation to prevent fuel freezing.

Bell Aerospace Company

d. Gimbal Ring and Engine Mount

The stainless steel gimbal ring included the engine mount as shown on Figures III-3 and III-4. The ring and engine mount calculations reflected the differences in the chamber definitions. The regen engine rings were attached to circumferential hat section supports which were considered welded to the chamber outer surface. Separate valve support structure was included. The ring/mount arrangement for the insulated columbium engine required a structural support cylinder attaching the gimbal ring near the throat station to the injector. The high columbium temperature and thermal expansion precluded gimbal ring attachment to the thrust chamber. The support cylinder eliminated the need for a separate valve mount.

The equations defining the gimbal ring and mount weights were established by layout and calculations of weights for several chamber diameters. The resulting parametric definitions were as follows:

Ring and Engine Mount Weight

$$\begin{aligned}\text{Drilled Al} &= \left(\frac{D_c + 5.5}{15} \right) & 21.5 \text{ lbs} \\ \text{Channel Wall} &= \left(\frac{D_c + 3.9}{15} \right) & 21.5 \text{ lbs} \\ \text{Insulated Columbium} &= \left(\frac{D_c + 6.2}{15} \right) & 21.5 \text{ lbs}\end{aligned}$$

Ring to Chamber Attachment and Valve Mount Weight

$$\begin{aligned}\text{Drilled Al} &= \sqrt{\frac{F}{6000}} & (0.21 D_c + 6.45) \\ \text{Channel Wall} &= \sqrt{\frac{F}{6000}} & \\ \text{Insulated Columbium} &= \sqrt{\frac{F}{6000}} & 3.2 + \left(\frac{D_c L}{88.8} \right) & 13.25\end{aligned}$$

Where

$$\begin{aligned}D_c &= \text{the chamber inside diameter} \\ L &= \text{length throat to injector}\end{aligned}$$

Bell Aerospace Company

e. Other Weights

The electrical ignition system valving and igniter for the LOX propellant combination (Figure III-6) was added as a constant 22.85 lbs by defining reasonable weights for each component of that subsystem.

Engine propellant line and flange weights were added as a function of the propellants volumetric flow rates to assure constant line pressure drop allocation. The propellant lines were defined without line flexures to accommodate gimbaling; the assumption was made that the line flexures were included in the system feed lines between the engine inlets and the propellant tanks.

Each point design engine weight total was multiplied by a factor of 1.05 for the final predicted weight to account for flight instrumentation and to provide a weight contingency.

A layout of the tube wall chamber was made at the nominal design conditions to establish a weight estimate for that chamber.

A separate study was made to determine the weight savings for engines with the gimbal ring and engine mount attached directly to the injector or a "head end mount". The nominal engine assembly weight reductions were reported as follows:

Insulated Columbium	-	12.38 lbs
Drilled Aluminum	-	4.50 lbs
Channel Wall	-	3.74 lbs

F. Predicted Engine Data

Nominal engine data provided by the ADEPT program is presented in Tables VIII and IX. The I_{sp} for the N_2O_4 /Amine Icb engines is approximately 6 sec. below the regeneratively cooled designs. The predicted fuel feed pressure of the Icb is about 20 psi below the CWR which in turn is about 13 psi below the DAR. The DAR engine is the lightest followed by the Icb and CWR. The tube wall regen has the highest weight. Use of silicone oil additive improves the regen engine I_{sp} by 3 seconds at the expense of about 20 lbs higher engine weight. The additive reduces the amount of film cooling to essentially zero using I_{sp} and increases the size (and weight) of the regen chamber divergent nozzle to a higher area ratio for the radiation cooled extension attachment. Operation with $N_2O_4/50-50$ at an O/F of 1.60 is predicted to reduce I_{sp} by 0.6 to 1.9 seconds relative to $N_2O_4/1^{st}$ at an O/F of 1.64.

Bell Aerospace Company

The LOX/Amine engines of Table IX show an I_{sp} improvement of about 20 seconds relative to N_2O_4 /Amine at the lower area ratios resulting from the reduced nominal P_c definition. The LOX/ C_3H_8 and LOX/RP-1 Icb engines' performance show little or no advantage relative to LOX/MMH. The LOX/RP-1 CWR engine has the same I_{sp} as its LOX/MMH counterpart and lower fuel feed pressure but over 20 lbs higher weight. The weight of the LOX regen engines is over 25 lbs higher than the N_2O_4 designs due to the ignition system and slightly larger chamber diameters for the lower nominal chamber pressure. The weight difference for the LOX Icb engines is about 40 lbs above the values predicted for N_2O_4 /Amine operation.

Samples of data from the final report of the Task I and II effort are shown in Table X and Figures III-20 through III-22. Approximately 1200 engine point designs were presented in Volume II of the report "Parametric Engine Data Report" No. 8693-953006, November 1972, in the format of Table X. Table X is a copy of the computer print-out. Each point design was characterized by up to 130 values of input data, and calculated performance, cooling margin, temperatures, pressure drop, material thicknesses, dimensions and weights. The description of the heading terms of Table X can be found in the report. A total of 254 data plots were presented in Volume I of the report. The samples of plotted data, Figures III-20 and III-21, show identification of operating conditions for where the cooling margin and maximum wall temperature limits could not be achieved without a large reduction in predicted I_{sp} .

The report of the Task I and II effort fulfilled all the requirements of the contract statement of work. The development of the ADEPT computer program with automatic machine plotting of selected parameters considerably simplified the preparation of the data. The program also insured that all interactions of the defining equations, input data, and the various thermal and mechanical limits were included in each point design. Each point design reflects all the engine definitions described in this section.

G. Engine Ratings and Recommendations

1. General

The contract work statement defined a comparative evaluation and rating of the various concepts of OME reusable thrust chamber. The evaluation was to include predicted design and operating characteristics, potential development risk, development and operational costs, maintenance and checkout. The approach taken

Bell Aerospace Company

to meet the work statement requirement consisted of the definition of technical rating factors and the numerical ranking of engines against those factors followed by an analysis which related the predicted engine operating characteristics and technical rating to engine and OMS development costs.

The technical rating will be described first and will be followed by a description of the cost comparison and recommendations made at the conclusion of the Task I and II effort. The recommendations are updated on the basis of test results and analyses which became available from the NAS 9-12803 and NAS 9-12802 demonstration testing. Those test results and analyses change the original recommendation of an insulated columbium engine and $\text{N}_2\text{O}_4/\text{MMH}$ propellants to an engine with a channel wall regeneratively cooled thrust chamber with the same propellant combination.

2. Technical Rating

The technical rating factors for the Task I and II chamber cooling concepts and propellant combinations are shown in Table 11. The listing of factors attempted to cover all operating and non-operating characteristics of the engines under the headings of

- Complexity
- Service and Maintenance
- Fabricability
- Start
- Steady State Operation
- Design Life

The heatings were defined by 5 to 8 factors. Each factor is described four ways with a corresponding numerical rating of 4, 3, 2 or 1. Certain factors are repeated; the requirements for "start auxiliary controls" (A5) and "feed system malfunction detection" (A6) define engine complexity and they were also included as part of the definition of service and maintenance, start and steady state operation. The repetition of those factors increases their impact on the total numerical rating for each engine. The "weight" four other factors was defined as 3. Those factors which were considered to represent high technical risk. The weighing of 3 recognizes the potential cost impact to the engine development program for problems resulting from the higher technical risk as will be described in the following section.

The "perfect" engine would have a total numerical score of 165 for the definitions of Table XI.

The selection of the individual factors and the 4 rating definitions of Table XI tried to include all engine characteristics which were applicable to the Task I and II engine definitions. The definitions of each element sought to provide a reasonable

ORIGINAL PAGE IS
OF POOR QUALITY

TABLE V-1

TASK I
NOMINAL ENGINE DATA
 $P_c = 125$ PSIA, DEX = 50, 80% BELL

PROPELLANTS CHAMFER COOLING CONCEPT	N_2O_4/MDH				$N_2O_4/M + S1$		$N_2O_4/50-50$		
	CHANNEL WALL REGEN	DRILLED AL REGEN	INSULATED COLUMBIUM	TUBE WALL REGEN	ANNEL WALL REGEN	DRILLED AL REGEN	CHANNEL WALL REGEN	DRILLED AL REGEN	INSULATED COLUMBIUM
$I_{sp\infty}$, SEC	316.40	316.2	310.50	316.40	319.30	319.30	315.80	315.80	308.60
O/F	1.64						1.60		
AREA RATIO	74.33						74.65		
FFP, PSIA	205.30	228.90	183.70	203.20	203.80	219.90	207.30	251.20	183.80
OFF, PSIA	190.60	190.70	184.60	190.60	190.60	190.60	190.60	190.60	184.60
WEIGHT, LB, TOTAL	194.80	183.70	191.40	208.68	216.30	201.70	194.20	184.50	191.30
LT, IN.	80.80	80.90	80.8			80.89	80.80		
D_{MAX} , IN.	66.73								
T_{MAX} OFF LIMITS, °F	-	-	2548	-	-	-	-	-	2513
BARRIER FLOW, %	3.59	3.73	7.65	3.32	0.01	0.01	4.69	4.68	8.65
EXTENSION A/AT	7.91	7.72		7.44	12.55	12.55	7.67	7.70	

Propellant Feed Temperature = 70 °F

*Based on 1° Gimbale Pitch and Yaw

TABLE V-2

TAS. II
NOMINAL ENGINE DATA

 $P_c = 100$ PSIA, DEX = 50, 80% BELL

PROPELLANT COOL CONCEPT	LOX/MEH			LOX/MEH + S1		LOX/MEH + S1			LOX/C ₂ H ₆	LOX/N ₂ H ₄	LOX/RP-1
	CHANNEL WALL	DRILL AL	INSULATED COLUMBIUM	CHANNEL WALL	DRILL AL	CHANNEL WALL	DRILL AL	INSULATED COLUMBIUM	INSULATED COLUMBIUM	INSULATED COLUMBIUM	CHANNEL WALL
I_{sp} , SEC.	333.20	333.20	329.60	336.0	336.0	335.0	335.7	327.20	315.9	331.2	333.3
O/F	1.0	1.0	1.10	1.0	1.0	1.0	1.0	1.00	2.30	0.70	2.40
AREA RATIO	58.96	58.96	54.54	58.96	58.96	59.40	59.40	59.34	60.15	59.25	61.23
FFP, PSIA	187.70	206.70	153.30	188.00	207.20	187.70	205.50	159.6	161.3	159.90	181.00
OFF, PSIA	159.80	159.80	150.70	159.80	159.80	159.80	159.80	159.8	159.7	159.80	159.60
WEIGHT, TOTAL	220.70	209.60	234.20	248.90	233.70	225.20	214.90	227.20	239.00	228.20	243.50
LT, IN.	81.3									81.3	84.9
D_{MAX} *	76.5										
BARRIER FLOW, %	4.97	5.06	8.51	1.83	1.12	4.63	4.55	9.98	5.90	10.02	0.02
EXT. A/A _t	4.75	4.59	-	9.84	13.73	5.66	5.66	-	-	-	8.19

FUEL FEED TEMPERATURE - 70°F

*±1% GIMBAL PITCH AND YAW

ORIGINAL PAGE IS
OF POOR QUALITY

TABLE X - COMPUTER PRINTOUT SAMPLE

CHARACTER WALL REEEN ENGINE - ADMINAL CONDITICNS														PRCPPELLANTS N2G4/PPH		PAGE 2	
THRST	ISP	ETAT	ETAB	C1	TC5	TT5	TE4	BT5	DEATI	L-CH	L-TM1	L-TM2	L-C/U	NVALV	L-ENG		
PC	CF	ETAN	ETAC	C2	TC4	TT4	TE4	BT4	DEACP	U-CH	U-TM1	U-TM2	U-C/U	UNUNT	L-MO2		
IC-ACZ	CPCK	CEAR	ETAK	C3	TC3	TT3	TE3	BT3	CAIAS	NHCLC	NHCLT	NHCLN	C/O-CA	NRING	IBELL		
EPS	CA	ETAC	ICURF	C4	TC2	TT2	TE2	BT2	CAICL	CHULC	CHGLT	CHGLN	L-TI	MMISC	OMAX		
C/F-C	ACCT	IBAR	MAHFC	CELEFC	TC1	TT1	TE1	BT1	LEFACH	VELC	VELT	VELN	D-TI	M-CH	MCH		
C/F-C	ADCS	IBCES	MAHFC	CELEFC	TC1	TT1	TE1	BT1	CAIAJ	C/A-C	C/A-T	C/A-N	C/O-TI	M-TI	WREG		
P-FL	T-FL	L*	MAHFC	CELEFC	TC1	TT1	TE1	BT1	CAICL	MG-C	MG-T	MG-N	T-CH	BYPAS	M-TMS		
P-CH	T-CH	CONTP	MAREO	CELEFC	TC1	TT1	TE1	BT1	CAICL	MG-C	MG-T	MG-N	T-CH	RED	M-TGT		
6000.	303.2	0.914	0.582	1833.	0.0	0.0	0.006	2.22	0.1630	11.169	4.749	4.870	6.285	42.02	82.15		
75.0	1.7886	0.556	0.589	3008.	0.0	0.0	0.020	30.06	0.3200	10.947	7.546	10.238	12.726	9.43	63.53		
50.000	1.6412	4220.	0.564	15.20	0.090	0.090	0.0	21.41	0.0	158	158	158	2.84	21.28	80.0		
43.70	9454.	0.557	0.550	590.0	0.075	0.075	0.0	5.96	0.3210	0.143	0.075	0.178	41.352	9.00	66.10		
1.640	19.79	8.24	0.126	22.7	0.030	0.030	0.0	6.17	0.2900	12.37	23.51	12.14	39.967	25.27	24.32		
2.054	18.07	7.67	0.458	58.1	20.0	5.613	0.320	25.89	0.2900	0.845	1.480	0.639	28.05	11.67	15.44		
158.4	188.2	30.00	-0.409	-15.3	0.900	70.***	***	3.56	0.0593	199.4	361.2	143.4	2400.	0.0	102.10		
143.4	125.2	2.10	0.277	17.1	1.120	70.	2647.	10.39	568.5	448.5	524.5	344.2	1400.	1.00	188.9		
6000.	317.3	0.931	0.581	1833.	0.0	0.0	0.006	2.23	0.1630	8.729	4.898	4.200	8.450	42.02	81.31		
170.0	1.8060	0.555	0.589	3008.	0.0	0.0	0.020	33.37	0.3200	10.447	6.504	9.543	14.277	9.39	69.07		
50.000	1.6415	4220.	0.584	15.20	0.090	0.090	0.0	21.03	0.0	136	136	136	5.23	20.56	80.0		
59.10	5553.	0.575	0.590	590.0	0.075	0.075	0.0	5.32	0.3210	0.166	0.075	0.269	50.805	4.16	66.48		
1.640	19.72	4.87	0.290	43.7	0.030	0.030	0.0	5.62	0.2500	11.97	26.45	12.30	44.309	31.05	15.22		
1.682	17.44	4.53	0.483	121.7	20.0	4.322	0.320	25.54	0.2900	1.024	2.008	0.755	45.78	7.85	25.43		
179.5	200.0	30.00	0.077	4.7	0.900	70.	3440.	3.29	0.0593	188.5	402.3	135.0	2400.	0.0	111.18		
164.4	119.6	2.58	0.432	37.7	1.120	70.	3302.	9.80	648.8	486.1	611.8	402.6	1400.	1.00	152.3		
6000.	315.4	0.936	0.580	1833.	0.0	0.0	0.006	2.22	0.1630	7.348	4.889	3.855	10.747	42.02	80.84		
125.0	1.8170	0.554	0.589	3008.	0.0	0.0	0.020	35.03	0.3200	10.009	5.800	8.637	16.314	9.26	66.10		
50.000	1.6744	4220.	0.585	15.20	0.090	0.090	0.0	21.30	0.0	121	121	121	7.91	19.94	80.0		
74.21	5802.	0.591	0.590	590.0	0.075	0.075	0.0	5.29	0.3210	0.185	0.076	0.311	55.752	9.28	66.73		
1.640	19.96	4.59	0.200	47.5	0.030	0.030	0.0	6.07	0.2900	1.094	29.21	12.51	45.752	37.24	14.14		
1.911	17.22	3.34	0.446	117.7	20.0	3.317	0.320	25.19	0.2900	1.185	2.678	0.848	62.34	5.90	29.85		
205.3	216.4	30.00	0.744	17.6	0.900	70.	3726.	3.14	0.0593	198.3	474.7	139.6	2400.	0.0	114.32		
160.6	118.8	2.58	0.458	46.4	1.120	70.	3615.	10.71	725.7	520.6	594.1	447.2	1400.	1.00	154.8		
6000.	318.9	0.938	0.580	1833.	0.0	0.0	0.006	2.23	0.1630	6.460	4.823	3.597	11.275	42.02	80.55		
150.0	1.8261	0.554	0.589	3008.	0.0	0.0	0.020	36.05	0.3200	9.623	5.281	7.954	16.484	9.15	66.87		
50.000	1.6851	4220.	0.585	15.20	0.090	0.090	0.0	20.38	0.0	110	110	110	5.74	19.38	80.0		
84.64	5619.	0.583	0.590	590.0	0.075	0.075	0.0	5.41	0.3210	0.200	0.076	0.300	58.309	9.23	66.92		
1.640	19.81	3.01	0.200	45.8	0.030	0.030	0.0	5.78	0.2900	1.006	31.77	12.46	46.572	39.27	14.05		
1.787	17.05	2.80	0.436	120.5	20.0	2.785	0.320	24.86	0.2900	1.322	3.218	0.946	77.77	4.96	30.96		
272.2	225.9	30.00	0.734	17.1	0.900	70.	3667.	2.85	0.0593	213.4	557.3	149.6	2400.	0.0	114.10		
215.4	119.1	3.32	0.540	57.8	1.120	70.	3741.	12.81	793.8	550.6	767.7	484.0	1400.	1.00	153.9		
6000.	322.2	0.940	0.575	1833.	0.0	0.0	0.006	2.24	0.1630	5.410	4.632	3.194	12.633	42.02	80.21		
200.0	1.8382	0.554	0.589	3008.	0.0	0.0	0.020	37.19	0.3200	8.967	4.558	6.977	17.303	8.97	67.93		
50.000	1.6984	4220.	0.585	15.20	0.090	0.090	0.0	20.17	0.0	95	95	95	14.41	13.44	80.0		
120.31	5640.	0.585	0.590	590.0	0.075	0.075	0.0	5.72	0.3210	0.222	0.076	0.300	61.700	9.25	67.18		
1.640	19.62	2.39	0.200	54.2	0.030	0.030	0.0	5.69	0.2900	12.46	71.95	13.54	47.548	41.55	11.14		
1.750	16.85	2.23	0.428	129.0	20.0	2.156	0.320	24.25	0.2900	1.575	4.254	1.083	108.40	3.71	34.47		
377.6	242.2	30.00	0.475	41.5	0.900	70.	4018.	2.43	0.0593	245.9	725.4	165.6	2400.	0.0	115.53		
264.7	120.0	3.87	0.593	72.7	1.120	70.	3927.	34.75	524.2	606.4	489.4	537.5	1400.	1.00	154.2		

Bell Aerospace Company

ORIGINAL PAGE IS
OF POOR QUALITY

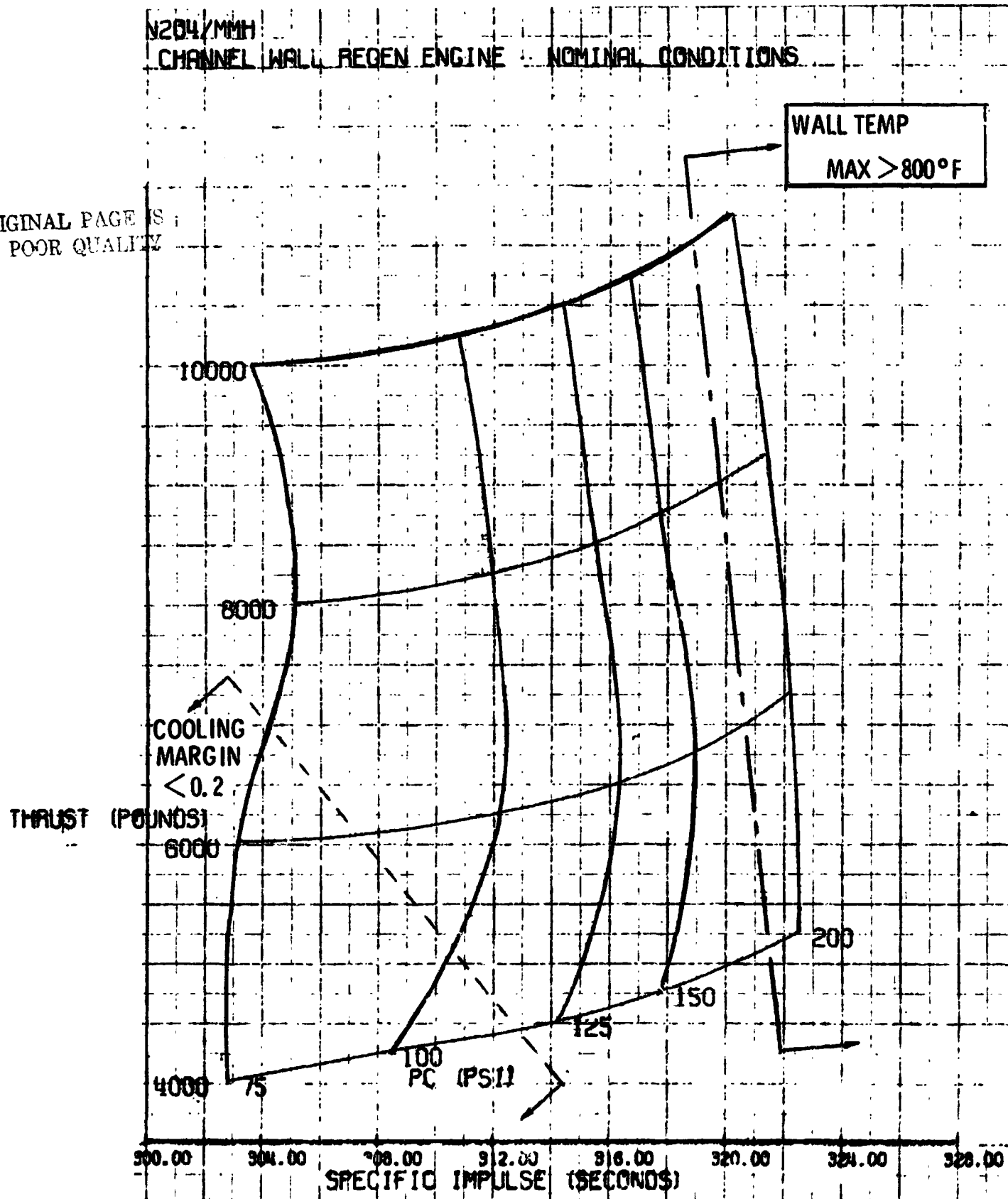


FIGURE III-20
THRUST AND P_C VERSUS SPECIFIC IMPULSE

Bell Aerospace Company

N204/MMH
CHANNEL WALL REGEN ENGINE - NOMINAL CONDITIONS

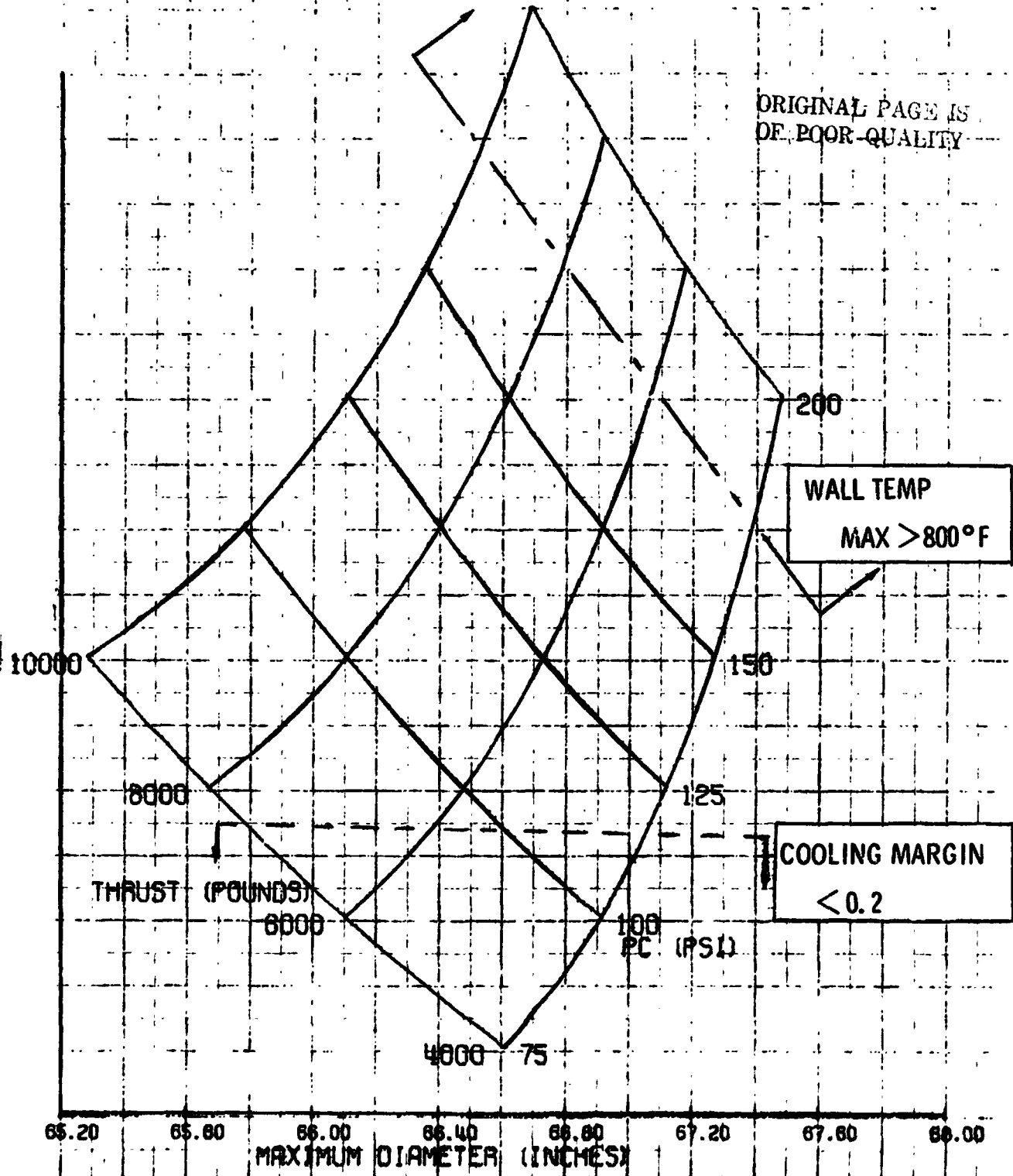


FIGURE III-21
THRUST AND P_c VERSUS MAXIMUM DIAMETER

Bell Aerospace Company

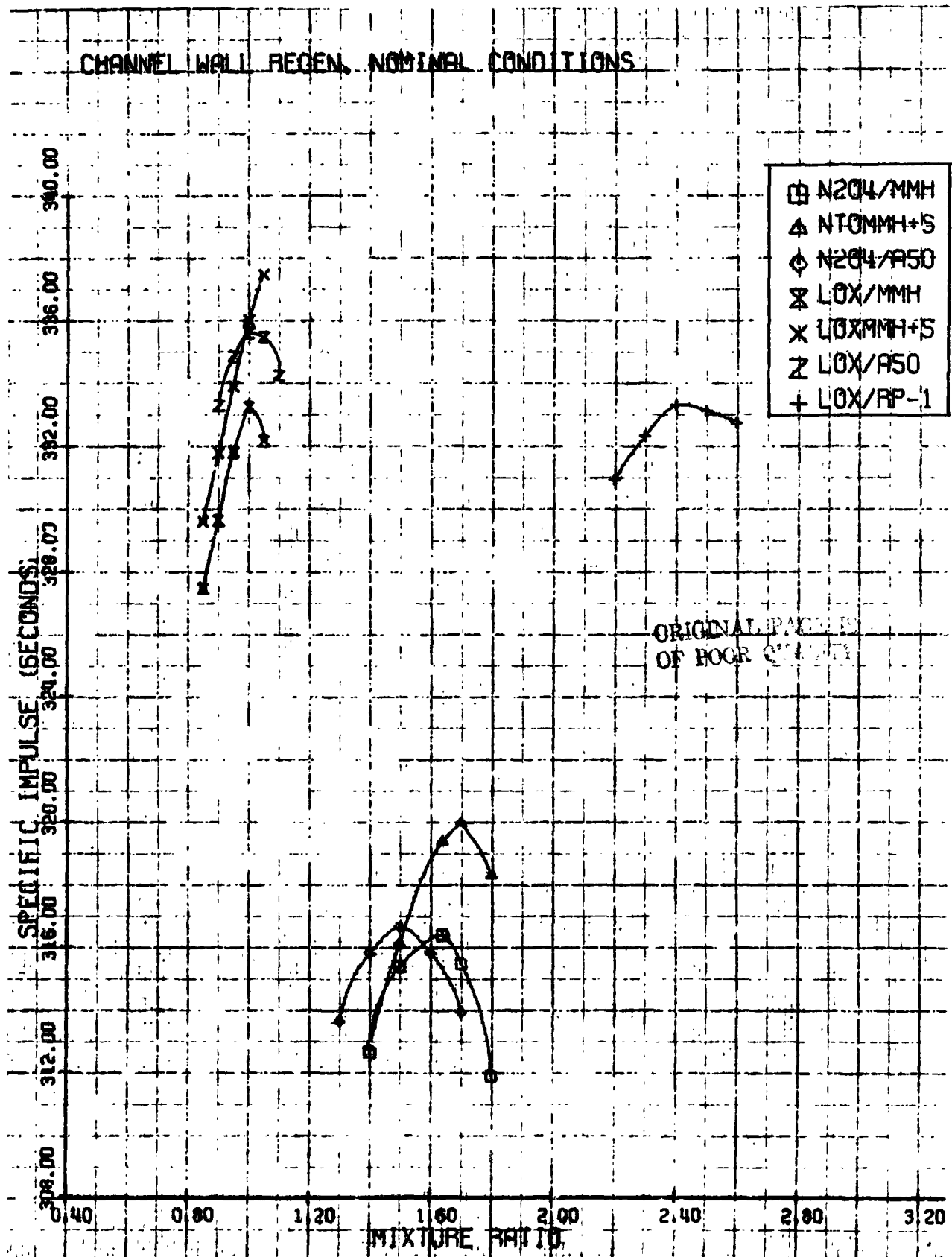


FIGURE III-22
SPECIFIC IMPULSE VERSUS MIXTURE RATIO

Bell Aerospace Company

self explanatory quantitative rating which would eliminate the qualitative judgement of the rater. The ranking definitions also reflected engine technology at the time of the rating and sought to include all areas of which presented potential development problems. The following comments provide further definition of the technical rating factors of Table XI.

- A1 - Number of mechanical joints; injector-to-chamber, chamber-to-extension.
- A2 - Number of metal-to-metal joints, chamber; weld, braze and individual electrodeposited metal joints.
- A4 - Insulation requirements; reference to the engine valve was made for the LOX propellant combinations.
- A5 - Start auxiliary controls; "auxiliary valves" covers chamber gas purges, "sequence" describes electrical timing of starting components.
- A6 - Feed system malfunction detection; sensors required to insure safe shutdown for ingested gas malfunction of the feed system.
- B1 - Compatibility; the nickel jacket of the CWR chamber is attacked by HNO_3 formed by moisture + N_2O_4 ; the DAR chamber has a potential problem of water corrosion of the drilled cooling passages.
- B2 - Inspectability, surface, visual; the liquid passages of the regen chambers cannot be visually inspected.
- B3, B4, B5 - Reflect additional components that require checkout and potential maintenance and servicing problems.
- D2 - Potential restart restrictions: < 5 min., is for example: engine cannot be restarted in less than 5 minutes after any duration firing.
- D4 - Malfunction Sensing (Time to P_c); an engine with a closely repeatable start transient, time to 90% P_c for example, could employ a timer tied into a P_c pickup to initiate shutdown if P_c is not obtained in the "nominal" time. The timer circuit could be employed for increased engine safety.
- E1 - Chamber cooling effect on injection; potential
(X3) change to engine combustion efficiency, heat rejection or stability due to regenerative heating of the propellants.
- E2 - Feed system malfunction detection sensitivity - time available to sense a malfunction before chamber temperatures exceed limit for thermal cycle life.
- E4 - Sensitivity to design point, I_{sp} calculated I_{sp} variation over the defined off limits operation requirement of $\pm 10\%$ P_c , $\pm 12\%$ O/F
- E5 - Confidence in predicted I_{sp} based on cooling required;
(X3) confidence in predicted vortex film cooling and heat rejected to regenerative coolant

Bell Aerospace Company

- E8 - Design margin off limits injector; the potential of
(X3) insufficient injector face or baffle cooling margin could lead to costly injector modification - impacts regenerative cooled chambers with N_2O_4 injector regen cooling. The chamber and extension margin can be improved as necessary by increasing film coolant, a change more easily made.
- F5 - Demonstration required; the demonstration of the
(X3) required engine cycle and accumulated firing life represents a relatively large development cost impact. The drilled Al concept has been demonstrated for over 1 hour of firing by the Agena Engine operating at 500 psia P_c and, therefore, limited additional demonstration would be required for OME. The I_{cb} demonstration can take advantage of subscale engine firings to demonstrate coating life. The CWR chamber has not been demonstrated and subscale testing is not applicable because the design is thermal cycle life limited. The reference to "extrapolate full duration" was intended to cover the testing of columbium chambers and nozzle extensions and assessment of one potential problem, Frittlement, by measuring the H_2 diffusion depth penetration at less than full duration and extrapolation of that quantity to full duration.

Table XII shows the engine ratings against the Table XI definitions. The insulated columbium approach with N_2O_4 /Amine propellants has the highest total (135.5) followed by the drilled aluminum N_2O_4 /Amine design (118.8) and the I_{cb} engine with LOX/MMH (110.5).

LOX/ C_3H_8 and LOX/ N_2H_4 can be considered only with the I_{cb} chamber because of the limited regen cooling potential of C_3H_8 and N_2H_4 . The use of N_2H_4 for vortex film cooling has no test verification which reduced its overall technical rating.

3. Cost Comparisons

The engine's cost comparisons are presented in Table XIII. The I_{sp} , feed pressure and engine weight Δ costs were developed from the McDonnell-Douglas OMS trade studies on the basis of the nominal engine design data. A separate baseline feed pressure was used for the Task I and Task II propellants because of the difference of nominal chamber pressure, 125 versus 100 psia. The "\$ Δ tech rating" is included in the cost comparison to estimate the change in OME program cost based on the engine's technical ratings. That Δ cost reflects the rating of the insulated columbium engine as baseline, the estimated engine manufacturer's cost of \$25,000,000 and a factor of 1.5 to reflect the cost to NASA. The 1.5 factor reflects the additional cost to the Δ subcontractor, and the shuttle prime contractor. The technical

TABLE V-3

TECHNICAL RATING FACTORS TASK I AND TASK II

WEIGHT		4	3	2	1
	A. COMPLEXITY				
1	1. NUMBER OF MECHANICAL JOINTS	0	1	2	> 2
1	2. NUMBER OF METAL TO METAL JOINTS, CH	0-1	2-3	4-6	> 6
1	3. COATINGS, OXIDATION RESISTANCE	NONE	NOZZLE EXTENSION	CHAMBER AND NOZZLE EXT.	TCA AND COOLING PASSAGES
1	4. INSULATION REQUIREMENTS	NONE	VALVE	COMBUSTION CHAMBER	VALVES AND C.C.
1	⑤ START AUXILIARY CONTROLS	NONE	AUXILIARY VALVES	AUX. VALVES AND SEQUENCE	AUX. VALVES SEQ. AND SENSING
1	⑥ FEED SYSTEM MALFUNCTION DETECTION	CHAMBER PRESSURE	P _c AND TEMP.	P _c , TEMP $\frac{w_o}{w_i}$	➔ PLUS OTHER
	B. SERVICING AND MAINTENANCE				
1	1. COMPATIBILITY PROPELLANT, FLUIDS	COMBAT DEMONSTRATED	POTENTIAL LONG TERM PROB.	REQUIRES PURGE	REQUIRES PURGE AND FLUSH
1	2. INSPECTIBILITY, SURFACE, VISUAL	EXCELLENT	GOOD	FAIR	NOT POSSIBLE
1	③ CHAMBER COMPLEXITY (ADD ITEMS A1-A4)	16	12	8	4
1	④ START AUXILIARY CONTROLS, (A5)	NONE	AUX. VALVES	AUX. VALVES AND SEQ.	AUX. VALVES SEQ. AND SENSING
1	⑤ FEED SYSTEM MALFUNCTION DET. (A6)	CHAMBER PRESSURE	P _c AND TEMP	P _c , TEMP $\frac{w_o}{w_i}$	➔ PLUS OTHER
	C. FABRICABILITY (CHAMBER)				
1	1. JOINING TECHNIQUES	WELD	+ BRAZE OR E.D.	+ BRAZE AND E.D.	DIFFUSION + BOND
1	2. FABRICATION METHODS (CHAMBER)	MACHINING	PLUS EDM	PLUS SPINNING OR E.D.	PLUS OTHER
1	3. INSPECTIBILITY, NDT	EXCELLENT	GOOD	FAIR	POOR
1	4. PROCESS CONTROLS	DEFINED	DEFINED FOR SMALLER	DEVELOPMENT REQUIRED	NEW PROCESS
1	5. TOOLING REQUIRED	NOMINAL	LOW COST RE- USABLE	LOW COST	HIGH COST

○ REPEATED FACTORS AND WEIGHT OF "START AUX CONTROLS" "FEED SYSTEM MALFUNCTION DETECTION" IS 3

E.D.M. - ELECTRODEPOSITED MACHINING

E.D. - ELECTRODEPOSITED

TABLE V-3

TECHNICAL RATING FACTORS TASK I AND TASK II (CONT'D)

WEIGHT		4	3	2	1
	D. START				
1	1. TYPE	HYPERGOLIC SPACE DEMO.	NON HYPER. SPACE DEMO	NON HYPER SL DEMO	NON HYPER NOT DEMOD
1	2. POTENTIAL RESTART RESTRICTIONS	NONE	< 5 MIN	5-15 MIN	> 15 MIN
1	③ AUXILIARY CONTROLS, AS	NONE	AUX VALVER	AUX. VALVES AND SFC	AUX. VALVES SEQ AND SENSING
1	4. MALFUNCTION SENSING (TIME TO P_c)	REPRODUCIBLE START TRANS.	CLOSELY REPRODUCIBLE	FAIRLY REPRODUCIBLE	ALT START TRANS. NOT DEFINED
	E. STEADY STATE OPERATION				
3	1. CHAMBER COOLING EFFECT ON INJECTION	NONE	HEATED PROP. DEMOD	HEATED FUEL NOT DEMOD	HEATED FUEL AND OX NOT DEMOD
1	2. FEED SYSTEM MALFUNCTION DETECT, SENSITIVITY	NOT SENSITIVE	> 1 SEC.	< 1 SEC	< 1 SEC
1	③ FEED SYSTEM MALFUNCTION DETECT, COMPLEXITY (AS)	CHAMBER PRESSURE	P_c AND TEMP	P_c , TEMP $\frac{w_o}{w_f}$ → PLUS OTHER	
1	4. SENSITIVITY TO DESIGN POINT, I_{sp}	NOT SENSITIVE	< 1% LOSS	> 1 < 2% LOSS	> 2% LOSS
3	5. CONFIDENCE IN PREDICTED I_{sp} BASED ON COOLING REQ'D	0	± 1%	± 2%	> ± 2%
1	6. DESIGN MARGIN, OFF LIMITS, CHAMBER	0.8	0.4	0.2	0
1	7. DESIGN MARGIN, OFF LIMITS, EXTENSION	> 0.8	> 0.4	> 0.2	> 0
3	8. DESIGN MARGIN, OFF LIMITS, INJECTOR	0.8	0.4	0.2	0
	F. DESIGN LIFE				
1	1. CHAMBER COATINGS	NOT APPLICABLE	DEMOM AT OPERATING COND	DEMOM AT TEMP	PARTIAL DEMOD
1	2. CHAMBER MATERIAL STRUCTURAL DESIGN CONFIDENCE	DESIGN TECH AND PROPERTIES AVAILABLE	EXTRAPOLATED MATERIAL PROPERTIES	POTENTIAL PROPERTY DEFINITION PROBLEM	CRITERIA AND PROPERTIES NOT DEFINABLE
1	3. GAS EMBRITTLEMENT, CHAMBER	LIFE DEMOD	NO INDICATION TESTING TO DATE	POTENTIAL PROBLEM	KNOWN PROBLEM
1	4. GAS EMBRITTLEMENT, NOZZLE EXTENSION	LIFE DEMOD	NO INDICATION, TESTING TO DATE	POTENTIAL PROBLEM	KNOWN PROBLEM
3	5. DEMONSTRATION REQUIRED	AVAIL DATA AND NOW FIRING	PLUS LIMITED FULL SCALE	EXTRAPOLATE FULL SCALE PLUS SUBSCALE	FULL SCALE TCA ONLY FULL LIFE FIRINGS

TABLE V-4

ENGINE RATINGS

OXIDIZER FUEL	N ₂ O ₄ MMH				N ₂ O ₄ MMH + Si		N ₂ O ₄ 50:50			LOX MMH			LOX MMH + Si		LOX RPI		LOX C ₂ H ₆ N ₂ H ₄	
	CWR	DAR	TWR	ICb	CWR	DAR	CWR	DAR	ICb	CWR	DAR	ICb	CWR	DAR	CWR	DAR	ICb	ICb
FACTOR																		
A	1	3	2	3	3	2	3	2	3	3	2	3	3	2	3	2	3	3
	2	1	2	1	3	1	2	1	2	3	1	2	3	1	2	2	3	3
	3	3	3	3	2	3	3	3	3	2	3	3	2	3	3	2	2	2
	4	4	4	4	2	4	4	4	4	2	3	3	2	3	3	2	1	1
	5	4	4	4	4	4	4	4	4	1	1	1	1	1	1	1	1	1
B	6	2	2	2	3	2	2	2	3	2	2	3	2	2	2	2	3	3
	1	2.5	1	3	4	2.5	1	2.5	1	4	2.5	1	4	1	2.5	1	4	4
	2	1	1	1	4	1	1	1	1	4	1	4	1	1	1	1	4	4
	3	2.8	2.8	2.8	2.5	2.8	2.8	2.8	2.5	2.5	2.5	2.5	2.5	2.5	2.5	2.5	2.5	2.5
	4	4	4	4	4	4	4	4	4	1	1	1	1	1	1	1	1	1
C	5	2	2	2	3	2	2	2	3	2	2	3	2	2	2	2	3	3
	1	3	4	2	4	3	4	3	4	3	4	4	3	4	3	4	4	4
	2	2	4	2	2	2	4	2	4	2	2	4	2	4	2	4	2	2
	3	3	3	2	3	3	3	3	3	3	3	3	3	3	3	3	3	3
	4	3	4	2	3	3	4	3	4	3	4	3	3	4	3	4	3	3
D	5	2	4	1	3	2	4	2	4	3	2	4	3	2	4	2	4	3
	1 (x3)	12	12	12	12	12	12	12	12	3	3	3	3	3	3	3	3	3
	2	2	2	2	4	2	2	2	4	2	2	4	2	2	2	2	4	4
	3	4	4	4	4	4	4	4	4	1	1	1	1	1	1	1	1	1
	4	3	3	3	4	3	3	3	4	1	1	1	1	1	1	1	1	1
E	1 (x3)	3	3	3	12	3	3	3	3	12	6	6	12	6	6	6	12	3
	2	1	2	1	3	1	2	1	2	3	1	2	3	1	2	1	3	3
	3	2	2	2	3	2	2	2	3	2	2	3	2	2	2	2	3	3
	4	3	3	3	3	3	3	3	3	2	2	2	2	2	2	2	1	1
	5 (x3)	9	9	9	9	9	9	9	9	6	6	6	6	6	6	6	6	3
F	6	2	2	2	4	2	2	2	4	2	2	4	2	2	2	2	4	4
	7	3	3	3	4	3	3	3	4	3	3	4	3	3	3	3	4	4
	8 (x3)	6	6	6	9	6	6	6	9	6	6	9	6	6	6	6	3	3
	1	4	3	4	2	4	3	4	3	4	3	2	4	3	4	3	2	2
	2	4	4	4	3	4	4	4	4	3	4	3	4	4	4	4	3	3
	3	3	3	3	2	3	3	3	3	2	3	3	2	3	3	3	2	2
	4	2	2	2	2	2	2	2	2	2	2	2	2	2	2	2	2	2
	5 (x3)	3	9	3	6	3	9	3	6	3	9	6	3	9	3	9	6	3
TOTALS		108.3	118.8	104.8	135.5	108.3	118.8	108.3	118.8	135.5	88.0	88.5	110.5	87.5	88.5	88.0	88.5	88.5

ORIGINAL PAGE
OF FOUR QUALITY

TABLE V-5
COST COMPARISONS $\times 10^5$

OX FUEL	N ₂ O ₄ MMH				N ₂ O ₄ MMH + S1		N ₂ O ₄ 50-50			LOX MMH			LOX MMH + S1		LOX RPI	LOX	
	Icb	DAR	CWR	TWR	CWR	DAR	CWR	DAR	Icb	CWR	DAR	Icb	CWR	DAR		CWR	Icb
\$ I _{sp}	0	-8.16	-8.45	-8.45	-12.60	-12.60	-7.59	-7.59	+2.72	-27.25	-27.13	-22.82	-30.47	-30.47	-30.05	-6.65	-24.74
\$ FEED PRESSURE	0	+7.23	+3.89	+3.60	+3.68	+5.95	+4.17	+10.36	+0.01	+5.04	+8.41	0	+5.10	+8.50	+2.97	0.392	+0.14
\$ ENGINE WEIGHT	0	-0.18	+0.08	+0.40	+0.60	+0.25	0.067	0.166	0	0.70	0.44	1.03	1.38	1.01	1.25	1.142	0.88
\$ TECH RATING ①	0	+0.23	+1.39	+11.0	+1.30	+0.53	9.42	5.27	0	21.6	15.2	7.95	20.6	1.2	21.6	11.6	19.2
\$ ONS ②	0	0	0	0	0	0	0	0	0	10	10	10	10	10	10	10	10
SUM	0	- .86	-3.09	+6.56	+6.93	-6.25	+6.07	+7.87	+2.73	+10.09	+6.92	-3.84	+6.61	+4.24	+6.77	+16.48	+5.48

CONVERSIONS	OX FUEL	N ₂ O ₄ AMINE	LOX AMINE	LOX C ₃ H ₈	LOX RPI
\$ I _{sp}		1.432	1.105	1.232	1.318
\$ FCI		0.141	0.177	0.196	0.184
\$ WEIGHT		0.104	0.034	0.024	0.021

McDONNELL DOUGLAS
ONS TRADE STUDIES
PROGRESS REPORT NO. 1
15 AUGUST 1972

① $1.5 \left[\frac{135.5}{\text{RATING}} - 1 \right]$ IS FACTOR OF 1.5 ESTIMATED CONVERSION BAC PRICE TO TOTAL PROGRAM COST

② COST ASSUMED AT \$10 $\times 10^5$ FOR LOX PROPELLANT COMBINATIONS

II-62

Bell Aerospace Company

rating weight of 3 was selected in order to impact the development cost from \$825,000 minimum to \$2,475,000 maximum for the high technical risk elements.

The last element of Δ cost was the estimated difference to the OMS for the Task II propellants. The 10 million dollars is primarily associated with the development and qualification costs of the insulated LOX tank.

4. Recommendations

The recommendation for the OME reusable thrust chamber and propellant combination based on the Task I and II effort resulted from the technical and cost ratings. The four "best" approaches were:

<u>Technical Rating</u>			<u>Cost Rating ($\times 10^{-6}$)</u>		
135.5	Icb	N ₂ O ₄ /Amine	-3.31	Icb	LOX/MMH
118.8	DAR	N ₂ O ₄ /Amine	-1.13	DAR	N ₂ O ₄ /MMH + Si
110.5	Icb	LOX/MMH	0.00	Icb	N ₂ O ₄ /MMH
108.3	CWR	N ₂ O ₄ /Amine	+1.10	CWR	N ₂ O ₄ /MMH + Si

The apparent high technical rating of the Icb with N₂O₄/Amine propellant appeared to offset the small cost advantages of the LOX/MMH propellant combination with the Icb chamber and the DAR design with N₂O₄/MMH + Si. Therefore, the insulated columbium thrust chamber engine with N₂O₄/MMH propellants was reported as the best choice based on the Task I and II studies and rates.

Subsequent effort under contract NAS 9-12803 as presented in this report, showed that both the Icb and CWR were capable of achieving their predicted performance with N₂O₄/MMH. The Icb design also met its nominal temperature definition of 2400°F. The heat rejection to the MMH regen coolant was shown to be significantly less than predicted providing higher thermal margins and allowing the use of an uncoated Haynes 25 nozzle extension in place of the coated columbium extension. A flat face injector with acoustic cavities was shown to provide damping for bomb induced combustion disturbances. The successful bomb testing showed that the Task I and II definition of an injector with a 5 leg baffle could be changed to an injector with no baffle and incorporating the acoustic cavities. Finally, analyses of the feed system gas ingestion malfunction showed that engine damage could be prevented by chamber pressure sensing only.

The subsequent tests and analyses change the technical and cost comparisons described above. Changes to the technical rating factors of Table XII are as follows:

Bell Aerospace Company

A6, B5, E3 - all engines change to a rating of 4, chamber pressure sensing only provides the necessary engine protection.

C2, C5-change CWR rating from 2 to 3 reflecting milling of liner cooling passages rather than EDM.

- E1 - Change rating of N_2O_4 regen engines from 3 to 12 (weight of 3), heated fuel shown to have no impact on performance or stability; LOX engines change 3 to 9.
- E2 - Change regen engine ratings from 1 or 2 to 3; chamber pressure sensing of feed system malfunction negates the effect of detection sensitivity.
- E5 - Raise regen chambers with N_2O_4 oxidizer to 12, LOX to 9 based on increased confidence of predicted I_{sp} .
- E6 - Raise regen chambers from 2 to 3, improved cooling margin demonstrated.
- E8 - Raise regen chambers from 6 to 9 for improved injector cooling margin by elimination of baffles and change from N_2O_4 face cooling to fuel face cooling permitted by lower heat input to fuel in chamber.
- E5 - Raise CWR from 3 to 6 based on thrust chamber firing demonstrations.

The result of the above changes on the ratings for the 6 "best" are as follows:

<u>Technical Rating</u>		<u>Cost Rating ($\times 10^{-6}$)</u>		
142.5	I_{cb} N_2O_4 /Amine	-6.93	CWR	N_2O_4 /MMH + Si
141.8	DAR N_2O_4 /Amine	-6.26	DAR	N_2O_4 /MMH + Si
137.3	CWR N_2O_4 /Amine	-3.84	I_{cb}	LOX/MMH
117.5	I_{cb} LOX/MMH	-3.09	CWR	N_2O_4 /MMH
113.5	DAR LOX/Amine	-0.88	DAR	N_2O_4 /MMH
109.0	CWR LOX/Amine	0.00	I_{cb}	N_2O_4 /MMH

The technical ratings of all engines increase. The difference in technical rating between I_{cb} and the regen chambers and between the DAR and CWR is reduced. The relative rating between N_2O_4 oxidizer and LOX oxidizer engines increases for the regeneratively cooled chambers. Therefore, with little technical rating difference between the various chambers the cost ratings would recommend either CWR and DAR with N_2O_4 and MMH with silicone oil additive. Prohibition of MMH + Si and LOX in order to have common propellants for the OMS and RCS makes CWR with N_2O_4 /MMH the overall choice.

Bell Aerospace Company

In conclusion, the large technology base established by the remainder of the program changes the recommended type of thrust chamber from Icb to CWR and confirms the selection of N_2O_4/MMH as the OME propellant combination.

Bell Aerospace Company

IV. 6000 LBF COLUMBIUM CHAMBER DESIGN, FABRICATION AND DEMONSTRATION TEST

A. ColumbiuM Thrust Chamber Design (Task III)

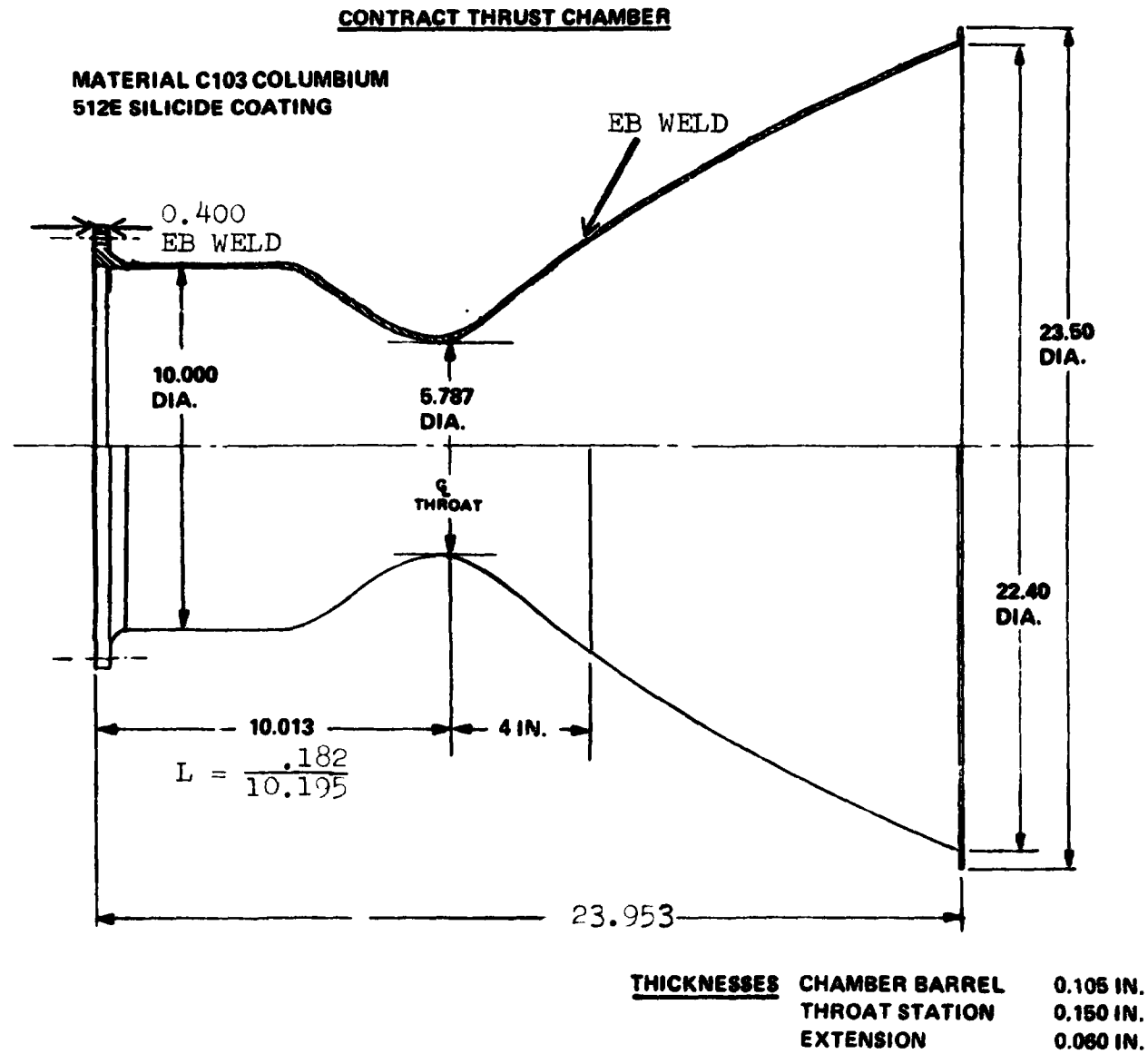
The columbiuM thrust chamber was designed in accordance with the Task I studies which set the chamber diameter at 10 inches, chamber and throat thicknesses at 0.105 and 0.150 respectively and the combustion chamber length at 10.013 inches. The chamber length provided an L^* of 30 inches with the combustion volume provided by the injector assembly. The design was consistent to the nominal N_2O_4/MMH 6000 lbf chamber at a chamber pressure of 125 psia. The divergent nozzle of the demonstration chamber was restricted to an area ratio of 15:1 by the altitude test facility at Bell. The development nozzle contour was established as a truncated section of the full nozzle contour rather than an optimized 15:1 shape. The contour selection was based on an agreement with the program monitor in order that the data generated would be comparable to the results generated under the second technology contract, NAS 9-12802. The chamber is shown in Figure IV-1.

The predicted operating characteristics for the columbiuM thrust chamber from the Task I studies included the following from Table VIII, Section III.

Design nominal maximum temperature (insulated)	2400°F
Off limits (-10% P_c , +12% O/F) maximum temperature (insulated)	2548°F
Nominal barrier flow (% of total flow)	7.657
$I_{sp\infty}$ (corrected to $\epsilon = 74.3$)	310.5 sec.

The chamber design reflected a study of alternate fabrication techniques to reduce cost and the fabrication schedule. The selected chamber definition included a weld-on injector mounting flange, a longitudinal weld seam in the barrel and convergent divergent nozzle, and a weld-on nozzle extension to an area ratio of 15:1. The extension was defined with two longitudinal weld seams. All welds were established as full penetration electron beam type. Testing at Bell on other programs has shown that no significant columbiuM property reduction is encountered across narrow beam E.B. welds. The demonstrated characteristics of the columbiuM E.B. welds permitted the multi-section chamber design. The chamber columbiuM alloy selected, C-103, was based on structural analyses that confirmed its adequacy, the superior

FIGURE V-3



Bell Aerospace Company

forming characteristics of that alloy relative to higher strength Cb alloys and the material availability. The multi-section approach and alloy selection minimized material, tooling and fabrication costs and insured a relatively short material procurement and chamber fabrication lead times.

The coating selected to prevent oxidation of the columbium shell and embrittlement from the combustion gas hydrogen species was HITEMPCO R-512E. The coating selection was based on its demonstrated compatibility with the propellants and all combinations of propellants, moisture and flushing fluids. The R-512E has demonstrated steady-state temperature life in combustion atmosphere (oxyacetylene torch) in excess of 212 hours at 2200°F and 80 hours at 2400°F. The coating has survived more than 10,000 thermal fatigue cycles to 2200°F.(x) Previous experience at Bell and elsewhere has shown that the coating is not easily damaged during normal handling. The columbium coating diffusion zone has a Vickers hardness of 1000 which provides a high resistance to scratch damage. The diffusion zone also reduces base metal hardness increase by hydrazine embrittlement. Essentially no columbium elongation or tensile strength changes have been noted after 10,000 seconds of firing with RCS units.

Use of Vac Hyde VH109 coating was considered prior to coating the second 6000 lbf columbium chamber (Task VI). Data from NASA CR712119 was reviewed. The relative merits of VH109 and R512E were also discussed with Lockheed, NASA Lewis and Air Force Material Laboratory personnel. The data and discussions confirmed the selection of the R512E for the demonstration columbium chambers.

B. Columbium Thrust Chamber Fabrication (Tasks IV and VI)

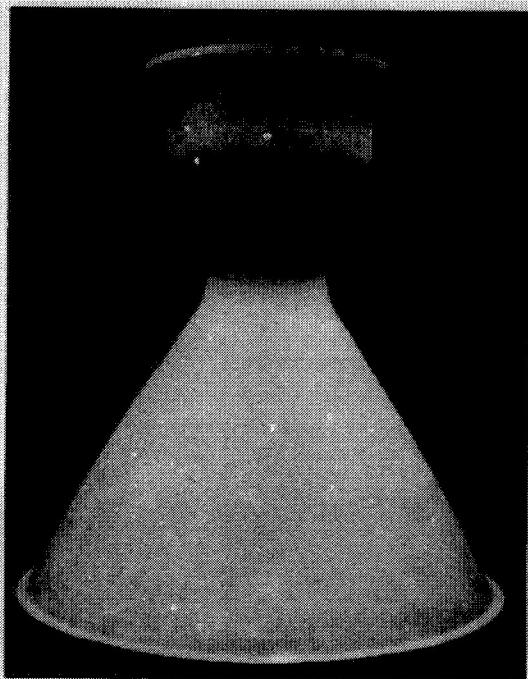
The procurement of material for chamber described above and the chamber fabrication under Task IV was accomplished over a 4 month time span through January 1973. Material lead time was approximately 2-1/2 months. The chamber components were fabricated as follows:

1. Injector Mounting Flange

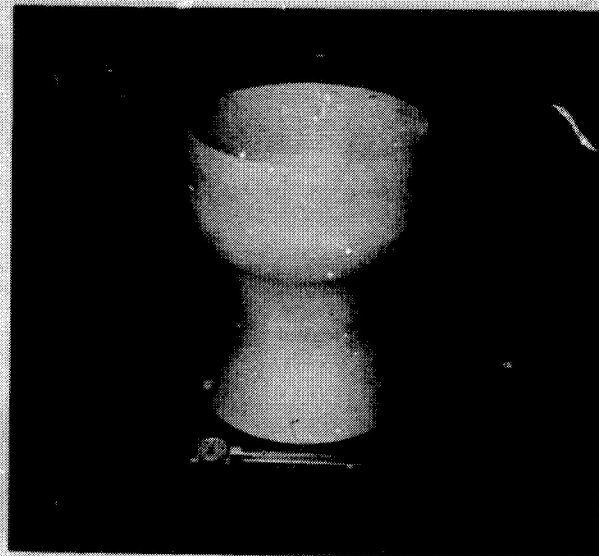
The flange was machined from a forged C103 billet with excess material to machine the injector mating surface and the I.D. to 10". The flange and the other chamber components are shown in Figure IV-2.

(x)Holloway, J. F. Jr., "Evaluation of Coated Columbium Alloys for Burner Application" AFML-TR-71-107, August 1971.

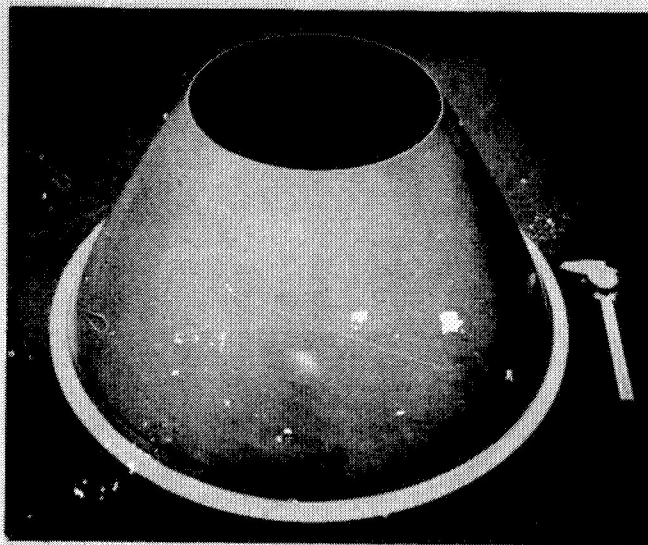
ORIGINAL PAGE IS
OF POOR QUALITY



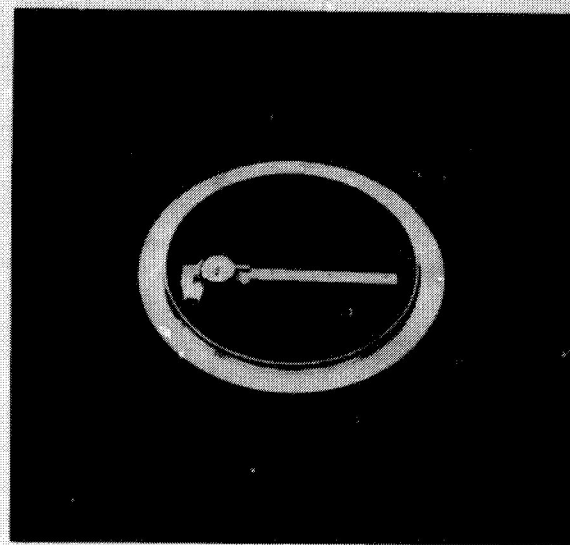
THRUST CHAMBER



CHAMBER/NOZZLE



NOZZLE SKIRT



MOUNTING FLANGE

FIGURE IV-2. ONE COLUMBIUM THRUST CHAMBER

Bell Aerospace Company

2. Barrel, Convergent - Divergent Nozzle

The section started as a cylinder rolled from plate stock to 8 inch I.D. and E.B. seam welded. One end was bulge formed to the 10 inch I.D. of the barrel section; the other end was tapered from 8 inch to 10 inch by bulge forming. The center section was spun to the approximate throat diameter and the contour upstream and downstream of the throat.

The forming of the throat required higher force and more annealing cycles than originally anticipated. Hand held spinning tools were replaced by hydraulic drive tools to complete the part. The manual spinning resulted in minor weld flows which were repaired.

3. Nozzle Extension

Two halves of the extension were rolled from .060 thick sheet stock to cone shape, seam welded and then bulge formed to final contour. The lip at the nozzle exit was formed by spinning. The use of constant thickness sheet stock was based on material availability and ease of fabrication. Machining to the necessary structural thickness of 0.020 inches was considered unnecessary for the planned demonstration firings.

4. Assembly

The assembly was accomplished by machining mating surfaces of the three chamber components to allow butt F.B. welds. The injector mounting flange to chamber weld was accomplished without incident. Some difficulties were encountered in the nozzle-to-nozzle extension weld which were precepitation hardened by a lack of penetration on the first weld. Subsequent welding of the chamber resulted in more distortion than acceptable and reforming and rewelding was required. A sound weld was completed by annealing the parts. The chamber and throat section were subsequently machined to drawing requirements.

Chamber coating inside and out with R-512E was completed as scheduled. The chamber assembly is shown in Figure IV-3. Thermocouples were subsequently resistance welded to the outside chamber wall after local coating removal. The thermocouple installation was painted with Pyrochrome to provide short term oxidation resistance of the columbium where the coating was removed.

The fabrication of the second chamber under Task VI paralleled the above description with the exception that the throat section employed hydraulic driven spinning tools only which expedited forming of that part. The second chamber was fabricated with a barrel section approximately two inches shorter than the first unit to permit testing with a reduced L*, 25 inches.

ORIGINAL PAGE IS
OF POOR QUALITY

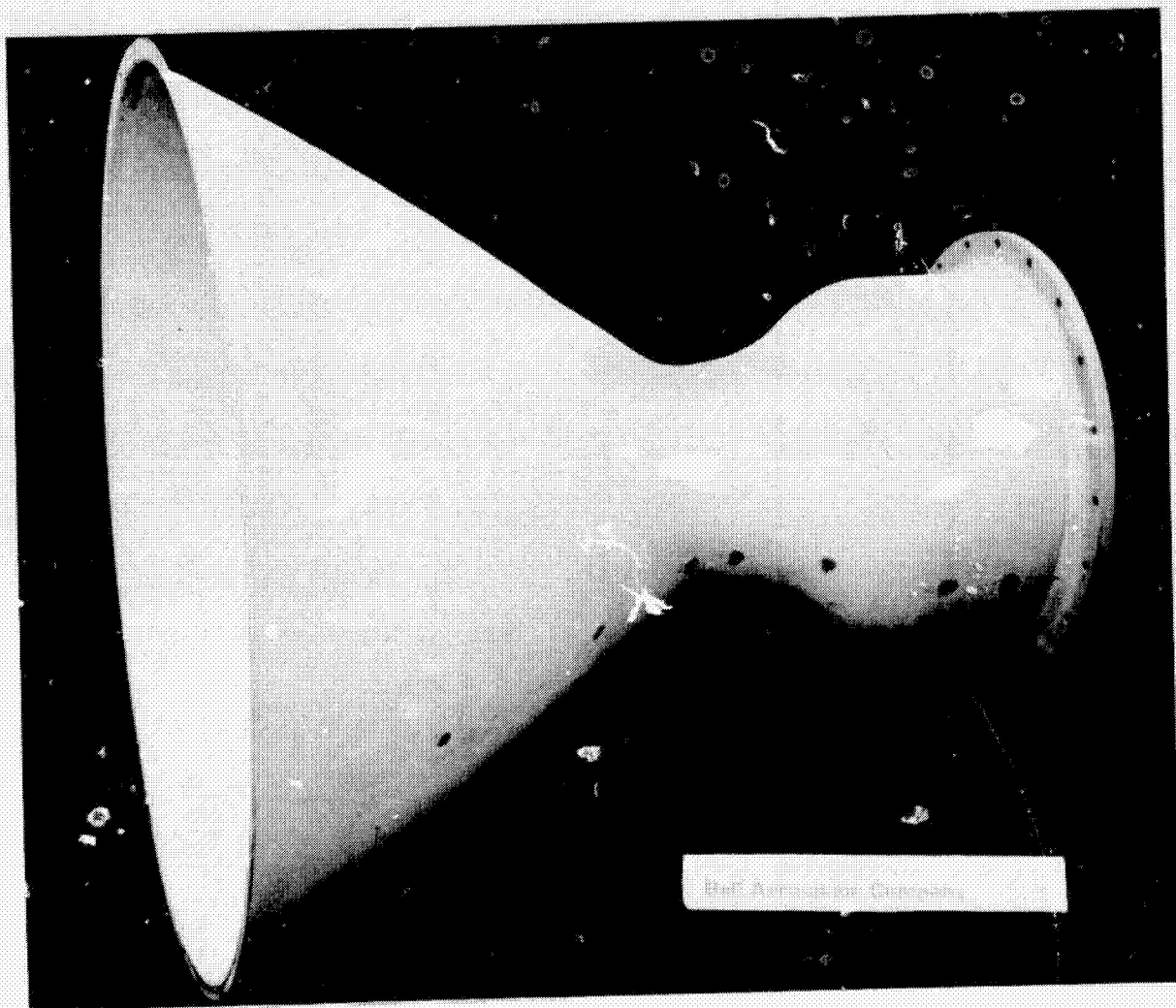


FIGURE IV-3. COATED COLUMBIUM THRUST CHAMBER

Bell Aerospace Company

C. Demonstration Testing (Task V and VIII)

1. General

The initial columbium chamber testing (Task V) with the 30 L* chamber was conducted in two phases. A five leg baffle stainless steel injector was used for the first test series. That injector was designed in accordance with the Task I and II OME definitions which included a 10 inch diameter chamber and injector. The injector incorporated triplet elements with an outer ring of unlike doublets. Test results with the stainless steel injector fell approximately 2% short of the predicted I_{sp} at the design operating conditions of 125 psia chamber pressure, N_2O_4/MMH propellants at a mixture ratio of 1.64 and a maximum insulated chamber temperature of 2400°F. The injector operation in the columbium chamber was characterized by non-uniform throat temperatures associated with the baffle configuration. An attempt to improve the temperature uniformity was successful but was achieved at the expense of combustion efficiency. The net result of the change was little or no I_{sp} improvement within the 2400°F maximum temperature restraint. With the agreement of the program monitor, the Task V testing was interrupted until a second injector became available.

The second 6000 lbf, N_2O_4/MMH , 10 inch diameter injector was fabricated from aluminum and incorporated acoustic cavities for the suppression of high frequency combustion instability. Fuel vortex film cooling was maintained as the approach to the gas film temperature reduction. The triplet injector element was used exclusively and the flat face design allowed the center-line of the triplet elements to be in line with the chamber radius. Aluminum was employed to expedite the injector fabrication. Testing with the second injector with the 30 inch L* chamber demonstrated operation within 0.5 seconds of the I_{sp} goal at the maximum temperature of 2400°F at nominal operating conditions. The tests confirmed the off-limits operation temperature predictions.

Tests under Task VIII, "Alternate Thrust Chamber and P Testing", evaluated operation with chamber L*'s of 26, 30 and 34 inches with a second aluminum injector. The second aluminum injector pattern was similar to the first; modifications were made primarily in the oxidizer inlet manifolding to improve the triplet element impingement. Tests with the second aluminum injector showed that the predicted I_{sp} could be exceeded by 1 sec. with an L* of 34 and that the I_{sp} with $N_2O_4/50-50$ blend was essentially equal to N_2O_4/MMH .

Bell Aerospace Company

2. Test Injector Descriptions

The stainless steel injector was designed with triplet elements (2 fuel on 1 oxidizer) with a single ring of unlike doublets near the outside diameter and separate orifice for fuel vortex film cooling. The injector design includes a 5 legged baffle (integral with the injector face) and acoustic slots designed for the first radial mode to assure stable operation in combination with the baffles (Figure IV-4). A view of the completed injector is shown in Figure IV-5. The injector baffle and faceplate are fuel cooled through radial feed holes with the fuel flowing radially outward through the baffle, then inward through the face coolant passages to the fuel orifices. The fuel vortex film separately fed to permit variation of fuel film flow independent of main injector flow. The injector propellant feed system consists of a single center feed fuel port and a single oxidizer port, each feeding their respective manifolds and orifices. All weld joints are designed so that any leakage would be overboard.

The first aluminum injector is shown in Figure IV-6 after several firings. The unit was designed with 184 radial triplet elements; the injection holes of each element are on a radius line. The face of the injector has electron beam welded ring sealing circumferential propellant manifold slots. The acoustic cavity/fuel vortex film coolant ring subassembly made provision for 8 cavities of 1.65 inches depth and 4 cavities of 0.76 inches as shown in Figure IV-7. The 8 deeper cavities were designed to damp the first tangential mode of instability; the 0.76 deep cavities were sized for the third tangential and first radial modes. The injector was designated AL #1 Mod A after manifold changes as described in the following section.

The second aluminum injector is shown in Figure IV-8. The number of triplet elements are increased to 196 to provide consistent spacing between the outer and second ring of elements. The fuel inlet is on the injector centerline supplying radial distribution holes. The oxidizer inlet is off center supplying a flat annular distribution manifold. The circumferential manifolds near the face required E.B. welded face rings.

The nominal injection orifice pressure drop of the second aluminum injector (AL #2) was designed for 40 psi, approximately 5 psi above AC #1 Mod A. The AC #2 injector utilized the same acoustic cavity vortex ring subassembly employed with AL #1 Mod A.

STAINLESS STEEL INJECTOR ASSEMBLY

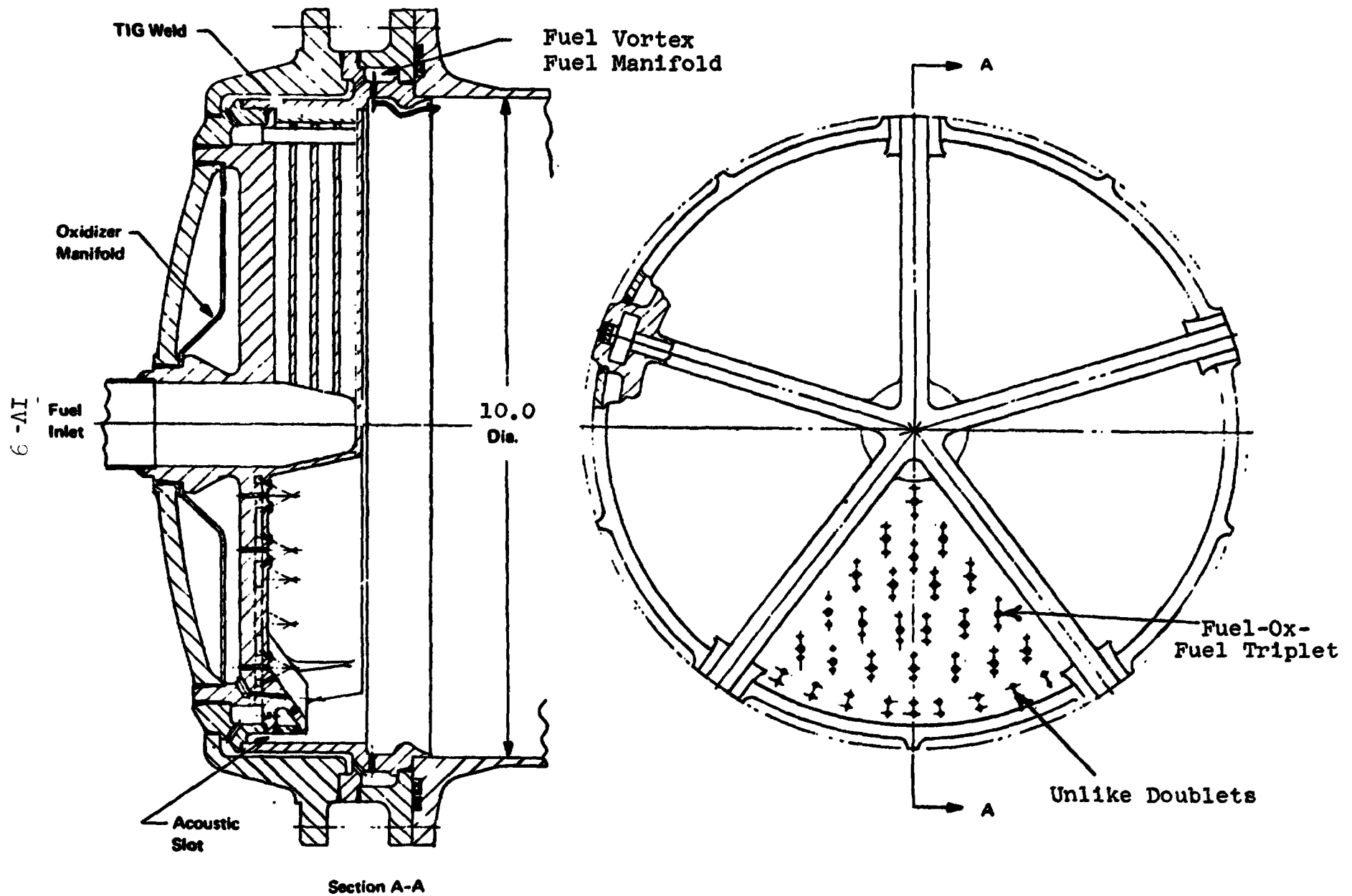


FIGURE IV-4

ORIGINAL PAGE IS
OF POOR QUALITY

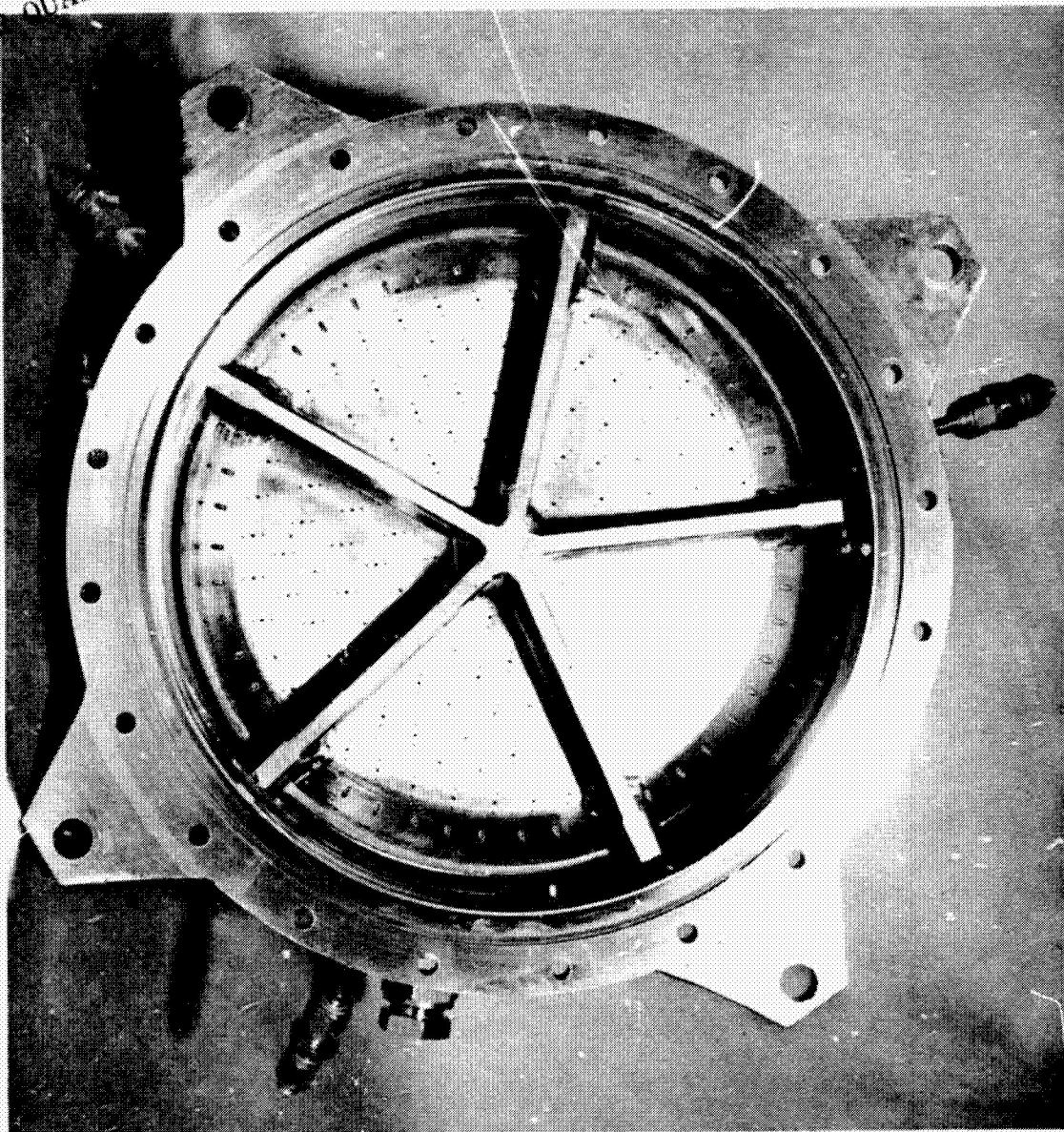
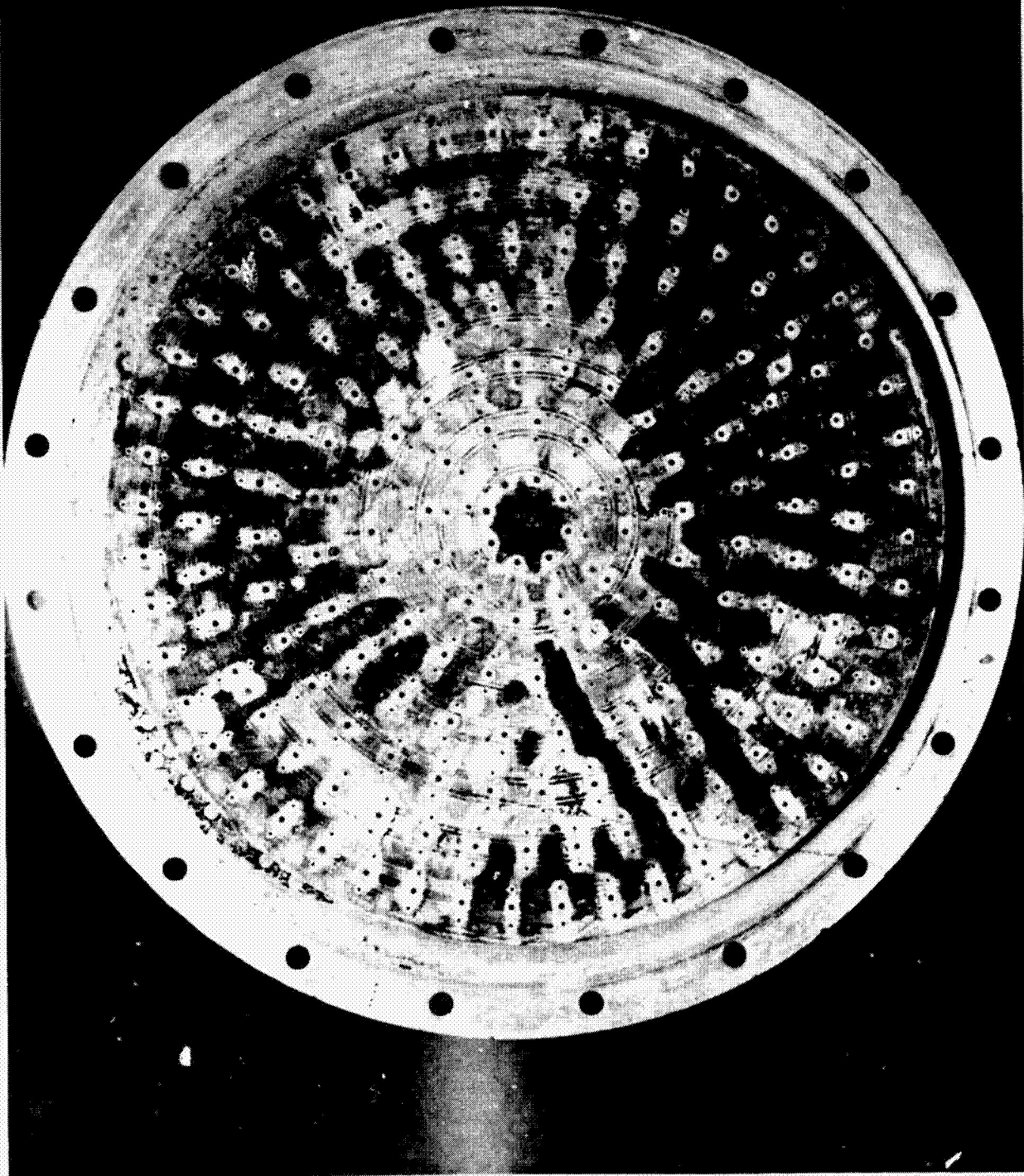


FIGURE IV-5. STAINLESS STEEL INJECTOR

ORIGINAL PAGE IS
OF QUALITY



ALUMINUM INJECTOR ASSEMBLY - DESIGN DATA

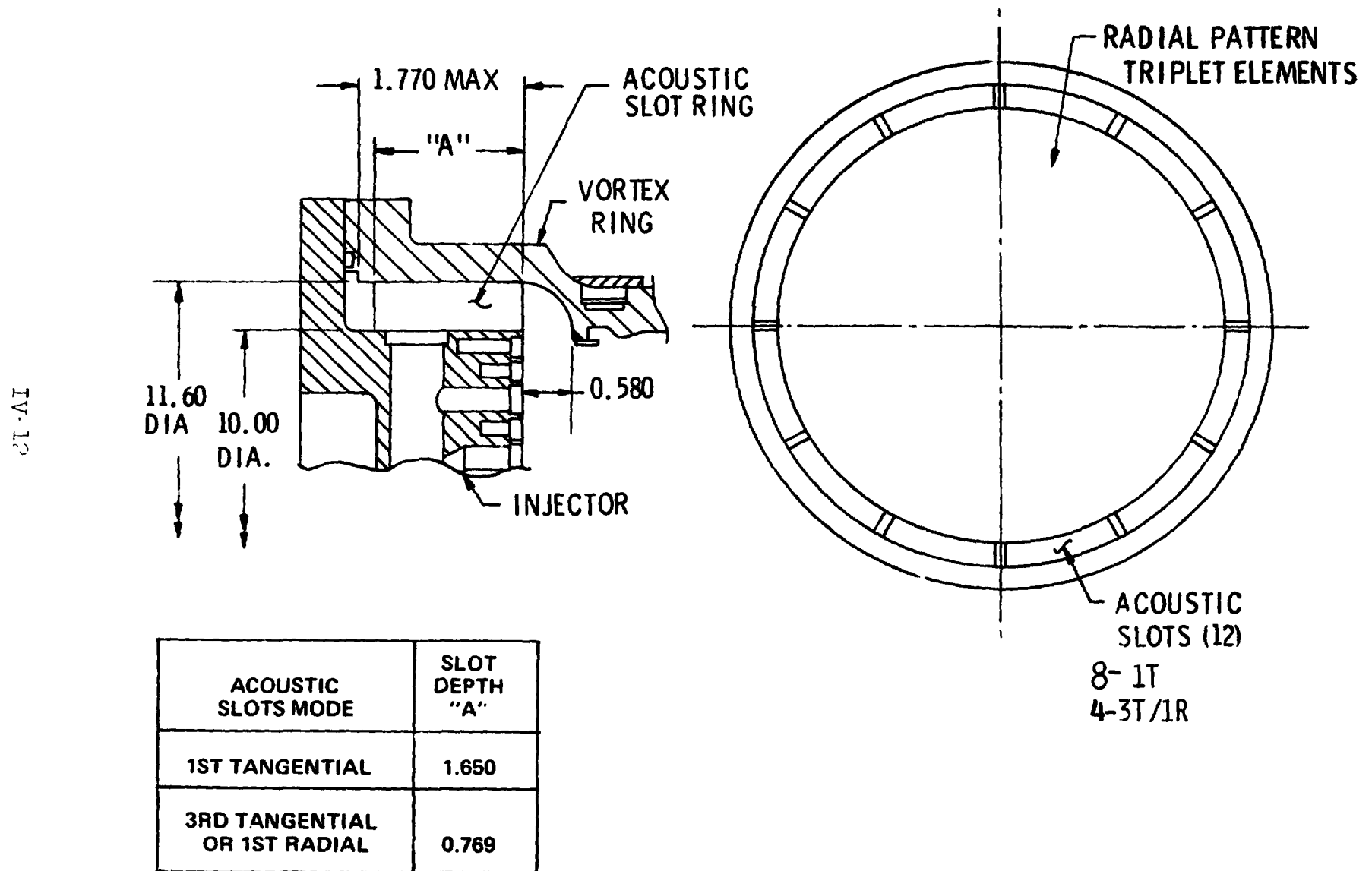


FIGURE IV-7

10 INCH DIA. ALUMINUM INJECTOR No. 2

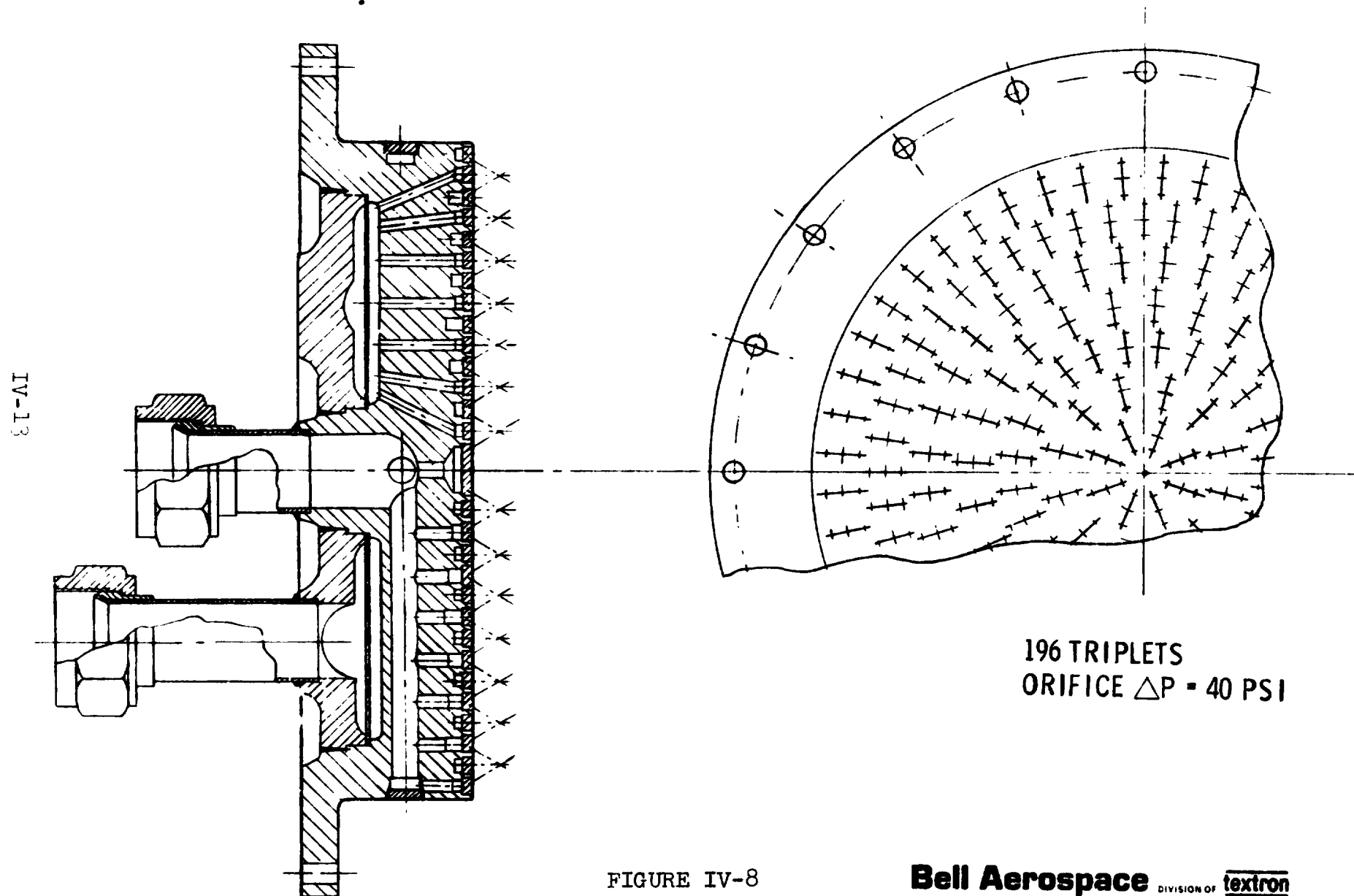


FIGURE IV-8

Bell Aerospace DIVISION OF **textron**

Bell Aerospace Company

3. Injector Check-out Firings

a. Stainless Steel Injector

Firing tests at sea level were conducted to define performance, c^* , as a function of chamber pressure, overall mixture ratio and percentage of fuel vortex film coolant. The tests also characterized the heat rejection to the throat section. The tests were conducted using a thrust chamber assembly consisting of an uncooled steel combustion chamber and a segmented water cooled nozzle, Figure IV-9. The longitudinally segmented nozzle was used to obtain a peripheral heat rejection signature for the injector.

A total of 15 tests were made for an accumulated run time of 201 seconds (See Table I). Testing was performed over a mixture ratio (O/F) range of 1.42 to 1.92, a chamber pressure range of 112.5 psia to 139.8 psia, and a vortex flow (ρ) range of 6.65% to 10.36%. Run durations were nominally 15.0 seconds duration except for the initial tests conducted and for one inadvertent fuel propellant exhaustion test, run 4407. During that test the fuel exhaustion was gradual and was attributed to vortexing around the feed tank stand pipe. The decrease in fuel flow caused a gradual drop in chamber pressure until the chamber pressure low level switch initiated shutdown at approximately 95 psia. This pressure transition was gradual and showed no signs of oscillatory combustion at the lower pressures.

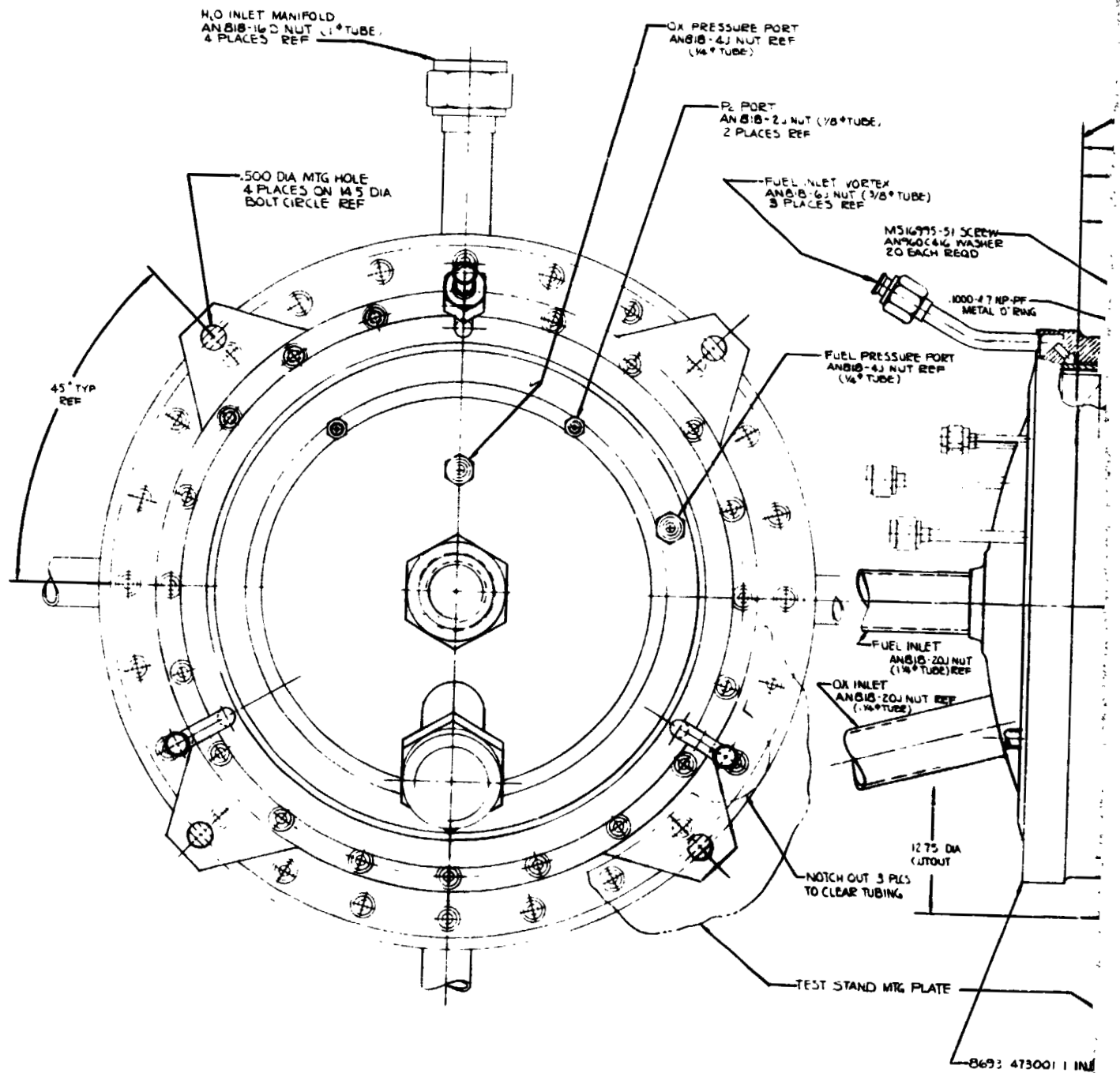
The basic test setup and instrumentation coverage is shown in Figures IV-10 and IV-11. The propellant was fed through a bipropellant valve. A separate flowmeter was employed for the fuel vortex film cooling. Two flowmeters were used in each of the three propellant feed lines. Thrust measurements were not made for the sea level tests.

The c^* data is plotted in Figure IV-12 as a function of film coolant, ρ , with lines of constant O/F inferred from the data. In general, the data follows the predicted c^* for the individual run conditions but at 0.4 to 1.3% lower values. The predicted c^* as used in the Task I studies was:

$$c^* = 4320 \rho + 0.99 (1 - \rho) c^*_{\text{core}}$$

The higher percentage differences were observed at low mixture ratio and nominal O/F at the higher percentages of film cooling. Chamber pressure variation from approximately 113 to 137 psia was observed to have little effect on the characteristic velocity, as predicted; c^*_{core} at a representative mixture ratio (2.2) changes approximately 14 ft/sec between $P_c = 110$ and 140 psia.

ORIGINAL PAGE IS
OF POOR QUALITY



⚠ APPLY EQUAL TORQUE TO SCREWS TO ENSURE UNIFORM COMPRESSION
OF -3 GASKET
NOTES:

FOLDOUT FRAME |

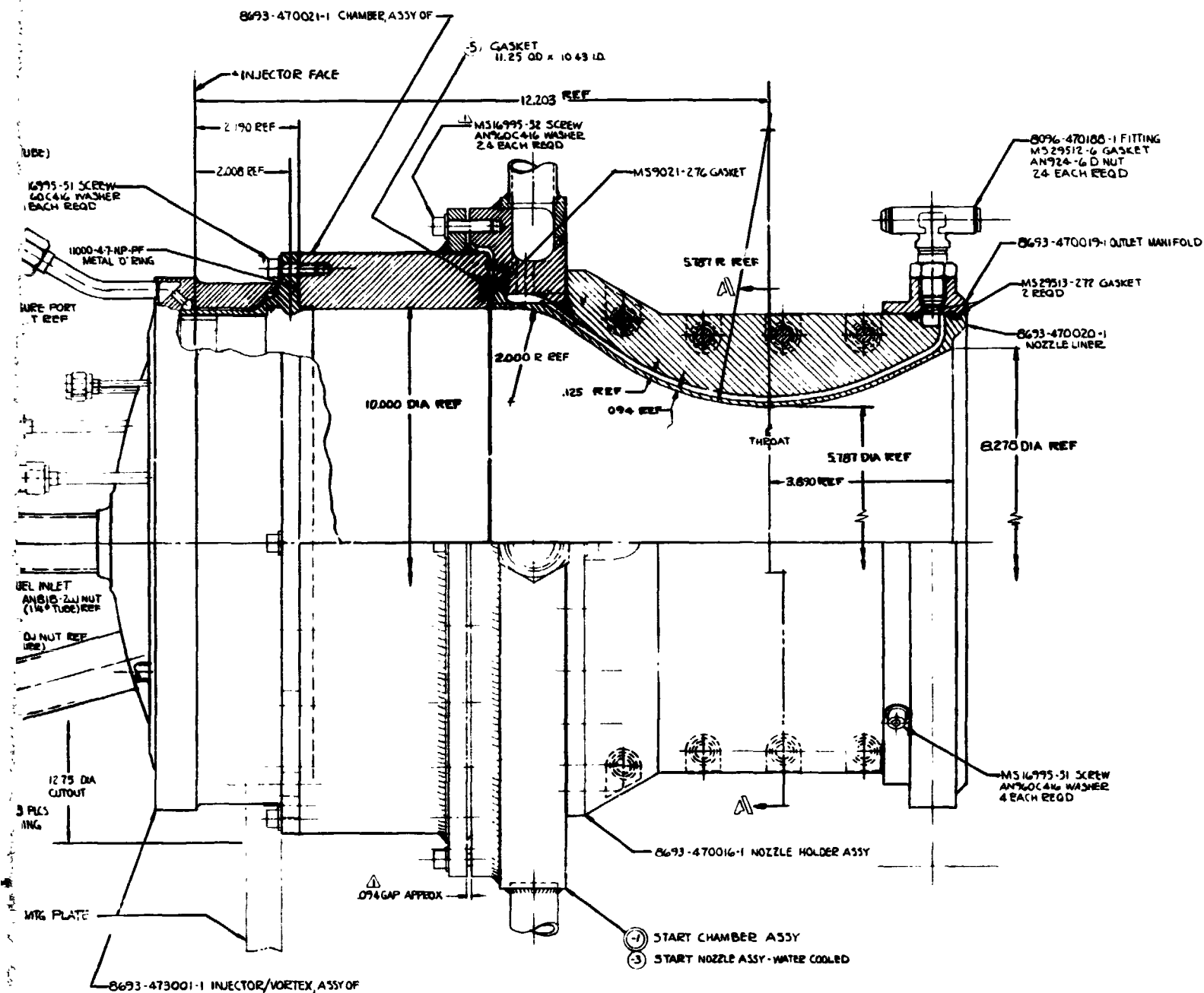


FIGURE IV-9
Start Chamber Assembly

IV-15

FOLDOUT FRAME 2

TABLE I
OME 6K THRUST PROGRAM
SEA LEVEL TEST DATA

TEST D-4	DUR. SEC.	DATA PT. SEC.	P _C CORR PSIA	R OVERALL	ϵ %	C* ^① CORR FT/SEC	η_{C*} %	Q/A _{NOZ} BTU/IN ² SEC	Q/A _{VORTEX} BTU/IN ² SEC	Q/A _{BAFF.} BTU/IN ² SEC
4395	2.0	1.5	123.6	1.703	10.36	5309	92.9	--	--	--
4396	7.8	7.3	124.1	1.655	10.04	5349	93.7	1.06	0.465	0.674
4397	15.5	15.0	123.7	1.635	10.16	5359	93.9	1.08	0.571	0.661
4398	15.1	14.6	123.5	1.596	8.39	5463	95.7	1.26	0.535	0.769
4399	15.4	14.9	124.0	1.604	7.47	5493	96.2	1.41	0.837	0.826
4400	15.1	14.6	122.6	1.677	10.17	5338	93.5	1.08	0.492	0.603
4401	15.1	14.6	121.9	1.921	6.64	5389	94.9	1.39	0.451	0.590
4402	15.3	14.8	122.2	1.855	9.83	5229	91.8	1.04	0.404	0.505
4403	15.1	14.6	124.6	1.421	10.18	5435	95.8	1.12	0.954	0.923
4404	14.8	14.3	124.5	1.447	7.17	5511	97.0	1.44	--	--
4405	13.6	14.3	110.6	1.686	6.91	5477	95.9	1.31	0.376	0.645
4406	15.0	14.5	112.5	1.672	9.80	5347	93.6	1.02	0.299	0.549
4407	② 7.2	6.0	134.3	1.661	7.29	5486	96.1	1.40	0.435	0.890
4408	15.0	14.5	134.7	1.662	7.50	5468	95.7	1.47	0.759	0.860
4409	15.1	14.6	134.6	1.631	10.03	5367	94.0	1.18	0.498	0.753
4410	2.3	1.8	124.1	1.728	8.87	5376	94.1	--	--	--
4411	2.2	1.7	122.8	1.681	7.11	5388	94.3	--	--	--
4412	15.1	14.6	120.7	1.671	9.36	5372	94.0	1.11	0.532	0.733

Hardware: Injector, Stainless Steel, 5 leg baffle; 8693-473001-1; S/N 1
Chamber, Steel 8693-470021-1; S/N 1
Nozzle, Aluminum, Water Cooled 8693-470016-1; S/N 1

Target 5497 C*

$\epsilon = 7.65$

P_C = 125

O/F = 1.64

① P_C correction factor is 0.983

② Abbreviated run due to exhaustion of fuel supply

ORIGINAL PAGE IS
OF POOR QUALITY

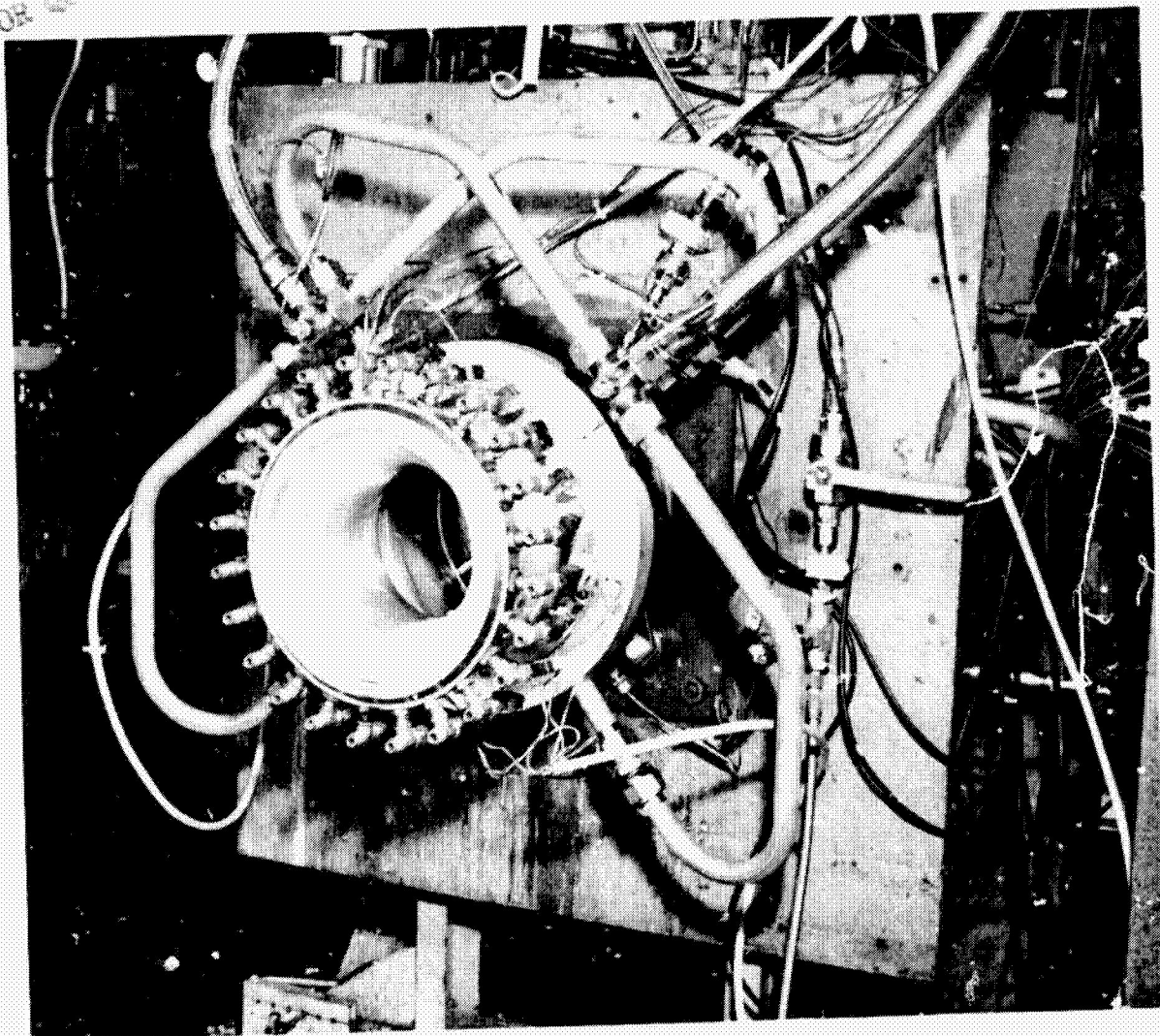


FIGURE IV-10. TEST STAND INSTALLATION

ORIGINAL PAGE IS
OF POOR QUALITY

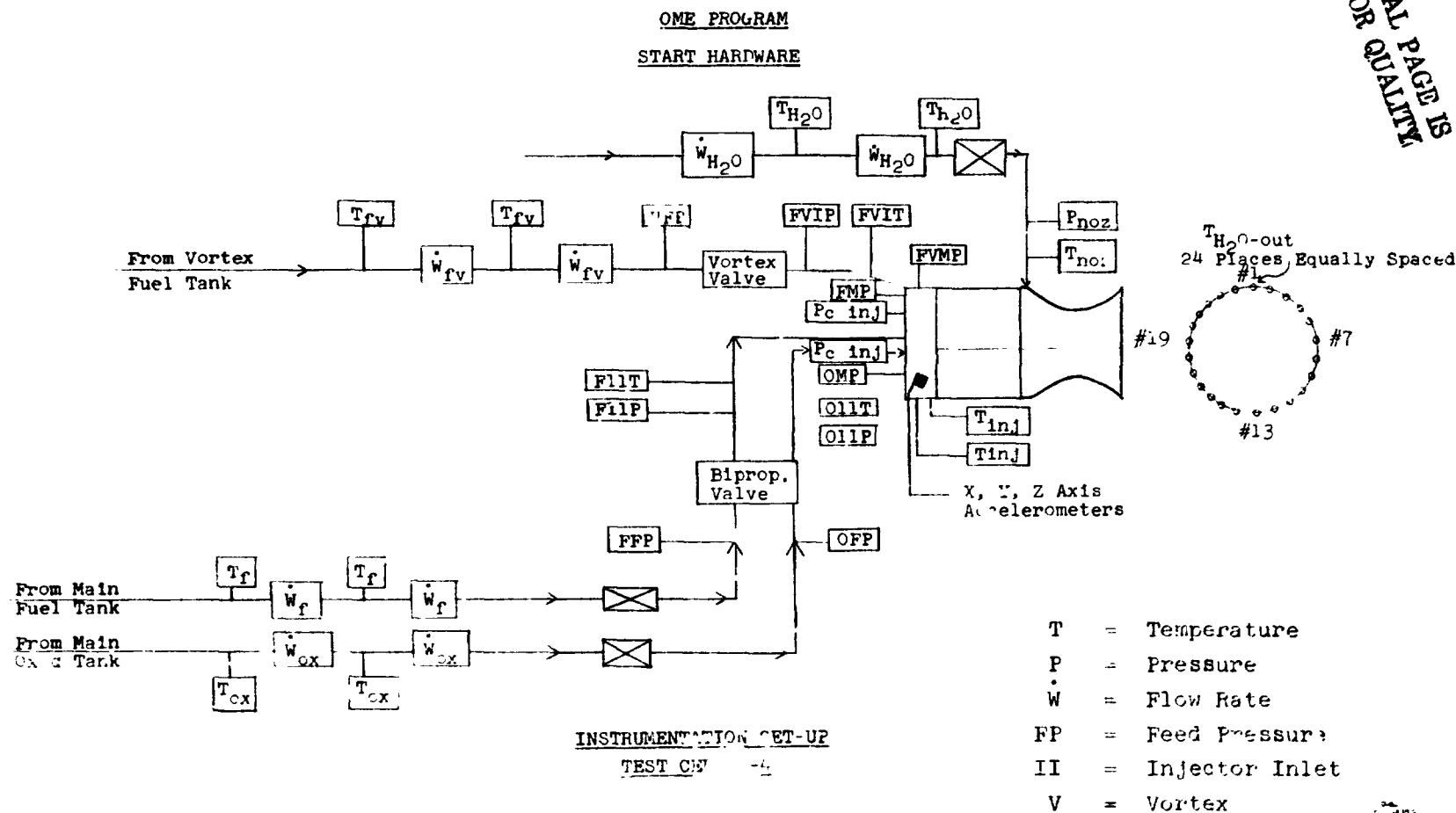


FIGURE IV-11

Bell Aerospace Company

C* vs
TEST CELL D-4
DATE: 2/22/73 TO 3/2/73

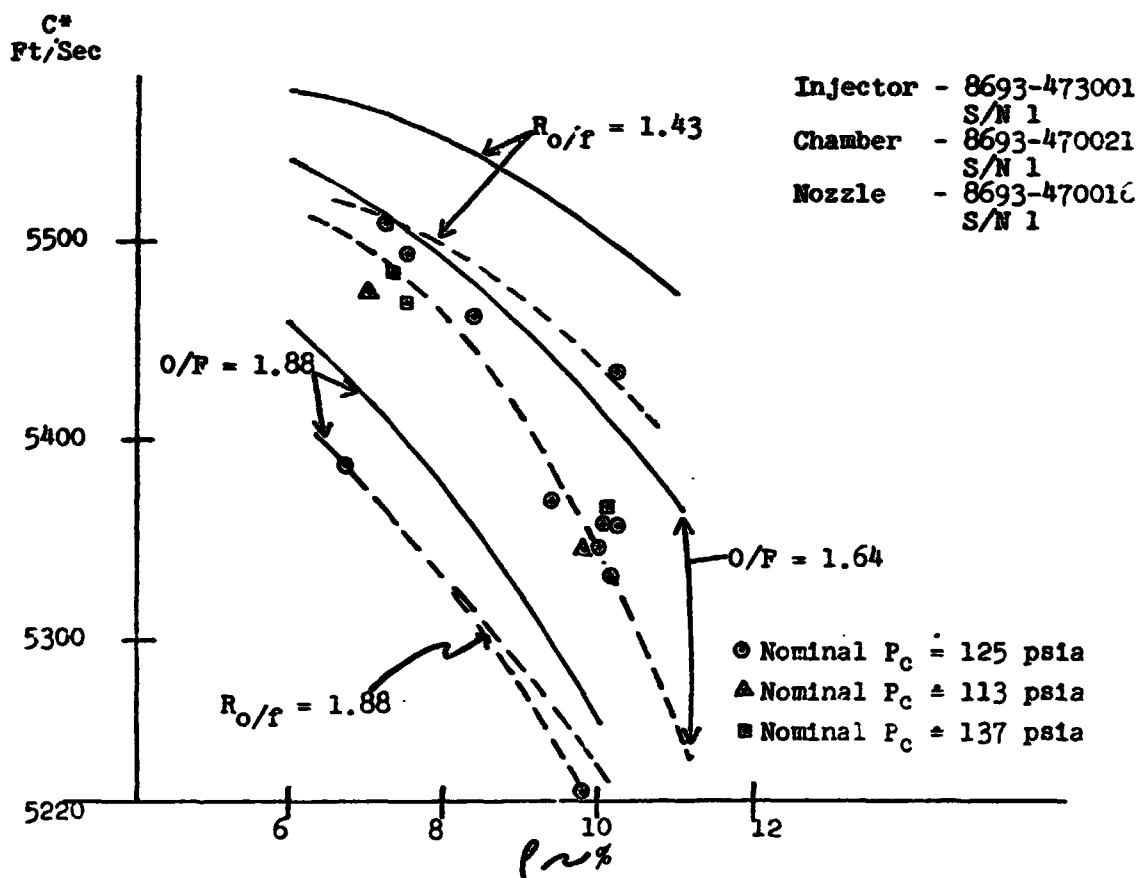


FIGURE IV-12

Bell Aerospace Company

Nozzle rejection data is shown in Figures IV-13 and IV-14. The total heat rejected as a function of ρ is less than predicted. The trend of increasing heat rejection with reduced O/F is consistent with the T film, ρ^* equation and the definition of ρ^* ; at lower O/F and higher c^* , ρ^* decreases and T film increase. The effect of chamber pressure is consistent with theory showing an increase of Q with $(P_c)^{0.8}$. The polar plot of Figure IV-14 suggests reasonably uniform circumferential heat rejection.

Measurement of fuel temperature after flow through the baffle and in the fuel vortex film manifold provided average Q/A for the baffles and the passages to the vortex manifold. The average Q/A for the baffle and the passages to the manifold agreed closely with predicted values.

Testing of the demonstration columbium chamber at altitude with the stainless steel injector was characterized by below goal c^* and non-uniform heat rejection as discussed in the following section. Injector modifications were evaluated to improve the heat rejection uniformity.

b. Aluminum Injector No. 1

The initial check firings of AL #1 showed performance improvement relative to the stainless steel injector; essentially the same c^* was obtained as a function of ρ but with an average water cooled nozzle heat flux reduction of 10%. Subsequent firings with a sea level columbium nozzle indicated that the goal c^* could be approached for insulated columbium operation of 2550°, 150° above the design temperature. The nozzle, barrel section and injector retained the characteristic length of 30 inches. The test set ups is shown in Figure IV-15. (The sea level columbium nozzle became available after the completion of the stainless steel injector check-out firings).

The firing data and observations from water flow testing lead to oxidizer manifold changes to improve the uniformity of triplet element impingement. Improvement was achieved but the impingement was still below standard. The injector was then designated AL #1 Mod. A.

Test data of AL #1 Mod. A with the sea level columbium nozzle is shown in Table II. The data indicated that the columbium chamber operating goals could be closely approached. The maximum "pyroscanner" temperature data will be described in the following section.

Bell Aerospace Company

Q_{nozzle} vs p
Test Cell D-4

Date: 2/22/73 to 3/2/73

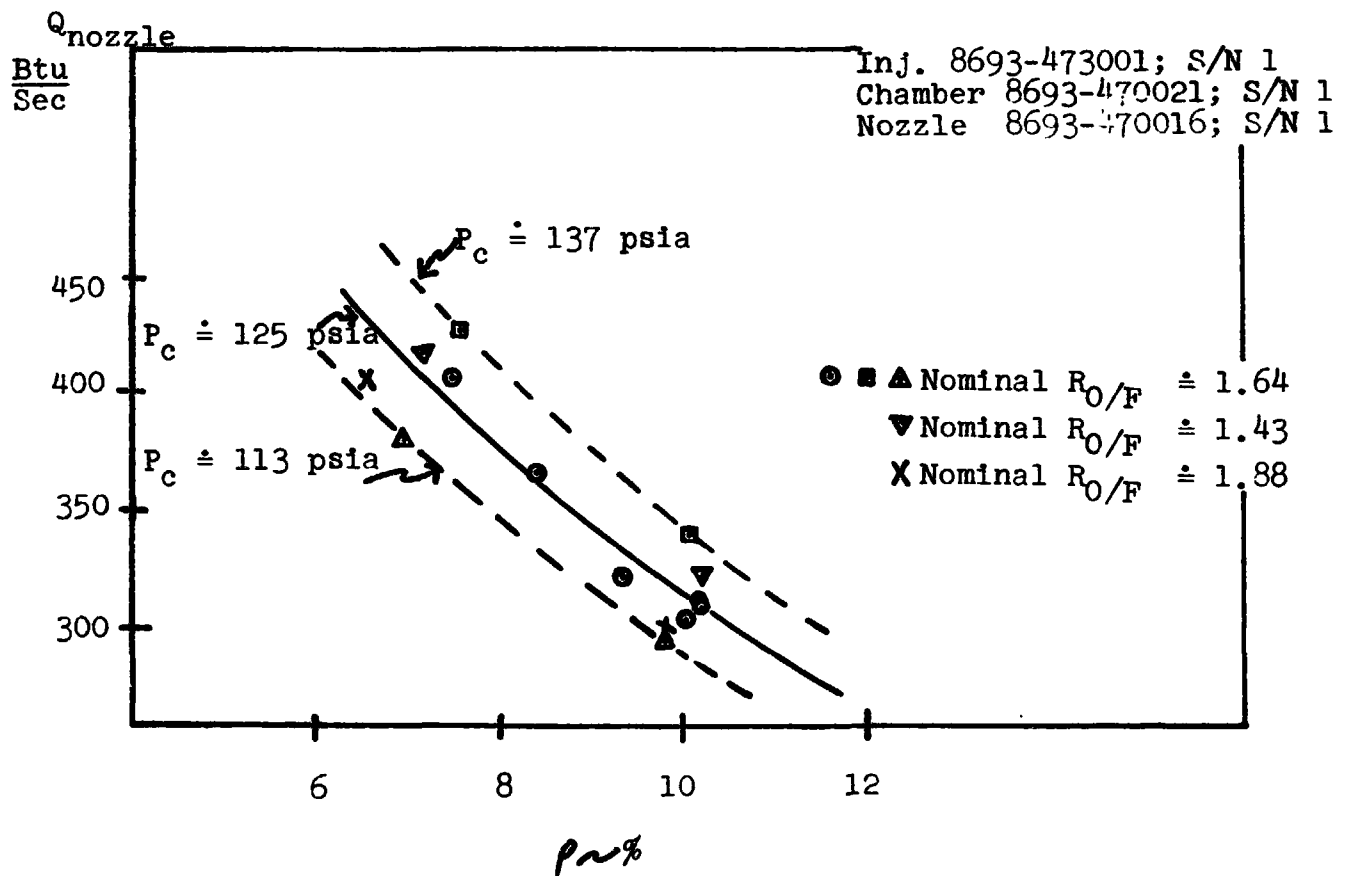
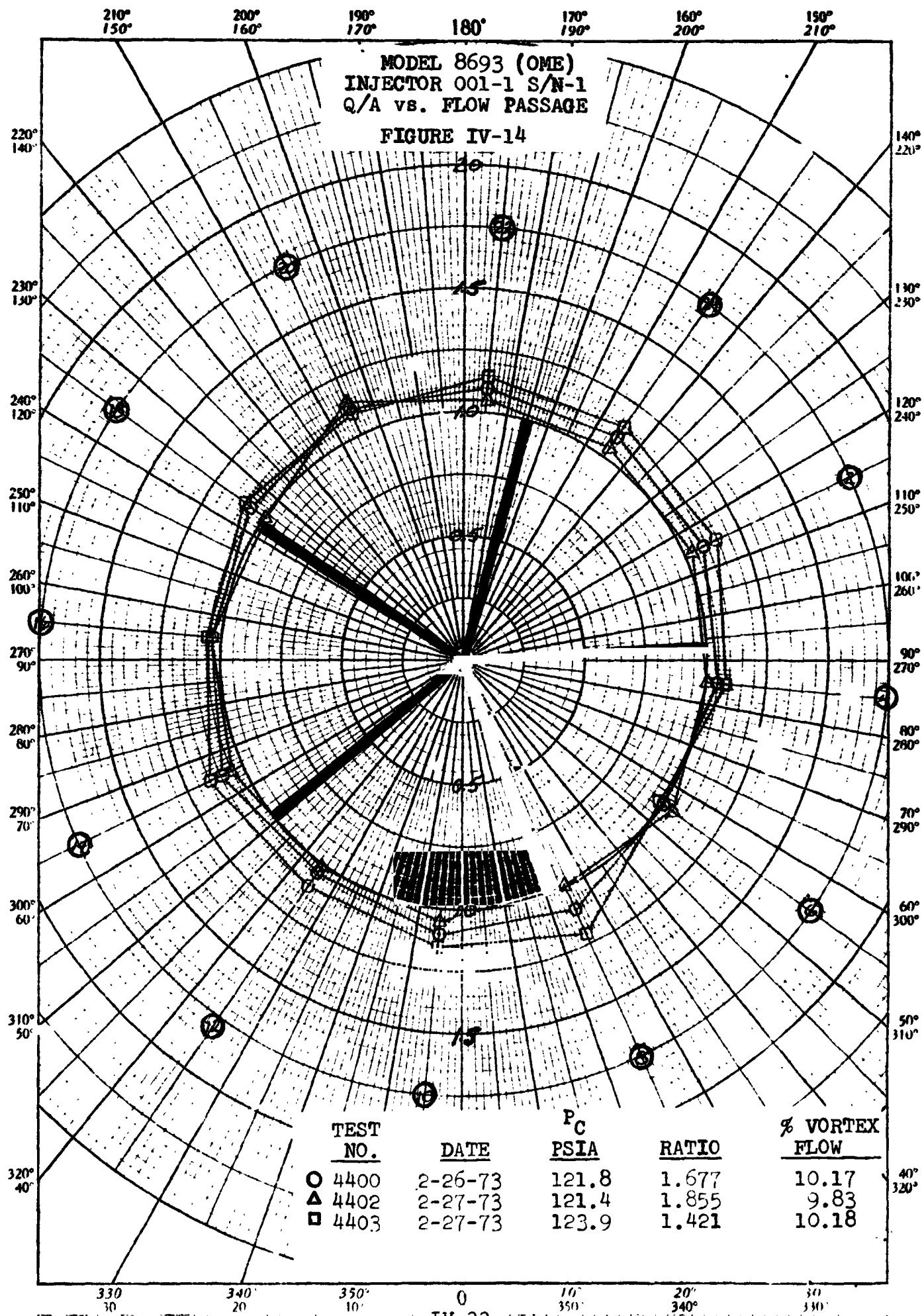


FIGURE IV-13



IV-23

ORIGINAL PAGE IS
OF POOR QUALITY

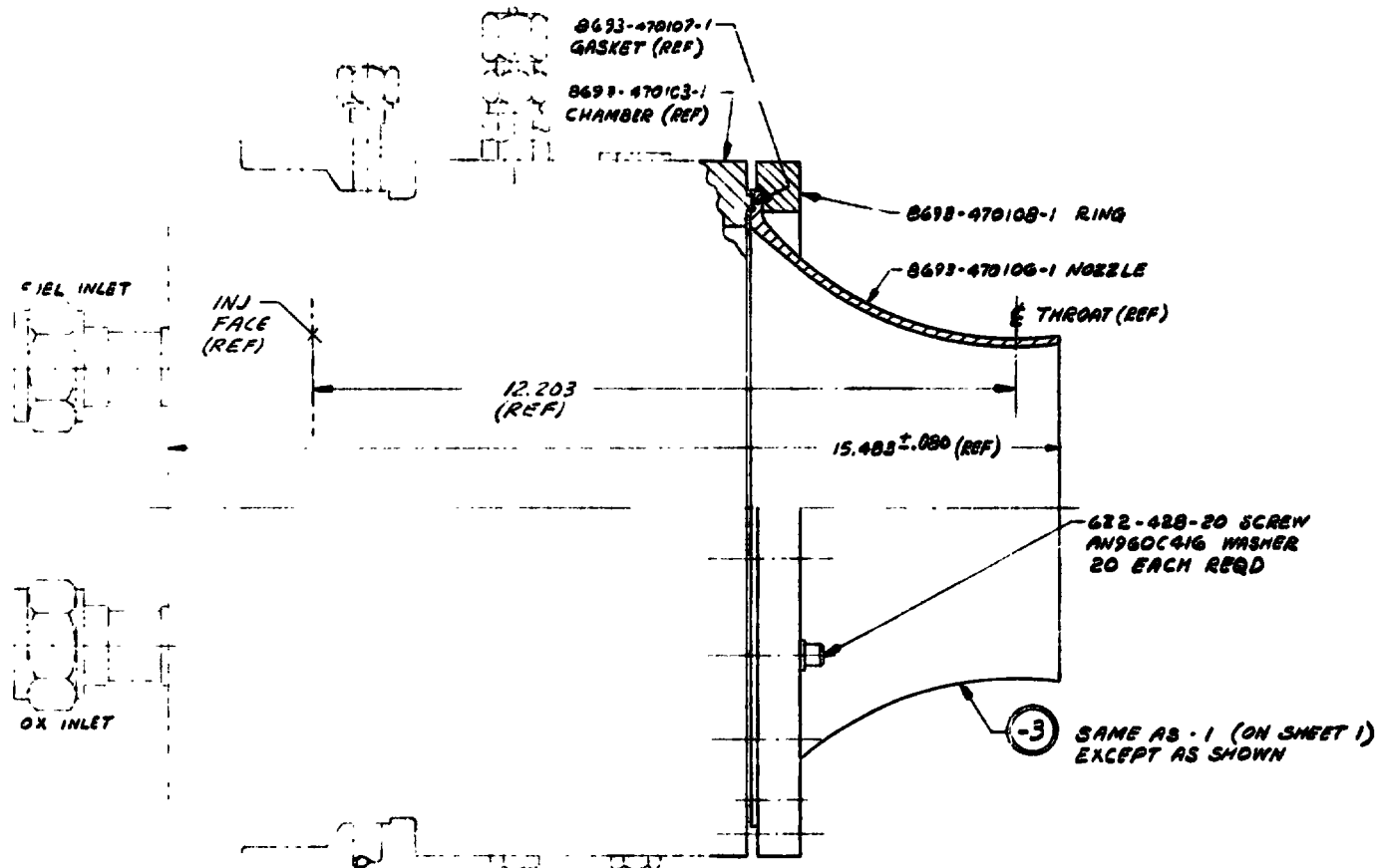


FIGURE IV-15

UNLESS OTHERWISE SPECIFIED DIMENSIONS ARE IN INCHES. TOLERANCES ON DECIMALS:				DESIGN & DRAWING 1-24-73		BELL AEROSPACE COMPANY	
.1	.11	.125	ANGLES:	GROUP		DIVISION OF TEXTRON INC.	
.13	.14	.15	± 0° 30'	APVD		POST OFFICE BOX ONE	
.16	.17	.18				BUFFALO, NEW YORK 14240	
.19	.20	.21		FILE		INJECTOR/VORTEX RING TEST ASSY-	
.22	.23	.24		UNLESS OTHERWISE SPECIFIED		10" OME WORKHORSE	
.25	.26	.27		BREAK EDGES .015 MAX RAD		SIZE	CODE IDENT NO
.28	.29	.30		OR CHAMFER		B	80070
.31	.32	.33		MACHINED SURFACES		8693-470109	
.34	.35	.36		EXCEPT AS NOTED		SCALE	1/2
.37	.38	.39				DEVELOPMENT	SH 2

ALUMINUM INJECTOR NO. 2

SEA LEVEL TEST DATA

TABLE II

CHECKOUT FIRINGS INJECTOR AL #1 MOD A

Test No.	Duration Sec.	P _c PSIA	O/F	%	C* Ft/Sec	T _{Max.} Pyro °F
4439	10	120	1.64	9.23	5439	2253
4440	8	124	1.59	8.49	5463	2325
4441	15	123	1.61	8.52	5476	2308
4442	15	122	1.62	8.49	5479	2204
4443	30	124	1.53	7.80	5523	2280

Goal 5500 C* @ T_{max} pyroscanner = 2300°F

Bell Aerospace Company

c. Aluminum Injector No. 2

The lack of desired triplet element impingement exhibited by AL #1 Mod. A was corrected with AL #2. Inlet manifolding was changed as described in the preceding section. The sea level test data from the unit is presented in Table III. More uniform pyroscanner temperatures were obtained than with A #1 Mod. A as shown by the agreement between the pyroscanner at 9:00 o'clock (S/N 5) and the pyroscanner at 3:00 o'clock (S/N 2). The characteristic velocity is essentially equal to that of AL #1 Mod. A. An improvement of c^* had been anticipated based on the improved injector impingement. A third pyroscanner was installed for test 4491 as a check on pyroscanner repeatability. The T_{max} from 10:00 o'clock agreed with that at 9:00 o'clock within 4°F or 0.2%.

4. Chamber Demonstration Tests, Task V

a. Test Facility

The altitude simulation system employed for the thrust chamber demonstration tests is located at the Bell Test Center. The facility is identified as LBN (Figure IV-16). The LBN facility was constructed for the development of the LM Ascent engine for the Apollo program and was later modified and used for the Space Shuttle APS reverse flow engine program (Contract NAS 3-14353). The altitude simulation system includes a 9 1/2 feet diameter by 24 feet long chamber (Figure IV-17) a water cooled diffuser duct, a water spray chamber, a six feet diameter vacuum isolation valve, a steam generator and a two stage non-condensing steam ejector. A mechanical vacuum pump is connected to this system for initial pumping down and calibrations prior to firing. The steam source for the ejector system is a gas generator which burns 19.3 pounds/second of alcohol, and 34.6 pounds/second of liquid oxygen which is quenched with 102 pounds/second of water to produce approximately 160 pounds/second of steam and CO_2 at 300 psig.

The LBN ejector sub-system included a center body diffuser just downstream of the engine exit to maintain a cell pressure of 90,000 feet equivalent altitude while hot firing the 3400 pound thrust LM Ascent engine for a duration of 600 seconds. The thermal load imposed by that engine exhaust was cooled to 1000°F in the water spray chamber by injecting water directly in the exhaust gas stream.

Thermal expansion of the ejector system is achieved by permitting all components to roll on tracked casters. Provision is also made to retract the entire system approximately two feet by a hydraulic cylinder to facilitate service on the test stand inside the altitude chamber.

TABLE III
CHECKOUT TESTS INJECTOR AL #2

TEST NO.	DURATION SECONDS	P _C PSIA	O/F	<i>P</i> %	C* FT/SEC.	PYROSCANNER	
						S/N 5	S/N 2
4491	10.5	125.8	1.58	7.77	5478	2284*	2183
4492	14.9	121.4	1.65	7.97	5470	2308	2213
4493	15.5	122.9	1.61	7.49	5500	2345	2279
4494	15.6	127.2	1.51	8.15	5479	2300	2292
4495	15.3	128.9	1.44	7.27	5539	2386	2329
4496	15.6	119.4	1.81	7.97	5429	2198	2152
4497	15.4	124.0	1.44	7.68	5548	2279	2273
4498	30.4	121.8	1.68	7.81	5487	2278	2241

* 3rd Pyro at 10:00 - 2288°F

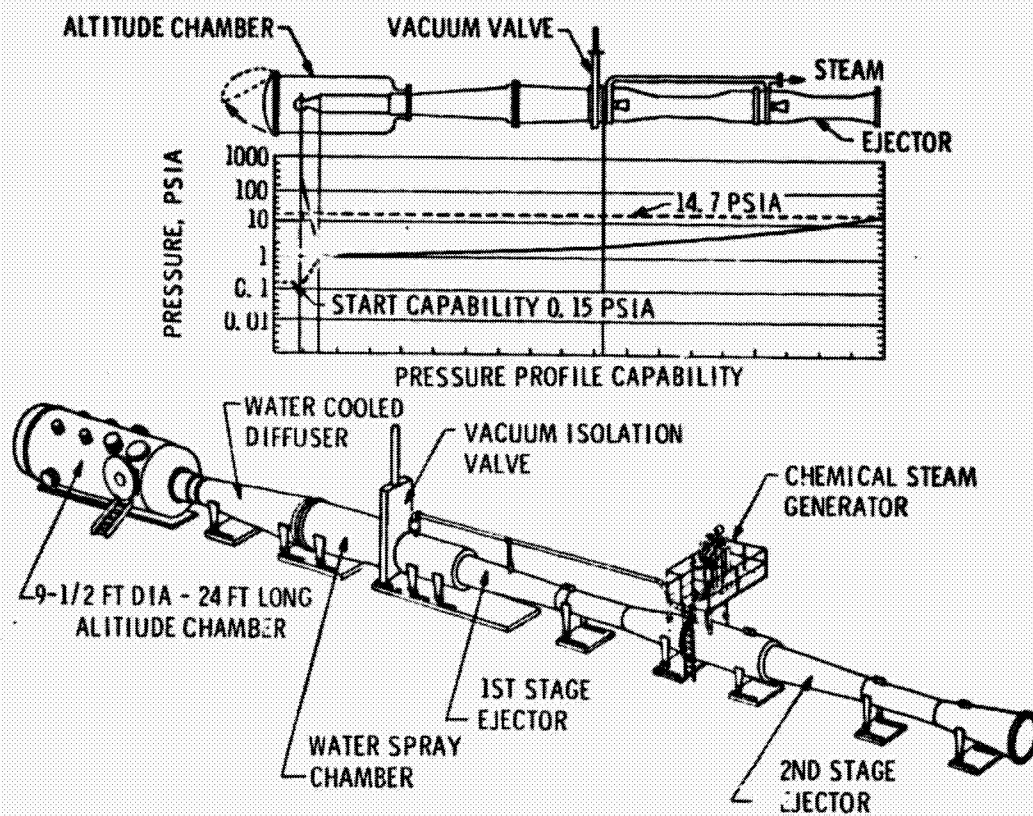


FIGURE IV-16. ALTITUDE FACILITY SCHEMATIC DIAGRAM

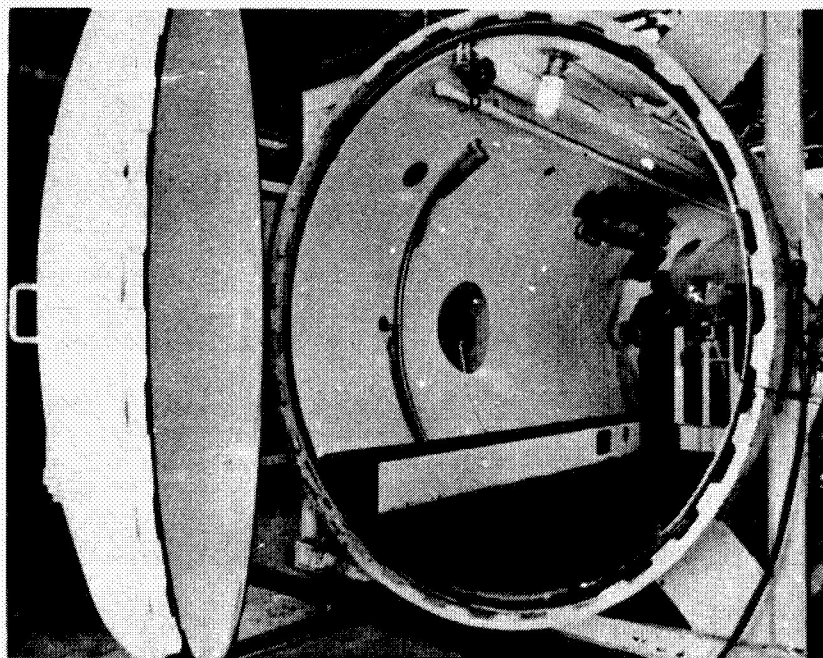


FIGURE IV-17. 1 BN ALTITUDE TEST CHAMBER

Bell Aerospace Company

The testing of the OME demonstration thrust chamber utilized the LBN facility with some modifications and additions. Since the centerbody diffuser was specifically designed for the LM engine it was used only as an interconnecting duct. A new cylindrical straight diffuser was designed, fabricated, and installed to assist in maintaining a vacuum pressure equivalent to approximately 100,000 ft. altitude. The O_2-H_2 plumbing from the NAS 3-14353 program was removed from the altitude chamber and the N_2O_4 and fuel lines were reinstalled. The thrust chamber assembly propellant feed system included a relatively closely coupled bipropellant valve assembly. The line lengths from valve outlet to injector inlet were approximately 3 feet long. The valve was an unmodified LM Ascent engine, series/parallel redundant assembly. The fuel feed line to the injector contained a branch line for the fuel vortex film cooling circuit. The film flow rate was adjusted by orifice. The vortex circuit volume was analyzed to provide essentially simultaneous injection of injector and film coolant flow at engine start. The oxidizer feed line from the bipropellant valve was designed for a nominal 60 ms. oxidizer lead.

The LBN facility included one channel of closed circuit television to monitor the thrust chamber assembly.

b. Instrumentation and Data Acquisition

(1) Instrumentation

Propellant feed pressures and chamber pressures were measured with Taber transducers, Model 226 or equivalent. The test cell ambient pressure was determined by 3 CEC strain gage transducers with a 0-2 psia range. Propellant flow rates were measured by redundant Fisher Porter turbine type flowmeters which were calibrated in place with water. Thrust measurement was obtained by a dual bridge Transducer Incorporated load cell mounted in a horizontal flexured thrust stand. The thrust monitoring installation included the capability for remote cell calibration at altitude with propellant feed pressure to the series/parallel redundant bipropellant valve. Platinum/Platinum-Rhodium thermocouples were used for columbium thrust chamber outside surface temperatures. Propellant feed temperatures employed Chromel/Alumel thermocouples. Columbium temperatures were also obtained for chamber operation without external insulation as described below.

Thermocouple thrust chamber skin temperatures were augmented by data measured by two optical brightness scanning pyrometers or pyroscanners stationed on both sides of the chamber. The instruments were jointly developed by Bell and the Instrument Development Laboratories of Attleboro, Massachusetts. Wall or

Bell Aerospace Company

skin temperatures in the range of 1,400°F to 4,000°F can be accurately measured. The device uses a unique image plane scanner - a rapidly moving endless belt containing small apertures in a geometric pattern. The light energy passes through the apertures and a monochromatic filter (653μ) to a photomultiplier. Synchronous pulses and internal calibration data are included in each "frame" of data. Each frame consists of 10 lines of scanned data and scan rates can be varied. Alternate frames or lines can be interlaced similar to a television raster. Typically, a field of interest 6 in. long by 3 in. high will have a spot resolution of 0.18 square inches. The sample field of interest is converted into a temperature matrix 90 x 40 at a frame rate of 15 pictures/second.

The data generated by the pyroscanner are recorded on the FM analog tape recorder system, played back into the High Speed Digital Acquisition System (Beckman), and digitized at an equivalent rate of 16,000 samples/second per channel. The data are then formatted by computer programs. Emissivity of the radiating body and calibration data are inputs to the computer program. Isotherms, time history plots and/or simple data/time tabulations may be obtained as outputs from the computer.

Calibration and alignment of the pyrometers are performed periodically. Pyroscanner calibration is traceable to NBS through NBS ribbon filament lamps manufactured by General Electric. Lamp brightness as a function of filament current is certified as $\pm 5^\circ\text{F}$ between 1900 and 2000°F and $\pm 12^\circ\text{F}$ at 3900°F. The accuracy of the pyroscanner is $\pm 50^\circ\text{F}$ (3σ, 90% UCL).

Pyroscanner printout data is presented in the following subsections.

2. Accelerometer Automatic Shutdown

Three Endevco Corp. Model 2273 accelerometers (range to 8 KHz) were used in conjunction with Kistler Model 504 electrostatic charge amplifiers to measure engine acceleration in three mutually perpendicular axes. The accelerometers were employed as the primary combustion monitor and were tied into the firing circuit to provide automatic shutdown in case of rough combustion. Normally, combustion pressure is monitored by a Kistler pressure transducer for automatic shutdown. However, the chamber opening for the Kistler pick-up would disturb the fuel vortex film on shutdown. The acceleration level which was immediate with no delay incorporated at the peak value.

3. Data Acquisition and Accuracy

The analog transducer signals are digitalized by Beckman systems and the digital data stored on magnetic tape. The digital tape

Bell Aerospace Company

data is presented in engineering units with selected derived parameters after processing by IBM 360 computers. Turbine type flowmeter cyclic data are digitized within the Beckman system and processed through the computers.

Provision was made for direct reading and oscillograph display of selected test parameters.

Table IV gives the frequency response and estimated overall data accuracy for the instrumentation and recording systems.

c. Test Results, Stainless Steel Injector

Twenty-one firing tests were carried out in the LBN facility with 30 inch c* columbium chamber and the stainless steel injector from 3/22 to 4/30/73. All firing tests provided usable data; each operation was characterized by acceptable stability, run and shutdown characteristics. There was no indication of low frequency or high frequency chamber pressure oscillations. The data is summarized in Table V. One of the run numbers allocated to the series of tests was used for LBN facility checkout and three runs were terminated before columbium chamber firing due to facility problems not associated with the test hardware.

Runs 790 through 813 of Table V were conducted without external insulation to assess maximum columbium temperature as a function of the percentage of fuel film coolant, chamber pressure and overall mixture ratio. The objective of the tests was the determination of the specific impulse which could be achieved with a maximum columbium chamber temperature of 2300°F. The 2300°F temperature, uninsulated, is equivalent to insulated chamber operation at 2400°F maximum. The insulated columbium chamber operation definition of 2400°F was established by the Task I and II studies. The last test, run 814, was carried out with external insulation.

The initial firing runs 790 and 791 indicated temperature variations in the throat region. Projections of the temperatures to steady state operation indicated unacceptable operation. The injector assembly was removed from the stand and water flow tested. The assembly of vortex ring and injector showed that part of the vortex was back flowing toward the injector face. The rotating back flow was stopped at each baffle leg resulting in a localized film flow buildup downstream of each leg. The back flow condition was not apparent in earlier water flow tests which were conducted on the ring and injector subassemblies. The localized buildup of film coolant was identified as contributing to the lack of throat temperature uniformity and lead to modification of the vortex "dam". The vortex cooling dam height (Figure IV-9) was reduced and the back flow was largely eliminated.

Bell Aerospace Company

TABLE IV

INSTRUMENTATION ACCURACY

	Digital Recorder		Oscillograph	
	Accuracy	Frequency Response	Accuracy	Frequency Response
1. Pressure Measurements	±0.5% F.S.	0-20 cps	±2.86% F.S.	Editor Only) 400 cps
2. Thrust	±0.7% F.S.	0-20 cps		60-70 cps
3. Flow Measurements (For water flow calibration)	±1.0% of Reading		±1.05%	200-300 cps
4. <u>Temperature</u>				
Chromel/Alumel Thermocouples	±0.4% of Reading		N/A	
Platinum/Platinum-Rhodium 10% Thermocouples	±0.25% of Reading		N/A	
Pyroscanner	±50°F		N/A	
<u>FM Tape</u>				
5. Accelerometers	Acceleration		Frequency Response	
	10%		0-5000 cps	

N/A - Not Applicable

F.S. - Full Scale

TABLE V
ONE DATA SUMMARY OF ALTITUDE TESTS

Test IBN	Duration (1) Seconds	P _c corr Psia	R _{O/F} O-A	ϵ	C* corr Ft/Sec	η_{c*} %	I_{sp}^{co} $\epsilon=75/1$ lbf-sec lbm	C _f $\epsilon=75/1$	Thermocouple T _{max} °F	Pyro T _{max}	Remarks
790	2.5	116.3	1.569	9.5	5357	93.9	303.0	1.81	894	--	
791	2.5	122.5	1.635	10.3	5312	93.0	303.1	1.836	779	--	
793	2.5	121.7	1.632	10.0	5327	93.3	300.1	1.812	793	--	Vortex Ring Modified between Runs 791 and 793
795	3.5	120.9	1.608	10.1	5338	93.5	300.9	1.814	1219	--	
796	4.4	121.4	1.612	10.1	5338	93.5	301.0	1.814	1486	--	
797	7.2	122.4	1.632	10.0	5341	93.5	301.1	1.814	1854	2084	
798	Facility Malfunction										
799	60.4	121.5	1.634	10.0	5356	93.8	Lost Thrust		2034	2222	
800	30.2	122.1	1.634	10.0	5353	93.7	302.7	1.819	1969	2077	
801	30.3	124.3	1.375	11.1	5379	95.3	301.5	1.801	1701	1976	
802	30.1	111.9	1.587	9.2	5401	94.7	302.6	1.803	1827	2225	
803	Facility Malfunction										
804	10.9	123.4	1.638	9.1	5397	94.6			2148	2323	SD on Max Temp (2300°F)
805	30.2	120.2	1.582	9.3	5378	94.3			2271	2200	Injector modified. New thrust load cell.
806	30.2	122.3	1.315	10.4	5393	96.1	Thrust Data Not Available		2151	2062	
807	29.9	118.7	1.737	8.7	5315	93.1			2136	2248	
808	30.3	123.2	1.515	8.7	5412	95.0	302.2	1.796	2234	2264	
809	4.7	125.6	1.317	9.5	5405	96.3	301.0	1.792	1564	1731	SD by Error
810	30.4	122.3	1.597	8.1	5407	94.7	302.5	1.800	2107	2278	
811	6.1	123.4	1.562	7.7	5434	95.2	303.7	1.798	1930	2300+	SD on Max Temp (2300°F)
812	30.1	123.5	1.591	7.9	5420	95.0	304.1	1.805	2260	2359	
813	29.9	123.7	1.726	7.5	5386	94.3	302.9	1.809	2162	2378	
814	30.1	122.7	1.650	7.7	5402	94.6	304.7	1.815	2253		Chamber Insulated

(1) P_c Correction Factor 0.981

ORIGINAL PAGE IS
OF POOR QUALITY

IV-32

Bell Aerospace Company

Fire testing was continued with increased duration firings approaching thermal equilibrium of the chamber (Runs 793 through 797). Firings of 30 and 60 second duration followed including operation at low O/F and low P_c . Attempts to reduce the vortex film coolant down to 9% to raise I_{sp} were not successful; run 803 was terminated at a run time of 10.9 seconds because the maximum columbium temperature had exceeded 2300°F. The lack of circumferential temperature uniformity in the throat region was evident throughout the tests. Pyroscanner data for runs 799 and 804 Figures IV-18, IV-19 and IV-20 indicate over 400°F circumferential variation at the throat plane. The higher temperatures were approximately inline with the center of each of the 5 injector sectors. Thermocouple data confirmed the temperatures as will be discussed in the following subsection. The lack of temperature uniformity and the higher than predicted film coolant flow limited I_{sp} (corrected to infinite altitude and an area ratio of 75:1) to approximately 302 seconds.

The stainless steel injector was modified between runs 804 and 805 to attempt to improve the temperature uniformity at the throat. Two oxidizer orifices were plugged in each of the 5 sectors near the sector centerline.

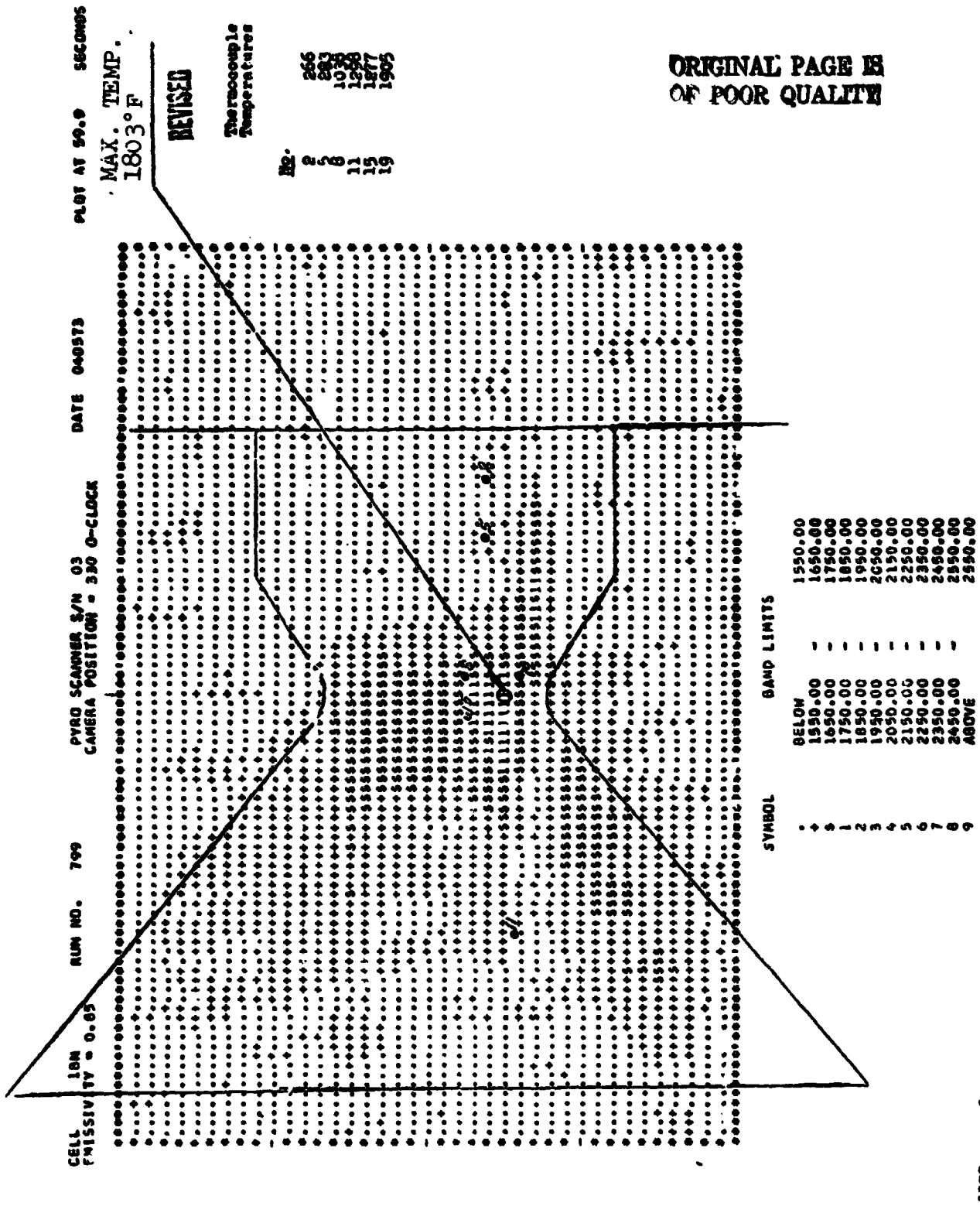
The modification was based on the original "pressure map" of the injector, and the apparent need to reduce the combustion gas generation on the sector centerline. The modification could also be made in a short period of time. While the plugging of the orifices was anticipated to improve the throat temperature uniformity it was also recognized that that benefit would be accompanied by a reduction of the combustion efficiency of the remainder of the elements.

Tests 805 through 813 (Table V) evaluated operation with the modified stainless steel injector. Far more consistent temperatures were achieved allowing operation at reduced vortex film cooling.

d. Test Results, Aluminum Injector #1

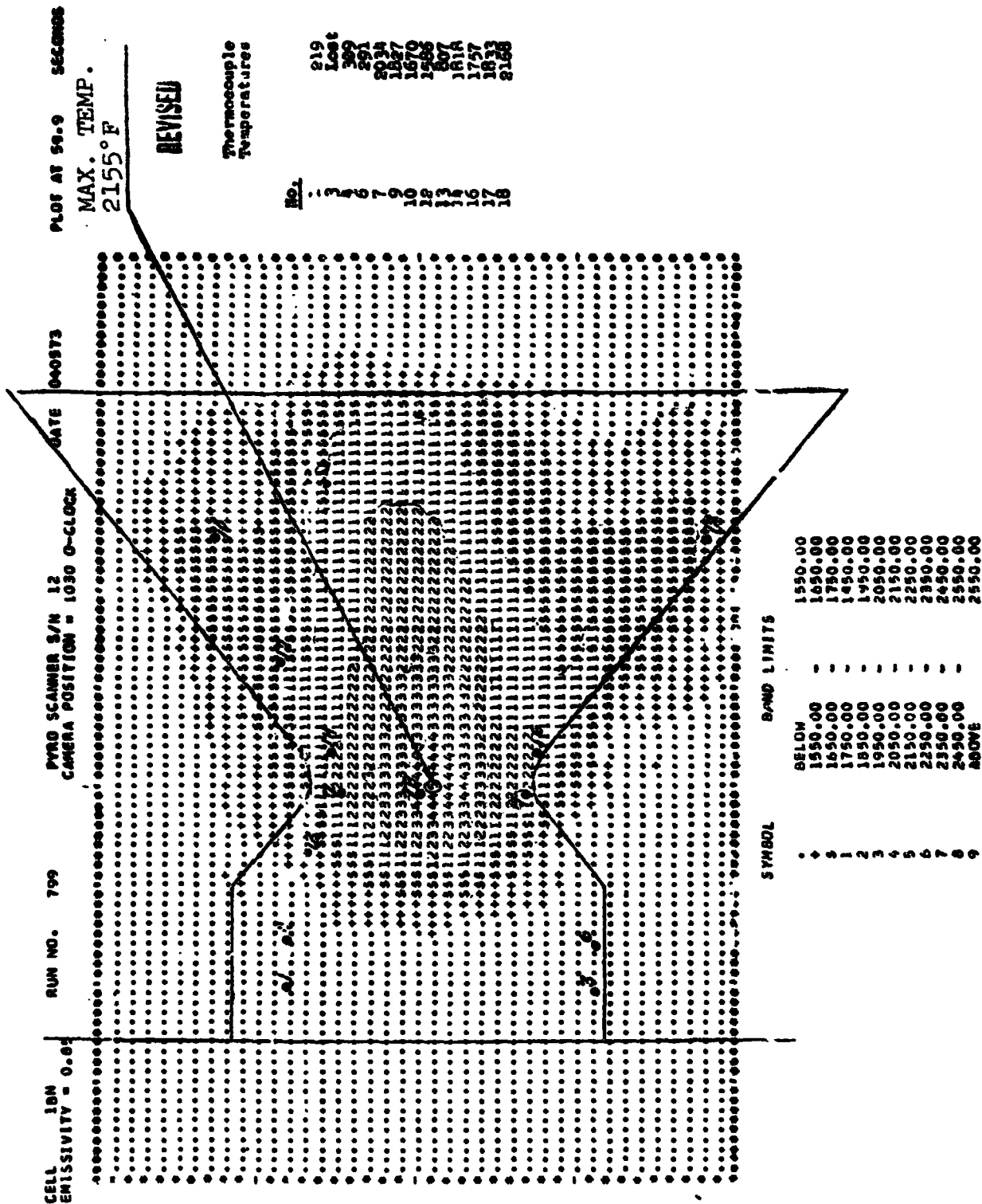
The next series of twenty-three tests were performed on the columbium chamber using the aluminum flat face injector. The features of this injector system were the builtin acoustic combustion stability dampers, and a fuel vortex film coolant ring.

Majority of the tests were of 20 seconds duration with the chamber radiation cooled. Two tests were of longer duration, 30 and 60 seconds, and with the chamber insulated. During the uninsulated testing the chamber wall temperatures were measured by pyroscanner while the wall temperatures were measured with thermocouples only during the insulated chamber tests. Satisfactory test results were obtained during the insulated tests, including



ORIGINAL PAGE IS
OF POOR QUALITY

FIGURE IV-18



CELL 1BN RUN NO. 804 PYRO SCANNER S/N 12 DATE 041073 PLOT AT 10.4 SECONDS
MAX. TEMP.
2323°F

PYRO S/N 3 LOST

Thermocouple
Temperatures

No. 1 2 3 4 5 6 7 8 9 10 11 12 13 14 15 16 17 18

257
264
282
289
Lost
1957
1173
1173
1082
906
102 Unreliat
1752
2148

ORIGINAL PAGE IS
OF POOR QUALITY



SYMBOL	BAND LIMITS
•	BELOW 1550.00
+	1550.00 - 1650.00
1	1650.00 - 1750.00
2	1750.00 - 1850.00
3	1850.00 - 1950.00
4	1950.00 - 2050.00
5	2050.00 - 2150.00
6	2150.00 - 2250.00
7	2250.00 - 2350.00
8	2350.00 - 2450.00
9	2450.00 - 2550.00
	ABOVE 2550.00

FIGURE IV-20

STOP
/6

Bell Aerospace Company

stable operation, acceptable start and shutdown transients, and an increase in performance over the stainless steel 5 leg baffle injector S/N 1 at approximately the same chamber wall temperature. A projected full area ratio nozzle performance of 310 seconds specific impulse was found to be representative for this injector in a columbium engine with a 75 to 1 area ratio nozzle. Improvements of local injector impingement anomalies were also considered to be an area for improvement. Where performance values for a similar, but improved manifold injector should exceed the 310 second Isp. The performance data obtained in this series are provided in Table VI.

Test Hardware

A Photograph of the thrust chamber assembly is shown in Figure IV-21. The 30 L* (8693-470006-1) columbium chamber is the same chamber previously tested with the stainless steel, 5 leg baffle injector. This chamber is fabricated from columbium C-103 material and coated with a silicide HiTemco 512E coating. The aluminum injector #1 mod A was fabricated from aluminum and utilizes triplet combustion elements. A removable stainless steel acoustic ring is used on the injector periphery to provide high frequency stability. This acoustic ring consists of twelve (12) acoustic slots (or cavities) with eight (8) slots designed for the third tangential/first radial mode. Further detail of this design is shown in Figure IV-22. The vortex ring is fabricated from stainless steel and is similar to the vortex ring used for testing the stainless steel injector S/N 1.

Test Results

The initial portion of this test series was conducted with the hardware uninsulated (Run Numbers 815 to 826) followed by two insulated tests (Run Numbers 827 and 828).

Results of these tests revealed achievement of the predicted 310 seconds specific impulse, but with wall temperatures at least 100°F above the desired level. Thermocouple temperature time histories are given for the 60 second duration insulated test in Figures IV-23 and IV-24. As listed in Table IX and shown in Figure IV-24 the maximum throat temperature measured was 2511°F, exceeding the goal of 2400°F. During the assembly of the hardware prior to this series a slight step was noted at the interface between the vortex ring and the chamber wall. Previous experience with both water flow and fire tests has shown that the vortex film can be affected by such a step. This is only true where the misalignment is an abrupt "step up" (flow must rise over a step). Interface discontinuities consisting of a "step down" (smaller diameter to larger diameter) have not appeared to cause any disturbance to the film flow characteristics. An effective temporary rework can be made by "filling"

ORIGINAL PAGE IS
OF POOR QUALITY

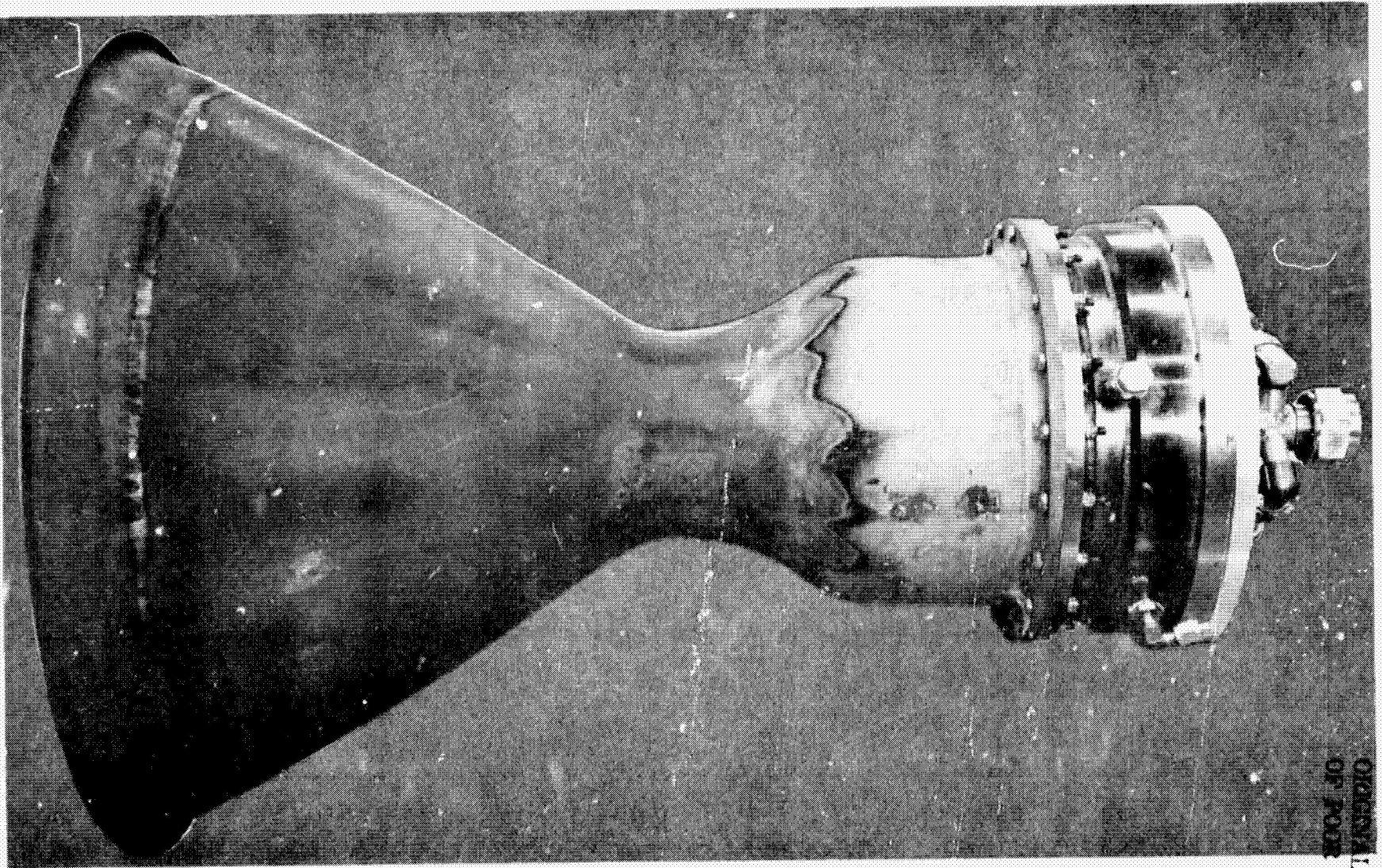


FIGURE IV-21. COLUMBIUM THRUST CHAMBER ASSY

TEST DATA SUMMARY - ALUMINUM No. 1 MOD A INJECTOR

TEST NO.	DURATION SEC	P _c PSIA	O/F	$\rho\%$	I _{sp∞} ε = 75:1	c* ① FT/SEC	C _f	T _{MAX} ② °F
816	20	123	1.56	7.9	311.1	5477	1.829	2469
817	20	121	1.57	7.9	310.9	5468	1.831	2377
818	20	122	1.70	7.6	310.4	5450	1.834	2427
819	20	124	1.59	8.0	310.2	5468	1.827	2389
820	20	125	1.33	8.8	308.4	5456	1.820	2357
821	20	123	1.79	7.4	309.9	5435	1.836	2449
822	20	126	1.57	8.0	310.2	5464	1.828	2434
823	20	136	1.77	7.5	310.5	5439	1.837	2416
824	20	112	1.42	8.5	308.2	5462	1.817	2224
825	20	114	1.78	7.5	309.1	5433	1.831	2554
826	20	136	1.45	8.4	310.7	5477	1.826	2505
INSULATED								
827	30	122	1.68	7.6	310.1	5460	1.829	2426 ③
828	60	122	1.67	7.5	312.3	5470	1.838	2511 ③

COMMENT: T_{MAX} HIGH, FILL IN STEP BETWEEN VORTEX RING AND CHAMBER WALL

NOTES: ① P_c INJECTOR X 0.981 CORRECTION
 ② PYROSCANNER MAXIMUM TEMPERATURE
 ③ THERMOCOUPLE

TABLE VI

Bell Aerospace DIVISION OF **textron**

TEST DATA SUMMARY - ALUMINUM No. 1 MOD A INJECTOR (CON'T)

TEST NO.	DURATION SEC	P _c PSIA	O/F	ρ %	I _{sp∞} ε = 75:1	c* ① FT/SEC	C _f	T _{MAX} F ②
829	20	111	1.42	8.5	307.4	5469	1.810	2175
830	20	137	1.47	8.5	310.0	5474	1.824	2172
831	20	112	1.66	7.8	308.9	5451	1.825	2302
832	20	134	1.65	7.9	309.9	5457	1.829	2257
833	20	122	1.68	7.8	309.6	5453	1.828	2291
835	20	114	1.76	7.5	308.7	5433	1.829	2434
836	20	136	1.75	7.6	310.1	5444	1.834	2356
837	20	135	1.49	8.4	310.1	5466	1.827	2271
838	20	123	1.77	7.5	309.4	5434	1.833	2396
839	20	124	1.45	8.5	308.9	5464	1.821	2223

NOTES: TEST 834 FACILITY MALFUNCTION

- ① P_c INJECTOR X 0.981 CORRECTION
- ② PYROSCANNER MAXIMUM TEMPERATURE
- ③ THERMOCOUPLE

TABLE VI

Bell Aerospace THE SIGN OF **textron**

ALUMINUM INJECTOR ASSEMBLY - DESIGN DATA

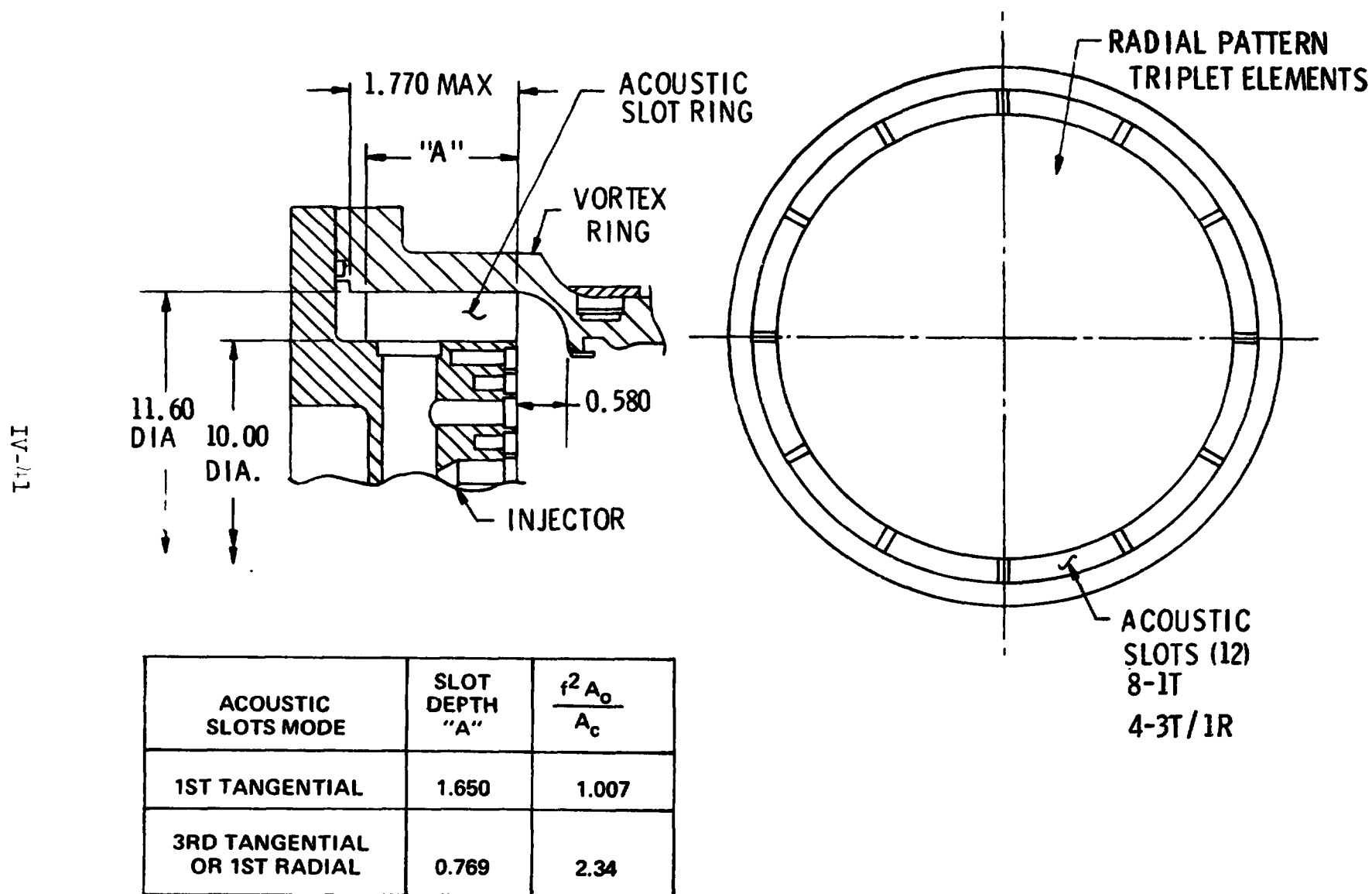


FIGURE IV-22

THERMOCOUPLE TEMPERATURE TIME HISTORY INSULATED TEST NO. 828 ALUMINUM INJECTOR NO. 1 MOD A

TEMPERATURE - °F

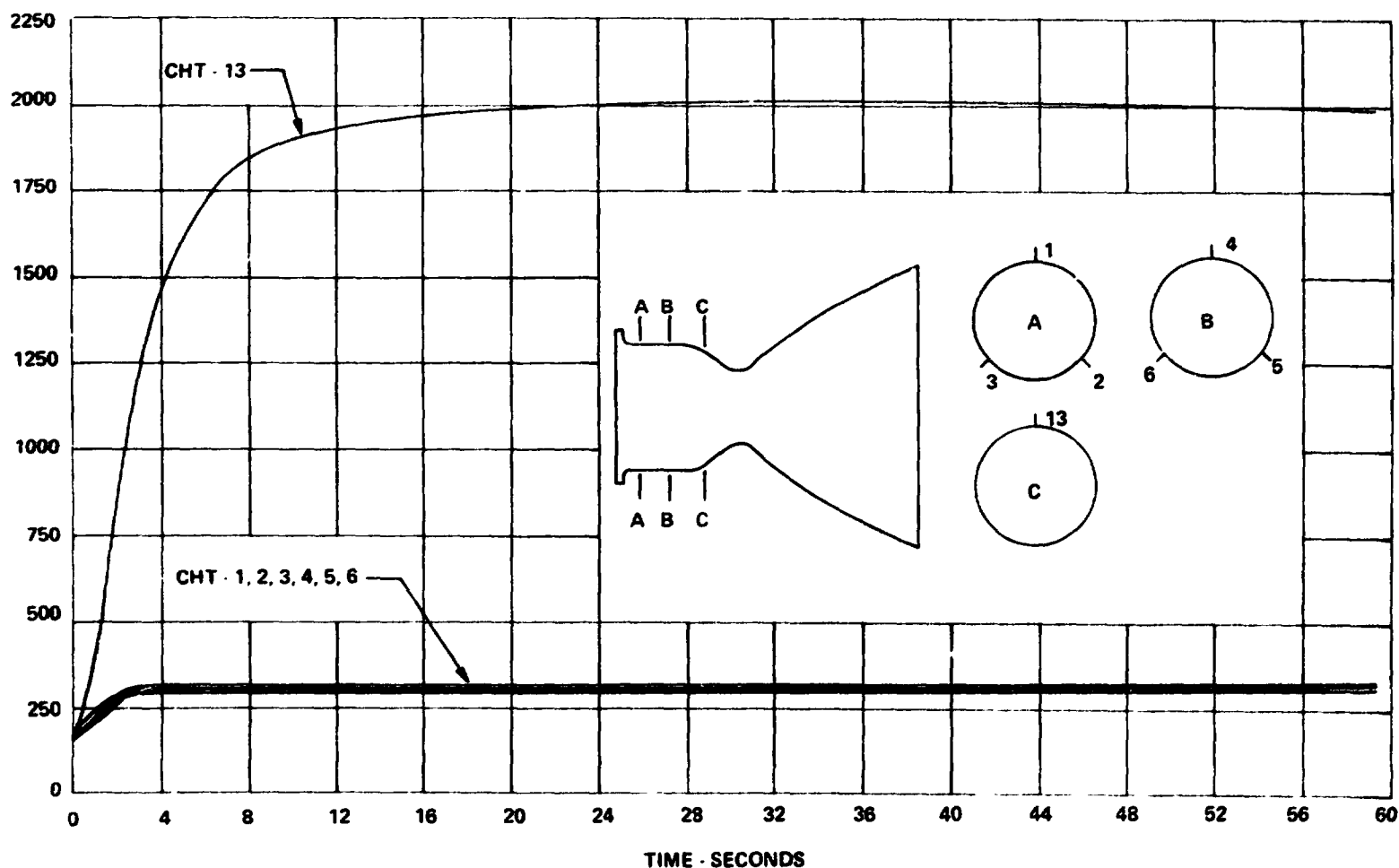


FIGURE IV-23

THERMOCOUPLE TEMPERATURE TIME HISTORY INSULATED TEST NO. 828 ALUMINUM INJECTOR NO. 1 MOD A

TEMPERATURE - °F

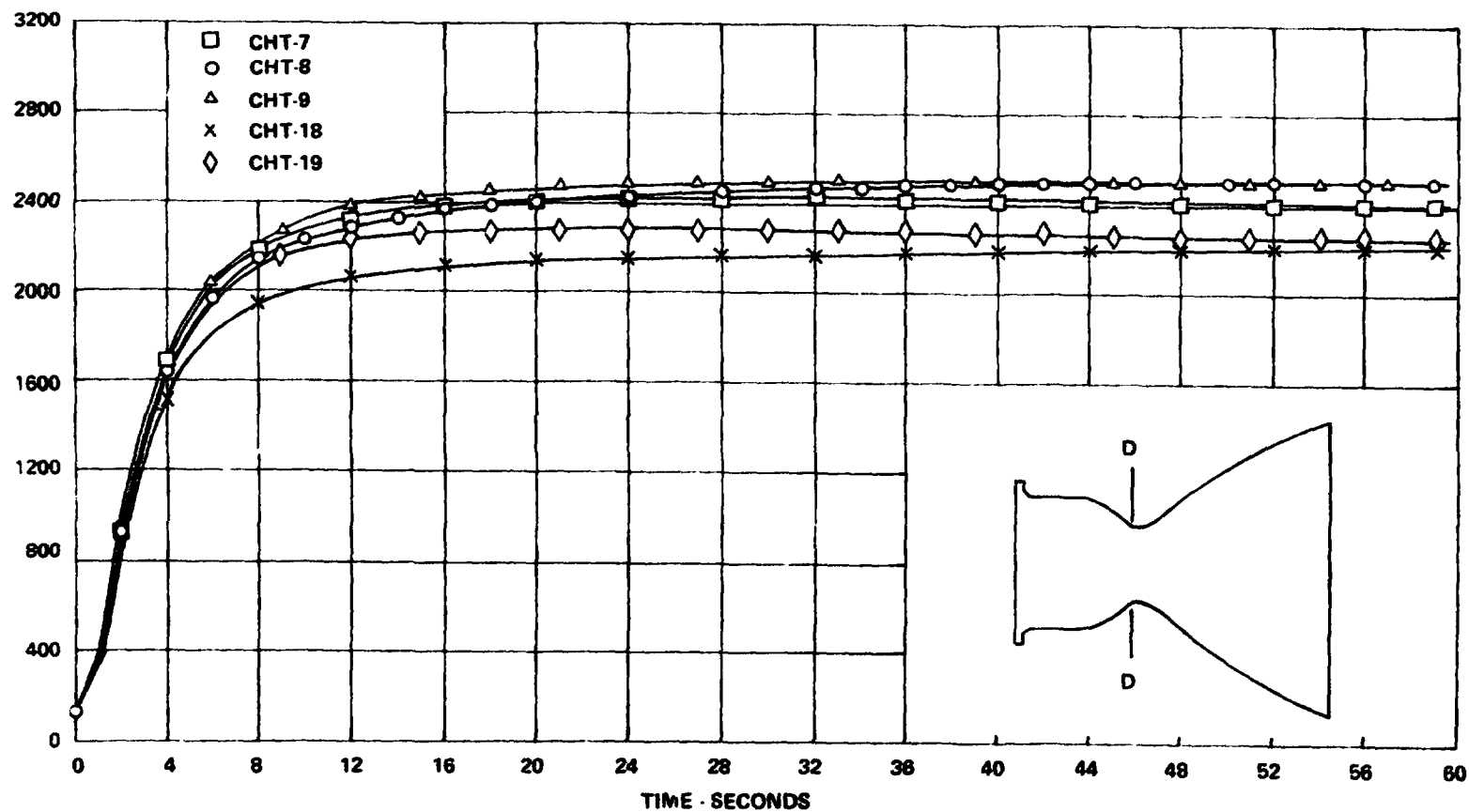


FIGURE IV-24

Bell Aerospace DIVISION OF **textron**

Bell Aerospace Company

the step with a high temperature ceramic cement producing a smooth flow surface for the film. This ceramic cement procedure was used on the chamber prior to run 829 to provide a smoother transition surface.

Following this rework additional tests were conducted in the radiation cooled condition (Run Numbers 829 to 839). The rework to smooth the chamber internal surface resulted in no performance variation (Figure IV-25), but maximum wall temperatures were reduced by more than 100°F , as given in Figure IV-26. The longitudinal temperature distribution was adjusted due to the smooth chamber wall for the 60 second insulated test using a predicted 2400°F gas temperature. A comparison of the actual temperature data obtained as tested with the "step up" condition versus the predicted insulated condition if the engine were tested with a smooth interface is provided in Figure IV-27. Note-the approximate 100°F reduction is effective from the convergent nozzle downstream.

Regression analyses were completed for these tests on the aluminum injector as listed in Figure IV-28. Low maximum residuals exist for c^* , C_F and maximum temperature (Pyroscanner). A plot of wall temperature versus overall (total) mixture ratio using the regression analysis equation is shown in Figure IV-29. A performance/temperature map utilizing the tests with the smooth chamber wall (Run Numbers 829 to 839) is provided in Figure IV-30. The predicted maximum wall temperature in the insulated condition versus the vortex cooling parameter is shown in Figure IV-31 same tests. This figure also shows the comparison to the data during (Task I and II) predicted value for heat rejection.

Data Comparison for Aluminum and Stainless Steel Injectors

A data comparison was made using the results of testing the unmodified and modified stainless steel injectors and the modified aluminum injector. A comparison of the representative uninsulated temperature data and performance is shown in Figure IV-32. The specific impulse displayed is again based on combustion efficiency and the performance expected from a 75 to 1 area ratio nozzle. Since the original unofficial performance objective of these tasks was to obtain 310 seconds specific impulse, it would appear this objective is not only feasible but should be obtained with reasonable development expenditures. The ability to obtain this performance is even more notable with considering, that the injector, can be improved by known design changes.

SPECIFIC IMPULSE ALUMINUM INJECTOR MOD A RUNS 816 - 839

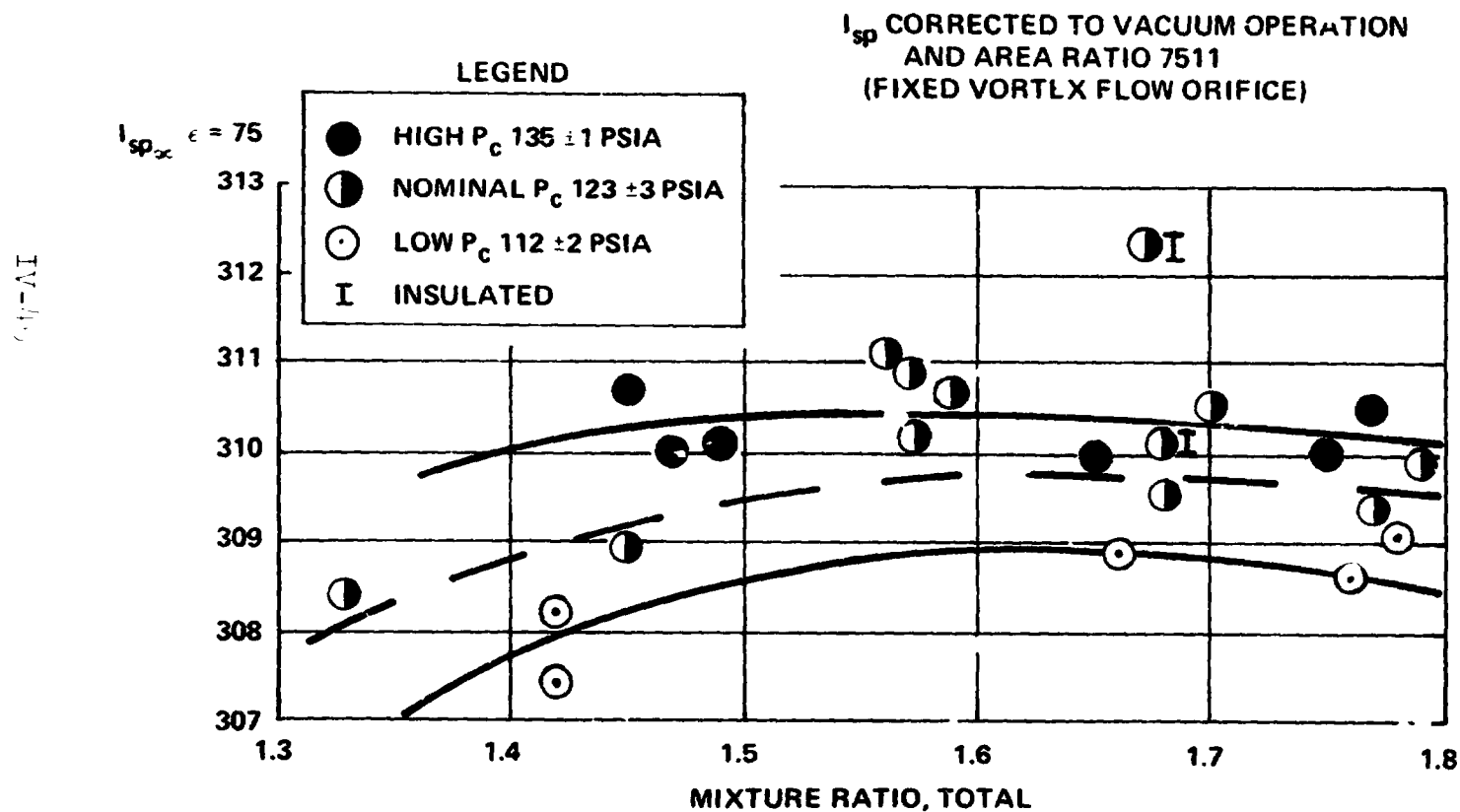
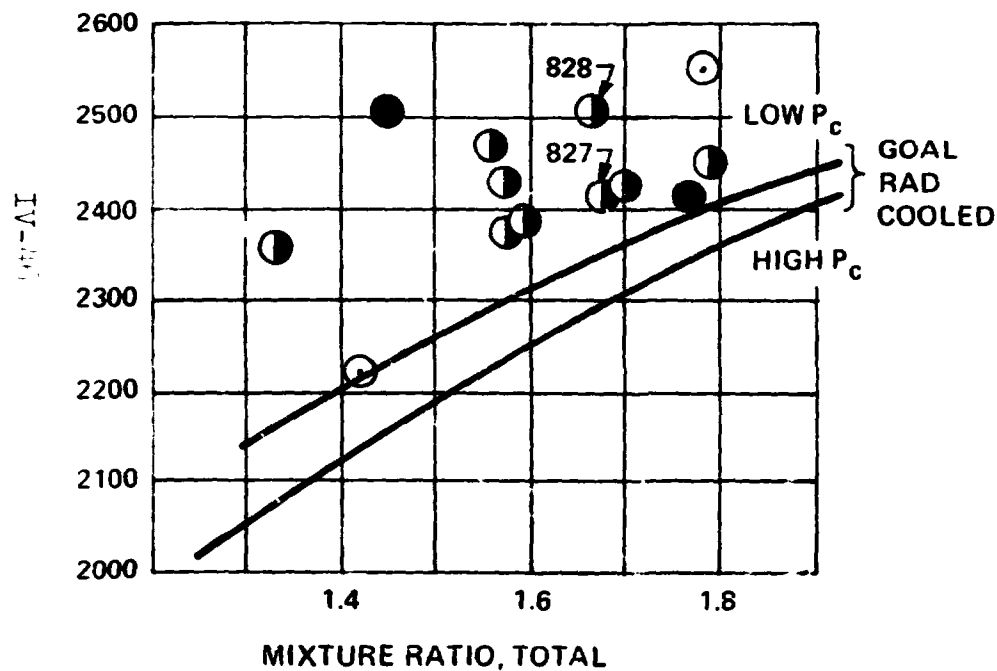


FIGURE IV-25

MAXIMUM TEMPERATURE ALUMINUM INJECTOR MOD A RUNS 816 - 839 (FIXED VORTEX FLOW ORIFICE)

(FIXED VORTEX FLOW ORIFICE)

RUNS 816 - 826 PYROSCANNER
827 and 828 INSULATED, THERMOCOUPLE



RUNS 829 - 839 PYROSCANNER
(STEP BETWEEN VORTEX RING
& CHAMBER WALL CORRECTED)

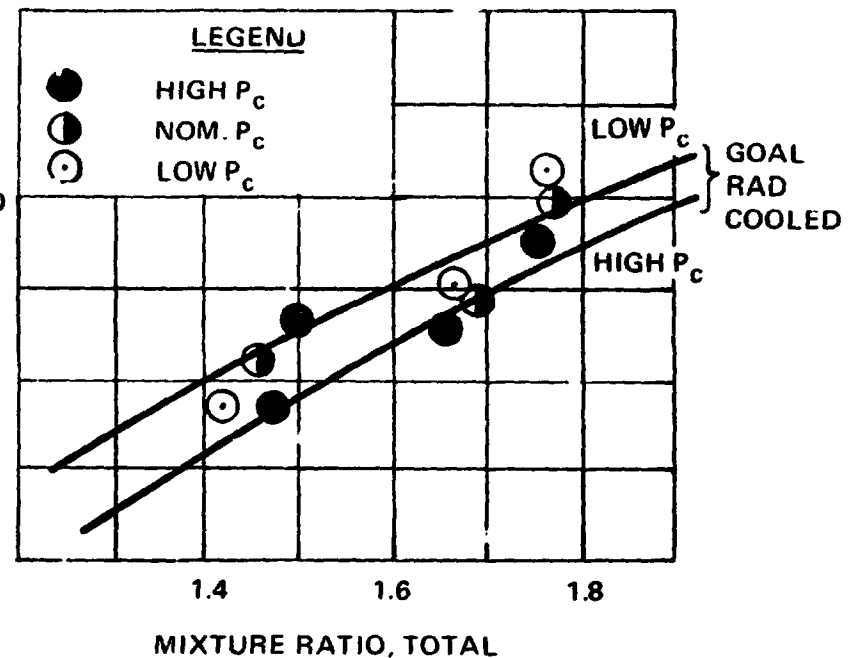
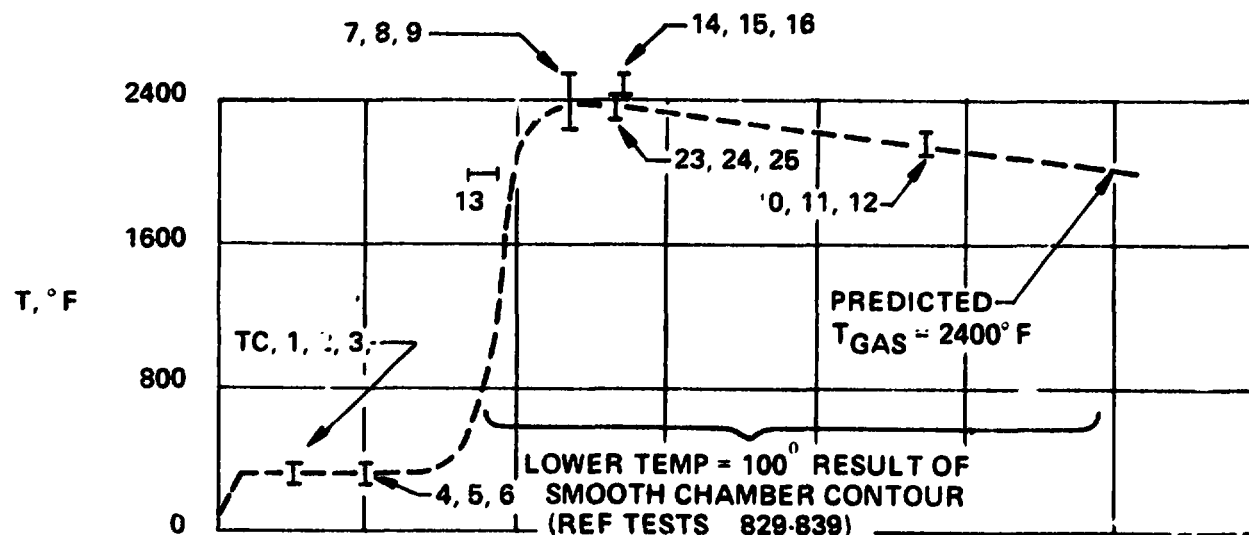


FIGURE IV-26

LONGITUDINAL TEMPERATURE DISTRIBUTION INSULATED TEST No. 828 60 SEC. DATA



MAXIMUM OUTSIDE BLANKET
TEMPERATURE $350^{\circ}F$

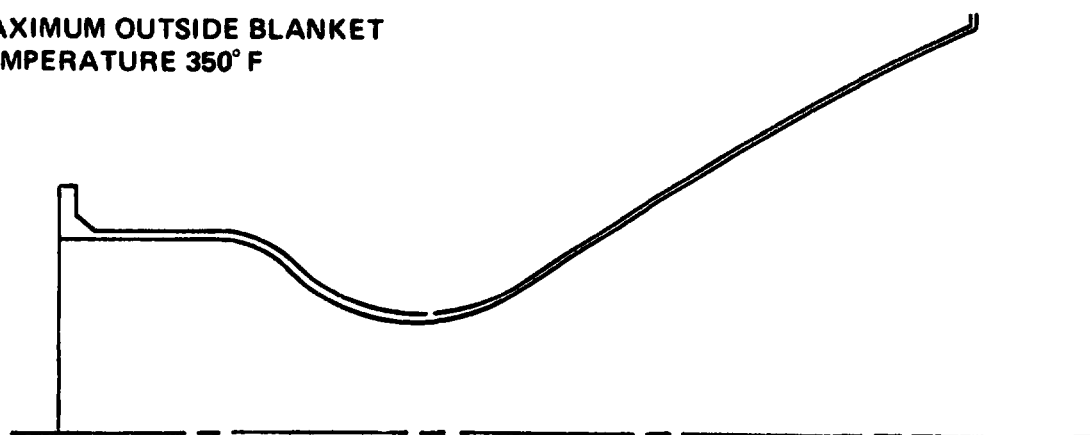


FIGURE V-7

Bell Aerospace DIVISION OF **textron**

DATA REGRESSION ANALYSES ALUMINUM INJECTOR MOD A

$$c^* \text{ (INJECTOR } P_c, \text{ CORE)} = 4919.7 + 0.23 P_c + 812.7 r_c - 230.5 r_c^2 - 2317.9 \rho \text{ (RUNS 816 - 839)}$$

$$\text{WHERE } r_c = \text{CORE O/F} = \frac{r_o}{1 - \rho - r_o \rho}$$

$$r_o = \text{TOTAL O/F}$$

$$\rho = \% \text{ VORTEX FLOW}$$

MAXIMUM RESIDUALS, + 21 FT/SEC

- 7 FT/SEC

$$C_{F_\infty} (\epsilon = 75.1) = 1.72606 + 0.03742 r_o + 0.00033 P_c \text{ (RUNS 816 - 839)}$$

$$\left. \begin{array}{l} \text{MAXIMUM RESIDUALS, + 0.0053} \\ - 0.0059 \end{array} \right\} \approx 0.3\%$$

$$T_{\text{MAX}} \text{ (PYROSCANNER)} = 3991.7 - 21445.8 \rho \text{ (RUNS 829 - 839)}$$

MAXIMUM RESIDUALS, + 57° F

- 47° F

FIGURE V-5

MAXIMUM WALL TEMPERATURE RADIATION COOLED AND INSULATED

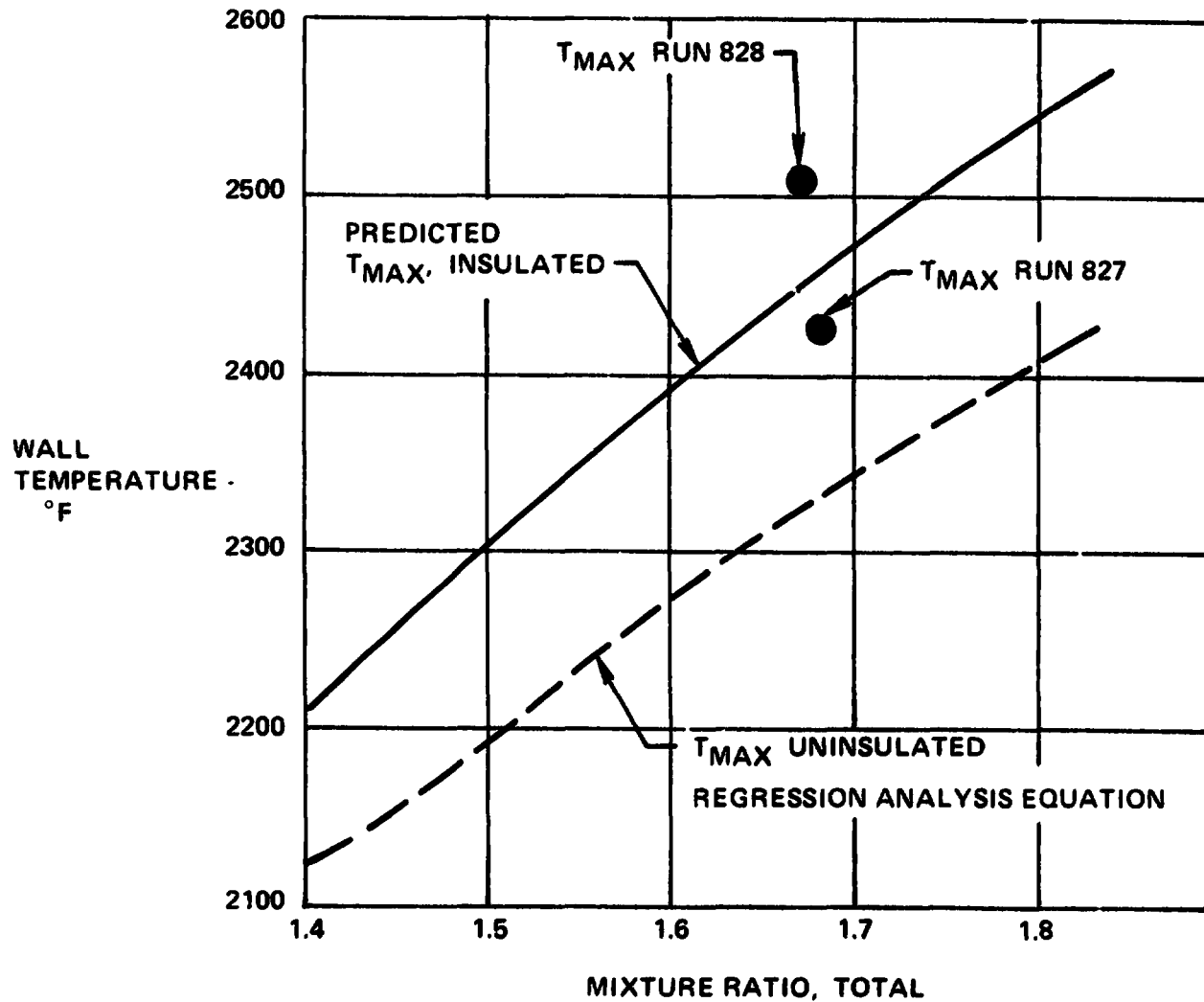


FIGURE IV-29

Bell Aerospace DIVISION OF **textron**

COLUMBIUM THRUST CHAMBER PERFORMANCE - TEMPERATURE MAP ALUMINUM INJECTOR TESTS 829 TO 839

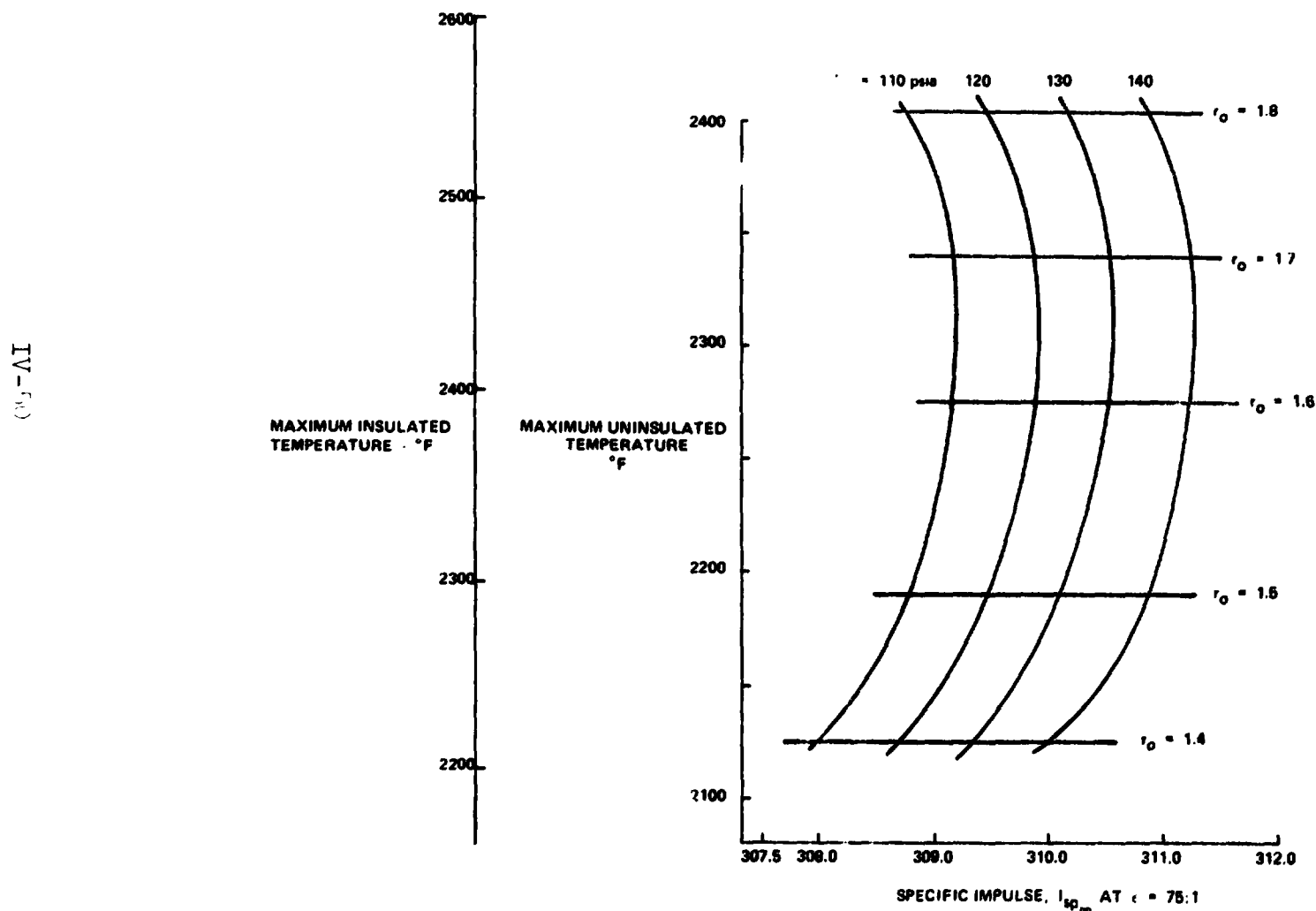
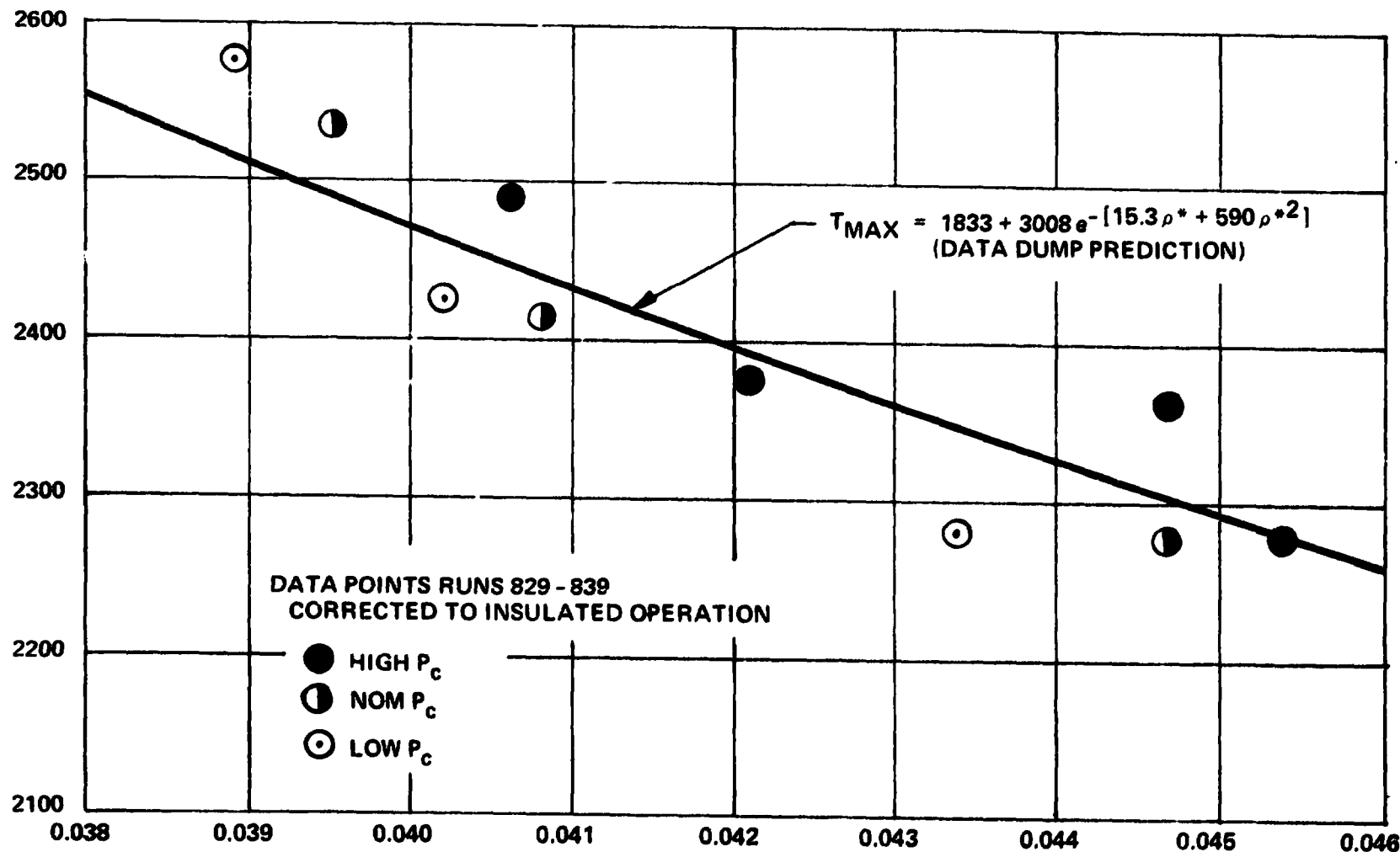


FIGURE V-6

PREDICTED T_{max} AND CORRECTED TEST DATA

T_{MAX} °F, INSULATED

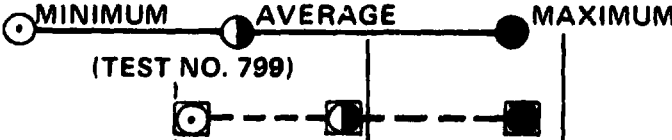
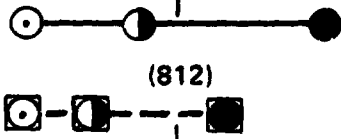
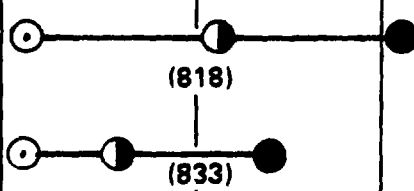


$$\rho^* = \frac{L}{D_c^{0.8}} \left(\frac{c^*}{P_c A_t} \right)^{0.2} ; \quad \begin{aligned} L &= 10.85 \text{ IN.} \\ D_c &= 10.00 \text{ IN.} \\ A_t &= 26.66 \text{ IN.}^2 \end{aligned}$$

FIGURE IV-31

Bell Aerospace DIVISION OF **textron**

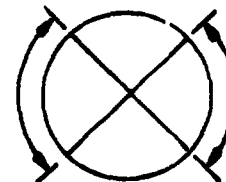
DEMONSTRATION TEST DATA SUMMARY

INJECTOR	REPRESENTATIVE UNINSULATED TEMPERATURE DATA					NOMINAL OPERATION	
	1600	1800	2000	2200	2400	ρ	I_{sp}^{∞} SEC $\epsilon = 75$
SS NO. 1						10.0	303
SS NO. 1 MOD A						7.7	305
AL NO. 1 MOD A						7.9	310



PYRO SCANNER

PYRO 2



PYRO 1



THERMOCOUPLE

FIGURE V-4

Bell Aerospace DIVISION OF **Textron**

Bell Aerospace Company

D. Demonstration Testing (Task VIII)

1. Chamber Demonstration Tests - Aluminum Injector #2

a. Test Results - Effect of L* and A50 Fuel

Testing to define the effect of L* on performance was accomplished after the availability of the second aluminum injector (See Task XI). Along with the L* (combustor length) evaluation, the effect on heat rejection of reducing the amount of vortex barrier, and the comparison of performance between MMH and A50 fuels were also tested with this injector. The method of obtaining these variables included the film coolant reduction by reducing the flow through the separate vortex manifold. The L* (combustor) variation was accomplished by using a shorter (alternate) columbium chamber for the 26 L* testing and a stainless chamber insert for the 34 L* testing. The A50 fuel tests were made so as to allow a direct comparison with MMH using both 34 and 30 L* chambers. The data accumulated during this testing is assembled in Table VII.

b. The Effect of Varying L* Using MMH Fuel

In order to establish the best estimate of engine performance as a function of the design and operating parameters, R_0 , ρ , L* and P_c , of the three L* configurations (26, 30 and 34), the performance data accumulated from all the tests, 841 through 869, on the columbium thrust chamber were subjected to statistical evaluation. Short duration firings were not considered and standard regression analysis techniques were employed.

Results indicated a linear trend in $I_{sp\infty}$ ($\epsilon=75:1$) with ρ , L* and P_c . The mixture ratio, R_0 , dependence was non-linear requiring higher order terms in the regression fit. The significance of each influence, including nonlinearities in parameters, was tested statistically.

All performance data were normalized to a ρ of 8% to provide a common reference for performance comparison of the three L* configurations. A plot of $I_{sp\infty n}$ with mixture ratio for the three L* configurations is shown in Figure IV-33. A high degree of consistency was achieved with maximum deviations between best fit and experimental results of less than $\pm 0.2\%$.

A comparison of maximum temperatures in the columbium chamber at 30 L* is also included as Figure IV-34.

TABLE VII
TEST DATA SUMMARY - ALUMINUM NO. 2 INJECTOR

TEST NO.	DURATION (SEC)	P _{corr} (PSIA)	O/F	ρ %	η_{C^*} %	I _{sp} _∞ ε=75:1	I _{sp} _{∞N} ε=75:1	C* (FT/SEC)	C _F	T _{MAX.} (°F)	L* (IN.)	PROPELLANTS
841	2.0	122.9	1.628	7.99	95.2	307.1	-	5437	1.819	NA	30	N ₂ O ₄ /MH
842	8.1	120.8	1.560	8.08	96.6	311.3	311.2	5509	1.820	2453	30	N ₂ O ₄ /MH
843	19.8	122.0	1.657	7.93	95.8	310.3	310.0	5471	1.827	2410	30	N ₂ O ₄ /MH
844	9.9	121.6	1.451	8.60	98.1	310.1	310.6	5513	1.811	2546	30	N ₂ O ₄ /MH
845	13.0	121.4	1.460	8.58	96.9	310.2	310.7	5503	1.815	2642	30	N ₂ O ₄ /MH
846	20.0	121.3	1.800	7.50	95.2	309.3	308.5	5428	1.835	2271	30	N ₂ O ₄ /MH
847	2.0	125.5	1.658	7.94	95.4	306.5	-	5452	1.810	NA	26	N ₂ O ₄ /MH
848	20.1	121.8	1.619	8.03	95.4	308.2	308.0	5447	1.822	1943	26	N ₂ O ₄ /MH
849	20.0	121.4	1.445	8.61	96.1	307.2	307.7	5455	1.814	NA	26	N ₂ O ₄ /MH
850	20.0	123.7	1.591	7.01	96.3	309.7	308.4	5499 ③	1.813 ③	2223	26	N ₂ O ₄ /MH
851	20.0	123.9	1.408	7.54	97.2	308.8	308.1	5504 ③	1.806 ③	2175	26	N ₂ O ₄ /MH
852	20.0	121.7	1.648	6.80	95.5	310.0	308.4	5457 ③	1.829 ③	2334	26	N ₂ O ₄ /MH
853	20.0	121.4	1.483	7.26	96.1	309.6	308.6	5465 ③	1.824 ③	2243	26	N ₂ O ₄ /MH
854	20.1	124.0	1.642	6.81	96.3	310.0	308.5	5498 ③	1.816 ③	2346	26	N ₂ O ₄ /MH
855	5.0	122.3	1.672	8.96	95.6	309.7	-	5461	1.826	1798	34	N ₂ O ₄ /MH
856	19.8	120.5	1.661	8.99	96.1	311.5	312.4	5488	1.828	2617	34	N ₂ O ₄ /MH
857	20.1	122.6	1.659	7.96	96.5	312.8	312.5	5515	1.827	2606	34	N ₂ O ₄ /MH
858	20.1	122.4	1.655	7.98	96.6	313.0	312.8	5517	1.827	2630	34	N ₂ O ₄ /MH
859	4.9	124.4	1.629	8.08	95.8	310.0	-	5485	1.820	1620	30	N ₂ O ₄ /A-50
860	20.0	121.8	1.635	8.02	95.9	310.5	310.6	5499	1.821	2268	30	N ₂ O ₄ /A-50
861	MALFUNCTION										30	N ₂ O ₄ /A-50
862	20.1	124.1	1.573	7.09	96.7	313.1	311.4	5540	1.820	2418	30	N ₂ O ₄ /A-50
863	19.8	122.7	1.628	6.82	96.4	312.5	310.3	5524	1.822	2466	30	N ₂ O ₄ /A-50
864	19.8	121.9	1.634	9.06	95.4	309.3	311.3	5463	1.823	2255	34	N ₂ O ₄ /A-50
865	MALFUNCTION										34	N ₂ O ₄ /A-50
866	20.0	123.3	1.589	8.17	96.0	312.9	313.2	5504	1.821	2451	34	N ₂ O ₄ /A-50
867	20.0	124.5	1.384	8.87	97.1	313.9	315.7	5543	1.823	2378	34	N ₂ O ₄ /A-50
868	19.7	122.4	1.617	6.96	96.8	313.5	312.1	5526	1.827	2530	34	N ₂ O ₄ /MH
869	20.1	122.0	1.686	6.67	96.7	313.8	312.1	5526	1.828	2543	34	N ₂ O ₄ /MH

- NOTES:
- ① P₀ injector x 0.981 correction
 - ② Pyroscanner maximum temperature
 - ③ Temperature for throat area based on pyroscanners
 - ④ Normalized to 2% ρ film cooling

IV-54
ORIGINAL PAGE IS
OF POOR QUALITY

Bell Aerospace Company

SPECIFIC IMPULSE VS MIXTURE RATIO ALUMINUM INJECTOR NO. 2-26L*, 30L*, 34L* CHAMBER RUNS 841-858, 868, 869

I_{SP} CORRECTED TO VACUUM OPERATION
AND AREA RATIO 75:1 AND NORMALIZED
TO 8% ρ FILM COOLING
 N_2O_4/MMH PROPELLANTS

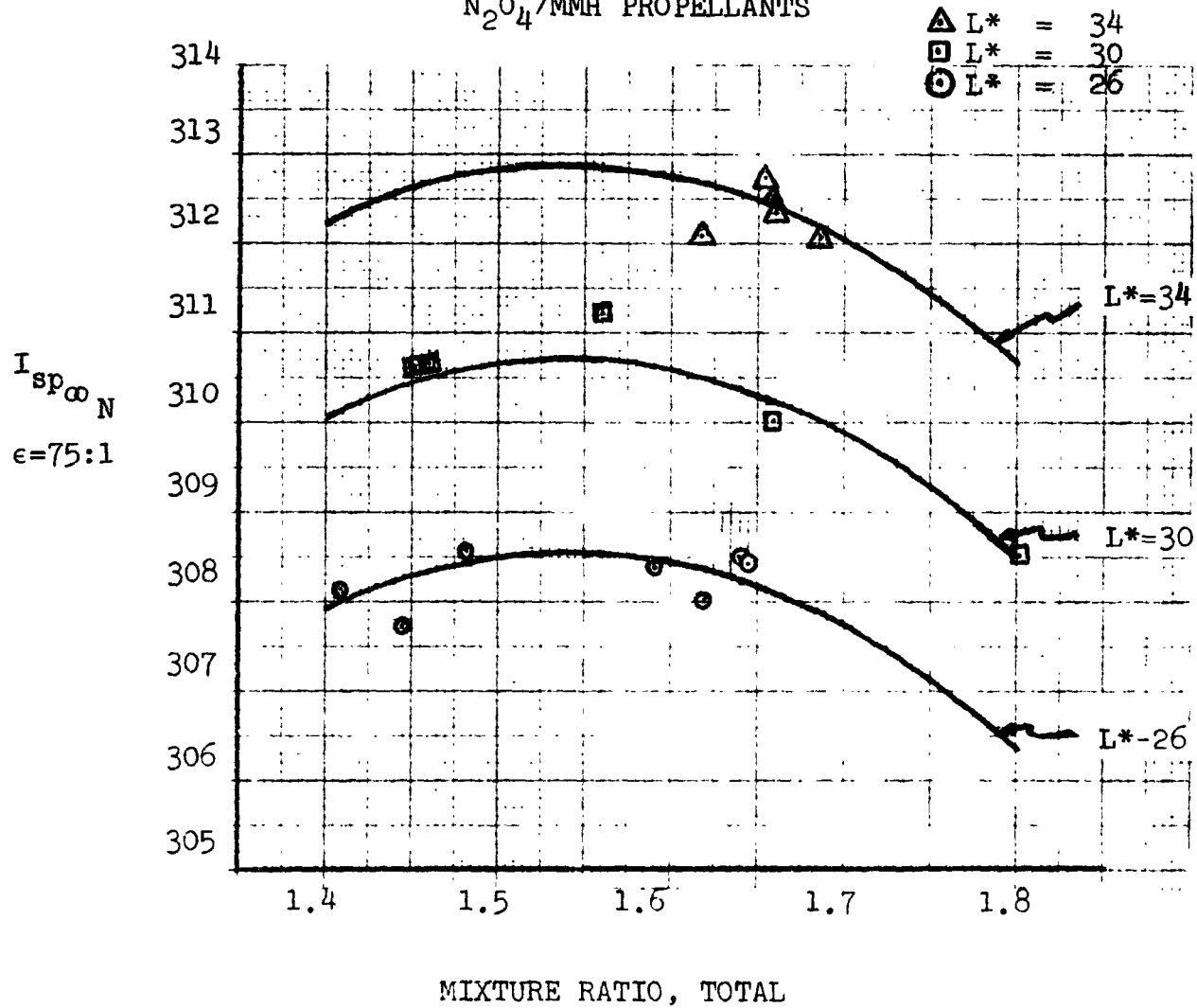


FIGURE V-8

Bell Aerospace Company

MAXIMUM PYROSCANNER TEMPERATURE

VS

MIXTURE RATIO

ALUMINUM INJECTOR NO. 2-30L* CHAMBER

RUNS 841-846

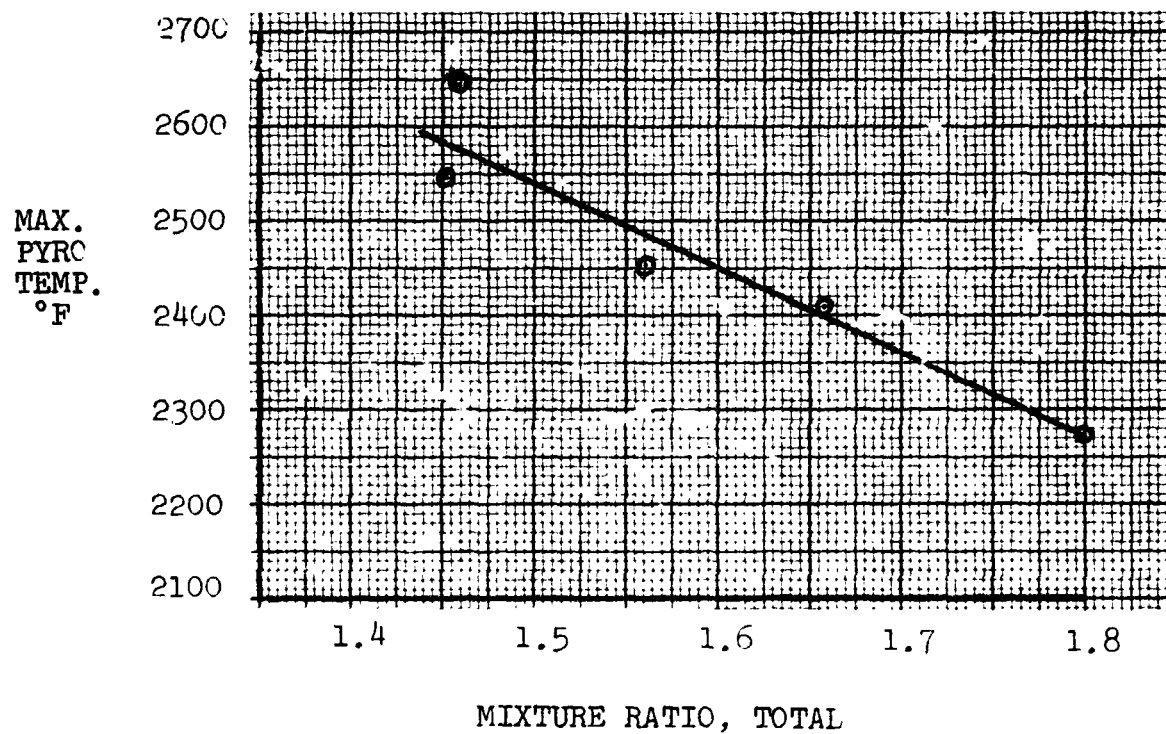


FIGURE V-9

Bell Aerospace Company

c. The Effect on Performance of Varying ρ

A series of tests were made varying ρ (film coolant percent of total propellants) at a constant 26 L*. These results are given graphically in Figure IV-35. The data presented approximates only two points and because of this scarcity of data, subsequent speculation related to design was not attempted. However, in the test region the results appear to produce a two second performance decrease, as a 1% increase in film coolant is injected.

d. Effect of ρ on Nozzle Temperatures

The data obtained with 34, 30 and 26 L* chambers relating the effect of changing the amount of film cooling (ρ) on the maximum chamber temperature is shown in Figures IV-36 and IV-37. The data plotted in both curves is as recorded although the shape of the curves shown in Figure IV-36 present some difficulty in interpretation and understanding. The 26 L* data appears straight forward and believable. However, the 30 L* and 34 L* data appear to be repressed in the expected effect of increasing the fuel flow.

The reason for this seeming reversal in effect of 30 and 34 L* fuel film effect has been examined both with respect to data accuracy and to possible causes. To date, it remains that the data accuracy is considered acceptable and the possible cause is unknown. The most reasonable explanation would appear that an "unknown" effect of mixing between the fuel film and the primary combustion was changing as the film coolant quantity changed and the resulting maximum temperature, at the throat, was as shown. Subsequent test data using the same instrumentation produced predicted results lending credence to the accuracy of the information.

A series of seven tests were conducted substituting A50 for the fuel. The objective of the tests was to provide data on the performance level and columbium chamber temperatures which would be expected of A50 were substituted for MMH as the fuel.

Tests 859 through 863 were performed with N₂O₄/A50 propellants in the 30 L* chamber, and tests 864 through 867 in the 34 L* chamber. The 30 L* tests covered ρ values from 6.82% to 8.02% and the 34 L* tests covered ρ values from 8.17% to 9.06%.

Performance in the 30 L* chamber was almost similar to that with N₂O₄/MMH propellants, specific impulse of 310 seconds versus 310.4 seconds, at rated ratio of 1.64.

These data were also subjected to statistical evaluation and normalized to a ρ of 8% to provide a direct comparison to the N₂O₄/MMH propellant data. A plot of $l_{sp_{\infty n}}$ with mixture ratio

Bell Aerospace Company

SPECIFIC IMPULSE VS MIXTURE RATIO ALUMINUM INJECTOR NO. 2 - 26L* CHAMBER

RUNS 847-854

I_{SP} CORRECTED TO VACUUM OPERATION
AND AREA RATIO 75:1

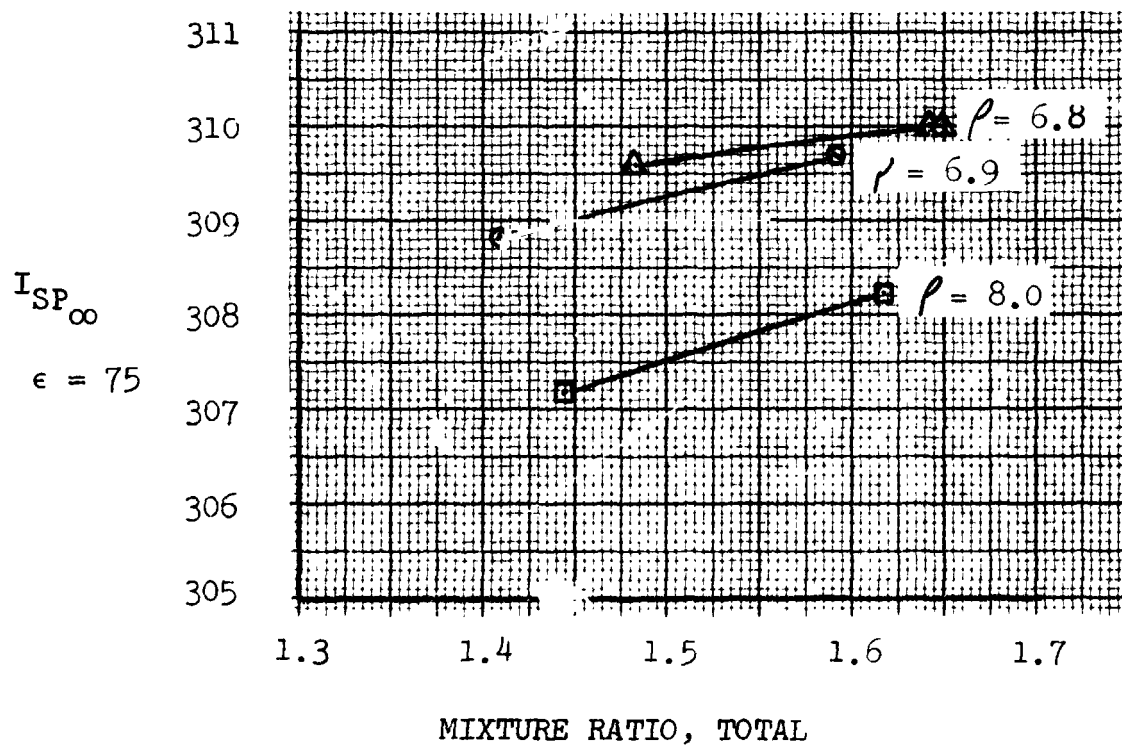


FIGURE V-10

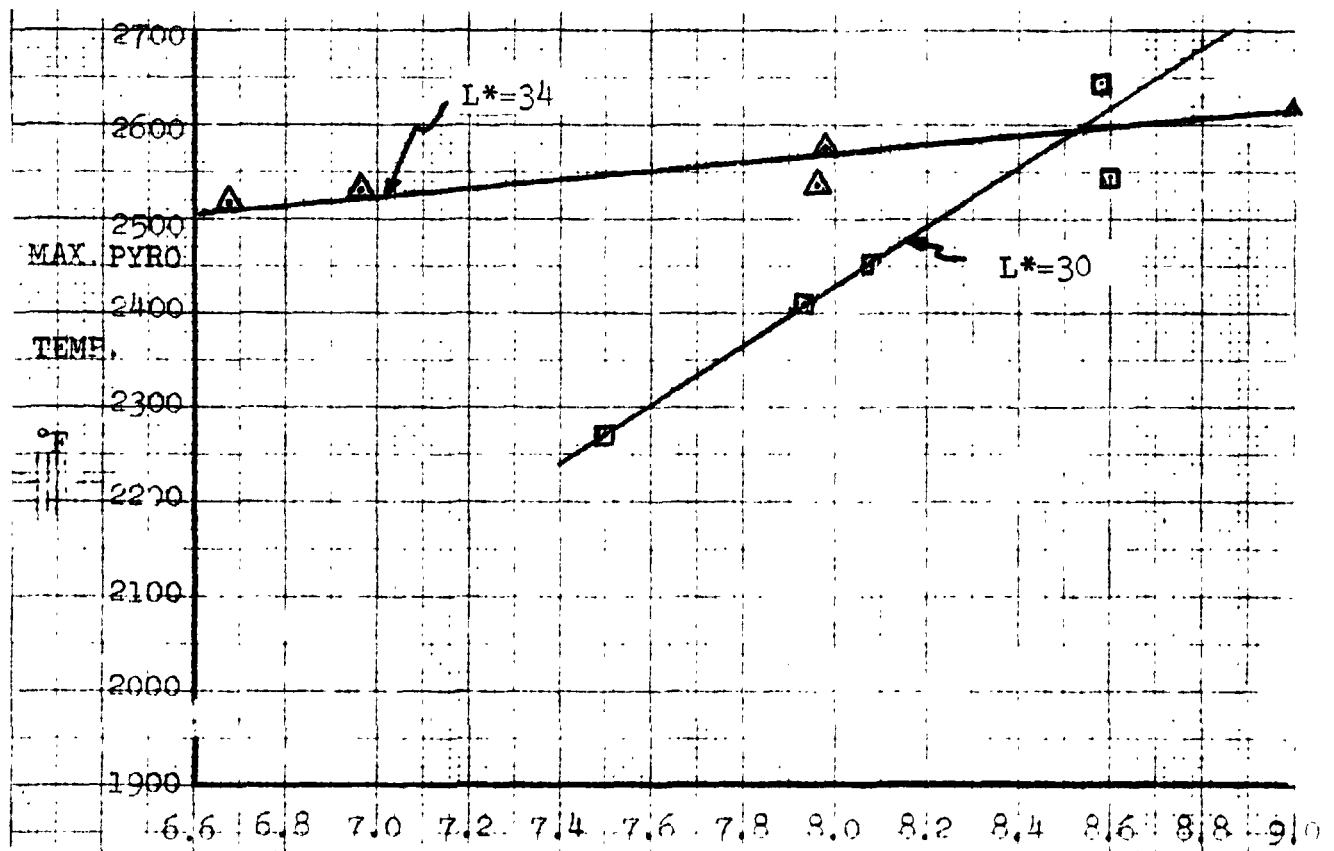
Bell Aerospace Company

MAXIMUM PYROSCANNER TEMPERATURE VS PERCENT VORTEX FLOW

ALUMINUM INJECTOR NO. 2 - 30L*, 34L*
RUNS 841-846, 855-858, 868, 869
N₂O₄/MMH PROPELLANTS

△ L* = 34

□ L* = 30



$\rho \%$

$\dot{V}_{w_f} / \dot{w}_t$

FIGURE V-11

Bell Aerospace Company

MAXIMUM PYROSCANNER TEMPERATURE

VS

PERCENT VORTEX FLOW

ALUMINUM INJECTOR NO. 2 - 26L* CHAMBER

RUNS 847-854

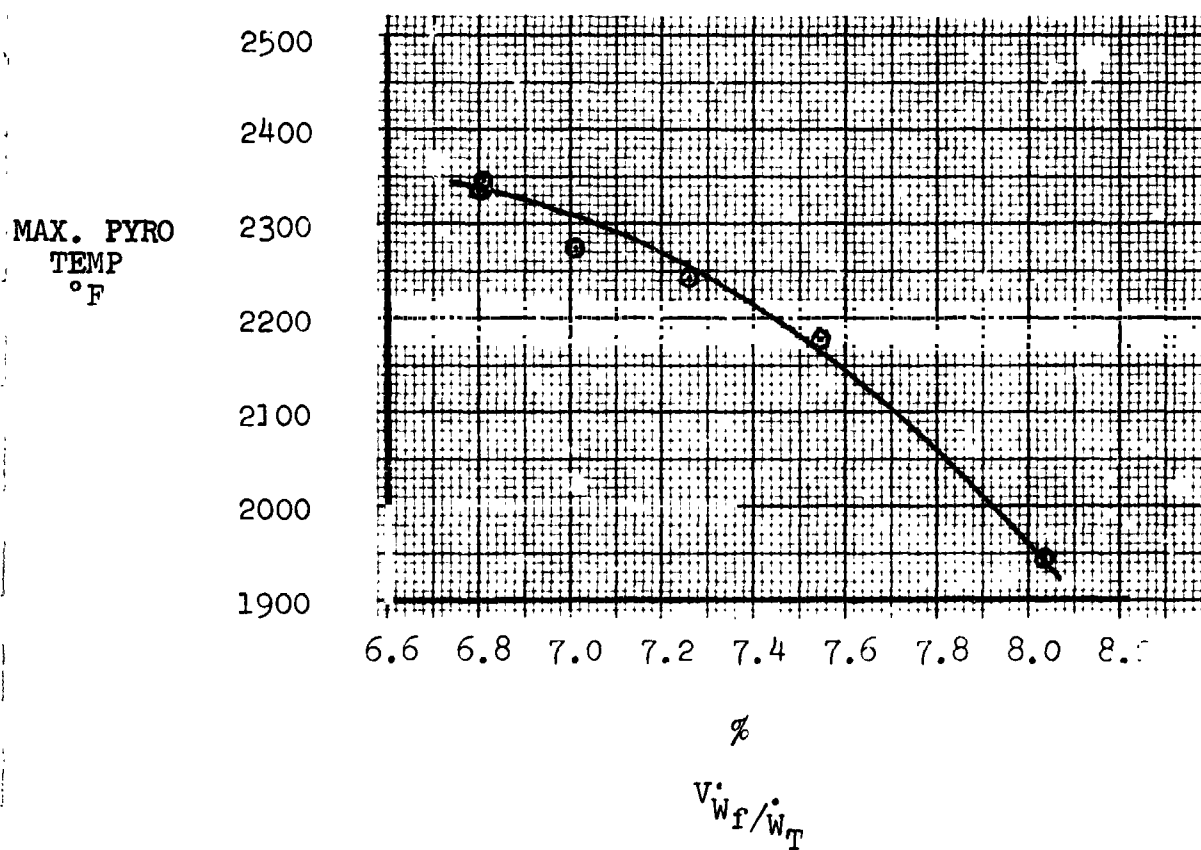


FIGURE V-12

Bell Aerospace Company

is shown in Figure IV-38.

Wall temperatures in both cases followed a similar pattern to the 26 L* $\text{N}_2\text{O}_4/\text{MMH}$ tests, decreasing with $P\%$, but opposite to the 30 L* and 34 L* $\text{N}_2\text{O}_4/\text{MMH}$ tests where wall temperature increased with $P\%$. The 2400°F design value was obtained at approximately $7.1\% P$ in the 30 L* chamber, with a corresponding performance of approximately 312 seconds specific impulse. The 2400°F value was obtained at $3.3\% P$ in the 34 L* chamber, with a corresponding specific impulse of approximately 311 seconds. The temperature data for both configurations are plotted in Figure IV-39.

The conclusion drawn from this testing was that the two fuels, A50 and MMH, are nearly interchangeable. Some adjustment in the amount of film coolant would be required to adjust wall temperatures, but the basic hardware would appear, on this cursory evaluation, to be readily usable for either propellant.

e. Conclusions From Testing

The extensive testing, conducted the columbium thrust chamber during the Task V and VIII effort proved that the operation of the columbium chamber was not only a viable concept but that operation could be predicted and adjusted to meet the design, operation and margin requirements of the engine. The fabrication of this engine was simple in comparison to most other contemporary concepts of reusable rocket thrust chambers. The simple use of a spun metal shell, coated and insulated far simplifies comparable multi-channel or multi-layer concepts of regenerative or ablative cooled units. However, with other non-perfect systems, a slight penalty would be paid with usage and this penalty would be in an increased wall coolant, and consequent performance, reduction to pay for the simplicity and low cost usage of the concept. With the achievement of 310 seconds in the current design, the performance penalty would be expected to be approximately $1\frac{1}{2}\%$ as compared to a regeneratively cooled thrust chamber. It is possible that this penalty could be reduced with further definition of coating capability or cycle reduction or metal improvement. However, at the present time it would appear that the current insulated columbium engine design would be limited to the materials and coatings currently being used.

Bell Aerospace Company

SPECIFIC IMPULSE VS MIXTURE RATIO ALUMINUM INJECTOR NO. 2 - 30L*, 34L* CHAMBER RUNS 859 - 867

I_{SP} CORRECTED TO VACUUM OPERATION
AND AREA RATIO 75:1 AND NORMALIZED
TO 8% ρ FILM COOLING

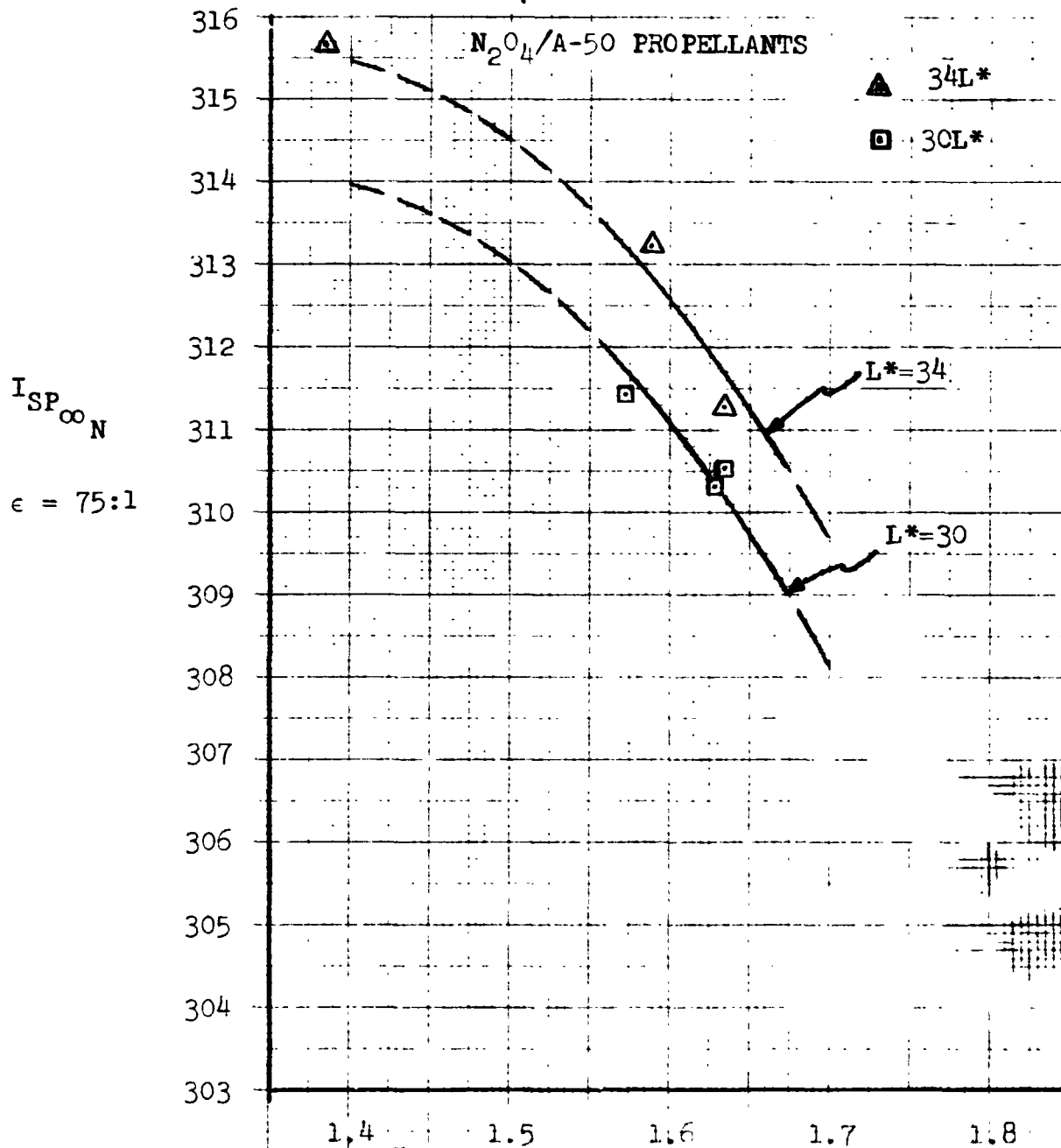


FIGURE V-13

Bell Aerospace Company

MAXIMUM PYROSCANNER TEMPERATURE

VS

PERCENT VORTEX FLOW

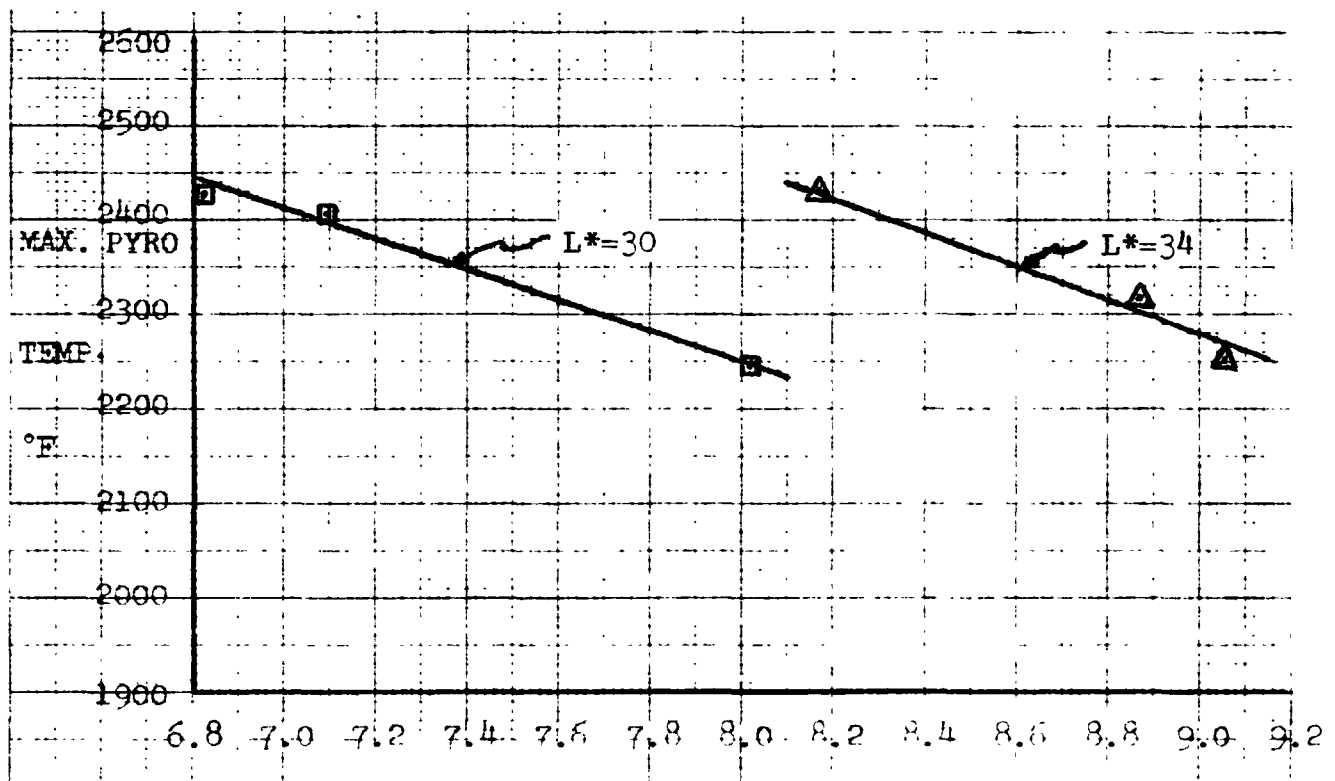
ALUMINUM INJECTOR NO. 2 - 30L*, 34L* CHAMBER

RUNS 859 - 867

$N_2O_4/A-50$ PROPELLANTS

Δ $L^* = 34$

\square $L^* = 30$



$\rho \%$

$\frac{V_{w_f}}{w_t}$

FIGURE V-14

Bell Aerospace Company

V. TASK VII - HEAT TRANSFER TESTING

It has been known for years that propellant additives can be used to decrease the heat rejection to a combustion chamber wall. Bell experiments with amine fuels dates back to the 50's and early 60's where medium chamber pressure (500 psia) operation was demonstrated but this additive coolant was not required. The demonstration was to add silicon oil (SO) in small quantities to the UDMH or MMH and the resultant oxidized precipitants have been theorized to coat the combustor wall presenting a thermal resistant surface to heat flux. Consistent heat rejection reductions of from 30 to 40% have been measured and one system has recently been made operational.

Since a similar thermal reduction would also provide margins for a low pressure engine such as the Space Shuttle, interest into heat transfer specifics at lower chamber pressure were generated within the scope of the OME program. Prior to this investigation, there was no awareness of information generated on the heat transfer characteristics and the possibility of cooling passage precipitants related to this lower chamber pressure operation.

The objective of the heated tube heat transfer test program was to determine, in an exploratory fashion, the effect of silicon additive to MMH and to 50-50. The results of this program were intended to support the Space Shuttle OME Technology Program. The program was conducted with and without silicon additive in both Hastelloy X and CRES 347 stainless steel, 1/8" O.D. tubes, with nominal velocities of 30 ft/sec., and 200 to 250 psia pressure. Generally, the tests were conducted by cycling up to and beyond the onset of nucleate boiling two or three times and then proceeding to the point of peak nucleate boiling with the associated tube burn out. Seven tubes were utilized, each of which were destroyed at the culmination of a test series. There were 25 heat-up and 18 cool-down half cycles. One tube was subjected to a 67 minute durability test consisting of 6 cycles each of which had about 6 minutes at temperature, 3 minutes to heat up, and 2 minutes to cool down.

Generally, the MMH with additive behaved the same as the clean MMH, a peak nucleate boiling point of between 5.0 and 5.3 Btu/in² sec., with the onset of nucleate boiling occurring at 2.0 to 2.3 Btu/in² sec., the heat transfer coefficient in the forced convection region was between .007 and .009 Btu/in² sec. °F. The long duration run seemed only to have the effect of raising the wall temperature somewhat but the peak nucleate boiling heat flux was unaltered. This probably means that an insulating film was deposited on the inside wall that reduced the effective film coefficient very slightly.

Bell Aerospace Company

The 50-50 had a slightly higher peak nucleate boiling, and the additive seemed to raise it a small amount, 5.64 and 6.17 Btu/in² sec., respectively, the onset of nucleate boiling was at 2.5 and 2.8 Btu/in² sec., and there was no difference in the forced convection film coefficient. The wall temperature in the nucleate boiling regime as a result was about 35°F higher with additive.

One particularly noteworthy finding, was that the onset of nucleate boiling appeared to take place at a lower temperature than the saturation temperature as indicated by the literature for MMH vapor pressure-temperature functionality for clean MMH with no and limited cycles. It is possible that film deposit disallowed decomposition of MMH that may have happened with a new tube.

A. Test Plan

The objective of this task was to determine the effects of certain variables on fuel blend heat transfer characteristics using resistance heated circular tubes. The program was to consist of cyclic heating of approximately seven tubes. Because of the limited scope, the program was intended to be exploratory in nature. Initially, it was considered desirable to do the test using CRES 347, however, due to a lack of available tubing a substitution of Hastelloy X was proposed, and was deemed acceptable. Two check cases were planned using steel and Hastelloy X with similar test conditions to further ascertain what this investigator had found on a previous program, that the choice of material was not significant.

The test specimens were to be subjected to cyclic heating to ascertain whether changes to the heat transfer characteristics did occur. Also, MMH and 50-50 were to be compared with each other and with additives that have been used to substantially reduce the gas side heat fluxes on other technology programs that have been conducted by this contractor.

Finally, a durability at temperature with repeated cycles was planned for MMH with one percent additive--Hexamethyldisilazine. The detailed test program as it was actually conducted is tabulated in the test results section.

B. Test Specimens

Each test specimen was constructed from a 10.7 inch section of either CRES 347S stainless steel or Hastelloy X seamed tubing. The nominal outside diameter of the tubes was 1/8 inch. The actual outside diameter varied between 0.1258 and 0.1265 inches. The wall thickness was 0.0149 ± 0.004, and 0.015 ± 0.002 inches for the stainless and Hastelloy X tubes, respectively.

Bell Aerospace Company

The 10.7 inch section allowed six inches for the heated section, four inches for the two electrodes, and 0.7 inches for attachments to the upstream and downstream adapter fittings.

Two predrilled copper sleeves were silver brazed onto the test specimens. This allowed for the attachment of large copper bus-bar clamps for electrical power input. Because of the very small resistance associated with this bus-bar clamp arrangement, almost all the resistance and thus temperature rise occurred in the six inch test section.

The heated length of six inches was selected because it provided sufficient electrical resistance to generate a heat flux well beyond the expected maximum burnout heat flux, and it was a convenient length with enough room to attach five surface thermocouples. The overall length of 10.7 inches was selected because it provided sufficient upstream length to establish turbulent flow before the heated portion of the test specimen.

The surface temperature thermocouples were made by tightly twisting number 28 gauge chromel-alumel wire together and forming a junction bead by arc welding. The thermocouple function bead was made as small and as smooth as possible and then turned to the inside as shown in Figure V-1.

The surface temperature thermocouples were electrically insulated from the tube surface by an initial uniform ceramic coating of aluminum oxide which was $0.005 \pm .001$ inch thick, see Figure V-2. After the initial 0.005 inch ceramic coating was applied, the outer-insulation of each thermocouple lead was pushed back to allow slipping the bead over the test specimen and onto the tube surface. The outer insulation was pulled down and a recheck made of each thermocouple bead to assure contact to the initial coating.

A second coating of Rokide "A", approximately 0.030 inches thick, was then applied over the entire length of test section of the tube to securely fasten the surface thermocouples.

C. Test Apparatus

Power was provided by four 28 volt VDC-750 ampere, compound-wound Hobart motor generators. These units were connected in an equalizer bus connection in the positive leg, which tied their series fields in parallel.

A contactor rated at 1000 amps d.c., complete with arc chute and blowout coil was installed in the negative leg of each machine, so that it could be switched on-line individually. The field

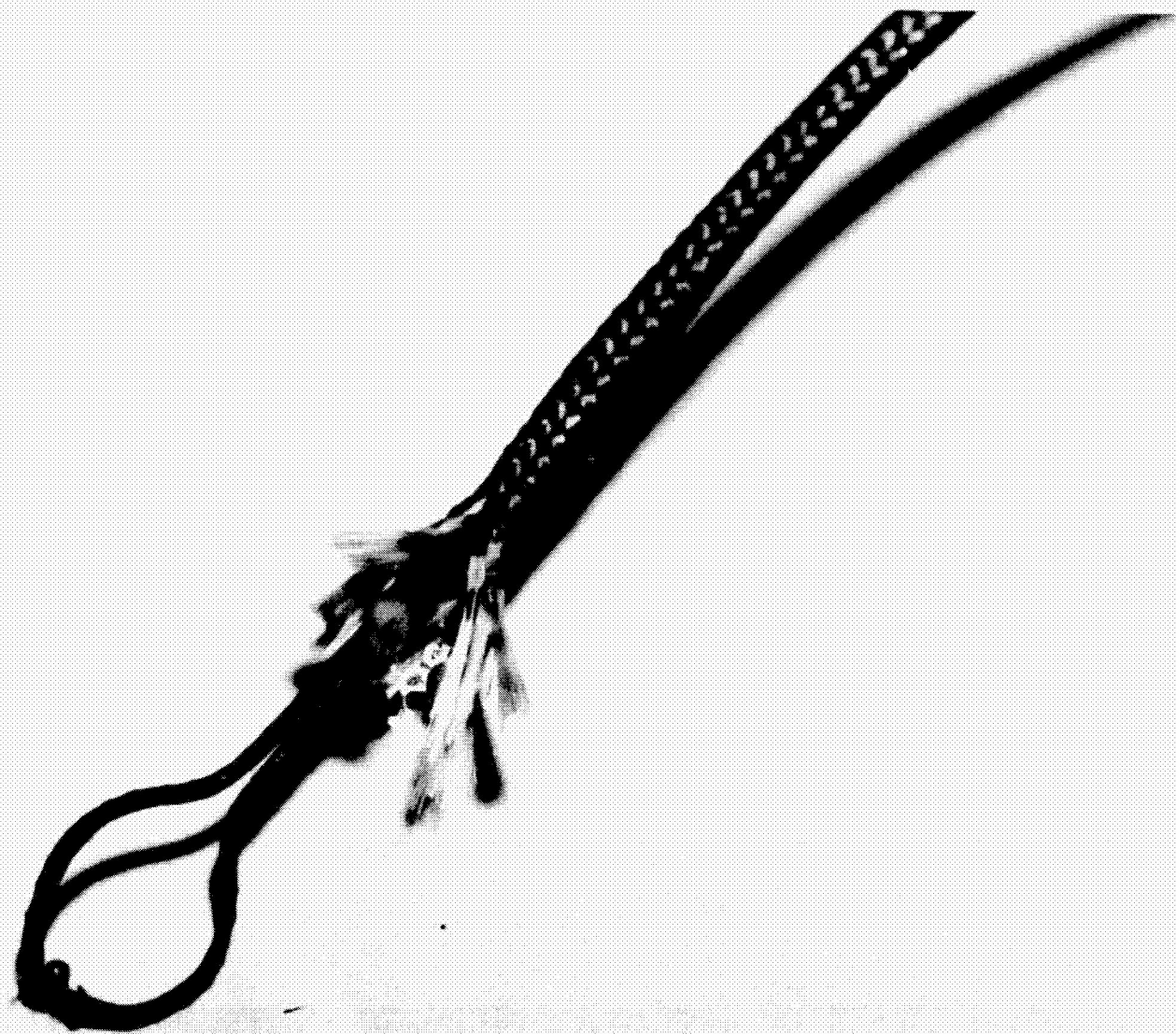


FIGURE V-1. THERMOCOUPLE BEAD

ORIGINAL PAGE IS
OF POOR QUALITY

V-5

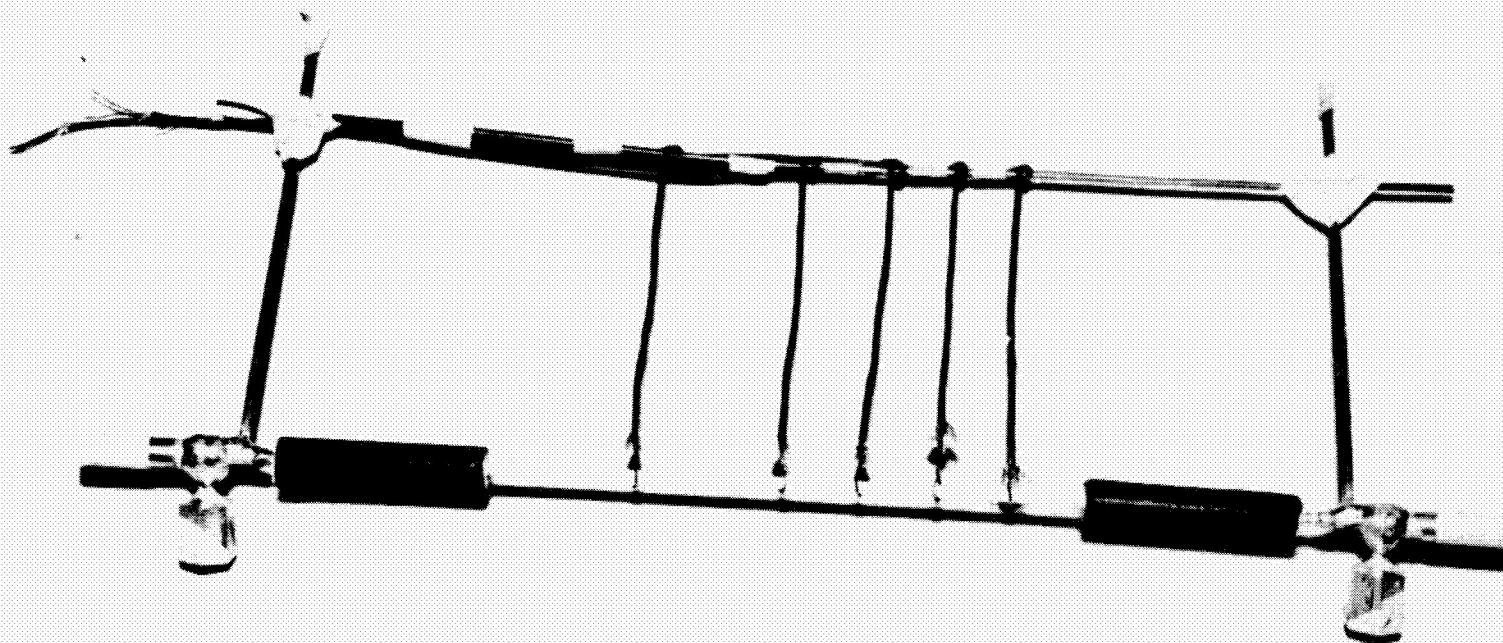


FIGURE V-2. ALUMINUM OXIDE COATED THERMOCOUPLES

Bell Aerospace Company

of each generator was separately excited by a 0-72 vdc supply, resulting in a saturation no-load terminal voltage of 50 vdc.

Generator bus bars and cable were sized for 1000 amps per machine. The entire system was wired for a capacity of 4000 amps.

When the tube failed the current ceased and the generators were shut down, the upstream and downstream propellant valves were closed and a CO₂ fire extinguishing system was automatically turn on. In all cases, the termination of the test was well controlled with no test stand damage.

The heat up-cool down cycles to approximately 70% of peak nucleate boiling was accomplished by increasing the power input in steps allowing the amperage and skin temperatures to stabilize before proceeding to the next step. After the power was shut-off, the liquid flow in the tube was shut off.

The power source characteristics map shown in Figure V-3 was constructed to depict the voltage and current values expected for each tube material. It can be seen that Hastelloy X has a considerably higher electrical resistance than stainless. Superimposed on the map are lines of constant heat flux covering the heat flux range for the fuels tested.

D. Propellant Supply System

The propellant supply system is shown schematically in Figure V-4.

The supply tank and receiver tank each have a capacity of 100 gallons and can be pressurized to 1200 psia. For this program the supply tank contained 55 gallons of propellant which allowed for test duration of up to 80 minutes for an 1/8 inch tube at 30 feet per second. Both the supply and receiver tanks were pressurized with a regulated gaseous nitrogen source to obtain the required 200 to 250 psia operating pressure at the test specimen.

The propellants were conditioned to the required inlet temperatures of 50°F by a system consisting primarily of a circulation pump, and a steam heat exchanger. The system is a closed loop system, circulating the propellant from the supply tank only, and can provide uniform propellant temperatures over the entire range of 30° to 200°F. The propellant was conditioned to the desired temperature prior to the start of each test, and during the test, the propellant conditioning system was isolated from the supply tank.

A 1/2 inch diameter line carried the propellant to the test section. Flow was controlled by two parallel valves (one for coarse adjustments, and one for fine adjustments) which were located downstream of the test section. The test section could

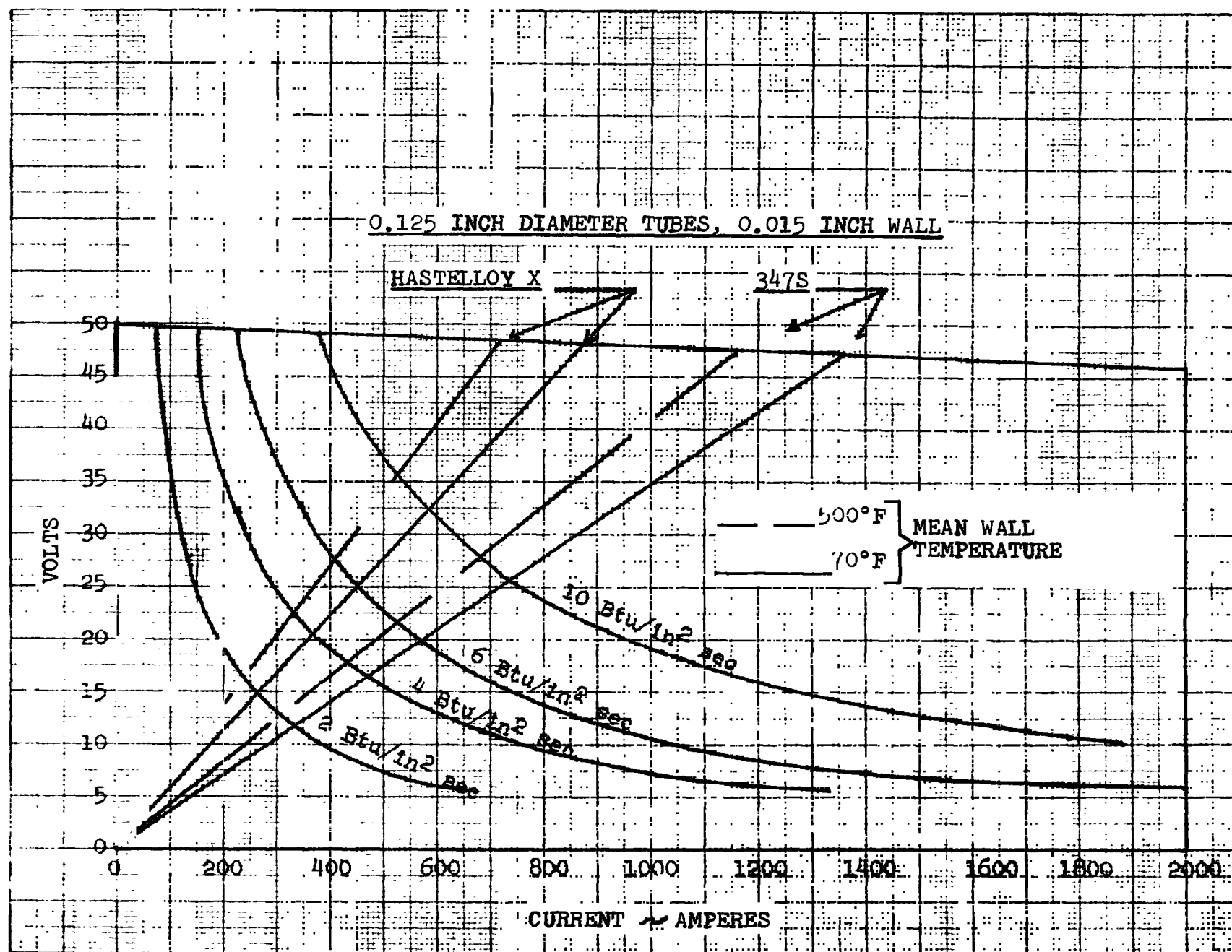
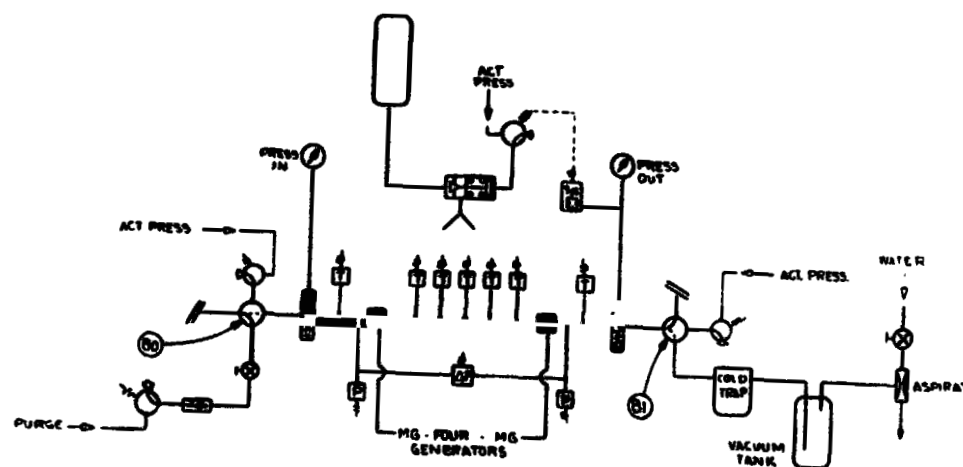
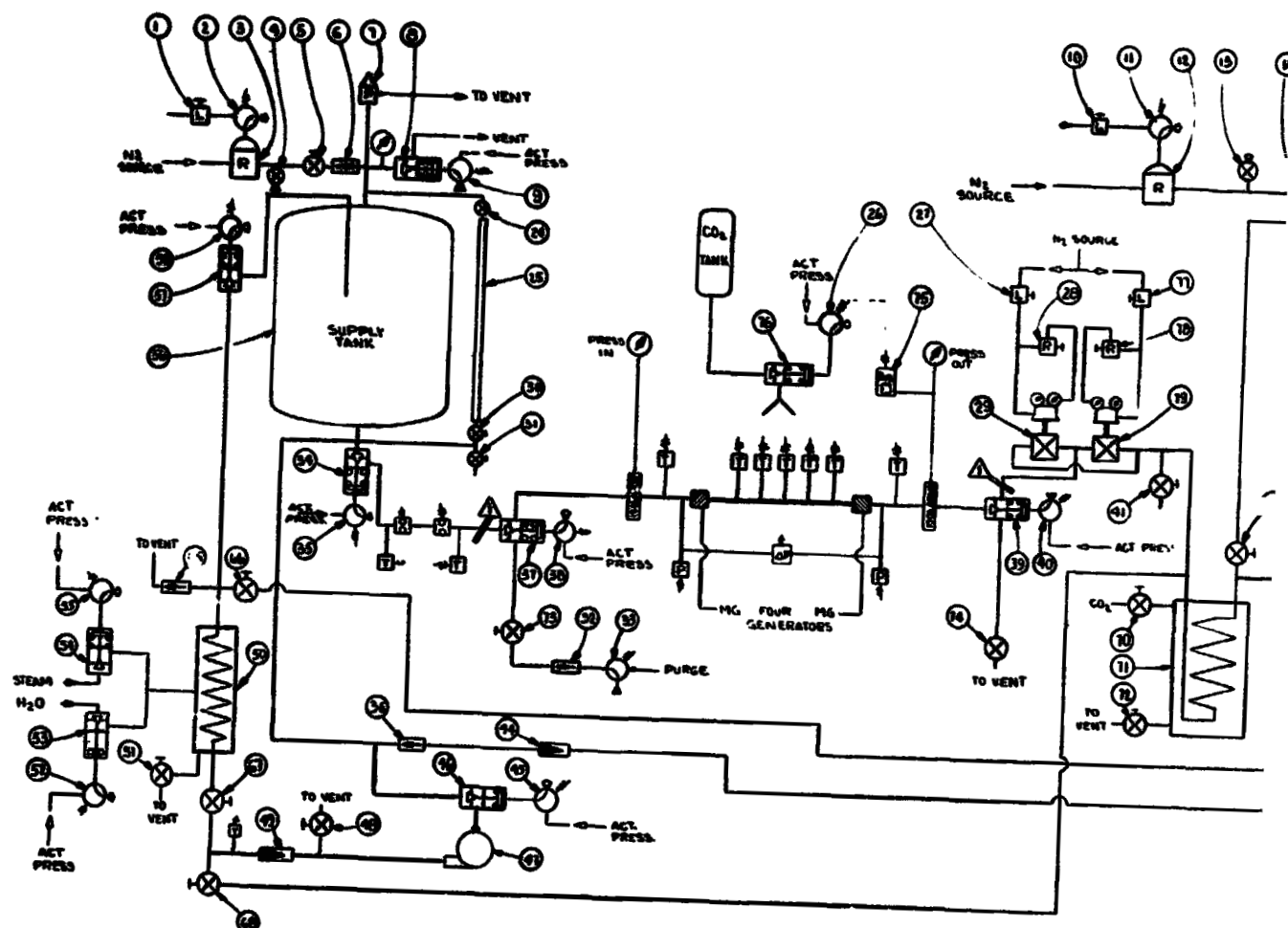


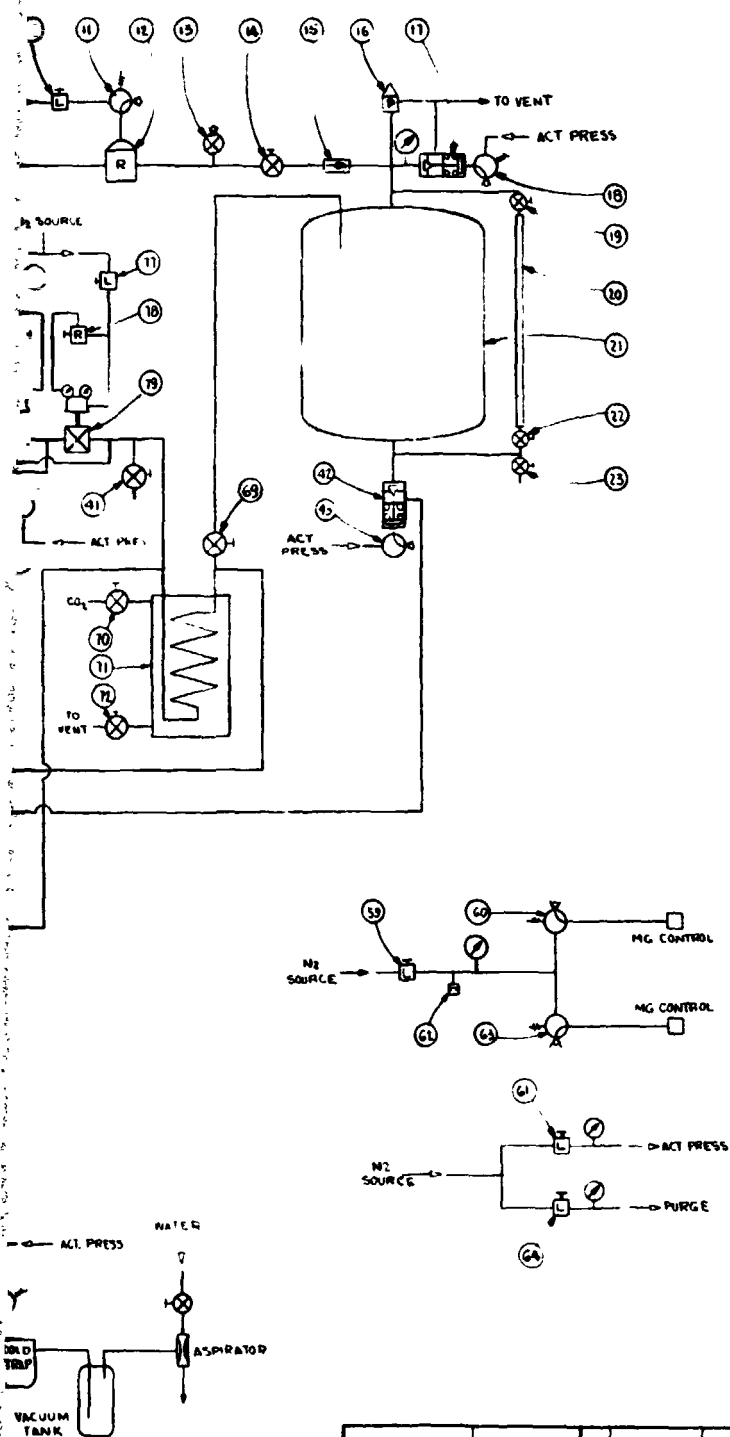
FIGURE V-3



VACUUM SHUTDOWN SET UP

⚠ FOR ALTERNATE CONFIGURATION SEE VACUUM SHUTDOWN SET UP
NOTES

FOLDOUT FRAME



ITEM NO.	LINE NO.	QUANTITY	DESCRIPTION	MAT'L	VENDOR OR PART NO.	FUNCTION OR LOCATION
			VALVE PNEU. OP.		*62-412-093 (BELL)	
			VALVE PNEU. OP.		*62-412-093 (BELL)	
			VALVE PNEU. OP.		ANNIN DOMOTOR	
			REGULATOR HAND		CONOFLOW	
			LOADER HAND			
			VALVE PNEU. OP. N.C.		TURANSKY	
			PRESSURE SWITCH			
			VALVE - HAND			
			VALVE - HAND			
			VALVE - HAND			
			HEAT EXCHANGER			
			VALVE HAND			
			VALVE - HAND			
			VALVE - HAND			
			VALVE - HAND			
			VALVE - CHECK			
			LOADER HAND			
			VALVE - 3WAY - SOL			
			BURST DISC ASSY			
			LOADER HAND			
			VALVE - 3WAY - SOL			
			LOADER HAND			
			VALVE - 3WAY - SOL		GROVE	
			VALVE - PNEU. OP. N.C.		GEN. CONT. AVIK-11A7	HEAT EXCHANGER OUTLET
			TANK		TURANSKY	
			VALVE - 3WAY - SOL			
			VALVE - PNEU. OP. N.C.			HEAT EXCHANGER - STEAM
			VALVE - PNEU. OP. N.C.			
			VALVE - 3WAY - SOL			HEAT EXCHANGER - WATER
			VALVE - HAND			
			HEAT EXCHANGER			
			FILTER 5/16 MICRON			
			VALVE - HAND			
			PUMP			
			VALVE - PNEU. OP. N.C.			
			VALVE - 3WAY - SOL			HEAT EXCHANGER INLET
			FILTER - 1/2 MICRON			
			VALVE - 3WAY - SOL			RECEIVER TANK VALVE
			VALVE - PNEU. OP. N.C.		TURANSKY	
			VALVE - HAND			
			VALVE - 3WAY - SOL			DOWN STREAM CUT-OFF
			VALVE PNEU. OP. N.C.			
			VALVE - 3WAY - SOL			UP STREAM CUT OFF
			VALVE - PNEU. OP. N.C.		TURANSKY	
			VALVE - CHECK			
			VALVE - 3WAY - SOL			SUPPLY TANK
			VALVE - PNEU. OP. N.C.		TURANSKY	
			VALVE - 3WAY - SOL			
			VALVE - CHECK			
			VALVE HAND			
			VALVE HAND			
			VALVE PNEU. OP.		ANNIN DOMOTOR	
			REGULATOR		CONOFLOW	
			LOADER - HAND		GROVE	
			VALVE - 3WAY - SOL		CO ₂ FOR FIRE	
			SIGHT GAGE			
			VALVE - HAND			
			VALVE - 3WAY - SOL			
			VALVE - PNEU. OP. N.C.		SST TURANSKY	RECEIVER TANK VENT
			VALVE - PRESS. RELIEF			
			VALVE - CHECK			
			VALVE - HAND			
			HAND VALVE			
			REGULATOR - DOME			
			VALVE - 3WAY - SOL		GEN. CONT. AVIK-11A7	RECEIVER TANK DOME
			LOADER HAND			
			VALVE - 3WAY - SOL		GEN. CONTROL AVIK-11A7	SUPPLY TANK VENT
			VALVE PNEU. OP. N.C.		SST TURANSKY	
			VALVE PRESS. RELIEF			
			VALVE - CHECK			
			VALVE - HAND			
			REGULATOR - DOME		GROVE	
			VALVE - 3WAY - SOL		GEN. CONTROL AVIK-11A7	SUPPLY TANK VALVE
			LOADER HAND		GROVE	

1300 PSI

ITEM NO. LINE NO. QUANTITY DESCRIPTION MAT'L VENDOR OR PART NO. FUNCTION OR LOCATION

HOLE TOLERANCES EXCEPT AS SHOWN

201 TO 200 - .001 - .001

200 TO 100 - .001 - .001

100 TO 50 - .001 - .001

FIGURE V-4. PROPELLANT SUPPLY SYSTEM SCHEMATIC

Bell Aerospace Company

be isolated from the supply and receiver system by upstream and downstream pneumatic operated valves. Under normal operating conditions, flow through the test specimen was remotely controlled by these valves, see Figure V-5; however whenever a rapid drop in pressure occurred (as is the case at tube destruction), a pressure switch automatically closed these valves isolating the test section (Figure V-6 and V-7).

The test specimen was simultaneously deluged with CO₂ from a nozzle located directly over the test specimens to preclude fire damage. The receiver tank was vented to sea level atmospheric conditions during all testing. Whenever necessary, the system back pressure was regulated by a remote controlled valve.

E. Test Instrumentation

The standard instrumentation set-up provided the capability of recording propellant flowrate, supply and receiver tank pressures, inlet and outlet pressure and temperature at the test specimen, surface temperatures at pre-determined points on the test specimen, and the current flow and voltage drop across the test specimen.

Pressure measurements were made with Tater Teledyne psia transducers and Statham psid transducers. The transducers used to measure the inlet and outlet pressures were electrically isolated from the heated test section by special insulation blocks. The demonstrated measurement uncertainty for this type of transducer is $\pm 0.7\%$ (three sigma) of nominal output.

Propellant temperatures were measured using Conax probe type chromel-alumel ungrounded thermocouples. The thermocouples are imbedded in a mineral insulated and protected from the propellants by a stainless steel sheath. The demonstrated measurement uncertainty for these thermocouple probes is $\pm 2.0^\circ\text{F}$ of nominal temperature.

Surface temperatures of the test tubes were measured with thermocouples made at Bell from number 28 gauge chromel-alumel wire with an asbestos/glass fiber insulation. The accuracy of these thermocouples is rated at $\pm 4.0^\circ\text{F}$ up to 530°F , and $\pm 0.75\%$ from 530°F to 1400°F .

All of the thermocouples, four propellant temperatures, and five surface temperatures, were referenced to 150°F using a Pace Reference Junction.

The power delivered to the test section was determined by measuring the current flowing in the circuit and the total voltage drop across the heated section of the tube. Current was measured with a shunt calibrated to generate 50 mv at 2000 amps. Voltage was measured directly across the test section by wires attached to the bus-bars. The measured

ORIGINAL PAGE IS
OF POOR QUALITY

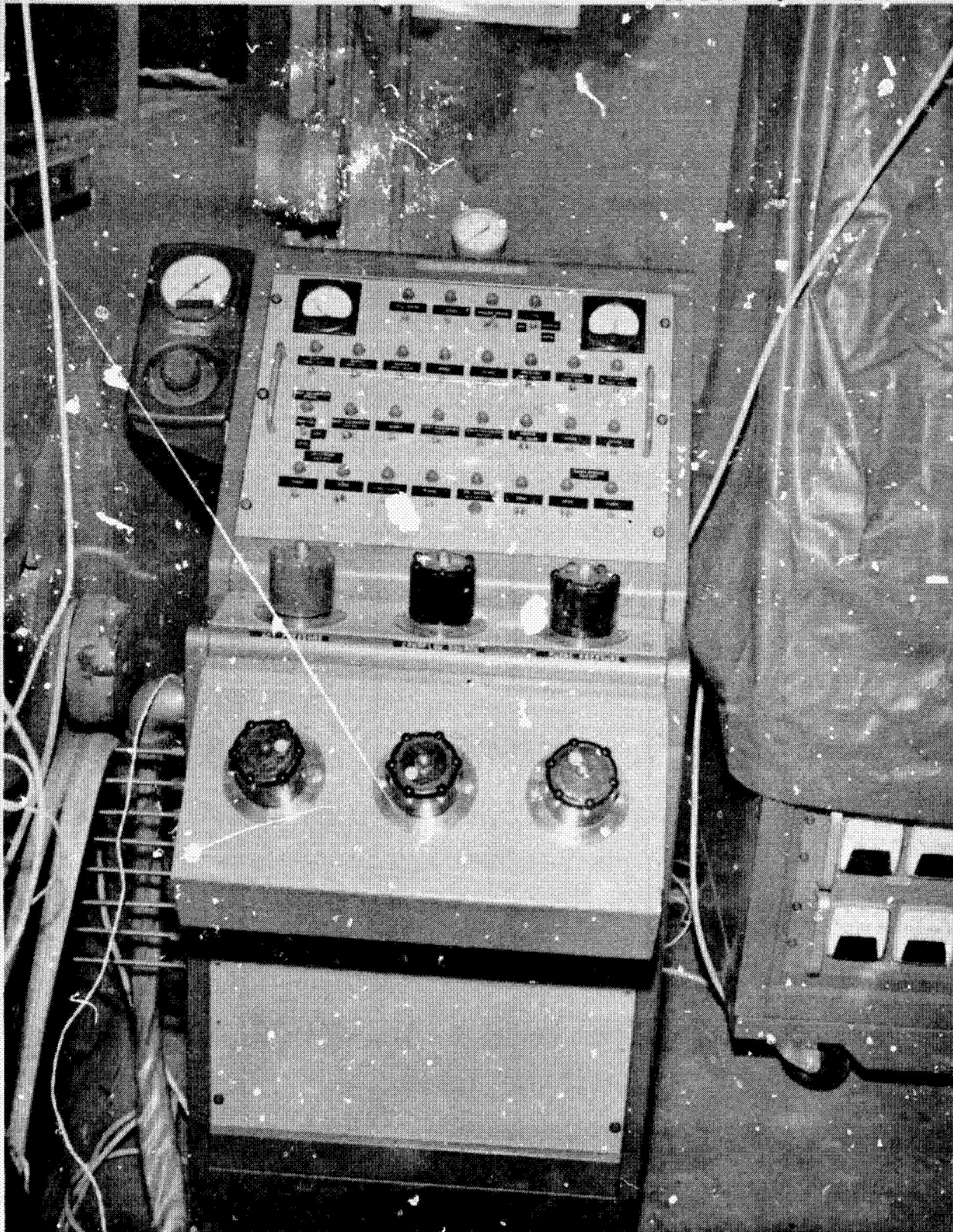


FIGURE V-5. FLOW CONTROL PANEL

ORIGINAL PAGE IS
OF POOR QUALITY

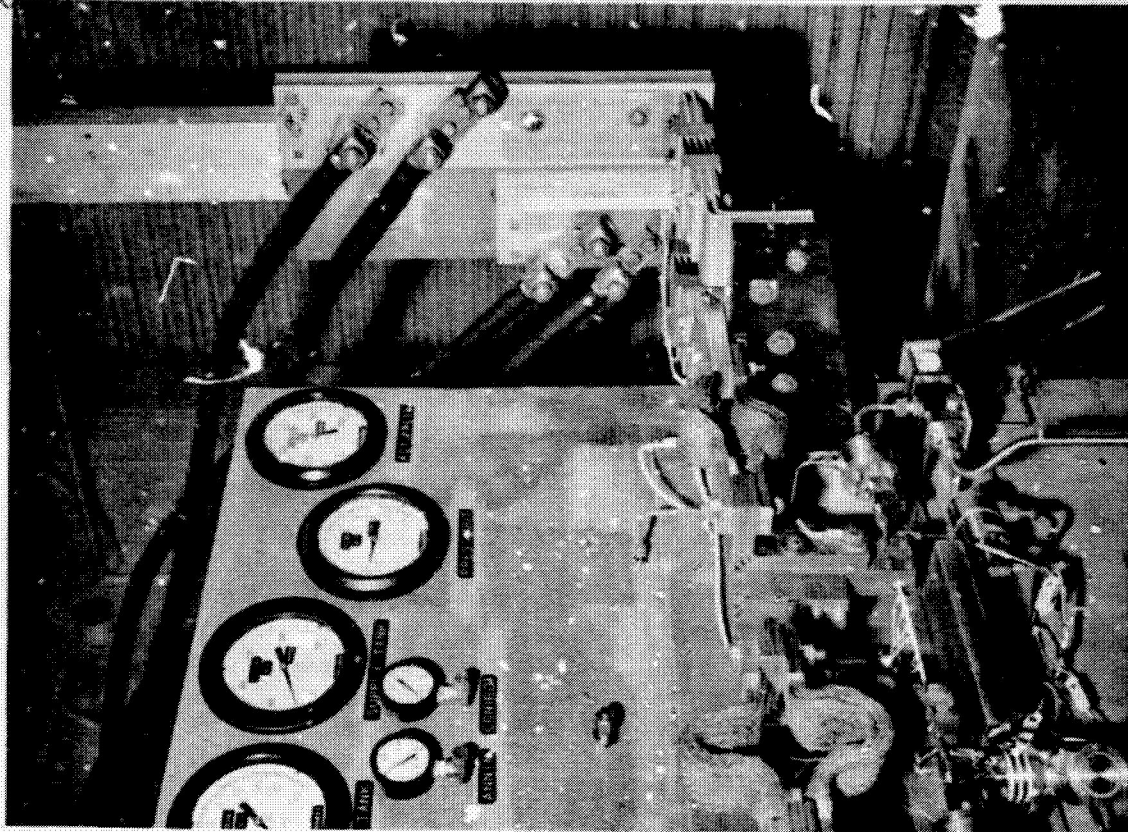


FIGURE V-7. HEAT TRANSFER TEST PANEL

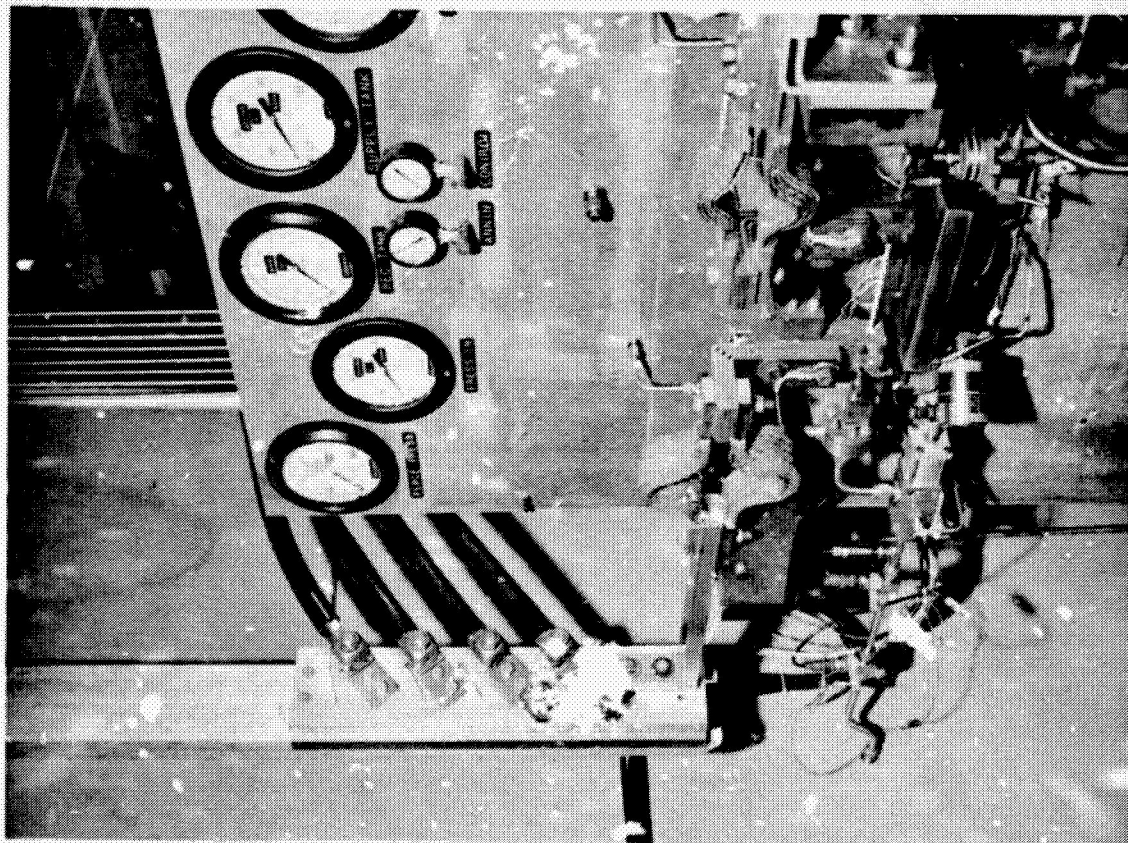


FIGURE V-6. HEAT TRANSFER TEST PANEL

Bell Aerospace Company

voltage was divided by a calibrated circuit to obtain a millivolt output.

Redundant Fischer-Porter turbine-type flowmeters were used to measure propellant flowrates. Prior to the initiation of the test program the flowmeters and their installation line was calibrated as a unit in water. At least two calibrations, over the expected region of operation, were conducted on the flowmeter set and an average sensitivity derived for test data reduction.

The measurement uncertainty associated with the type of flowmeters used for the test program has been demonstrated to be approximately $\pm 1.0\%$.

The millivolt outputs of the transducers and the current level and voltage drop across the test specimen were patched to signal conditioners and recorded on a Brush Recorder, with an accuracy of $\pm 3\%$ of full scale; a CEC Oscillograph, with an accuracy of less than $\pm 5\%$ over the range of the galvanometer used; and on a Beckman Model 210 Data Acquisition System, with an accuracy of $\pm 0.1\%$ for 20 millivolt full scale input.

The Beckman 210 Data Acquisition System converts the conditioned millivolt outputs of the various transducers and measuring devices to a digital data bit, and records the data on magnetic tape in a format suitable for data reduction on an IBM 360 Model 44 computer.

F. Test Procedure

The general procedure for conducting a test was to first condition the propellant to the desired inlet temperature by circulating the propellant from the supply tank through the heat exchanger. The test specimen was installed in the test stand pressure test, and an instrumentation check made. The next step was to pressurize the propellant system to the annin valves by means of the gaseous nitrogen regulator. The flow control valves were then adjusted to obtain the proper inlet velocity and operating pressure at the test specimen. Once the desired propellant system conditions were obtained, a 10 second data file of the test parameters, such as supply pressure, flowrate, test specimens, inlet and outlet temperature and pressure, and receiver tank pressures were recorded on magnetic tape.

Power was then applied to the test specimen in pre-determined increments. Once steady state was attained at each increment, as evidenced by a visual recording (Brush Recorder) of the test specimen outside wall thermocouples, a 10 second data file of all pertinent parameters was recorded on magnetic tape.

Bell Aerospace Company

G. Data Reduction

The test data were obtained from the electrical output of the various pressure transducers, flowmeters, and thermocouples. These electrical outputs were converted and recorded as digital data on a magnetic tape. These data were then used as inputs to a series of assembler and Fortran language programs which performed the calculations necessary to produce engineering units and data essential for assessing the test results. The data reduction programs also require as input data, the physical properties of the tube materials and propellants. These data were obtained from References 12, 13, 14, and 15.

The following describes the engineering rationale and resultant equations which were programmed for the computer.

$$T_W = \frac{-A + \sqrt{A^2 + 2B \left\{ AT_s + \frac{B}{2} T_s^2 - \phi \left[\frac{1 - \left(\frac{I.D.}{O.D.} \right)^2 \cdot \ln \left(\frac{O.D.}{I.D.} \right) - \frac{I.D.}{4} \right] \right\}}}{B}$$

where: A and B are the coefficients of the appropriate thermal conductivity relationship.

The energy transfer into the system is given by the following equation:

$$Q_{in} = 0.000984 (\Delta E) (I) \frac{BTU}{sec}$$

The energy transfer out of the test area was given the following equation:

$$Q_{out} = \dot{W} \bar{C}_p \left[T_o - T_i - (T_o - T_i) \phi = 0 \right]$$

Bell Aerospace Company

This equation assumes that all of the electrical energy released into the system is removed by the enthalpy increase in the fuel. The heat losses due to convection and radiation have been calculated and found to be insignificant, and are therefore neglected. Changes in the kinetic energy of the fluid as it passes through the system is also negligible. The equation for one phase flow is used because the small amount of vapor formed at the liquid-tube wall interface will be mixed with the cooler liquid and condensed before reaching the outlet bulk temperature thermocouple. The $(T_o - T_i)\phi = 0$ term is included to account for frictional effects and thermocouple errors which are present before power is applied.

The flowrate used in the equation above was derived from the measured volumetric flowrates:

$$\dot{W} = \rho \cdot q$$

Where:

q is the measured volumetric flowrate.

and

ρ is the propellant density and is derived from the propellant temperature measurements at the turbine flowmeters.

The heat transfer coefficient can be calculated at any station by applying the equation shown below.

$$h = \phi / (T_w - T_B)$$

Flow velocity is calculated by applying the simple one-dimensional continuity equation,

$$V = \dot{W} / \left[\pi \rho \frac{r^2}{144} \right]$$

where density is given above and r is the inside radius of the appropriate test specimen.

The computer was also programmed to calculate the following dimensionless correlation parameters with fluid properties evaluated at local bulk temperatures and estimated mean film temperatures.

Bell Aerospace Company

$$\text{Nusselt Number} \quad Nu = \frac{(h) (I.D.)}{K_L}$$

$$\text{Reynolds Number} \quad Re = \frac{(I.D.) (V) (\rho)}{\mu}$$

$$\text{Prandtl Number} \quad Pr = \frac{(C_p) (\mu)}{K_L}$$

The heat flux into the liquid at any point is given by the following equation:

$$\phi = \frac{(0.000948) (\Delta E) (I)}{\pi (I.D.) (L)} \quad \frac{\text{BTU}}{\text{sec-in}^2}$$

The heat flux was treated as a constant along the length of the tube.

The bulk temperature at any station is given by the following equation:

$$T_B = T_i + (T_o - T_i) \frac{X}{L} \quad ^\circ\text{F}$$

This assumes that no significant change in temperature occurs outside the heated section of the tube in the 2 1/2 inch sections between the thermocouples and the heated section. It is also assumed for simplicity, that the temperature variation along the length of the tube is linear. This assumption will introduce some error into the calculated bulk temperature as C_p varies somewhat with temperature, the greatest error occurring near the center of the test section.

The equation for local static pressure is similar to the equation for bulk temperature. The pressure, however, is assumed to drop linearly between the two pressure taps which are placed at either end of the 11-inch test section. The pressure is therefore given by the following equation:

$$P = P_i - (P_i - P_o) \frac{2.5 + X}{11}$$

The inside wall temperature at each thermocouple station along the heated section of the tube was calculated from the thermal conductivity of the tube material and the measured power input, surface temperature, and tube dimensions i.e.,

$$K_{\text{metal}} = A + BT_s$$

Bell Aerospace Company

H. Results of Test Program

The results of the test program are summarized in Table 1. Typical Q/A vs inside wall temperature functionalities are shown in Figures V-8, V-9, and V-10 for MMH no cycling, 50-50 and MMH with cycling. The additive used with MMH was 1% hexamethyldisilazane, and 1% methylcyanoethylpolysiloxane was added to 50-50. The following statements are made based on the limited number of tests that were conducted.

MMH

For MMH with and without additive there is no apparent difference in the heat transfer characteristics whether the specimen be Hastelloy X or CRES 347 stainless steel. The peak nucleate boiling point appears to be independent of number of cycles or time at temperature. The onset of nucleate boiling was very consistent for all tests with and without additive at $2.15 \pm .15$ Btu/in² sec., rather remarkable reproducibility. The temperature at which the nucleate boiling occurs seems to increase with increased numbers of cycles or time at temperature or both. It can be noted that the first two test series using clean MMH had the onset of nucleate boiling occur at a lower temperature than saturation. This occurred with the first two MMH with additive tests, but to a lesser degree. The long duration series 1191 through 1196, and the subsequent burnout 1197 had a Q/A vs. inside wall temperature more like one would expect. Perhaps some decomposition takes place within the tube until a film is built up on the tube wall.

Another slight variation that might have some bearing is that the later tests were run at about 60 psia lower pressure. The forced convection film coefficient tended to be slightly lower with additive than without and it seemed to decrease slightly with repeated cycling 1191 through 1196, see Figure V-10.

50-50

There were only two series run, one with clean 50-50, tests 1177-1180; and with additive--tests 1181-1183. It would appear as though the onset of nucleate boiling was delayed and the peak nucleate boiling point was increased from 5.6 to 6.2 Btu/in² sec going from clean propellant to additive. The temperature at which boiling begins to occur appears to be about 35°F higher with additive. Similar kinds of tests conducted by this investigator using these same propellants but at 750 psia, and velocities of 50 and 80 ft/sec., resulted in 3 to 4 Btu/in² sec. increment, however, these specimens were not cycled. When a test was conducted with additive and cycled this effect was found to be 1 to 1 1/2 Btu/in² sec. less. That test was conducted by evacuating the tube to 100,000 ft. simulated altitude on

NOTE: A - Beginning
B - End Point } 5 Minute High Temp.
C - End

TABLE I
RESULTS OF TEST PROGRAM

TUBE NO.	TUBE S/N	RUN NO.	PROPELLANT	TUBE SIZE	VELOCITY Q/A MAX.	PRESSURE		BURN-OUT	ONSET N. B.	HIGHEST Q/A	P.N.B.	F.C. h_L	ΔT_{WALL} ONSET	$T_{IN WALL}$ OF N.B.	SAT. TEMP.	BULK TEMP AT B.O.	SAT. BULK TEMP.	V ΔT $\times 10^{-3}$
						IN	OUT											
1	22	1172	MCH	Hast. 1/8"	28.2	259	254	Yes	2.3	-	5.35	.0088	104	350	402	221	181	5.1
2	35	1173	MCH	Steel 1/8"	29.3	240	226	No	2.2	3.15	-	.0088	68	349	395	-	-	-
	35	1174	MCH	Steel 1/8"	29.3	251	236	No	2.1	2.4	-	.0078	65	355	397	-	-	-
	35	1175	MCH	Steel 1/8"	29.6	248	235	No	2.1	2.5	-	.0078	66	358	397	-	-	-
	35	1176	MCH	Steel 1/8"	27.9	252	247	Yes	2.2	-	5.18	.0081	67	359	400	239	161	4.5
3	14	1177	50-50	Hast. 1/8"	28.6	222	210	No	2.5	2.56	-	.0086	104	373	365	-	-	-
	14	1178	50-50	Hast. 1/8"	29.6	245	233	No	2.5	2.9	-	.0086	103	380	375	-	-	-
	14	1179	50-50	Hast. 1/8"	28.4	224	211	No	2.5	5.6	-	.0086	103	369	365	-	-	-
	14	1180	50-50	Hast. 1/8"	27.4	234	222	Yes	2.5	-	5.64	.0086	103	375	371	234	137	3.8
4	7	1181	50-50 + 1%	Hast. 1/8"	29.6	238	222	No	2.8	4.06	-	.0084	123	407	375	-	-	-
	7	1182	50-50 + 1%	Hast. 1/8"	29.7	240	225	No	2.8	4.86	-	.0084	112	408	375	-	-	-
	7	1183	50-50 + 1%	Hast. 1/8"	26.1	243	229	Yes	2.8	-	6.17	.0084	111	419	375	259	116	3.0
5	13	1184	50-50 + 1%	Steel 1/4"	44.0	462	449	No	5.0	7.58	-	.0135	146	450	442	-	-	-
6	15	1185	MCH + 1%	Hast. 1/8"	29.6	210	196	No	2.0	3.9	-	.0073	82	353	377	-	-	-
	15	1186	MCH + 1%	Hast. 1/8"	28.4	210	196	No	2.1	4.	-	.0073	84	371	377	-	-	-
	15	1187	MCH + 1%	Hast. 1/8"	28.7	212	197	Yes	2.0	-	5.04	.0073	83	368	377	221	156	4.5

TABLE I (CONT'D)
RESULTS OF TEST PROGRAM

TUBE NO.	TUBE S/N	RUN NO.	PROPELLANT	TUBE SIZE	VELOCITY Q/A MAX.	PRESSURE		BURN-OUT	ONSET N. B.	HIGHEST Q/A	P.N.B.	F.C. $\frac{P}{L}$	ΔT_{WALL} $T_{IN WALL}$ ONSET OF N.B.		SAT. TEMP.	BULK TEMP AT B.O.	SAT. BULK TEMP.	$v \Delta T \times 10^{-3}$	$T_{IN W}$ AT PEAK Q/A	$T_{OUT W}$
						IN	OUT													
-	25	11149	MMH + 1%	Steel 1/8"	28.8	201	187	No	2.1	4.0	-		65	352	365	-	-	-		
	25	11150	MMH + 1%	Steel 1/8"	29.5	203	194	No	2.1	4.2	-		64	365	365	-	-	-		
	25	11150	MMH + 1%	Steel 1/8"	29.3	200	184	Yes	2.1	-	.1		64	352	365	219	146	4.3		
V-18	23	11131A	MMH + 1%	Hast. 1/8"	29.6	206	190	No	2.1	3.70	-	.0071	84	370	-	-	-	-	372	520
	23	11131B	MMH + 1%	Hast. 1/8"	29.3	207	192	No	-	3.78	-	-	-	-	-	-	-	-	385	535
	23	11131C	MMH + 1%	Hast. 1/8"	29.3	208	192	No	-	3.65	-	.0064	84	395	-	-	-	-	390	534
	23	11132A	MMH + 1%	Hast. 1/8"	29.3	208	193	No	2.0	3.67	-	.0070	84	374	-	-	-	-	395	529
	23	11132B	MMH + 1%	Hast. 1/8"	29.2	208	193	No	-	3.45	-	-	-	-	-	-	-	-	389	526
	23	11132C	MMH + 1%	Hast. 1/8"	29.1	208	193	No	-	3.41	-	.0063	84	399	-	-	-	-	392	527
	23	11133A	MMH + 1%	Hast. 1/8"	28.4	207	192	No	2.0	3.61	-	.0069	84	378	-	-	-	-	392	535
	23	11133B	MMH + 1%	Hast. 1/8"	28.2	206	191	No	-	3.59	-	-	-	-	-	-	-	-	395	537
	23	11133C	MMH + 1%	Hast. 1/8"	28.1	205	190	No	-	3.56	-	.0062	84	403	-	-	-	-	395	536
	23	11134A	MMH + 1%	Hast. 1/8"	28.0	203	188	No	2.0	3.63	-	.0068	84	382	-	-	-	-	397	540
	23	11134B	MMH + 1%	Hast. 1/8"	27.9	202	1		-	3.58	-	-	-	-	-	-	-	-	392	533
	23	11134C	MMH + 1%	Hast. 1/8"	27.8	201	186		-	3.54	-	.0061	84	407	-	-	-	-	404	543

TABLE I (CONT'D)
RESULTS OF TEST PROGRAM

TUBE NO.	TUBE S/N	RUN NO.	PROPELLANT	TUBE SIZE	VELOCITY Q/A MAX.	PRESSURE		BURN-OUT	ONSET N. B.	HIGHEST Q/A	P.N.B.	F.C. h_L	ΔT_{WALL} $T_{IN WALL}$ ONSET OF N.B.		SAT. TEMP.	BULK TEMP AT B.O.	SAT. BULK TEMP.	$V \Delta T \times 10^{-3}$	T_{IN}^W AT PEAK Q/A	T_{OUT}^W
						IN	OUT													
3	23	1195A	MMH + 1%	Hast. 1/8"	27.7	200	185	No	2.0	3.65	-	.0067	84	386	-	-	-	-	400	543
	23	1195B	MMH + 1%	Hast. 1/8"	27.5	199	184	No	-	3.60	-	-	-	-	-	-	-	-	410	551
	23	1195C	MMH + 1%	Hast. 1/8"	27.5	198	183		-	3.57	-	.0060	84	411	-	-	-	-	415	554
	23	1195A	MMH + 1%	Hast. 1/8"	27.5	195	181		2.0	3.66	-	.0066	84	390	-	-	-	-	419	560
	23	1196B	MMH + 1%	Hast. 1/8"	27.4	194	180		-	3.52	-	-	-	-	-	-	-	-	416	553
	23	1196C	MMH + 1%	Hast. 1/8"	27.4	193	179		-	3.43	-	.0059	84	415	-	-	-	-	422	555
4		1196	MMH + 1%	Hast. 1/8"	27.8	192	175	Yes	2.0	-	5.39	.0066	84	392	367	233	134	3.7	455	650

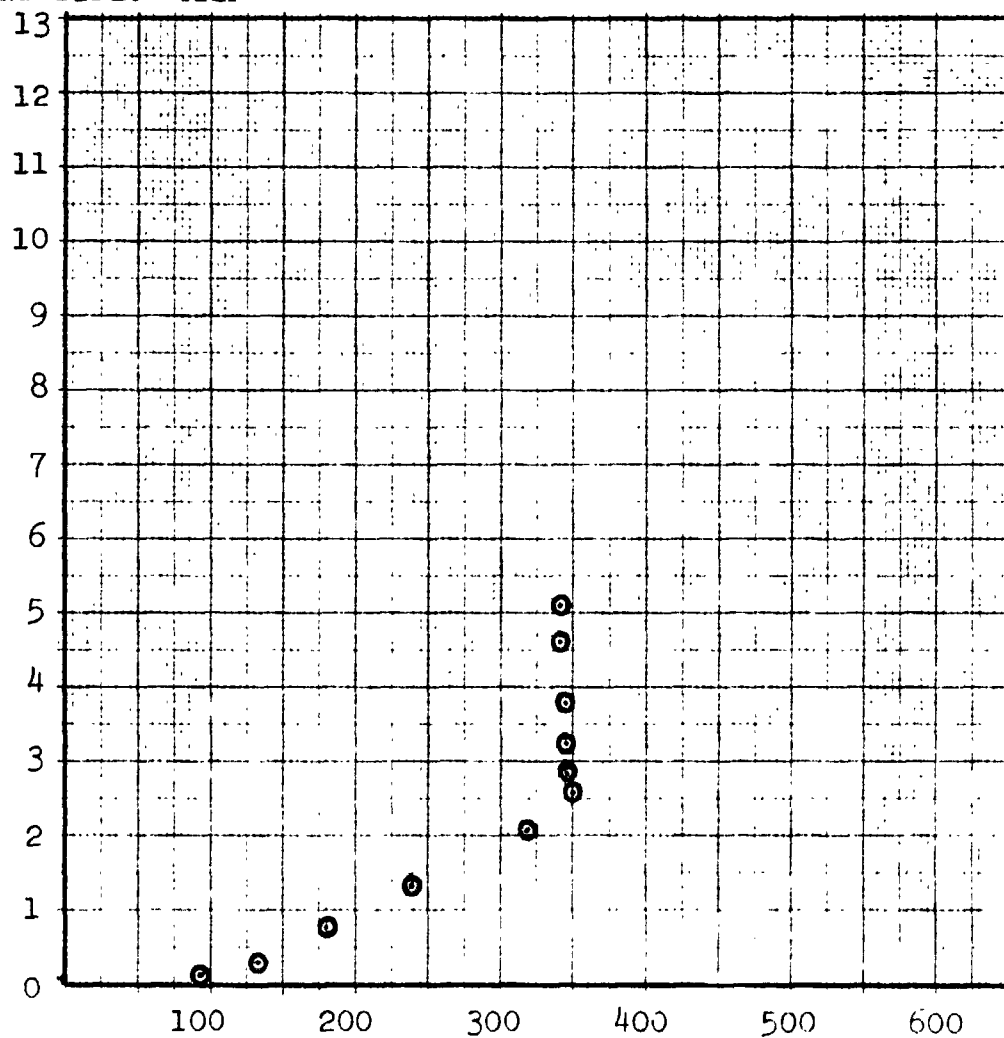
V-19

ORIGINAL PAGE IS
OF POOR QUALITY

Bell Aerospace Company

TEST NO. 1172 CELL X-1
TEST DATE: 8/11/72
PROPELLANT TEMPERATURE: 90°F
INLET VELOCITY: 30 FT/SEC
METAL TYPE: HASTELLOY
TUBE SIZE: 1/8"
PROPELLANT TYPE: MMH

Ø HEAT FLUX
BTU/SEC-IN²



AVERAGE INSIDE WALL TEMPERATURE ~°F

FIGURE V-8

Bell Aerospace Company

TEST NO. 1177 - CELL X-1

TEST DATE: 8/15/72

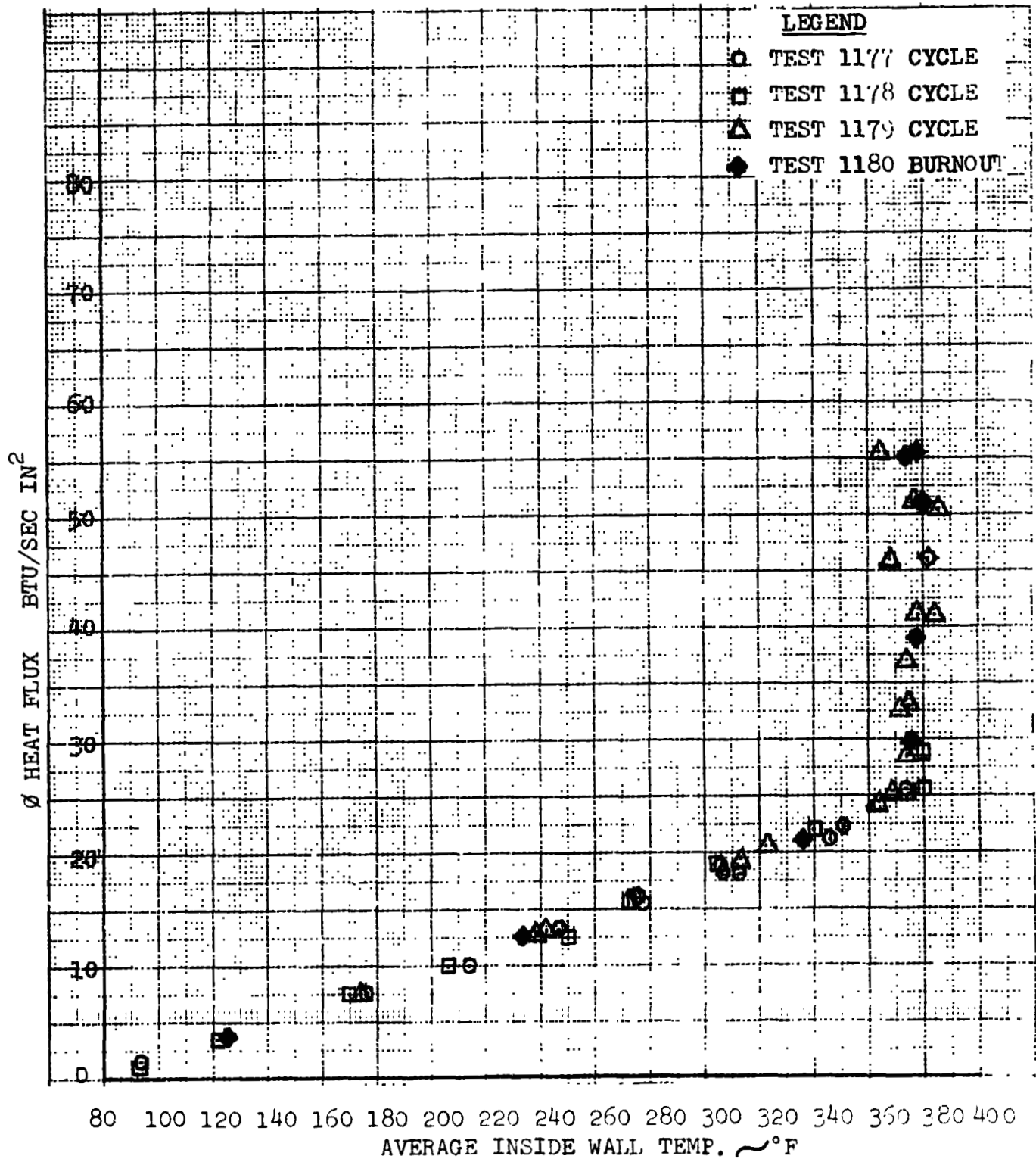
PROPELLANT TEMPERATURE: 90°F

INLET VELOCITY: 30 FT/SEC

METAL TYPE: HASTELLOY

TUBE SIZE: 1/8"

PROP. TYPE: 50/50



Bell Aerospace Company

FIGURE V-10

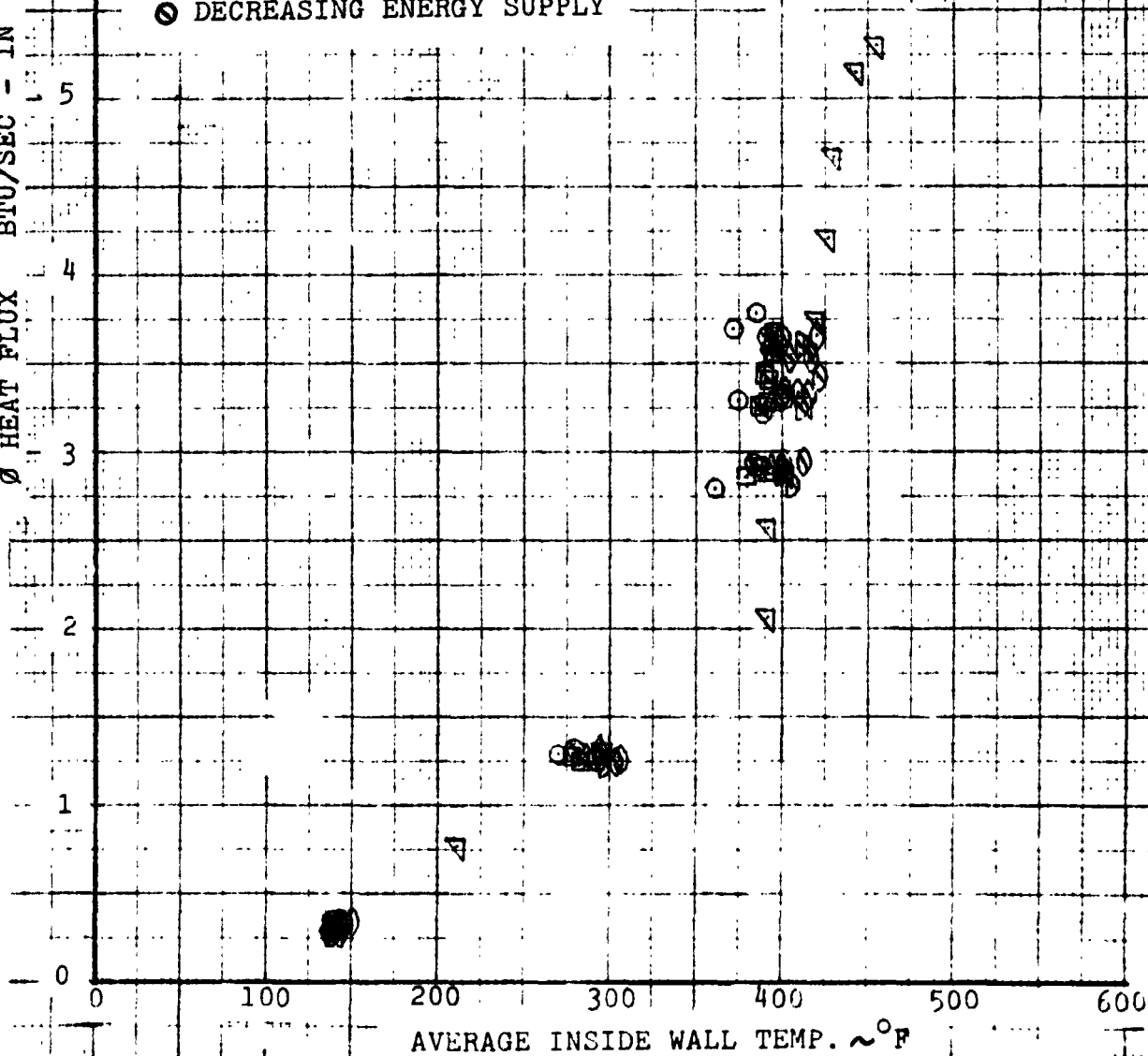
TEST NO. 1191 - CELL X1
 TEST DATE 8/22/72
 PROP. TEMP. 90°F
 INLET VELOCITY 30 FT/SEC.
 METAL TYPE HASTALLOY
 TUBE SIZE 1/8"
 PROP. TYPE MMH + 1% SILICONE OIL

ORIGINAL PAGE
 OF POOR QUALITY

LEGEND

- TEST 1191 CYCLE
- TEST 1192 CYCLE
- △ TEST 1193 CYCLE
- ◇ TEST 1194 CYCLE
- ◐ TEST 1195 CYCLE
- ◑ TEST 1196 CYCLE
- ▽ TEST 1197 BURN-OUT
- INCREASING ENERGY SUPPLY
- DECREASING ENERGY SUPPLY

Ø HEAT FLUX BTU/SEC - IN²



Bell Aerospace Company

shut down. Since the series 1181-1183 was cycled, it is possible that peak nucleate boiling point was suppressed.

J. Conclusions

Although this test series was very limited, certain tentative conclusions can be set forth. The results did provide additional questions that could be answered with a more exhaustive test series.

This test series points up the following conclusions:

The MMH heat transfer characteristics were unaltered by the silicone additive.

The onset of nucleate boiling with MMH occurred below the purported saturation temperature when the tube was clean or had very little time at temperature. Subsequently, a change appeared where it was hypothesized that a film builds up on the inside of the tube that either insulates the tube wall or prevents decomposition because of passivation or that the fuel does not contact the Hastelloy X or CRES 347.

The cycling or time at temperature had no effect on the peak nucleate boiling heat flux, however, the tube wall temperature was substantially higher, $\approx 100^{\circ}\text{F}$.

Bell Aerospace Company

VI. TASK IX - INJECTOR CHARACTERIZATION AND STABILITY TESTING

During the course of this contract, two basic thrust chamber concepts were being evaluated for use on the OME. The two concepts being the insulated columbium chamber described in previous tasks, and the regeneratively cooled chamber, actively pursued on other NASA contracts. Comparative data between these contracts had indicated some concern related to the performance of conventional injectors when the fuel temperature was elevated to the temperature exiting from the regenerative chamber jacket and consequently entering the injector. Due to this concern, and other contract experience, the triplet injector was subjected to simulated regenerative chamber operation, to evaluate its performance and stability at those conditions. The simulated regen operation was performed with tests at elevated fuel temperatures (200 to 250°F) and ambient oxidizer. This increased fuel temperature simulated the heat pick up of the regeneratively cooled jacket and differed from the ambient temperature fuel testing was used for the insulated columbium chamber.

This task was performed in three sub-tasks. The first subtask being the characterization of performance with increased fuel temperature (with mixture ratio and chamber pressure variations), after testing to show injector acceptability. The second and third test tasks were performed, both concerning continued stability and included a short test stand and system checkout series with the baffled stainless steel injector, and the series test evaluation of the #1 aluminum acoustic damper stabilized injector.

A further change incorporated in this test series, was in the amount of vortex cooling required during the testing. Previously during this contract, the operation of the columbium chamber required the fuel film cooling amount to be 6 to 8% of the propellants injected. The regeneratively cooled chamber only requires from 2 to 4% of the propellants as fuel cooling, allowing a modest increase in performance and also somewhat different wall operating conditions. Thus, the test objectives of this task was to evaluate as closely as practical, the triplet injector at the conditions simulating operation in a regeneratively cooled OME engine.

A. Injector Tests at Elevated Propellant Temperatures

Fire tests conducted at sea level on the aluminum flat face injector S/N 1 were performed to investigate the effect of

Bell Aerospace Company

heated propellants on performance and heat rejection. The test objective was to evaluate performance at simulated maximum propellant temperatures for a regeneratively cooled chamber. The injector arrangements for these tests differ (from previous installations only) in the use of a low flow vortex cooling ring required to simulate the conditions for the regeneratively cooled chamber. All testing was completed with a steel "work-horse" chamber and a water cooled aluminum nozzle.

Baseline tests were initially conducted for two purposes. First, to establish correct sequencing and operation with the different vortex hardware, and second to establish a baseline on both the hardware and instrumentation for comparison to high temperature operation. The heated propellant tests were of 10 seconds duration. Heat rejection data in the water cooled nozzle were determined by chromel/alumel thermocouple probes in water jacket inlet and outlet manifolds.

Satisfactory test results were obtained with heated fuel and heated fuel/heated oxidizer. No performance decay was noted with heated fuel (240°F) and less than 1% performance decay with combined heated fuel (240°F) and heated oxidizer (110°F). The performance data obtained in this series are listed in Table I.

The characterization of the aluminum triplec injector configuration at various temperatures was added to this task as required if consideration was given to stability at the different cooling schemes. Since concern has been noted that performance might be materially effected at fuel temperatures, representative of regen operation, it was the object of this task to check out the injector operation at the higher temperatures as a prerequisite of bombing a "representative" injector. Testing was thus conducted at the elevated temperatures to establish a performance pattern and indeed the desirability of bombing the available injector.

B. Test Hardware

A cross section of the test hardware is shown in Figure VI-1. The injector and acoustic cavity is the same as previously tested with the columbium chamber. The vortex ring was modified to accept the lower film flow of a regen configuration. The only instrumentation change incorporated was the addition of added fuel flow meters such that fuel was measured with two sets of dual flowmeters where the oxidizer flowrates were measured with one set of dual flowmeters.

TEST DATA SUMMARY HEATED PROPELLANT TESTING ALUMINUM INJECTOR NO. 1 MOD A

TESTING	DUR SEC	P _c (PSIA)	O/F	% P	C* (P _c INJ. CORR)	FIIT (°F)	OIIT (°F)	Q (BTU/SEC)
4444-4455	2	CHECKOUT FIRINGS						
4456	10	127	1.65	4.2	5534	77	74	477
4457	15	126	1.62	4.2	5535	78	74	485
4458	15	105	1.46	4.5	5518	78	73	406
4459	15	105	1.77	4.0	5513	78	74	431
4460	15	138	1.74	4.0	5532	78	74	529
4461	10	123	1.66	3.7	5542	78	72	484
4462	2	CHECKOUT FIRING						
4463	10	125	1.66	2.9	5558	78	72	504
4464	2	CHECKOUT FIRING						
4465	10	104	1.54	3.0	5542	78	72	426
4466	10	103	1.92	2.6	5509	77	72	450
4467	10	137	1.82	2.8	5541	78	73	548
4468-69	5	CHECKOUT FIRINGS						
4470	10	126	1.69	2.9	5580	243	78	503
4471	10	124	1.56	3.1	5585	244	78	493
4472	10	137	1.89	2.8	5541	240	78	549
4473	10	102	1.81	2.8	5504	234	78	426
4474	10	104	1.52	3.2	5542	236	78	416
4475	10	124	1.90	2.8	5529	236	78	510
4476	10	101	1.67	2.9	5495	235	104	405
4477	10	104	1.83	2.8	5496	235	102	421
4478	10	100	1.70	2.9	5463	242	103	395
4479 ^①	10	100	.	.	.	244	103	384
4480	10	122	1.62	3.0	5514	243	103	475
4481	10	136	1.84	2.8	5502	243	103	537

① FUEL FLOW CHANGE DURING RUN - DATA NOT RELIABLE

TABLE I

TEST HARDWARE - HEATED PROPELLANT TESTS

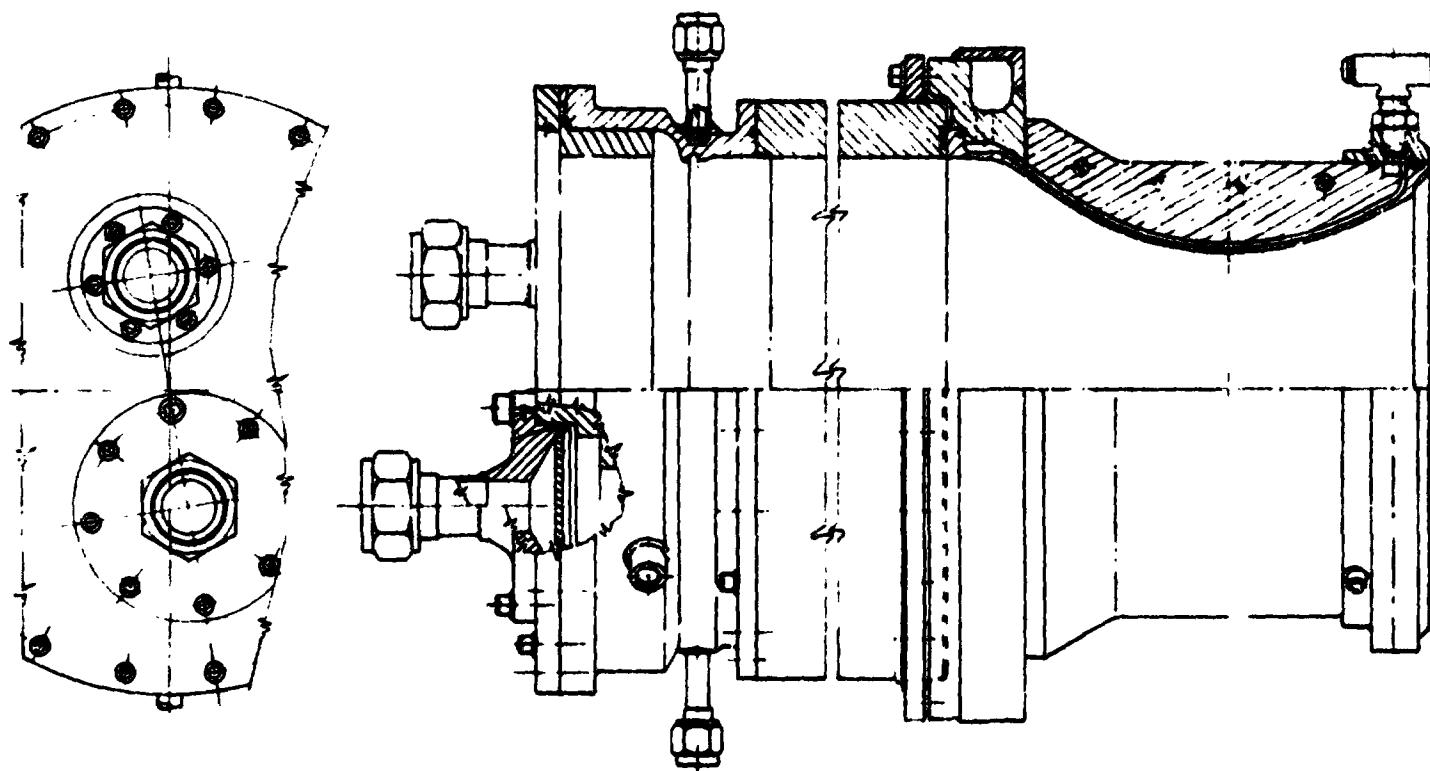


FIGURE VI-1

Bell Aerospace DIVISION OF **Textron**

Bell Aerospace Company

C. Test Results

The characterization of the triplet injector with heated propellants has been successfully demonstrated during this series. The test duration of 10 seconds is sufficient to assure high temperature propellant to reach the injector as shown in Figure VI-2. Heat rejection data was basically stabilized also within this duration. The ambient temperature baseline performance data are plotted in Figure VI-3 with data at three chamber pressure levels and three levels of fuel vortex cooling across the mixture ratio range. Testing at various mixture ratios and chamber pressures with the fuel heated to approximately 240°F revealed no performance degradation as given in Figure VI-4. Raising the oxidizer temperature had a greater effect and some performance loss was encountered (< 1%) when the oxidizer was heated to approximately 110°F (Figure VI-5). A comparison of the heat rejection data for ambient and heated propellants is made in Figure VI-6.

A regression analysis was made with the heated propellant data revealing very small residuals for performance and heat rejection with heated fuel. Data for this analysis is given in Figure VI-7. These small residuals identify the negligible effect with heated fuel. The analysis with the combined heated fuel and heated oxidizer flow performance loss of approximately 2/3% with also a slight reduction in heat rejection.

D. Conclusions From Injector Characterization With Heated Propellant

Results from this test series agree well with previous subscale testing of triplet elements with heated propellants.¹ No noticeable performance decrease with fuel heated to 240° was expected at full scale while the effect of oxidizer was more pronounced. Even the effect of oxidizer temperature was found to be negligible within the specified 100°F temperature range indicating that regeneratively cooled chamber operation with this injector would not produce any so-called "blow apart" phenomena or performance degradation. This conclusion, and the test results, presumed this injector to be fully qualified as a representative injector for further stability testing.

E. Bomb Chamber Checkout Tests

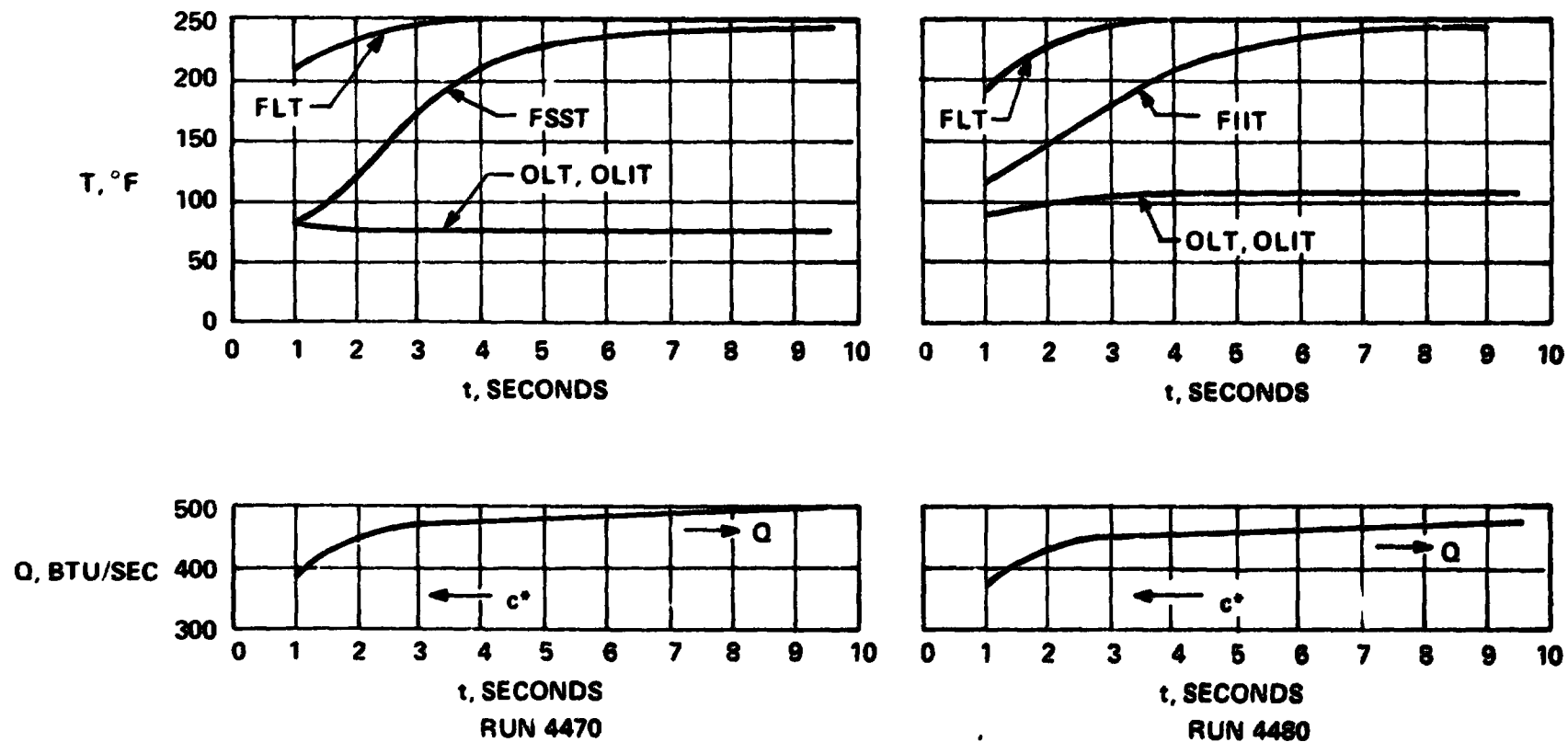
As series of tests were made with the stainless steel injector S/N 1 to insure the operation of the combustion stability systems installed in the test cell. These systems included the bomb detonation sequence wiring and timing, the instrumentation for monitoring results, the automatic shutdown systems and the bombs themselves. These tests were completed with the results shown in Figure VI-9 and the test engine was immediately changed to use the acoustic damper injector.

¹ 600# thrust subscale tests were conducted up to 150°F fuel inlet temperatures without a performance decrease.

HEATED PROPELLANT TESTS

DATA TIME HISTORIES

VI-2

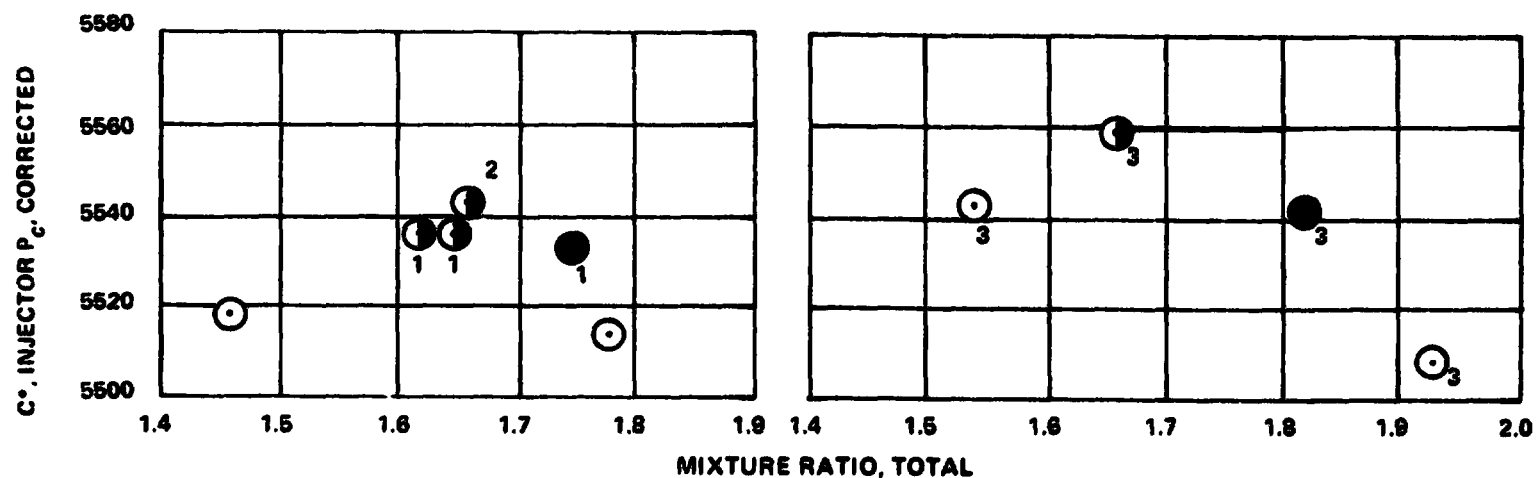


LEGEND: FLT FUEL LINE TEMPERATURE,
FIIT FUEL INJECTOR INLET TEMPERATURE

FIGURE VI-2

Bell Aerospace DIVISION OF **Textron**

C* VERSUS TOTAL O/F AMBIENT PROPELLANTS 10 INCH ALUMINUM INJECTOR, MOD A



LEGEND

- HIGH P_c 137 ± 2 PSIA
- ① NOM P_c 125 ± 2 PSIA
- ⊙ LOW P_c 103 ± 2 PSIA
- 1 % ρ, NOMINAL = 4.2
- 2 % ρ, NOMINAL = 3.7
- 3 % ρ, NOMINAL = 2.9

FIGURE VI-3

C^* VERSUS TOTAL O/F HEATED FUEL, AMBIENT OXIDIZER $\%P(\text{NOMINAL PC, O/F}) = 2.9$

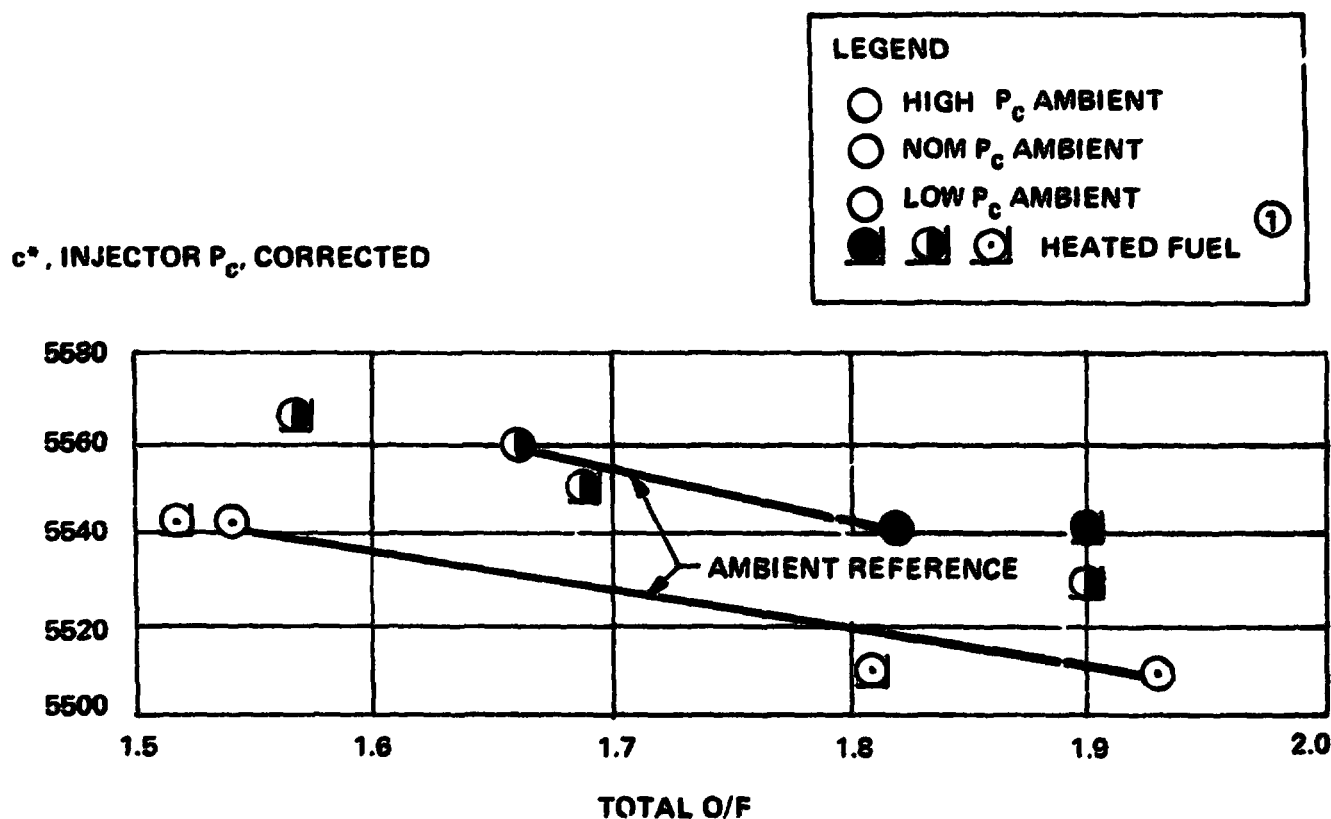
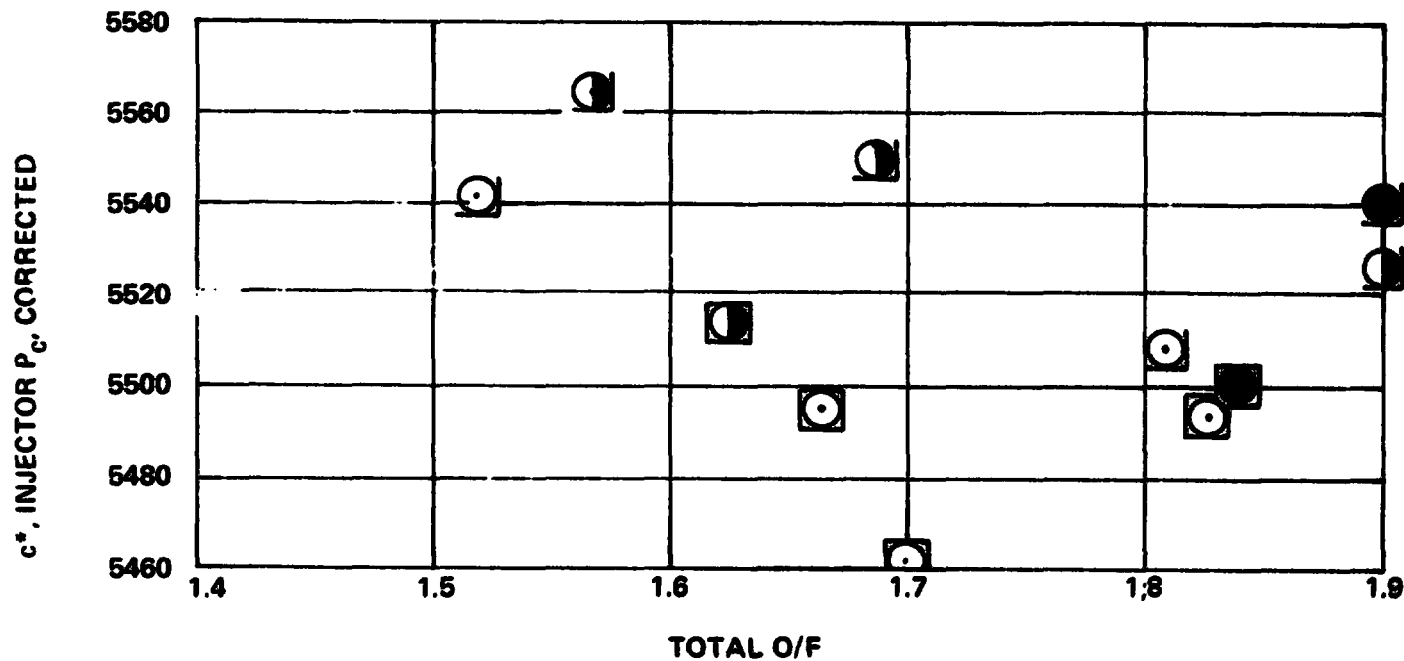


FIGURE VI-4

C* VERSUS TOTAL O/F **HEATED FUEL, AMBIENT OXIDIZER AND** **HEATED FUEL, HEATED OXIDIZER^①**



① HEATED FUEL FIIT, 235 TO 244°F
 HEATED OX. OIIT, 102 TO 104°F

LEGEND

- HIGH P_c , HEATED FUEL
- ◐ NOM. P_c , HEATED FUEL
- ◑ LOW P_c , HEATED FUEL
- ◐ ◑ HEATED FUEL AND HEATED OX.

FIGURE VI-5

INSULATED COLUMBIUM ENGINE : PROJECTED OPERATION

	<u>$I_{SP\infty}$</u>	<u>INSULATED T MAX</u>
CURRENT BEST ASSESSMENT	310.2 OR 310.0	2425° F 2400° F
	(1 SEC $I_{SP} = 100^\circ F$)	
POTENTIAL IMPROVEMENTS		
CHAMBER LENGTH OPTIMIZATION (LOWER c^* TESTING TASK IX)	310.0	2250° F
INJECTOR IMPROVEMENTS (ALUMINUM INJECTOR NO. 2)	312.0	2450° F
VORTEX IMPROVEMENTS		

FIGURE VI-8

DATA ANALYSIS

HEATED PROPELLANT TESTING

ALUMINUM INJECTOR No. 1, MOD A

A. AMBIENT PROPELLANTS, HEATED FUEL AND AMBIENT OX

$$c^* = 5334.8 + 0.92 P_c + 242.3 r_c - 90.45 r_c^2 - 1337.2 \rho$$

MULTIPLE CORRELATION COEFFICIENT 0.93

RESIDUALS +12 FT/SEC

- 14 FT/SEC

$$\ln Q = 0.83 \ln \left(\frac{P_c}{125} \right) - 0.186 \ln \rho + 5.567$$

MULTIPLE CORRELATION COEFFICIENT = 0.99
(+4, -11 BTU/SEC)

NEGLIGIBLE EFFECT
OF HEATED FUEL

B. HEATED FUEL AND HEATED OX

c^* LOSS APPROX 2/3%

Q SLIGHTLY LOWER THAN ABOVE

FIGURE VI-7

Bell Aerospace DIVISION OF **Textron**

INSULATED COLUMBIUM ENGINE : PROJECTED OPERATION

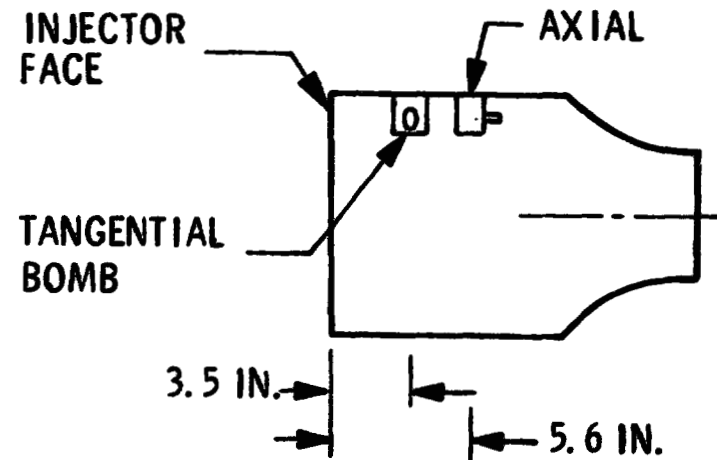
	<u>$I_{sp\infty}$</u>	<u>INSULATED T MAX</u>
CURRENT BEST ASSESSMENT	310.2 OR 310.0	2425° F 2400° F
	(1 SEC I_{sp} = 100° F)	
POTENTIAL IMPROVEMENTS		
CHAMBER LENGTH OPTIMIZATION (LOWER c^* TESTING TASK IX)	310.0	2250° F
INJECTOR IMPROVEMENTS (ALUMINUM INJECTOR NO. 2)	OR	2450° F
VORTEX IMPROVEMENTS		

FIGURE VI-8

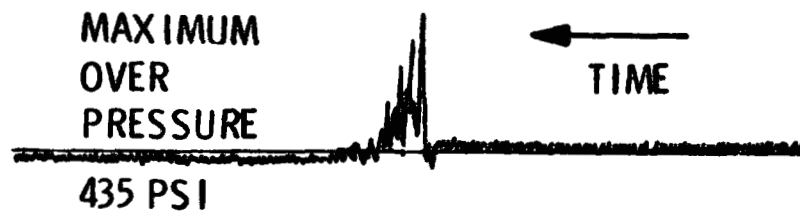
SS INJECTOR No. 1 BOMB TEST

RUN NO.	P _c PSIA	O/F	%	BOMB LOCATION	DAMP TIME MS
4484	125.0	1.67	7.3	AXIAL	3.5
4485	108.9	1.40	7.3	TANGENTIAL	3.5
4486	106.6	1.80	7.5	TANGENTIAL	3.2
4487	128.7	1.60	7.9	TANGENTIAL	5.0
4488	131.7	1.80	7.5	TANGENTIAL	5.8

BOMB LOCATIONS
(10 GRAIN PETN)



RESPONSE TO TANGENTIAL BOMB



RUN NO. 4484

FIGURE VI-9

Bell Aerospace Company

F. Acoustic Damper Stability Testing

A series of tests were conducted in the bomb test chamber using aluminum injector #1. This program was initially defined to be a screening program where a general idea of the 10 inch flat face injector combustion stability could be examined. The projected program was designed to make several bomb tests, modify the damper as required to obtain stability and retest. Originally, 4 such iterations were planned. The test results were somewhat different as the initial design produced stable results and the additional tests took the form of limit and alternate operating condition examinations.

The damper arrangement tested is shown in Figure VI-10. The damper consists of 8 deep and 4 shallow grooves at the injector periphery. The 8 deep grooves were to damp the first tangential mode and the 4 shallow grooves for the third tangential or first radial modes. Actually, the shallow damper slots were sized for the mid point between the third tangential and first radial, these frequencies being only a few hundred cycles/second apart.

A sketch of the bomb chamber tested is shown in Figure VI-11. The data obtained is included in Table II.

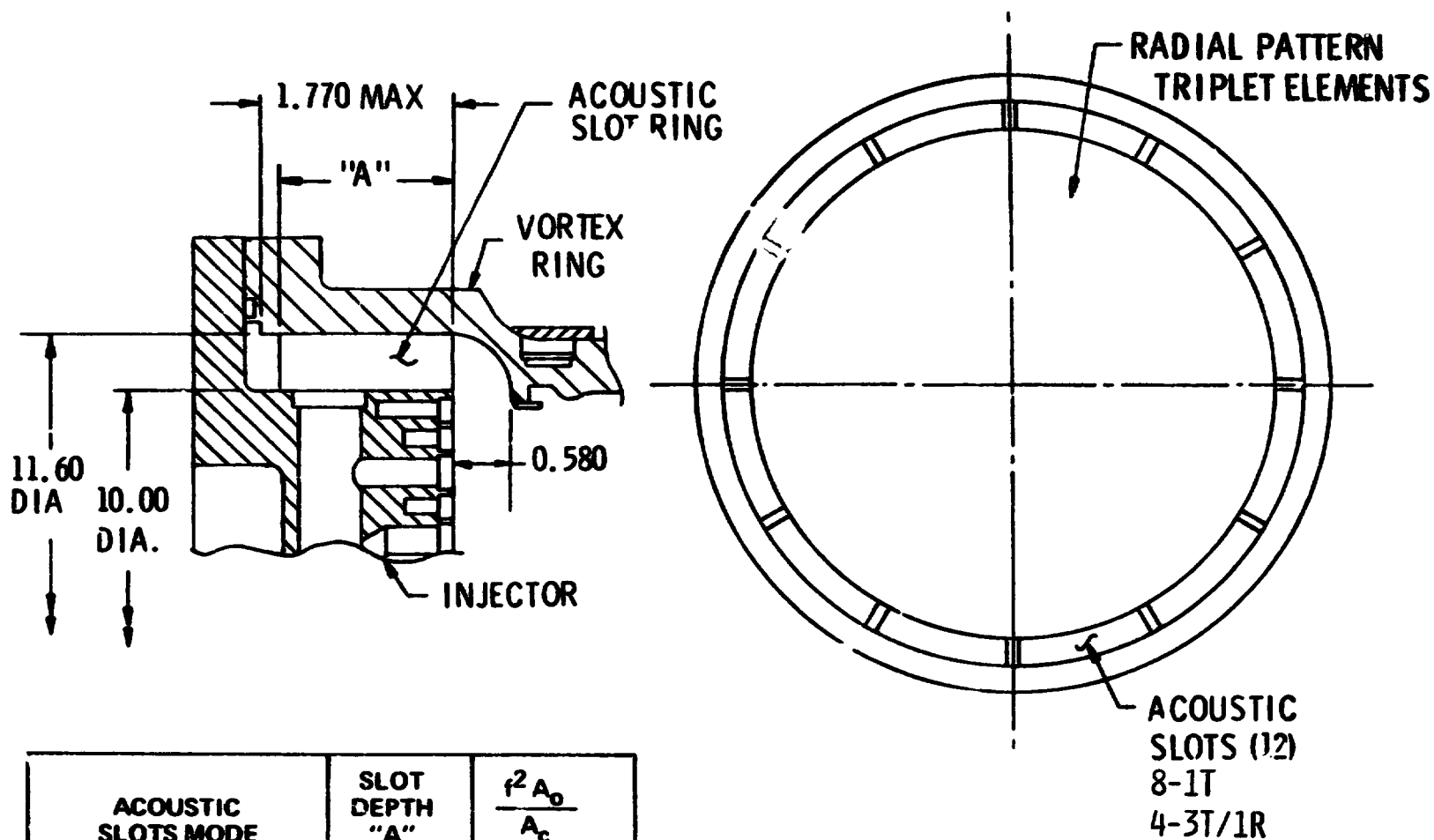
All tests produced stable results. Over pressures with the bombs used appeared to be sharp enough and of such magnitude as to produce stringent damping requirements. The bombs were 10 grain PETN/RDX and were detonated in two positions in the chamber.

Two bombs per test were normally used except when either an unusual test condition, or bomb installation change was incorporated.

Initial testing was conducted with ambient propellants as would be normally encountered with the non-regen columbium chamber. The test matrix evaluated included the normal variations in mixture ratio and chamber pressure.

Successful stabilization of this matrix allowed several added tests to be conducted and these were made at longer times into a test, to ensure a steady state operation other than transient, and to evaluate increased fuel temperature, to simulate regen operation. No difference in the damping capability of the thrust chamber was noted with the later tests. The data obtained during this testing is listed in Table I.

ALUMINUM INJECTOR ASSEMBLY - DESIGN DATA



ACOUSTIC SLOTS MODE	SLOT DEPTH "A"	$\frac{f^2 A_o}{A_c}$
1ST TANGENTIAL	1.650	1.007
3RD TANGENTIAL OR 1ST RADIAL	0.769	2.34

FIGURE VI-10

BOMB TEST ASSEMBLY

C-3

VI-11

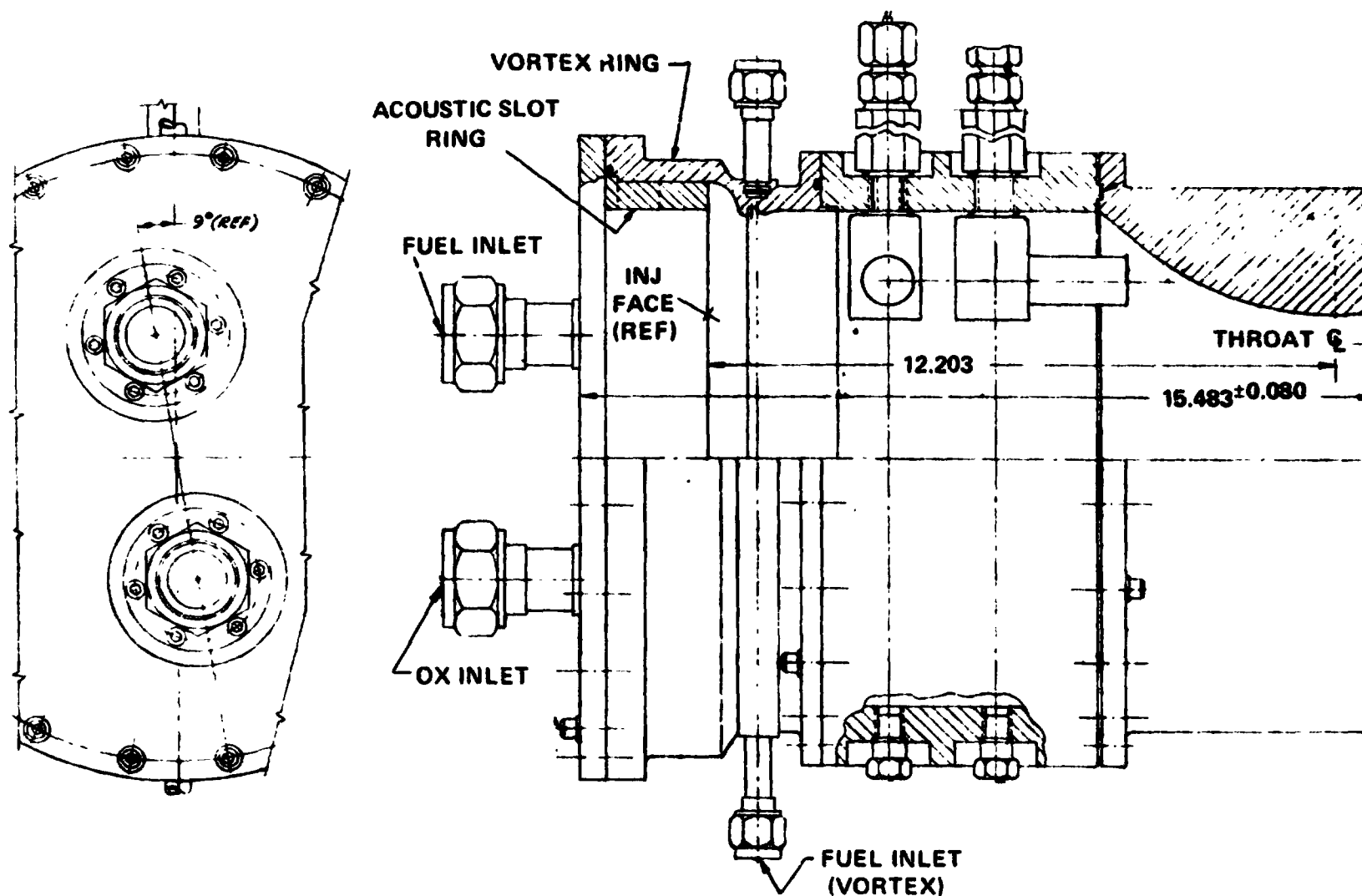


FIGURE VI-11

BELL AEROSPACE COMPANY
TABLE II
FLAT FACE INJECTOR BOMB TESTS
(ALUMINUM INJECTOR NO. 1)

TEST NO.	P _C PSIA	O/F	% W VORTEX	F11T °F	O11T °F	BOMB LOCATION	MAX OVER- PRESSURE PSI	BOMB TIME SEC.	RECOVERY TIME MILLISECONDS
4502	127	1.67	2.9	78	75	1	512	.48	3.0
4503	127	1.65	2.9	76	74	2	524	.48	3.0
4504	126	1.83	0.0	78	74	2	512	.48	3.0
						1	488	.75	3.0
4506	105	1.44	3.3	84	81	2	478	.48	3.0
						1	413	.75	2.5
4507	106	1.68	3.2	84	84	2	435	.48	2.5
						1	293	.75	2.5
4508	137	1.42	3.0	84	81	2	315	.48	2.5
						1	337	.75	2.5
4509	135	1.81	3.0	87	84	2	450	.48	2.5
						1	567	.75	2.5
4510	127	1.72	2.7	86	85	2	287	.48	2.5
						1	227	--	2.5
4511	127	1.68	2.8	80	77	1	375	2.5	2.0
4513	127	1.73	2.9	72	71	2	213	2.5	2.0
4514	125	1.78	3.0	227	70	2	232	2.5	2.0
4515	127	1.68	3.1	224	73	1	387	2.5	2.0

VI-17

Bell Aerospace Company

G. Conclusions From Bomb Tests

The original objective of this task was to perform a screening of information to indicate dynamic combustion stability could be achieved on a 10 inch diameter OME injector stabilized with acoustic slot type dampers. The task was approached with some concern that the 10 inch diameter chamber would require significantly more damping than previously demonstrated by other contractors at smaller diameters. The test results of this task indicated this concern to be unwarranted, at least within the confines of the tests conducted.

Although the data generated was somewhat meager by previous development program standards, the almost immediate damping of this injector when subjected to the test bombs, indicated excellent results and encouragement that the 10 inch acoustic damper application was warranted. These successful results also provided encouragement that further testing at other operating conditions should be conducted to more adequately examine the full range of OME operating conditions.

Bell Aerospace Company

VII. TASK X - REGENERATIVELY COOLED THRUST CHAMBER DEMONSTRATION

The successful demonstration of the use of the triplet injector with hot fuel allowed the extension of testing with this injector to a regeneratively cooled thrust chamber. The regeneratively cooled channel wall chamber was furnished to the program and the task evaluation consisted of obtaining performance and heat rejection information. The test assembly consisted of the S/N 2 aluminum injector with its associated vortex cooling ring, the channel wall regenerative thrust chamber furnished by Bell, a columbium nozzle extension (to nozzle area ratio of 15) and a propellant valve adopted to the flow quantities for this engine. The nozzle area ratio was determined by the altitude test facility where testing of this assembly was conducted. This altitude test facility was previously rated at 3500# thrust and the throat section of the duct restricted the size of engine operation to the 15 to 1 nozzle area ratio used. The expense of modifying this facility to accept the full size OME nozzle was not considered to be necessary for the preliminary testing scheduled.

A. Test Hardware

The test engine consisted of four basic components including the Injector/Vortex Ring Assembly a channel wall regeneratively cooled thrust chamber, a nozzle extension (area ratio 6 to 15) and a Bipropellant Valve. An assembly drawing of the company sponsored thrust chamber is shown in Figure VII-1 with the injector shown in Figure VII-2. The acoustic damper vortex ring detail is included as Figure VII-3. The regeneratively cooled chamber is a channel wall configuration at a nominal internal diameter of (10) inches as shown in Figure VII-4.

The main portion of the inner liner was machined from a 304-L stainless steel forged billet. This part of the liner contains 60 flow channels of a constant depth of 0.045 inch and vary in width from 0.248 inch to 0.469 inch. The lands are a constant width of 0.060 inch. The hot gas side wall thickness of the inner liner is .050 inch.

A flange ring is EB welded to the forward end of the inner liner. A flanged concial ring containing 120, 1/8 inch diameter coolant holes is EB welded to the aft end of the inner liner. Both these flanged rings are constructed of 304-L stainless steel.

VII-2

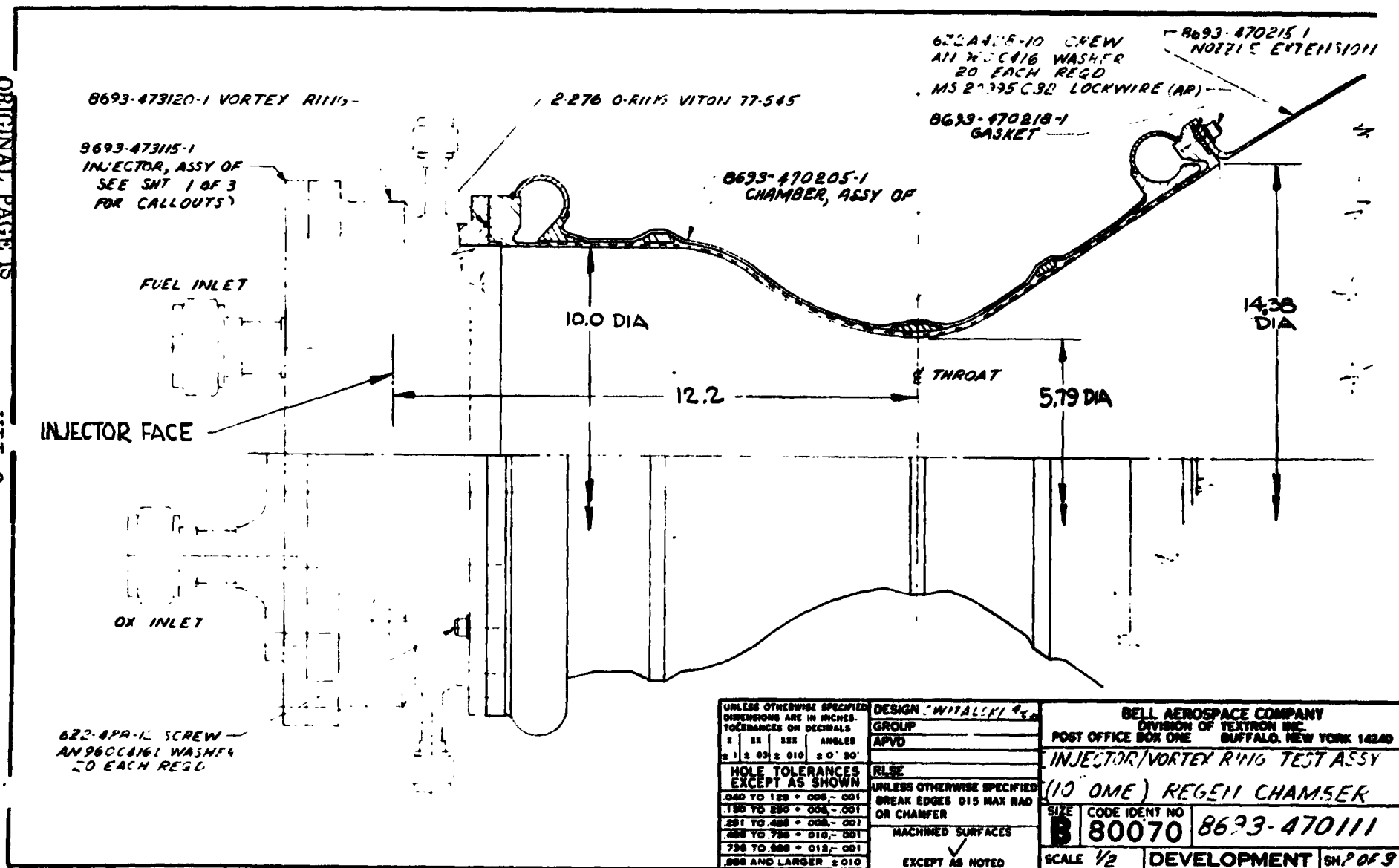
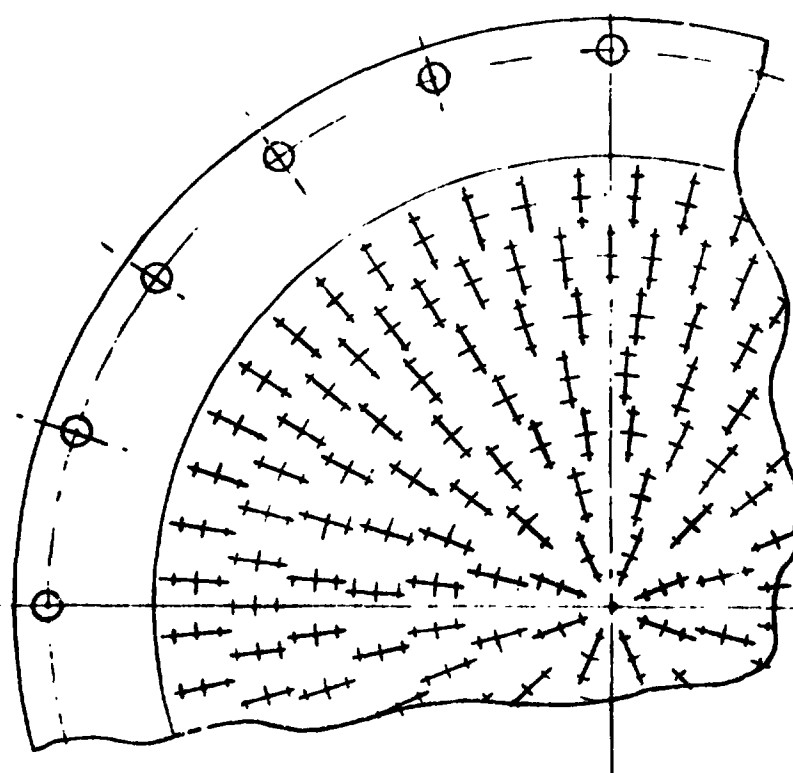
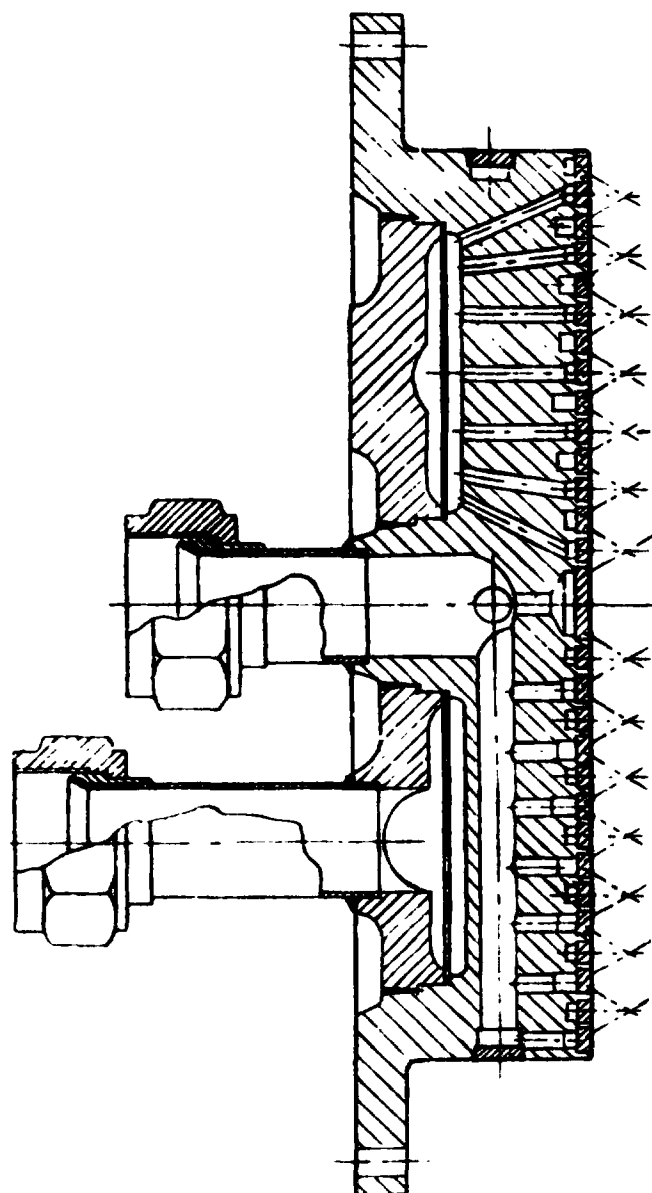


FIGURE VII-1

10 INCH DIA. ALUMINUM INJECTOR No. 2

VII-3

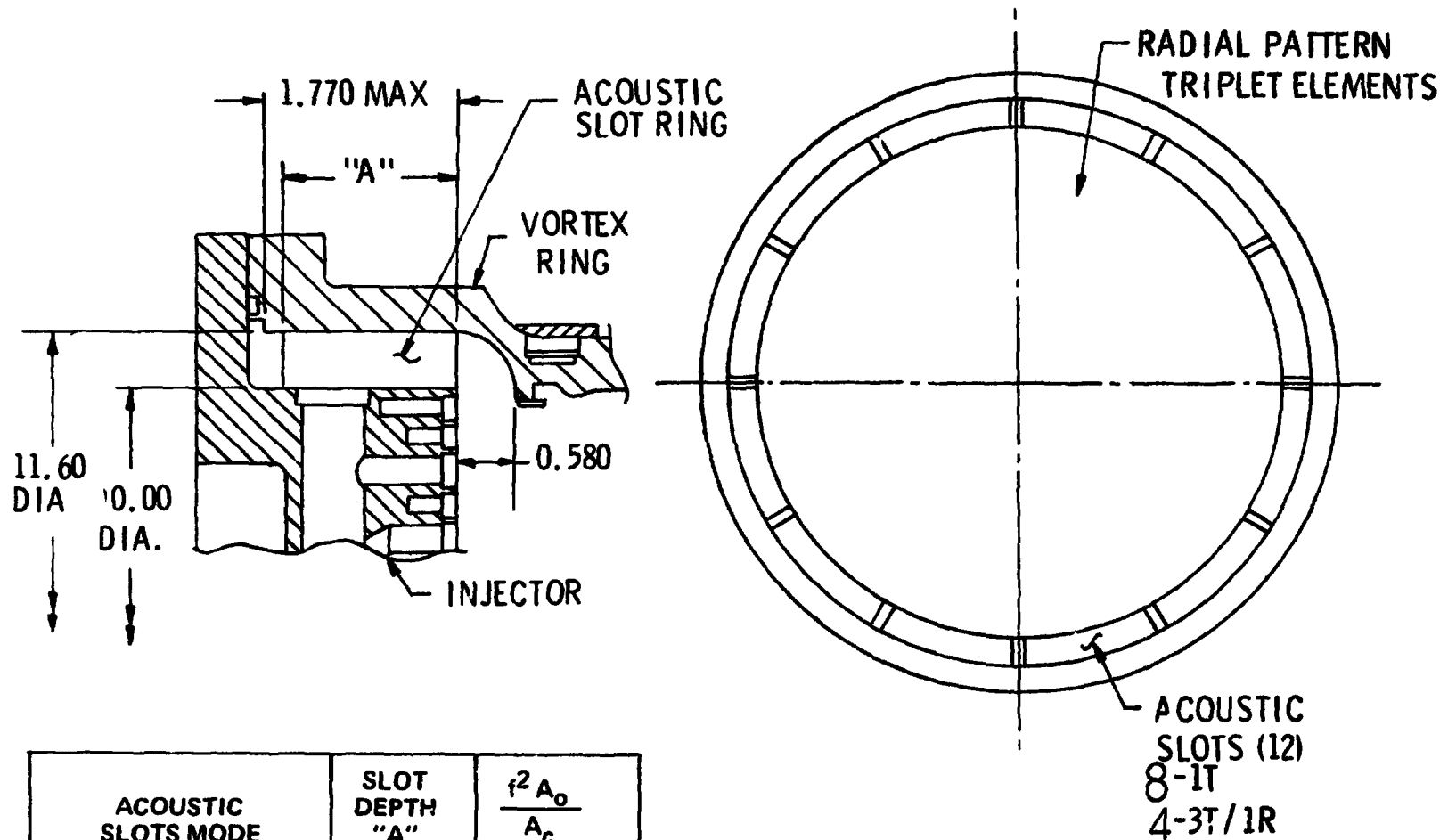


196 TRIPLETS
ORIFICE $\Delta P = 40$ PSI

FIGURE VII-2

Bell Aerospace DIVISION OF **Textron**

ALUMINUM INJECTOR ASSEMBLY - DESIGN DATA



ACOUSTIC SLOTS MODE	SLOT DEPTH "A"	$\frac{f^2 A_o}{A_c}$
1ST TANGENTIAL	1.650	1.007
3RD TANGENTIAL OR 1ST RADIAL	0.769	2.34

FIGURE VII-3

DEMONSTRATION CHAMBER ASSEMBLY

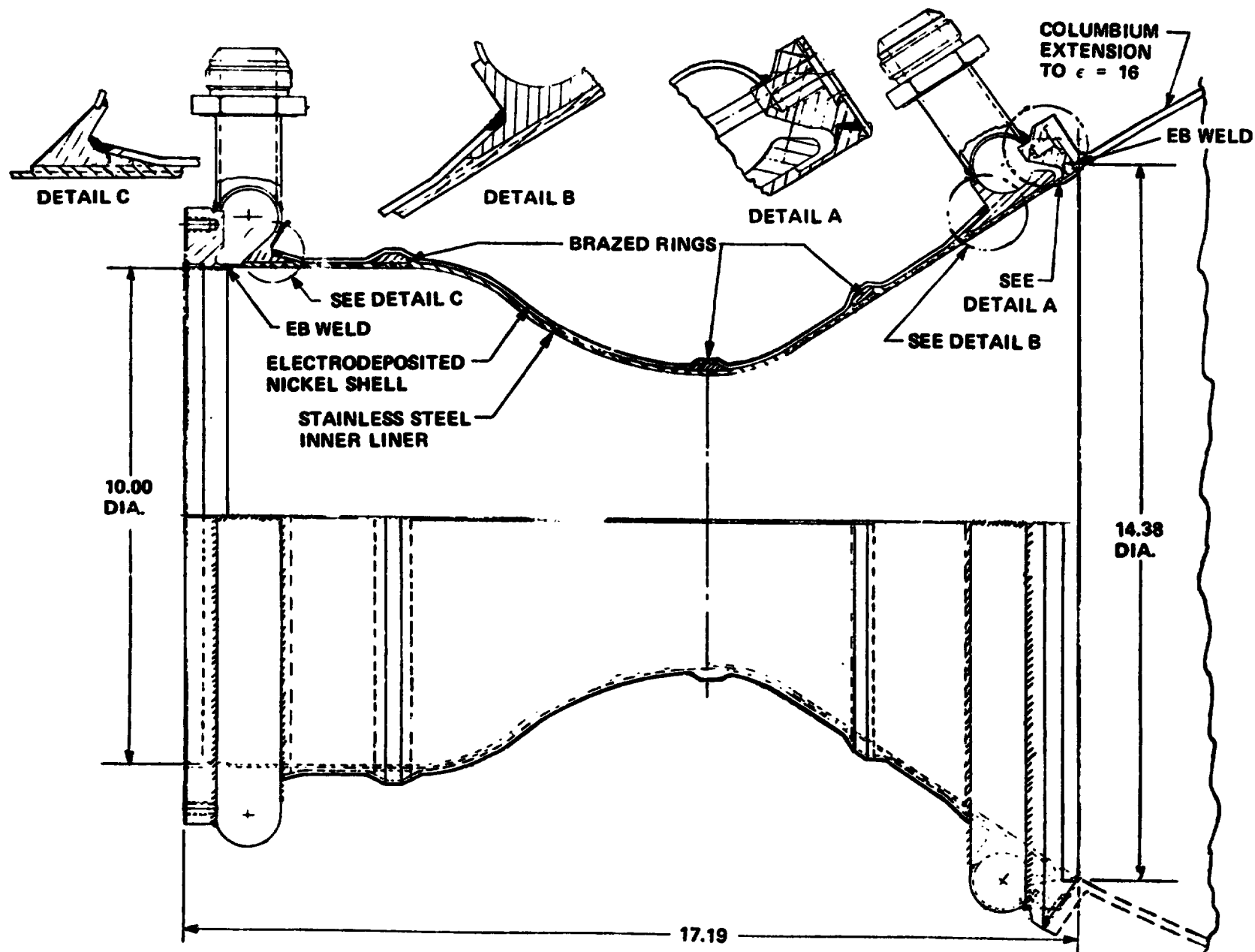


FIGURE VII-4

Bell Aerospace Company

Four stainless steel reinforcement rings are provided over the lands of the inner liner. The outer shell is fabricated by electrodepositing pure nickel over the lands, channels and flange ends. The approximate thickness of the shell is 0.055 inches. A stainless steel torus manifold is welded at each flange end which closes out the coolant circuit. Propellant line connection fittings are welded to each torus manifold. The exit area ratio of the channel nozzle is 6:1.

A columbium nozzle extension was used for all testing at BAC with an exit area ratio of 15:1. This columbium C-103 nozzle extension is coated with a silicide 512-E coating and interfaces with the regenerative chamber at an area ratio of approximately 6:1. (Shown in Figure VII-5.) The interface with the regenerative chamber is sealed using a velbestos gasket.

The engine valve is a LM ascent valve (Bell P/N 8258-472225-23 valve assembly) with the exception that a normally open solenoid valve has been installed on the valve assembly. The reason for the addition of this solenoid is to augment the actuator spring load. This was required due to test cell configurations and the use of the LM valve for OME development tests. Feed pressures up to 350 psig were required which resulted in higher than normal ball and shaft torque loadings. Because of this increase, the actuator return springs were marginal in closing of the valve. See Figure VII-6 for a schematic of this solenoid installation.

The normally opened solenoid is electrically connected in parallel with the four LM valve solenoids. When the four LM solenoids are deactuated closed, the actuating pressure is vented overboard which permits the actuator return springs to start closing of the balls. At the same time, the N.O. solenoid is de-energized opened which permits a present N₂ gas pressure to enter the spring cavity of each actuator which helps the spring to insure full closing of each ball. See Figure VII-7 for the recommended actuating pressure and spring cavity pressure for various inlet feed pressure conditions.

The nominal pressure drop for the valve at the 6000 lbf OME condition is as follows:

<u>Oxidizer</u>	<u>Pressure Drop (psid)</u>
Filter Assembly	14.0
Flow Bodies	<u>4.0</u>
Total	18.0

SCHEMATIC OF SOLENOID INSTALLATION

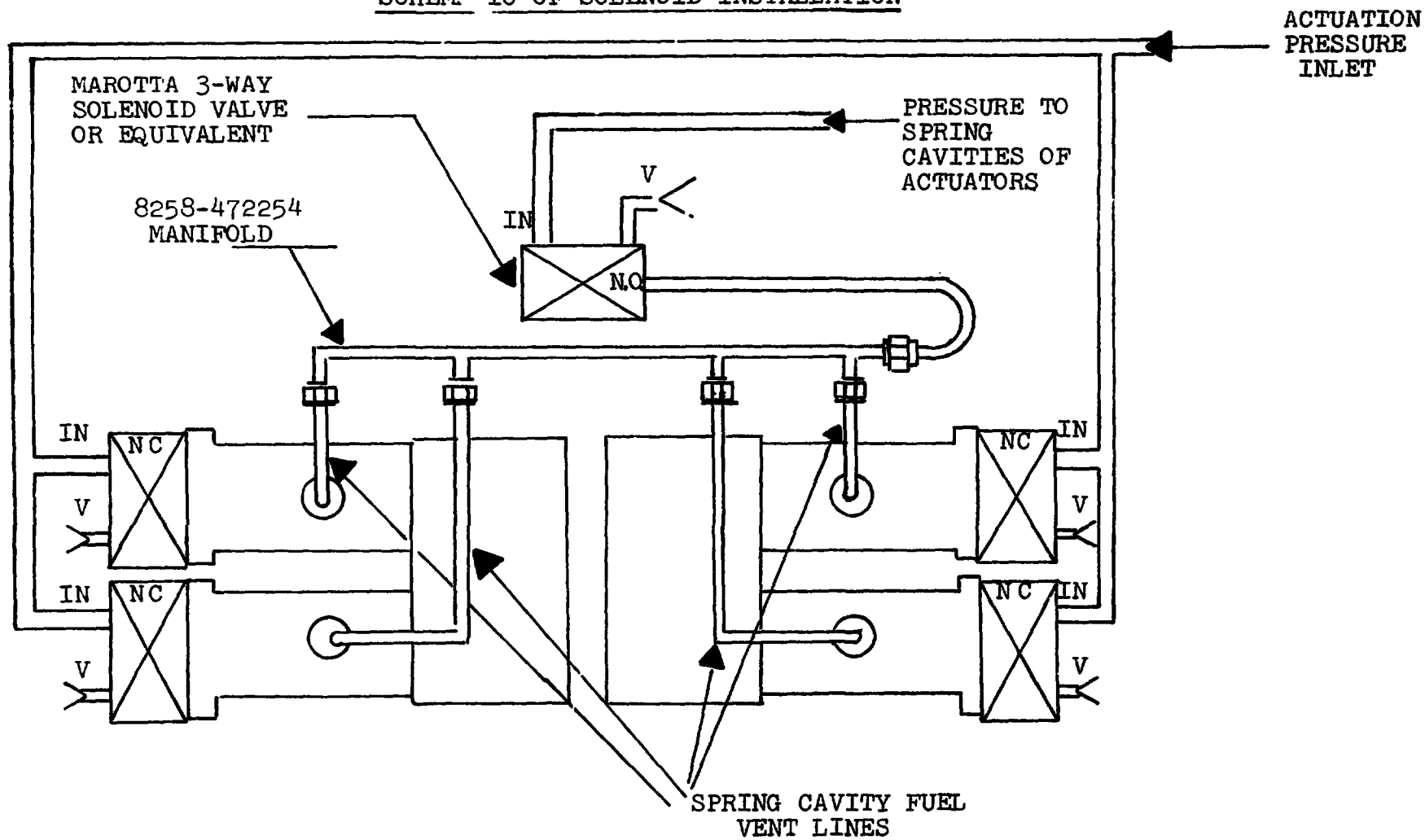


FIGURE VII-6

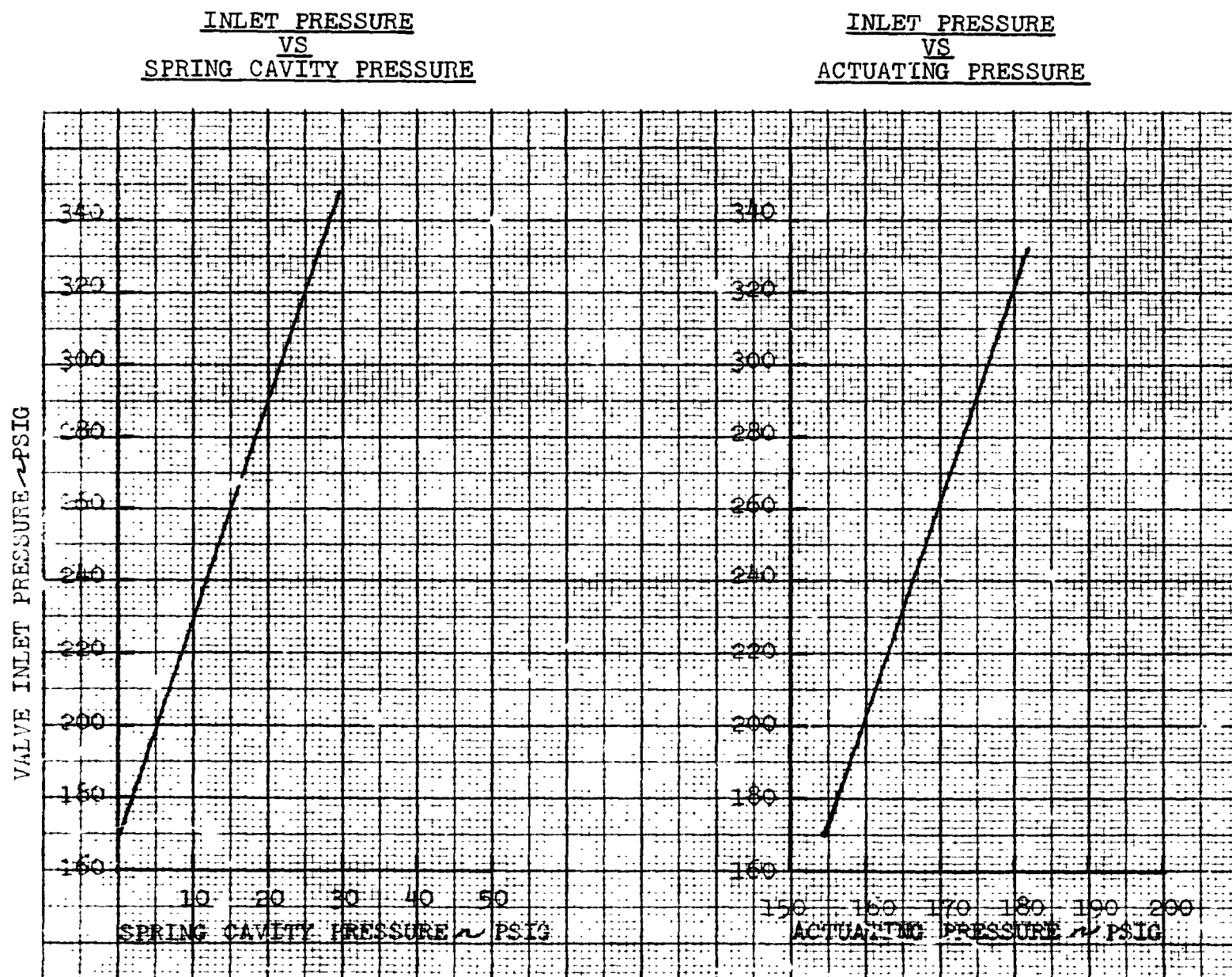


FIGURE VII-7

Cell Aerospace Company

<u>Fuel</u>	<u>Pressure Drop (psid)</u>
Filter Assembly	8.2
Flow Bodies	<u>2.8</u>
Total	11.0

<u>Name</u>	<u>Part Number</u>
Aluminum Injector S/N 2	8693-4, 3050-1
Acoustic Ring (1T and 3T/1R)	8693-743133-1
Vortex Ring	8693-473140-3
Channel Wall Regenerative Chamber	8693-470205-1
Columbium Nozzle Extension ($\epsilon = 15:1$)	8693-470215-1
Adapter (Nozzle Extension) ($\epsilon = 72:5$)	8693-470228-1

B. Regeneratively Cooled Thrust Chamber Test Results

The regeneratively cooled 6,000 pound thrust 10 inch diameter channel wall chamber was test fired in accordance with the test plan outlined in Report 8693-928002. Eighteen test firings with an accumulated run time of 199 seconds were conducted somewhat exceeding the 17 test firings with an accumulated run time of 158 seconds called for in the Test Plan.

The attached Table I shows the comparison of planned to actual test conditions.

The main changes were in test series II. The high/low P_c tests were replaced by high/low O/F ratio tests, and 15 and 25 second tests were made prior to the 30 second test. The effect of mixture ratio changes were considered to be of more importance at this time than the chamber pressure series. The 15 and 25 second tests were added to obtain a better definition of hardware thermal characteristics prior to the 30 second test.

Table II is a summary of the test data.

The high vortex flow at nominal chamber pressure (125 psia) and nominal mixture ratio (1.65) was 4.1% with specific impulse for $\epsilon = 75:1$ of 313.8 $\frac{\text{lb}_f\text{-sec}}{\text{lb}_m}$. The regen chamber jacket temp-

erature rise was 90°F and the jacket pressure drop was 27 psid,

TABLE I

REGEN CHAMBER TESTING

TEST SERIES	TEST NO.	TEST DESCRIPTION	R ₀ /F	P _c PSIA	ℓ %	TEST SERIES	TEST NO.	TEST DESCRIPTION	R ₀ /F	P _c PSIA	ℓ %			
IA	1	1.5 sec. checkout	1.65	125	4	IA	1	2.0 sec. checkout	1.69	126	4.1			
	2	1.5 sec. checkout					2	9.2 sec. checkout	1.70	124	4.1			
	3	5 sec. checkout					3	10.0 sec. perf.	1.68	124	4.1			
	4	10 sec. perf. eval.					4	10.3 evaluation	1.69	133	4.1			
	5	10 sec. perf. eval.		5			9.9 evaluation	1.68	114	4.1				
	6	10 sec. perf. eval.		115										
			135				41.4 Total							
IB	7	5 sec. checkout	1.65	125	4/2	IB	6	4.9 sec. checkout	1.65	124	4/1.9			
	8	5 sec. checkout					7	10.0 sec. per. eval.	1.65	124	4/1.9			
	9	10 sec. perf. eval.					8	10.2 sec. per. eval.	1.65	133	4/1.9			
	10	10 sec. perf. eval.					9	10.2 sec. per. eval.	1.66	113	4/1.9			
	11	10 sec. perf. eval.		10			15.0 sec. per. eval.	1.64	125	4.1				
	12	15 sec. perf. eval.		115										
			125	4			50.3 Total							
II	13	5 sec. checkout	1.65	125	4/2	II	11	1.8 sec. checkout	1.58	126	4.1			
	14	10 sec. perf. eval.					12	5.0 sec. checkout	1.62	124	4/1.9			
	15	10 sec. perf. eval.					13	10.3 sec. per. eval.	1.63	123	4/1.9			
	16	10 sec. perf. eval.					14	10.1 sec. per. eval.	1.46	124	4/2			
	17	30 sec. perf. eval.		135			4		15	9.9 sec. per. eval.	1.80	124	4/1.8	
									16	15.1 sec. per. eval.	1.65	124	4/1.9	
			125				17	25.2 sec. per. eval.	1.64	125	4/1.9			
							18	30.0 sec. per. eval.	1.62	125	4/1.9			
								107.4 Total						

TOTAL

199.1

BELL AEROSPACE COMPANY
TABLE II
6K OME REGEN CHAMBER
TEST SUMMARY AT ALTITUDE

ORIGINAL PAGE IS
OF POOR QUALITY

TEST SUMMARY AT ALTITUDE																	REGEN FUEL	CHAMBER JACKET					
Date	Test	Dur.	Data Pt.	Pc corr	R	ρ	C* corr	η_{C^*}	Isp test	Isp ∞	Isp ∞	Isp ∞	Isp ∞	F test	Cf	CHT		PYRO MAX.	NET		Temp Rise	Press Drop	
																Therm.	Max.		Therm.	Max.			
1973	IBN-	Sec.	Sec.	PSIA	o/f	%	ft/sec	%	$\epsilon=15/1$	$\epsilon=15/1$	$\epsilon=75/1$	$\epsilon=75/1$	$\epsilon=75/1$	lb ϵ	$\epsilon=75/1$	No.	°F	°F	No.	°F	°F	°F	°F
9/16	870	2.0	Checkout	Firing																			
9/16	871	9.2	8.6	124.4	1.696	4.13	5593	97.90	271.5	280.0	314.6	316.98	5107	1.811	1	151	NA	NA	NA	97.9	25.0		
9/17	872	10.0	9.4	124.2	1.685	4.13	5572	97.53	271.1	279.5	314.0	316.39	5101	1.815	1	147	NA	NA	NA	94.2	24.9		
9/17	873	10.3	9.7	133.4	1.693	4.08	5574	97.57	272.0	280.4	315.1	316.74	5490	1.820	1	149	NA	NA	NA	95.7	23.6		
9/18	874	9.9	9.3	114.3	1.684	4.11	5568	97.47	270.7	279.0	313.5	316.61	4688	1.813	1	149	NA	NA	NA	92.5	21.3		
9/19	875	4.9	Checkout	Firing																			
9/19	876	10.0	9.4	123.8	1.653	1.91	5627	98.51	273.5	281.8	316.7	316.80	5074	1.812	1	157	NA	8	1399	113.3	27.0		
9/19	877	10.2	9.6	133.0	1.646	1.92	5617	98.20	273.6	282.1	317.0	316.40	5466	1.817	1	158	NA	6	1492	111.0	33.1		
9/19	878	10.2	9.6	113.4	1.662	1.90	5590	97.80	272.4	281.0	315.7	316.57	4662	1.818	1	158	NA	8	1367	114.2	21.7		
9/20	879	15.0	14.0	125.0	1.636	4.11	5575	97.61	270.6	279.3	313.8	316.12	5104	1.812	1	154	1711	8	1604	99.0	27.1		
9/27	880	1.8	Checkout	Firing																			
9/28	881	5.0	Checkout	Firing																			
9/28	882	10.3	9.7	122.8	1.631	1.89	5626	98.51	272.4	281.1	316.0	316.15	5019	1.809	2	173	NA	6	1416	114.5	25.9		
9/28	883	10.1	9.5	124.1	1.458	2.03	5615	98.84	270.9	279.5	314.0	314.18	5049	1.801	2	165	NA	6	1350	104.1	30.3		
9/28	884	9.9	9.3	123.8	1.801	1.78	5610	98.36	272.9	281.8	316.6	316.55	5083	1.817	2	179	NA	6	1456	124.5	23.7		
9/28	885	15.1	14.5	123.5	1.653	1.88	5622	98.42	271.8	281.6	316.4	316.49	5035	1.812	2	175	1673	7	1597	119.0	25.9		
10/1	886	25.2	10.0	124.4	1.643	1.89	5623	98.44	272.6	281.3	316.0	316.04	5090	1.810	2	170	NA	5	1451	115.9	26.2		
			20.0	125.3	1.643	1.88	5621	98.41	271.1	281.4	316.1	--	5099	1.811	1	173	NA	7	1681	119.2	26.7		
			24.0	125.4	1.645	1.87	5621	98.40	270.5	281.3	316.1	--	5090	1.811	1	178	1761	7	1701	119.9	26.8		
10/1	887	30.0	10.0	125.4	1.618	1.90	5626	98.53	272.8	281.6	316.4	316.36	5131	1.811	2	171	NA	5	1448	117.3	26.0		
			20.0	124.5	1.632	1.88	5622	98.41	271.2	281.6	316.4	--	5065	1.812	2	175	NA	7	1665	122.0	25.4		
			25.0	124.6	1.620	1.87	5623	98.47	270.3	281.4	316.2	--	5056	1.811	2	176	NA	7	1700	121.9	25.9		
			29.0	124.7	1.614	1.85	5625	98.52	269.8	281.5	316.3	--	5048	1.810	2	176	1784	7	1718	122.2	26.0		

(1) Pc correction factor 0.981

(2) Normalized to 1.9% ρ film cooling and Pc = 125 psia

Bell Aerospace Company

while the maximum skin temperature was 154°F and occurred at the injector end of the chamber for the 15 second firing. The maximum indicated temperature in the columbium nozzle extension was 1711°F.

The low vortex flow at nominal chamber pressure and mixture ratio was 1.9% with a specific impulse for $\epsilon = 75/1$ of 316.4 $\frac{\text{lb}_f - \text{sec}}{\text{lb}_m}$. The regen chamber jacket temperature rise was

119°F and the jacket pressure drop was 26 psi, while the maximum skin temperature was 175°F and occurred at the injector end of the chamber for the 15 second firing. The maximum indicated temperature on the columbium nozzle extension was 1597°F.

The 30 second duration firing at nominal chamber pressure and mixture ratio indicated the following performance values:

$I_{sp}\epsilon = 75/1$	= 316.3 $\frac{\text{lb}_f - \text{sec}}{\text{lb}_m}$
Jacket ΔT	= 122°F
Jacket ΔP	= 26 psi
Skin Max Temp	= 176°F
Extension Max Temp	= 1718°F

Very little performance difference is noted between the 15 second and 30 second runs indicating that the engine is operating at or near equilibrium. It is also noted that there is a specific impulse gain of 2.5 $\frac{\text{lb}_f - \text{sec}}{\text{lb}_m}$ when vortex flow is reduced from 4.1% to 1.9%.

REGENERATIVELY COOLED CHAMBER PROPELLANT FLOW SCHEMATIC

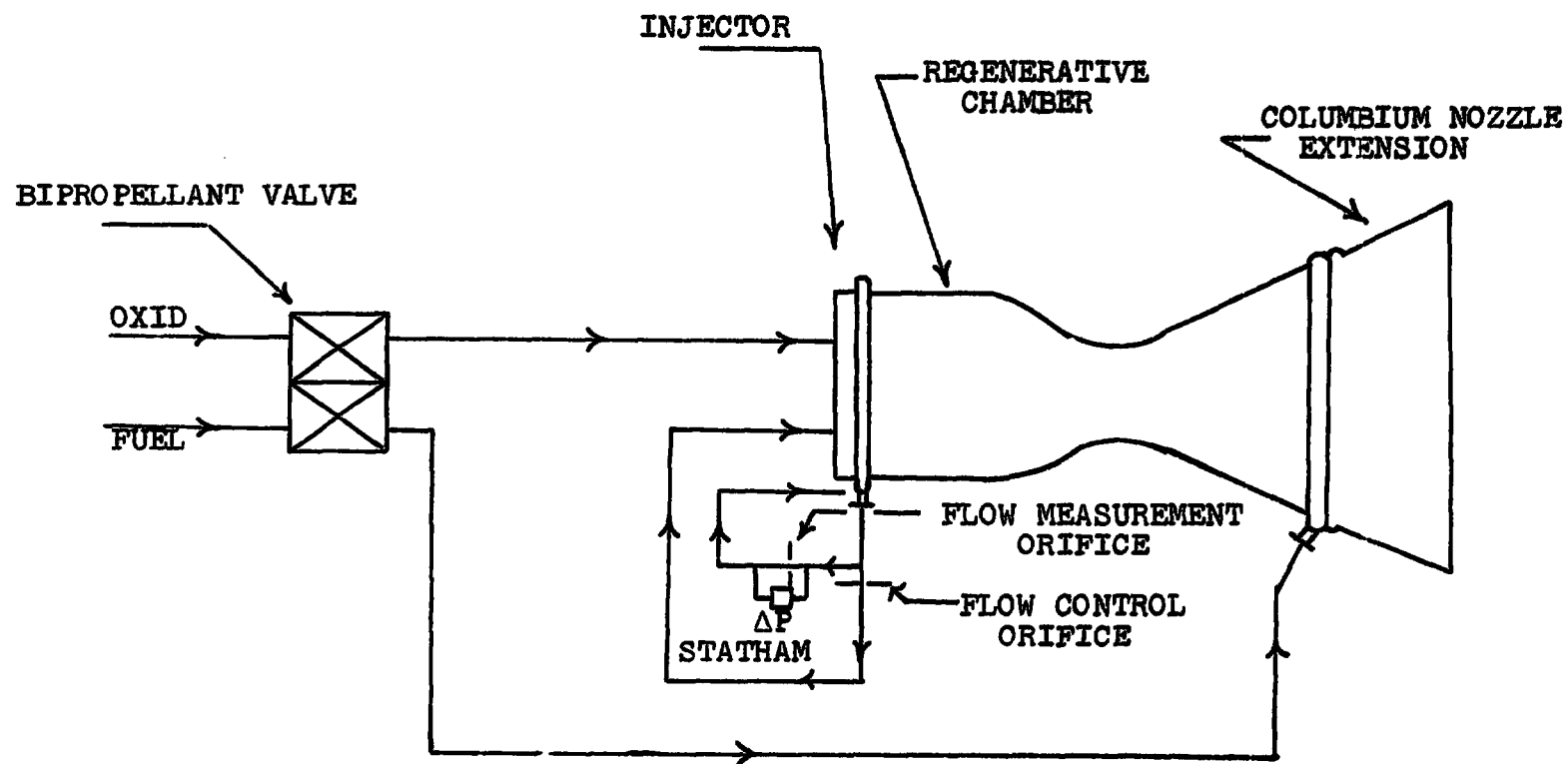


FIGURE VII-8

Bell Aerospace Company

1. Performance

The performance data are presented in plots of specific impulse and characteristic velocity versus mixture ratio for all test durations of 10 seconds or greater. The specific impulse versus mixture ratio is shown in Figure VII-9 for fuel vortex percentages of 4.1% and 1.9% at high, nominal and low chamber pressure.

A similar plot for characteristic velocity versus mixture ratio is given in Figure VII-10.

The specific impulse and characteristic velocity versus test duration for the 30 second test (LBN-887) is shown in Figure VII-11. Stabilization of specific impulse was achieved after approximately 5 seconds duration. Characteristic velocity shows a slight decrease with duration due to apparent throat area change which was not applied to these data.

2. Heat Rejection

The fuel jacket temperature rise effect versus mixture ratio is shown in Figure VII-12 for the two vortex flow conditions and at the three chamber pressure levels. These data are presented at the 10 second point. The fuel jacket temperature rise versus test duration for the 30 second test is given in Figure VII-13. The total chamber heat load vs chamber pressure is shown in Figure VII-14.

3. Shell and Nozzle Temperature

The external shell of the regeneratively cooled chamber was instrumented with a total of fifteen (15) chromel/alumel thermocouples as shown in Figure VII-15. Thirteen (13) of these being located on the outer surface of the chamber in two circumferential locations (12 o'clock and 9 o'clock) and two (2) being located on the chamber flange. The injector was instrumented with two (2) flange thermocouples. The columbium nozzle extension was instrumented with three (3) chromel/alumel and six (6) platinum/platinum-rhodium thermocouples for all tests.

Bell Aerospace Company

OME PERFORMANCE

$I_{SP \infty}$ VS O/F

$\epsilon = 75:1$

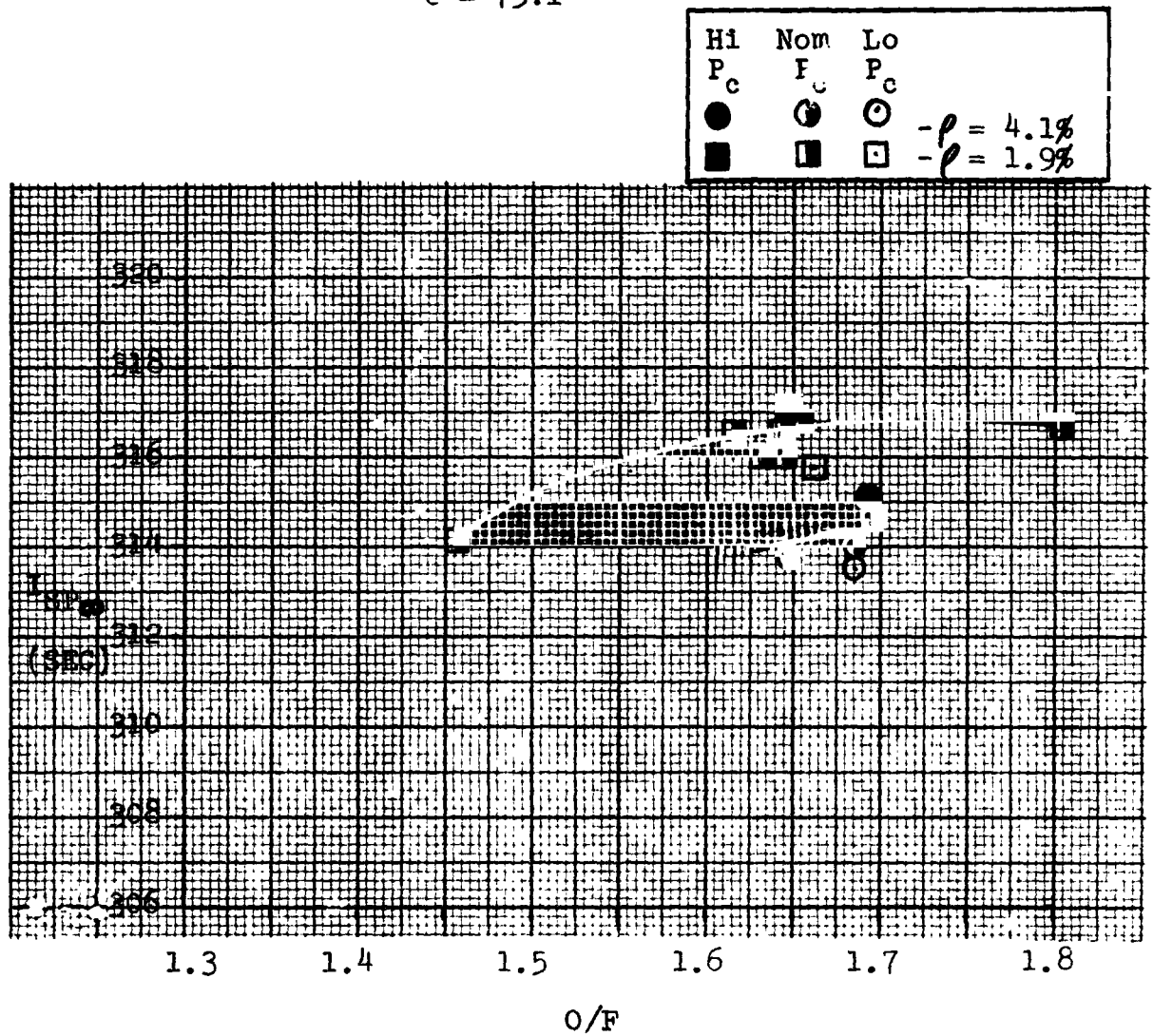


FIGURE VII-9

OME PERFORMANCE

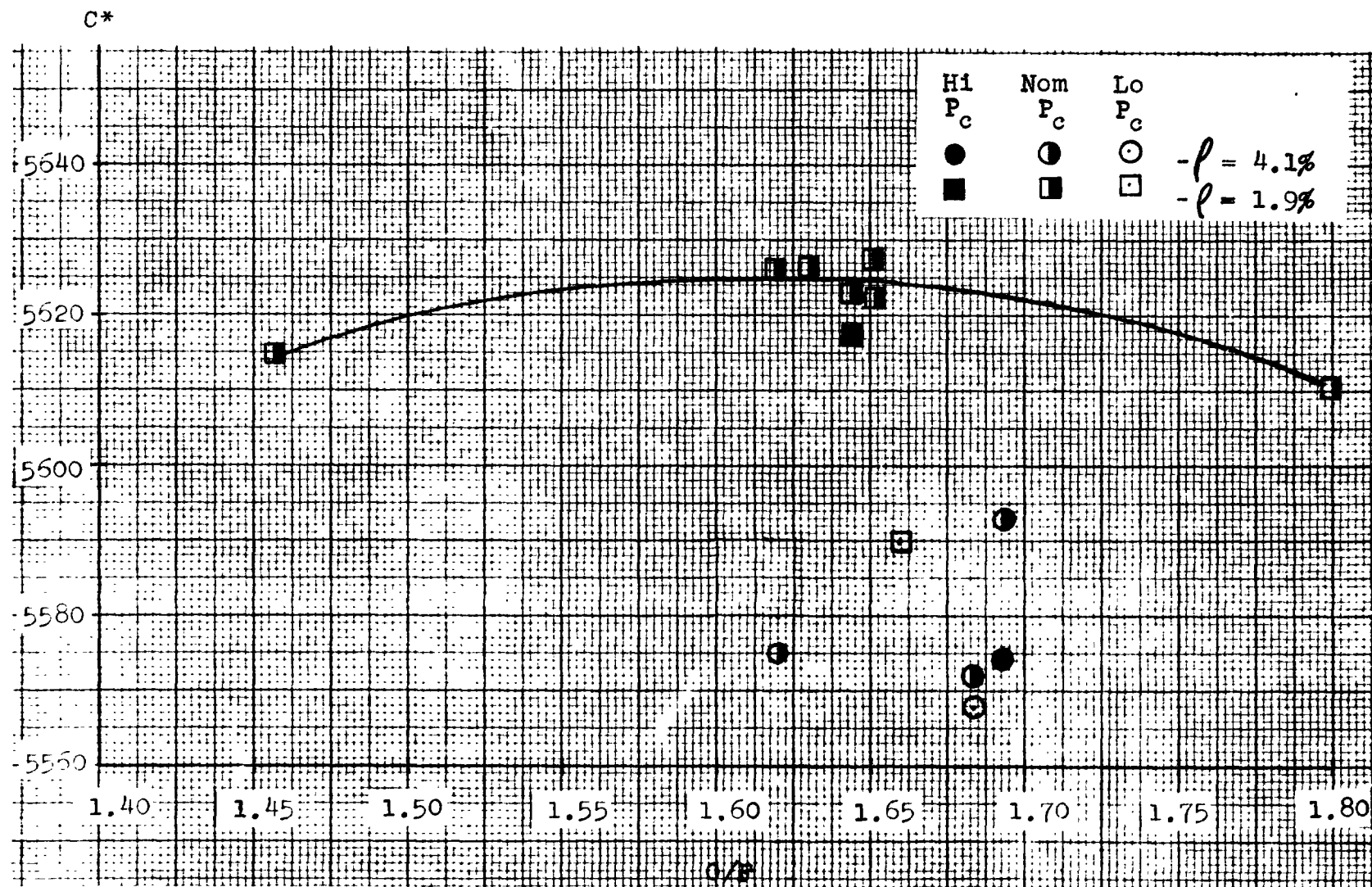
C* VS O/F

FIGURE VII-10

81-IIA

I_{SP} ($\epsilon = 75$)

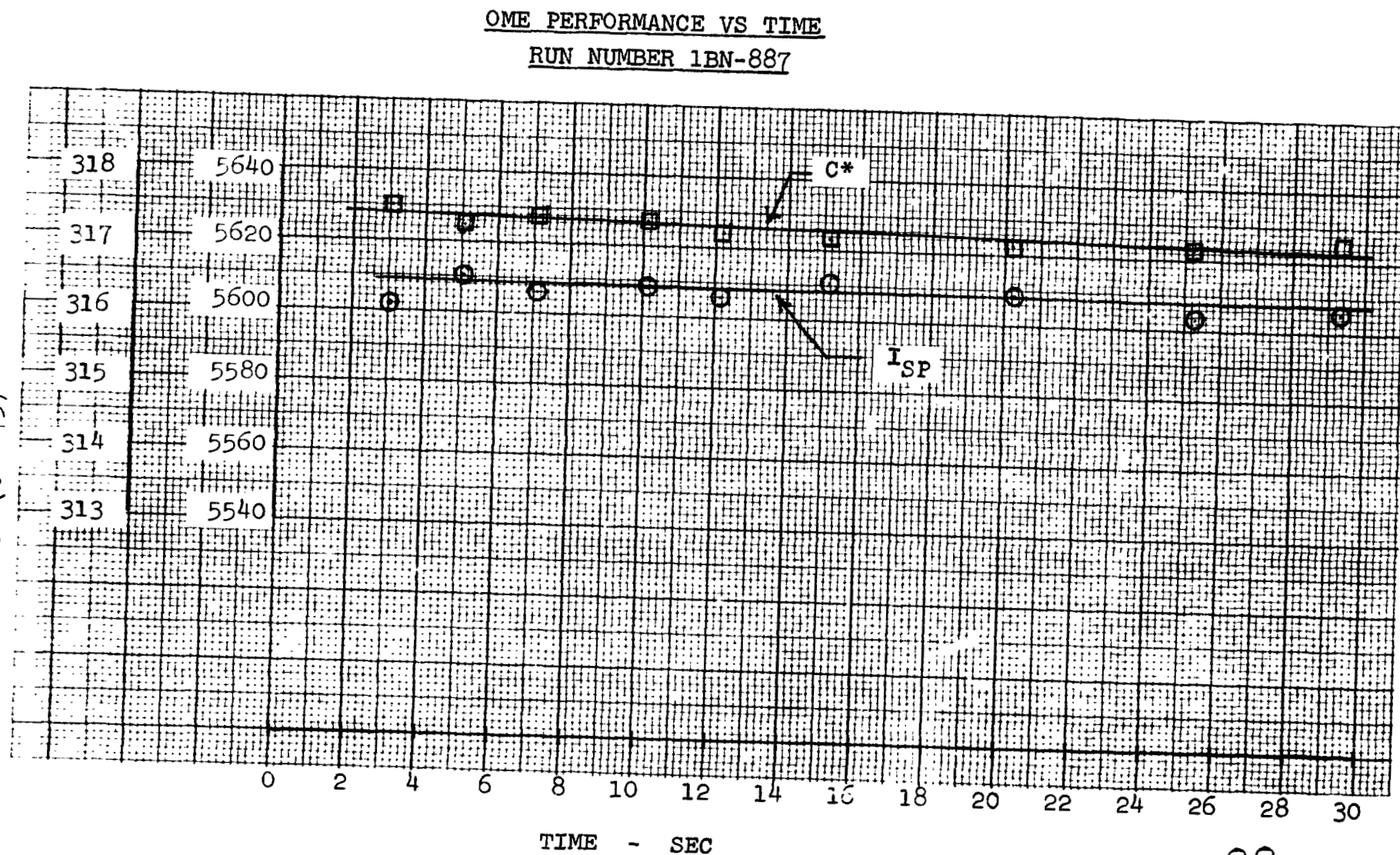


FIGURE VII-11

ORIGINAL PAGE IS
OF POOR QUALITY

OME PERFORMANCE

JACKET FUEL TEMP
RISE VS O/F
10 SEC DATA POINT

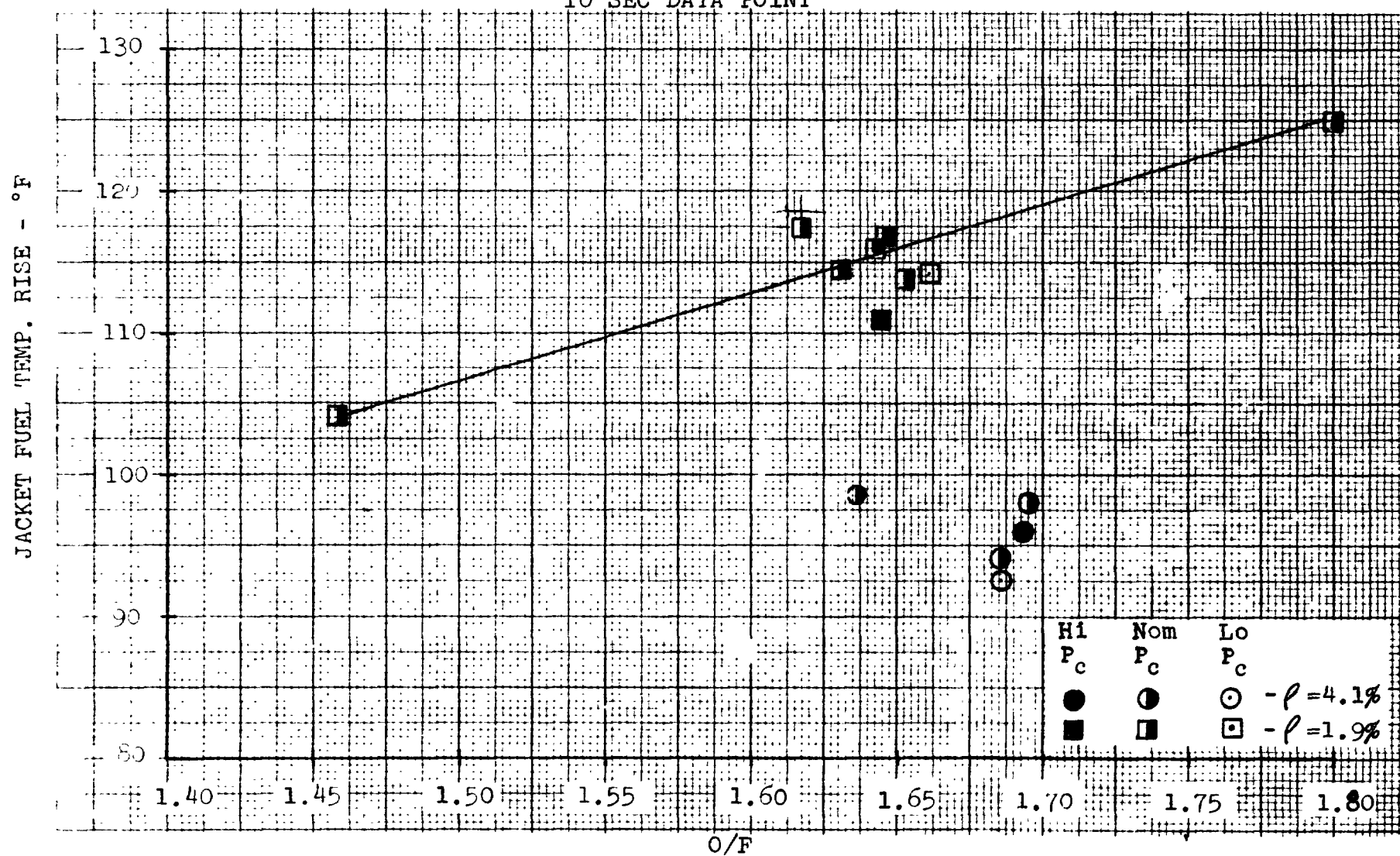


FIGURE VII-12

OME-REGENERATIVE CHAMBER
FUEL JACKET TEMPERATURE RISE
VS TIME
RUN NO. 1BN 887-30 SECONDS

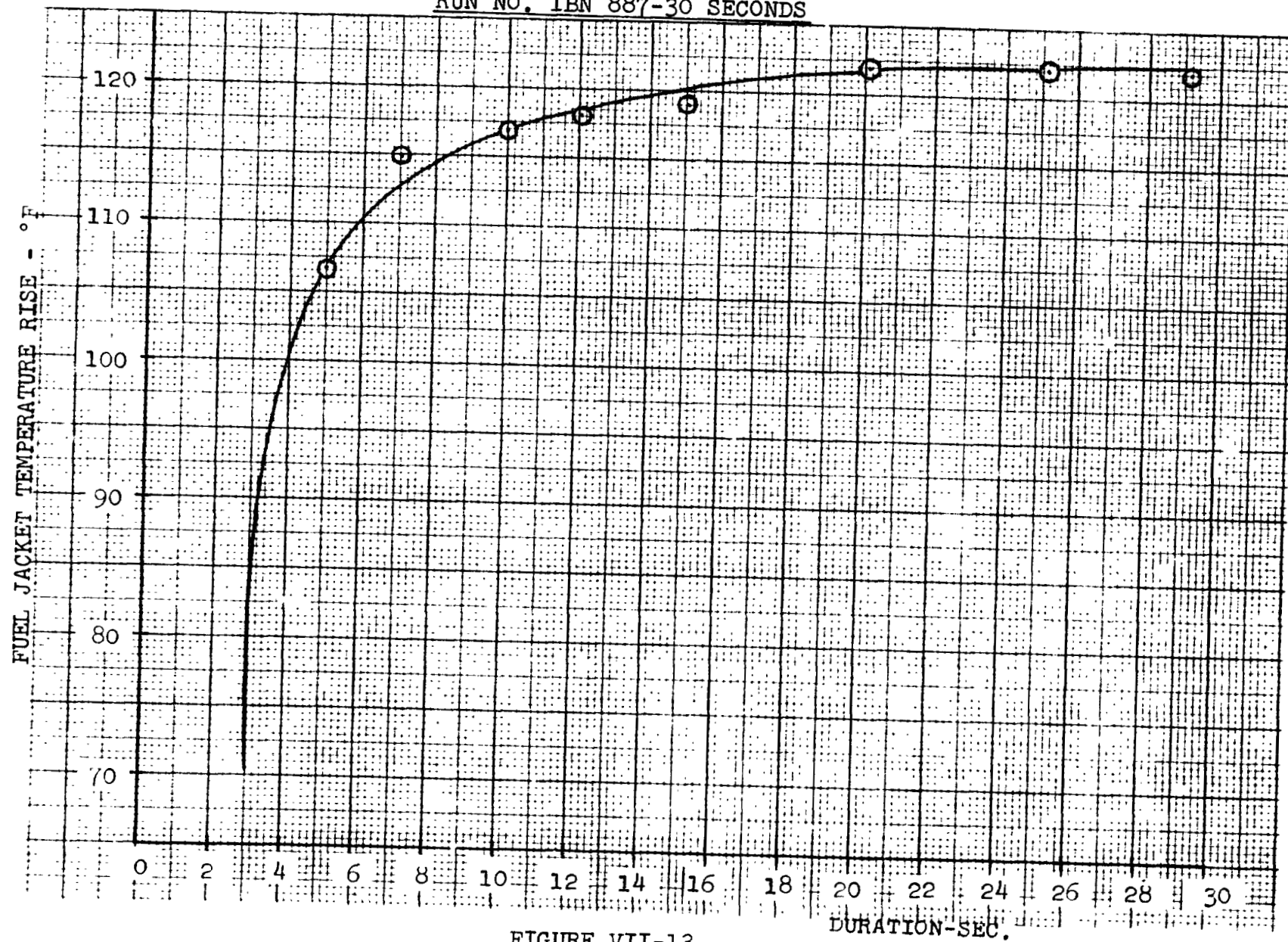


FIGURE VII-13

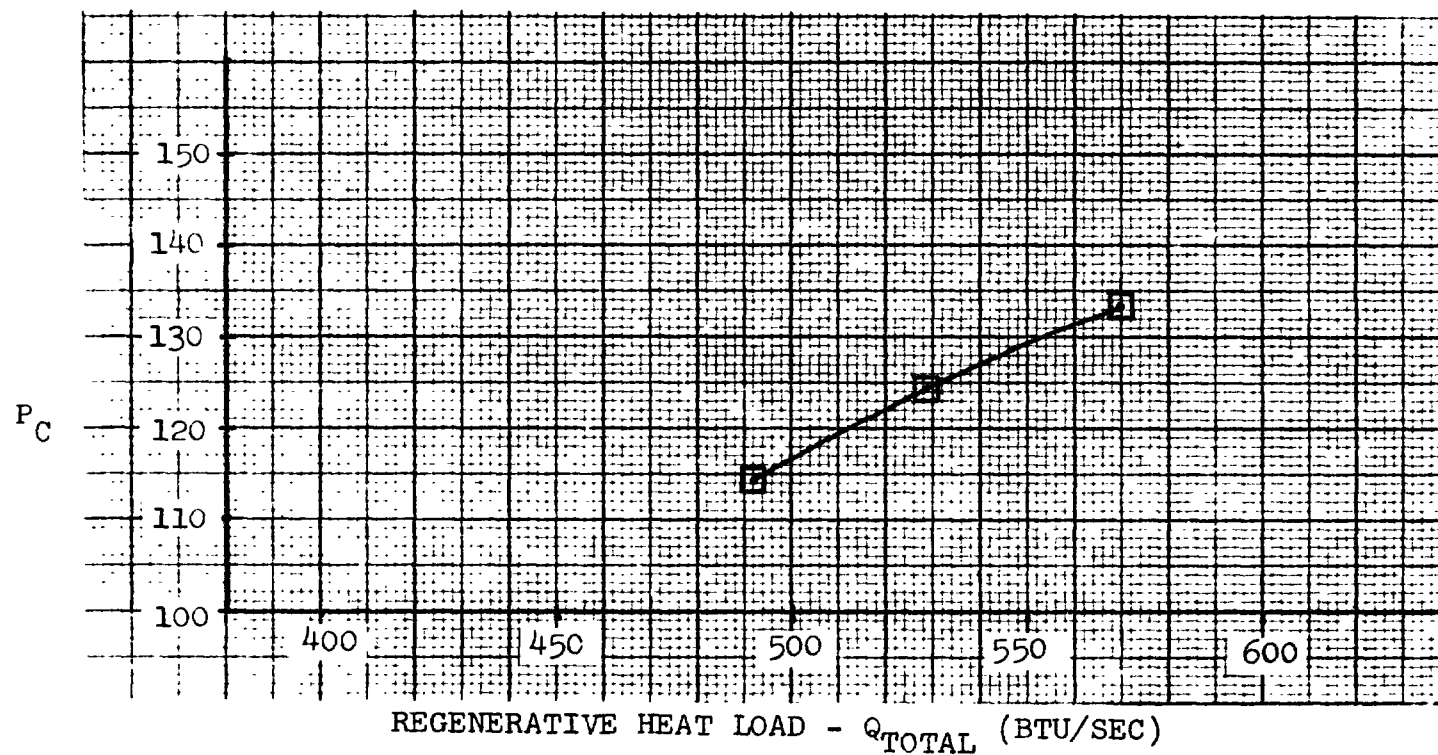
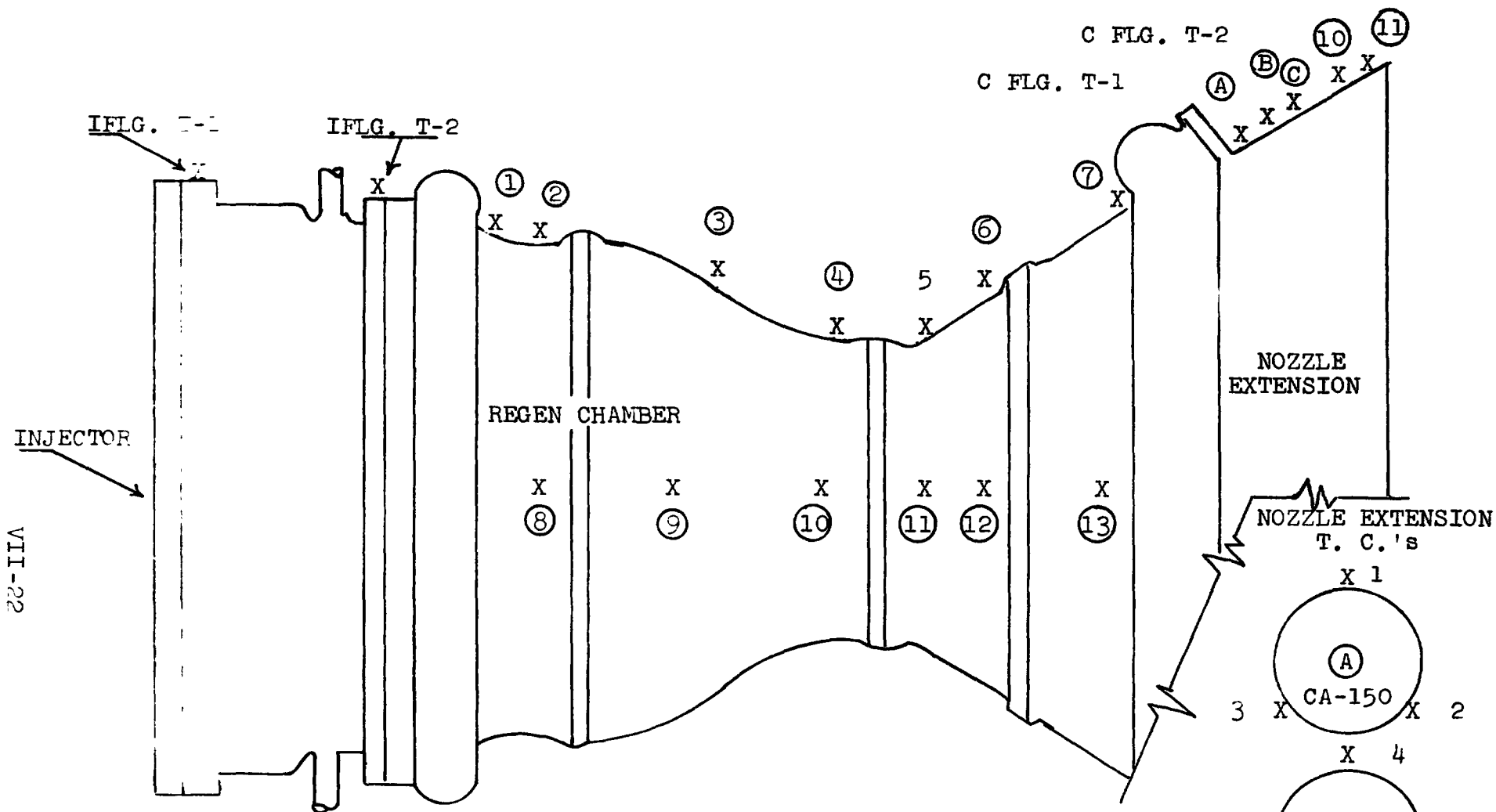
TOTAL HEAT LOAD VS CHAMBER PRESSURE

FIGURE VII-14



NOTE: Chamber Temperatures #1-7 and Flg. Temperatures at 12 o'clock; Chamber temperatures #8-13 at 9 o'clock. (All chamber thrust chambers are C/A)

REGENERATIVE CHAMBER THERMOCOUPLE LOCATIONS

FIGURE VII-15

Bell Aerospace Company

Two (2) additional platinum/platinum-rhodium thermocouples were added for the latter test series from test number 1BN-880 to 887.

The maximum chamber skin temperature versus mixture ratio is shown in Figure VII-16 for all tests of 10 seconds duration or greater. The data presented are for all 10 second points. The maximum temperature measured is located at the injector end of the chamber (thermocouple T-1 or T-2). The increase of maximum chamber temperature between the 10 second data point and the thermally stabilized end of run data point is less than 10°F.

The temperature profile of the chamber skin temperatures and nozzle extension temperatures for the 30 second duration test is shown in Figure VII-17 (at the end of run data points).

The temperature plots of all the chamber and nozzle extension thermocouples except extension thermocouples 10 and 11 are listed for the 30 second duration test in Figures VII-18 through VII-23.

4. Start Transients

Starting of the regeneratively cooled engine was predicated on several set up requirements. These being an oxidizer lead requirement and also that the fuel film coolant and main fuel flows enter as simultaneously as possible to eliminate possible flashback and overheating. Unfortunately, in this separately fed hardware, to achieve this type of propellant timing required orificing and volume changes because of different flow adjustments to the film manifold. While this criteria (fill time entry) was accomplished, the feed system used was much more involved than normal, leaving very little useful data to project to a final flight engine transient analysis. However, the starts achieved were useful in defining altitude start information and can be used as a criteria of successful operation.

Two basic systems were used for the regen chamber testing to accommodate vortex flows of approximately 4% and 2%. The 4% vortex system was simpler and available when the regen chamber was available for initial testing, and consequently was used first. The 2% vortex system required a bypass system utilizing a parallel line circuit with a valve and orificed line arrangement, as shown in Figure 23. This system was used to obtain proper propellant sequencing on start transients without adding additional volumes between the bipropellant valve and combustion chamber ($P = 4\%$ on start), and permitted operating at a 2% vortex flow during steady-state. The 2% flow resulted when the valve was closed at the 2.5 second point of the test firings.

OME PERFORMANCE
MAXIMUM CHAMBER SKIN TEMPERATURE (AT INJECTOR
END) VS O/F

10 SECOND DATA POINTS

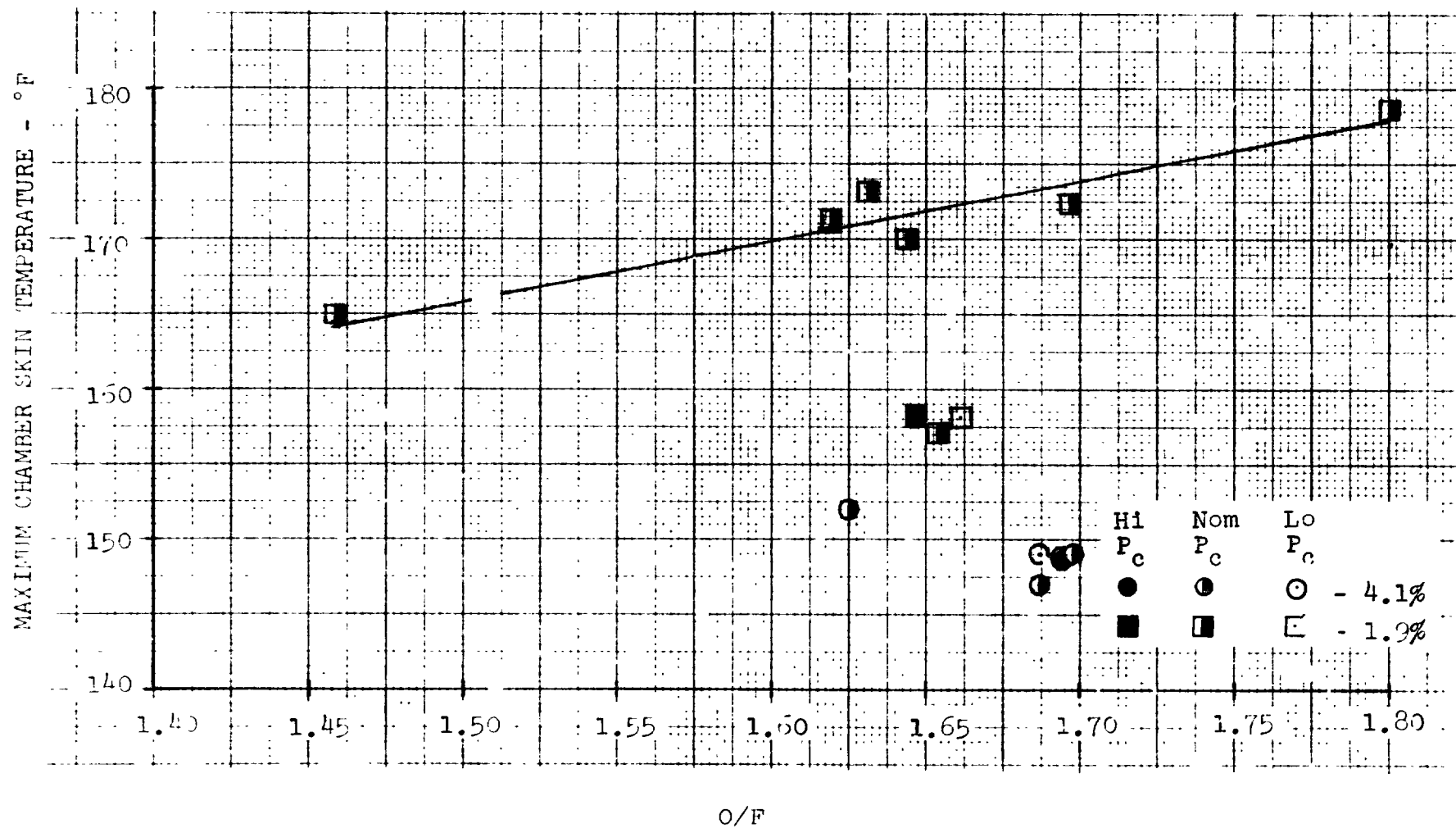
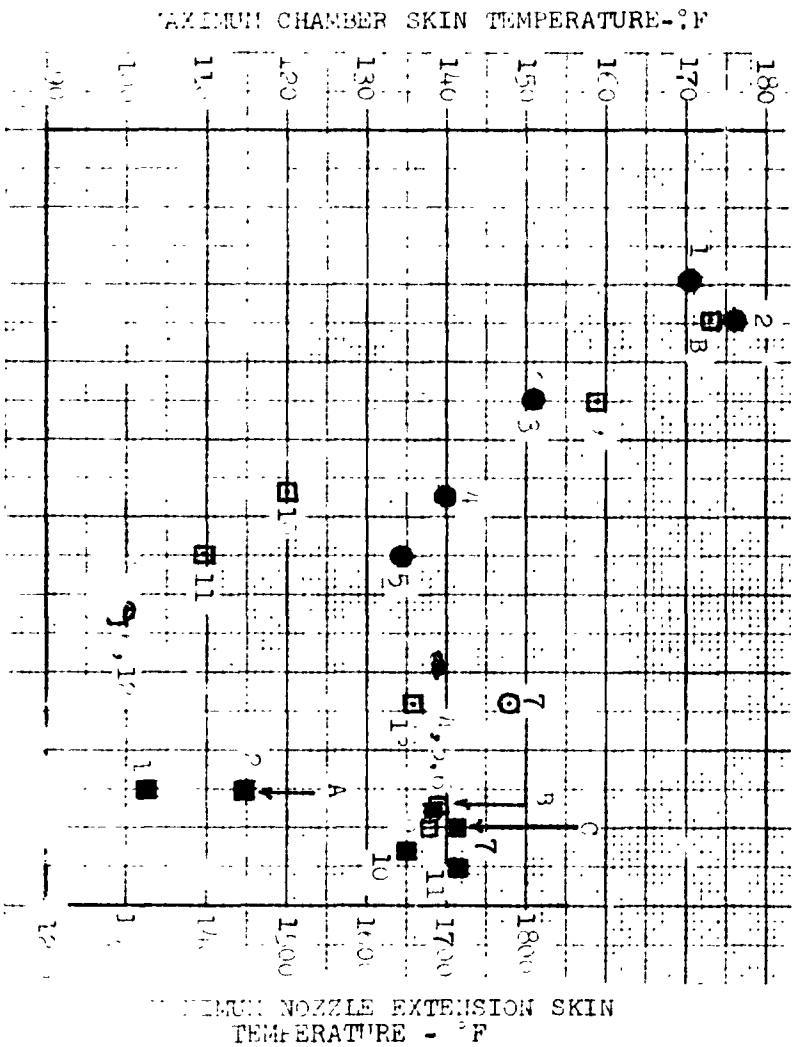
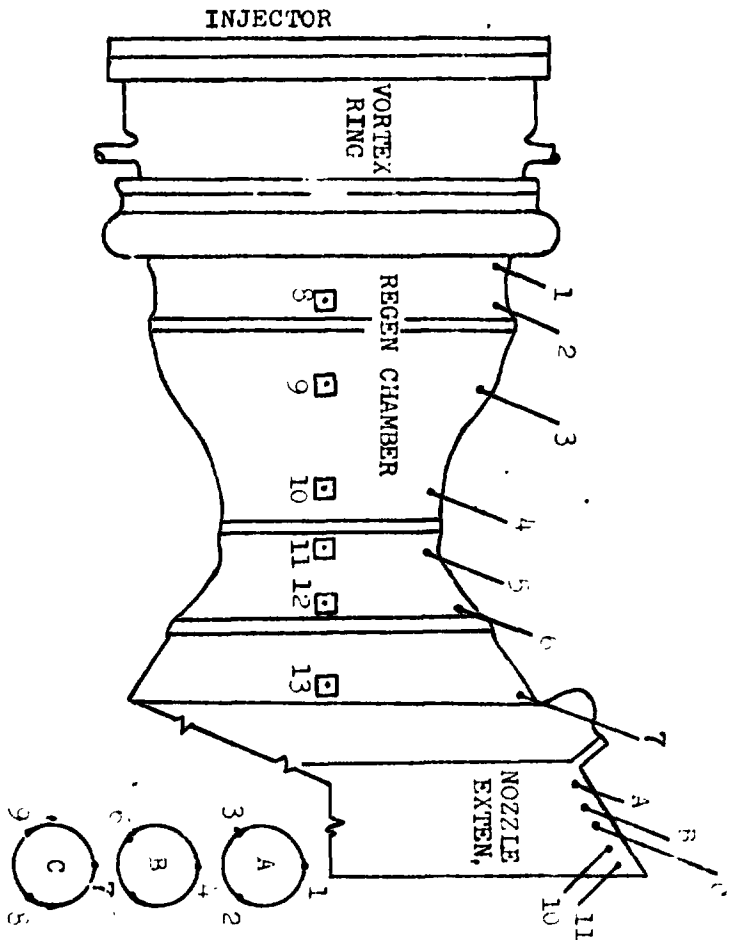


FIGURE VII-16

FIGURE VII-17
ONE - REGEN CHAMBER
TEMPERATURE PROFILE, RUN NO. 1BN-887, 80 SEC



BELL AEROSPACE COMPANY DIVISION OF TEXTRON
 MODEL 8693 OME 5K THRUST REGENERATIVELY COOLED CHAMBER
 CELL 1BN RUN NC. 887 DATE: 10-01-73

ORIGINAL PAGE IS
 OF POOR QUALITY

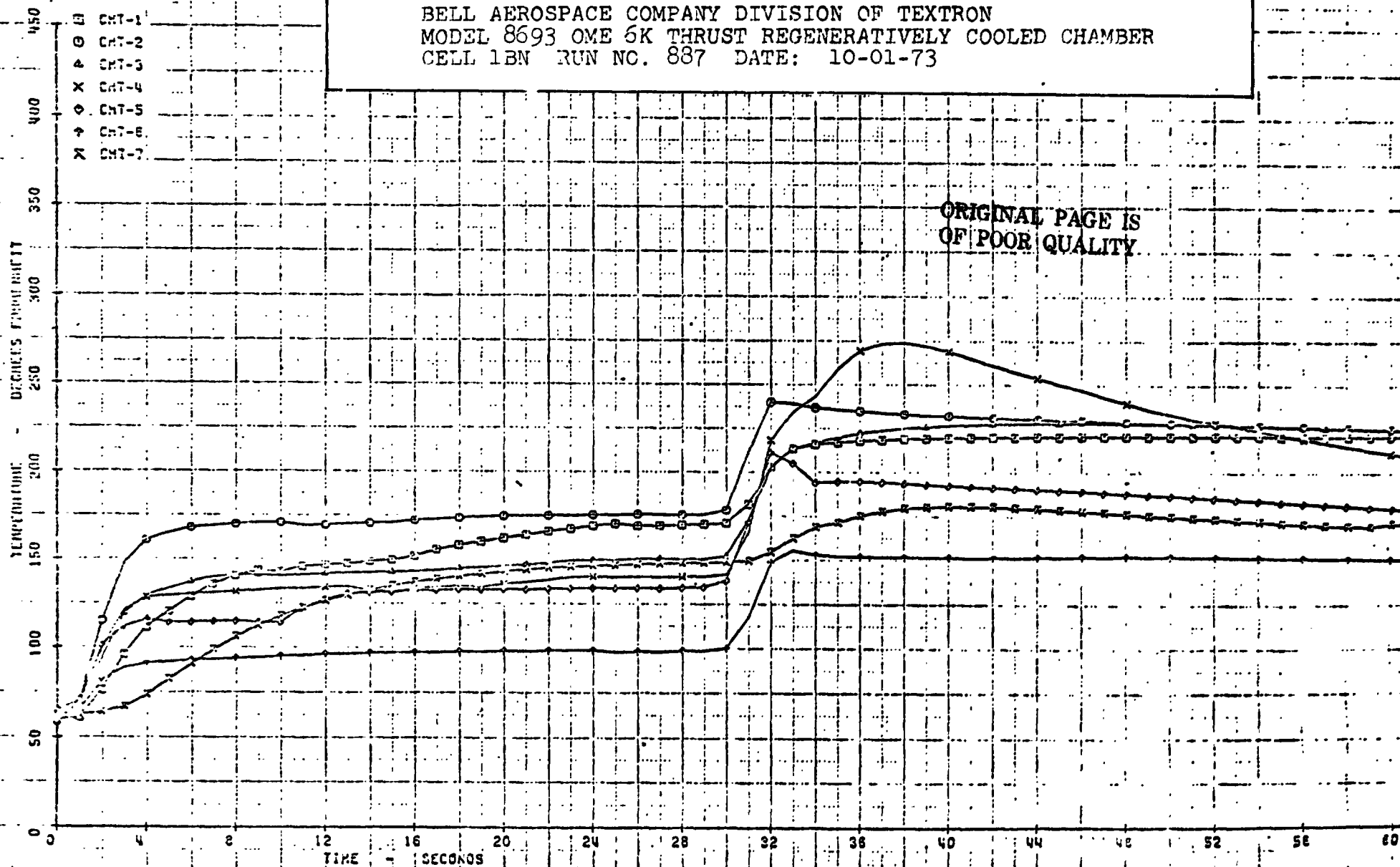


FIGURE VII-18

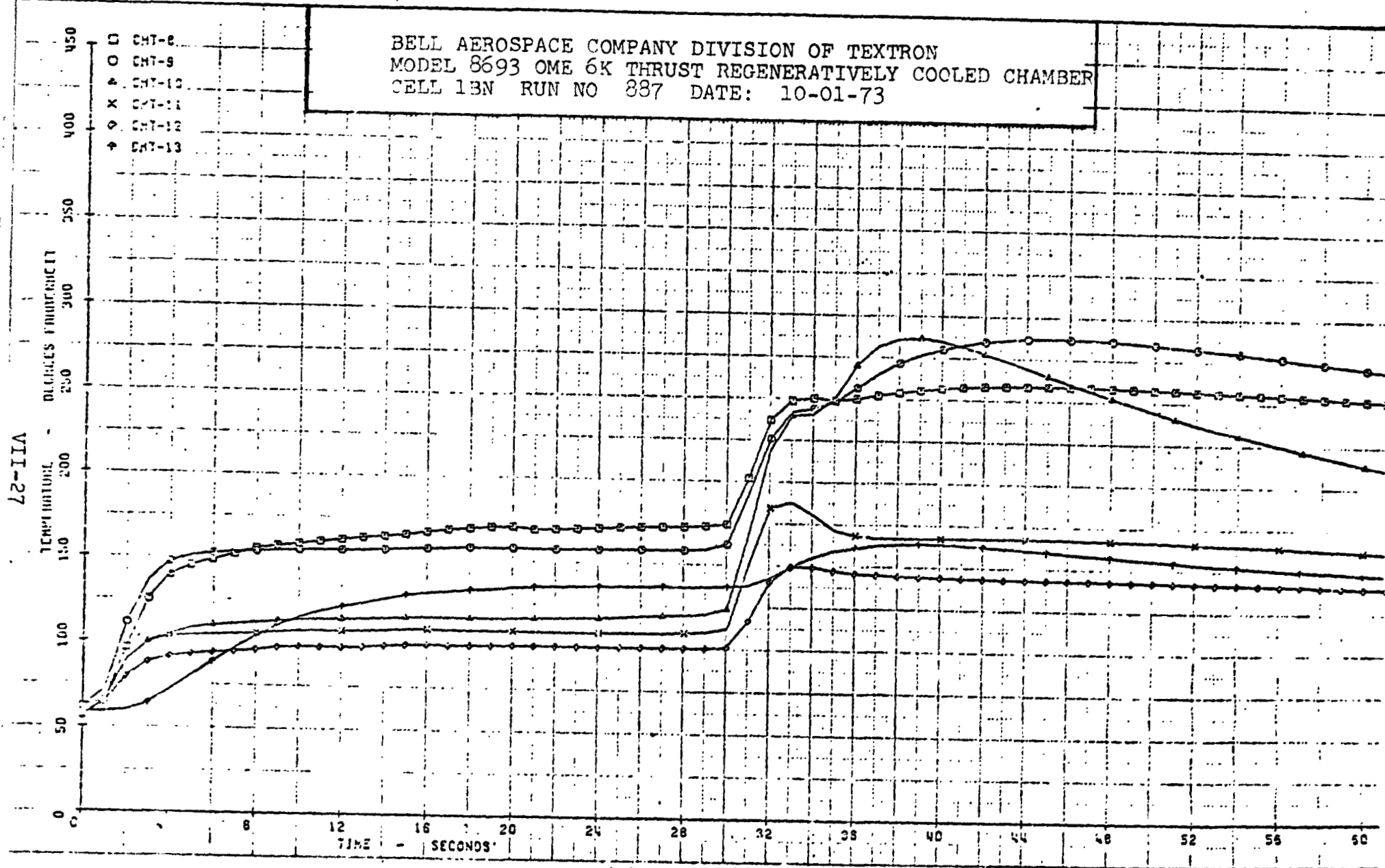


FIGURE VII-19

BELL AEROSPACE COMPANY DIVISION OF TEXTRON
 MODEL 8693 OME 6K THRUST REGENERATIVELY COOLED CHAMBER
 CELL 1BN RUN NO. 887 DATE: 10-01-73

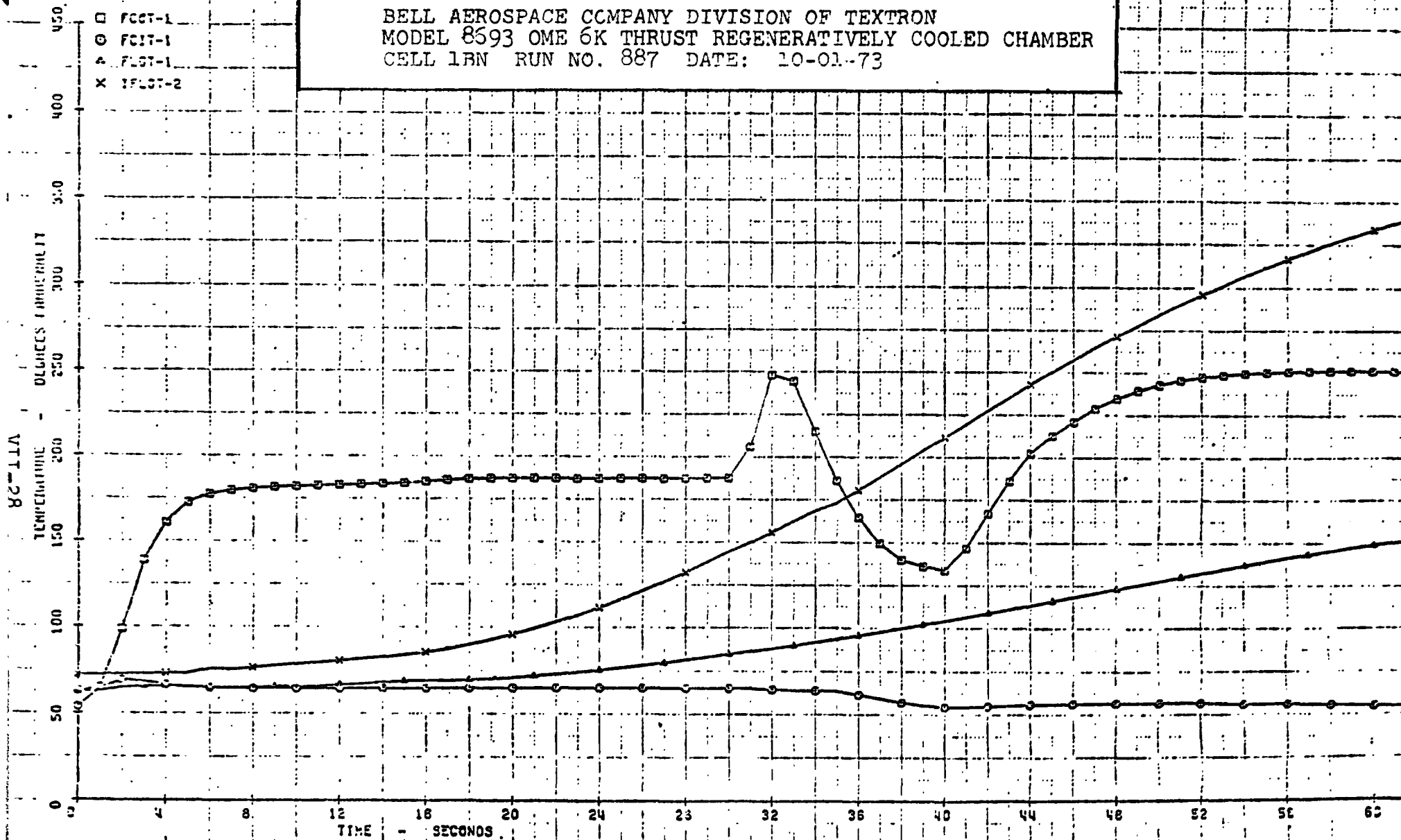


FIGURE VII-20

VII-29

BELL AEROSPACE COMPANY DIVISION OF TEXTRON
 MODEL 8693 OME 6K THRUST REGENERATIVELY COOLED CHAMBER
 CELL 1BN RUN NO. 887 DATE: 10-01-73

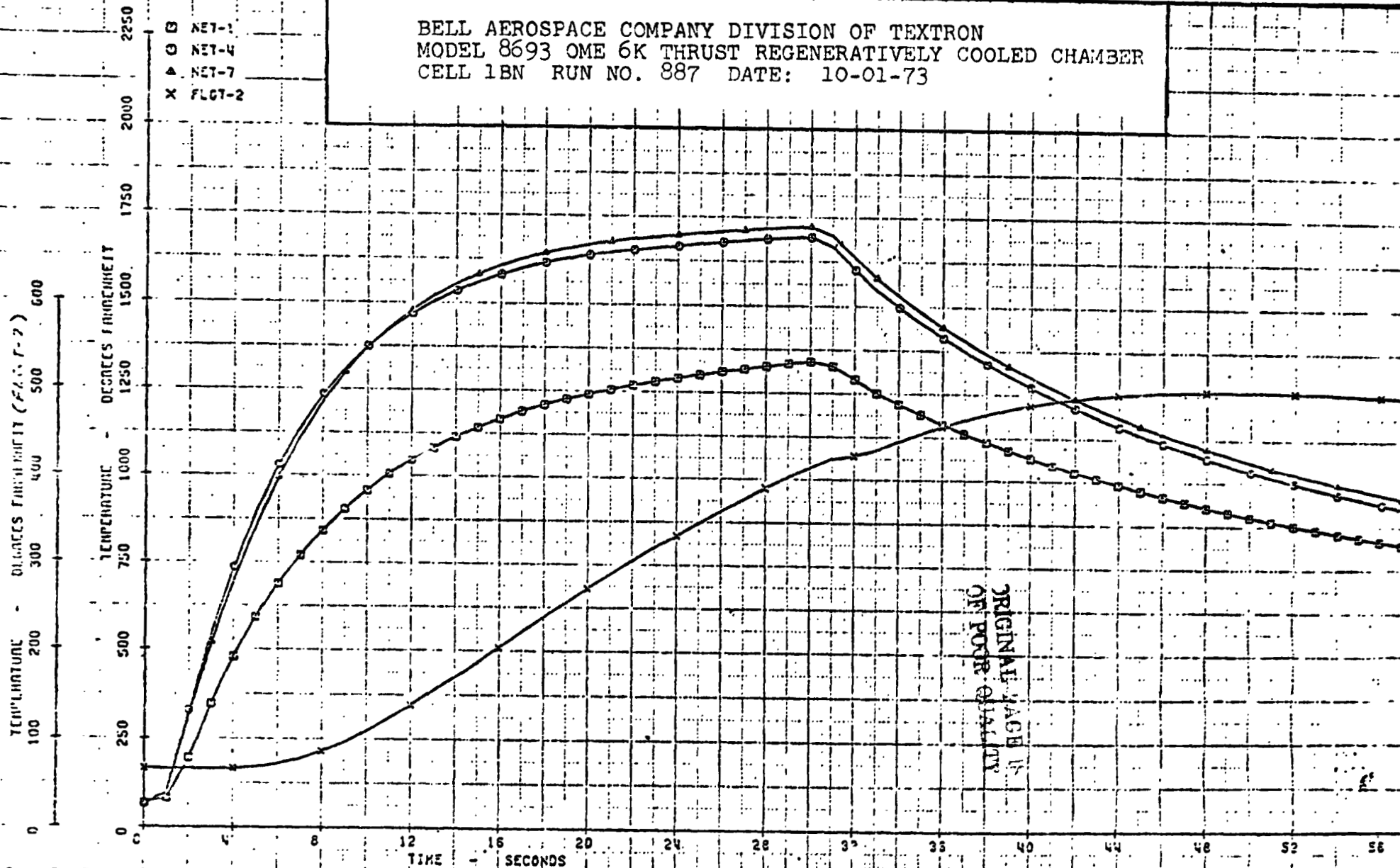


FIGURE VII-21

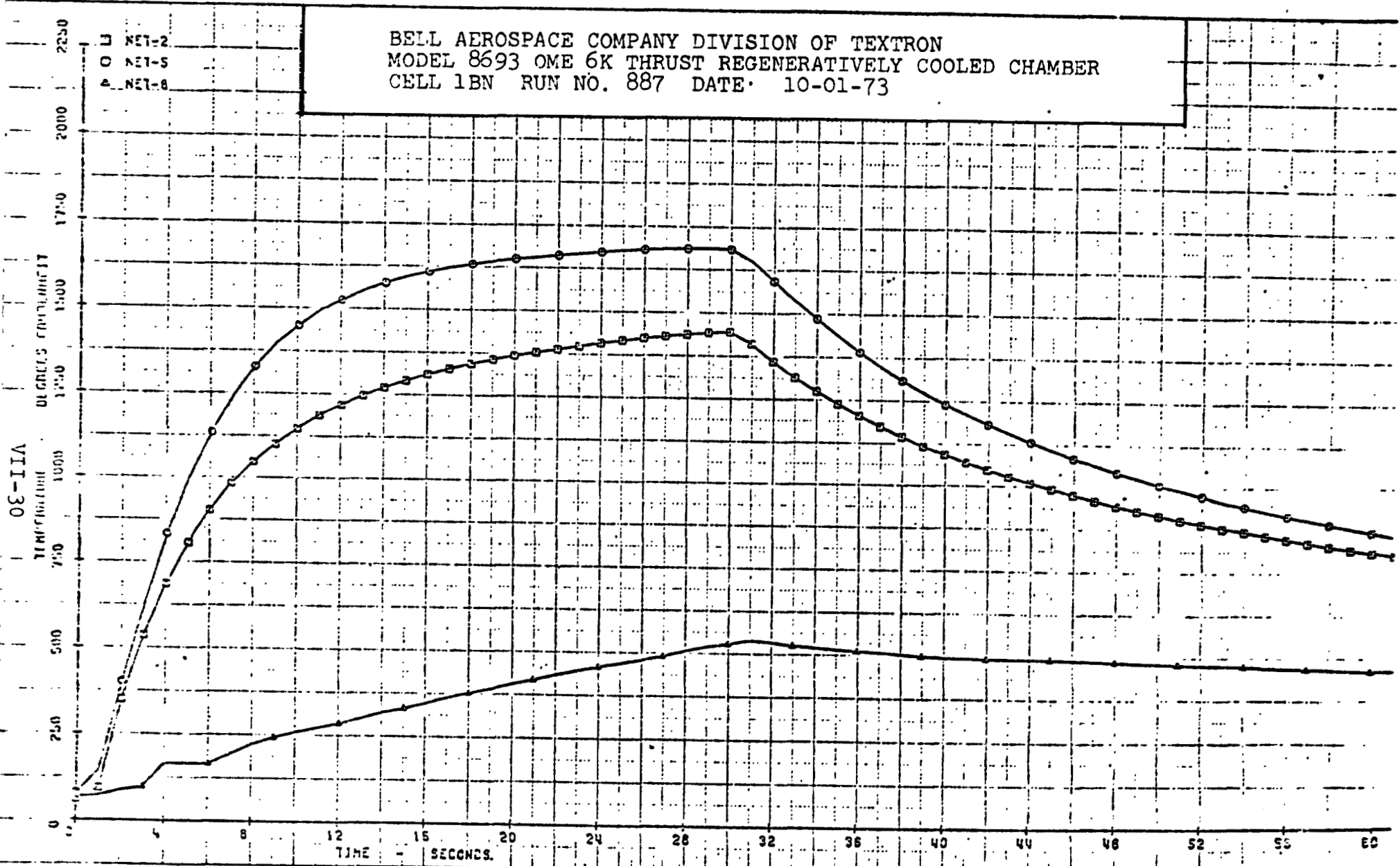


FIGURE VII-22

VII-31

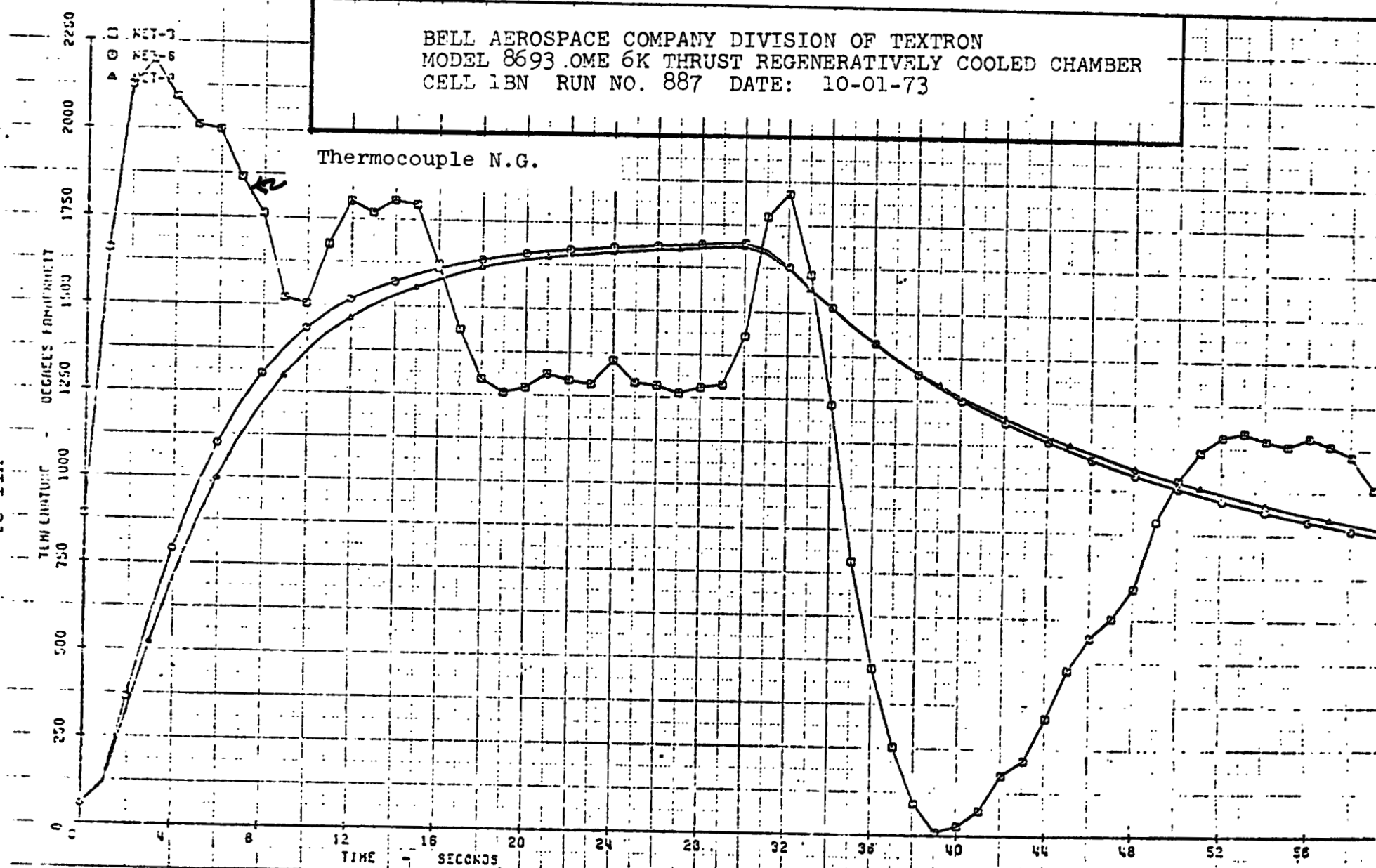


FIGURE VII-23

Bell Aerospace Company

The volumes and orifice diameters were determined with a start and shutdown transient model.

Prior to installation in the test cell, that portion of the feed system containing the orifices was water calibrated and modified until the desired vortex flow and orifice pressure drops were obtained. The complete propellant system was then flow calibrated in the test cell to assure that oxidizer preceded the fuel into the chamber, and that the vortex fuel flow reached the chamber within 100 milliseconds of the injector fuel flow.

Bell Aerospace Company

VIII. TASK XI - OME MODEL INJECTOR

The original intent of this contract was the development of information leading to reusable thrust chambers which would prove the acceptability of cooling systems proposed for use on the OME. The initial tasks of this contract carried through the parametric trade studies, selection of a design, design, fabrication, and demonstration of the chamber to prove the cooling concepts to be real and viable. To accomplish this task, injection systems were furnished to the program. However, with the advent of more stringent and varied stability criteria, the complete use of an injector, modified to suit the program needs, was required. As a consequence, the designated injector S/N 2 which was designed as a company sponsored project, (Figure VIII-1) with its associate vortex cooling assembly, was transferred to the program.

This injector (8693-473050-1) was fabricated from aluminum. The injector was designed for construction from stainless steel, with all internal hydraulic passages of flight design. The flight design concept was also maintained in the face thickness and manifolds such that flight characteristic orifice L/D hydraulics and manifold velocities were examined. However, the construction was carried out in aluminum as a cost reduction item. In this case, the cost reduction was warranted due to both funding limitations and also because the primary injector parameters could be demonstrated with either type material.

The cost reduction attributed to the aluminum construction is primarily associated with decreased machining time in both formed parts and injection orifice fabrication. The two primary parts forming the injection system are the 8693-473150-1 injector, and the 8693-473140-1 vortex assembly. This vortex assembly is comprised of the manifold, injector orifices, and vortex coolant generation slots for the fuel film coolant of the thrust chamber.

This injector was a second generation injector based on the original flat-face injector S/N 1. The design evolution was made with changes in the propellant manifolds to reduce velocity and therefore, cross flow effects at the entrance of the injection orifices. The water flow tests of the original S/N 1 injector pointed out the orifice distortion and immediate changes were made in this unit (S/N 1A) to reduce the degrading manifold effect. Unfortunately, the feed system on that injector was not adequate to allow a completely efficient symmetrical propellant supply and the redesign of the manifolds resulted. The incorporated manifold changes made to the design of the S/N 2 injector were highly effective and this injector was considered applicable for all future testing operations.

ORIGINAL PAGE IS
OF POOR QUALITY

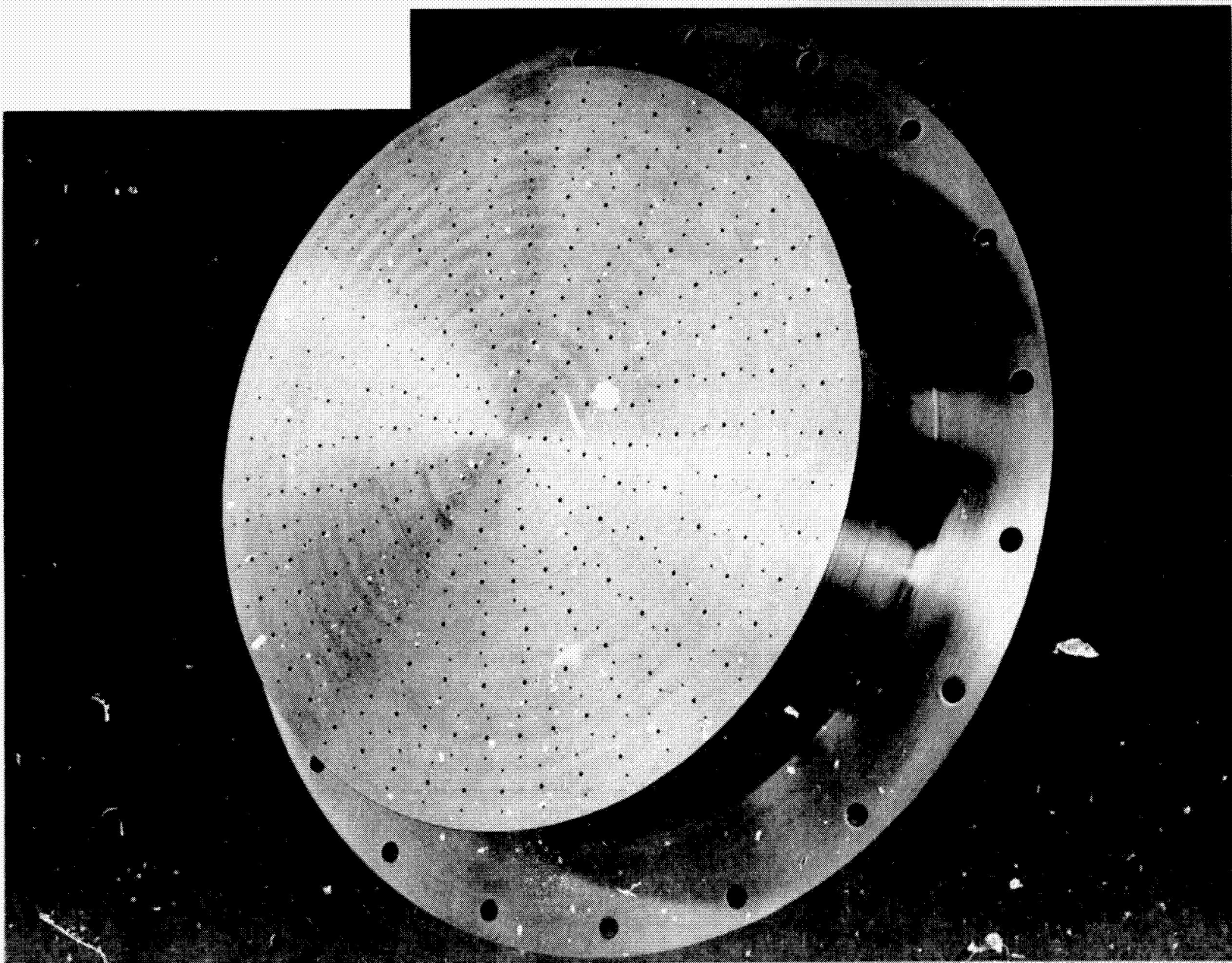


FIGURE VIII-1. ALUMINUM INJECTOR NO. 2

Bell Aerospace Company

TABLE I

INJECTOR CORE DESIGN

	<u>10 INCH DIAMETER (S/N 2)</u>
DIAMETER (INCH)	10
THRUST (LBS)	6000
ELEMENT TYPE	TRIPLET
NUMBER OF ELEMENTS (PRIMARY)	196
THRUST/ELEMENT (LBS)	31
OX MANIFOLD VELOCITY (FT/SEC)	< 8
FUEL MANIFOLD VELOCITY (FT/SEC)	< 9.5
PROPELLANT FLOW/A _C (LBS/IN ²)	0.24
NUMBER OF ELEMENT ROWS	7
<u>ELEMENT CONFIGURATION</u>	
● IMPINGEMENT DISTANCE (INCH)	0.397
● IMPINGEMENT ANGLE (°)	32
● OX ORIFICE DIAMETER (INCH)	0.0492/0.0465
● FUEL ORIFICE DIAMETER (INCH)	0.0295/0.0276
● L/D OX	4.0
● L/D FUEL	5.0
● ΔP OX (PSI)	41
● ΔP FUEL (PSI) (2% <i>p</i>)	43.5
● FACE RING WIDTH (INCH)	0.250

Bell Aerospace Company

The critical design information used for this injector is included in Table I with the injector drawing included as Figure VIII-2. In addition, the vortex ring used to inject the fuel film cooling is also included as Figure VIII-3. These two parts complete the injection system with approximately 93% of the propellants injected through the primary injector, and approximately 7% of the propellants, as fuel, in the vortex film cooling. This propellant distribution was used for the testing of the insulated columbium thrust chamber.

The regeneratively cooled thrust chamber required much less fuel film cooling, and only 2% of the propellants, or less, was injected through the vortex ring when testing the regenerative chamber.

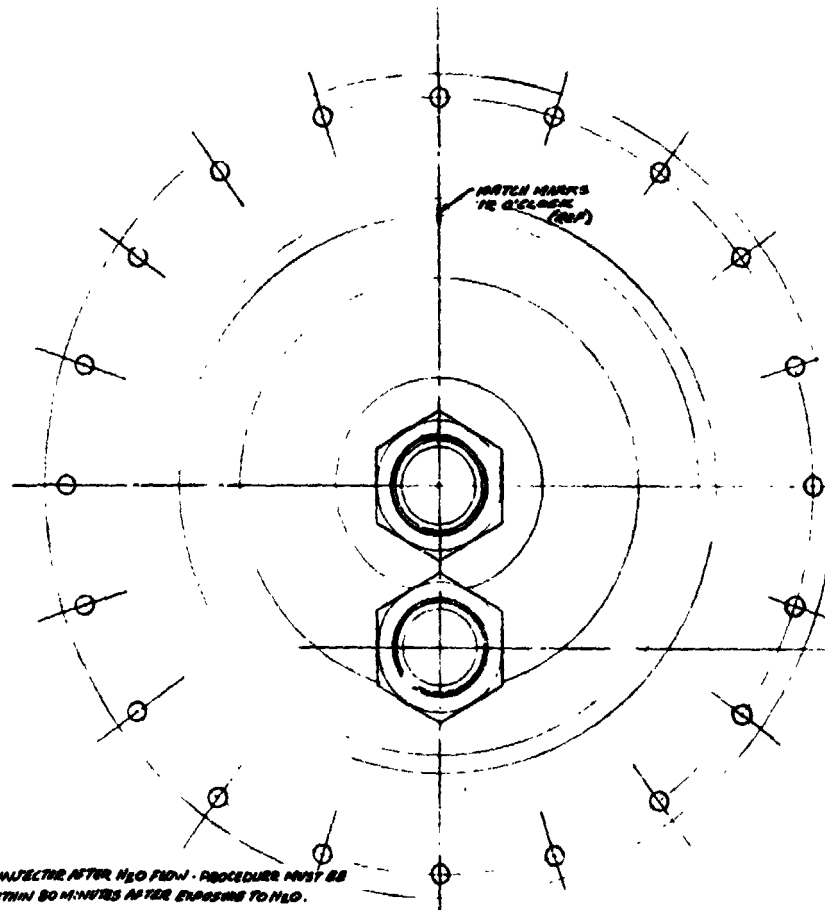
A series of acceptance tests were performed on the S/N 2 injector. The tests were conducted on a sea level test stand with a thrust chamber consisting of an uncooled steel chamber and a columbium throat arrangement. Testing was conducted in this manner to observe the throat temperature and also to examine for streaking of the injector. Since the injector was originally designated for use with an insulated columbium chamber, this acceptance procedure was not only applicable but presented a measure of acceptance of temperature distribution. The acceptance test data is shown in the following table.

TABLE II
ALUMINUM INJEC OR S/N 2

Run D-4	Dur. Sec.	Data Point Sec.	$R_{o/f}$	P_c corr Psia	c^* Ft/Sec	ρ %	Pyro Maximum °F
4489	2.7	2.2	1.630	129.8	5393	3.81	-
4490	2.4	1.9	1.719	124.4	5411	7.58	-
4491	10.5	10.0	1.582	125.0	5478	7.77	2284
4492	14.9	14.4	1.65	121.4	5478	7.97	2308
4493	15.5	15.0	1.611	122.9	5479	7.49	2340
4494	15.6	15.1	1.512	127.2	5488	8.15	2340
4495	15.3	14.8	1.436	128.9	5548	7.27	2386
4496	15.6	15.1	1.810	119.4	5438	7.97	2279
4497	15.4	14.9	1.438	124.0	5557	7.68	2279
4498	30.4	29.9	1.680	121.8	5487	7.81	2278

ORIGINAL PAGE IS
OF POOR QUALITY

8625-478
FUEL INLET



LINE UP FASTEN MARKS ON -
THE BLANK, CENTERED ON FUEL
PRIOR TO G.W. (1/2 DIA
8625-47805-1 BAY, ONE

8625-47805-1 COVER PLAT.

ELECTRON BEAM WELD
300 °C PENETRATION
BEFORE MACHINING FACE OF HJ

ANBIS-200 NOT CORPUS
N5 2019-20 0 SLIP, FLAME FUEL
(TYP 2 PLACES)

FUEL INLET
(R.M.)

1.250 X .060 WALL AL. AL.
LOW TENSILE (TYP 2 PLACES) AS SHOWN

OXID INLET
(R.M.)

ELECTRON BEAM WELD
300 °C PENETRATION
BEFORE MACHINING FACE

8625-47805-1 H

- 11 - DRYING OF INJECTOR AFTER H₂O FLOW - PROCEDURE MUST BE STARTED WITHIN 30 MINUTES AFTER EXPOSURE TO H₂O.
- 11.1 - DRAIN AS COMPLETELY AS POSSIBLE
- 11.2 - FULLY IMMERSE IN ACETONE (M.E.K. IS ACCEPTABLE SUBSTITUTE) FILLING ALL Voids, FOR 30 MINUTES
- 11.3 - RINSE FROM ACETONE & DRAIN AS COMPLETELY AS POSSIBLE
- 11.4 - WITHIN 2 HRS (MAX) OF STEP 11.3, PLACE IN VACUUM OVEN PREHEATED TO 150°F FOR 2 HRS. EVACUATE OVEN TO 26 IN. (H.G.)
- 11.5 - PACKAGE IN POLY-B BAG, PURGE BAG WITH H₂ & HEAT SEAL OPENING.
- 12 - ALL H₂O USED FOR FLOW TEST MUST BE IMMERSED WITH CHROMIC ACID, 0.10% BY WEIGHT.

H₂O FLOW TEST PER ENGRG. INFORMATION.

ALL WELD JOINTS & ADJOINING SURFACES ARE TO BE SURFACED WITH LINTLESS CLOTH SANDING WITH CHLOROSOLVENT (M.E.K.) OF M.E.K. IMMEDIATELY PRIOR TO WELDING.

7 - ALL DETAILS TO BE CLEANED PRIOR TO WELDING PER STEEL DETAIL TYPE 2 AND INFORMATION. IMMEDIATELY AFTER QUALIFIED H₂O FLOW DOWN H₂O FROM PART & IMMERSA IN ACETONE (OR M.E.K.). DRAIN ACETONE FROM PART & PLACE IN VACUUM OVEN PREHEATED TO 150°F (MIN) FOR 2 HOURS. EVACUATE OVEN TO 26 IN. (H.G.) HEAT SEAL IN "H₂O C" BAG OR EQUIV.

ALL CENTER LINES OF EACH SET OF HOLES & BORE & POINT OF IMPINGEMENT TO INTERSECT WITHIN .001

ALL HOLES ARE TO BE PRODUCED BY ELECT DISCHARGE MACHINING (EDM) TO A SURFACE FINISH EQUAL TO 64/ RMS.

SHARP EDGES ARE TO BE CHAMFERED (BENT) AT ALL FUEL & OXIDIZER ENTRIES

REWORKING WITH SURFACE MARKED "FACE" SURFACED.

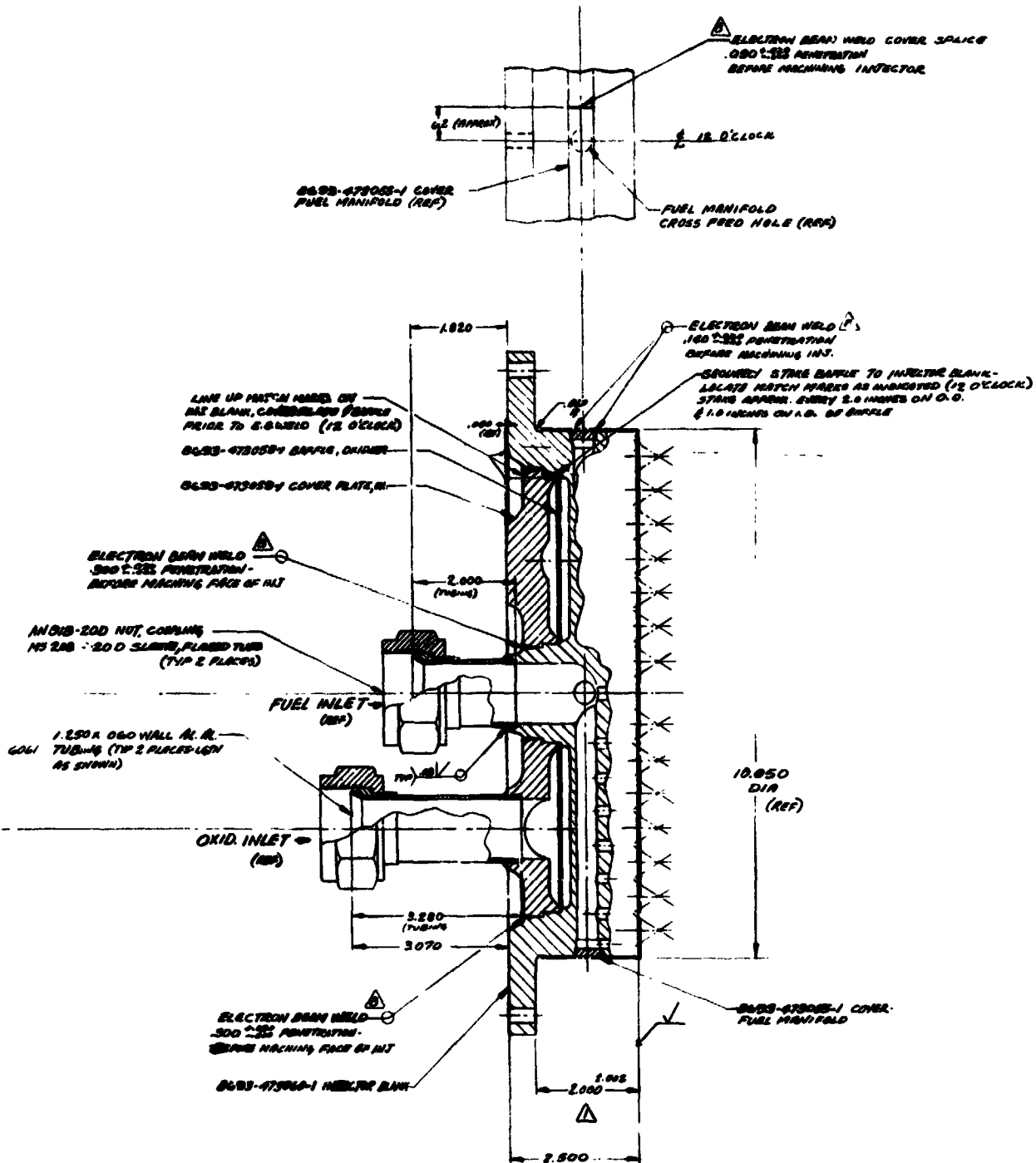
CONCENTRIC WITHIN .001 TIR

INJECTOR FACE & 9990 DIA TO BE MACHINED AFTER WELDING & BEFORE ORIFICE MACHINING.

NOTES:

FOLDOUT FRAME

IS
ITV



FOLDOUT FRAME



FOLDOUT FRAME

ORIGINAL PAGE IS
OF POOR QUALITY

10 TRIPLETS EQUALLY SPACED (AS SHOWN) WITHIN .085 TIE
40 ORDIZER ORIFICES .0492 DIA.
30 FUEL ORIFICES .0295 DIA.

40 TRIPLETS EQUALLY SPACED (AS SHOWN) WITHIN .085 TIE
40 ORDIZER ORIFICES .0492 DIA.
30 FUEL ORIFICES .0276 DIA. } THESE DIMENSIONS FOR THIS
PART OF THE INJECTOR ONLY

32 TRIPLETS EQUALLY SPACED (AS SHOWN) WITHIN .085 TIE
32 ORDIZER ORIFICES .0492 DIA.
24 FUEL ORIFICES .0295 DIA.

24 TRIPLETS EQUALLY SPACED (AS SHOWN) WITHIN .085 TIE
24 ORDIZER ORIFICES .0492 DIA.
16 FUEL ORIFICES .0295 DIA.

24 TRIPLETS EQUALLY SPACED (AS SHOWN) WITHIN .085 TIE
24 ORDIZER ORIFICES .0492 DIA.
16 FUEL ORIFICES .0295 DIA.

12 TRIPLETS EQUALLY SPACED (AS SHOWN) WITHIN .085 TIE
12 ORDIZER ORIFICES .0492 DIA.
8 FUEL ORIFICES .0295 DIA.

8 TRIPLETS EQUALLY SPACED (AS SHOWN) WITHIN .085 TIE
8 ORDIZER ORIFICES .0492 DIA.
4 FUEL ORIFICES .0295 DIA.

96 TOTAL TRIPLETS

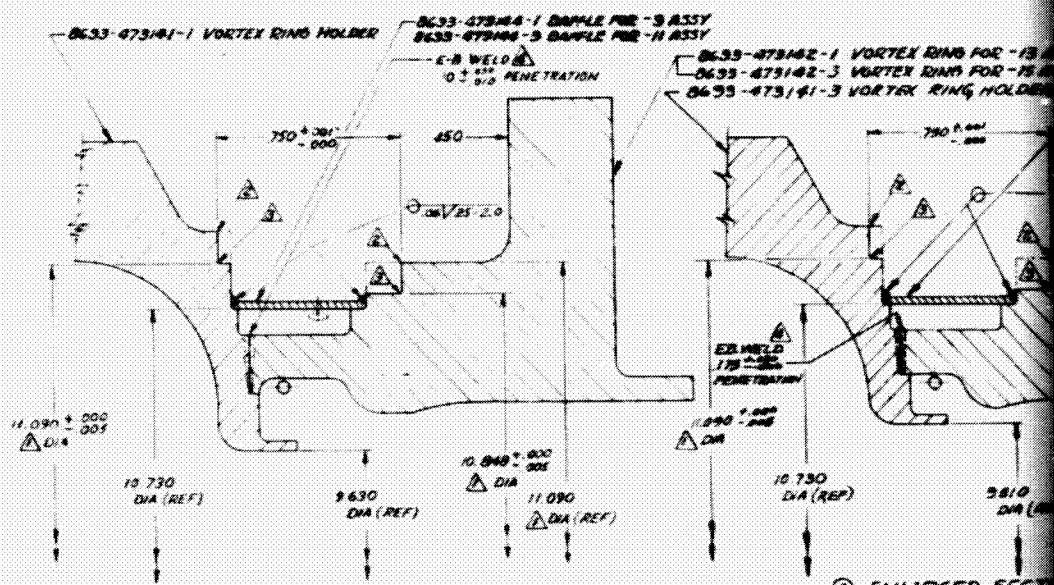
48 TOTAL .0492 DIA ORDIZER ORIFICES
48 TOTAL .0492 DIA ORDIZER ORIFICES
296 TOTAL .0295 DIA FUEL ORIFICES
96 TOTAL .0276 DIA FUEL ORIFICES

WORKHORSE ASSY OF 10" DIA WORKHORSE (ALUM) INJECTOR P 80070 8693-43050 SCALE 1/2" = 1" DEVELOPMENT		BELL & HOWELL COMPANY 1000 N. 10TH ST. MILWAUKEE, WIS. 53233 TEL. 442-1111 CABLE: BELL & HOWELL WORKHORSE ASSY OF 10" DIA WORKHORSE (ALUM) INJECTOR P 80070 8693-43050 SCALE 1/2" = 1" DEVELOPMENT
---	--	--

FIGURE VIII-2.
10 INCH DIAMETER
ALUMINUM INJECTOR NO. 2

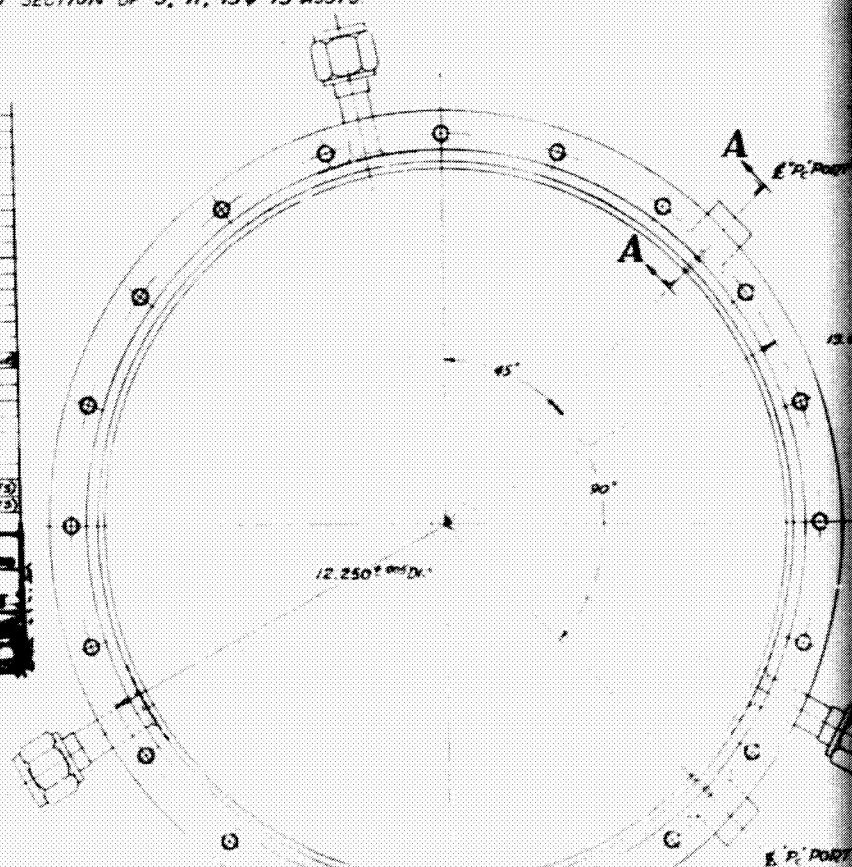
VIII-5

FOLDOUT FRAME 2



ENLARGED SECTION OF -9, -11, -13 & -15 ASSYS

					0633-473-42-2	VORTEX KING
					0678-473-41-3	VORTEX KING HOLDER
			3	3	AN618-BJ	NUT
			3	3	M520815-BJ	SCREW
					0633-473-40-25	VORTEX KING ASSY, ASSY
					0633-473-40-23	VORTEX KING (CD WELD) ASSY
			2	2	02-362-155-1	BOSS (FEMALE WELD ON)
					0633-473-44-5	SCREW
					0633-473-43-5	CD WELD NUT
					0633-473-40-3	BAFFLE
					0633-473-43-1	BAFFLE
					0633-473-43-1	COVER NUTS
					0633-473-40-3	VORTEX KING
					0633-473-42-1	VORTEX KING
					0633-473-41-1	VORTEX KING HOLDER
					0633-473-40-21	VORTEX KING
					0633-473-40-19	VORTEX KING ASSY OF (P. 1) N. (CD WELD)
					0633-473-40-17	TUBE (CD WELD)
			3	3	0633-473-40-25	VORTEX KING (CD WELD) ASSY
					0633-473-40-13	VORTEX KING (CD WELD) ASSY
					0633-473-40-11	VORTEX KING (BAFFLE) ASSY
					0633-473-40-9	VORTEX KING (BAFFLE) ASSY
					0633-473-40-7	NUTS KING
					0633-473-40-5	NUTS KING
					0633-473-40-3	NUTS KING ASSY OF (20 HOLES)
					0633-473-40-1	NUTS KING ASSY OF (20 HOLES)



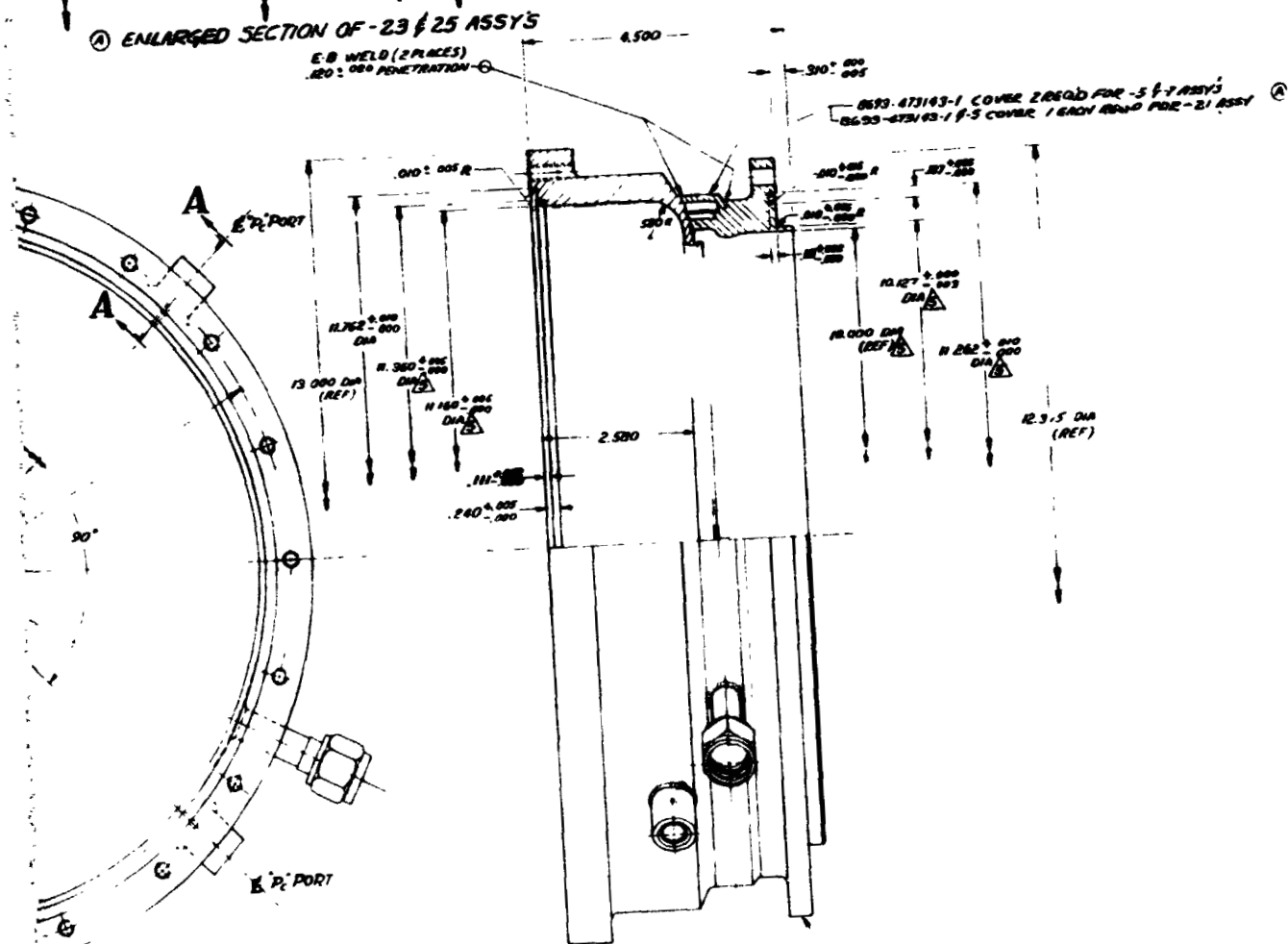
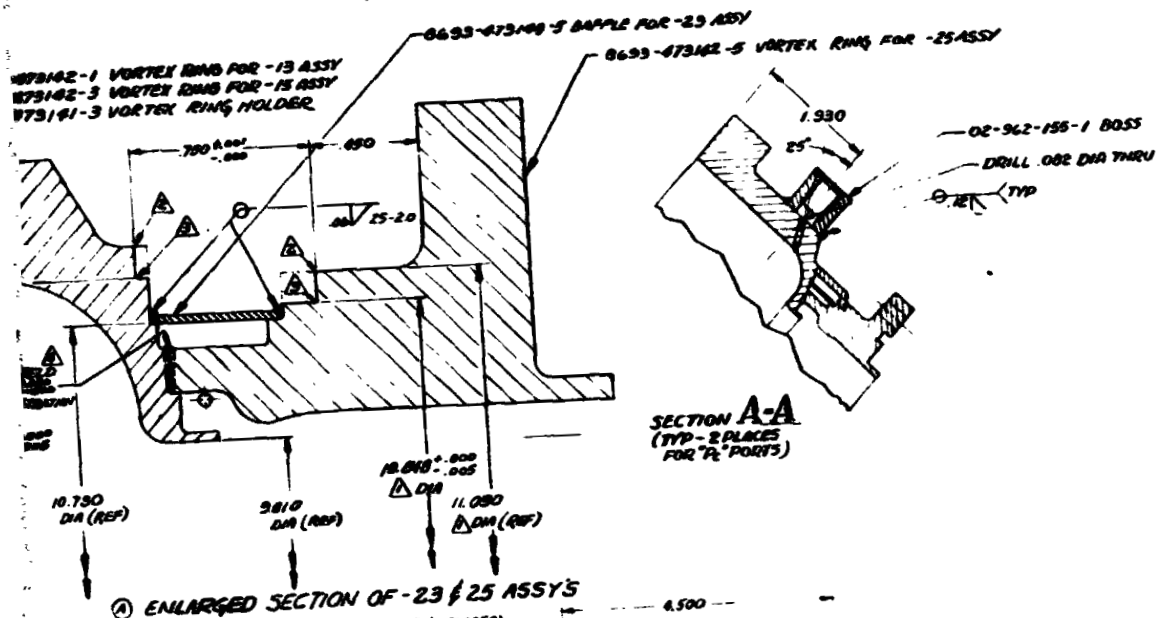
- ⚠️ THESE DIAMETERS TO BE CONCENTRIC WITHIN .002T.
- ⚠️ CLEAN UP ANY WELD SPLATTER AFTER COMPLETION OF E-B WELDING BEFORE WELDING 8693-473483-1 COVERS IN PLACE.
- ⚠️ CORNER RADIUS NOT TO EXCEED .010R
- ⚠️ SHARP EDGE PREFERRED. RADIUS OF CHAMFER NOT TO EXCEED .005
- ⚠️ THESE DIAMETERS TO BE CONCENTRIC WITHIN .002T/2

NOTES

TAP DRILL THRU
TAP 2500-28 UNF-3B THD
DEPTH 500 MIN (PERFECT THD)
20 HOLES EQUALLY SPACED WITHIN

FOLDOUT FRAME

ORIGINAL PAGE IS
OF POOR QUALITY



TAP DRILL THRU
TAP 2500-28 UNF-3B THD
DEPTH .500 MIN (PERFECT THD)
20 HOLES EQUALLY SPACED WITHIN .005

- ① VORTEX RING, ASSY OF
- ② VORTEX RING
- ③ VORTEX RING, ASSY OF
- ④ VORTEX RING
- ⑤ VORTEX RING, ASSY OF
- ⑥ VORTEX RING

FOLDOUT FRAME

ORIGINAL PAGE IS
OF POOR QUALITY

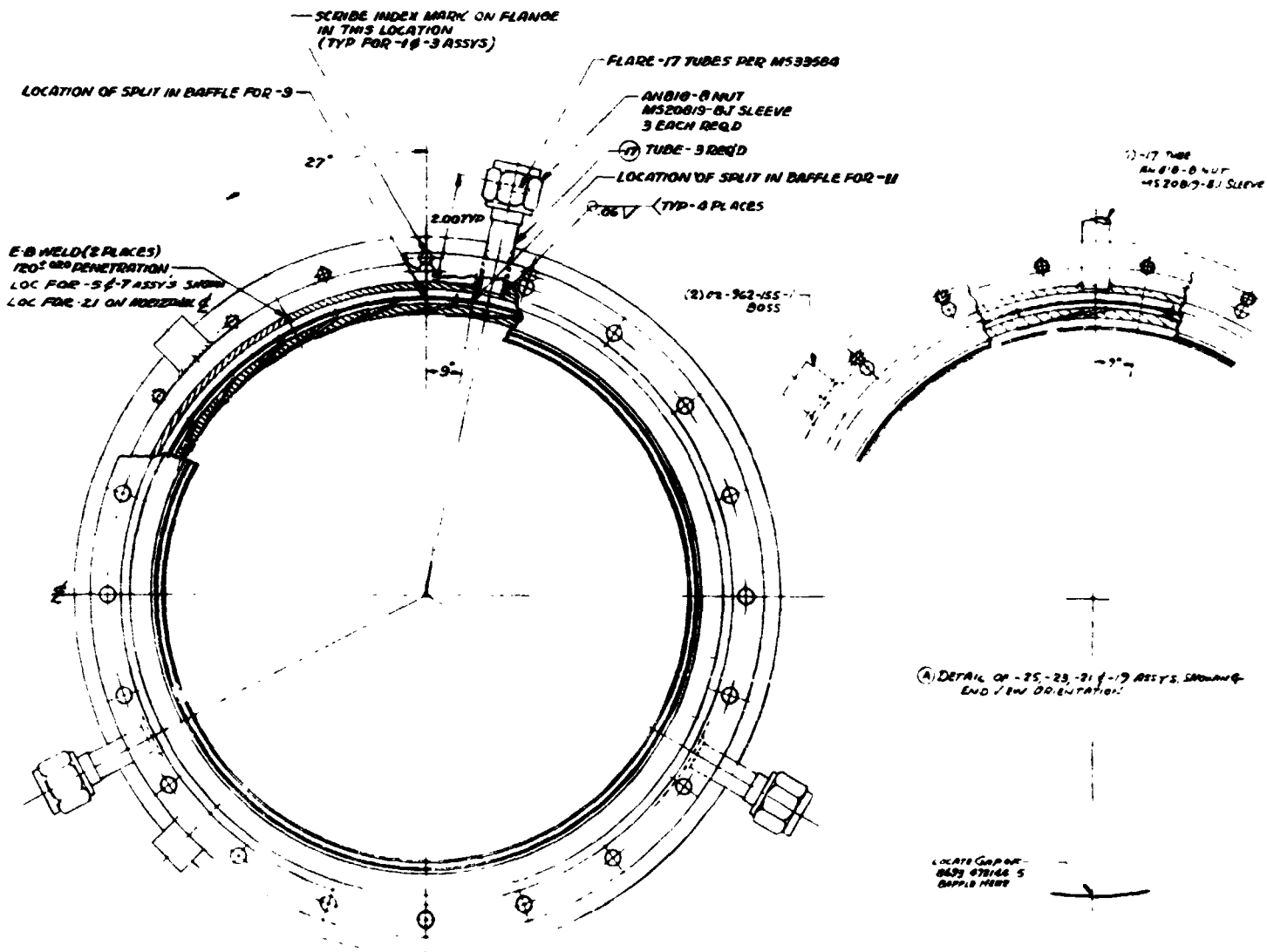


FIGURE VIII-3. VORTEX RING

Bell Aerospace Company

IX. TASK XII - HEATED PROPELLANT INJECTOR **STABILITY TESTING**

The principal objective of this task was to obtain high frequency combustion stability data using an injector representative of regenerative chamber operation. This representation was accomplished by heating the fuel to a temperature expected from the outlet of a cooling jacket and detonating bombs at intervals in the starting transient.

To insure stability or at least a representative condition, it was also desired to evaluate the temperature in the acoustic cavity. The cavity temperature was of concern as the original design was based on an acoustic frequency, which in turn is based on temperature. Some tests related to this program, had previously indicated that the cavity temperatures could be significantly above the design values. Since a substantial increase in temperature should reduce (or at least change) the stabilizing effectiveness of the cavity, knowledge of this temperature was considered necessary to obtain a reasonable assessment of the test data or to make recommendation resulting from test data. As a consequence, the initial test was of 10 seconds to obtain acoustic cavity, time-temperature data. Ten seconds of operation was considered sufficient time to reach equilibrium conditions in the acoustic cavities.

The bomb thermal detonation time also became a restriction when it was found that cavity thermal equilibrium occurred after the normal maximum detonation time of 2.5 seconds. The temperature data obtained indicated that some 6 to 10 seconds operating time in the chamber would be required if full thermal stability was to be achieved. It was suspected that the bomb would not last more than 3 to 5 seconds and indeed this was confirmed in testing. As a consequence of these initial tests, the test duration was programmed for approximately 7 seconds and a bomb insertion device designed which would allow the bomb to remain out of the chamber until the needed time.

Sixteen tests were conducted as the combustion stability task of this program. The stability tests were conducted with an objective of defining a limit where the injector was marginal or produced instability. To accomplish this end, a building block acoustic damper arrangement was used where the open area could be varied to reduce both open area and depth of the individual cavities. With these variations, the 12 deep (1T) cavities could have depths of 1.65, .78 and 0 inches (from the injector face). The percent open area could be incrementally

Bell Aerospace Company

adjusted to have 7.8, 11.6, 13.7 and 15.6%. The four shallow cavities could only have .78 and 0 depths and open areas of 7.8, 3.9 and 0%.

The test sequence was such that the deep cavities were varied from 15.6 to 11.6 to 0 to 7.8% open area where the testing to date indicated stability at 11.6% open area and instability at 7.8%. The shallow cavities (3T) were varied down to 0 without unstable results. Recovery from the bombs on the stable tests, occurred in less than 5 milliseconds in all cases. No apparent recovery was noted on any of the three unstable tests after the first bomb was detonated.

The manner in which the tests were conducted was somewhat unusual. Prior to the test series, temperature recordings in the cavities had shown temperatures in excess of design values. These temperatures recorded were in the order of 3000°F where the original "guess" from literature was in the order of 600°F. Concern was expressed at the cavity capability to damp and a test procedure evolved which would take advantage of this high temperature. Since a substantial time was required for the temperature to come to equilibrium (7 to 10 seconds), a bomb sequence was incorporated detonating charges at 0.5, 2.0 and 7 seconds representing approximately 1000, 2000 and 3000°F in the acoustic cavity. It was suggested that by bombing over this temperature range, a broad spectrum of conditions relating to the speed of sound would be covered and should produce a large amount of useful data with a modest number of tests.

In retrospect, no effect of temperature in the cavity has been found to date. There were only two occurrences of instability noted and these occurrences were with the 1T cavities reduced to 3T depths. Both tests were stable until the bomb was detonated, and neither bomb test recovered after detonation of the first bomb. The test results are summarized in Tables I with the individual tests tabulated in Table II. All bombs had a PETN base charge of 6.9 grains.

A. Preliminary Test Results

The initial tests in this task were conducted to obtain information on the thermal stabilization time of the acoustic cavities. Previous bomb tests had been conducted in the first 1 to 2 seconds of chamber operation, and some related program data had indicated the acoustic cavities to be in a thermal transient in this time period. As a consequence, an acoustic manifold was instrumented to obtain transient data on tests conducted. In addition, the normal bomb insulation which has been used in testing has provided thermal protection for only 4 or 5 seconds. If a longer test was required, then a redesigned

TABLE I
TEST SUMMARY

<u>1T</u>	<u>3T</u>	<u>RESULT</u>	<u>NO. TESTS</u>	<u>NO. BOMBS</u>	<u>REMARKS</u>
15.6	7.8	S	4	1	CAVITY TEMP > 3000°F THERMAL BOMB - OLD STYLE
15.6	7.8	S	6	17	NEW BOMBS DAMP < 5 MS
11.6	7.8	S	5	15	DAMP < 5 MS
0	23.4	U	2	3	BOTH TESTS UNSTABLE
7.8	15.6	U	1	3	INITIAL BOMB UNSTABLE TO SHUTDOWN
11.6	3.9	S	1	3	DAMP < 5 MS
11.6	0	S	1	3	DAMP < 5 MS

TABLE II
TEST SUMMARY OF BOMB TESTS - BOMB STABILITY PROGRAM, TASK XII

DATE	TEST NUMBER	DURATION SEC.	DATA POINT SEC.	R ₀ /F	P _{CC} IN. PSIA	C* FT/SEC	P %	C ₁ LT °F	P ₁ LT °F	MAXIMUM % OVERPRESSURE					MAXIMUM CAVITY TEMPERATURE & DETONATION OF			(1) NO. OF BOMBS	(% OF CHAMBER)		COMMENTS
										CHAMBER		CAVITY			BOMB 1	BOMB 2	BOMB 3		CAVITY AREA		
										P _{C-1}	P _{C-2}	P _{C-5}	P _{C-3}	P _{C-4}					.1T	.3T/1R	
3/1/74	4560	2.2	1.0	1.862	110.9	5643	2.1	57	128	216	140	130	327	-	1229	1770	N.A.	2 (2)	15.6	7.9	All recovery times less than 5 MS
3/4/74	4561	6.0	6.0	1.791	125.6	5622	2.2	85	231	--	113	141	305	-	1320	1720	3025	3			
3/4/74	4563	6.0	6.0	1.335	17.1	5535	2.6	85	209	--	132	228	394	-	1430	1800	--	3			
3/5/74	4564	7.0	6.0	1.865	152.7	5609	2.1	86	220	147	77	93	295	246	--	--	--	3			
3/5/74	4565	7.0	6.0	1.720	16.5	5539	2.3	85	203	250	131	248	350	492	--	--	--	3			
3/6/74	4566	7.0	6.0	1.467	151.3	5538	2.5	68	211	184	114	98	252	160	--	--	--	3			
3/8/74	4567	6.0	6.0	1.546	125.7	5562	2.3	60	173	252	115	324	312	277	1730	2440	2825	3	11.6	7.9	All recovery times less than 5 MS
3/8/74	4568	6.0	6.0	1.495	101.3	5510	2.5	67	199	218	116	--	443	378	1670	3205	2530	3			
3/8/74	4569	7.0	6.0	2.054	104.1	5455	2.1	61	184	200	157	--	196	344	2065	2875	2480	3			
3/11/74	4570	7.0	6.0	1.940	149.4	5531	2.1	70	225	244	99	--	--	179	2120	2740	2775	3			
3/11/74	4571	7.0	6.0	1.489	149.8	5556	2.5	60	206	203	79	--	265	184	1585	3250	3620	3			
3/14/74	4572	0.7	0.45	1.753	122.1	--	2.3	37	23	202	94	--	254	308	2015	--	--	1 (3)	0	23.6	Unstable-Automatic shutdown (ASD). Unstable 2 to 8.1 sec. ASD did not operate. ASD did not operate. Unstable from 1st bomb to shutdown ASD did not operate since unstable overpressures (30 psi) was less than 40 psi limit. Recovery time less than 5 MS
3/15/74	4573	6.1	6.0	1.791	119.8	5614	2.3	66	217	135	118	--	334	396	--	2915	--	2 (4)	0	23.6	
3/26/74	4574	6.1	6.0	1.603	125.2	5476	2.3	66	198	173	98	--	197	414	1910	2280	1965	3	7.85	15.75	
4/11/74	4575	6.0	6.0	1.670	129.3	5595	2.2	65	213	231	135	159	410	521	1580	2840	2795	3	11.6	3.9	
4/12/74	4576	6.0	6.0	1.536	125.3	5584	2.3	71	215	218	154	155	319	-	1680	2080	2750	3	11.6	0	

(1) BOMB DETONATION TIMES WERE APPROXIMATELY 0.5, 2.0, AND 6.9 SEC. FOR EACH RUN.

(2) BOMB DETONATION TIMES 0.5 AND 2 SEC.

(3) BOMB DETONATION TIME 0.5 SEC.

(4) BOMB DETONATION TIMES 2.0 SEC., AND BETWEEN 6.9 AND 8.1 SEC.

N.A. - NOT APPLICABLE

Bell Aerospace Company

bomb thermal protection or an insertion device would be desirable. To confirm that this added effort was needed, a bomb was inserted into a chamber and tested to thermal detonation. The results of these preliminary tests showed that thermal equilibrium was not achieved until 7 to 9 seconds and that the bomb thermal detonation occurred at 4.2 seconds. These results indicated the need for the longer bomb run and the bomb inserter was designed as a result of the tests.

By using a longer run time and by using multiple bombs, the stability program was redesigned to present a more comprehensive stability survey.

The three bombs were considered to represent entirely different temperature (and possibly acoustic) conditions in the damper cavities. The bomb detonation times of .5, 2.0 and 7.0 seconds roughly approximate temperatures of 1000°F, 2000°F, and 3000°F in the acoustic damper cavity (PR #16). This test procedure was devised to take advantage of the high temperature of these cavities, especially since the temperature transient is sufficiently slow, so that the bomb can be detonated with some time latitude without being too far away from the expected temperature condition.

1. Hardware Changes for Preliminary Testing

Acoustic Damper - As a result of separate studies, some additional cooling for the acoustic damper was indicated. Original estimates of cavity temperatures were much lower than those encountered in test. As a result of this information, active cooling, and consequently cavity size changes were indicated and incorporated into the injector chamber interfaces.

The changes consisted of a 0.015 inch increase in the cavity width to compensate for the thicker lands, thus maintaining a baseline open area that was the same as that on previously demonstrated hardware. The land thickness of the acoustic ring was increased to allow the incorporation of coolant passages on future designs. To define stability margin, the acoustic ring was designed to permit variations to the acoustic cavity open area by the attachment of inserts to the lands (Figure IX-1). These rings were designed so that the 1T tangential cavities (deeper one) could be varied to have from 15.7 to 11.6% open area. The third tangential cavities could have 7.8 to 3.9% open area. The basic symmetry of the acoustic cavities was maintained, eliminating concern or effect of unequal area distribution, and also simulating the configuration expected on the final design. Provisions have also been made to vary the cavity depth from 1.65 to 1.77 inch depth from the injector face.

ACOUSTIC DAMPER INSTALLATION
10 INCH INJECTOR

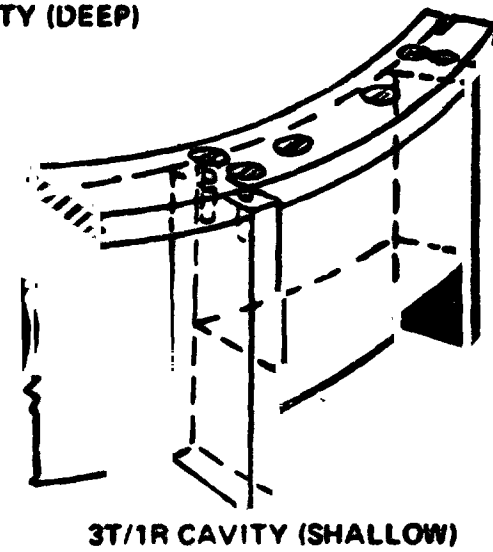
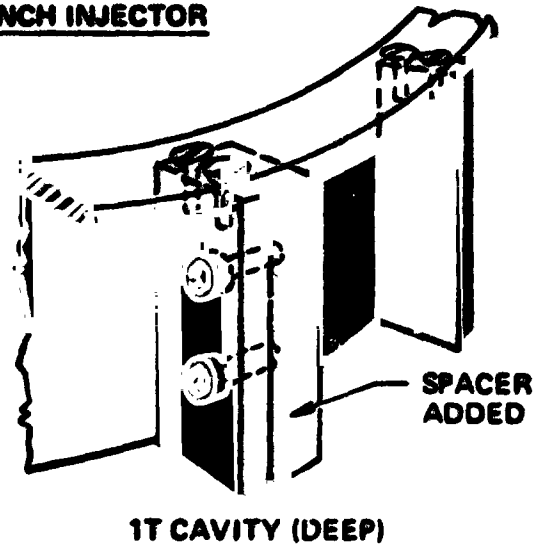
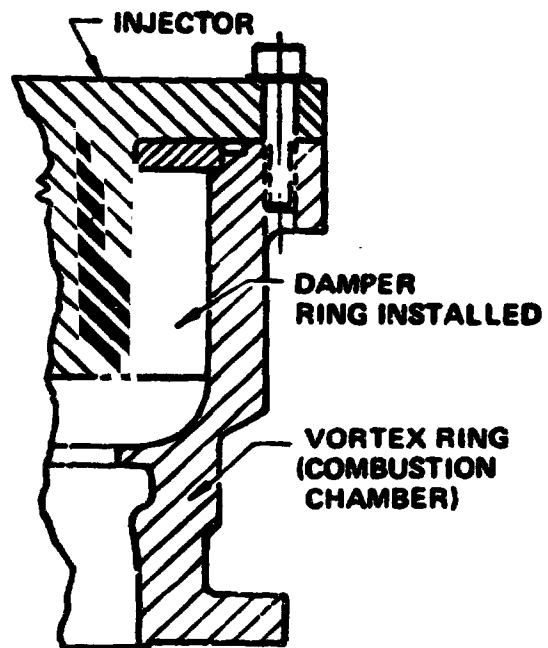
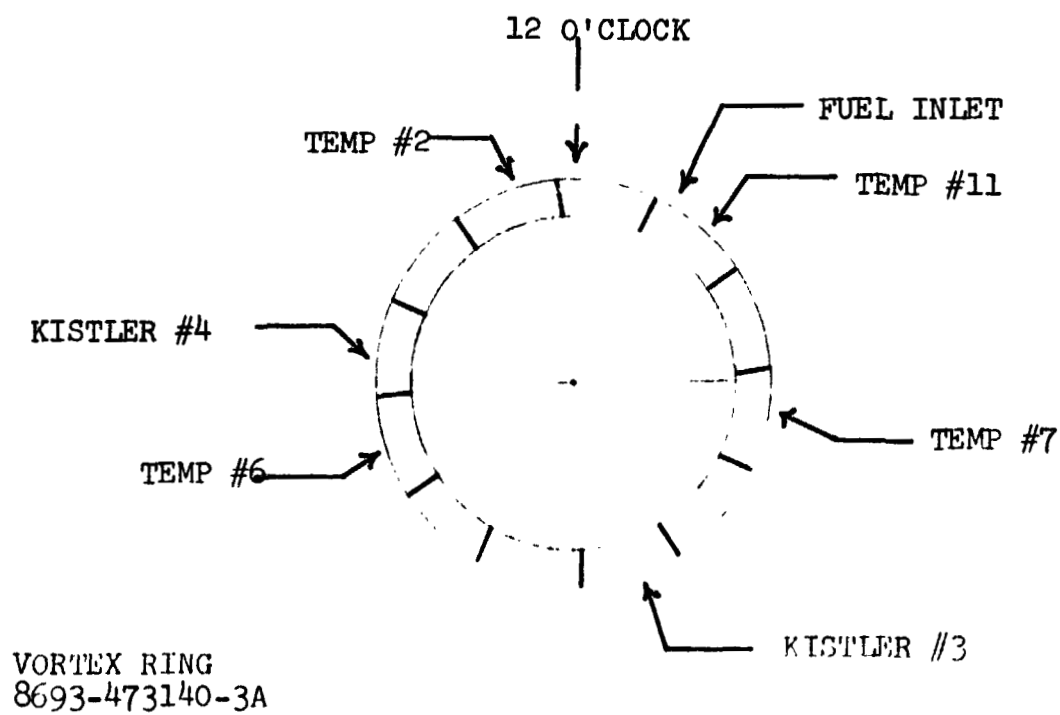
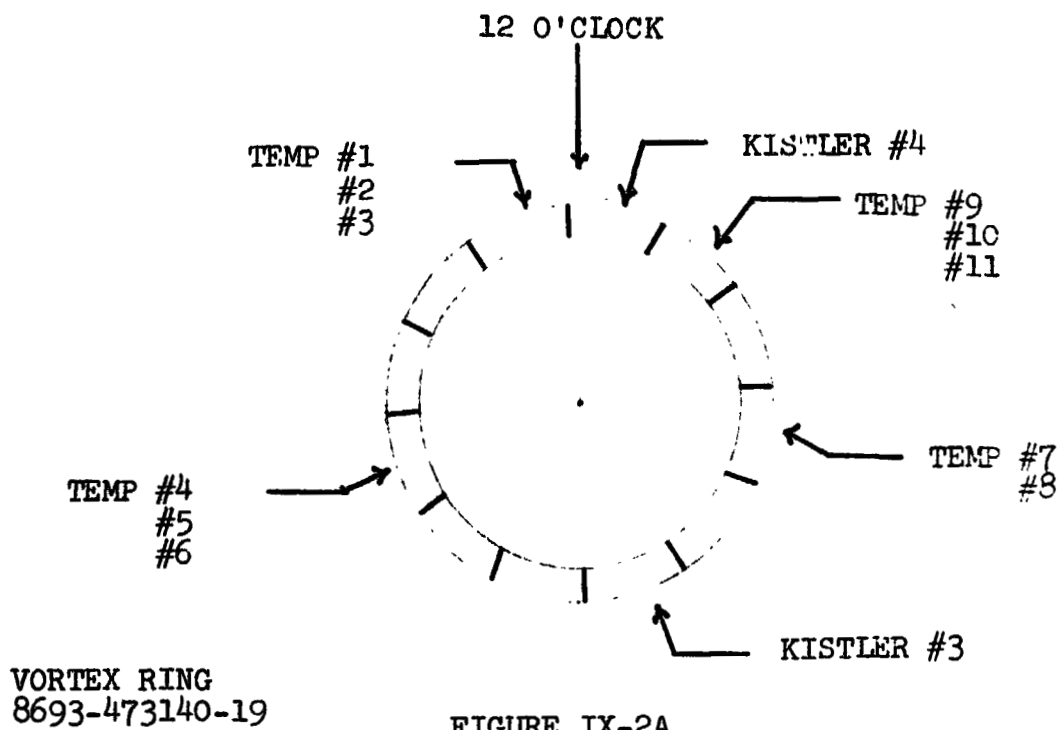


FIGURE IX-1

Bell Aerospace Company

VORTEX RING INSTRUMENTATION



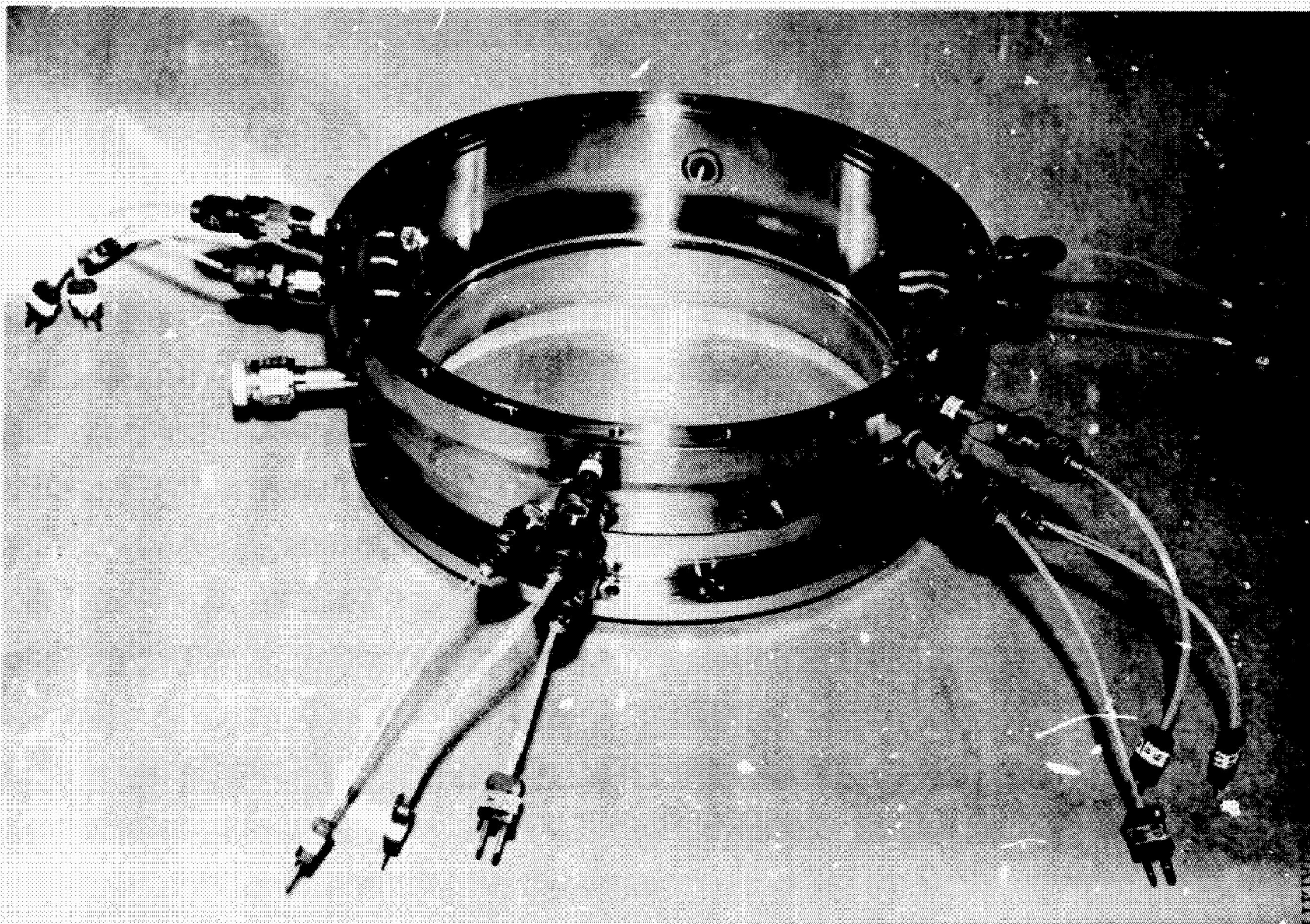
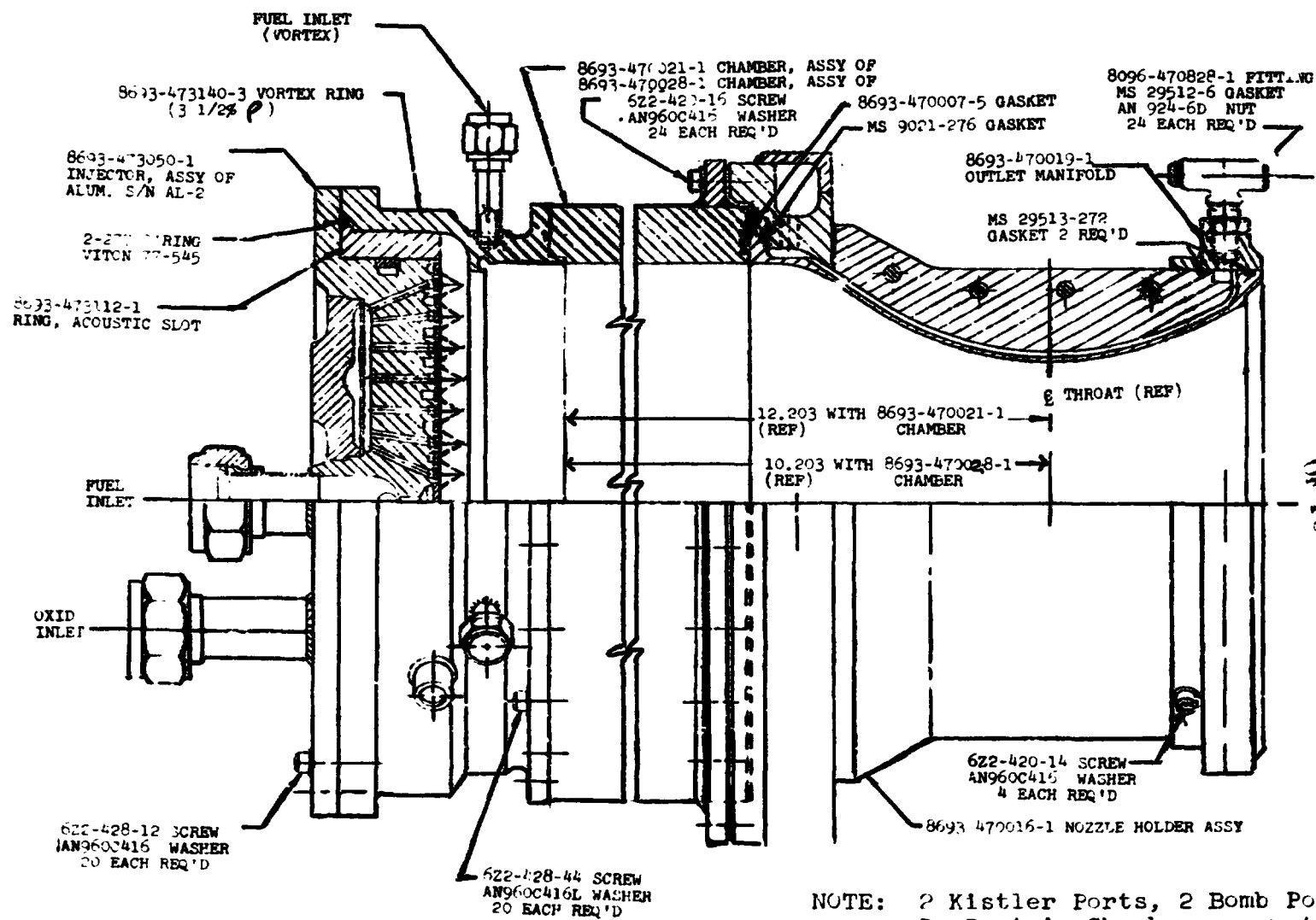


FIGURE IX-3. THERMOCOUPLE INSTALLATION FUEL VORTEX RING (8693-473140-19)



NOTE: 2 Kistler Ports, 2 Bomb Ports and P_c Port in Chamber are not shown.

ORIGINAL PAGE IS
OF POOR QUALITY

FIGURE IX-1

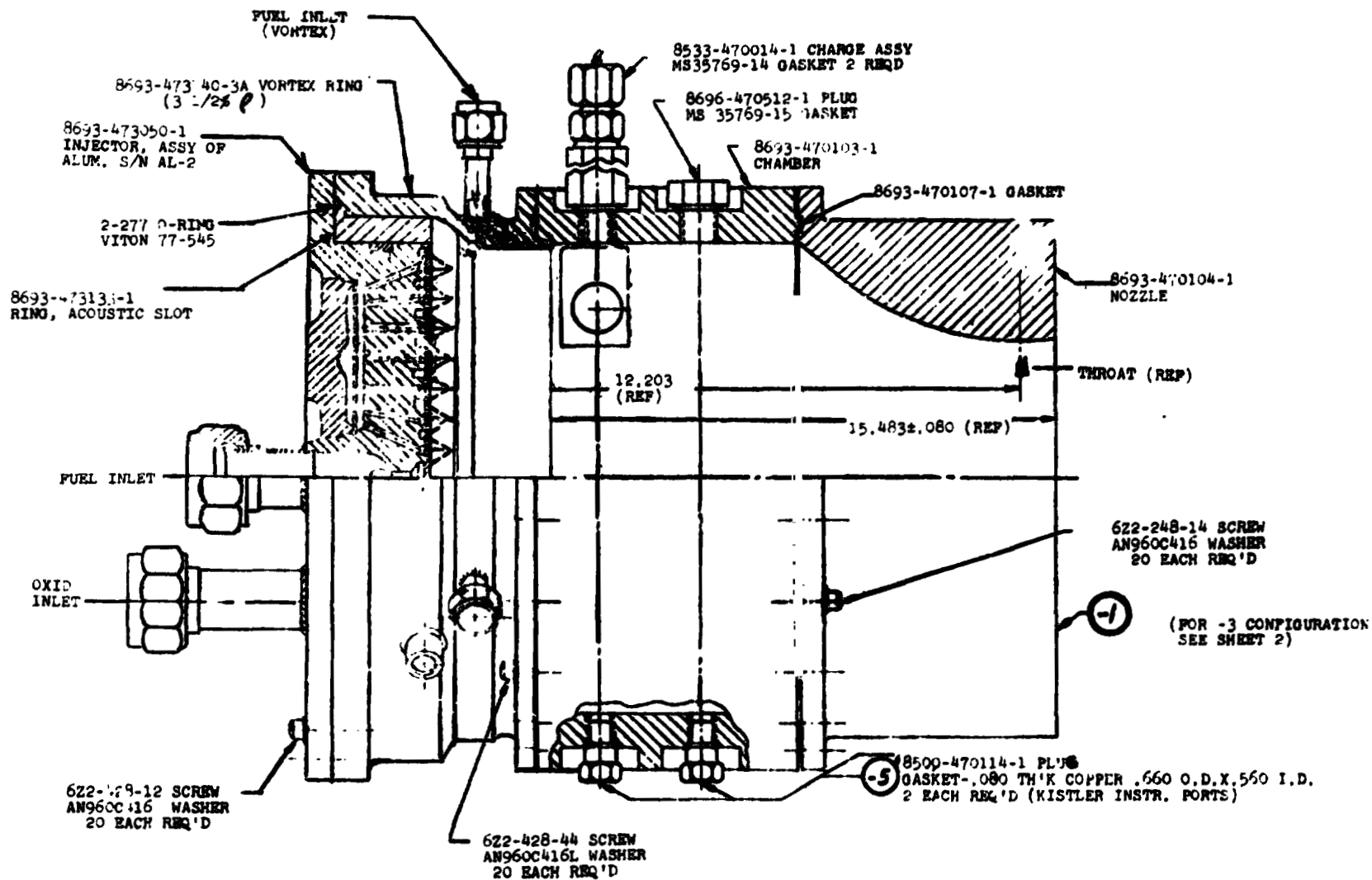


FIGURE IX-1

TABLE III
TEST SUMMARY OF CHECKOUT RUNS
BOMB STABILITY PROGRAM

DATE	RUN #	DUR. (SEC)	DATA POINT (SEC)	R ₀ /F	P _{CC} (PSIA)	t	V* (FT/SEC)	MAX CAVITY TEMP. (°F)	BOMB SIZE (GRAINS)	BOMB TIME (SEC)	MAX. OVERPRESSURE				RECOVERY TIME (MILLISECONDS)
											P _C #1	P _C #2	P _C #3	P _C #4	
1/03/74	4556	3.1	2.5	1.811	121.8	2.14	5545	2844	-	-	-	-	-	-	-
1/14/74	4557	10.2	4.0	1.654	121.0	2.03	5516	3320	-	-	-	-	-	-	-
1/15/74	4558	3.1	2.0	1.644	122.0	2.10	- (1)	1760 (3)	-	-	-	-	-	-	-
1/17/74	4559	4.5	3.5	1.645	124.2	2.19	5456 (2)	3100	10	4.23	296	216	468	336	5

(1) DATA NOT VALID DUE TO NOZZLE THROAT PROBLEM

(2) DATA QUESTIONABLE DUE TO PATCHBOARD PROBLEM

(3) MAX CAVITY TEMPERATURE @ 2.5 SEC. 1930°F

Bell Aerospace Company

TABLE IV

HARDWARE CONFIGURATION

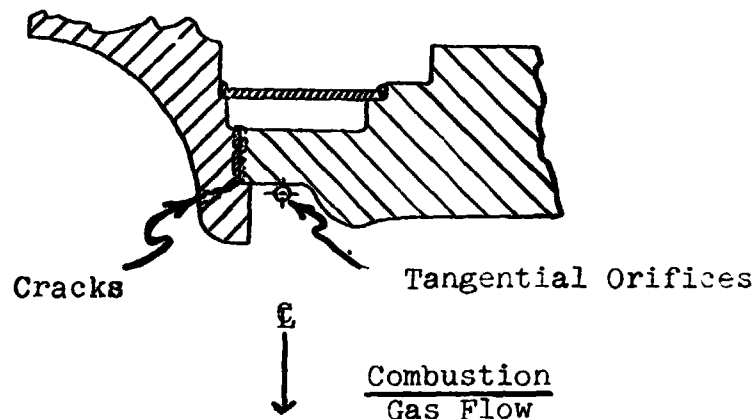
HARDWARE DESCRIPTION	RUN D-4			
	4556	4557	4558	4559
Aluminum Injector, S/N 1A (8693-473115-1)	x	x		
Aluminum Injector, S/N 2 (8693-473050-1)			x	x
Fuel Vortex Ring, S/N 1 (8693-473140-19)	x	x		
Fuel Vortex Ring, S/N 1A (8693-473140-3A)			x	x
Acoustic Cavity Ring, S/N 1 (8693-473112-1)	x	x	x	x
Bomb Chamber, S/N 1 (8693-470103-1)				x
Bomb Chamber, S/N 1A (8693-470021-1A)	x	x	x	
Heat Sink Nozzle, S/N 1 (8693-470104-1)				x
Water Cooled Nozzle, S/N 1 (8693-470016-1)	x	x	x	
Bipropellant Valve, S/N 1 (8612-470010)	x	x	x	x

Bell Aerospace Company

The 10 second duration test produced a mixture ratio (O/F) of 1.664, vortex flow at 2.03% and chamber pressure at 121.0 psia. The maximum gas temperature recorded in the acoustic cavity was 3320°F (Temp. No. 3) and occurred in deep cavity number 1, and was at the top (gas side) of the cavity.

The tungsten/rhenium thermocouples operated very satisfactorily during the test and produced a believable time history. On the other hand, the platinum-platinum/rhodium thermocouples opened at the combustor intersection, where temperatures apparently exceeded the couple capability. Figures IX-6 through IX-9 are temperature time histories. The temperature results indicated that a much longer bomb time than the previously used 2 seconds was required to reach stabilization. From this data, it was concluded that approximately seven seconds would be the minimum bomb detonation time that could be used to represent a stabilized temperature.

Post run examination of the hardware revealed several cracks on the vortex ring just upstream of the tangential orifices as shown below.



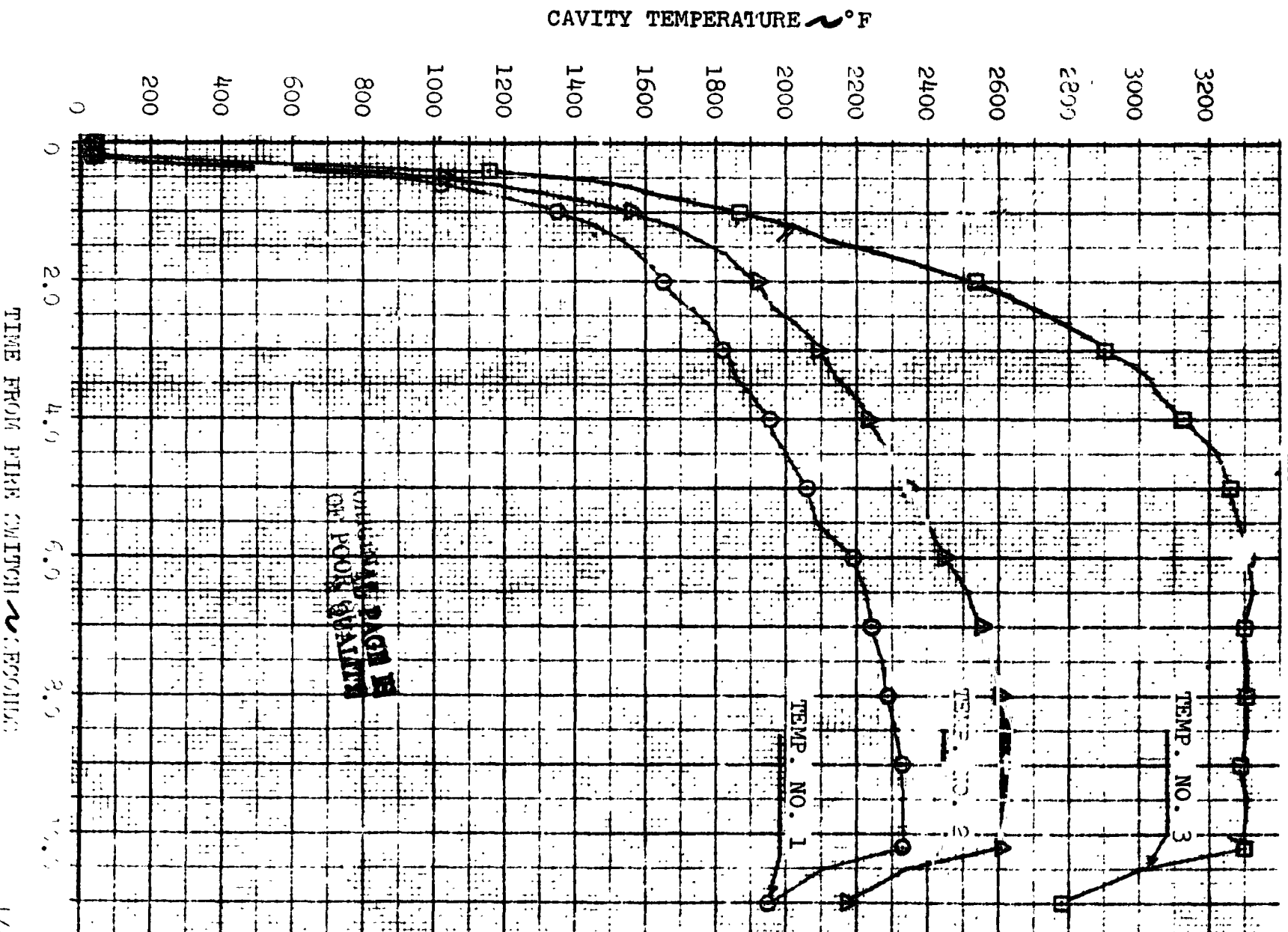
It appears that the cracks may have originated at the weld joint where high stress concentrations are likely. Repair of this unit was not considered productive and the part was set aside and replaced with vortex ring 8693-473140-3A for the next test.

Due to the requirement to change the hardware, a reorificing test was also scheduled for test 4558. The result of the test was a confirmation of the high temperatures in the acoustic cavity, resulting from test 4557. Since the primary objective of the program was to confirm the high temperature, it was

Boell Aerospace Company

FIGURE IX-6
ACOUSTIC CAVITY GAS TEMPERATURE
VS
TIME

CAVITY NO. 1
 TEST D-4: 4557
 DATE: 1/4/74



CAVITY NO. 1
 TEST D-4: 4557
 DATE: 1/4/74

TIME FROM FIRE SWITCH ~ SECONDS

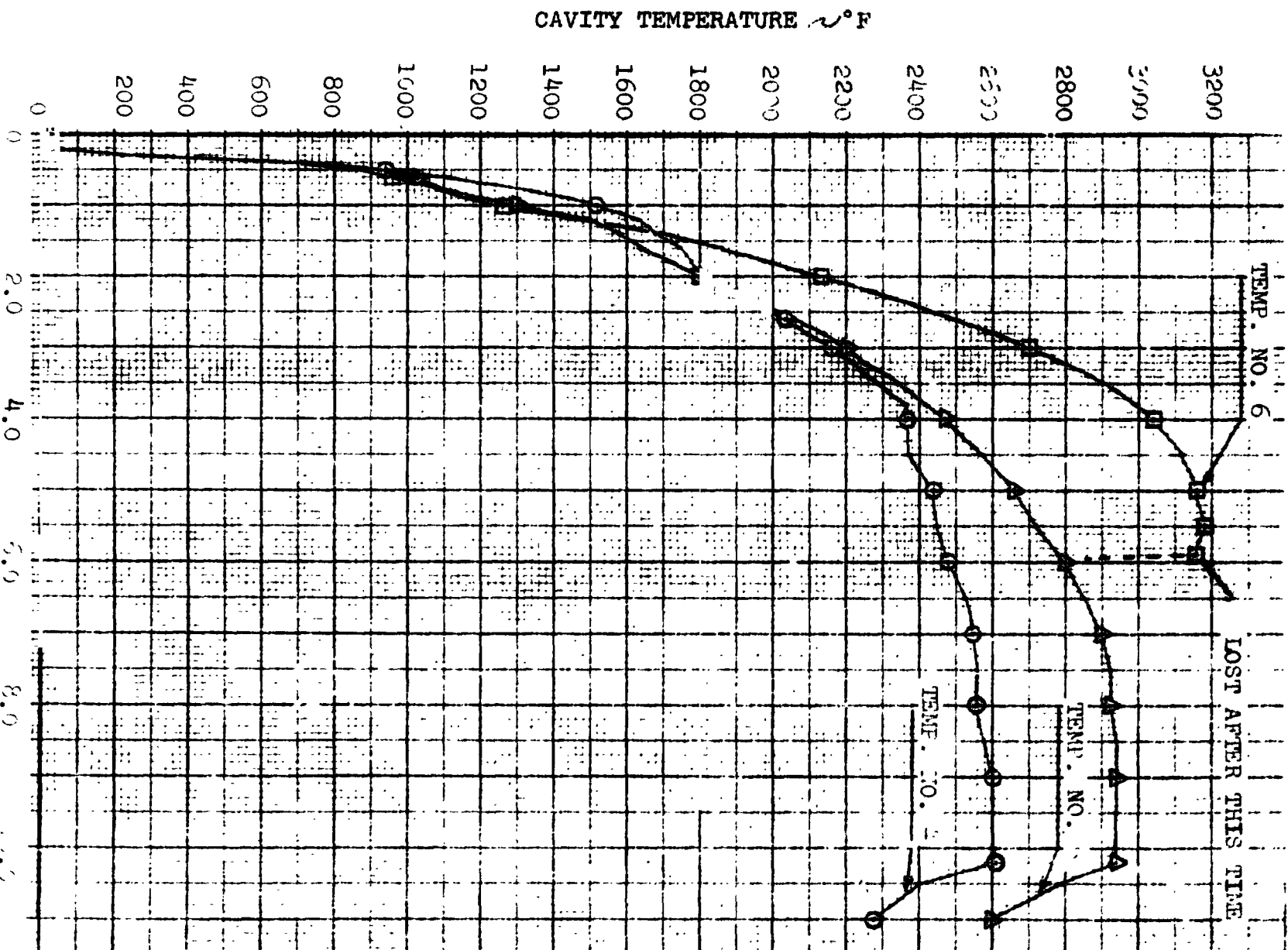
1/4/74

Dell Aerospace Company

FIGURE IX-7
ACOUSTIC CAVITY GAS TEMPERATURE

VS
TIME

CAVITY NO. 6
TEST NO. 1557
DATE: 1/4/74

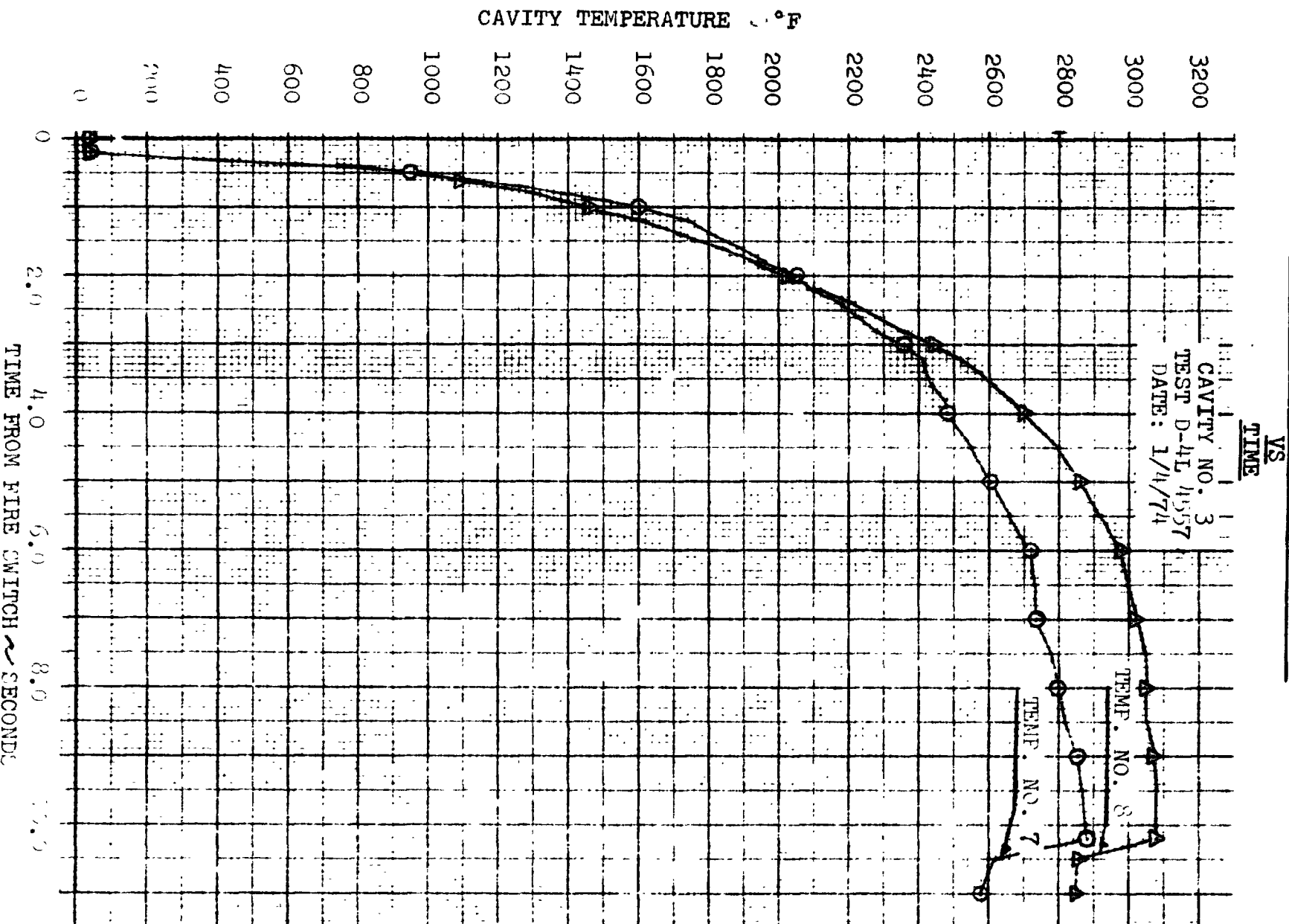


TIME FROM FIRE SWITCH / C/S FREQ. 100

Bell Aerospace Company

FIGURE IX-8

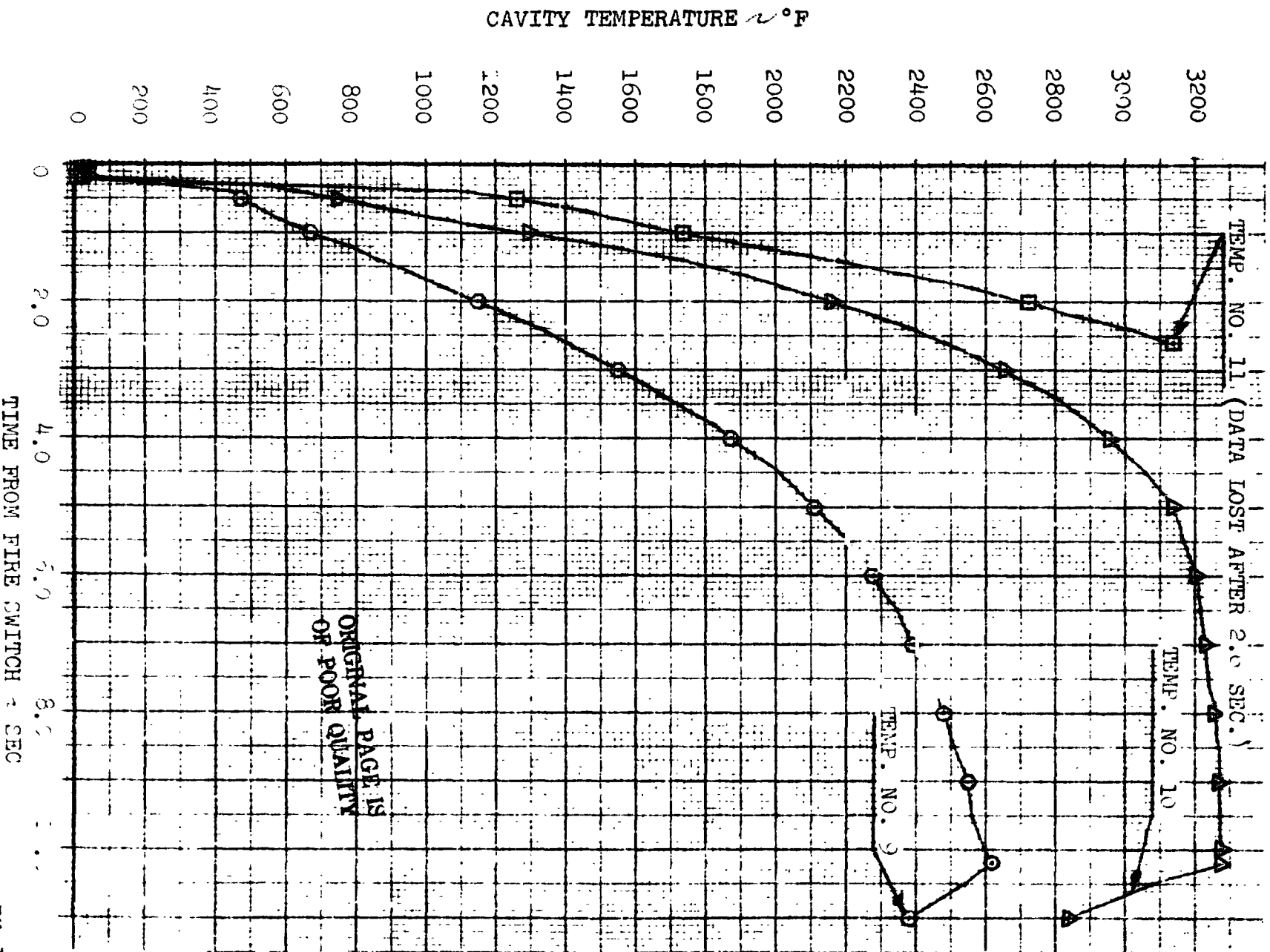
ACOUSTIC CAVITY GAS TEMPERATURE



Bell Aerospace Company

FIGURE IX-9
ACOUSTIC CAVITY GAS TEMPERATURE
VS
TIME

CAVITY NO. 4
TEST D-4: 4557
DATE: 1/4/74



Bell Aerospace Company

considered that further testing to confirm temperatures was not warranted. The three second checkout test resulted in a mixture ratio (O/F) of 1.644, vortex flowrate of 2.10%, and chamber pressure of 122.9 psia. The decision to change to the bomb durability tests also helped by some hardware damage resulting from the test. The water cooled liner of the nozzle was damaged in the test and repairs were required. Since further testing of the water cooled nozzle did not appear necessary, the bomb duration test was set up immediately.

The set-up for this run 4559 is also depicted in Figure IX-5 with the hardware listed in Table IV. The objective of this test was to define the time for thermal detonation of a bomb. More precisely, since 6 seconds of operation was required to represent equilibrium temperatures, the test was made to see if the current bomb decision would last that long in the thrust chamber. A 10 grain bomb was installed in the upstream port. Provisions were also made for electrical detonation if the expected thermal detonation did not occur.

The bomb detonated thermally at 4.23 seconds from fire switch and shutdown was made at 4.5 seconds. The test was made at a mixture ratio (O/F) of 1.645, $P = 2.19\%$ and $P_c = 124.2$ psia. Maximum acoustic cavity temperature of 3080°F was recorded and occurred at the top of cavity number 1.

A temperature time history plot is shown in Figure IX-10. The four second data point was plotted on figures IX-6, IX-7, IX-8, and IX-9 for comparison with the results of test 4557 and are tabulated below:

<u>Temp. No.</u>	<u>Data Time (Sec)</u>	<u>Run 4557 Temp. (°F)</u>	<u>Run 4559 Temp. (°F)</u>	<u>Cavity Configuration</u>
2	4.0	2230	2400	Deep
6	4.0	3040	2550	Deep
11	4.0	--	3080	Deep
7	4.0	2480	2450	Shallow

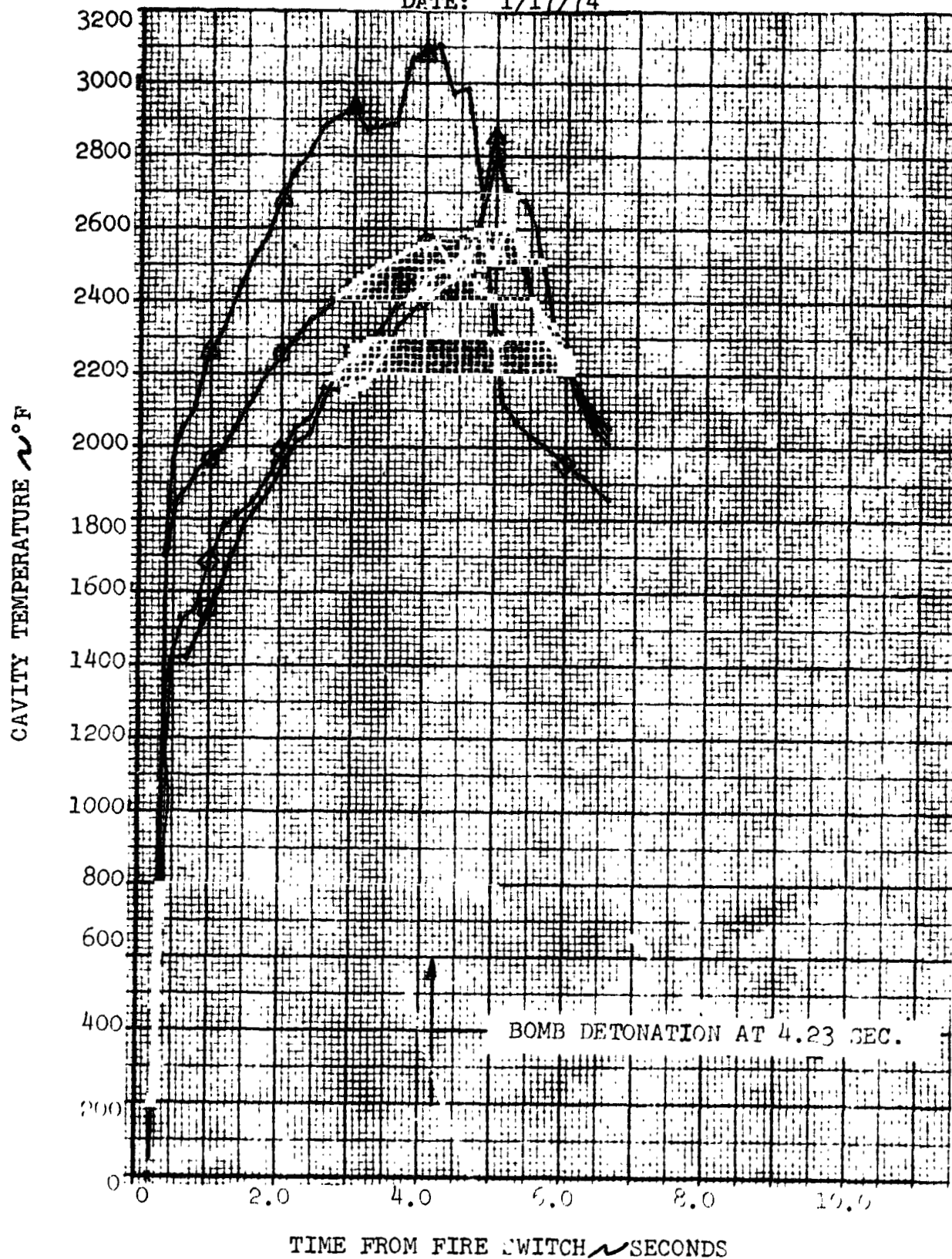
The four second temperatures were of specific interest to ensure that the higher temperatures (up to 3000°F) were encountered near or at the time of bomb detonation. Also, some concern had been exhibited in that the longer bomb detonation time would occur at a higher cavity temperature than previously encountered.

Bell Aerospace Company

FIGURE IX-10
ACOUSTIC CAVITY GAS TEMPERATURE
VS
TIME

- ◇ Temp #2 - Cavity #1
- Temp #6 - Cavity #2
- △ Temp #11 - Cavity #3
- Temp #7 - Cavity #4

TEST NO. D-4: 4559
DATE: 1/17/74



Bell Aerospace Company

The test was conducted without incidence. The bomb detonated thermally at a slightly longer operating time (4.2 seconds) than originally predicted (3.5 seconds). Recovery was 5 milliseconds, comparable to previous tests.

4. Preliminary Test Conclusions

Two conclusions were made from these tests. The first being related to a longer run time requirement for the acoustic damper stabilization than originally anticipated. The second being a much higher acoustic cavity temperature than literature information had indicated. As a consequence to the above conclusions, it was decided to reconfigure the bomb chamber to incorporate the capability of both long and short duration bombs by having a wall mounted bomb for short durations, and a bomb inserter to be used for detonating bombs at durations greater than 4 seconds.

a. Bomb Inserter

The technique of inserting bombs into a combustion chamber was developed during the LM Ascent engine program and readily accomplished. Unfortunately, that program has been completed for several years and all related equipment scrapped. Thus, also with the bomb inserters. On the current program, it was decided to design and fabricate a new inserter, one of reduced complexity and therefore cost. The design selected is shown in Figure IX-11.

Operation of the inserter is pneumatic. The bomb is mounted in the inserter such that the top insulating cap is flush with the chamber wall. On command, the inserter is actuated, pushing the bomb and its protective cover into the chamber. An electrical signal then detonates the bomb at the time designated.

B. Heated Propellant Stability Test Results - Test Hardware

The hardware used for this stability evaluation is listed in Table V and the assembly is shown in Figure IX-12. Figure IX-12 also shows the location of the 3 bomb ports and the 5 high frequency response transducers. The stationary bomb and inserter bomb assemblies are shown in Figure IX-13. Figure IX-14 shows the location of thermocouples 2, 6, 7 and 11 which were used for this test effort.

Figures IX-15 through IX-17 are photographs of the injector acoustic ring (11.6% 1T and 3.9% 3T/1R), stationary bomb installation and bomb inserter assembly respectively.

BOMB INSERTER ASSEMBLY

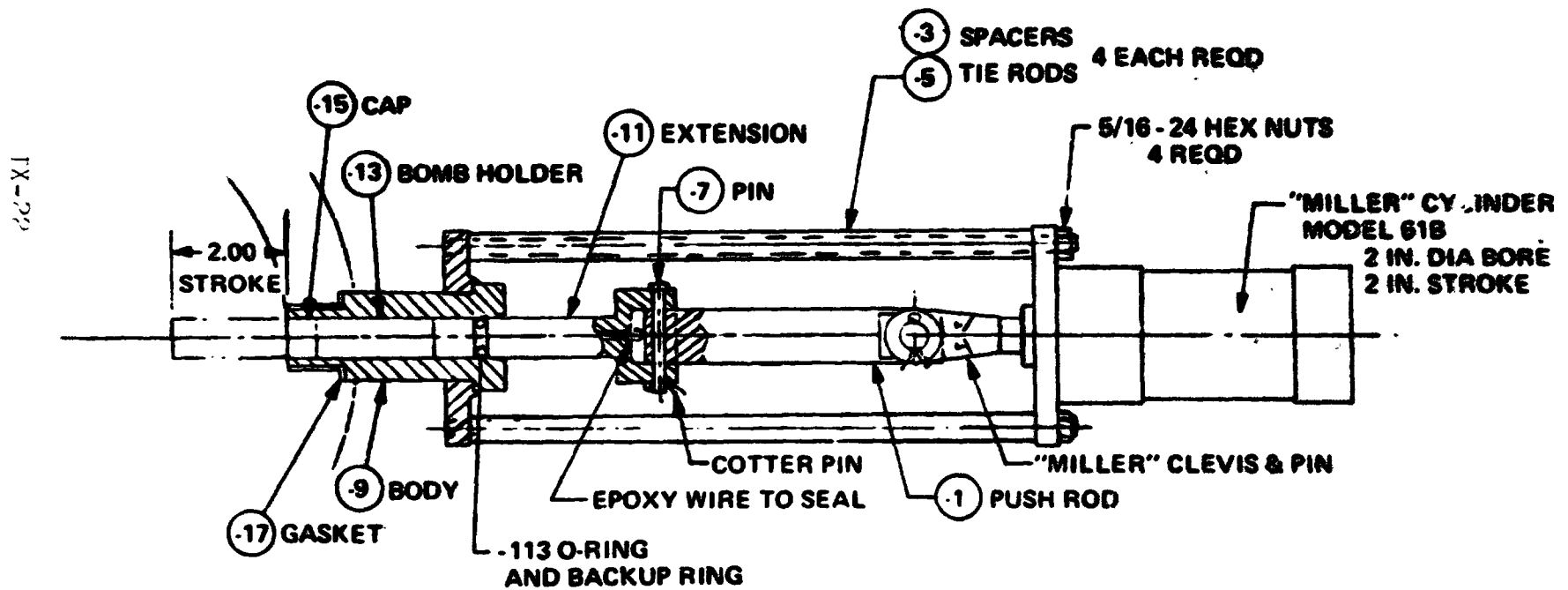
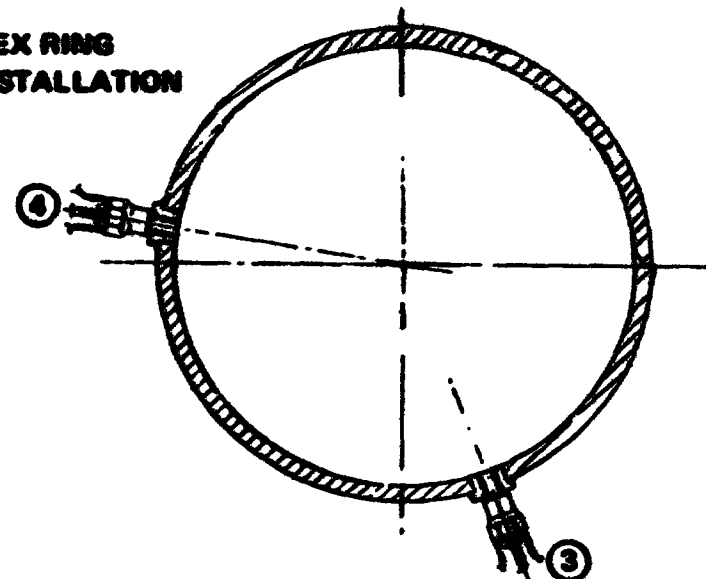


FIGURE IX-11

THRUST CHAMBER ASSEMBLY
(BOMB TEST)

**VORTEX RING
KISTLER INSTALLATION**



**CHAMBER BOMB AND KISTLER
INSTALLATION**

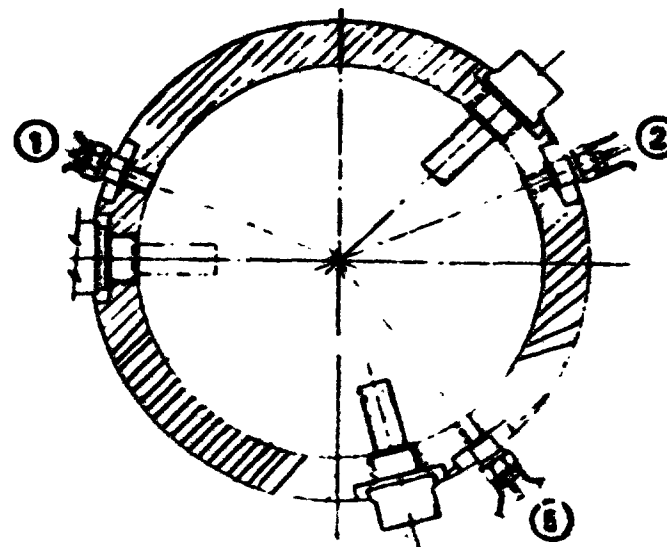
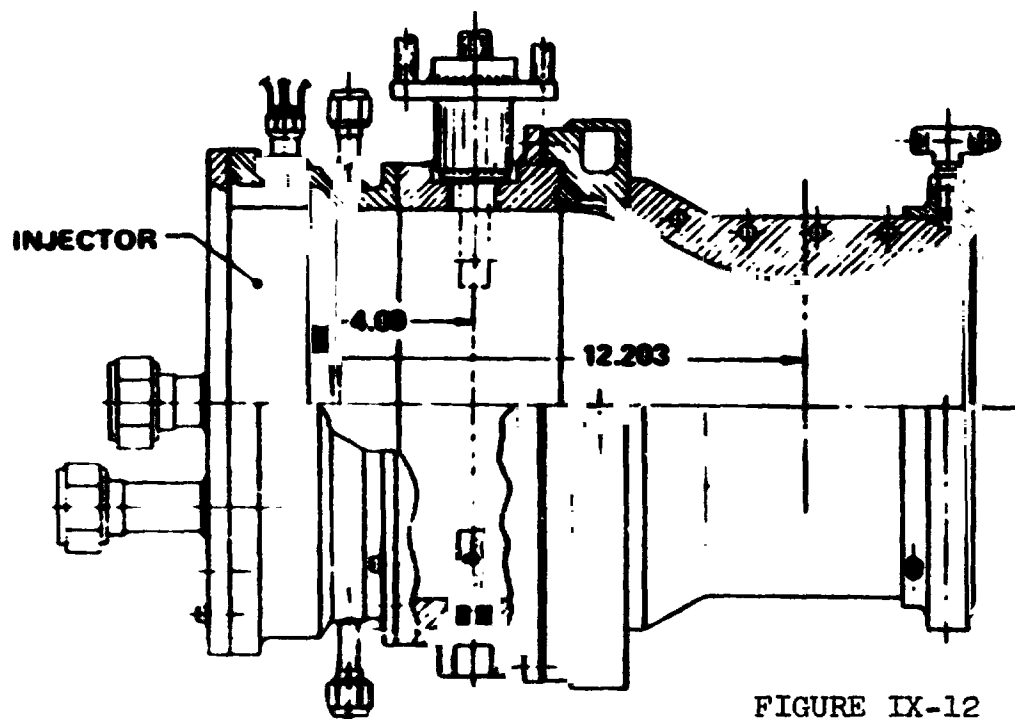


FIGURE IX-12



IX-24

ORIGINAL PART OF POB QCA

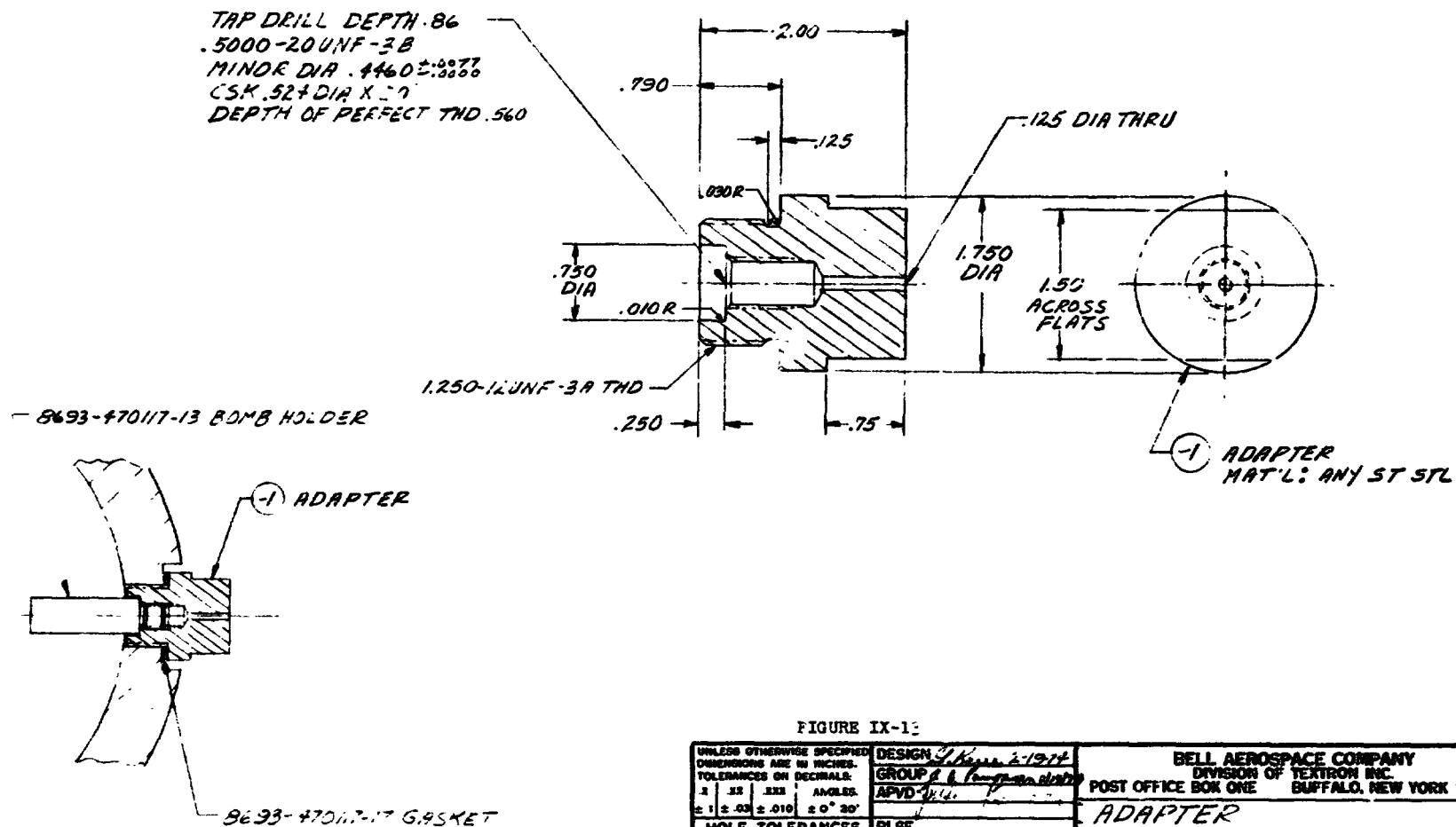
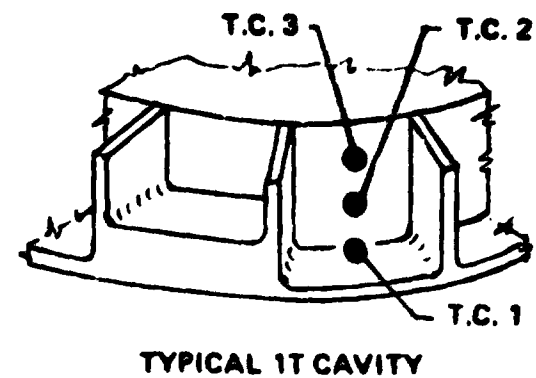
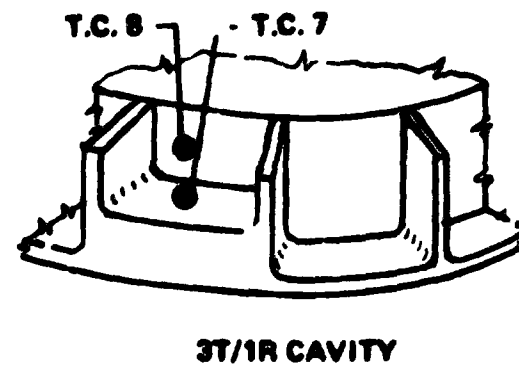
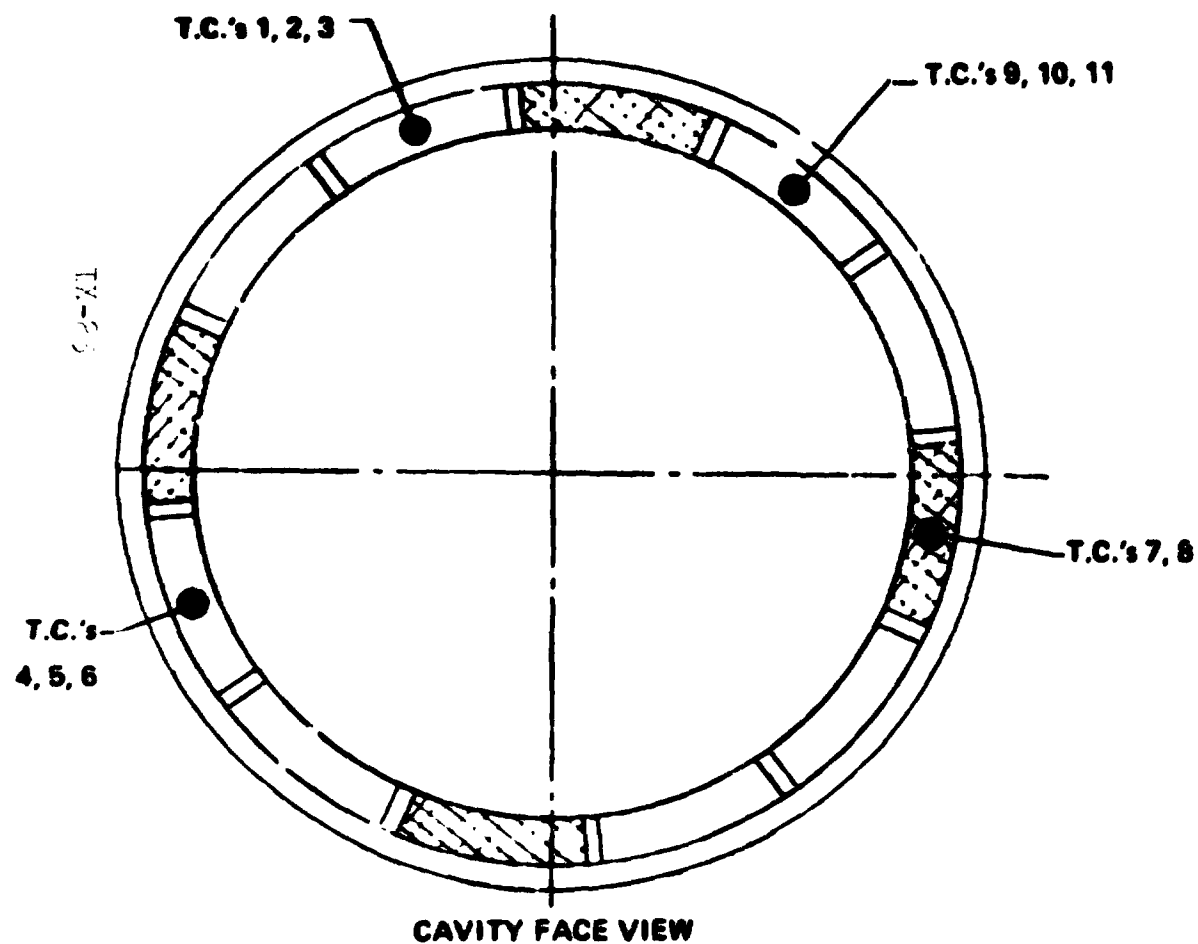


FIGURE IX-13

UNLESS OTHERWISE SPECIFIED DIMENSIONS ARE IN INCHES. TOLERANCES ON DECIMALS:		DESIGN <i>J. K. 2-1974</i>		BELL AEROSPACE COMPANY DIVISION OF TEXTRON INC. POST OFFICE BOX ONE BUFFALO, NEW YORK 14240	
1	.XX	XXX	ANGLES	ADAPTER	
± 1	± .00	± .010	± 0° 30'	BOMB INSTALLATION	
HOLE TOLERANCES EXCEPT AS SHOWN			RLSE	SCALE <i>FULL & HALF</i>	
0.04 TO .120	± .005	± .001	UNLESS OTHERWISE SPECIFIED BREAK EDGES .015 MAX RAD OR CHAMFER	SIZE	CODE IDENT NO
.130 TO .250	± .005	± .001		B	80070
.261 TO .488	± .005	± .001	MACHINED SURFACES	8693-470119	
.499 TO .750	± .010	± .001	EXCEPT AS NOTED	DEVELOPMENT SH	
.750 TO .988	± .015	± .001			
.989 AND LARGER	± .010				

CAVITY TEMPERATURE TEST THERMOCOUPLE LOCATIONS



NOTE: Only thermocouples 2, 5, 7 and 11 were used in this test effort.

FIGURE IX-14

ORIGINAL PAGE IS
OF POOR QUALITY

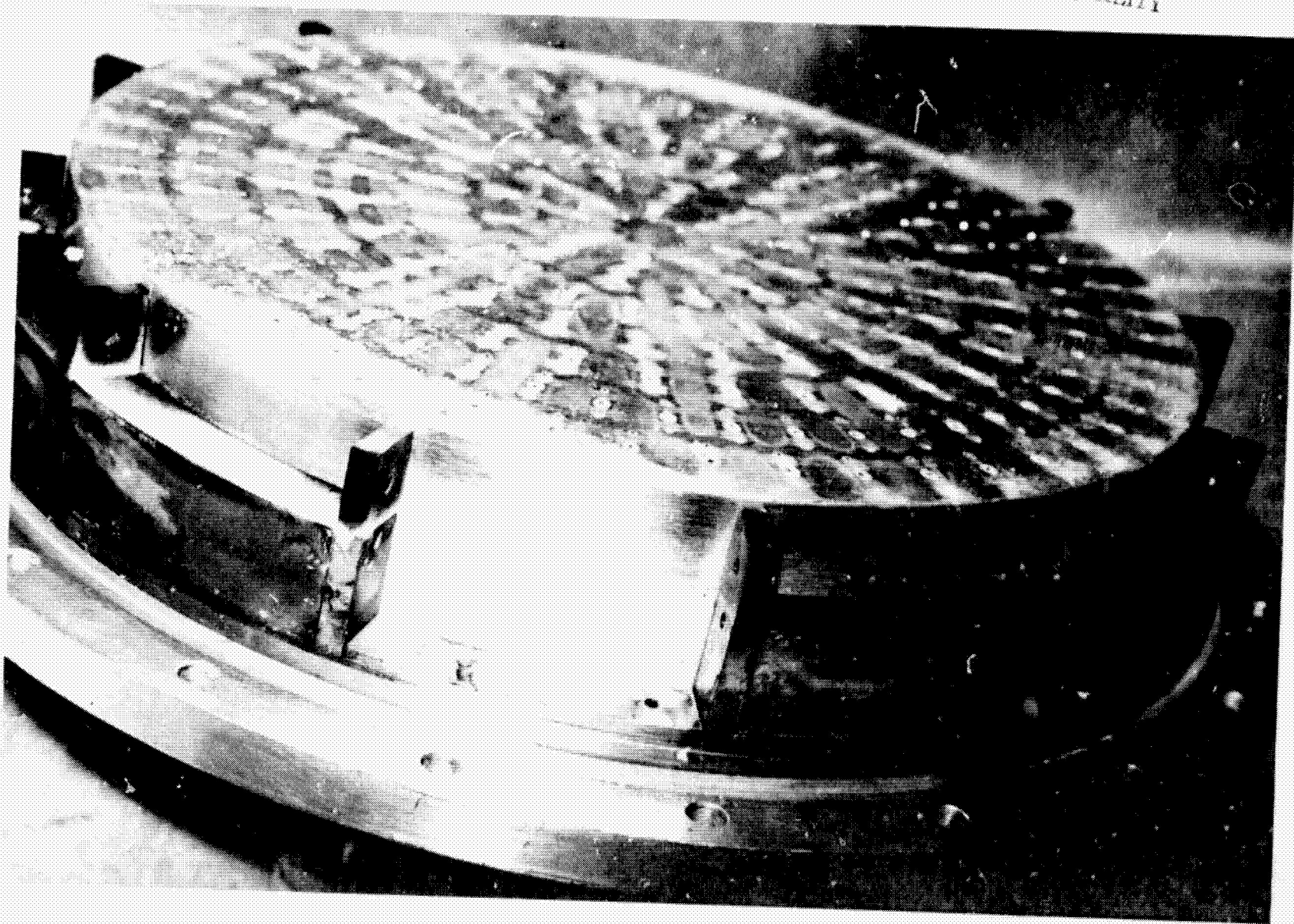
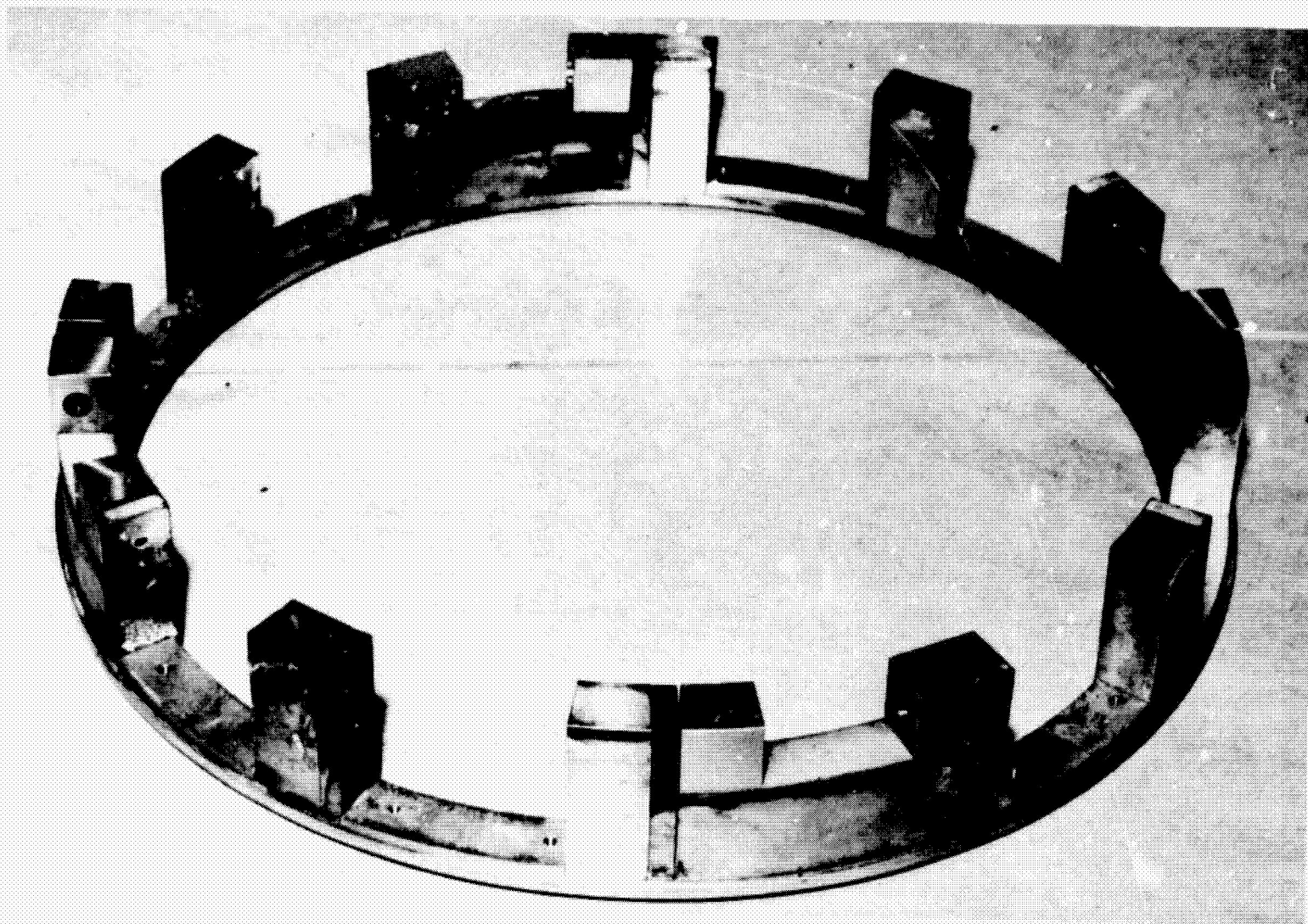


FIGURE IX-15. INJECTOR AND DAMPER RING (4 DEEP (17) - 8 SHALLOW (3T) CAVITIES)

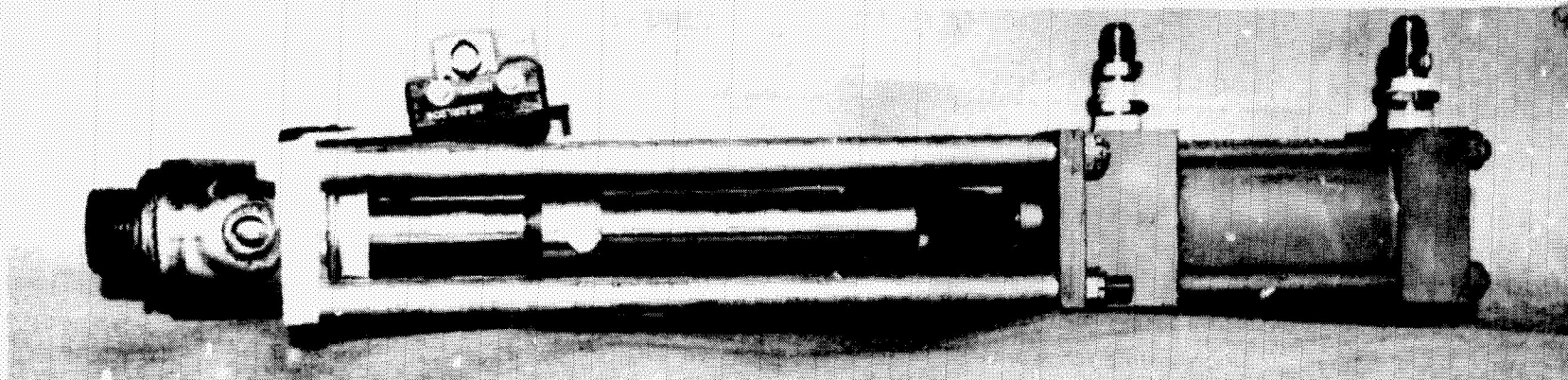
ORIGINAL PAGE IS
OF POOR QUALITY



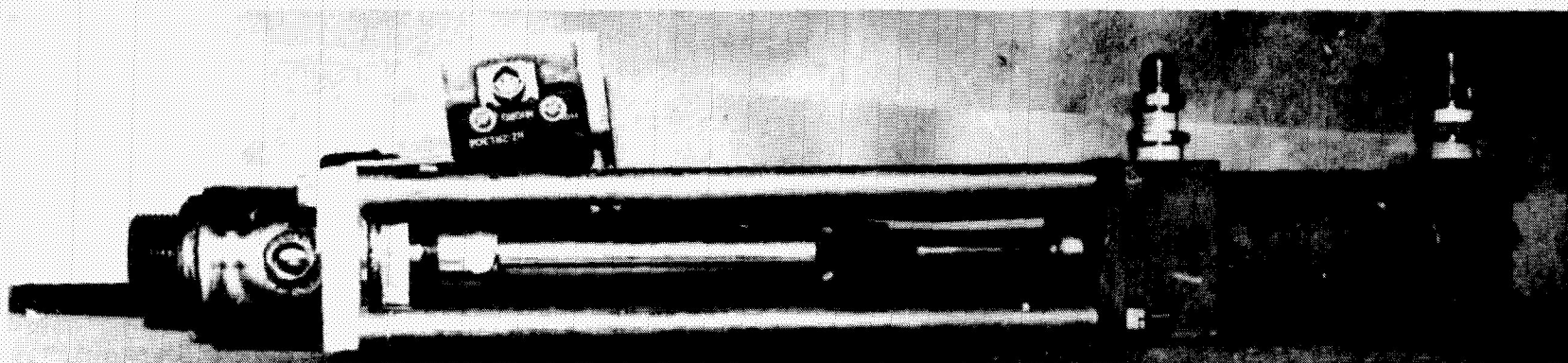
IX-27

FIGURE IX-16. ACOUSTIC RING (11.6% OPEN AREA 1T - 3.9% OPEN AREA 3T)

ORIGINAL PAGE IS
OF POOR QUALITY



RETRACTED POSITION



EXTENDED POSITION

FIGURE IX-17. BOMB INSERTER

Bell Aerospace Company

TABLE V

HARDWARE CONFIGURATION

(Reference Figure 1)

<u>Item</u>	<u>Part Number</u>	<u>Serial Number</u>
Aluminum Injector	8693-473050-1	S/N 2
Fuel Vortex Ring	8693-473140-3A	S/N 1A
Acoustic Cavity Ring	8693-473112-1	S/N 1
Bomb Chamber	8693-470021-1A	S/N 1A
Water Cooled Nozzle	8693-470016-1	S/N 1

1. Test Results - Series 1 (Tests 4560 - 4566)

The initial (baseline) stability series was conducted with an acoustic cavity configuration consisting of a 1T open area of 15.6%, and a 3T/1R open area of 7.8% (Figure IX-18 and Figure IX-19). The series consisted of 6 tests with 17 bomb detonations. All tests were stable. There was no noticeable effect on stability characteristics with variations in mixture ratio, chamber pressure, and acoustic cavity gas temperature. Chamber pressure overpressure maximums were generally greater in the acoustic cavities than in the chamber. The per cent overpressure in the acoustic cavities ranged from 160% to 394%, and in the chamber ranged from 77% to 250%. These maximum pressures occur immediately after bomb detonation.

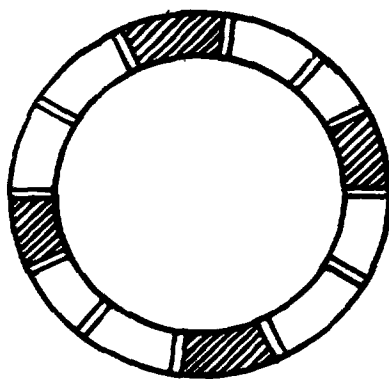
The maximum cavity gas temperatures recorded for this series at detonation of bombs 1, 2, and 3 were approximately 1325°F, 1750°F and 3000°F respectively, and are based on limited temperature data.

2. Test Results - Series 2 (Tests 4567 - 4571)

The second test series was conducted with an acoustic cavity configuration consisting of a 1T open area of 11.6% and a 3T/1R open area of 7.9% (Figure IX-18). The series consisted of five tests with 15 bomb detonations. All tests were stable and there was no noticeable effect on stability characteristics with variations in mixture ratio, chamber pressure and acoustic cavity gas temperature. The percent overpressure in the acoustic cavities ranged from 179% to 443%, and in the chamber from 79% to 324%.

The acoustic cavity gas temperatures varied considerably from run to run at the three bomb detonation times. The gas temperature ranged from 1585°F to 2120°F at the time of detonation of bomb 1; ranged from 2440°F to 3250°F at time of detonation of

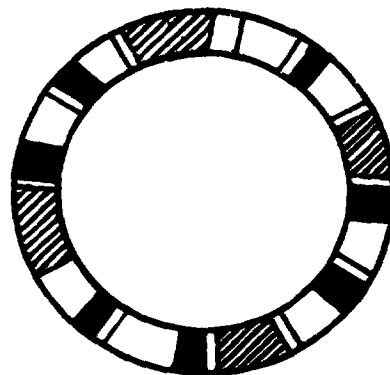
ACOUSTIC CAVITY ARRANGEMENTS



BASELINE

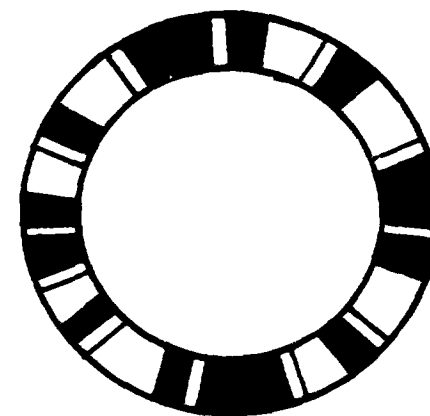
15.6% 1T

7.8% 3T



11.6% 1T

7.8% 3T



11.6% 1T

0 3T

ADDITIONAL ARRANGEMENTS

0%

7.8% 1T

7.8%

15.7% 3T

FIGURE IX-18



OPEN AREA 1T

OPEN AREA 3T

ACOUSTIC DAMPER DETAIL

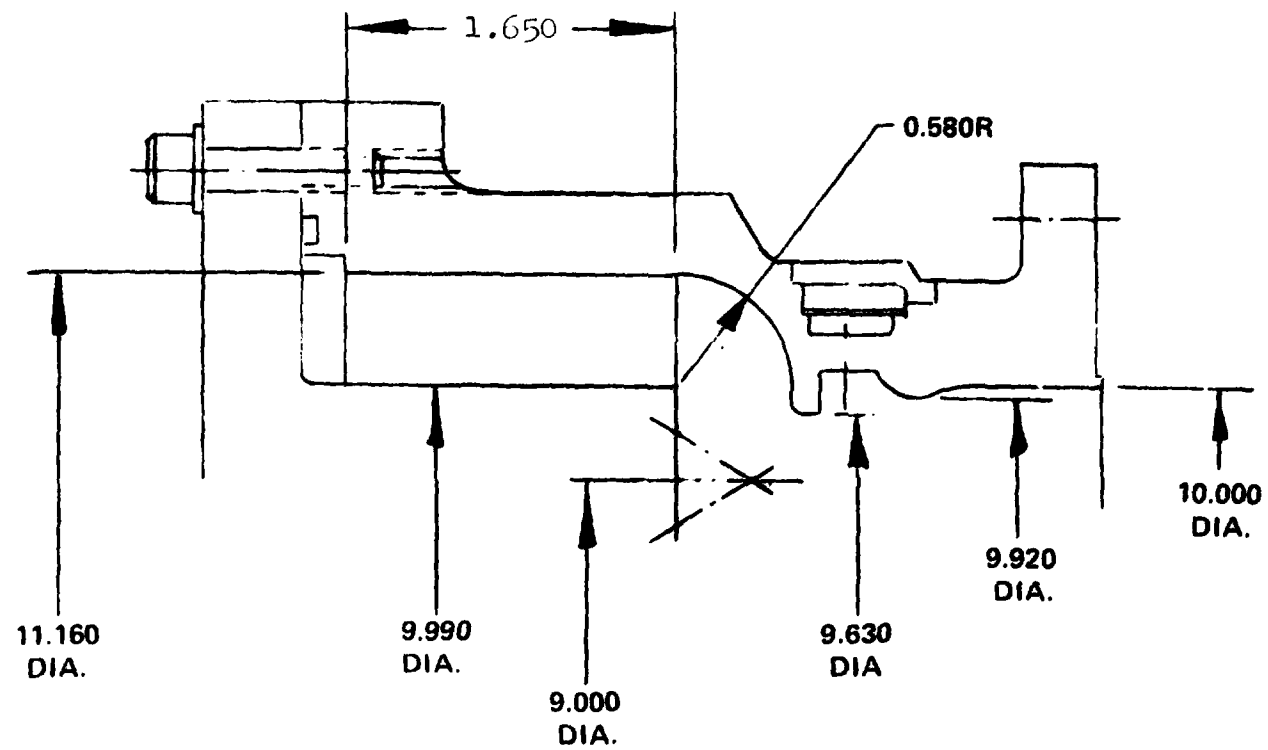


FIGURE IX-19

ORIGINAL PAGE IS
OF POOR QUALITY

Bell Aerospace Company

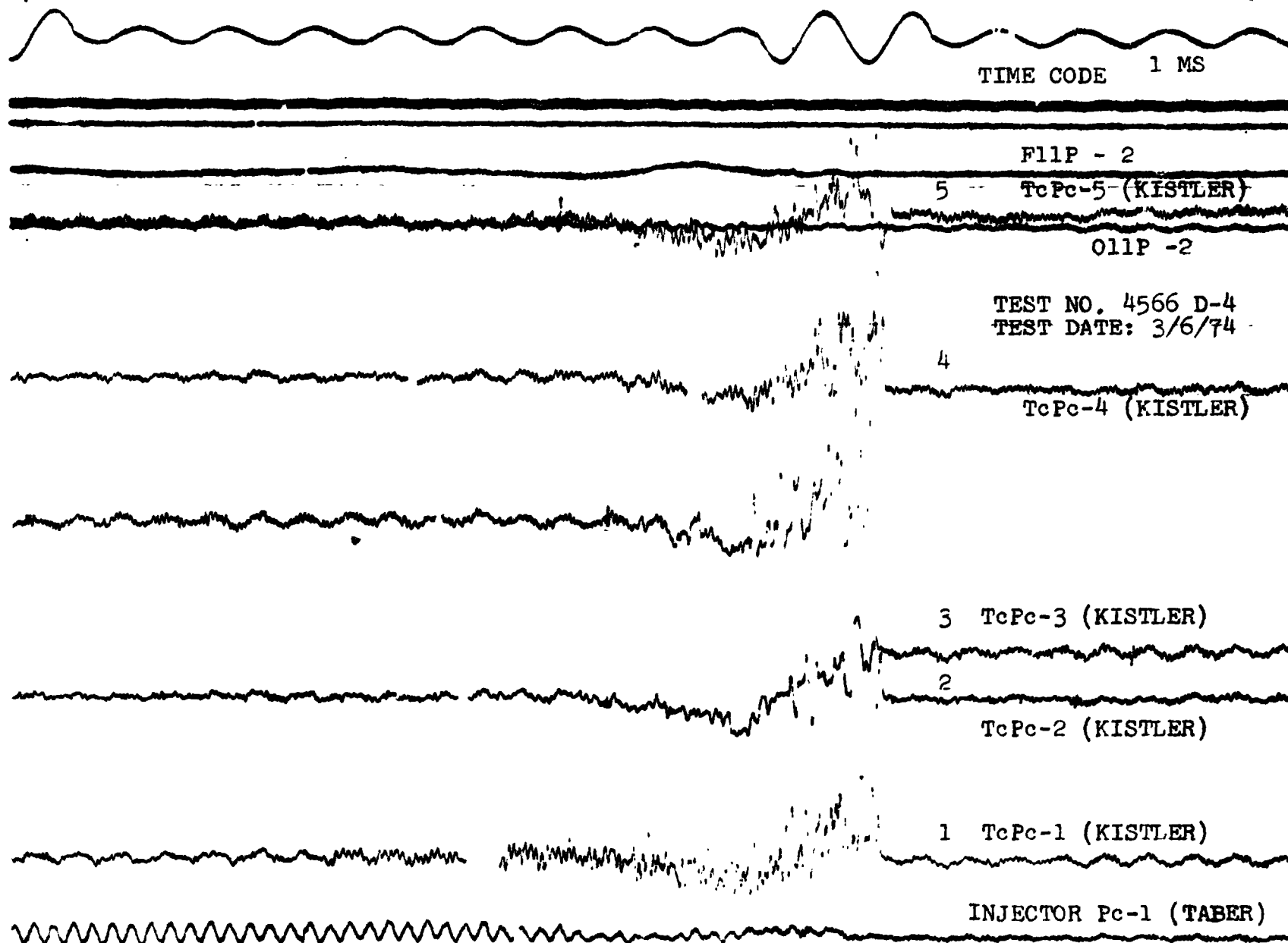


FIGURE IX

Bell Aerospace Company

3693 OME INJECTOR S/N 2
CAVITY TEMP. VS TIME, TEST NO. 4567 D-4
DATE: 3-8-74

INJECTOR PC CORR = 125.7; RATIO = 1.55

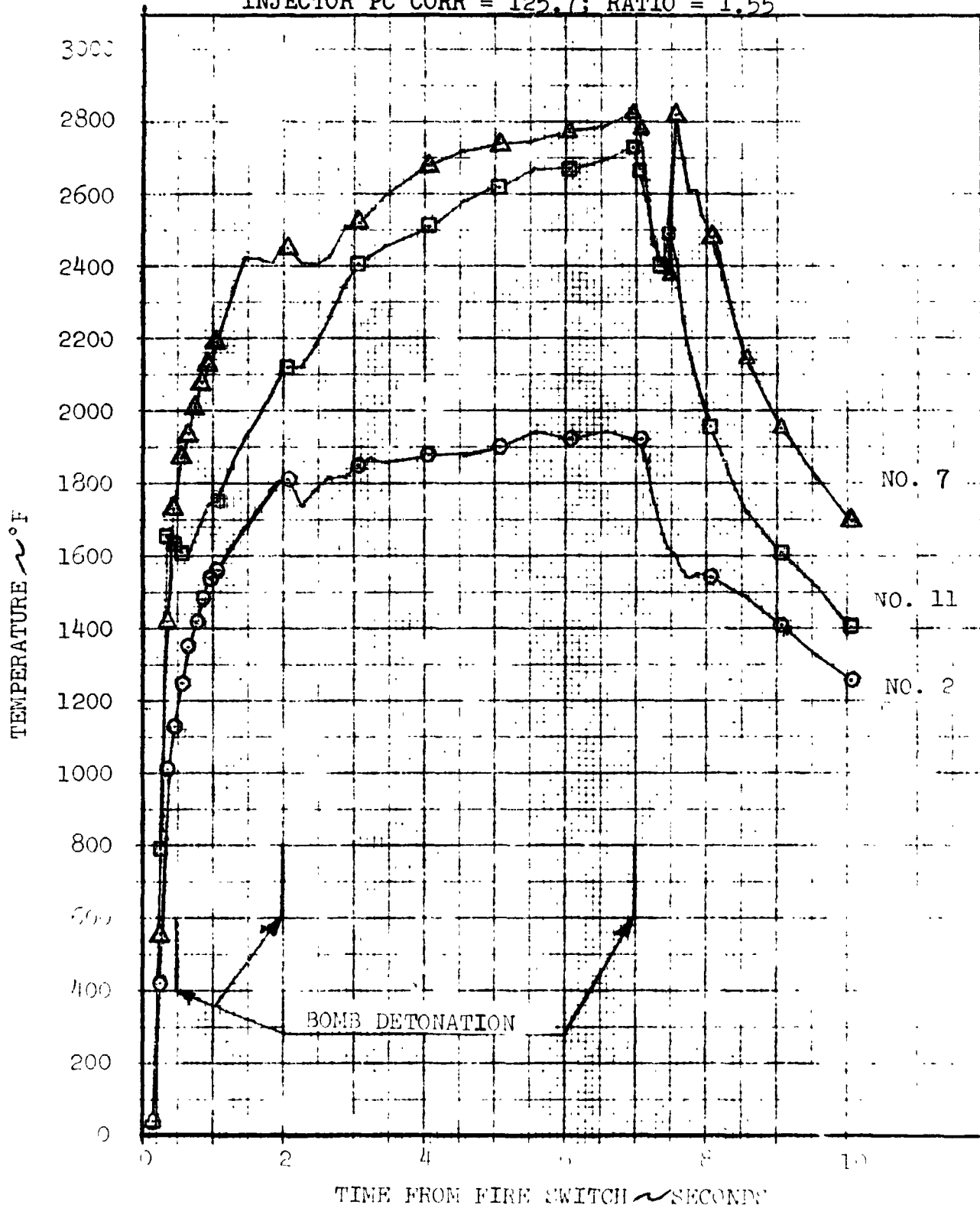


FIGURE IX-21

8693-ONE INJECTOR S/N-2

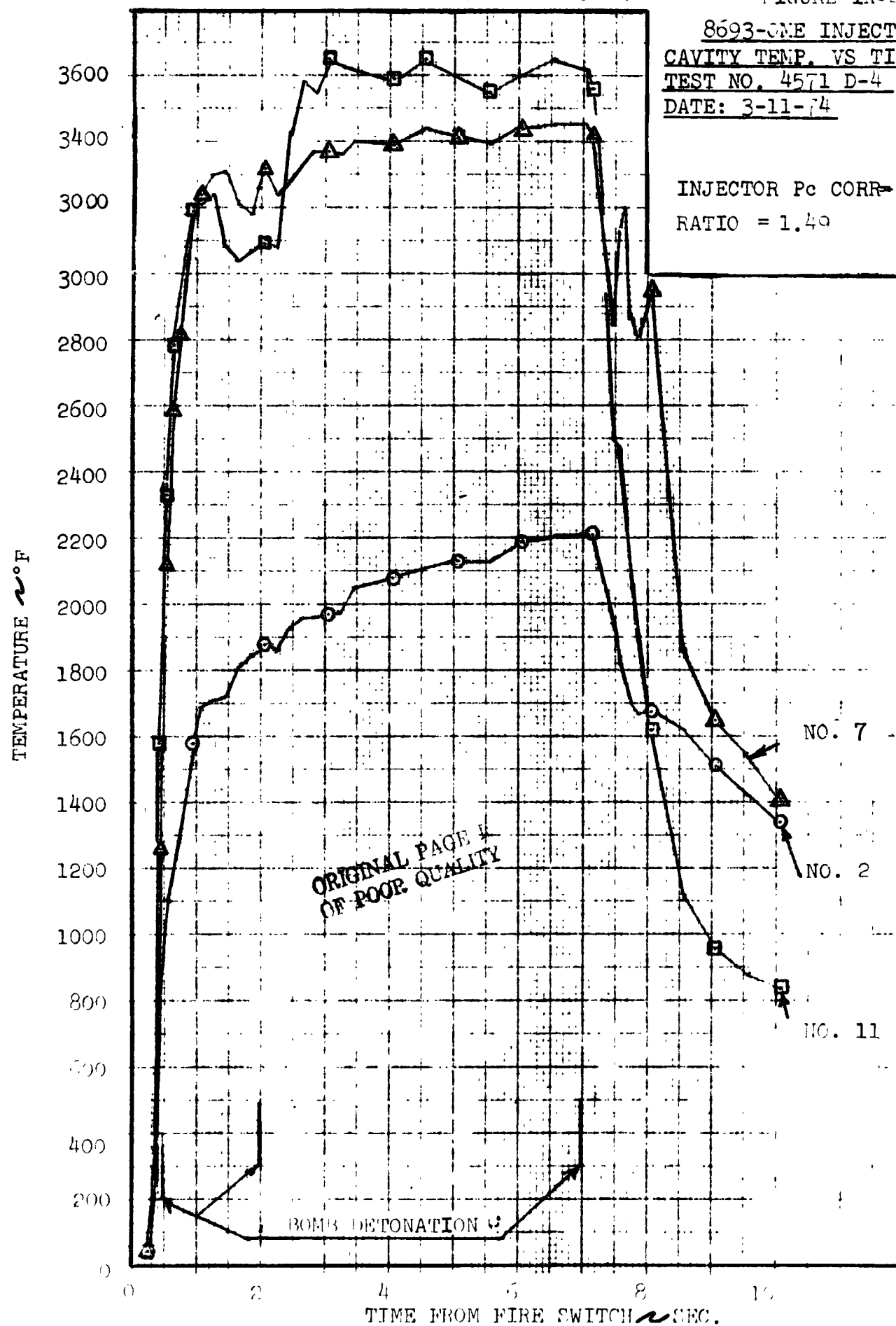
CAVITY TEMP. VS TIME

TEST NO. 4571 D-4

DATE: 3-11-74

INJECTOR Pc CORR=149.4 PSIA

RATIO = 1.40



Bell Aerospace Company

of bomb 2; and 2480°F to 3620°F at time of detonation of bomb 3.

Temperature time histories of the acoustic cavity gas temperature are shown in Figures IX-21 and IX-22.

A typical recovery time record is shown in Figure IX-23.

3. Test Results - Series 3 (Tests 4572, 4573)

On the third test series all of the acoustic cavities were of a 3T/1R configuration. It was decided to "jump" to this arrangement as tests at another facility had indicated stability with a shorter cavity length.

On the first test, the first bomb was detonated at 0.5 second. At bomb detonation the engine became unstable and the ASD circuit shut the engine down at 0.7 second. The frequency observed was approximately 2620 Hertz which was considered to be a first tangential mode.

The time of bomb detonation and resultant instability is shown on an oscillograph reproduction in Figure IX-24. The acoustic cavity pressures (Injector P_{c-3} and Injector P_{c-4}) generally showed greater amplitudes than the pressures ($T_{cP_{c-1}}$ and $T_{cP_{c-2}}$) in the combustion chamber. Maximum overpressure in the acoustic cavity ranged from 254% to 308%, and in the chamber from 94% to 202%. The traces are oscillating at a frequency of approximately 2620 Hertz. Superimposed frequencies, of reduced magnitude of approximately 5,100 Hertz, and 13,000 Hertz can be detected.

The second test was made to determine if instability would occur when a bomb was detonated at a later time into the run. The bomb was detonated at 2.0 seconds and followed again by unstable operation. Unfortunately, during this second test the ASD system was not activated and a full 8 second test resulted. Thermal detonation of the inserted bomb also was encountered with no effect on the combustion. The long time exposure to unstable operation (approximately 6 seconds) resulted in some scalloping at outer edge of the injector which is shown in Figure IX-25. Some damage also occurred to the vortex ring acoustic cavity entrance and the vortex ring lip which pilots into the chamber. The hardware was readily repaired and testing resumed.

Maximum overpressure in the acoustic cavities ranged from 334% to 396%, and in the chamber from 118% to 135%.

BOMB DAMP TIME

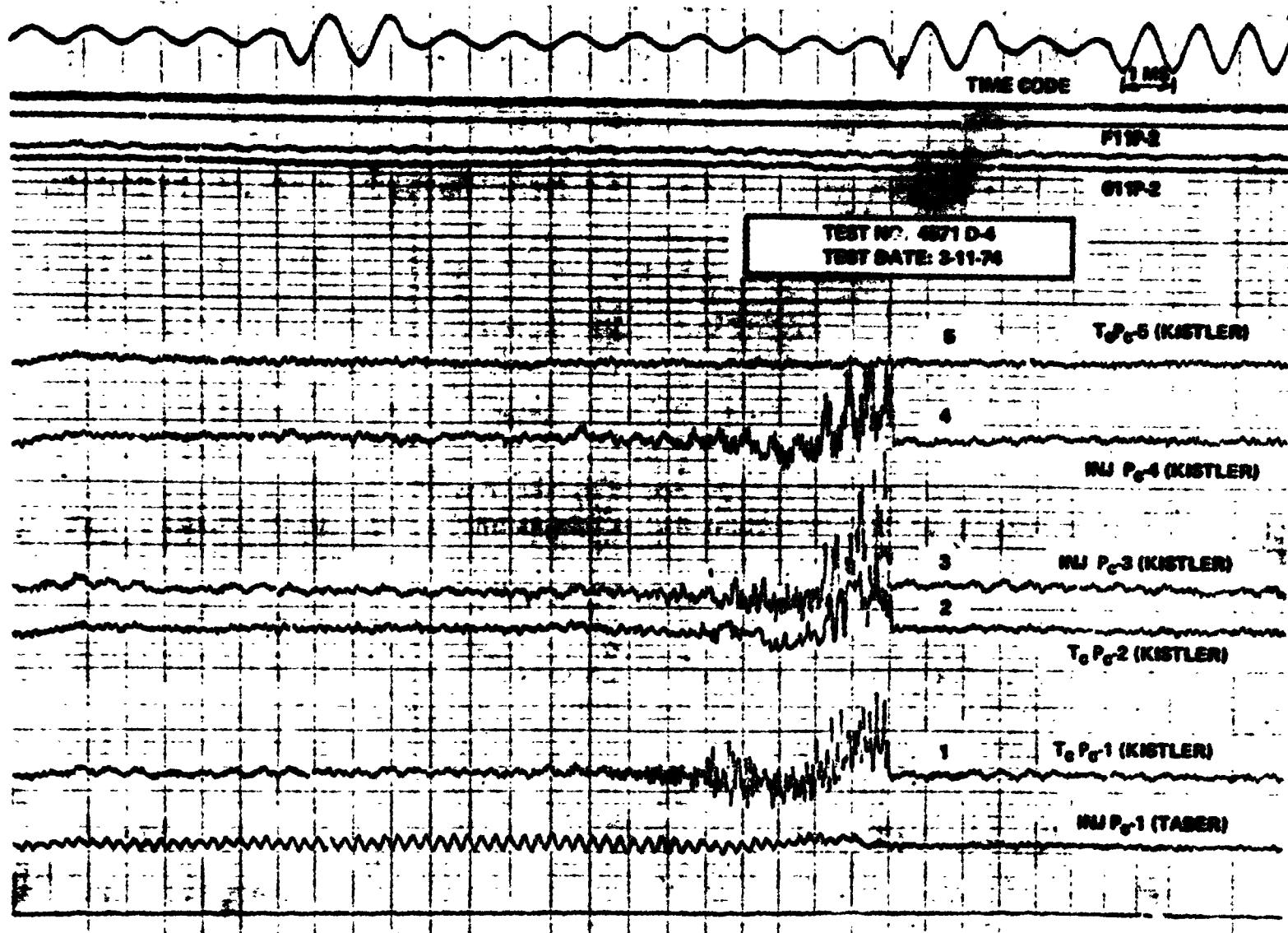


FIGURE IX-23

**UNSTABLE TEST NO. 4572 D-4
OSCILLOGRAPH RECORD
(0.5 SECOND BOMB - 12:3T CAVITIES)**

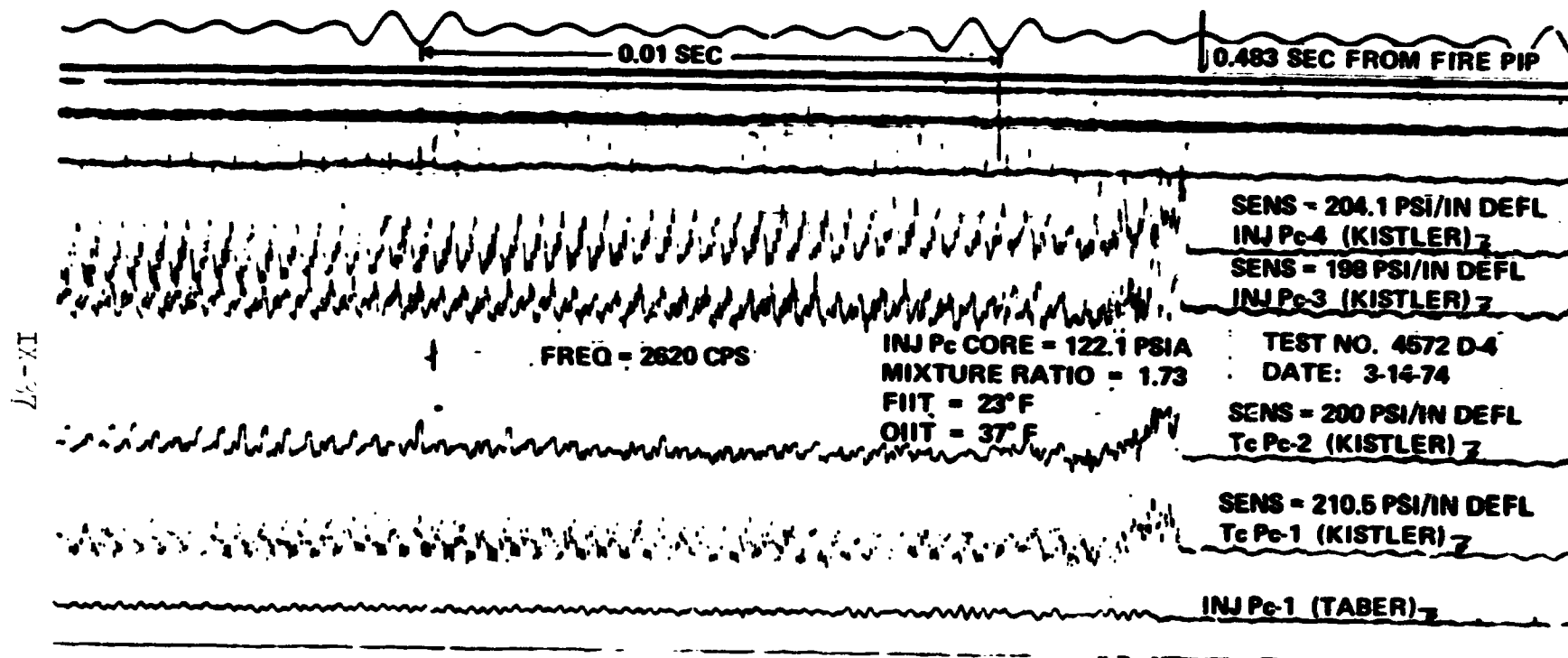


FIGURE IX-24

ORIGINAL PAGE IS
OF POOR QUALITY

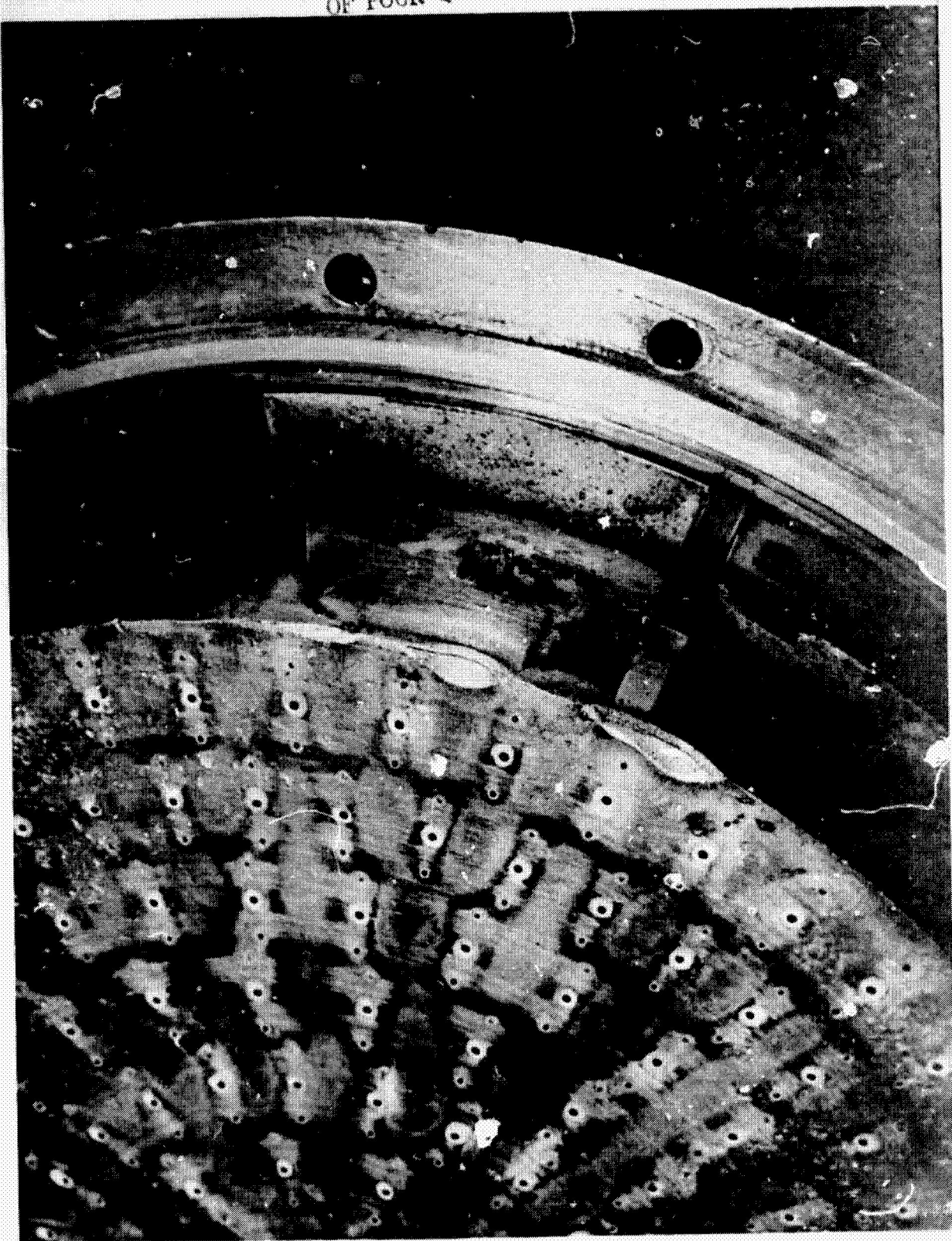


FIGURE IX-25. INJECTOR DAMAGE AFTER UNSTABLE FIRE TEST

Bell Aerospace Company

The time of the first bomb detonation and the resultant instability is shown on an oscillograph reproduction in Figure IX-26. Figure IX-27 is a temperature/time history of the acoustic cavity gas temperatures during the unstable operation. A noticeable change in the temperature time history is seen at the 2 second duration point where the initial bomb was detonated. The erratic behavior of thermocouple #7 is due to an open circuit. The temperature transition from stable to unstable operation appears to be quite rapid from these traces. Interestingly, although the temperature traces close to the combustion (Numbers TC-6 and TC-11) both accelerate quite rapidly, the stabilization appears to be below temperatures measured during stable testing.

4. Test Results - Series 4 (Test 4574)

The fourth test series was to be conducted with an acoustic cavity configuration with 7.8% 1T open area and 15.6% 3T/1R open area. The first test of the series went unstable at the first bomb detonation and further testing was negated. Unfortunately, this run also continued in an unstable mode as the ASD was set to high (40 psi) to be triggered by the chamber pressure oscillations (\approx 30 psi) Figure IX-26. Consequently, the engine operated for 8 seconds, at which time a timer limit circuit terminated the run.

One obvious implication from this test was that the pressure peaks were reduced when some 1T (7.8% open area) cavities were incorporated. This data was compared to a prior test where the ASD circuit was actuated by the instability noted when no deep cavities were used.

Again, some damage was noted at the outer edge of the injector but repairs were readily made. Detonation over pressure in the acoustic cavity ranged from 197% to 414% and at the chamber measuring points from 98 to 198%.

The thermocouples in the acoustic damper will also be monitored for this test and a comparison made with the next stable test. This chart is shown in Figure IX-29. Somewhat surprisingly, the cavity temperature appear to be lower than on stable tests. No real explanation has been given for these lower temperatures, especially observing the erosion on the periphery of the injector. Speculation would predict that some mixture ratio shift is probably occurring and that more fuel is being brought into the local areas of the thermocouples.

UNSTABLE TEST NO. 4573 D-4
OSCILLOGRAPH RECORD
(2 SECOND BOMB - 12:3T CAVITIES)

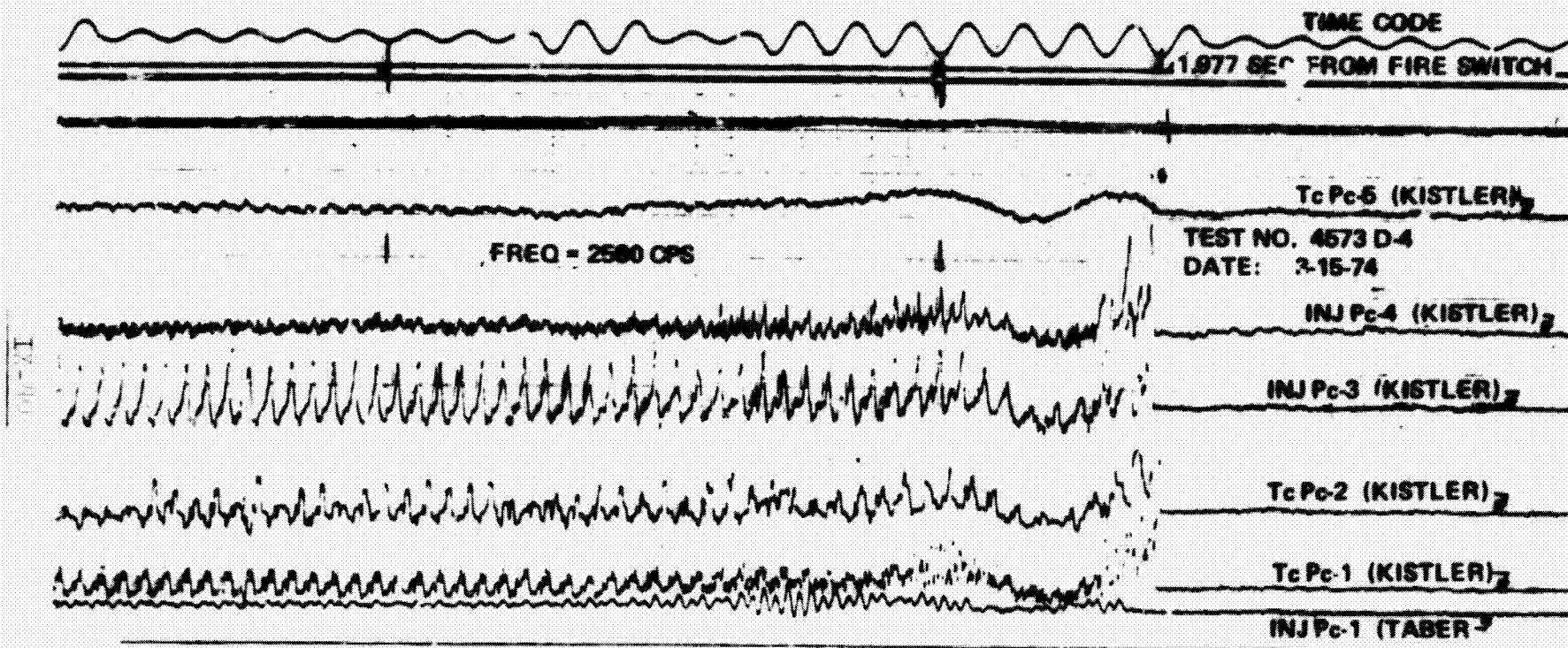


FIGURE IX-26

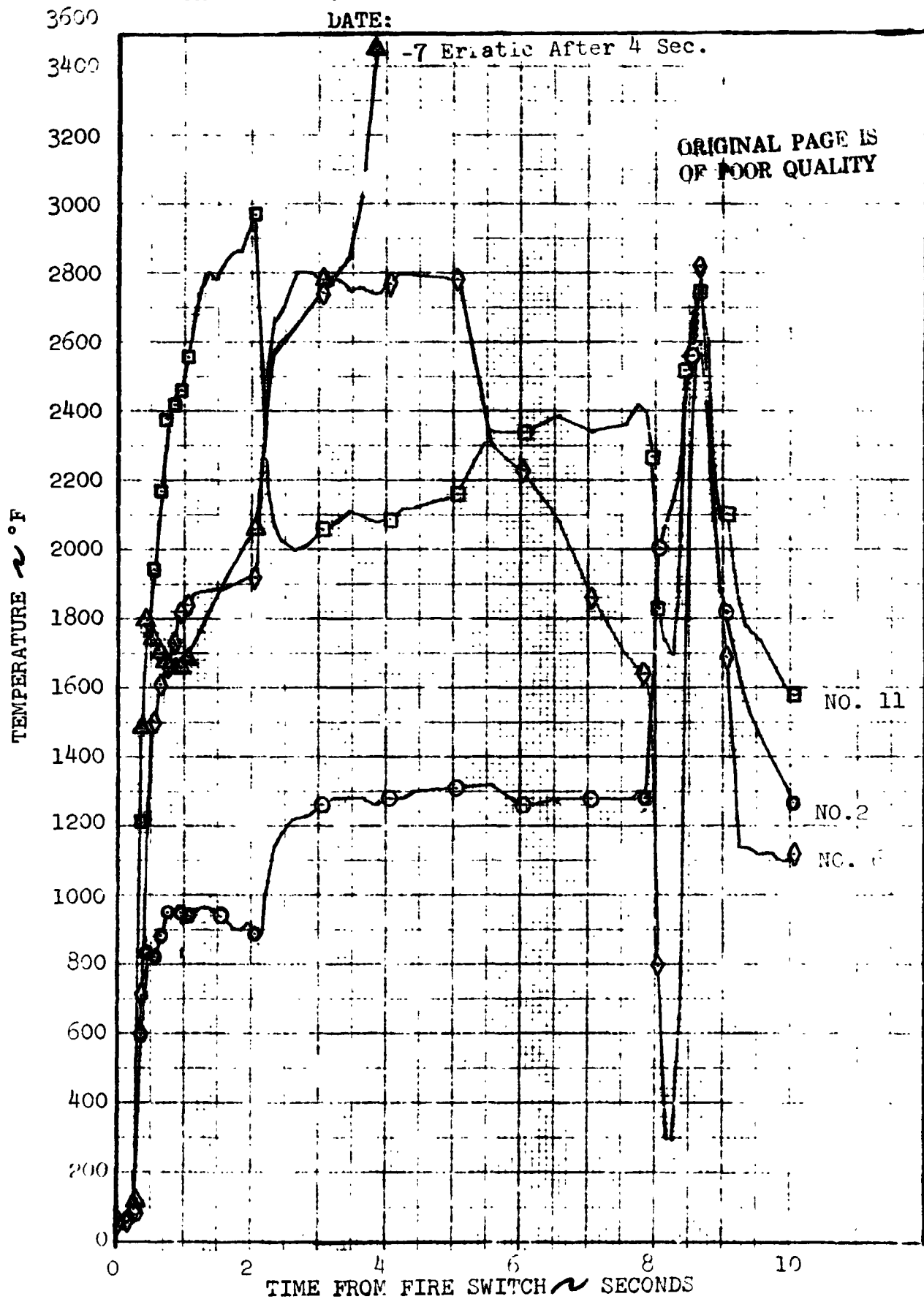
Bell Aerospace Company

FIGURE IX-27

8693 OME INJECTOR S/N -2

CAVITY TEMP. VS TIME: TEST NO. 4573 D-4

DATE:



UNSTABLE TEST NO. 4574 D-4
OSCILLOGRAPH RECORD
(0.5 SECOND BOMB - 4:1T CAVITIES; 8:3T CAVITIES)

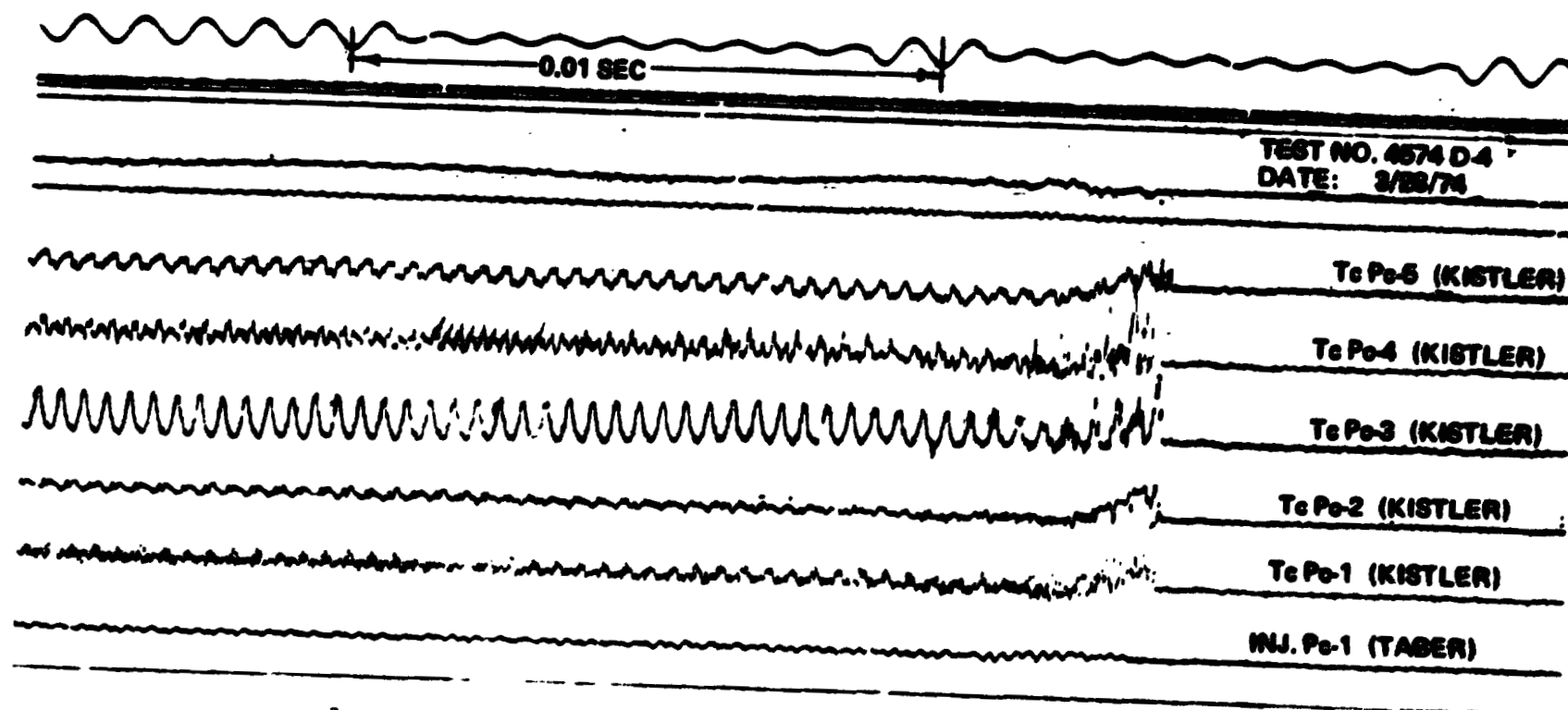


FIGURE IX-23

CAVITY TEMPERATURES UNSTABLE AND STABLE TESTS

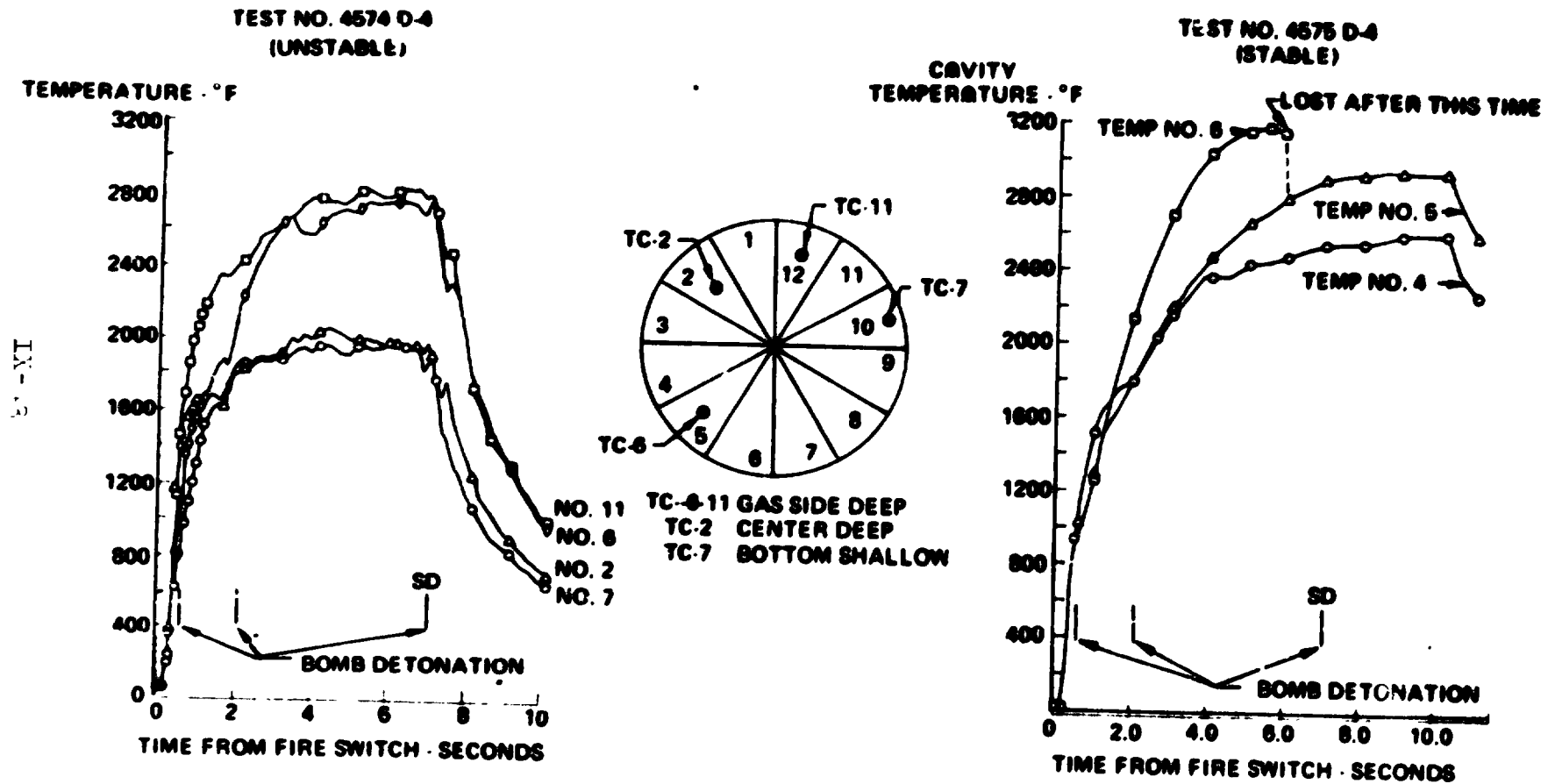


FIGURE IX-2

Bell Aerospace Company

5. Test Results - Series 5 (Test 4575)

On the fifth test series, the 1T cavities were again opened up to 11.6% open area and the test objective concentrated on a reduced 3T/1R area to 3.9%. One test was made with 3 bomb detonations. The test was stable and there was no noticeable effect on stability characteristics with variations in acoustic cavity gas temperature. The gas temperature ranged from 890°F to 1580°F at the time of detonation of bomb 1; from 1955°F to 2840°F at time of detonation of bomb 2; and ranged from 1880°F to 2795°F at time of detonation of bomb 3. All recovery times were less than 5 ms.

Maximum bomb overpressures in the acoustic cavity ranged from 410% to 521% and in the chamber from 135% to 231%.

6. Test Results - Test Series 6 (Test 4576)

The sixth test configuration further reduced the 3T/1R area to 0, with 11.6% open area 1T. One test was made with 3 bomb detonations. The test was stable with all three bomb recoveries made in about the same time for period. The gas temperature time history is shown in Figure IX-30. All recovery times were less than 5 ms.

The gas temperature ranged from 1200°F to 1700°F at the time of detonation of bomb 1; ranged from 1900°F to 2080°F at time of detonation of bomb 2; and ranged from 2280°F to 2750°F at time of detonation of bomb 3. Acoustic cavity thermocouple #7 was not recorded in the closed-off 3T/1R cavity.

Maximum overpressure in the acoustic cavity was 319% (second high frequency instrument removed), and in the chamber ranged from 155% to 218%.

C. Acoustic Cavity Gas Temperatures

Acoustic cavity gas temperatures generally showed large variations from test to test and from cavity to cavity. In general, the thermocouples near the entrance to the cavities (#6 and #11) were higher than those inside the cavity (#2 and #7).

A comparison of an unstable run with a stable run (Figure IX-29) shows a more rapid rise in temperature during unstable operation with temperature overshoots near the beginning and end of the test.

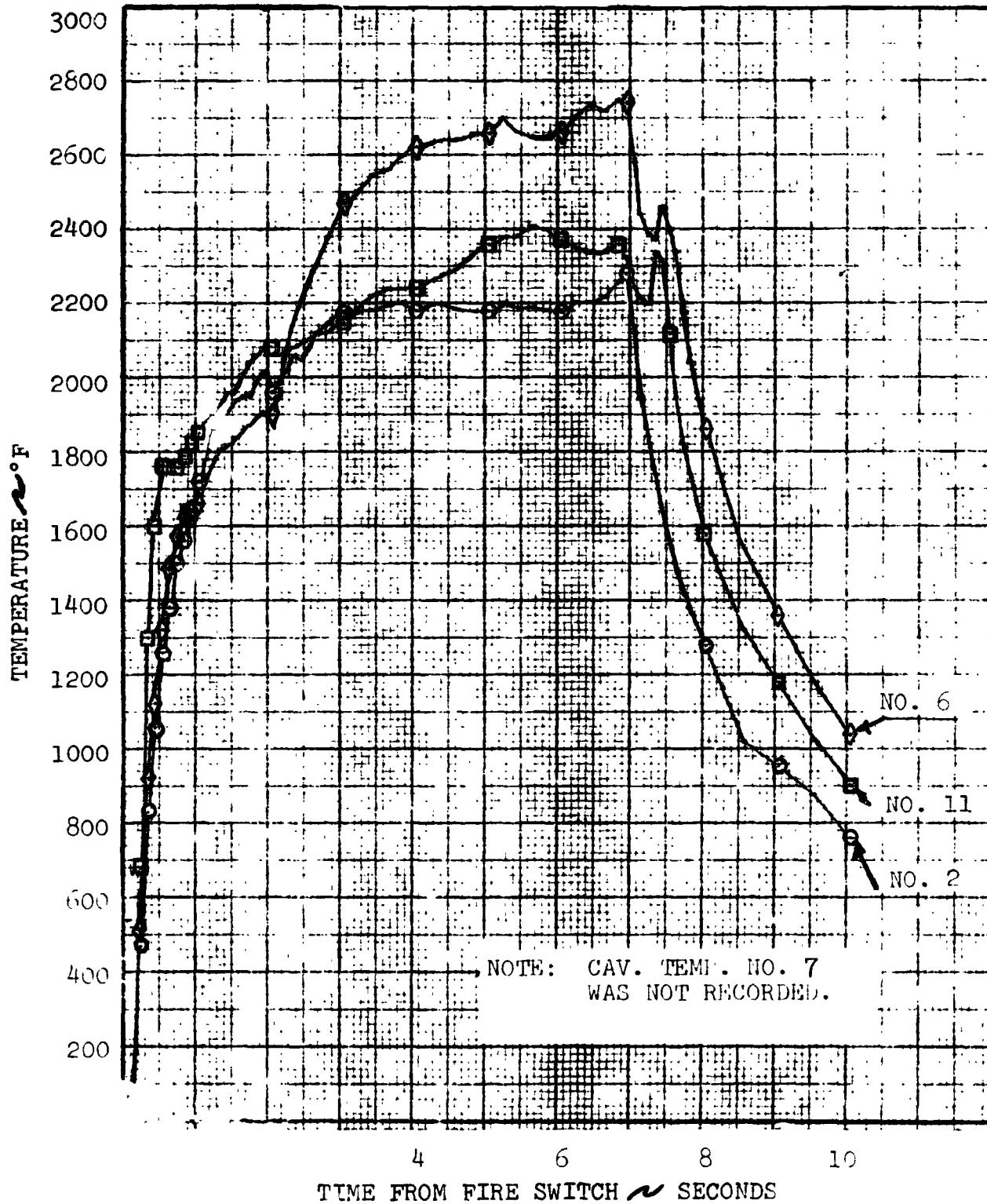
A temperature comparison at the 4 second time point indicated a lower gas temperature by 400-500°F at the acoustic cavity entrance during unstable operation, but a higher gas temperature at the midpoint of the deep cavity.

Bell Aerospace Company

FIGURE IX-30
8693 OME INJECTOR S/N-2

CAVITY TEMP. VS TIME: TEST NO. 4576 D-4

DATE: 4-12-74



Bell Aerospace Company

TEMPERATURE COMPARISON

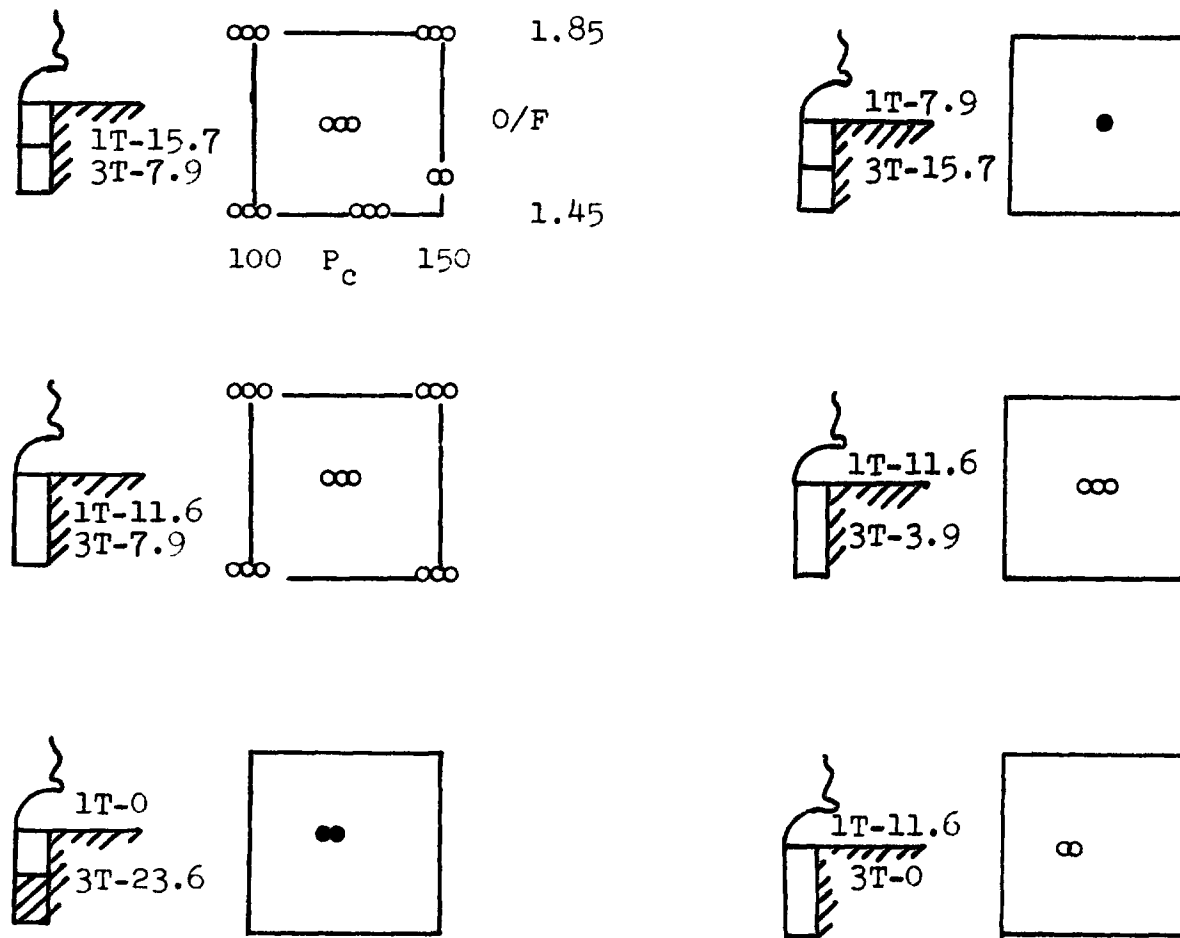
<u>Data Thermocouple Point Numbers Sec.</u>	<u>Unstable Test (4574) °F</u>	<u>Stable Test (4575) °F</u>
2	2280	1950
6	2200	2620
7	1700	2040
11	2275	2780

D. Conclusions Resulting From Tests

The test results obtained have been plotted in block form in Figure IX-31. The primary result of this series is that instability results as the cavities are shortened and the area of 1T significantly reduced. There did not appear to be a significant relation between the cavity temperature and the ability of the cavity to stabilize. The following items are considered the primary observations resulting from these tests.

- Minimum open area appears 11.6% or less
- Cavity temperature effect is not obvious
- 3T requirement not demonstrated

TASK XII - STABILITY TEST RESULTS
(FUEL VORTEX COOLING)



- STABLE
- MARGINAL
- UNSTABLE

1T - 1ST TANGENTIAL OPEN AREA %
 3T - 3RD TANGENTIAL/1ST RADIAL OPEN AREA %

FIGURE IX-31

Bell Aerospace Company

X. TASK XIII - WSTF TEST AND ANALYSIS SUPPORT

A group of tests to evaluate the performance of the ten inch diameter injector; a regeneratively cooled thrust chamber and a large area ratio nozzle were conducted at the White Sands Test Facility (WSTF) in October and November 1973. The uncooled stainless steel divergent nozzle (nozzle extension) was furnished by the NASA, WSTF, and was mounted to the Bell Aerospace Company regeneratively cooled thrust chamber with an uncooled adapter section. The test objective was to define performance for this thrust chamber assembly at a simulated altitude of approximately 100,000 feet with N_2O_4/MMH propellants. Sub-objectives addressed the performance variation with excursions of mixture ratio, chamber pressure, combustion length, helium saturated propellants and heated propellants.

A total of 47 altitude test firings were conducted at WSTF using the 76.7 area ratio nozzle extension. Data are supplied for these tests as well as comparison with data from testing at BAC with a 15:1 area ratio nozzle extension and projected to a typical OME vehicle nozzle envelope at an area ratio of 72.7.

These tests with N_2O_4/MMH propellants confirmed the BAC performance predictions which were determined by the JANNAF procedures. The WSTF data indicated a slightly higher performance (0.2%) than predicted from the BAC data (I_{sp} of 317.5 vs 317.0 seconds). No noticeable performance differences were observed with increased chamber length (30 L^* to 34 L^*) or with helium saturated propellants versus unsaturated propellants. A chamber pressure variation resulted in a performance change of about 0.03% seconds $I_{sp}/psi P_c$. A detectable increase in performance of about 0.3% was also noted when propellant temperatures were increased.

No combustion instability was noted during the test series and the projection of maximum nozzle extension temperature was lower than the original study value but almost identical to the temperature predicted from the 15:1 area ratio nozzle tests at BAC.

Due to the use of uncooled hardware for the fuel vortex assembly, vaporization of the fuel in the vortex manifold resulted during the initial test sequences. This was attributed to heat soak back during the short "down times" used in the early series. Changing this test sequence eliminated the problem which would not be encountered on properly cooled flight hardware.

Bell Aerospace Company

A. Test Hardware

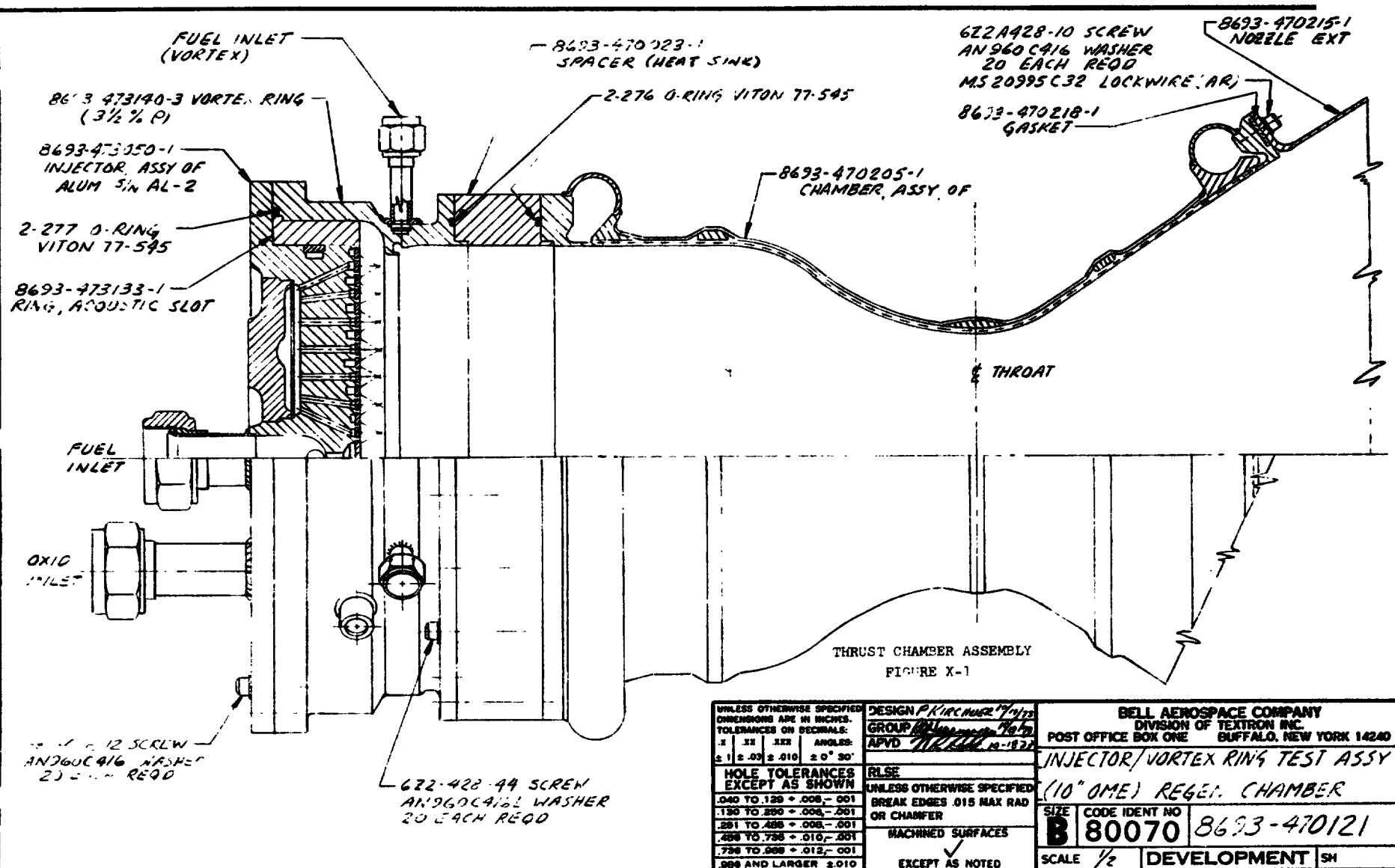
The hardware used for this test program consisted of a 10 inch diameter triplet injector (S/N 2) utilizing acoustic cavities for high frequency stability and fuel vortex film cooling, a fuel regeneratively cooled thrust chamber, a NASA supplied nozzle extension and a bipropellant valve. The hardware was designed for complete flexibility with all components bolted together and sealed with appropriate seals. As shown in Figure X-1 subcomponents are used to provide the hardware interchangeability. A photograph of an exploded view is given in Figure X-2.

The injector is an aluminum, flat face design consisting of 196 two fuel on one oxidizer triplet elements (Figure X-3). A replaceable stainless steel acoustic cavity ring is located at the injector periphery and consists of 12 cavities, 8 designed for the 1T frequency range and 4 designed for the 3T/1R frequency range (Figure X-4). A stainless steel fuel vortex film coolant ring is used to provide uniform film cooling and serves also as an outer closeout for the acoustic cavities (Figure X-5). This vortex ring contains 16 tangential orifices which distribute the fuel uniformly along the chamber wall. This vortex ring is supplied from the chamber outlet manifold with flow controlled by use of an orifice.

A heat sink chamber length adapter is located between the injector and regeneratively cooled chamber to allow L^* variation. The 10 inch diameter regeneratively cooled chamber consists of 60 rectangular coolant passages with the inner wall and lands fabricated from 304L stainless steel (Figure X-6). The passages are closed out with electroformed nickel (Figure X-7). The combustion chamber length is 17.3 inches with a throat diameter of 5.787 inches and a contraction ratio of 3.1. The expansion ratio of the regeneratively cooled nozzle exit is 6. The thrust chamber was designed for the temperature profile given in Figure X-9. Channel sizes were designed for sufficient safety margin to meet the most severe of design conditions at a fuel inlet temperature of 100°F, chamber pressure of 112 psia and a mixture ratio of 1.85. The coolant liner and nickel closeout design is flight weight but the inlet and outlet manifolds are not, to allow a reduction in fabrication cost. The updated design of this chamber has resulted in reduced weight in both the liner and the nickel closeout. A second uncooled in face section was mounted to the aft thrust chamber flange to allow the mounting of the uncooled nozzle section. The thrust chamber/adapter/extension interface is shown in Figure X-8.

Instrumentation provisions have been incorporated on the hardware to measure coolant inlet and outlet pressures and temperatures, injector inlet pressures, and chamber pressure at the acoustic cavity region.

ORIGINAL PAGE IS
OF POOR QUALITY



UNLESS OTHERWISE SPECIFIED DIMENSIONS ARE IN INCHES. TOLERANCES ON DECIMALS:			
.X	.XX	.XXX	ANGLES:
± .1	± .03	± .010	± 0° 30'
HOLE TOLERANCES EXCEPT AS SHOWN			
.040 TO .120 + .008 - .001			
.125 TO .250 + .008 - .001			
.251 TO .438 + .008 - .001			
.439 TO .750 + .010 - .001			
.751 TO .999 + .012 - .001			
1.000 AND LARGER ± .010			
DESIGN <i>PK 1000000-1012</i>			
GROUP <i>APVD 10-10-70</i>			
APVD <i>THRU 10-10-70</i>			
RLSE			
UNLESS OTHERWISE SPECIFIED BREAK EDGES .015 MAX RAD OR CHAMFER			
MACHINED SURFACES			
EXCEPT AS NOTED			

BELL AEROSPACE COMPANY DIVISION OF TEXTRON INC. POST OFFICE BOX ONE BUFFALO, NEW YORK 14240			
INJECTOR/VORTEX RING TEST ASSY (10" OME) REGEN. CHAMBER			
SIZE	CODE IDENT NO	8693-470121	
B	80070		
SCALE	1/2	DEVELOPMENT	SH

X-4

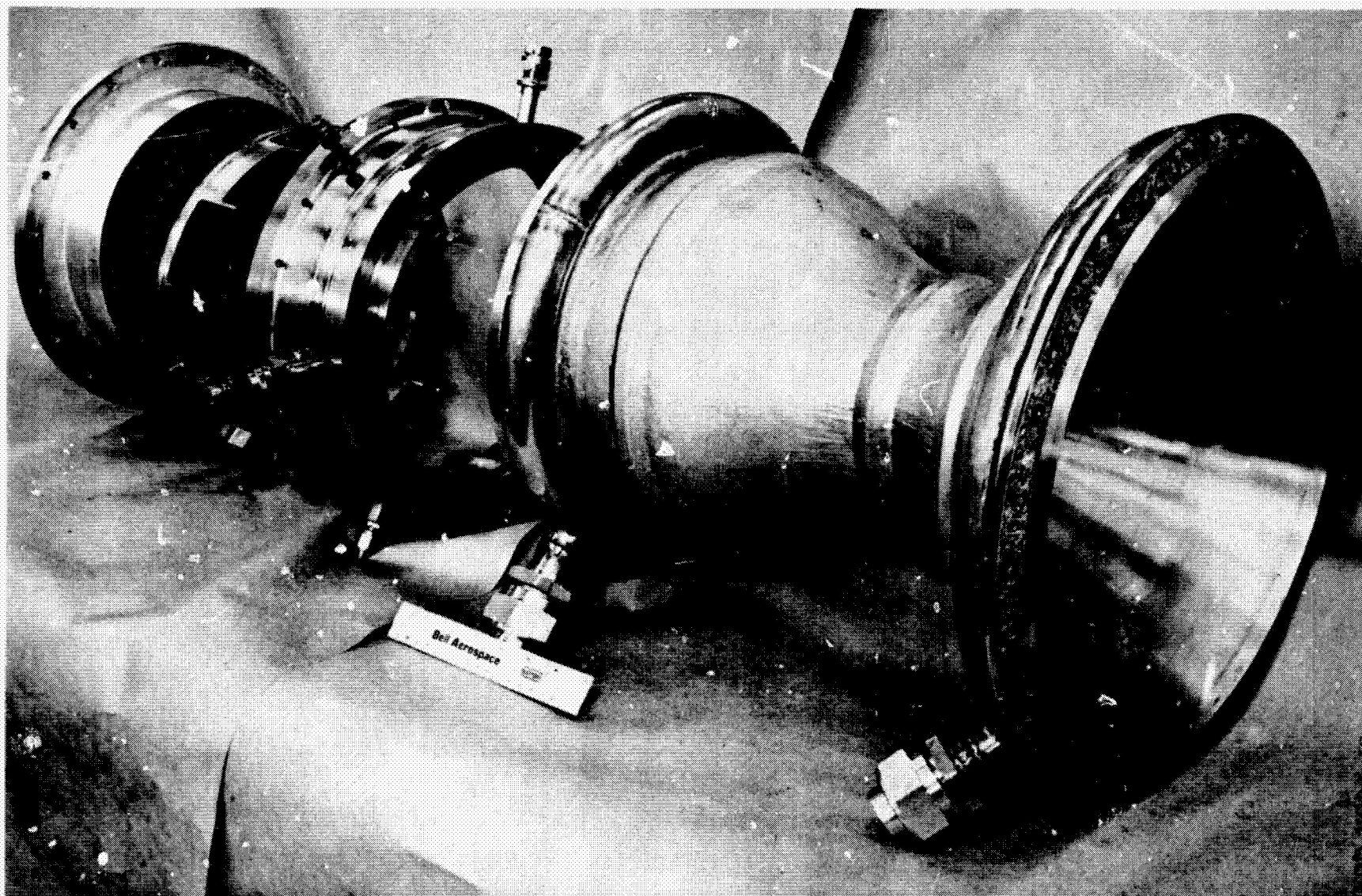


FIGURE X-2. THRUST CHAMBER ASSEMBLY EXPLODED VIEW

ORIGINAL PAGE IS
OF POOR QUALITY

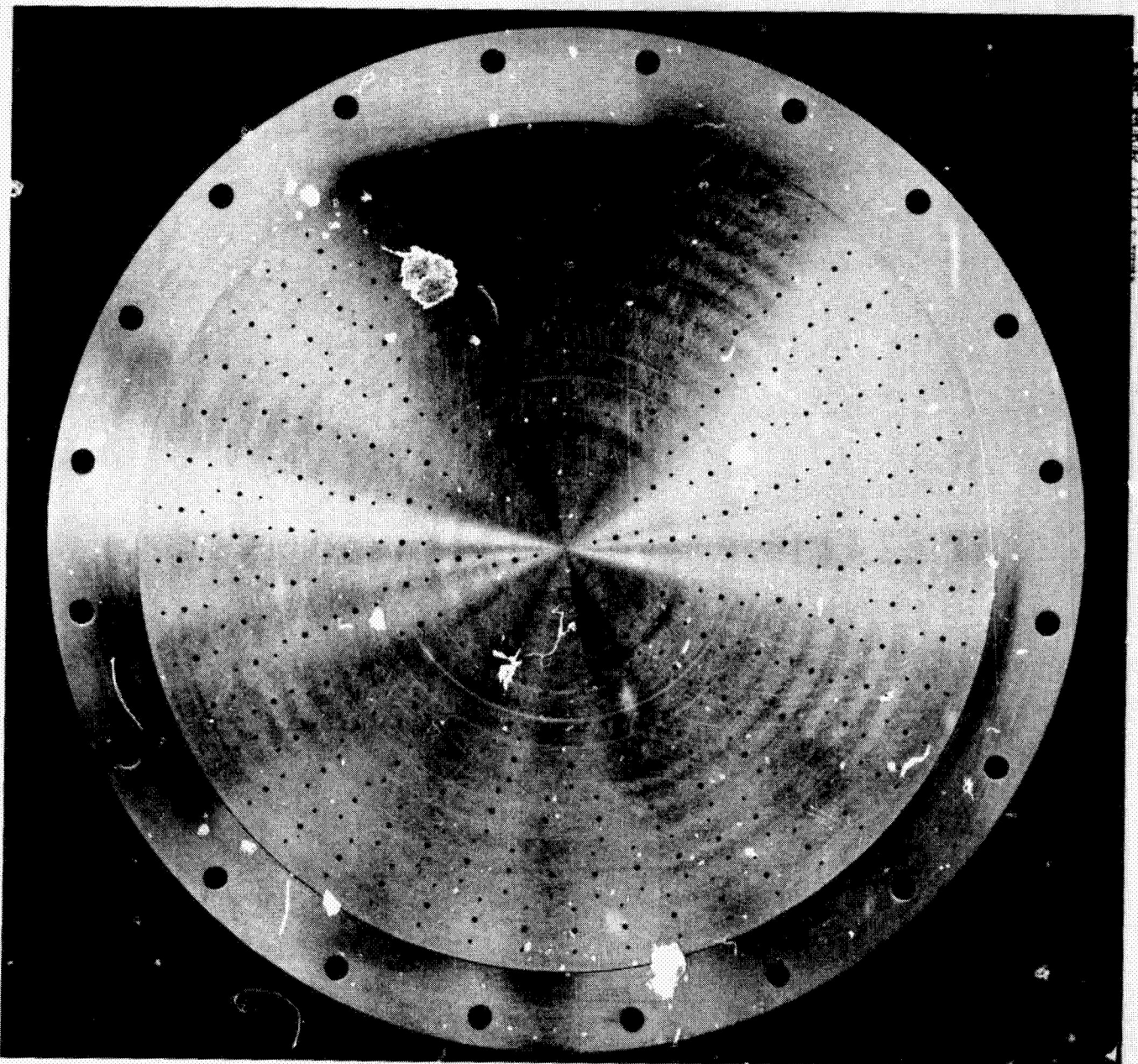
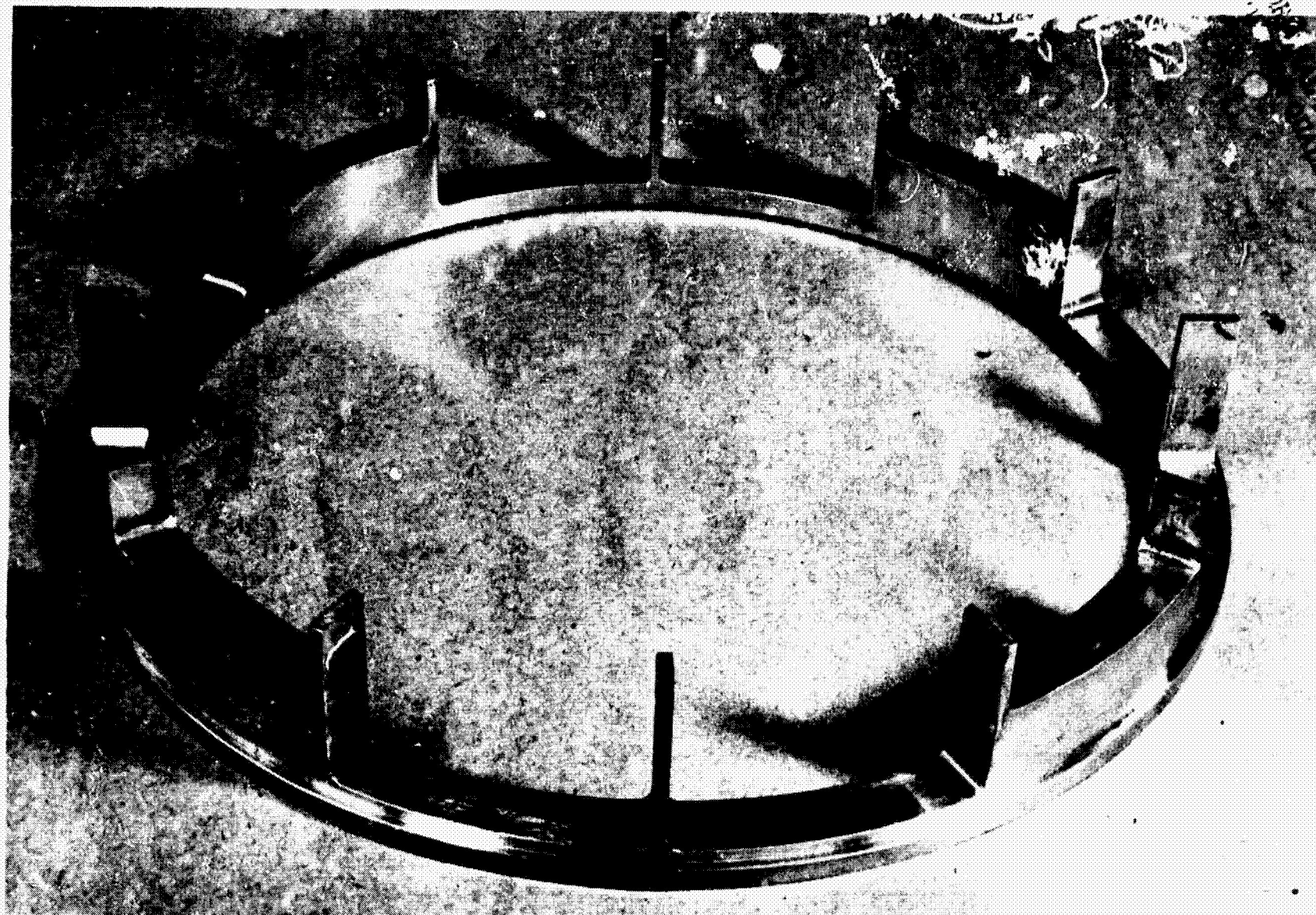


FIGURE X-3. TRIPLET ELEMENT INJECTOR



PAGE 15
QUALITY

FIGURE X-4. ACOUSTIC RING

ORIGINAL PAGE IS
OF POOR QUALITY

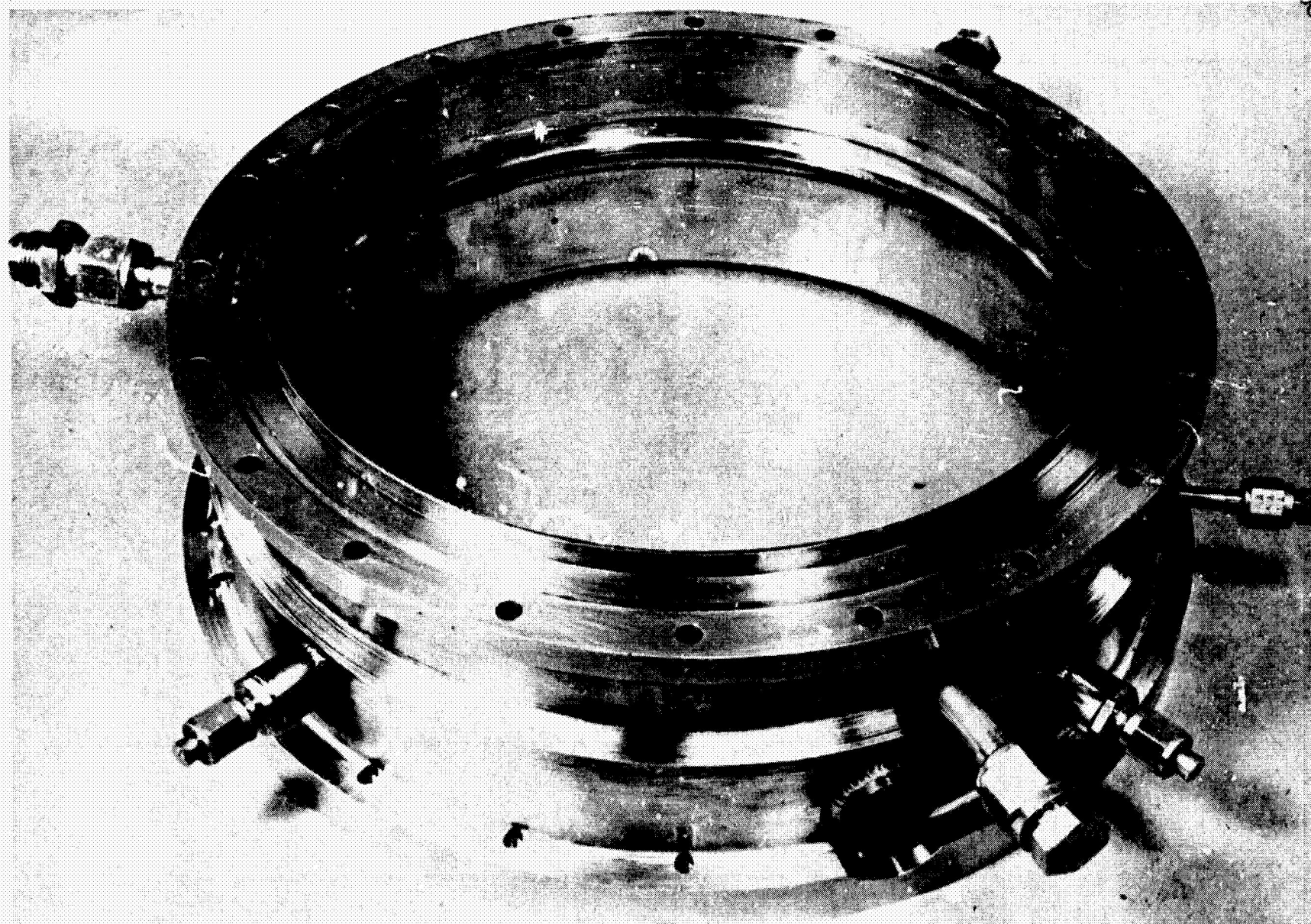
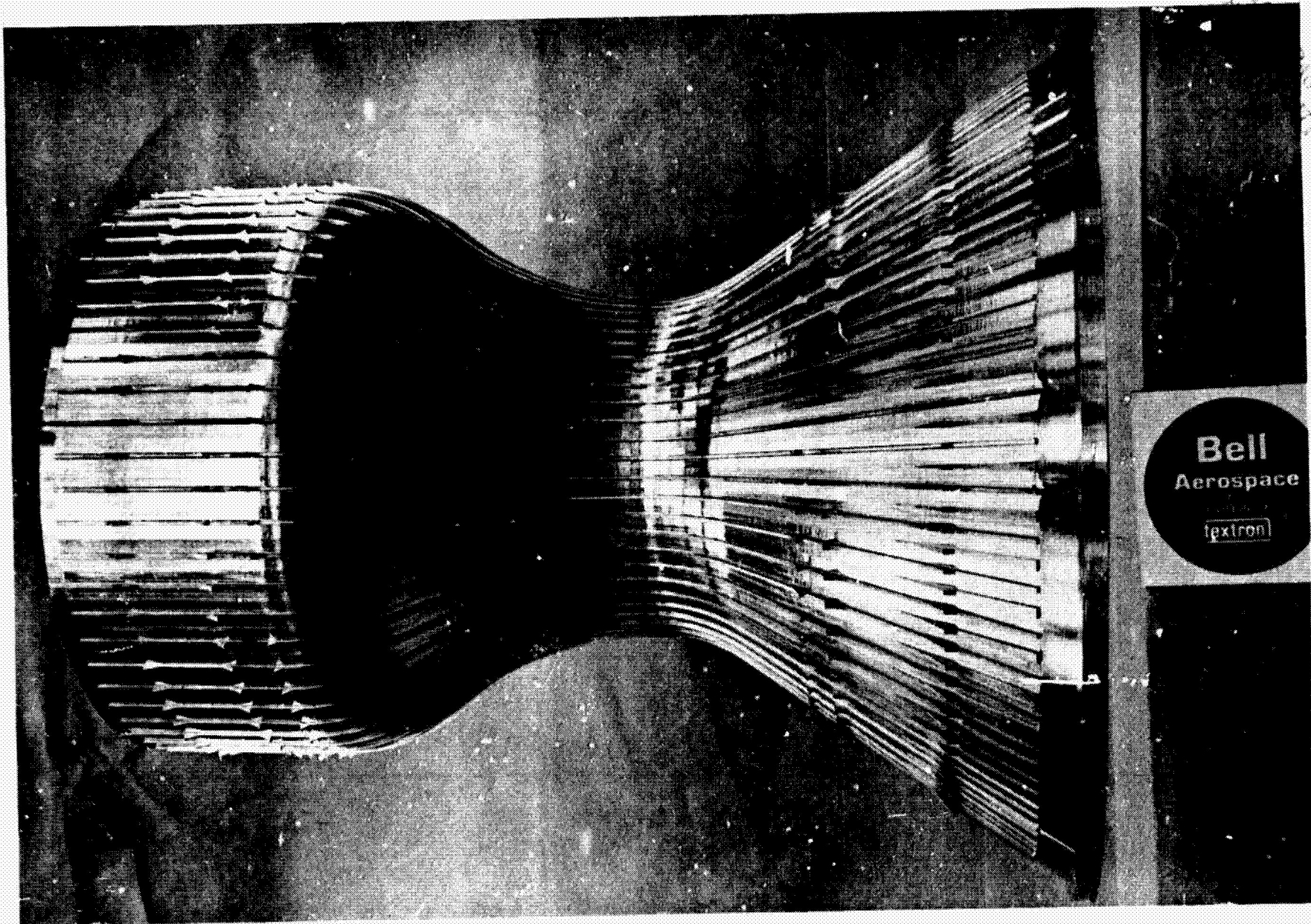
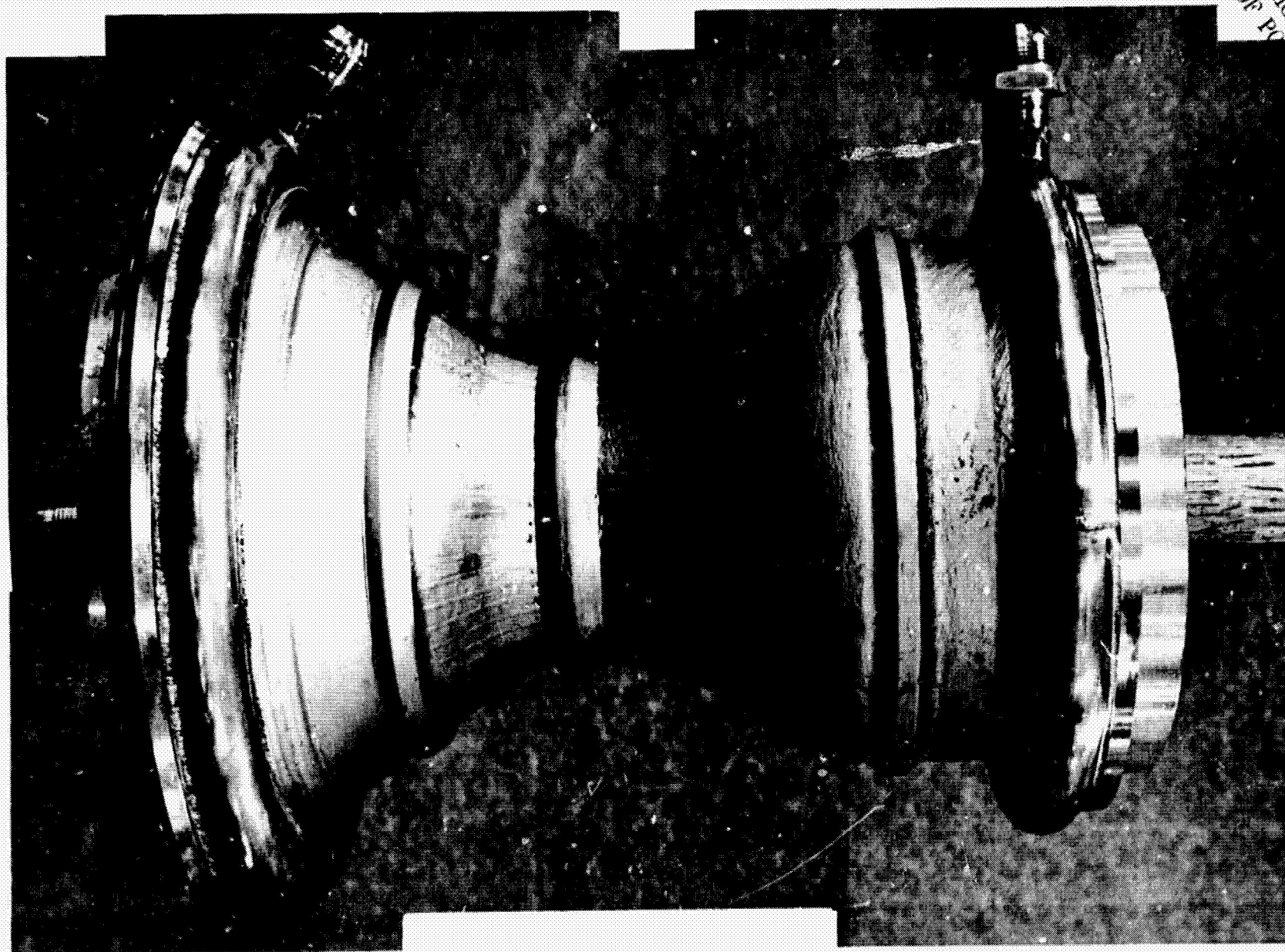


FIGURE X-5. FILM COOLANT RING





ORIGINAL PAGE IS
OF POOR QUALITY

FIGURE X-7. REGENERATIVE THRUST CHAMBER

X-10

8693-470228-5
ADAPTER - NOZZLE EXTENSION

8693-470218-1
GASKET

O-RING

612A428-10 SCREW
AN960C416 WASHER
40 EACH REQ'D

R5006094 X ROCKETDYNE
NOZZLE EXTENSION ASSY.
HEAT SINK "ONE"

8693-470226-1 -
CHAMBER, ASSY OF

7.170 TO ~~4~~ THROAT - 949

FIGURE X-

REV. A 100 1035

BELL AEROSPACE COMPANY DIVISION OF TEXTRON INC. POST OFFICE BOX ONE BUFFALO, NEW YORK 14240			
INTERFACE, ASSY OF REGEN TEST HARDWARE			
SIZE B	CODE IDENT NO 80070	8693-478030	
SCALE 1/1	DEVELOPMENT		SH 2052

Bell Aerospace Company

CALCULATED CHAMBER TEMPERATURES

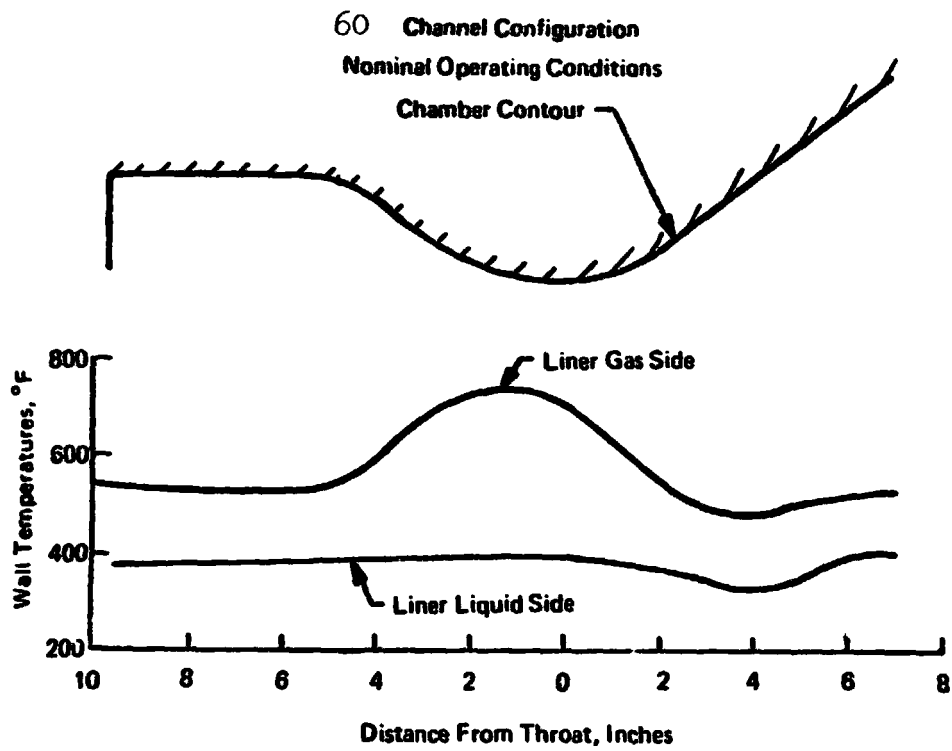


FIGURE X-9

Bell Aerospace Company

A complete summary of the regeneratively cooled chamber and injector design characteristics are given in Table I and II respectively with a hardware summary used in the test series listed in Tables III and IV.

B. Test Facility

The thrust chamber was tested at Bell Aerospace Company's Bell Test Center Facility prior to shipment and evaluation at Test Cell Area 401 of the White Sands Test Facility at simulated altitudes of about 100,000 feet. Testing at the WSTF was conducted with a nozzle area ratio of 76.7:1, whereas at BAC the nozzle area ratio was 15:1.

1. White Sands Test Facility

A photograph of the installation in the White Sands Test Facility is shown in Figure X-10 and a test cell schematic given in Figure X-11. Propellant tank capacities were 2000 gallons for both the fuel and oxidizer. The altitude system was initially pumped down to a pressure of approximately 0.1 psia, and then a gas generator-driven ejector system pumped the capsule down to a pressure of 0.06 to 0.07 psia, equivalent to an altitude in excess of 100,000 feet. Facility pressure drops at rated flow conditions were 25 psi for the oxidizer circuit and 15 psi for the fuel circuit.

Thrust measurements were made using a multi-axis measuring system with three axial dual bridge load cells for recording the main thrust. A general list of facility and engine instrumentation is given in Table V and a detailed list is provided in Table VI. The type of instrumentation and the quantities were similar to that used at BAC.

The test operation was initiated with a vacuum pump evacuation approximately 2-3 hours prior to the actual test operation. The pre-fire engine test operation was completed with the assurance the engine was ready for testing. The gas generator driven ejector system was brought up to full operation, thus bringing the altitude cell to the final run pressure.

The OME countdown covered from T10 second until T+35 second and counted every second.

The engine purges were initiated at T₀ second on both sides. At T₀ the bipropellant fire valve was opened and purging stopped. At shutdown the engine was purged for 15 seconds. This procedure was used for all the test series.

Bell Aerospace Company

TABLE I

DEMONSTRATOR THRUST CHAMBER DESIGN CHARACTERISTICS

COMBUSTOR

Contraction Ratio	3
Length, Inches	17.3

NOZZLE

Regen Section Expansion Ratio	To 6:1
Contour	Parabolic
Nozzle Extension Expansion Ratio	6:1 to 76.7:1

COOLANT

Circuit	
Number of Regen Coolant Channels	60
Coolant Pressure Drop, PSID	15
Coolant Bulk Temperature	120
Auxiliary Film Coolant	2.0% of Total Propellant

MATERIALS

Hot Wall (0.050 inch) and Lands	304L Stainless Steel
Cold Wall (0.050 inch)	Electroformed Nickel

Bell Aerospace Company

TABLE II

INJECTOR CHARACTERISTICS

Diameter, Inches	10
Number of Elements	196
Number of Rows	7
Type of Elements	Triplet, 2 fuel on 1 oxidizer
Oxidizer Element Diameter, Inch (Minimum/Maximum)	0.0465/0.0492
Fuel Element Diameter, Inch (Minimum/Maximum)	0.0276/0.0295
Number of Acoustic Cavities	8/4
Mode Suppression	1st Tangential 3rd Tangential, 1st Radial

Bell Aerospace Company

TABLE III
TEST HARDWARE FOR TEST SERIES 1

DESCRIPTION	P/N	S/N	QTY.
Injector - Aluminum	8693-473050-1	2	1
Regen Chamber - Stainless Steel with Nickel Cover	8693-470205-1	1	1
Vortex Ring - Stainless Steel ($\rho = 3-1/2\%$)	8693-473140-3	1	1
Acoustic Slot Ring - Stainless Steel	8693-473133-1	2	1
Nozzle Adapter Ring-Stainless Steel	8693-470228-1	1	1
Injector Mounting Ring - Stainless Steel	8600-986330-1	1	1
Bipropellant Valve - Al/S.S.	8258-472225	65	1
Accelerometer Block-Cemented to Upstream Side of Injector			1
ΔP Transducer (B386061) - Used to Measure Vortex Flow			1
Oxidizer Line(1-1/4" O.D. Tubing)			
Fuel Line - Chamber Outlet to Inj. (1-1/4" O.D. Tubing) Includes 0.619" Dia. Orifice			
Vortex Line (1/2" O.D. Tubing)			
Vortex Loop (1/2" O.D. Tubing) Includes a Turansky Valve and 0.126" Diameter Orifice			
Fuel Line - Bipropellant Valve to Chamber Inlet (1-1/4" O.D. Tubing)			
Bipropellant Valve Flange			
Accelerometers			
Accelerometer Leads			
NASA Supplied Nozzle Extension ($\epsilon = 76.7$)			
Pressure Test Hardware			
Nozzle Throat Plug - Al	8693-470027	1	1
Injector Pressure Plate	8693-470015-1	1	1

Bell Aerospace Company

TABLE IV
HARDWARE CONFIGURATION FOR TEST SERIES 2

DESCRIPTION	P/N	S/N	QTY.
Injector - Aluminum	8693-473050-1	2	1
Regen Chamber - Stainless Steel With Nickel Cover	8693-470205-1	1	1
Vortex Ring - Stainless Steel ($\phi = 3-1/2\%$)	8693-473140-3	1	1
Acoustic Slot Ring - Stainless Steel	8693-473133-1	2	1
Nozzle Adapter Ring - Stainless Steel	8693-470228-1	1	1
Injector Mounting Ring - Stainless Steel	8600-986330-1	1	1
Bipropellant Valve - Al/Stainless Steel	8258-472225	65	
Accelerometer Block - Cemented to Upstream Side of Injector			1
ΔP Transducer (B3860161) - Used to Measure Vortex Flow			1
Two Inch Barrel Section	8693-470023-1	1	1
Oxidizer Line (1-1/4" O.D. Tubing)			
Fuel Line - Chamber Outlet to Injector (1-1/4" O.D. Tubing) Includes 0.619" Diameter Orifice			
Vortex Line (1/2" O.D. Tubing)			
Vortex Loop (1/2" O.D. Tubing) Includes a Turansky Valve and 0.126" Diameter Orifice			
Fuel Line - Bipropellant Valve To Chamber Inlet (1-1/4" O.D. Tubing)			
Bipropellant Valve Flange			
Accelerometers			
Accelerometer Leads			
NASA Supplied Nozzle Extension ($\epsilon = 76.7$)			
Pressure Test Hardware			
Nozzle Throat Plug - Al	8693-470027	1	1
Injector Pressure Plate	8693-470015-1	1	1

ORIGINAL PAGE IS
OF POOR QUALITY

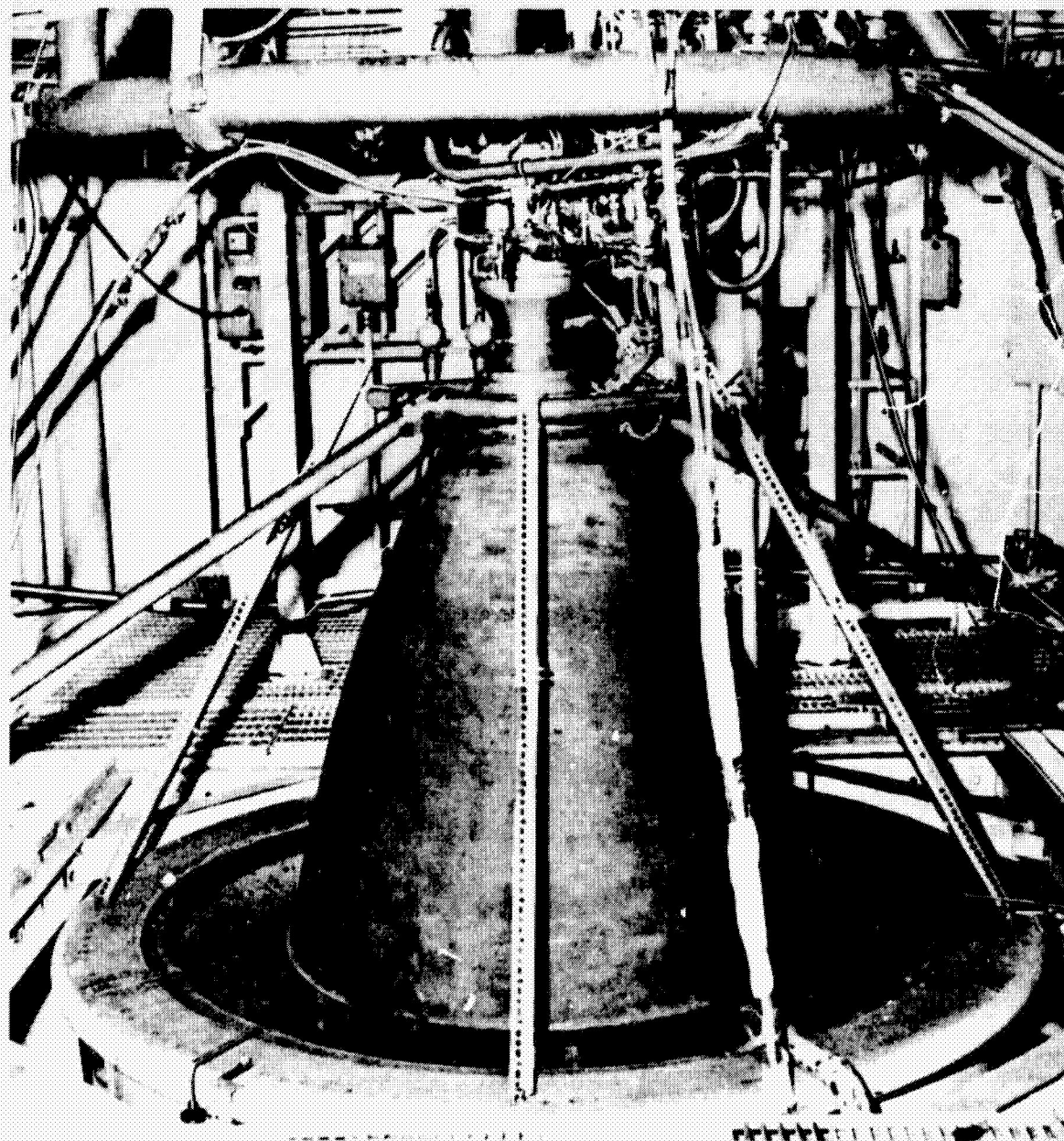


FIGURE X-10. THRUST CHAMBER MOUNTED IN WSTF ALTITUDE TEST CELL AREA 401

ORIGINAL PAGE IS
OF POOR QUALITY

FIGURE X-11

REGENERATIVE CHAMBER INSTRUMENTATION LOCATION

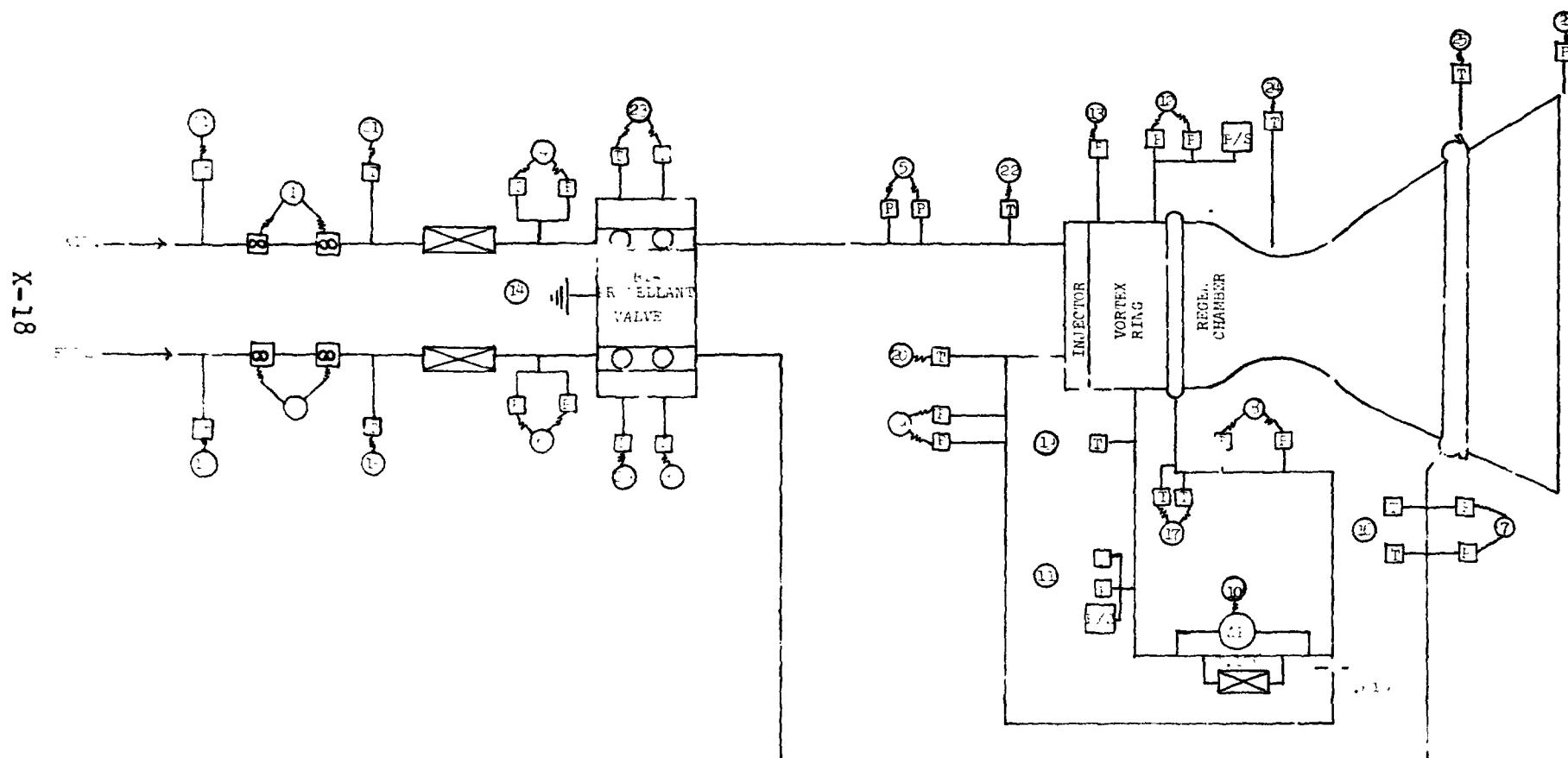


TABLE V
GENERAL INSTRUMENTATION LIST

NO.	SYMBOL	PARAMETER	NO. OF PARAMETERS
1	\dot{W}_{ox}	Oxidizer Flowrate	2
2	\dot{W}_f	Fuel Flowrate	2
3	\dot{W}_{H_2O}	Duct Coolant Water Flowrate	2
4	OFP	Oxidizer Feed Pressure	2
5	OII P	Oxidizer Injector Inlet Pressure	2
6	FFP	Fuel Feed Pressure	2
7	FCIP	Fuel Chamber Inlet Pressure	2
8	FCOP	Fuel Chamber Outlet Pressure	2
9	FIIP	Fuel Injector Inlet Pressure	2
10	FVO Δ P	Fuel Vortex Orifice Δ Pressure	1
11	FVIP	Fuel Vortex Inlet Pressure	2
12	P _{Inj.}	Chamber Pressure	2
13	P _{Inj.}	Chamber Pressure (Close Coupled)	1
14	F	Thrust	1
15	FLT	Fuel Line Temperature	2
16	FCIT	Fuel Chamber Inlet Temperature	2
17	FCOT	Fuel Chamber Outlet Temperature	2
18	FVIT	Fuel Vortex Inlet Temperature	1
19	FIIT	Fuel Injector Inlet Temperature	1
20	OLT	Oxidizer Line Temperature	2

Bell Aerospace Company

TABLE V (CONT'D)

GENERAL INSTRUMENTATION LIST

NO.	SYMBOL	PARAMETER	NO. OF PARAMETERS
21	OIIT	Oxidizer Injector Inlet Temp.	1
22	VT	Valve Temperature	2
23	CH-T	Chamber Temperature	13
24	FLG.-T	Flange Temperature	2
25	DIT	Water Duct Inlet Temperature	2
26	DOT	Water Duct Outlet Temperature	2
27	P _{NE}	Pressure - Nozzle Exit	3
28	VAPL	Valve Actuation Pressure - Low	1
29	VAPH	Valve Actuation Pressure - High	1

ORIGINAL PAGE IS
OF POOR QUALITY

TABLE VI

SAC 6K OMS
ENGINE TECHNOLOGY SUPPORT PROGRAM
FACILITY AND ENGINE INSTRUMENTATION LIST

MEASUREMENT NUMBER	DESCRIPTION	RANGE
1001P	He inlet pressure fuel	0-5000 psia
1002P	Hi reg out fuel	0-2000 psia
1003P	Lo reg out fuel	0-500 psia
1005T	Fuel tank bottom temperature	32-150°F
1006H	Fuel up flow 1	0-100 gpm
1007R	Fuel down flow 2	0-100 gpm
1010P	Fuel FM inlet pressure	0-500 psia
1011T	Fuel FM inlet temperature	32-150°F
1013P	Fuel FM out pressure	0-500 psia
1014T	Fuel tank end temperature	32-150°F
1015T	Fuel interface temperature	32-150°F
1020V	Fuel pre valve command	0-30 VDC
GXD535P	Fuel tank pressure	0-500 psia
GXD537P	Oxidizer tank pressure	0-500 psia
2001P	He inlet pressure Ox	0-5000 psia
2002P	Hi reg out Ox	0-2000 psia
2003P	Lo reg out Ox	0-500 psia
2005T	Ox tank bottom temperature	32-150°F
2006R	Ox up flow 1	0-100 gpm
2007R	Ox down flow 2	0-100 gpm
2010P	Ox FM inlet pressure	0-500 psia
2013P	Ox FM outlet pressure	0-500 psia
2014P	Ox tank end temperature	32-150°F
2015T	Ox interface temperature	32-150°F
2020V	Ox pre valve command	0-30 VDC
3001P	Vert force 1A	0-3500 lbf
3002P	Vert force 1B	0-3500 lbf
3003P	Vert force 2A	0-3500 lbf
3004P	Vert force 2B	0-3500 lbf
3005P	Vert force 3A	0-3500 lbf
3006P	Vert force 3B	0-3500 lbf
3007P	Horiz force 1A	0-200 lbf
3008P	Horiz force 1B	0-200 lbf
3009P	Horiz force 2A	0-200 lbf
3010P	Horiz force 2B	0-200 lbf
3011P	Horiz force 3A	0-200 lbf
3012P	Horiz force 3B	0-200 lbf
3013P	Cal cell 1A	0-10000 lbf
3014P	Vert force A total	0-10000 lbf
3015T	Load cell temperature	32-150°F
4001P	Fuel interface pressure	0-400 psia
4002P	Oxid interface pressure	0-400 psia
4003P	T/C coolant in pressure	0-300 psia
4004X	Chamber pressure switch	ON/OFF
4005P	T/C coolant out pressure	0-300 psia
4006V	Eng valve voltage	0-30 VDC
4007T	T/C coolant out temperature -1	32-300°F
4008	Vacant	
4009P	Fuel injector pressure	0-300 psia
4010P	Oxid injector pressure	0-300 psia
4011P	Chamber pressure -1 (c-c)	0-200 psia
4012P	Chamber pressure -2	0-200 psia
4013P	Chamber pressure -3	0-200 psia
4014X	ISO A closed	ON/OFF
4015X	ISO B closed	ON/OFF
4016X	Prop A closed	ON/OFF
4017X	Prop B closed	ON/OFF
4018	Vacant	
4019P	Fuel Vortex ORF PI	-1 psia
4020T	Oxid injector temperature	32-150°F
4021P	Fuel injector temperature	32-150°F
4022X	Vortex in pressure switch	ON/OFF
4023T	T/C coolant in temperature -2	32-300°F
4024X	ISO A open	ON/OFF
4025X	ISO B open	ON/OFF
4026X	Prop A open	ON/OFF
4027X	Prop B open	ON/OFF
4028L	X-axis vibration	10 g
4029L	Y-axis vibration	10 g
4030L	Z-axis vibration	10 g

TABLE VI (CONT'D)
BAC 6K OMS
ENGINE TECHNOLOGY SUPPORT PROGRAM
FACILITY AND ENGINE INSTRUMENTATION LIST

MEASUREMENT NUMBER	DESCRIPTION	RANGE
4031C	ISO valve A current	0-5 ADC
4032C	ISO valve B current	0-5 ADC
4033P	Fuel vortex inlet pressure	0-300 psia
4034T	Vortex Flange Top Temperature	32-300°F
4035T	Vortex BLC temperature	32-300°F
4036T	Vortex Flange bottom temperature	32-300°F
4037T	T/C coolant in temperature -2	32-300°F
4038T	T/C-nozzle flange temperature (-0)	32-300°F
4039T	T/C coolant out temperature -2	32-300°F
4040T	T/C-nozzle flange temperature (-90)	32-300°F
4041T	Chamber surf 1 (0, -8.0 in)	32-300°F
4042T	Chamber surf 2 (0, -7.0 in)	32-300°F
4043T	Chamber surf 3 (0, -4.25 in)	32-300°F
4044T	Chamber surf 4 (0, -0.75 in)	32-300°F
4045T	Chamber surf 5 (0, +0.75 in)	32-300°F
4046T	Chamber surf 6 (0, +2.75 in)	32-300°F
4047T	Chamber surf 7 (0, +5.0)	32-300°F
4048T	Chamber surf 8 (90, -7.0 in)	32-300°F
4049T	Chamber surf 9 (90, -4.25 in)	32-300°F
4050T	Chamber surf 10 (90, -0.75 in)	32-300°F
4051T	Chamber surf 11 (90, +0.75 in)	32-300°F
4052T	Chamber surf 12 (90, +2.75 in)	32-300°F
4053T	Chamber surf 13 (90, +5.0 in)	32-300°F
4054T	Nozzle surf (0, +9.8 in)	32-2000°F
4055T	Nozzle surf (0, +10.4 in)	32-2000°F
4056T	Nozzle surf (0, +12.5 in)	32-2000°F
4057T	Nozzle surf (0, +14.3 in)	32-2000°F
4058T	Nozzle surf (0, +18.8 in)	32-2000°F
4059T	Nozzle surf (0, +31 in)	32-2000°F
4060T	Nozzle surf (0, +43 in)	32-2000°F
4061T	Nozzle surf (0, +60 in)	32-2000°F
4062T	Nozzle surf (90, +9.8 in)	32-2000°F
4063T	Nozzle surf (90, +10.4 in)	32-2000°F
4064T	Nozzle surf (90, +12.5 in)	32-2000°F
4065T	Nozzle surf (90, +14.3 in)	32-2000°F
4066T	Nozzle surf (90, +18.8 in)	32-2000°F
4067T	Nozzle surf (90, +31 in)	32-2000°F
4068T	Nozzle surf (90, +43 in)	32-2000°F
4069T	Nozzle surf (90, +60 in)	32-2000°F
5001P	Nozzle exit pressure - 0	0-0.5 psia
5002P	Nozzle exit pressure - 120	0-0.5 psia
5003P	Nozzle exit pressure - 240	0-0.5 psia
EQ7801P	Fuel injector purge	0-300 psia
EQ7802P	Oxid injector purge	0-300 psia
EQ7501P	Alt cell hi -Z L.L.	0-15 psia
EQ7511P	Alt cell lo -Y L.L.	0-0.5 psia
EQ7512P	Alt cell lo -Z L.L.	0-0.5 psia
9000X	Engine fire switch	ON/OFF
9011T	Oxid FM Inlet Temperature	32-150°F

Bell Aerospace Company

Propellant flow started very nearly simultaneously. An oxidizer lead was assured by the proper design of volumes and resistances downstream of the bipropellant valve and the facilities volumes and resistance upstream of the bipropellant valve. The oxidizer lead was generally about 20 milliseconds.

The test were automatically terminated after the predetermined duration by removing power from the bipropellant valve.

During the purge cycle, the propellant tank pressures were reset to the predetermined levels for the next test. The time required for each test was between 30 and 120 seconds, the variation generally depended upon the magnitude of the tank pressure change. Following the last test of a sequence, the engine was purged as before. On completion of the purge, the altitude cell isolation valve was closed and the hyperflow steam generator system shutdown. The altitude cell pressure was then returned to ambient by bleeding in gaseous nitrogen.

C. Test Program

The test program consisted of a total of 47 tests with 1) two variations in chamber L^* ; 2) ambient and hot propellants; 3) unsaturated and helium saturated propellants; 4) variations in chamber pressure and mixture ratio. The program was completed in two series, the first with the 30 L^* chamber configuration, and the second with a 34 L^* chamber configuration (utilizing a 2-inch spacer between the injector and chamber). Majority of the tests were of 8 seconds duration, with two shorter duration tests of 1.5 and 5.0 seconds for checkout purposes and one 20 second duration test to verify thermal equilibrium. A general summary of the test series including the various sequences is listed in Table VII.

The test setup was similar to that utilized at BAC where a high fuel vortex flow (4.1%) was initiated on start and then reduced to a low vortex flow (1.9%) for steady state conditions. This was accomplished through a switching circuit at 2.5 seconds into the test utilizing an externally supplied dual orifice arrangement to the fuel film coolant vortex manifold.

In addition to the vortex flow checkout tests and the long duration tests with the 30 L^* chamber, one sequence of 10 tests was conducted with unsaturated propellants and one sequence of 10 tests was conducted with helium saturated propellants.

Bell Aerospace Company

TABLE VII

TEST PROGRAM SUMMARY

<u>SERIES</u>	<u>SEQUENCE</u>	<u>NUMBER OF TESTS</u>	<u>CONDITION</u>
1	1	2	30L* - Checkout
1	2	10	30L* - Unsaturated Propellants P _c - M/R Variations
1	3	10	30L* - Saturated Propellants P _c - M/R Variations
1	4	1	20 Sec. - Unsaturated Propellants 30L*
2	1	8	34L* - Unsaturated Propellants P _c - M/R Variation
2	2	8	34L* - Unsaturated Propellants 104°F - Fuel 94°F - Ox
2	3	8	34L* - Saturated Propellants P _c - M/R Variation

Bell Aerospace Company

Three sequences of 8 tests each were conducted with the 3- L* chamber. They were with unsaturated propellants, hot propellants, and helium saturated ambient temperature propellants.

The first test series, first sequence, was originally planned to consist of a 1.5 second, 5.0 second and 12.0 second test, but was reduced to the first two tests when problems were encountered with the ΔP vortex transducer. The problem was improper instrumentation set up which was corrected for subsequent testing.

The first series, second sequence, was planned to consist of ten-10 second tests, but was modified to two-10 second tests and eight-8 second tests. The eight second tests were incorporated to conserve altitude cell propellants. The eight second tests reduced heat applied to the nozzle extension, thus allowing a reduced down time between tests.

An additional test time change was incorporated when the data showed the chamber pressure reading was drifting during tests 5 through 10 of the first series, second sequence and that the vortex ΔP instrument was erratic. The hypothesis forwarded related to vortex manifold fuel "boiling" and was attributed to the short coast maximum heat input to the manifold. Based on the evaluation of these tests the following changes were made:

1. The test series was reduced from 10 to 8 tests.
2. Four tests were made per steam time. Each series consisting of one 10-second and three 8-second tests.
3. Data review after the four tests limited the restart to a 250°F hardware temperature on the test hardware.

All subsequent test series were made in this fashion except for the one 20 second duration test. No subsequent vortex fuel pressure fluctuations were noted in the balance of the testing.

D. Test Results

The test conditions and steady state data summary for the White Sands Test Facility tests conducted on the Bell Aerospace Company regeneratively cooled thrust chamber are summarized in Table VIII. A total of 47 tests were conducted for a cumulative

ORIGINAL PAGE IS
OF POOR QUALITY

TABLE VIII

6K ONE REGEN CHAMBER

ALTITUDE TEST SUMMARY AT WSTF - 10/27/73 TO 11/2/73

Series	Seq.	Test No.	Dur. Sec.	Data Pt. Sec.	P _c corr ⁽¹⁾ Psia	R O/F	ρ %	C* corr Ft/Sec	η %	F _{test} $\epsilon=76.7$	I _{sp} $\epsilon=76.7$	I _{sp} $\epsilon=76.7$	C _f $\epsilon=76.7$	I _{sp} $\epsilon=72.7$	I _{sp} $\epsilon=72.7$	Cht Max °F	Net Max °F	Regen Fuel Temp Rise °F	Chamber Jacket ΔP	L*	Test Condition
I	I	1	1.6	1.3	121.6	1.494	4.53	5628	98.7	5563	312.1	--	1.784	--	--	71	80	3.2	17.7	30	Checkout
I	II	2	5.0	4.5	119.3	1.541	2.02	5621	98.6	5498	313.6	--	1.795	--	--	140	357	99.6	16.1	30	Checkout
I	II	1	10.1	7.5	122.7	1.612	1.93	5617	98.3	5718	315.2	316.29	1.805	316.1	316.75	154	507	114.3	15.2	30	Unsat.
I	II	2	8.0	7.5	126.2	1.435	2.02	5621	98.9	5839	313.9	313.89	1.797	314.8	314.86	159	920	110.0	17.2	30	N ₂ O ₄ /N ₂ H ₄
I	II	3	8.1	7.5	133.9	1.463	2.02	5624	98.3	6203	313.8	313.09	1.795	314.7	313.92	154	1072	106.6	21.0	30	
I	II	4	8.1	7.5	133.9	1.619	1.92	5641	98.7	6238	317.1	316.35	1.808	318.0	317.15	168	1226	117.5	16.0	30	
I	II	5	8.1	7.5	134.4	1.729	1.79	5641	98.6	6289	318.5	317.72	1.916	319.4	318.37	174	1318	123.8	13.7	30	
I	II	6	8.1	7.5	125.6	1.729	1.73	5628	98.5	5874	317.7	317.73	1.816	319.6	318.33	178	1332	127.9	12.0	30	
I	II	7	8.1	7.5	116.5	1.745	1.65	5619	98.5	5442	316.8	317.72	1.814	317.7	318.23	181	1306	132.0	10.8	30	
I	II	8	8.1	7.5	116.3	1.630	1.66	5631	98.6	5401	315.8	316.74	1.804	316.7	317.26	177	1292	126.0	12.1	30	
I	II	9	8.1	7.5	116.6	1.516	1.77	5629	98.9	5392	313.7	314.60	1.793	314.6	315.26	167	1249	119.0	15.1	30	
I	II	10	10.1	7.5	123.3	1.648	1.63	5658	99.0	5729	317.2	316.87	1.803	318.1	317.56	172	1253	126.0	14.7	30	
I	III	1	10.1	7.5	123.3	1.605	1.95	5657	99.0	5706	316.0	316.15	1.797	316.7	317.00	160	1620	114.4	15.6	30	He Sat
I	III	2	8.1	7.5	125.3	1.472	2.03	5620	98.9	5789	312.9	313.12	1.791	314.0	314.02	157	1054	107.7	16.9	30	N ₂ O ₄ /N ₂ H ₄
I	III	3	8.1	7.5	132.9	1.463	2.05	5624	99.0	6147	313.4	312.72	1.793	314.3	313.63	155	1027	106.2	20.4	30	
I	III	4	8.1	7.5	133.8	1.619	1.94	5653	98.8	6224	316.7	316.05	1.802	317.7	316.88	161	1088	115.7	16.0	30	
I	III	5	8.1	7.5	134.5	1.735	1.86	5640	98.6	6294	318.6	317.90	1.818	319.6	318.57	172	1233	123.0	14.9	30	
I	III	6	8.1	7.5	126.2	1.724	1.82	5629	98.5	5900	318.1	317.76	1.818	318.7	317.40	176	1290	124.0	12.8	30	
I	III	7	8.1	7.5	117.2	1.739	1.76	5616	98.4	5476	316.6	317.29	1.814	317.5	318.00	179	1286	129.2	10.6	30	
I	III	8	8.1	7.5	115.8	1.602	1.81	5634	98.8	5358	315.0	315.91	1.799	315.9	316.60	176	1287	122.6	11.5	30	
I	III	9	8.1	7.5	115.8	1.483	1.87	5629	98.9	5333	313.2	314.20	1.790	314.2	314.94	171	1291	115.7	13.0	30	
I	III	10	10.1	7.5	123.2	1.637	1.74	5645	98.8	5725	316.8	317.23	1.806	317.6	317.39	175	1292	123.4	13.0	30	
I	IV	1	20.1	7.5	123.4	1.622	1.94	5619	98.3	5725	314.4	316.48	1.800	315.3	315.50	150	454	113.1	15.5	30	Nominal,
I	IV			9.5	123.3	1.620	1.94	5628	98.5	5737	315.5	316.48	1.803	316.4	316.60	153	560	116.0	15.5	30	Long
I	IV			19.5	121.8	1.618	1.93	5593	97.9	5712	314.8	316.40	1.811	315.7	316.00	160	1002	119.0	15.2	30	Duration
II	I	1	10.1	7.5	126.5	1.625	1.93	5650	98.9	5876	316.3	316.51	1.801	317.2	316.56	154	462	117.8	16.3	34	Unsat.
II	I	2	8.1	7.5	126.5	1.422	2.09	5617	99.1	5814	311.7	311.50	1.785	312.6	312.34	155	954	108.1	17.2	34	N ₂ O ₄ /N ₂ H ₄
II	I	3	8.1	7.5	135.6	1.610	1.96	5649	98.1	6315	317.0	315.90	1.806	317.9	315.61	164	2016	120.7	16.5	34	
II	I	4	8.1	7.5	135.4	1.820	1.79	5640	98.7	6366	319.5	318.47	1.823	320.4	319.00	178	2090	136.2	14.3	34	
II	I	5	10.1	7.5	114.5	1.630	1.94	5634	98.7	5305	315.4	316.60	1.799	316.3	317.35	172	1754	123.8	10.9	34	
II	I	6	8.1	7.5	114.8	1.860	1.78	5617	98.7	5369	317.5	318.38	1.818	318.4	318.94	184	1951	139.9	9.6	34	
II	I	7	8.1	7.5	125.4	1.830	1.80	5638	98.8	5873	318.6	318.50	1.818	319.5	319.06	178	2021	136.8	12.1	34	
II	I	8	8.1	7.5	125.9	1.615	1.95	5659	99.0	5840	316.9	316.79	1.802	317.8	317.48	173	2073	125.0	14.1	34	
II	II	1	10.1	7.5	126.3	1.591	1.97	5695	99.7	5833	316.8	316.74	1.790	317.7	316.60	183	501	115.7	17.6	34	Hot
II	II	2	8.1	7.5	126.3	1.414	2.10	5629	99.3	5814	312.3	311.35	1.785	313.2	317.00	182	857	105.4	20.5	34	Prop.
II	II	3	8.0	7.5	136.1	1.600	1.95	5670	99.2	6339	318.1	316.21	1.805	319.0	316.87	192	941	117.8	19.7	34	
II	II	4	8.1	7.5	135.5	1.806	1.82	5649	98.8	6371	320.1	318.29	1.823	321.0	318.82	209	1137	113.1	13.3	34	
II	II	5	10.1	7.5	114.3	1.615	1.96	5653	99.0	5290	315.8	315.93	1.797	316.7	316.65	203	543	124.8	10.4	34	
II	II	6	8.1	7.5	114.3	1.798	1.83	5647	99.1	5325	317.9	318.04	1.811	318.8	318.62	208	947	136.1	9.4	34	
II	II	7	8.1	7.5	125.3	1.810	1.83	5603	99.2	5860	319.3	318.43	1.814	320.2	318.99	205	1018	134.4	12.8	34	
II	II	8	8.1	7.5	125.6	1.604	1.95	5672	99.2	5833	317.4	316.48	1.800	318.3	317.18	201	1131	123.2	14.4	34	
II	III	1	10.1	7.5	126.0	1.611	1.96	5668	99.2	5845	316.4	317.11	1.796	317.3	317.70	176	534	118.5	16.3	34	Hot
II	III	2	8.1	7.5	125.2	1.407	2.12	5612	99.0	5749	310.6	310.52	1.781	311.5	311.40	174	898	107.3	17.2	34	Prop.
II	III	3	8.1	7.5	135.8	1.616	1.95	5664	99.1	6316	317.2	316.10	1.802	318.1	316.78	182	1933	120.5	18.4	34	He Sat.
II	III	4	8.1	7.5	135.7	1.805	1.80	5652	98.9	6369	319.5	318.45	1.819	320.4	318.95	196	1866	132.5	14.2	34	
II	III	5	10.1	7.5	113.7	1.597	1.98	5635	98.7	5243	313.3	316.53	1.789	314.2	314.13	198	601	125.8	8.9	34	
II	III	6	8.1	7.5	113.7	1.803	1.83	5638	98.9	5287	316.7	317.70	1.807	317.6	318.23	201	982	138.3	9.5	34	
II	III	7	8.1	7.5	125.5	1.815	1.83	5671	99.3	5854	319.0	318.89	1.810	319.9	319.43	196	1021	136.2	12.0	34	
II	III	8	8.1	7.5	125.0	1.631	1.95	5659	99.0	5802	316.5	316.52	1.800	317.4	317.18	191	1140	126.6	13.8	34	

(1) P_c correction factor 0.981

(2) Normalized to P_c=125 psia and nominal propellant temp.

(3) Normalized to 1.9% ρ film cooling and P_c=125 psia, unsaturated and nominal propellant temp.

X-26

Bell Aerospace Company

duration of 375 seconds. Chamber pressure ranged from 114 psia to 136 psia and mixture ratios (O/F) from 1.41 to 2.12.

1. Transient Characteristics

The start and shutdown transients of a thrust chamber depend on valve design and sequencing, engine and facility flow resistances and volumes, ambient pressure and level of steady-state operating conditions. A typical start transient for the engine is shown in Figure X-12.

The oxidizer injector pressure shows a gradual rise until the fuel reaches the injector, and then a rapid rise as the injector orifices flow fully. The incipient oxidizer pressure rise precedes the fuel pressure rise by approximately 400 milliseconds and is attributed to the vaporization of the oxidizer, which has a high vapor pressure. There was no significant over pressure in chamber pressure and the start transient was gradual.

When the bipropellant valve closes the fuel, oxidizer and chamber pressures start to decay simultaneously (Figure X-13).

The injector/thrust chamber combination tested at WSTF demonstrated safe starts and shutdowns over a range of propellant inlet conditions using a bipropellant valve.

2. Stability Characteristics

There was no high or low frequency instability recorded over the steady-state operating ranges of chamber pressure and mixture ratio with N_2O_4/MMH propellants. The damping configuration consisted of acoustic cavities without baffles to maintain stable operation. Accelerometers were installed on the upstream side of the injector-to-monitor loads in three mutually perpendicular axes. Typical loads of less than 20g's were noted at start and no significant loads during steady-state operation.

WSTF Test Data

The raw test data was plotted in Figures X-14 through X-20. The graphs attempt to show comparisons of 30 L* and 34 L* (Figure X-1), unsaturated and helium saturated propellants @ 30 L* (Figure X-15), and @ 34 L* (Figure X-16), ambient and heated propellants at 34 L* (Figure X-17), and chamber pressure effects at 30 L* and 34 L* (Figures X-18 and X-19). The data scatter is such that it is difficult to define a curve or curves for L* comparison, and for unsaturated and saturated propellants comparisons. Although there is scatter, trends are discernable for ambient and heated propellants, and chamber pressure effects (Figures X-17, X-18, and X-19).

FIGURE 12
START TRANSIENT
TEST 1-4-1
29 OCT 1973

Chamber Pressure

Oxidizer Injector Pressure

Fuel Injector Pressure

Fuel Coolant Pressure

Axial Accelerometer

100 Milliseconds

FIGURE 13
SHUTDOWN TRANSIENT
TEST 1-4-1
29 OCT 1973

Oxidizer Injector Pressure

Fuel Injector Pressure

Fuel Coolant Pressure

Axial Accelerometer

100 Milliseconds

Bell Aerospace Company

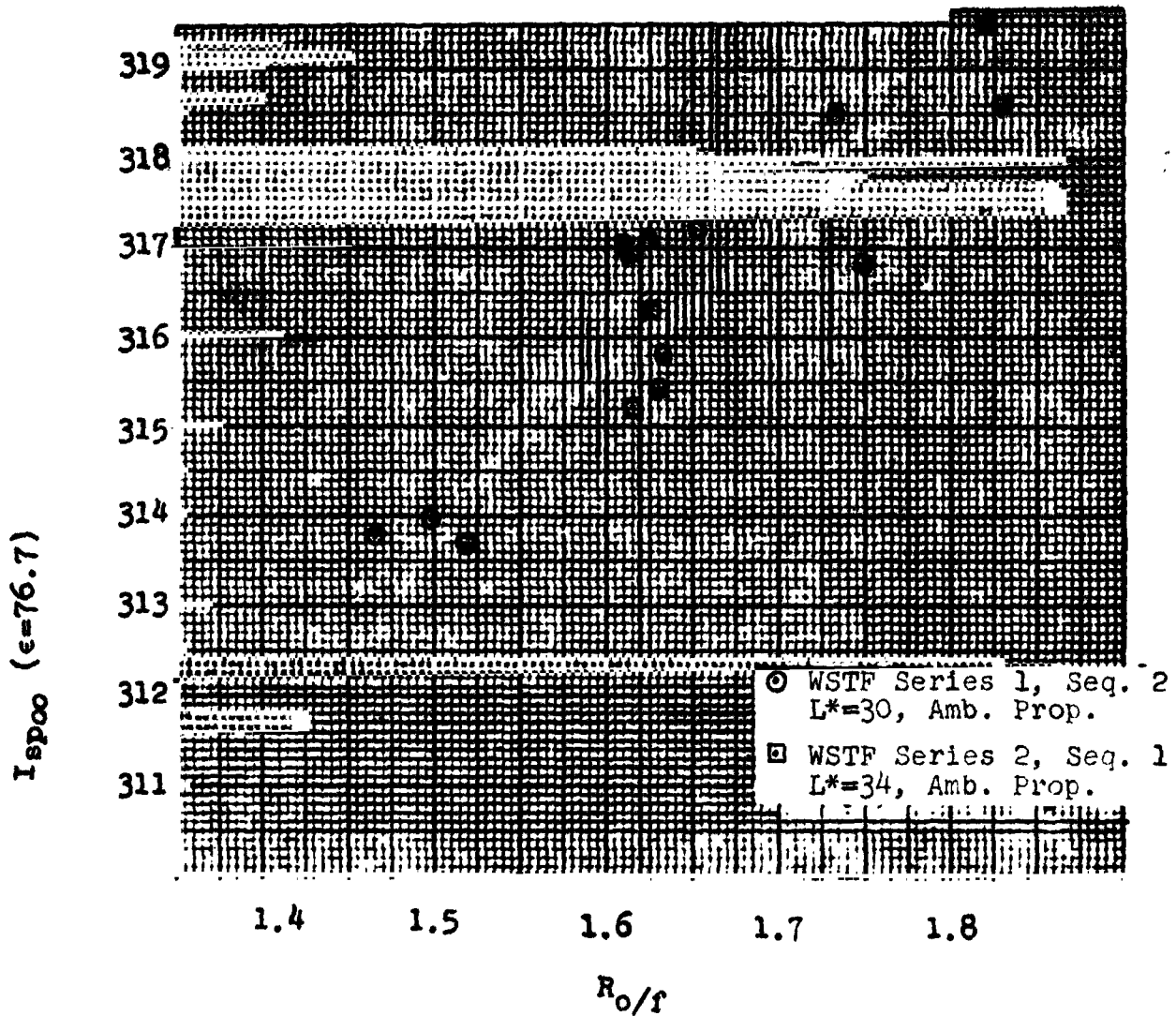
FIGURE X-14

$I_{sp\infty}$ ($\epsilon=76.7$) vs R_o/r - 6K ONE REGION

COMPARISON OF 30L* AND 34L*

A1 INJECTOR S/N 2

PROPELLANTS: N_2O_4/MMH



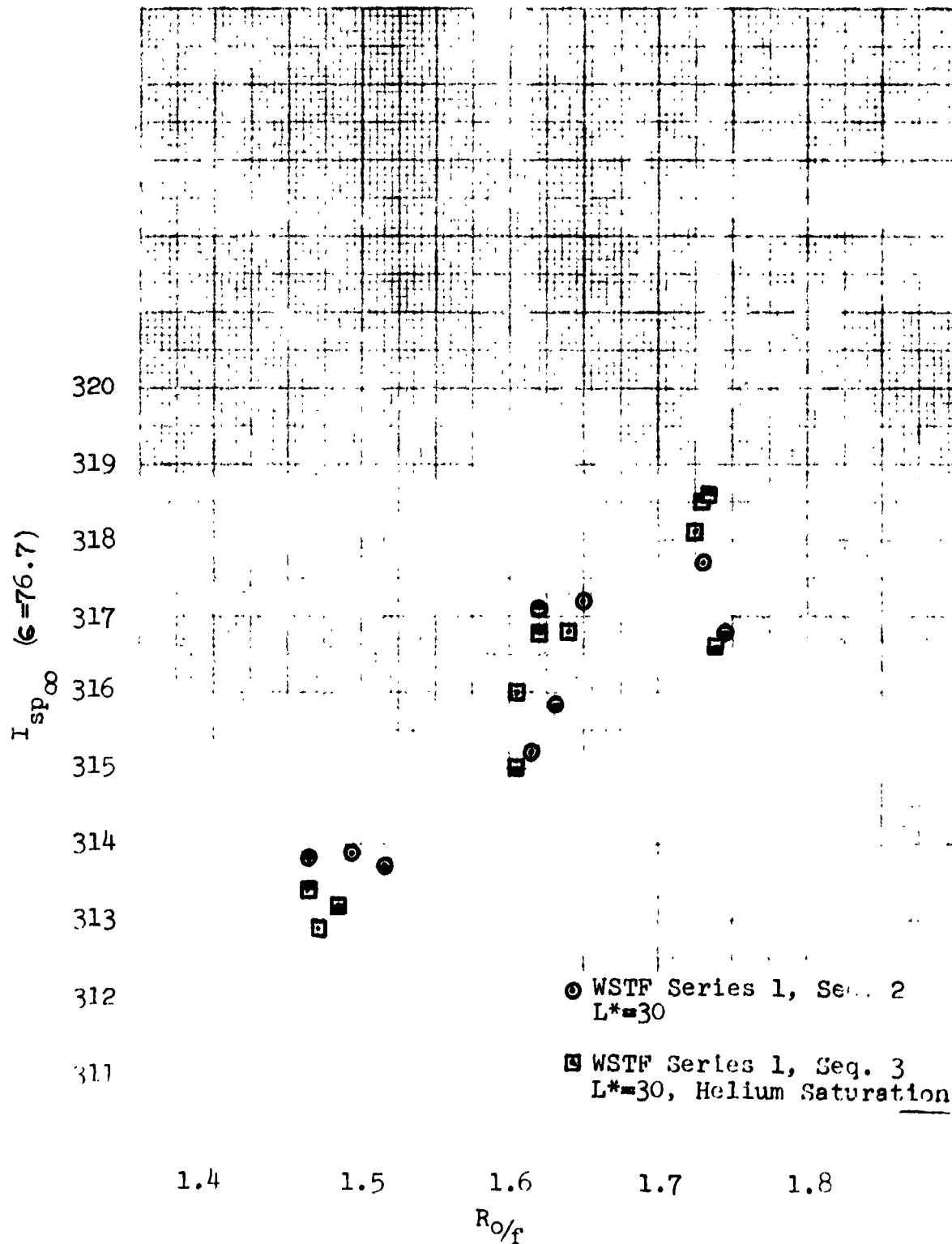
Bell Aerospace Company

FIGURE X-15

$I_{sp\infty}$ ($\epsilon=76.7$) vs $R_{o/f}$ - 6K OME REGEN
COMPARISON OF UNSAT. AND SAT. PROP. @ 30L*

AL INJECTOR S/N 2

PROPELLANTS: N_2O_4/MMH

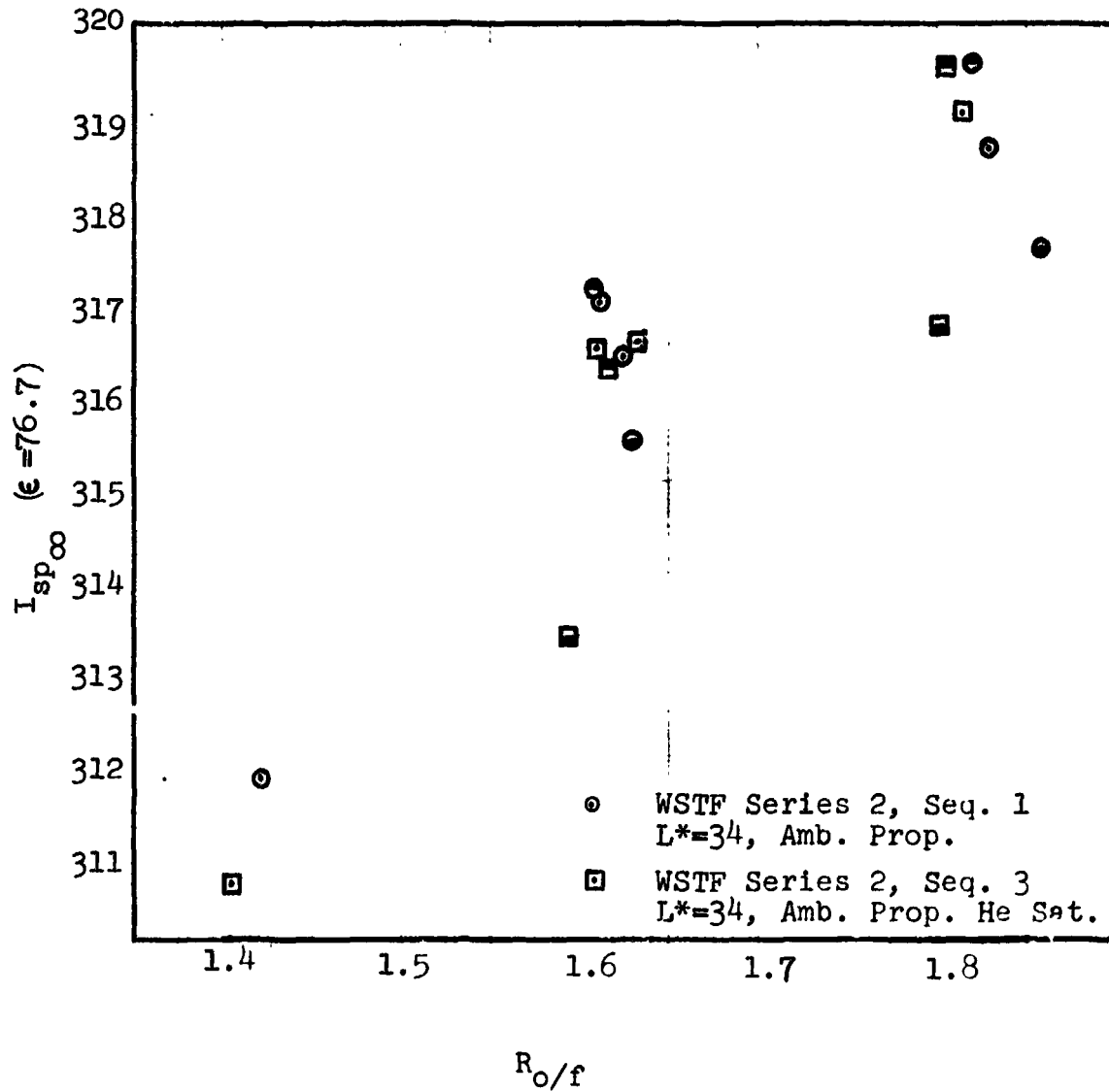


Bell Aerospace Company

FIGURE X-16

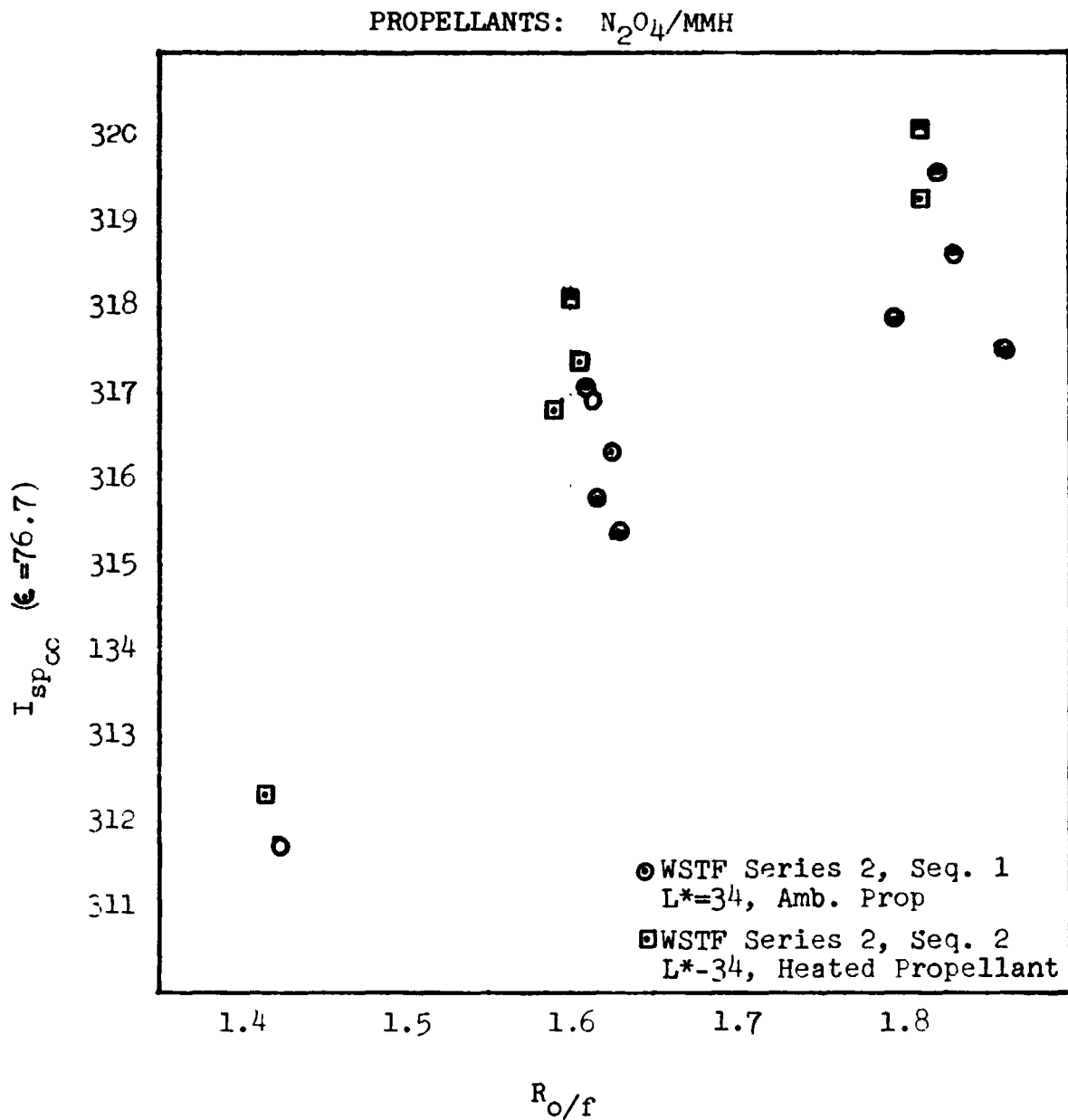
$I_{sp\infty}$ ($\epsilon=76.7$) vs R_o/f - 6K OME REGEN

COMPARISON OF UNSAT. AND SAT. PROPELLANT @ 34 L*



Bell Aerospace Company

FIGURE X-17
 $I_{sp\infty}$ ($\epsilon=76.7$) vs R_o/f - 6K OME REGEN
COMPARISON OF AMBIENT AND HEATED PROPELLANT
Al INJECTOR S/N 2
TEST DATA



Bell Aerospace Company

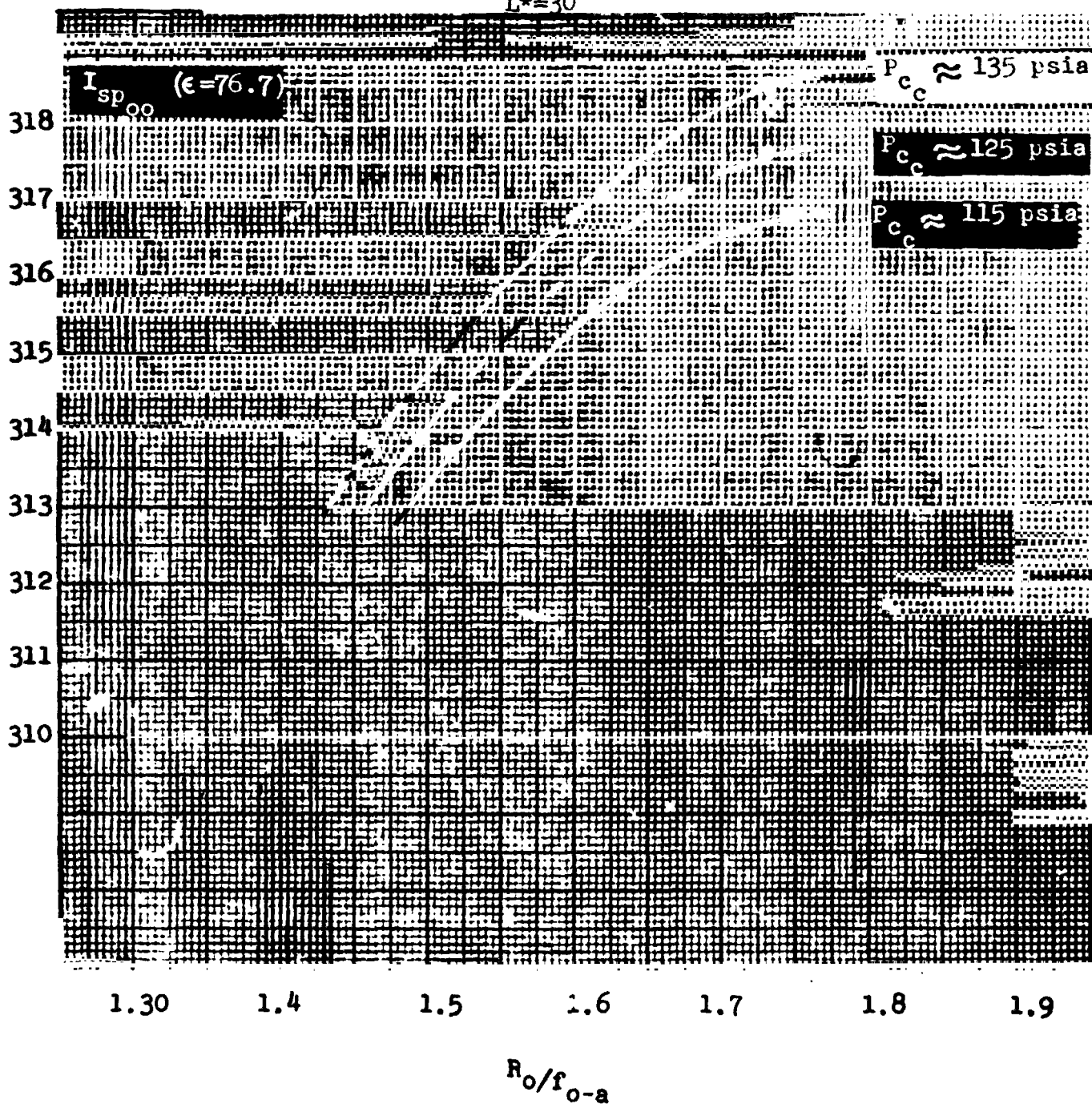
FIGURE X-18

WSTF DATA

COMPARISON OF PERFORMANCE WITH CHAMBER PRESSURE

$I_{sp_{oo}} (\epsilon = 76.7)$ vs R_o/f_{o-a}

$L^* = 30$



ORIGINAL PAGE IS
OF QUALITY

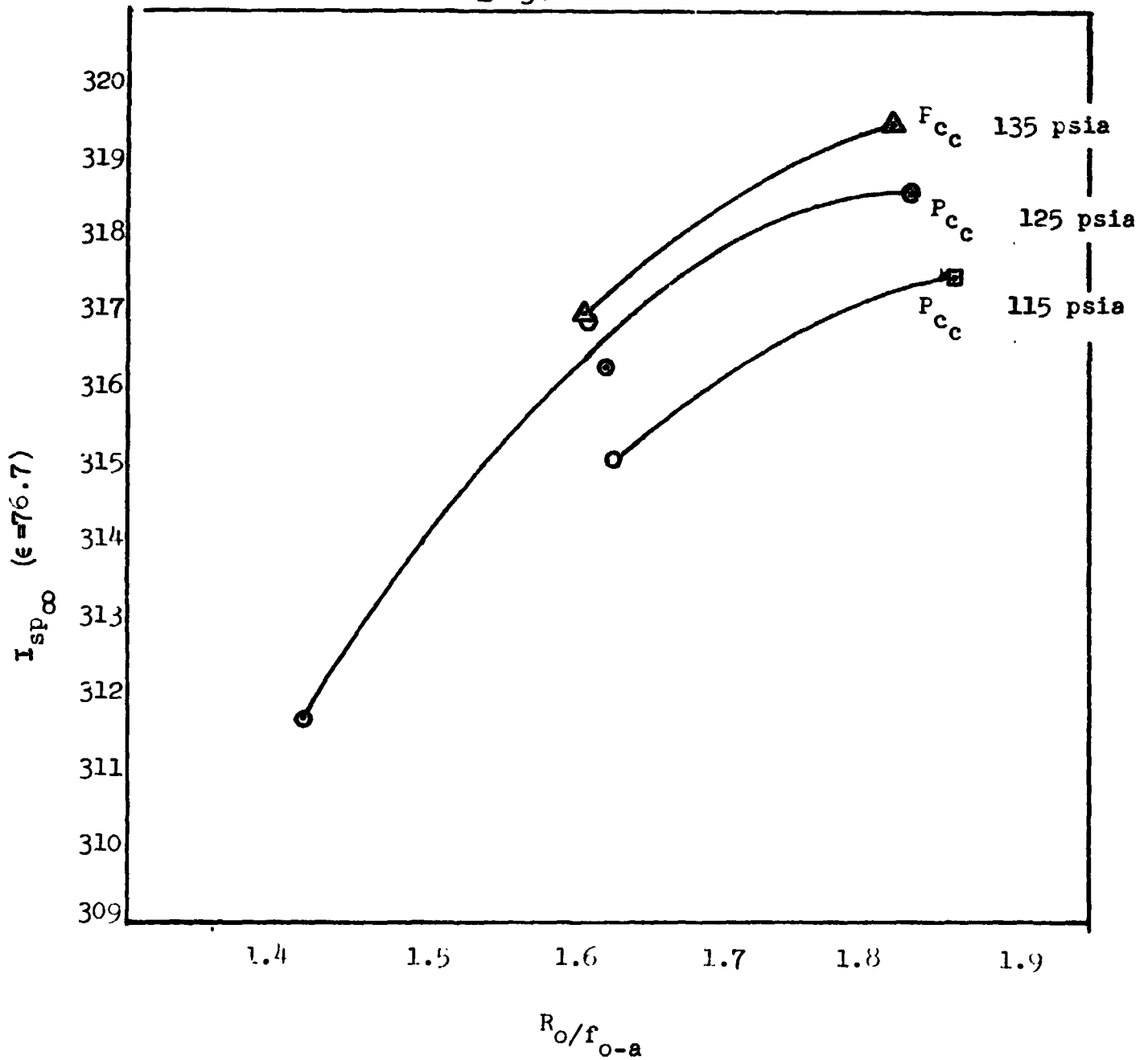
Bell Aerospace Company

FIGURE X-19

WSTF DATA

$I_{sp\infty}$ ($\epsilon=76.7$) vs R_o/f_{o-a}

L^*-34



Bell Aerospace Company

The data scatter is attributed to the normal difficulties of setting up precise test point, and was further examined by a normalization technique which is discussed in the subsequent section.

The initial series of tests conducted resulted in what was hypothesized as overheating in the fuel vortex manifold near the end series of 10 second tests. Since this overheating could compromise data, a single burst 20 second test was conducted to define steady state values and compare the data to the end 10 second test. The results of the 20 second test confirmed the original data and relieved any concern that any pulse performance was recorded due to the somewhat unrealistic test sequence. An obvious byproduct of the test was the obtainment of more thermal data to predict temperatures of the nozzle extension (divergent nozzle).

The regen chamber fuel temperature rise appears to be near stabilization within the 20 seconds as temperature rise varies from 113°F at 7.5 seconds to 119°F at 19.5 seconds.

E. Normalization of Test Data

1. General

It seldom happens that test data are obtained with such precision that parametric influences can be directly examined. Graphical plots of such data frequently appear to contain considerable random scatter which many times is associated with measurement error.

A more accurate assessment of such data can be made if the data can be adjusted to a standard set of conditions prior to presentation on a plot. Occasionally such correction formulas are available from purely analytical considerations. More often they are not and knowledge of them may actually have been a principal reason for conducting the test program in the first place.

In the latter case proper correction formulas can be derived by applying statistical regression techniques. The procedure used for the WSTF test data was the development of a "best fit" expression to describe the influence of each variable upon the parameter of interest. A plot of corrected data was then developed as follows:

The independent variable for the plot was selected (e.g. mixture ratio). No correction is applied for variations in this variable since it is the influence of this variable which is to be graphically presented.

Bell Aerospace Company

A set of standard or nominal conditions for the remaining independent variables was selected (e.g. P_c , ρ , etc.).

Each data point was adjusted to the nominal conditions by using the regression equation to determine how the dependent variable changes when conditions are changed from those of the test to those selected as nominal.

These were the procedures used to develop the plots in the present report. Generally the overall mixture ratio was selected, one was treated as a parameter. When plotting data on such plots the convention normally followed is to group the data within selected bands of one parameter and correct data to the nominal value associated with that band. Thus, for example, one may select P_c and R_o as the independent plot variables and may elect to plot the P_c influence parametrically at three levels such as 110, 120 and 130 psia. Test data obtained in the P_c range 110 \pm 5 may then be corrected to a P_c of 110 before plotting. Tests in the range 120 \pm 5 are corrected to 120 and so on.

In general the test data presented in this report have been corrected to the following conditions.

$$P_c = 125$$

$$\rho = 1.9\%$$

$$\text{Propellant Temperatures} = \text{Ambient } (75 \pm 10^\circ\text{F})$$

In one case a plot is presented comparing the BAC test cell LBN data with WSTF data. Data from LBN were obtained with a 15/1 area ratio nozzle. Those at WSTF were for $\epsilon = 76.7/1$. In this case one must pre-correct data for one geometry to operation with a nozzle of the other geometry or must correct both sets of data to a third nozzle configuration. The latter course was selected and all data were analytically pre-corrected to a nozzle configuration having an $\epsilon = 72.7/1$ and a length equal to 59.1 inches. This geometry was considered typical for Space Shuttle applications.

2. WSTF Test Data Normalized

When the WSTF test data were normalized and plotted, the effects of the test variables became more apparent and data scatter was significantly reduced. On the various graphs, the nominal curve is based on the 45 tests normalized to 125 psia chamber pressure and ambient propellant temperatures. The 1.5 second and 5.0 second tests are not included because of their short run durations.

Bell Aerospace Company

A comparison of Figure X-20, where 5 of the 47 WSTF tests are plotted after being normalized, and Figures X-1, X-2, and X-3 (data not normalized) illustrates the reduction in data scatter.

A comparison of normalized unsaturated and saturated data indicated that the effects of helium in the propellants is insignificant and that these results compare well with the nominal curve which includes all test data (Figure X-21).

The effects of L^* variation appeared to be insignificant over the range of test conditions and indicated the insensitivity of the triplet injector design to L^* 's between 30 and 34 inches (Figure X-22).

The effects of propellant temperature were significant as shown in Figure X-23 where heated propellant tests are compared with ambient propellant results for the 34 L^* chamber at a chamber pressure of 125 psia. At a mixture ratio (O/F) of 1.65 the gain in performance was 0.83 seconds of impulse or 0.27% when oxidizer temperature is raised from approximately 75°F to 94°F and fuel is raised from 75°F to 104°F.

Chamber pressure effects were also significant as shown in Figure X-24 where 125 psia data is compared with 135 psia and 115 psia data. Both 30 L^* and 34 L^* data were used since there was no significant performance difference between them. The test data points for each chamber pressure range (115±2.2, 125±1.5, 135±1.1) were normalized to nominal values 1.3
2.3 2.1

of 115, 125 and 135 psia in the plot and the curves for 115 psia, 125 psia and 135 psia are based on test data in those ranges. At a mixture ratio 1.65, the specific impulse for the three chamber pressures varied as follows:

	P_c Psia	$I_{sp\infty}$ ($\epsilon = 76.7$) lb _f - sec lbm	ΔI_{sp} lb _f -sec lbm	%
Nominal	135	317.8	+0.9	+0.28
	125	316.9	-	
	115	316.0	-0.9	-0.28

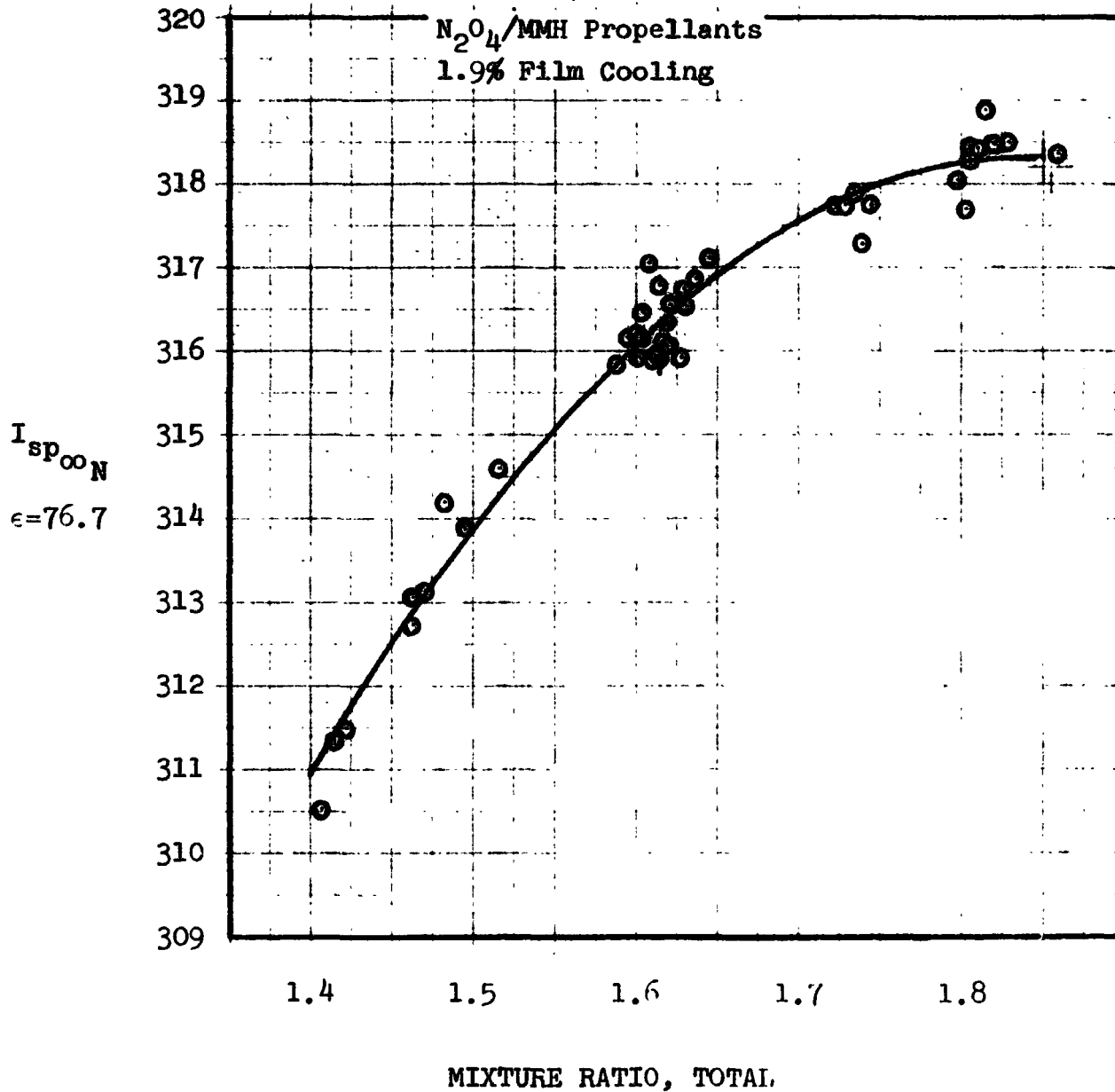
This indicated that a 10 psi increase or decrease in chamber pressure from the nominal would result in a 0.28% increase or decrease in impulse performance respectively.

Bell Aerospace Company

FIGURE X-20
SPECIFIC IMPULSE VS MIXTURE RATIO
6K OME REGEN CHAMBER - 30L*, 34L*
ALUMINUM INJECTOR NO. 2

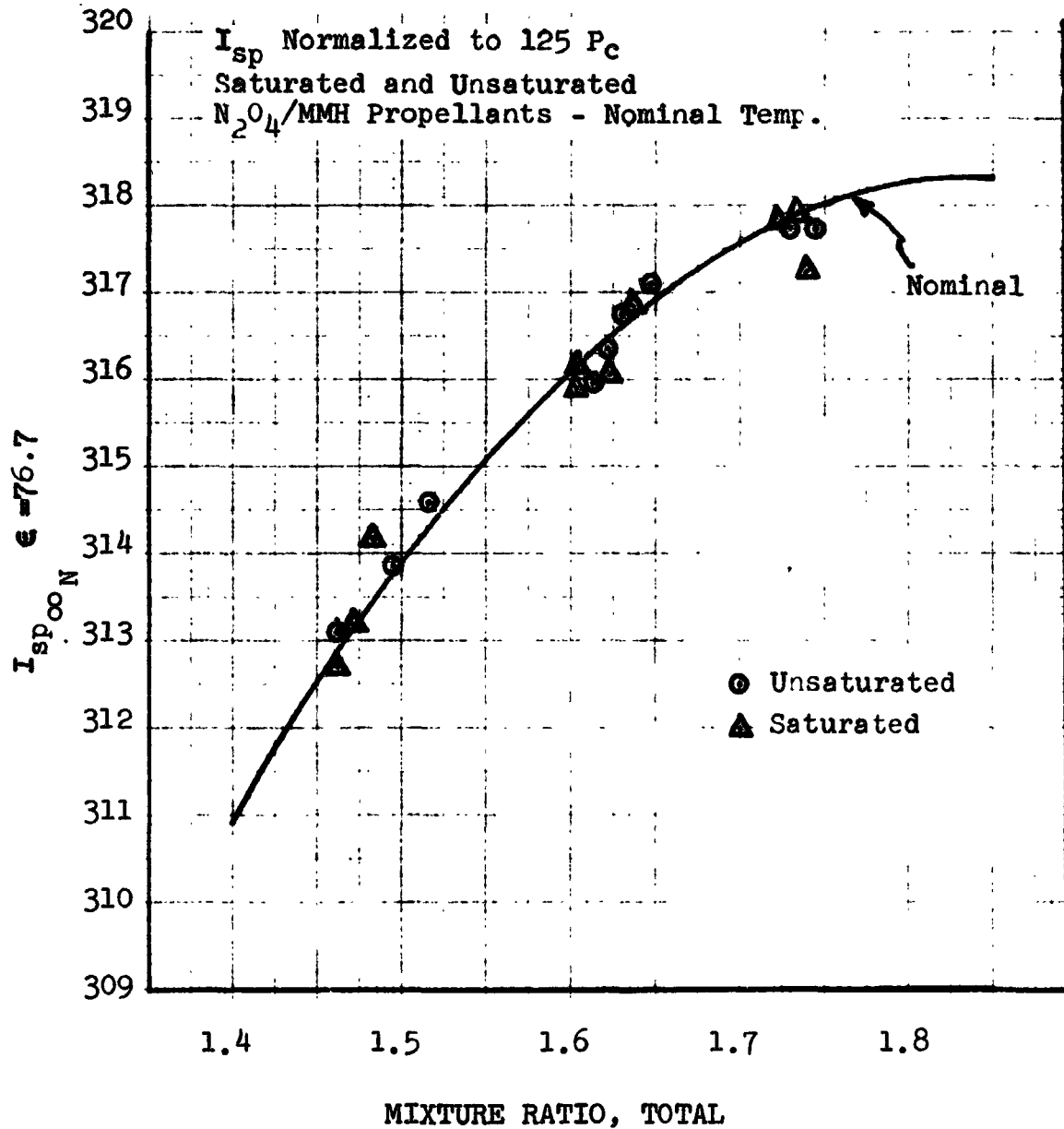
WSTF TEST DATA

I_{sp} Normalized to 125 Pc and Nominal Propellant Temperature



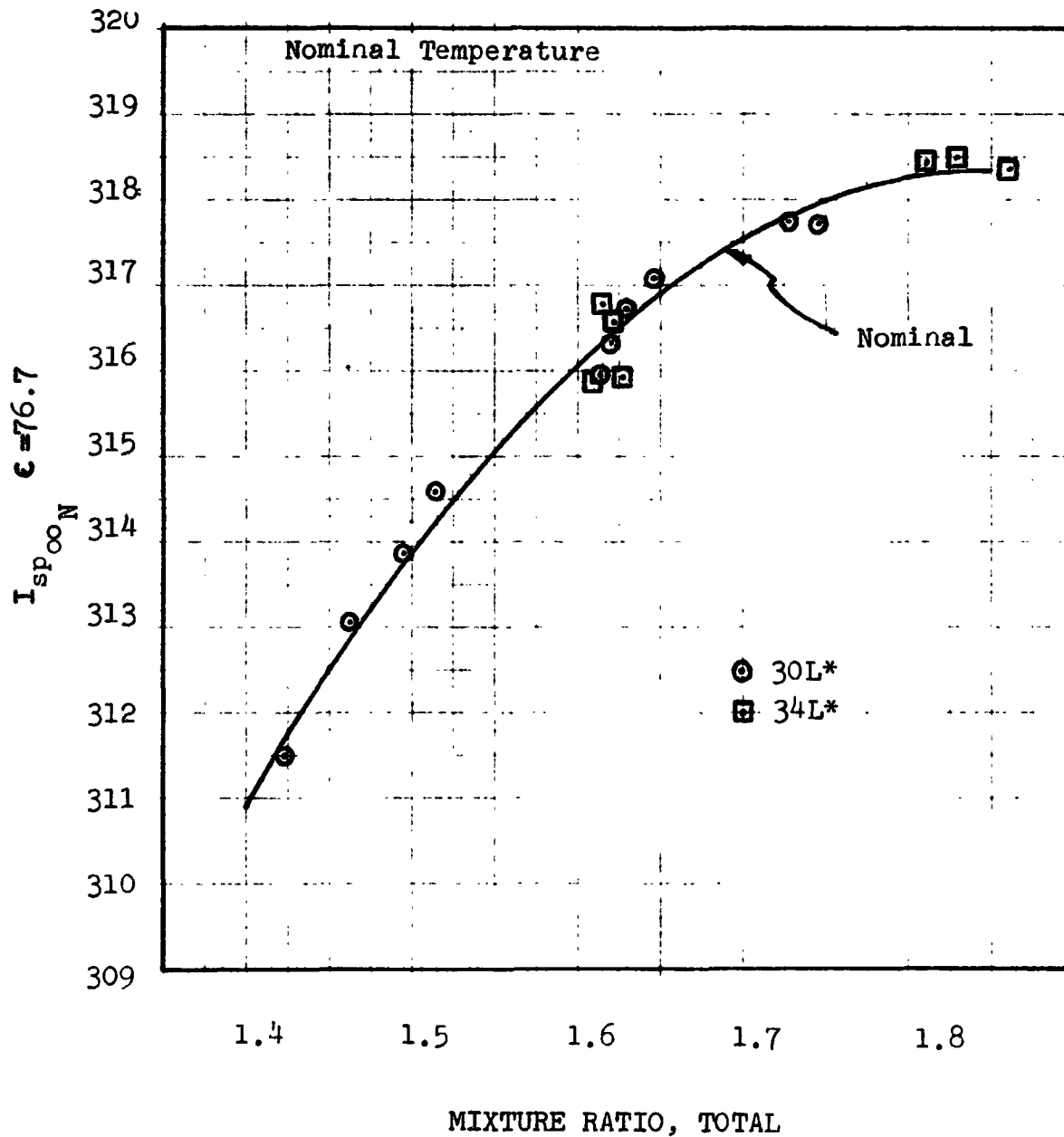
Bell Aerospace Company

FIGURE X-21
SPECIFIC IMPULSE VS MIXTURE RATIO
6K OME REGEN CHAMBER - 30 L*
ALUMINUM INJECTOR NO. 2
WSTF TEST DATA



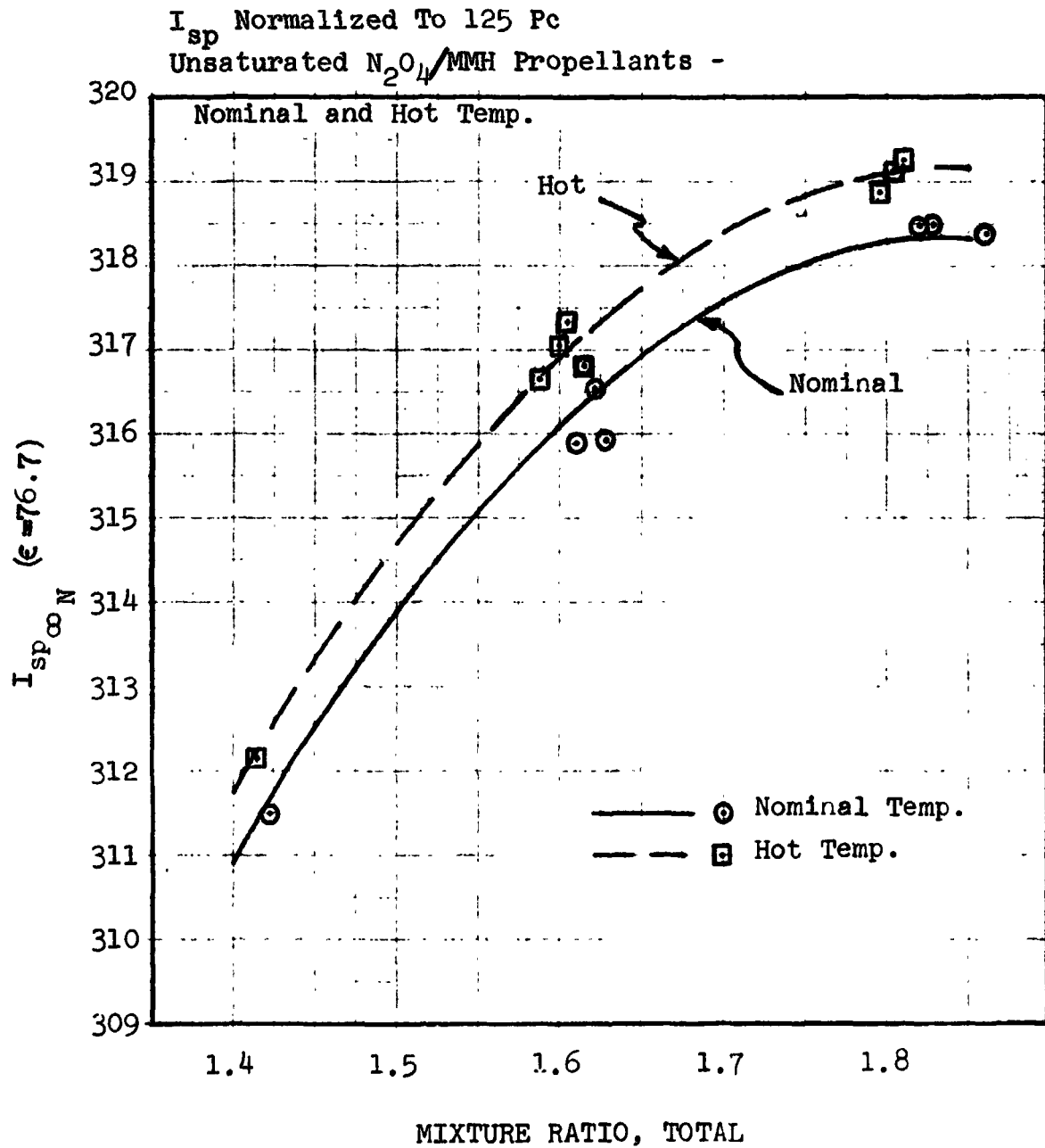
Bell Aerospace Company

FIGURE X-22
SPECIFIC IMPULSE VS MIXTURE RATIO
6K OME REGEN CHAMBER - 30L*, 34L*
ALUMINUM INJECTOR NO. 2
WSTF TEST DATA
 I_{sp} Normalized To 125 P_c
Unsaturated N_2O_4 /MMH Propellants-
Nominal Temp.



Bell Aerospace Company

FIGURE X-23
SPECIFIC IMPULSE VS MIXTURE RATIO
6K OME REGEN CHAMBER - 34 L*
ALUMINUM INJECTOR NO. 2
WSTF TEST DATA



Bell Aerospace Company

FIGURE X-24

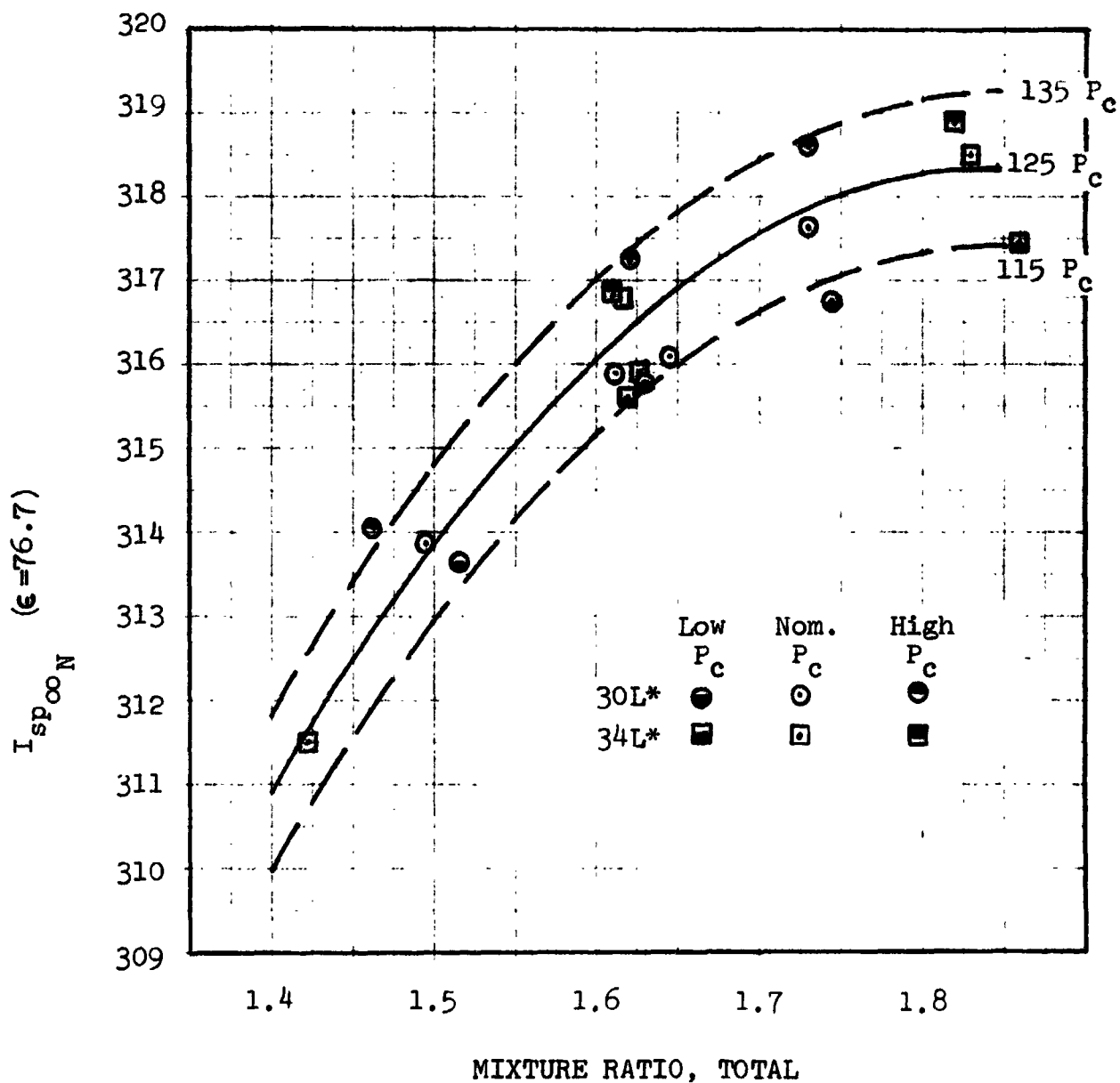
SPECIFIC IMPULSE VS MIXTURE RATIO

6K OME REGEN CHAMBER - 30L*, 34L*

ALUMINUM INJECTOR NO. 2

WSTF TEST DATA

Unsaturated N_2O_4/MMH Propellants -
Low, Nom. and High Chamber Pressure



Bell Aerospace Company

The $I_{sp\infty N}$ ($\epsilon=76.7$) in Table VIII was normalized to 125 psia chamber pressure and nominal propellant temperature in accordance with the following equation:

$$I_{sp\infty N} (\epsilon = 76.7) = 180 + 0.093 P_{cc} + 0.83 (\text{Hot}) \\ + 137.267 R_{o/f} - 37.18 R_{o/f}^2$$

where: P_{cc} = Total chamber pressure at entrance to nozzle

$R_{o/f}$ = Overall propellant mixture ratio

Adjustments to the values in Table VIII for chamber pressure and propellant temperature can be made as follows:

For P_{cc} use Δ from 125

For hot propellants use factor of 1.0

3. WSTF and BAC Data Comparison

One of the original objectives of the WSTF test program was to obtain direct data comparison between facilities, in this case the BAC altitude test cell 1BN and the WSTF facility. Tests were to be conducted at WSTF with the $\epsilon=15$ nozzle so that the direct data comparison could be made. Unfortunately these tests were not conducted, and the comparison was made on the basis of a JANNAF extrapolation from the 15 to 76.7 ϵ nozzle.

Comparisons of the WSTF data and BAC data were made and performance values analyzed by means of a multiregression correlation analysis. The influence coefficients were determined for chamber pressure, mixture ratio, propellant saturation, propellant temperature, chamber L^* and vortex flow. Performance was normalized for a chamber pressure of 125 psia, chamber L^* of 30, 1.9% vortex flow, unsaturated and nominal propellant temperature. The specific impulse versus mixture ratio corrected to vacuum operation and nozzle area ratio of 72.7:1 is shown in Figure X-25.

The normalization was accomplished by using the derived correlation equation of the test data:

Bell Aerospace Company

ORIGINAL PAGE IS
OF POOR QUALITY

FIGURE X-25

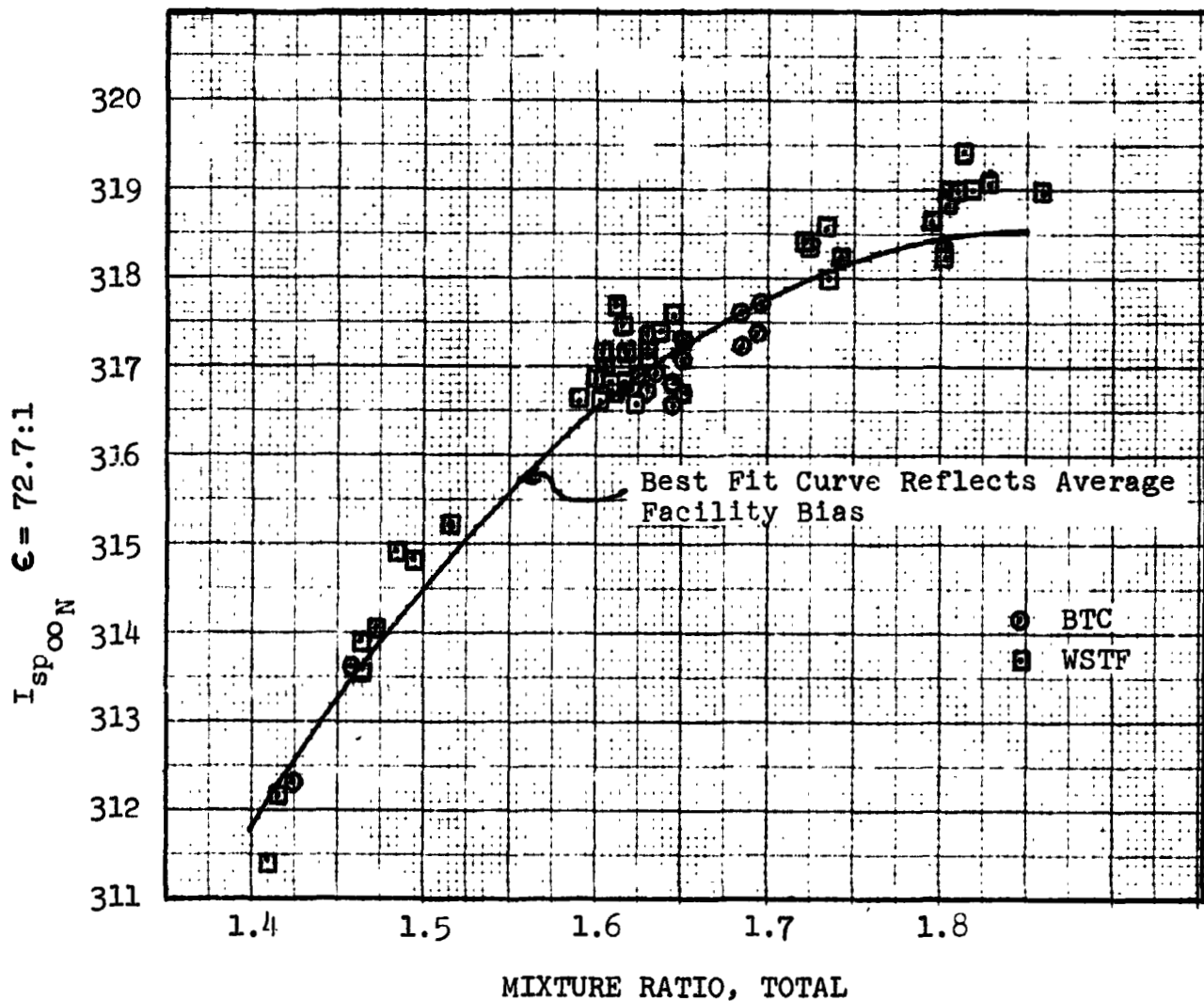
SPECIFIC IMPULSE VS MIXTURE RATIO

6K OME REGEN CHAMBER

ALUMINUM INJECTOR NO. 2

COMBINED WSTF/BAC DATA

I_{sp} Corrected to Vacuum Operation and Area Ratio 72.7:1,
Normalized to 125 P_c , 30 L^* , 1.9% Film Cooling, Unsaturated
and Nominal Propellant Temperature - N_2O_4/MMH Propellants



Bell Aerospace Company

$$I_{sp\infty} (\epsilon = 72.7) = 189.5 + 0.073 L^* - 117.2 \rho + 0.094 P_{cc} \\ + 0.086 Sat + 0.85 Hot + 127.9 R_o - 34.8 R_o^2 - 0.5 (1BN)$$

where:

- R_o = Overall propellant mixture ratio
- ρ = Vortex flow percentage
- P_{cc} = Total chamber pressure at entrance to nozzle
- L^* = Chamber size
- Sat = 1.0 for saturated propellants
- Hot = 1.0 for hot propellants
- 1BN = Facility bias

The WSTF data indicates somewhat higher performance over the mixture ratio range tested. At nominal conditions, the specific impulse measured at WSTF is about 0.3% higher than BAC values (Reference Figure X-26). Based on the data on both facilities, a specific impulse of at least 317 seconds is indicated at the nominal operating conditions of $P_c=125$ psia, $R_o/r=1.65$ and $\rho=1.9\%$ in an 30 L^* chamber, whereas WSTF data indicates a specific impulse of 317.5 seconds. These results are based on a nozzle $\epsilon=72.7$ which would be typical for Space Shuttle envelope.

All $I_{sp\infty} N (\epsilon = 72.7)$ in table are normalized to 125 P_{cc} , 1.9% film cooling, unsaturated and nominal propellant temperature, 30 L^* . Changes can be made to any other conditions with following equation:

$$I_{sp\infty} = 189.5 + 0.073 L^* - 117.2 \rho + 0.094 P_{cc} \\ + 0.086 Sat + 0.85 Hot + 127.9 R_o - 34.8 R_o^2$$

Example: for Sat propellants use factor 1.0 (+0.1 sec.)
 for Hot propellants use factor 1.0 (+0.9 sec.)
 for P_{cc} (use Δ , ex 115-125 = -10, $-10 \times 0.094 = -.9$)

FIGURE X-26

SPEC. FIC IMPULSE VERSUS MIXTURE RATIO

6K OME REGEN CHAMBER

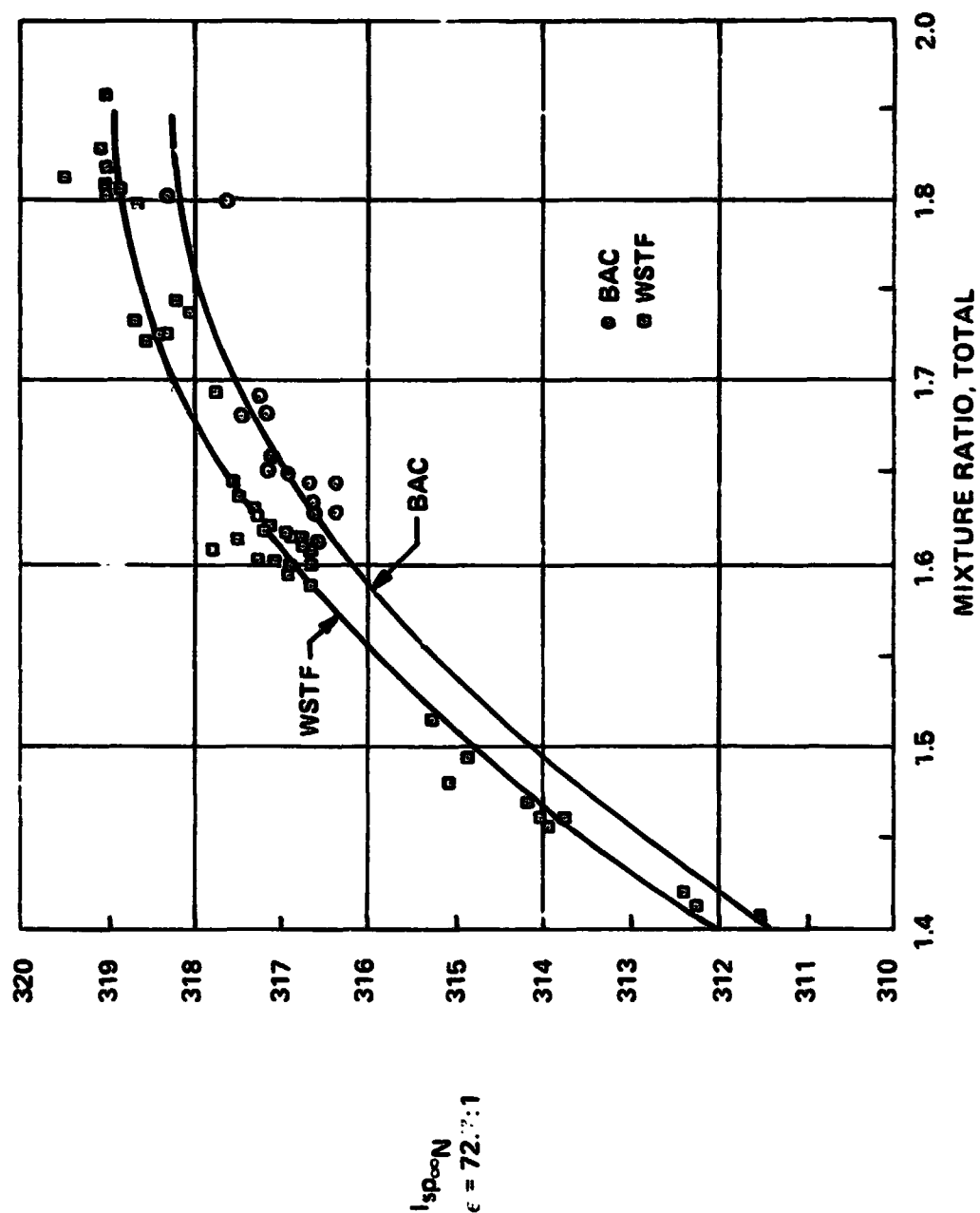
ALUMINUM INJECTOR NO. 2

COMBINED WSTF/BAC DATA

I_{sp} CORRECTED TO VACUUM OPERATION AND AREA RATIO 72.7:1, NORMALIZED TO

125 P_c, 30L*, 1.9% FILM COOLING, UNSATURATED AND NOMINAL PROPELLANT

TEMPERATURE - N₂O₄/H₂ MH PROPELLANTS



Bell Aerospace Company

4. Thermal Data

Thermal data taken during these tests included regen chamber fuel inlet and outlet temperatures, regen chamber back wall temperatures and radiation cooled nozzle extension temperatures. This data plus heat loads are summarized in Table IX.

5. Regen Chamber Coolant Temperature Rise and Heat Load

The operating conditions and thermal data are also tabulated in Table IX. The fuel inlet and outlet temperatures were measured in their respective manifolds of the regen chamber. The bulk temperature rise of the coolant fuel was calculated from these parameters, and then multiplied by the fuel flow rate through the jacket and the specific heat of the fuel to determine the heat transferred to the fuel.

The regen chamber fuel temperature rise for the 20 second test appears to be near stabilization within the 20 seconds as temperature rise varies from 113°F at 7.5 seconds to 119°F at 19.5 seconds (Figure X-27).

The response of the coolant outlet temperature is shown in Figure X-29. At six seconds this temperature is approximately 96% of the steady state value of 186°F. After shutdown the temperature rises to 209°F before decaying indicating that considerable margin exists between measured temperatures and the design maximum backwall temperature of 600°F.

In Figure X-28 the heat loads are plotted against chamber pressure for the 30 L* and 34 L* configurations. These data follow the variation with chamber pressure to the 0.8 power. The open symbols represent ambient temperature, unsaturated propellants; the partially closed symbols represent ambient temperature, helium saturated propellants; the fully closed symbols represent heated, unsaturated propellants.

There was no significant effect on heat loads from either saturating the propellants with helium or heating the propellants. The mixture ratio trends are generally in the same direction and data scatter is within plus or minus 6.5%. This latter fact may obscure trends that may be due to mixture ratio.

The change in L^* was accomplished by the addition of a 2 inch section at the head end of the chamber. Thus the heat load variation in the regen chamber section, if any, could be attributed to the diminishing effectiveness of the film coolant resulting from the increased distance of the regen chamber from the injector. A comparison of the 30 L* and 34 L* data (Figure X-2) indicated the heat loads were higher for the 34 L* section at the higher mixture ratios, indicating a low degree of sensitivity in the range tested.

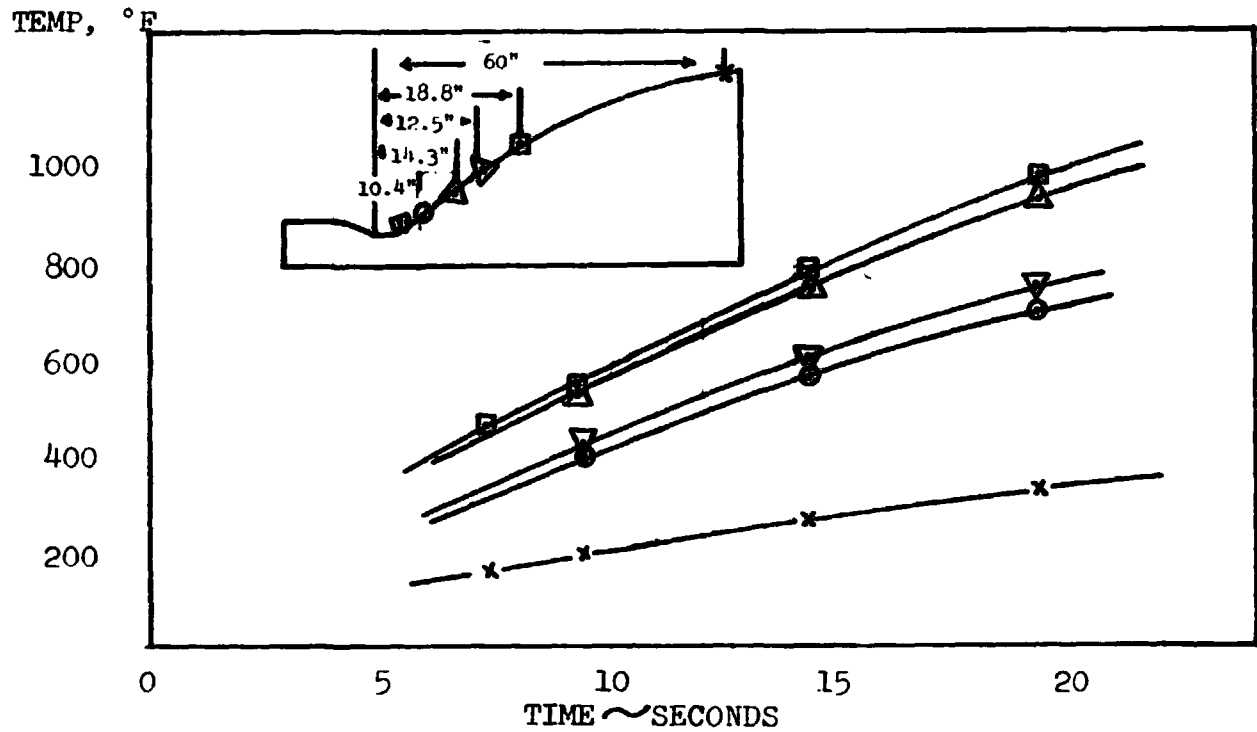
Bell Aerospace Company

FIGURE X-27

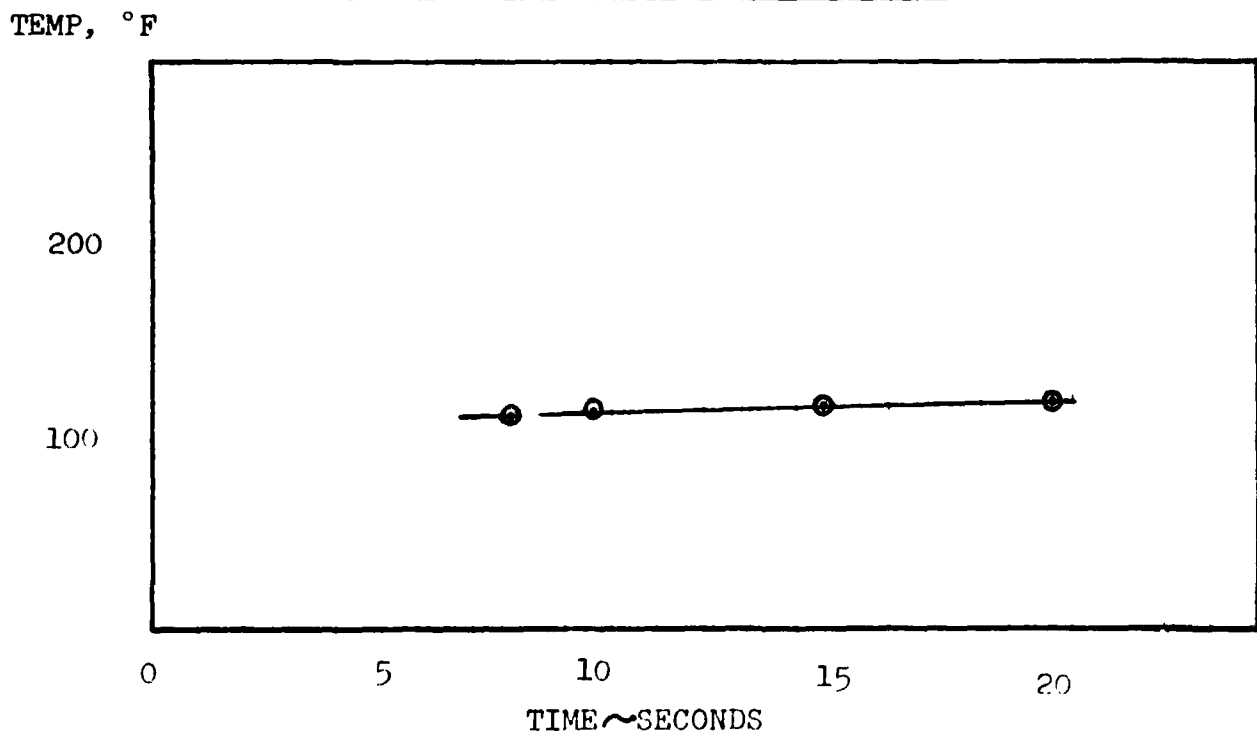
TEST: WSTF, SERIES 1, SEQ. 4, TEST 1

$L^* = 30$ IN

NOZZLE EXTENSION TEMPERATURE VS TIME



REGENERATIVE TEMPERATURE FUEL ΔT VS TIME



ORIGINAL PAGE IS
OF POOR QUALITY

Bell Aerospace Company

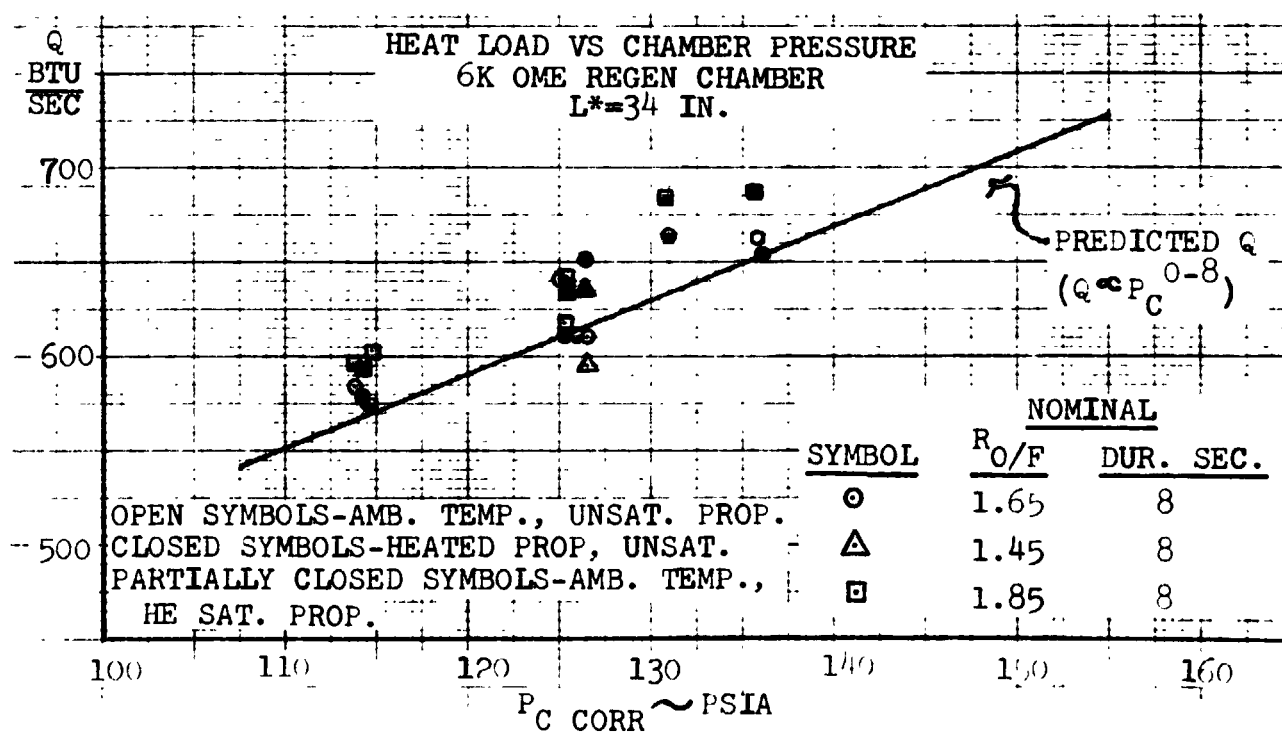
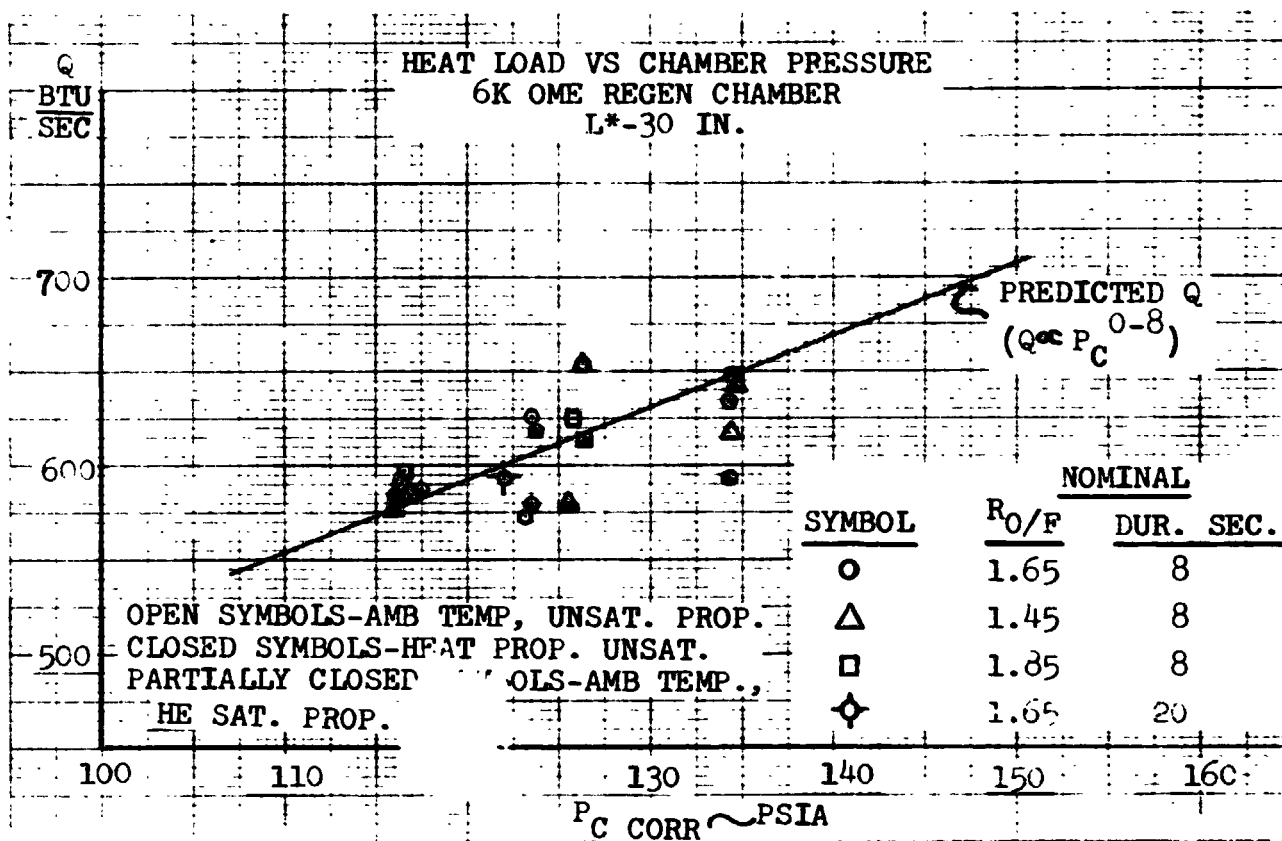


FIGURE X-28

Bell Aerospace Company

Temp. °F

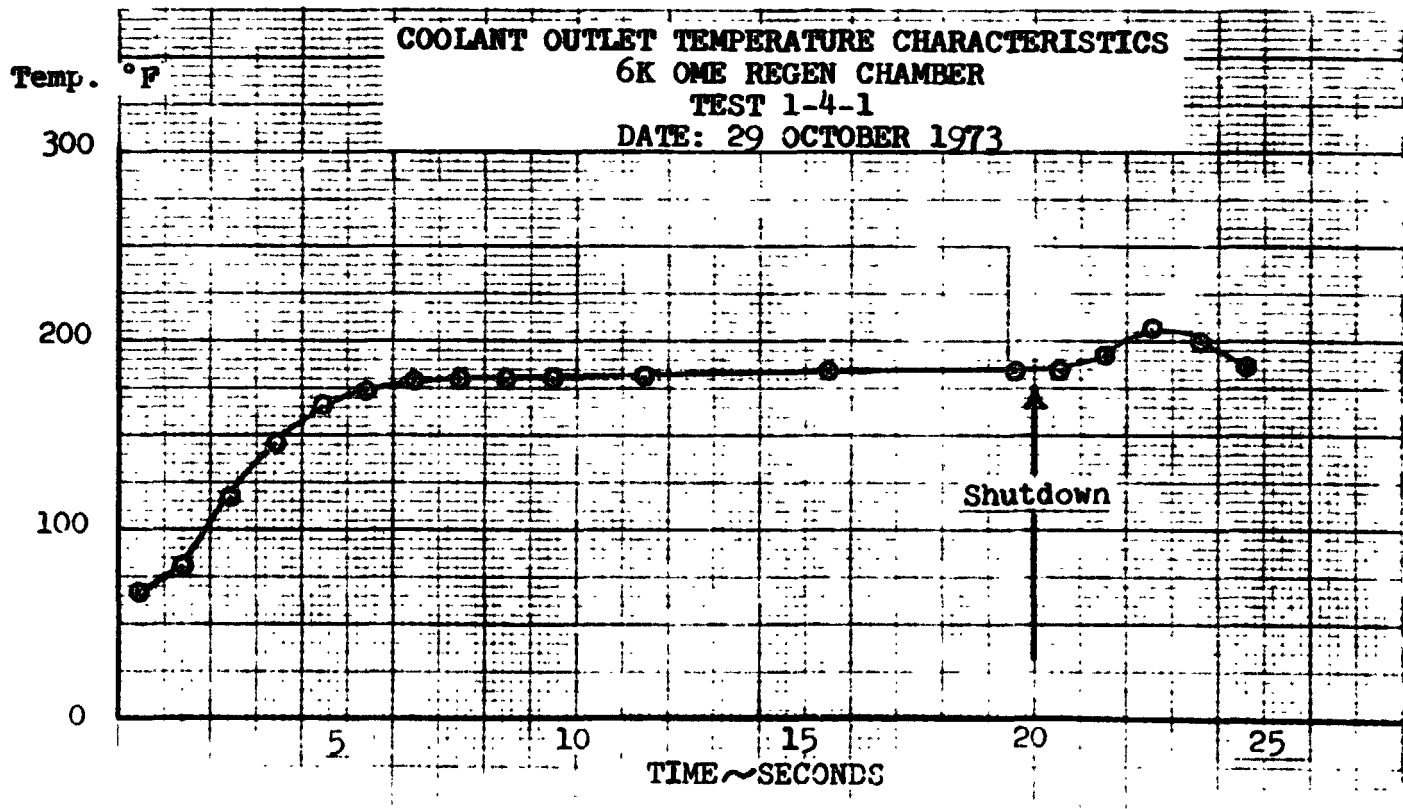
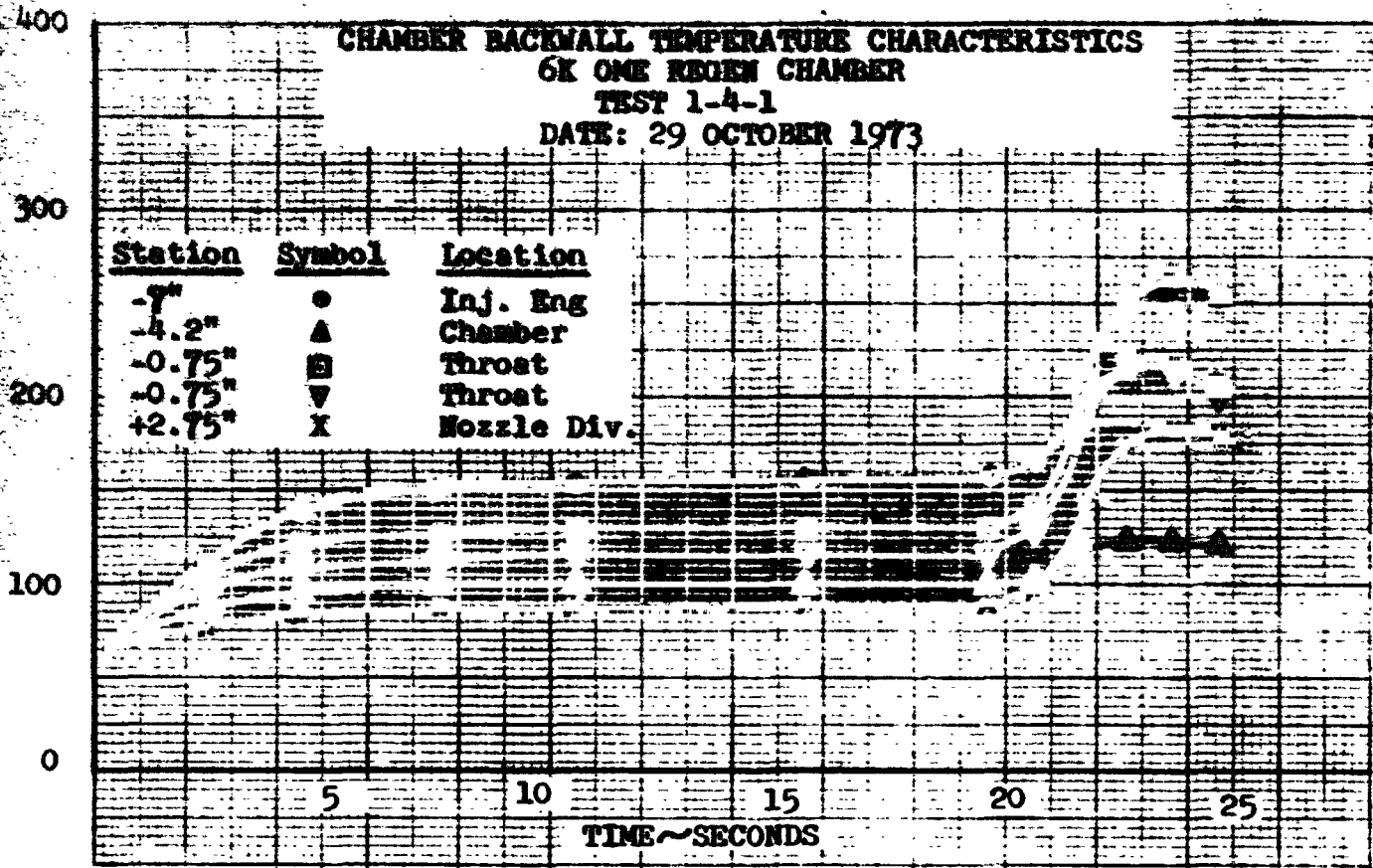


FIGURE X-29

JACKET PRESSURE DROP VS COOLANT FLOWRATE

6K ONE REGEN CHAMBER



TABLE IX
REGENERATIVELY COOLED THRUST CHAMBER THERMAL DATA

SEQ.	TEST NO.	DUR. SEC.	DATA POINT SEC.	P _c CORR PSIA	R O/F	P	W _{FC} (LB/SEC)	INLET TEMP. °F	OUTLET TEMP. °F	REGEN FUEL TEMP RISE °F	Q BTU/SEC	CHAMBER BURNER TEMPERATURE							CHAMBER JACKET ΔP	L ²	TEST CONDITION
												T-1	T-2	T-3	T-4	T-5	T-6	T-7			
I	1	1.5	1.3	121.6	1.494	4.53	7.29	66	69	3	15	70	69	68	72	71	67	65	17.7	30	Checkout Checkout
	2	5.0	4.5	119.3	1.541	2.01	7.03	65	165	100	497	140	139	95	120	110	85	87	16.1		
II	1	10.1	7.5	122.7	1.612	1.93	7.02	67	182	115	572	157	156	103	129	118	92	124	15.2		Unsat. H ₂ O ₂ /N ₂ H ₄
	2	8.0	7.5	126.2	1.495	2.02	7.57	68	178	110	654	159	157	104	131	117	93	132	17.2		
	3	8.0	7.5	133.9	1.463	2.02	8.13	68	175	107	616	154	152	105	127	115	92	129	21.0		
	4	8.1	7.5	133.9	1.619	1.92	7.62	69	186	117	632	168	165	111	138	122	96	138	16.0		
	5	8.1	7.5	134.4	1.729	1.79	7.34	69	193	124	647	174	171	115	143	126	99	143	13.7		
	6	8.1	7.5	125.6	1.729	1.73	6.88	69	197	128	626	178	176	118	146	129	100	145	12.0		
	7	8.1	7.5	116.5	1.745	1.65	6.36	69	201	132	597	181	177	121	147	132	102	146	10.8		
	8	8.1	7.5	116.3	1.630	1.66	6.60	69	195	126	591	177	174	121	144	128	99	144	12.1		
	9	8.1	7.5	116.6	1.516	1.77	6.93	69	188	119	585	167	165	120	137	123	97	140	15.1		
	10	10.1	7.5	123.3	1.648	1.63	6.92	69	196	126	624	173	171	123	142	127	99	145	14.7		
III	1	10.1	7.5	123.3	1.605	1.95	7.03	73	189	114	579	163	162	105	134	123	97	125	15.6		Helium Saturation H ₂ O ₂ /N ₂ H ₄
	2	8.1	7.5	125.3	1.472	2.03	7.59	73	181	108	581	158	157	105	131	120	96	131	16.9		
	3	8.1	7.5	132.9	1.463	2.05	8.07	74	177	106	-	-	-	-	-	-	-	-	20.4		
	4	8.1	7.5	133.8	1.619	1.94	7.60	74	189	116	592	162	161	110	135	123	98	132	18.0		
	5	8.1	7.5	134.5	1.735	1.85	7.33	74	197	123	641	173	171	114	141	129	101	143	14.9		
	6	8.1	7.5	126.2	1.724	1.82	6.92	74	199	124	615	177	173	118	143	131	103	146	12.8		
	7	8.1	7.5	117.2	1.739	1.76	6.41	74	203	129	588	180	177	121	146	134	105	145	10.6		
	8	8.1	7.5	115.8	1.602	1.81	6.64	74	197	123	581	176	174	121	143	130	103	144	11.5		
	9	8.1	7.5	115.8	1.483	1.87	6.97	74	190	116	575	172	169	120	139	126	101	142	13.0		
	10	10.1	7.5	123.2	1.637	1.74	6.15	74	199	123	618	175	174	124	144	131	103	146	13.0	30	
IV	1	20.1	7.5	123.4	1.622	1.94	7.00	66	185	113	-	160	153	100	130	118	94	136	15.5	30	Nominal, Long Duration
			9.5	123.3	1.620	1.94				116	591								15.5		
I			19.5	121.8	1.618	1.93				119									15.2		
	1	10.1	7.5	126.5	1.625	1.93	7.16	58	178	118	610	156	156	45	121	110	82	102	16.3	34	Unsat. H ₂ O ₂ /N ₂ H ₄
	2	8.1	7.5	126.5	1.422	2.09	7.82	59	167	109	597	155	154	68	118	106	82	118	17.2		
	3	8.1	7.5	135.6	1.610	1.95	7.74	59	180	121	661	164	162	81	124	112	85	123	16.5		
	4	8.1	7.5	135.4	1.820	1.79	7.16	60	196	136	689	178	173	129	132	121	91	133	14.3		
	5	10.1	7.5	114.5	1.630	1.94	6.50	60	185	124	575	174	170	78	129	118	88	127	10.9		
	6	8.1	7.5	114.8	1.860	1.78	6.01	60	201	140	602	184	180	92	137	127	94	133	9.6		
	7	8.1	7.5	125.4	1.830	1.80	6.61	60	197	137	643	179	174	106	134	124	82	135	12.1		
	8	8.1	7.5	125.9	1.615	1.95	7.16	60	185	125	633	173	168	117	129	117	88	133	14.1		
II	1	10.1	7.5	126.3	1.591	1.97	7.19	93	210	116	601	188	185	166	148	136	113	121	17.6		Not Propellant
	2	8.1	7.5	126.3	1.414	2.10	7.82	94	199	105	586	182	179	161	146	133	113	134	20.5		
	3	8.0	7.5	136.1	1.600	1.95	7.76	96	214	118	655	192	188	169	132	120	118	143	19.7		
	4	8.1	7.5	135.5	1.806	1.82	7.19	97	230	113	686	209	204	184	163	149	124	157	15.3		
	5	10.1	7.5	114.3	1.615	1.96	6.49	92	217	125	580	204	198	179	156	144	119	162	10.4		
	6	8.1	7.5	114.3	1.798	1.83	6.09	91	227	136	593	208	204	185	162	148	121	158	9.4		
	7	8.1	7.5	125.3	1.810	1.83	6.62	95	229	134	636	205	198	181	160	147	121	150	12.8		
	8	8.1	7.5	125.6	1.604	1.95	7.15	96	219	123	630	201	196	177	158	144	121	155	14.4		
III	1	10.1	7.5	126.0	1.611	1.96	7.15	82	202	118	611	180	177	158	141	128	104	119	16.3		Ambient Propellant Helium Saturation
	2	8.1	7.5	125.2	1.407	2.12	7.96	82	190	107	613	175	172	153	137	125	103	134	17.2		
	3	8.1	7.5	135.8	1.616	1.95	7.71	83	204	120	665	182	178	160	142	130	106	135	18.4		
	4	8.1	7.5	135.7	1.805	1.80	7.20	83	216	132	684	196	191	171	151	138	111	147	14.2		
	5	10.1	7.5	113.7	1.597	1.98	6.52	81	207	126	586	198	192	172	149	137	110	166	8.9		
	6	8.1	7.5	113.7	1.803	1.83	6.06	81	219	138	597	202	197	178	155	142	113	153	9.5		
	7	8.1	7.5	125.5	1.815	1.83	6.61	83	219	136	642	196	191	172	151	139	111	144	12.0		
	8	8.1	7.5	125.0	1.631	1.95	7.06	83	210	127	640	192	187	168	148	135	110	148	13.8	34	

P_c correction factor 0.981

X-53

Bell Aerospace Company

The test results show good comparison with the predicted Q for the 30 L*, but are somewhat higher for the 34 L* as expected. This is so, since the predicted value was based on a 30 L* chamber at $P_c = 125$ psia, $R_o/f = 1.65$ and film coolant flow of 2.0%.

6. Regen Chamber Back Wall Temperature

The regeneratively cooled back wall temperatures were measured to demonstrate that steady state values are within the maximum OME requirement of 600°F.

Maximum steady-state backwall temperature occurred at the injector end of the chamber and reached a value of 158°F during a 20 second firing. Maximum heat soakback temperature also occurred at the injector end and reached a value of 265°F (Figure X-29) confirming that considerable margin exists between measured temperatures and the design maximum.

7. Regen Chamber Coolant Jacket ΔP

The regeneratively cooled chamber coolant jacket pressure drops are shown in Table IX, and graphically as a function of coolant flowrate in Figure X-30. Inlet and outlet pressures were measured in the chamber manifolds.

A comparison of ΔP vs flowrate was made between unsaturated, helium saturated and heated propellants. No significant difference was observed.

F. Conclusions

Sufficient data has been generated at the White Sands Test Facility and at the Bell Aerospace Company test facility to draw conclusions on the performance, thermal capabilities and stability characteristics of the BAC designed and fabricated OME regeneratively cooled thrust chamber/injector combination.

1. Safety

The engine demonstrated the capability of operating safely at both nominal design conditions and at off-rated conditions of mixture ratio and chamber pressure. Safe operation was demonstrated with both helium saturated propellants and with heated propellants.

2. Performance

Measured performance data demonstrated specific impulse performance of > 315 seconds with the $\epsilon = 76.7:1$ test nozzle. Based on the WSTF test data a specific impulse of 317.5 seconds is indicated at nominal operating conditions of $P_c = 125$ psia,

Bell Aerospace Company

$R_o/r = 1.65$ and film coolant is 1.9% in a 30 L*, 10 inch diameter chamber, and a nozzle fitting the OME compartment length.

3. Heat Transfer

The hardware temperatures were substantially lower than expected, indicating higher safety factors. This would allow a reduction in the amount of film coolant which may result in higher performance. The low nozzle temperatures suggest that a lower temperature material may be substituted for the nozzle extension or that the regen chamber/nozzle extension joint may be relocated to reduce weight. The regen chamber backwall temperature did not exceed 300°F during operation or after shutdown.

4. Stability

There was no incidents of combustion instability on the 47 tests operated over the chamber pressure range of 114 psia to 136 psia and mixture ratio (O/F) range of 1.41 to 2.12. Although no bomb tests were performed at WSTF, bomb tests were performed at BAC to verify a stable injector/thrust chamber assembly.

Bell Aerospace Company

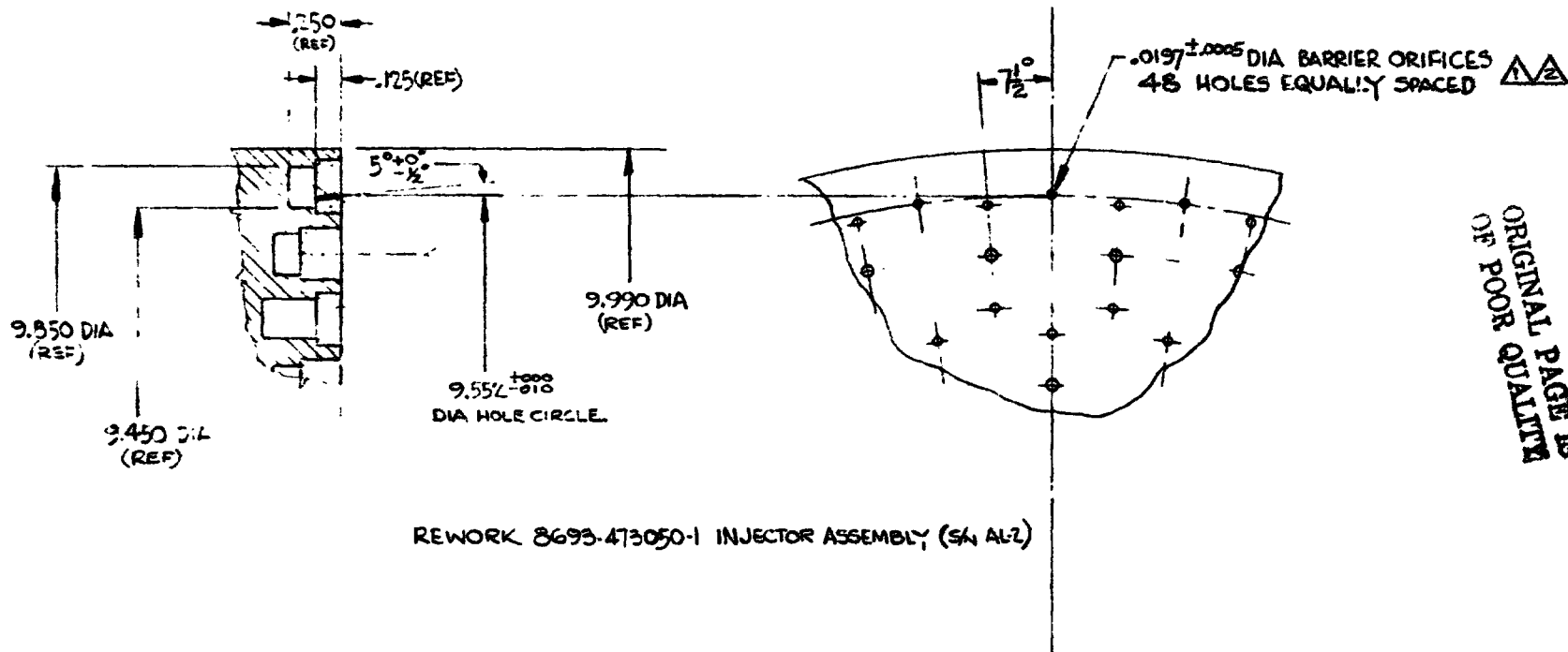
XI. TASK XIV - TRIplet INJECTOR DYNAMIC STABILITY VERIFICATION

This task amplifies the stability findings of Task XII by conducting additional analyses and stability testing on the full scale, 10 inch diameter OME type triplet injector. The task included: 1) modification of the injector to incorporate injector end fuel film coolant; and 2) changes in the acoustic cavity inlet configuration to evaluate its effect on damping characteristics. The available aluminum injector S/N 2, building block acoustic cavity ring and test thrust chamber from Task XII were used. A new acoustic cavity ring adapter assembly was used to allow variations at the inlet.

It may be noted that the change to film cooling of the injector was precipitated by competitive engine designs. The Bell vortex cooling is unique and as a consequence presented some difficulty in correlation of stability test data with other investigators. Since this chamber vortex wall cooling is injected downstream of the acoustic cavity, significant differences in cavity temperatures could be expected when different amounts and manner of coolant injection was added upstream of the cavity entrance. Needless to say, a secondary objective of the stability program became the consideration of the fuel film coolant on combustion stability.

A. Design Definition

The 10 inch diameter injector was redesigned to include 48 film coolant orifices equally spaced between the 48 outer triplet elements (Figure XI-1), and was designed for a film coolant flowrate of 2% of the total flow at nominal test conditions. This design permits the use of a reasonable quantity of film coolant orifices compatible with the outer row spacing of elements and a reasonable orifice diameter of 0.0197 inches. The criteria for selecting the impingement angle of the fuel film coolant on the chamber wall was to impinge as close to the injector end of the chamber as possible, but provide stream clearance for any desirable acoustic cavity entrance configuration. All previous stability testing conducted at BAC on the OME type injector utilized a fuel vortex ring with a small protrusion (lip) extending into the combustion chamber (See Sketch).



ORIGINAL PAGE IS
OF POOR QUALITY

FIGURE XI-2

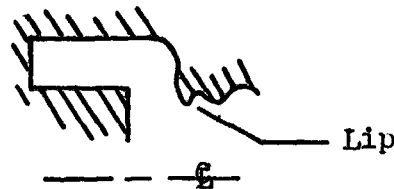
P. 2%

▲ SHARP EDGE REQUIRED ON EXIT & ENTRANCE OF ORIFICES
▲ ORIFICES TO BE PRODUCED BY ELECTRICAL DISCHARGE MACHINING (EDM)
TO A SURFACE FINISH EQUAL TO 63 RMR

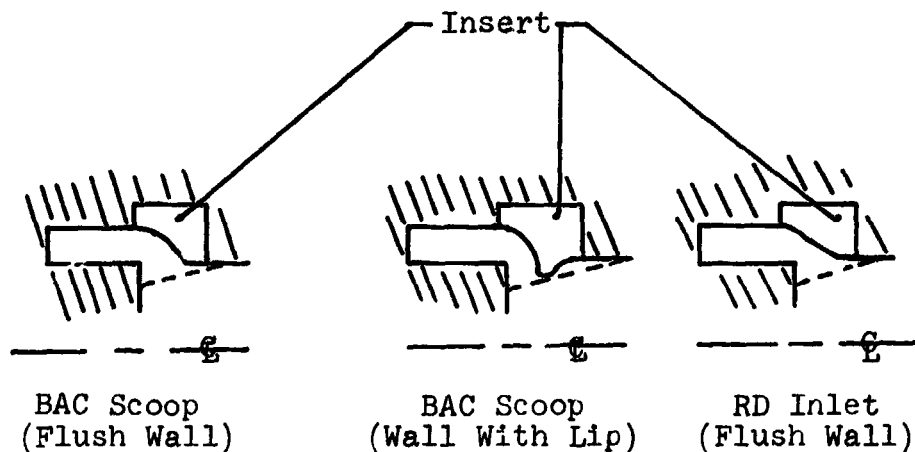
NOTES

UNLESS OTHERWISE SPECIFIED DIMENSIONS ARE IN INCHES. TOLERANCES ON DECIMALS:		DESIGNER (HARDER 5-15-14)		BELL AEROSPACE COMPANY	
.1	.125	.125	ANGLES:	DIVISION OF TESTRON INC.	
±.1	±.02	±.010	±.0° 30'	POST OFFICE BOX ONE	
HOLE TOLERANCES EXCEPT AS SHOWN			APPROVED	BUFFALO, NEW YORK 14240	
.040 TO .125 ± .005 - .001			DATE	INJECTOR SN AL2 REWORK	
.125 TO .250 ± .005 - .001			UNLESS OTHERWISE SPECIFIED	(ADD FUEL BARRIER ORIFICES)	
.251 TO .400 ± .005 - .001			BREAK EDGES .015 MAX AND	SIZE CODE IDENT NO	
.401 TO .750 ± .010 - .001			OR CHAMFER	80070 8693-473061	
.751 TO .999 ± .015 - .001			MACHINED SURFACES	SCALE 2/1 DEVELOPMENT SN	
1.000 AND LARGER ±.010			EXCEPT AS NOTED		

Bell Aerospace Company



It was therefore considered practical to include a similar capability with the discrete fuel film coolant orifice configuration. Provision for a 0.130 inch lip with the BAC cavity inlet defines a 5° angle for the fuel film coolant orifices. This 5° angle also is sufficient to assure fuel stream impingement on the chamber wall (without concern of splashing into the cavity inlet), for accommodating a Rocketdyne (RD) tapered acoustic cavity inlet (See Sketches).



The only design changes necessary to accommodate the above inlet configurations was a new acoustic ring adapter (Figure XI-2) which includes replaceable cavity inlet inserts (flush and with lip) as shown in detail in Figure XI-3.

The cavity depth and open area capability remained unchanged from the original configuration; with 1.65 inches the maximum cavity depth and 23.4% the maximum open area with cavity dividers (lands) flush with the injector face. The acoustic cavity ring and replaceable inserts are available from Task XII with open area change capability in the circumferential direction. An additional set of depth blocks were provided. The following summarizes the depth and open area capability:

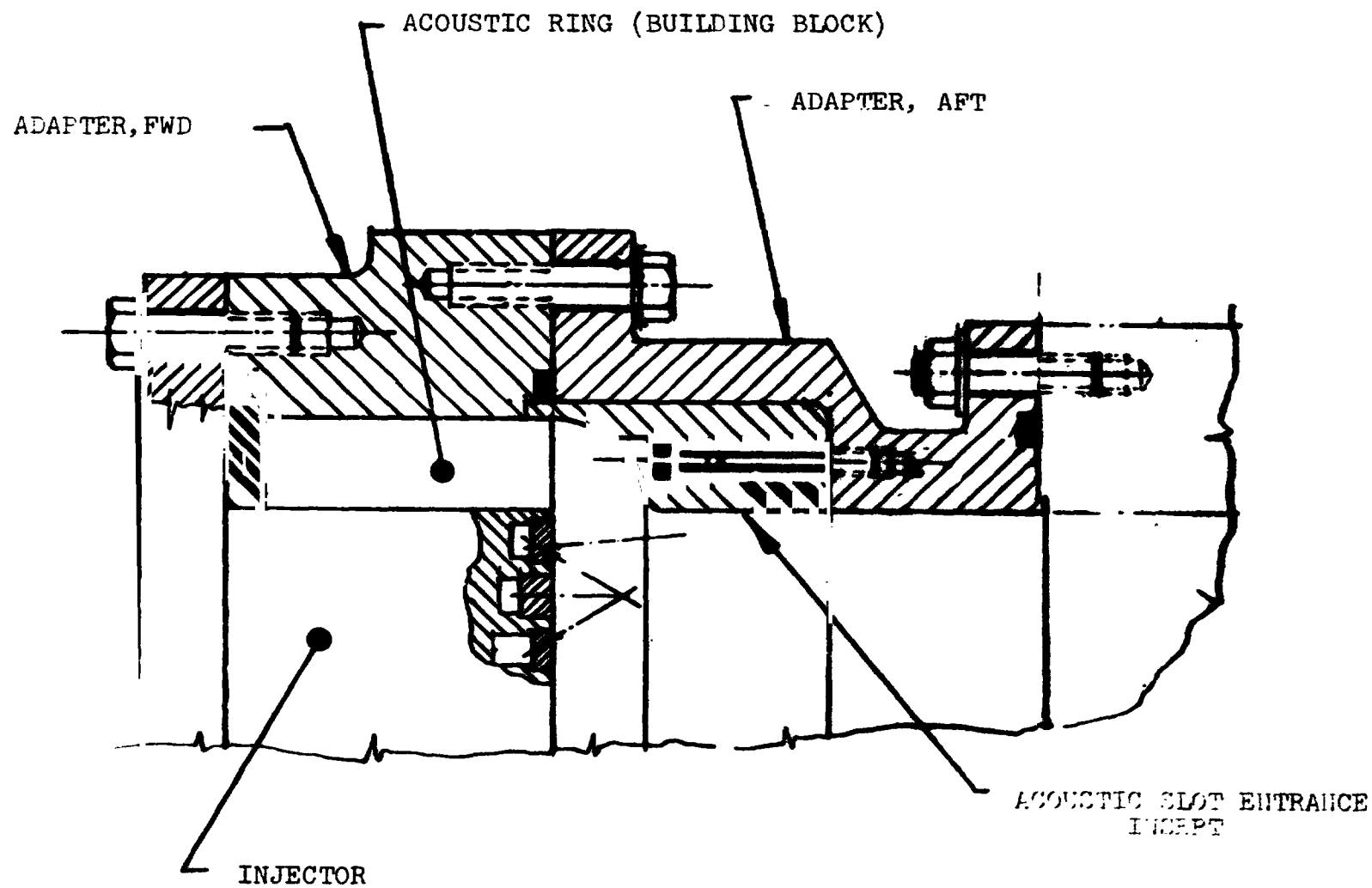
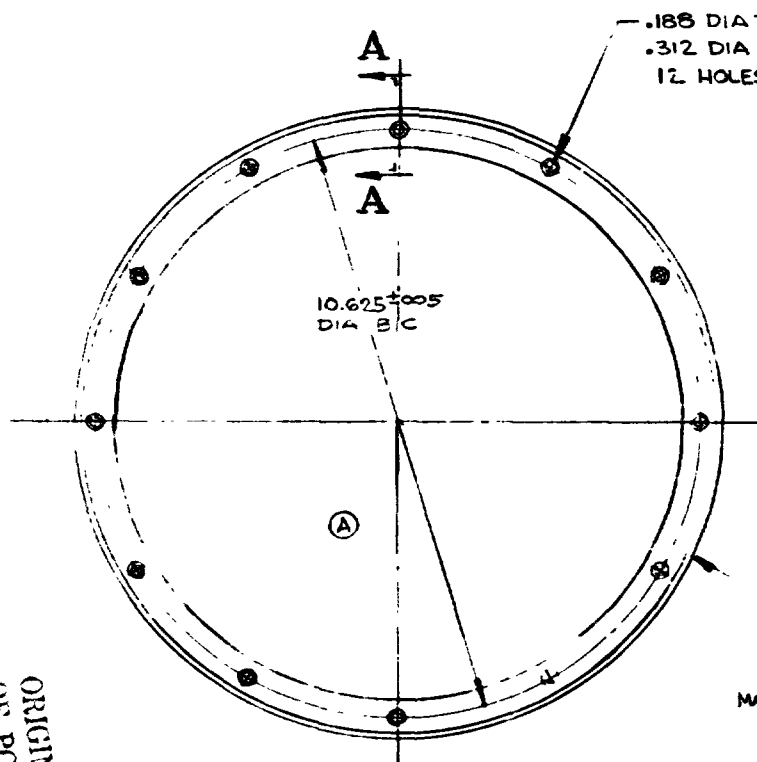
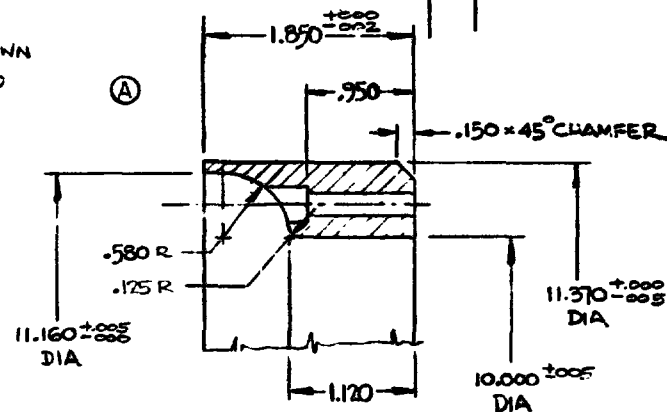


FIGURE XI-2

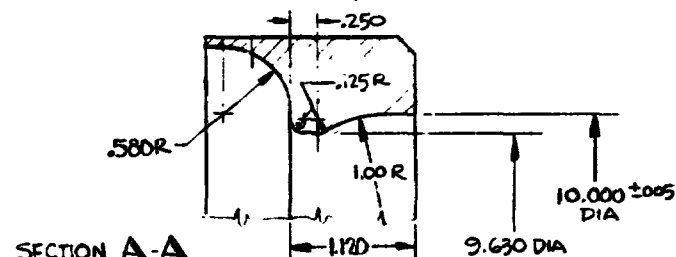
ORIGINAL PAGE IS
OF POOR QUALITY



(-1) INSERT
(-3) INSERT
MATERIAL: ANY 300 SERIES
ST. S.T.L.



SECTION A-A
-1 ONLY SCALE 1/2



SECTION A-A
-3 ONLY (SAME AS -1 EXCEPT AS SHOWN)

REV		
A	REMOVED .250 TRI-LED HOLES	RCM 5/8/71

FIGURE XI-1

UNLESS OTHERWISE SPECIFIED DIMENSIONS ARE IN INCHES. TOLERANCES ON DECIMALS:		DESIGNER: HAARMETER T-474		BELL AEROSPACE COMPANY DIVISION OF TEXTRON INC. POST OFFICE BOX ONE BUFFALO, NEW YORK 14240	
1	2	3	4	5	6
1	2	3	4	5	6
1	2	3	4	5	6
HOLE TOLERANCES EXCEPT AS SHOWN		RISE		INSERT, ENTRANCE, ACOUSTIC SLOT (BELL TYPE - .580 OPENING)	
.040 TO .125 ± .005, -.001		UNLESS OTHERWISE SPECIFIED		SIZE CODE IDENT NO	
.130 TO .250 ± .004, -.001		BREAK EDGES .015 MAX RAD OR CHAMFER		B 80070 8693-470124	
.261 TO .400 ± .003, -.001		MACHINED SURFACES		SCALE 1/2 SHOLD DEVELOPMENT SH	
.400 TO .750 ± .010, -.001		EXCEPT AS NOTED			
.750 TO .900 ± .012, -.001					
.900 AND LARGER ± .010					

REV. A

Bell Aerospace Company

	<u>Depth (Inches)</u>	<u>% Open Area</u>
1T Cavity	1.65 } Available 0.76 } New Block 1.10 }	11.6 } Available 15.6 }
3T Cavity	0.76 } Available 0 }	7.8 } Available 0 }

Both flush and full fin acoustic damper cavity separators were also made available for test.

The acoustic cavities had the same instrumentation as the Task XII effort, which included four thermocouples (one thermocouple in each of three 1T cavities and one in a 3T 'R cavity).

B. Stability Bomb Configuration Evaluation

With the incorporation of multiple bomb detonation techniques in a single test, the cost of the bombs as well as injector damage attributed to the bomb, is of increasing importance. The Bell test injectors, being fabricated from aluminum, have been particularly subject to bomb damage. In fact, the initial bomb configuration (Figure XI-4) was originally developed to keep all shrapnel off the injector face.

Primarily due to cost, a bomb redesign was undertaken. Several ground rules were imposed, the first being that the bomb size should be 6.9 grain and the second being the bomb would be used both for the inserter and as stationary bombs. Some considerations in cost for the redesign were that the elimination of the machined casing or insulation, and retaining of a production detonator squib would be cost effective. In the final design, a molded insulation was used, but there were no available plastic detonator squibs so that a non-production unit was finally incorporated.

A test series with a group of bomb materials (Figure XI-5) was made to check on damage to an aluminum surface. Interestingly enough, it was found that the metal detonator was probably the most damaging, as though the casing materials absorbed some of the shrapnel momentum from the squib. The shrapnel absorption was most noticeable with the teflon. However, the material was hard enough to impose some damage on its own.

The lowest damage on these tests appeared with the molded cork (Insul Cork) presenting the opportunity for molding the casing, as well as having a low damage quotient. By molding in a standard aluminum cap plug (Figure XI-6), a very inexpensive

BOMB INSTALLATIONS

XI-7

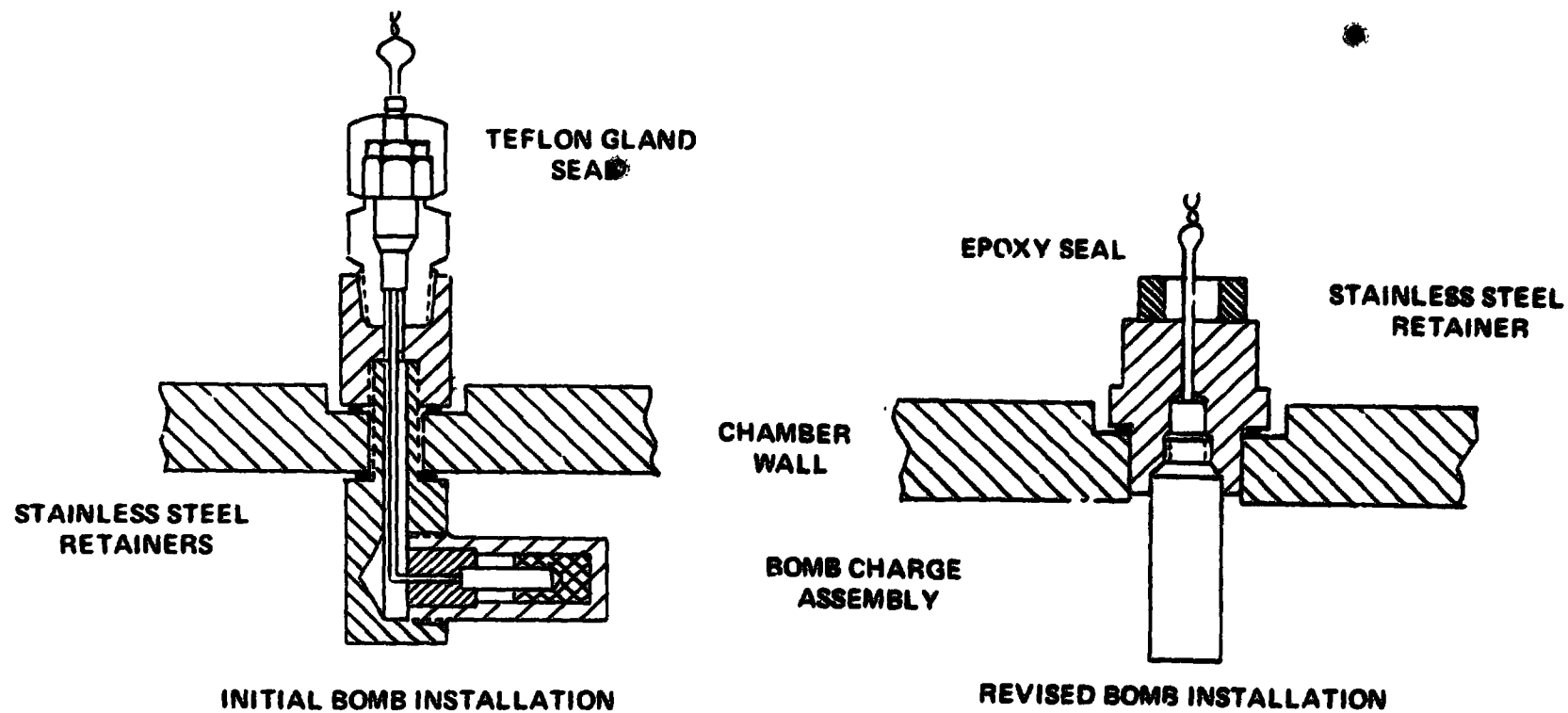
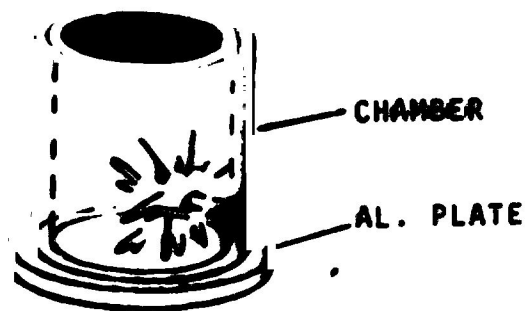


FIGURE XI-4

4-IX

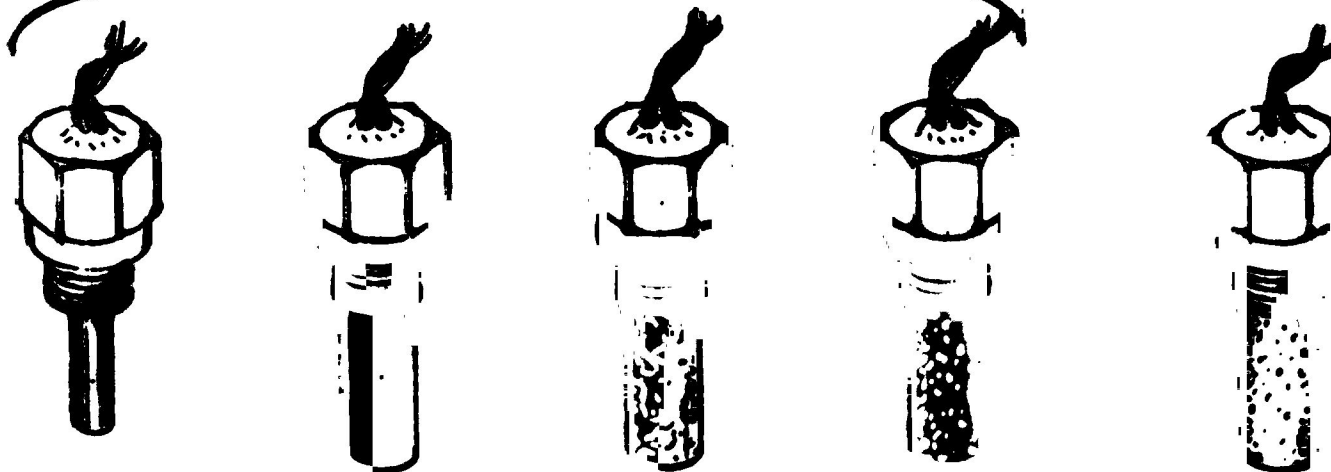
BOMB SHRAPNEL EVALUATION

TEST SETUP



ALUMINUM METAL CASE
DETONATOR (6.9 GRAINS)

PLASTIC
DETONATOR
(6.9 GRAINS)



TYPE OF
CASE



DET. ONLY

TEFLON

NATURAL
CORK

INSUL.
CORK

INSUL.
CORK

INJ. FACE
DAMAGE
POTENTIAL



HIGHEST

MODERATE

HIGH
MODERATE

LOW

LOWEST

| FIGURE XI-5

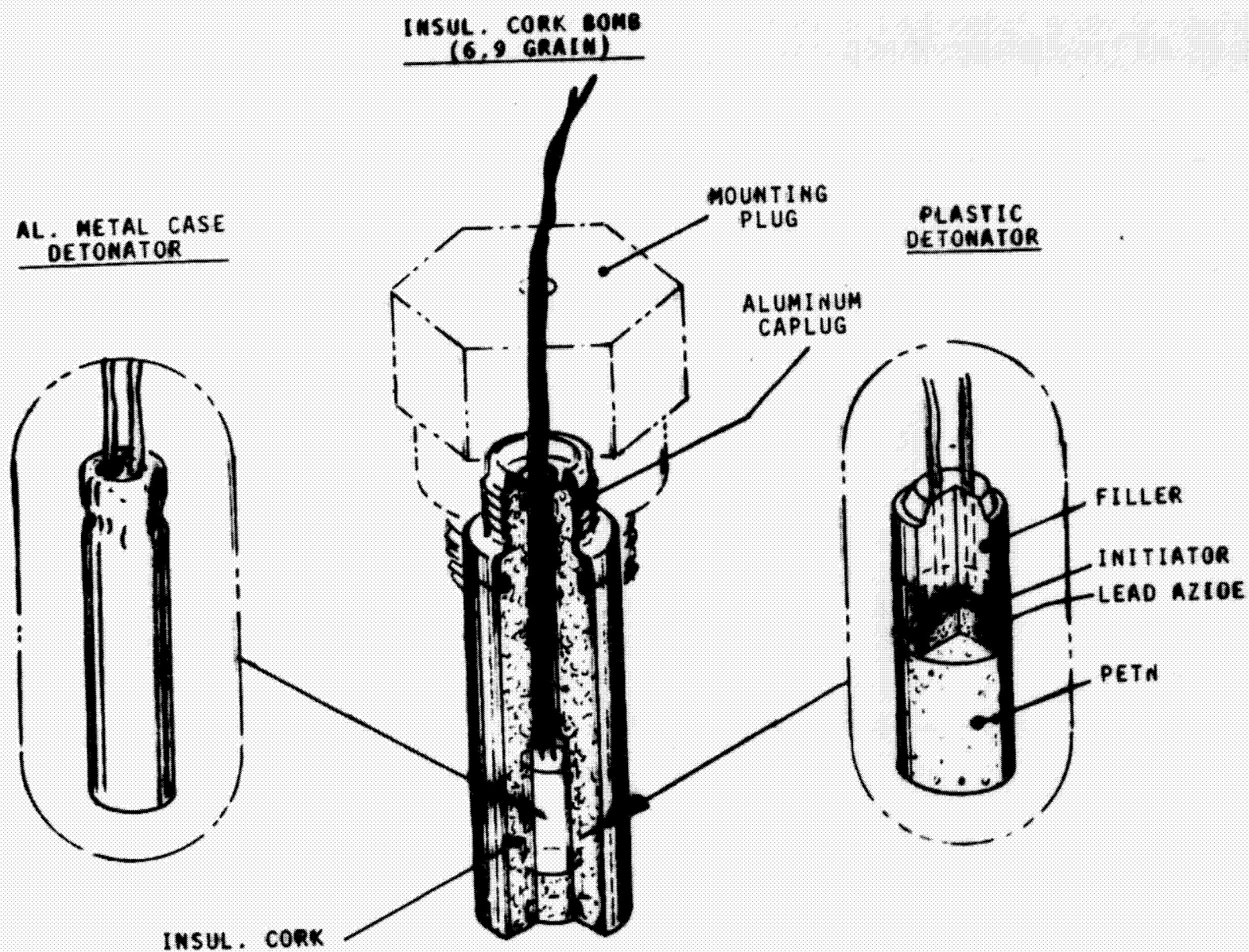


FIGURE XI-6

Bell Aerospace Company

casing was designed with the only machining and handling operation being the drilled holes for the insertion of the detonator. This hole could also be molded on subsequent parts but time and circumstances did not warrant this refinement on the initial procurement.

One additional cost saving procedure used in procuring the bombs was the testing and assurance of each charge. Original bombs were tested and rechecked for continuity and probability of detonation. Examination of past records, both in fabrication and test showed that bomb failures were almost negligible, at least within the record history of this fabrication.

In addition, with the multiple bomb technique of testing, if one bomb was lost, the other detonations were considered normally sufficient to evaluate the condition. With these considerations the testing after fabrication and assembly of the bomb was eliminated at a probable saving which would have doubled the cost of the bomb. The approximate cost for the final bomb was approximately \$25 where the original cost was approximately \$156. The design of the bomb used in Task XIV and XV testing is shown in Figure XI-7.

One final evaluation was made for the bombs, that is to monitor tests for both pulse strength and damage. Observations of the aluminum injector after Tasks XIV and XV showed the damage to be significantly reduced but not altogether eliminated. The strength of the bomb pulse did not appear to be affected as illustrated in Figure XI-8). While the values of the recorded pressure for the bomb detonations are quite varied, the average pulse produced does not appear different for the two types of bombs evaluated.

C. Stability Test Results

The stability tests in this task were primarily designed to examine the entrance of the acoustic damper and its effect on stabilization. Experiments at other facilities on 8 inch diameter engine hardware had shown suspected effects of the entrance geometry on stabilization. Also, tests in Task XII had indicated some deviation from accepted theory with stabilization in cavities operating well above the designed temperature. As a result, the test hardware was redesigned so that adjustments could be made to both the entrance size and shape.

To ensure comparative data, the injector was also reworked to incorporate a fuel film coolant in the outer injector face ring (Figure XI-2). The region of the acoustic cavity is shown in this figure where the adjustments in the damper and entrance could be made. The various arrangements examined are shown in Figure XI-9.

Bell Aerospace Company

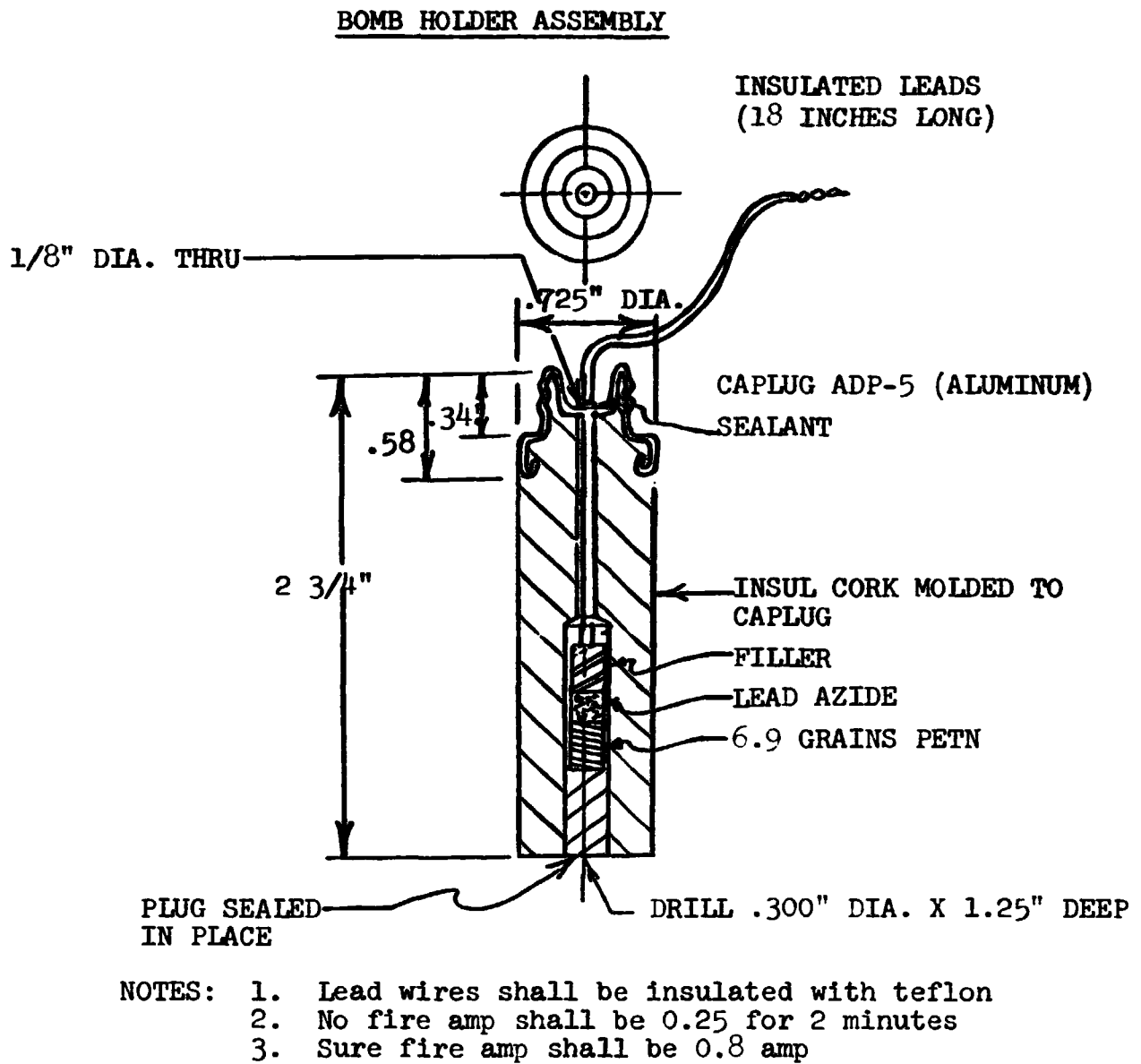


FIGURE XI-7

BOMB OVERPRESSURE COMPARISON

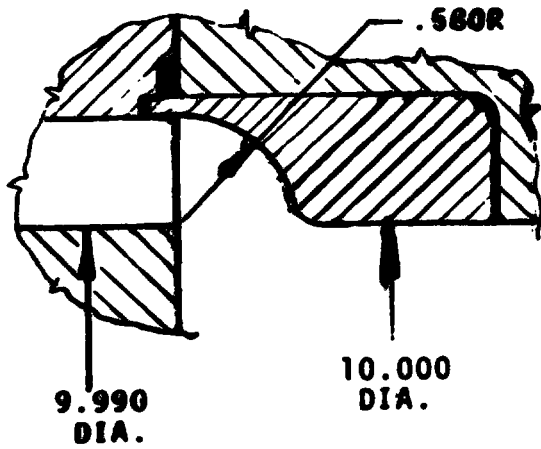
	OVERPRESSURE ~% OF P _C				
	K-1	K-2	K-3	K-4	K-5
INSUL CORK CASE	77-315	82-420	115-404	139-577	74-254
TEFLON CASE	58-244	52-157	106-443	110-492	65-325

ALL BOMBS INCLUDED TESTS 4560 THROUGH 4574 AND 4577 THROUGH 4608

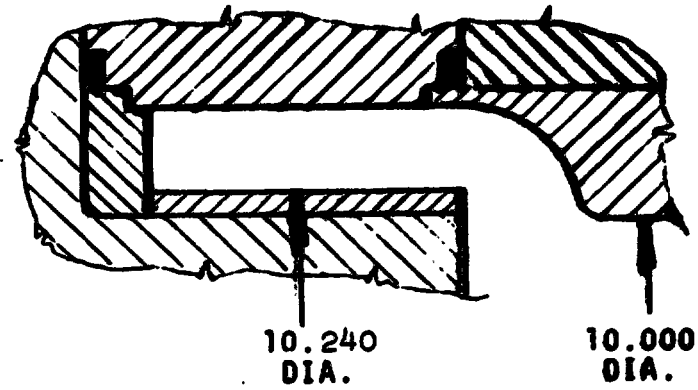
ALL BOMBS HAD 6.9 GRAIN CHARGE

FIGURE XI-8

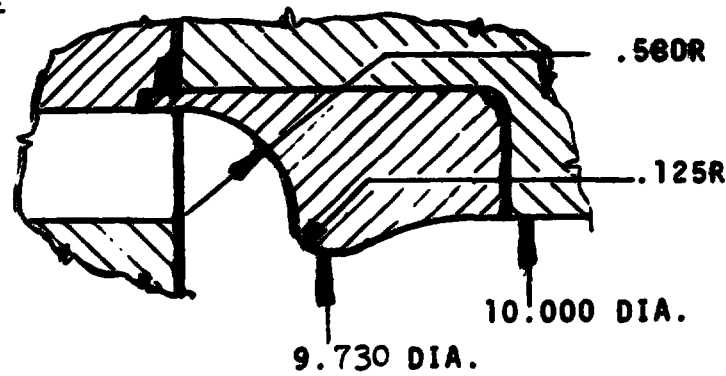
ACOUSTIC DAMPER CONFIGURATIONS



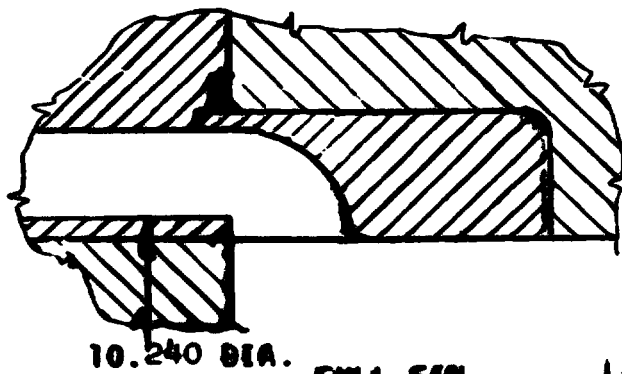
STANDARD DIAMETER



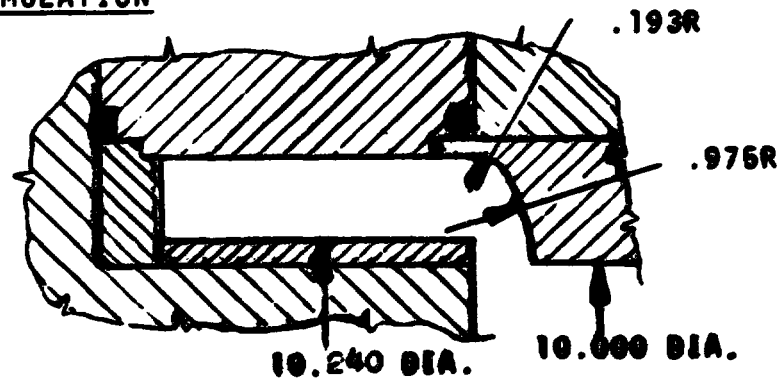
INJECTOR EXTENSION



VORTEX SIMULATION



FULL FIN



SMALL ENTRANCE

| FIGURE XI-9

Bell Aerospace Company

Mention should also be made of one parameter having particular importance and that is the overlap between the chamber and the O.D. of the injector, forming the inside diameter of the acoustic cavity. The center sketch of the Figure XI-9 shows the type of installation tested in Task XII. Actually, the hardware had a greater overlap than shown here, but the film coolant became a very awkward arrangement if a smaller diameter were used. A simulated overlap was arranged in three other configurations as indicated by the sketches showing the injector extension. The complete list of tests conducted during this task is displayed in Table I. The results are plotted in a P_c/MR form in Figure XI-10. The following remarks will be to compare data for different hardware variable to examine their effect on stability.

1. Fuel Vortex vs Fuel Film Coolant

Figure XI-11 is presented to compare the data obtained with the film cooled and vortex cooled injectors. Unfortunately, like many experiments the data is tainted with two variables. The second variable in the test is the chamber overlap where the vortex cooled version had approximately .180 inch overlap, and the film cooled unit .130 inch overlap. Since an overlap larger than .130 would have compromised the design of the film coolant orifices (by striking the lip at the 5° wall angle drilling), the tests were conducted to show general conditions rather than compare only the difference between film and vortex cooling. In retrospect, an experiment where both types of ancillary cooling were blocked and an equal lip used would have been interesting to evaluate.

One very interesting observation was made in examination of frequencies when instability was encountered on the film cooled experiments. The observation was that there appeared to be very little if any definable and sustained 3T/1R mode activity. In some cases, these frequencies were observed but they appeared to be somewhat intermittent, and did not predominate as an established mode.

The conclusion of the experiment showed that more information was needed to compare film and vortex cooling effects. An obvious unstable condition due to the free fuel film at the acoustic damper entrance did not materialize. However, since the vortex cooling does allow a different head end protrusion configuration, the vortex cooled version appeared to gain points in the comparison.

Figure XI-12 is also presented to show that not only was there no startling differences in the film and vortex stability, but there also were no startling differences in the temperatures.

ORIGINAL PAGE IS
OF POOR QUALITY

Legend:
X Detonated
U Unstable
D Damped 20-30 MS

X_T Detonated Thermally
∞ Did Not Damp
(2) Avg. of 2 Max Kistler Values
(3) Damped 45 MS

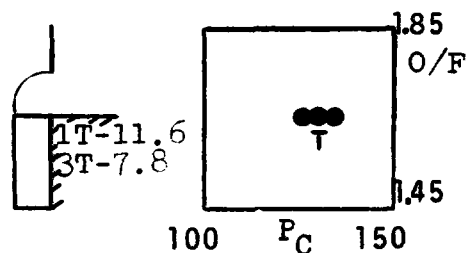
TABLE I
TEST SUMMARY OF BOMB TESTS
BOMB STABILITY PROGRAM, TASK XIV

TEST NUMBER	DURATION (SEC)	R _O /F	P _{cc} -in. (Psi)	C* (Ft/Sec)	O ₁ IT (°F)	F ₁ IT (°F)	BOMB POSITION			DAMP TIME (MSEC)			AVG. MAX. PRESS SPIKE(2) ABOVE P _c (PSI)			NOZZLE AVERAGE HEAT FLUX		AVERAGE ACOUSTIC CAVITY GAS TEMPERATURE (°F)	ACOUSTIC CAVITY		KISTLER FREQUENCIES				
							1	2	3	1	2	3	1	2	3	Q/A (BTU/in ² SEC)	Q (BTU)		K ₃	K ₄	HERTZ				
																					K ₁	K ₂	K ₅		
4577	1.1	1.83	124		80	143	(X)			∞			262						2510	{2527 5023 10046 2528 2560	2520 2560 2510				
4578	1.1	1.78	123		79	135	(X)			∞			192												
4579	7.3	1.75	123	5576	78	181	(X)	X _T		24.6	7.7	∞	210	1.74	502	2344									
4580	1.8	1.70	128		74	148	(X)		X			8.9	165	209	320	1.78	513	2461							
4581	6.9	1.73	128	5588	75	202				∞			252						{2473 4945	2473					
4582	0.6	1.95	150		65	142	(X)																		
4583	1.4	1.84	154		69	139		X _T			7.9		128												
4584	7.0	1.91	154	5586	72	160			X			5.3	238	2.10	608	2540									
4585	8.0	1.56	155	5608	62	180	X	X		4.3	4.8		175	256		2.03	586	2916							
4586	1.4	1.43	104		66	151	X			4.7			170												
4587	1.5	1.50	104		65	160		X _T			4.2		290												
4588	7.0	1.52	104	5552	61	189			X			4.0	211	1.44	417	2194			{2460 2489	{2460 2489	{2460 2489	2489			
4589	1.6	2.05	101		60	143	(X)	(X)		4.5	∞		190	195											
4590	6.9	2.08	101	5468	61	176			X			5.1	269	1.50	432	1963									
4591	6.9	1.65	130	5596	71	180	X	X	X	5.0	5.0	3.7	223	270	209	1.78	513	2590							
4592	1.5	1.88	153		79	165	X	X _T		4.8	5.5		222	276											
4593	6.9	1.87	154	5583	72	197			X			5.0	246	2.11	610	2411									
4594	6.9	1.91	105	5538	72	193	X	X	X	5.2	4.5	4.2	180	226	238	1.54	444	2048							
4595	7.0	1.52	155	5597	73	200	X	X	X	4.1	7.7	8.1	160	282	216	2.04	590	2756							
4596	6.9	1.47	105	5556	72	194	X	X	X	4.5	6.4	4.3	165	178	238	1.45	419	2281							
4597	6.9	1.58	128	5593	75	192	X	X	X	5.0	6.5	4.5	146	168	204	1.96	566	2482							
4598	1.2	1.78	157		70	141	(X)	(X)		22.5	∞		178	166					{2495 2530	4949		2542			
4599	6.9	1.85	155	5592	74	198		X _T	X			4.6	220	2.17	627	2571									
4600	6.9	1.79	104	5538	69	201	X	X	X	8.6	5.9	4.3	216	201	232	1.51	436	2120							
4601	1.1	1.63	137		66	160	(X)			∞															
4602	1.3	1.62	130		68	170				∞			174						{2825 5650	5660 5505	5660 4450	4405			
4603	6.9	1.64	130	5589	68	201		X _T	(X)			∞	193	1.83	528	2538									
4604	1.1	1.66	127	5589	67	187	X	X	X	4.7	5.5	3.3	153	211	202	1.78	513	2690							
4605	7.0	1.84	155	5593	66	203	X		X	4.5	5.6	4.0	166	202	206	2.18	629	2636							
4606	6.9	1.87	102	5529	63	201	X	X	X	3.7	4.0	3.9	166	151	210	1.51	435	2281							
4607	6.9	1.49	153	5589	55	198	X	X	X	5.0	6.2	4.7	181	182	225	2.05	592	3234							
4608	6.9	1.53	104	5547	54	190	X	X	X	5.7	4.1	3.8	172	196	162	1.49	431	2877							

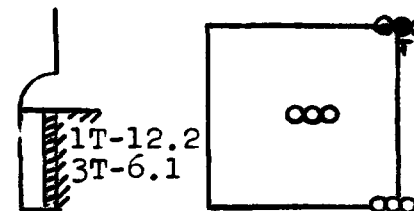
All Performance and Temperature Data at 5.5 Sec.

XI-15

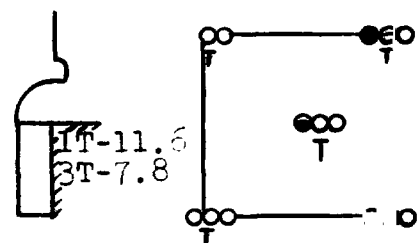
FIGURE XI-10
TASK XIV - TEST RESULTS



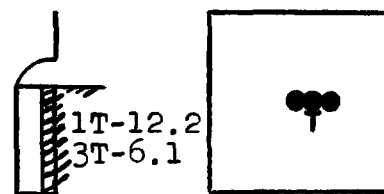
Standard Diameter



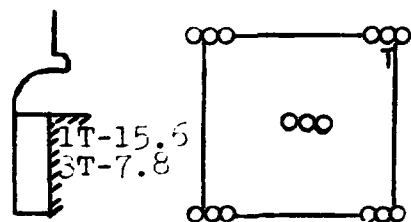
Injector Extension



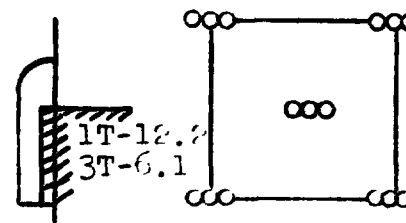
Vortex Simulation



Small Entrance



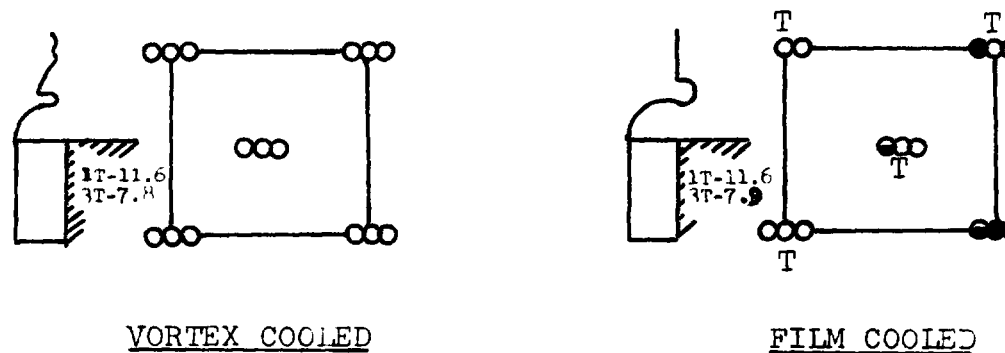
Vortex Simulation



Full Pin

- | | |
|------------|--|
| ○ STABLE | 1T - 1ST TANGENTIAL OPEN AREA % |
| ● MARGINAL | 3T - 3RD TANGENTIAL/1ST RADIAL OPEN AREA % |
| ● UNSTABLE | O/T - THERMAL DETONATION |

TASK XIV - TEST RESULTS
VORTEX VS FILM COOLED INJECTOR



OBSERVATIONS

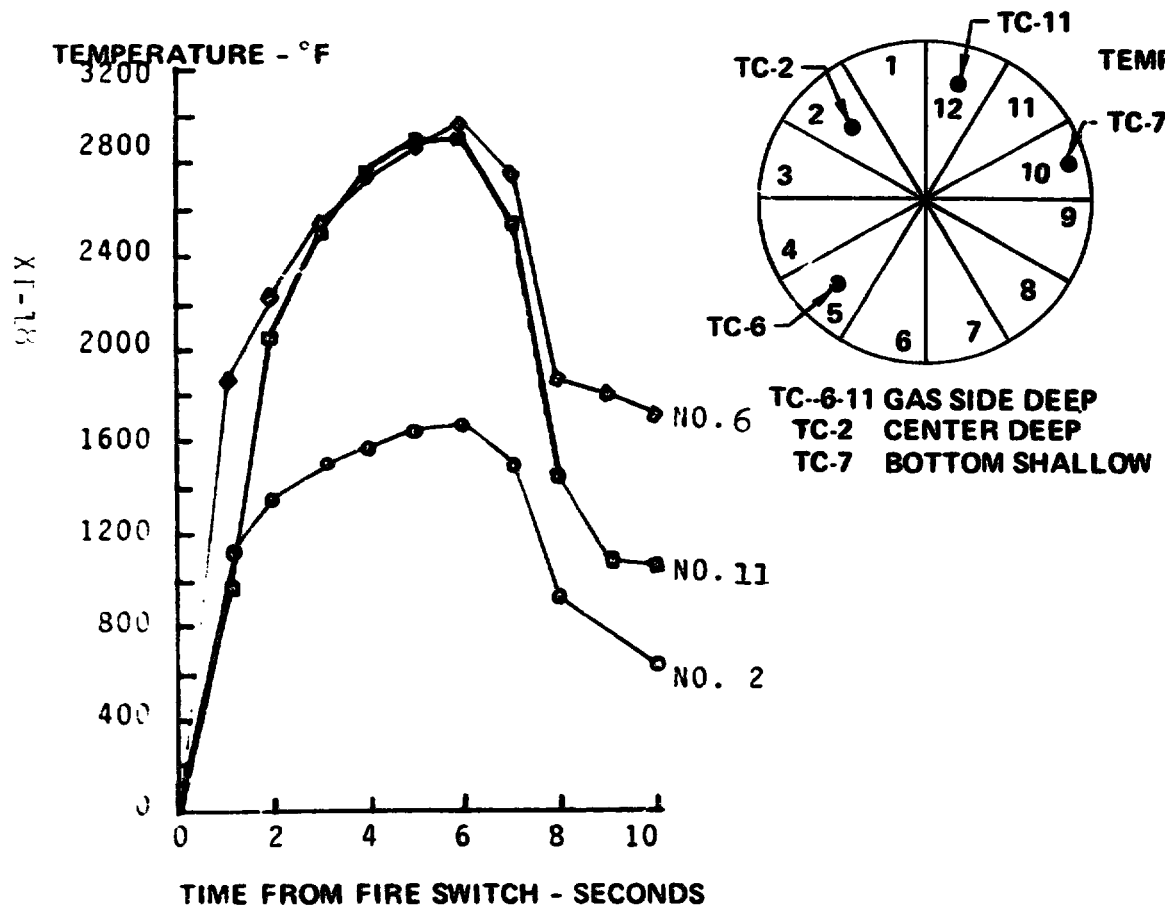
- VORTEX COOLED CONFIGURATION SIGNIFICANTLY MORE STABLE THAN FILM COOLED CONFIGURATION.
- DIFFERENCE IN STABILITY CHARACTERISTICS MAY BE PARTLY RELATED TO GEOMETRY (INJECTOR-CHAMBER OVERLAP).
- NO APPARENT 3T/1R ACTIVITY IN VORTEX CONFIGURATION

FIGURE XI-11

CAVITY TEMPERATURES FILM COOLING AND VORTEX COOLING TESTS

FILM COOLING

TEST NO. 4581 D-4
(STABLE)



VORTEX COOLING

TEST NO. 4575 D-4
(STABLE)

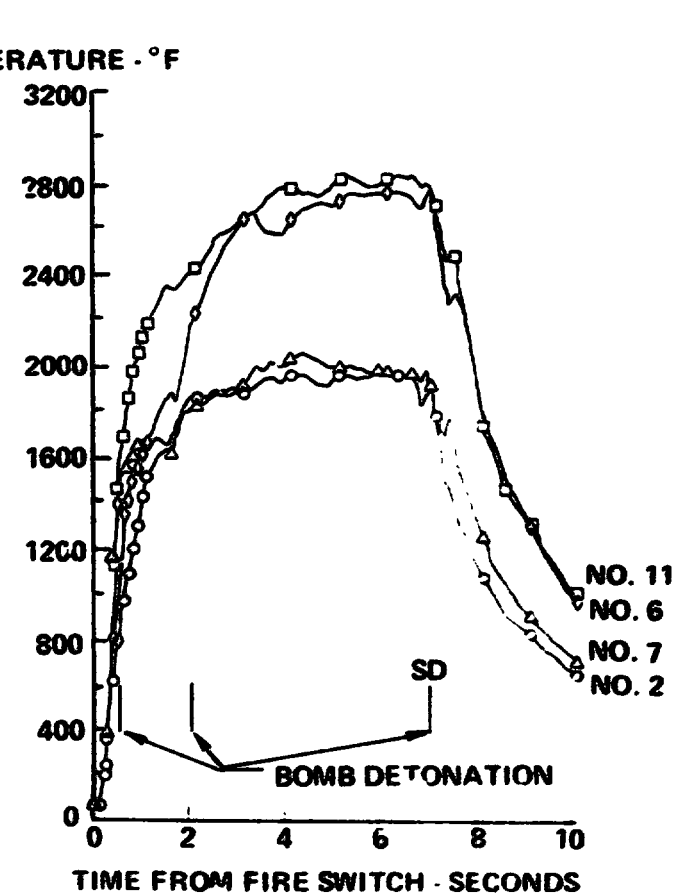


FIGURE XI-12

Bell Aerospace Company

It could be argued that the lower thermocouple (2) represented a lower average cavity temperature. However, if anything, this should have produced a stabilizing effect which was not borne out by test. After examination of the data, it was concluded that there was no significant difference in the temperature of the acoustic cavity and very probably a contributory factor in the little if any stability difference attributed to the film cooled injector.

2. Effect of Chamber Overlap

The first three unstable tests conducted on this program left little doubt that the entrance was important, and the chamber overlap a critical factor in stabilization. These tests also confirmed findings at other facilities which had been evaluated on different diameter hardware. Since the original overlap was in the form of the vortex lip, the overlap was eliminated on the film injector work. Since this design produced unstable operation, the next step was to expand the injector diameter to form a similar overlap. The test results of this experiment are shown in Figure XI-13. The 10% 1T open area was insufficient for stability but the 15.6% was stable with the vortex lip overlap. The 12.2% open area with the expanded injector resulted in marginal stability. This 12.2% open area was limiting for this experiment, as a larger open area require a substantial hardware rework.

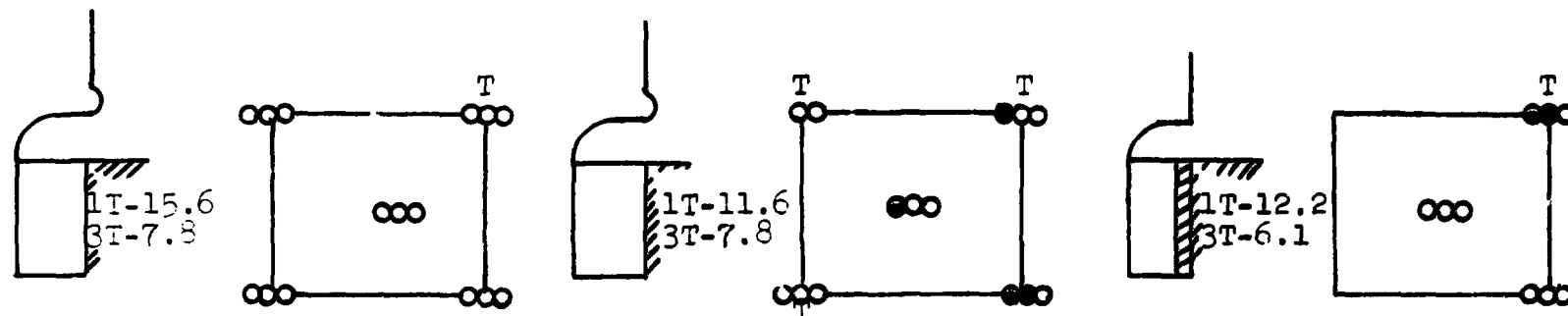
Considering both above and the Task XII test results, another interesting speculation results in that with .180 inch overlap 11% open area was stable (7.8% unstable) and with .130 and .120 overlap, 11.6% and 12.2% was marginal.¹ The obvious implication is that overlap and open area are related and should both be considered when extrapolating test results.

3. Flush and Full Fin Damper Separators

Testing to date on acoustic dampers has maintained the 12 segment peripheral sections of the original investigators. However, the full separators were originally cut off at the injector face due to heat rejection and hardware configuration considerations. Since other investigators had tested the full fin type damper arrangement, and there was concern relative to the effective length of the opening with and without the fin, comparative tests were made. Figure XI-14 shows the results of these tests where with the full fin baffle, stable operation was achieved with the minimum overlap over the chamber pressure, mixture ratio matrix.

1 Marginal in this case meaning that stability was noted at rated conditions and low chamber pressure but the high chamber pressure lean (high O/W) mixture ratio condition was unsatisfactory.

TASK XIV - TEST RESULTS
CHAMBER LIP VS INJECTOR EXTENSION
(FILM COOLED)



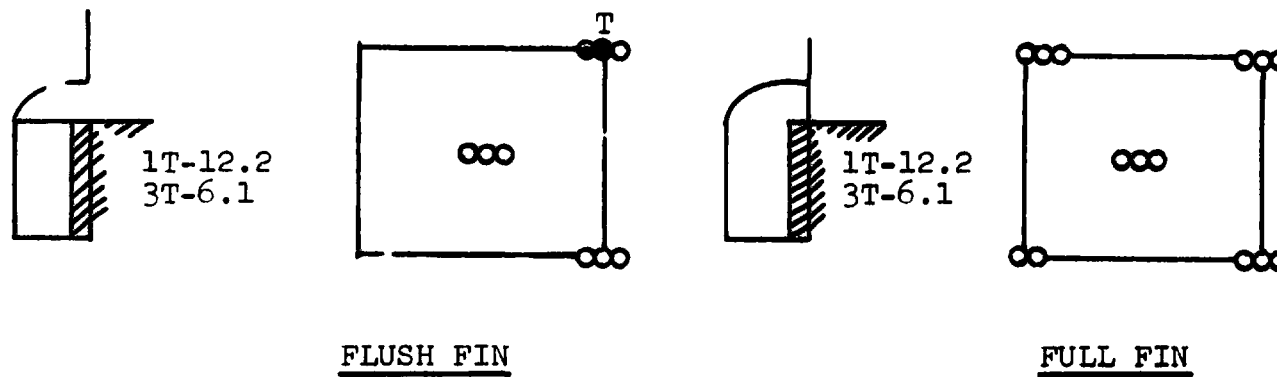
OBSERVATIONS

- CHAMBER LIP NOT DEFINABLY MORE STABLE THAN INJECTOR EXTENSION
- RECOMMENDATION FOR INJECTOR EXTENSION OF INCREASED OPEN ARE
(PROBABLY REQUIRES LESS THAN A 15.6/7.8 1T/3T COMBO)

FIGURE XI-13

TASK XIV - TEST RESULTS

FLUSH FIN VS FULL FIN



OBSERVATIONS

- FULL FIN MORE STABLE THAN FLUSH FIN
- DEGREE OF FULL FIN STABILITY INCREASE NOT OBVIOUS FROM DATA

FIGURE XI-14

Bell Aerospace Company

4. Reduced Entrance Size

An experiment was also conducted to evaluate the reduction in area to the entrance of the acoustic damper. Originally, the concept was to increase the viscous resistance in this local area and/or to "tune" the entrance to the cavity width. Since the original hardware fabrication was conducted long before testing began, an arbitrary 1/2 width was selected. This entrance proved very unsatisfactory and in retrospect was probably a poor test choice. Relating to the cavity width the .29 inch entrance opening was far short of the .45 inch width and probably afforded no tuning at all.

One very interesting result was noted on these tests, however, that being the substantial increase in the 3T/1R frequency activity. Since this frequency was not sustained on any of the unstable tests with the larger opening, this increase in activity was of interest in that the opening appears to not only effect the amount of damping, but also the frequency at which it is recorded. Again, the limited funding of the program restricted further effort to examine other opening configurations. However, it is strongly suspected that by changing the opening, both damping and frequency are effected together.

5. Comparison of Stable Configurations

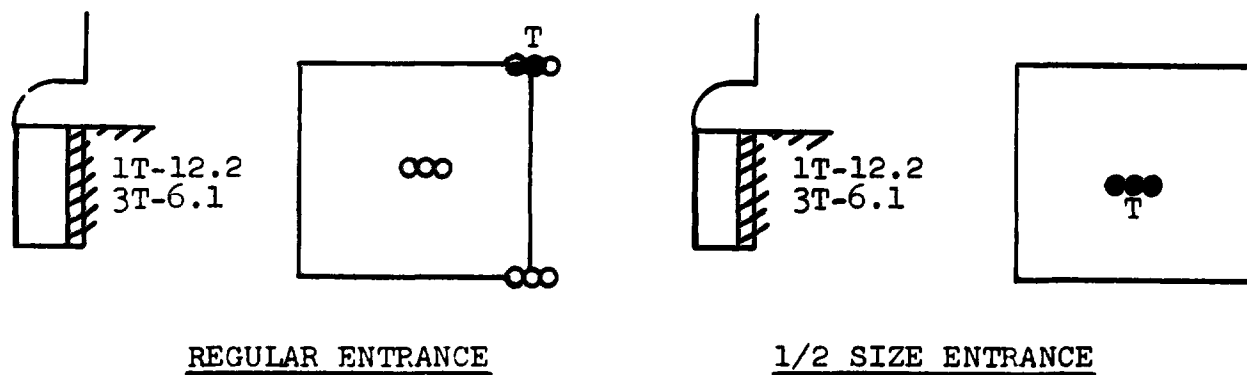
Two of the test configurations displayed stable operation over both the mixture ratio and the chamber pressure range. Of the two configurations, one had an overlap protruding into the chamber and the other had the extended injector diameter full fin damper combination. The test records of each configuration were examined to see if either configuration would display a greater statistical stability and therefore a direction for design. The test results shown in Figure XI-16 were used.

For the statistical examination, the mean damp time in (milliseconds) was used, as well as the σ (standard deviation) for each group. These values are as follows:

<u>Group</u>	<u>Mean Damp Time M.S.</u>	<u>σ</u>	<u>F (Comparison of σ's)</u>	<u>T (Comparison of Means)</u>
Chamber Lip	5.2	1.274	2.19	1.562
Full Fin	4.6	0.86		

TASK XIV - TEST RESULTS

REDUCED ENTRANCE SIZE

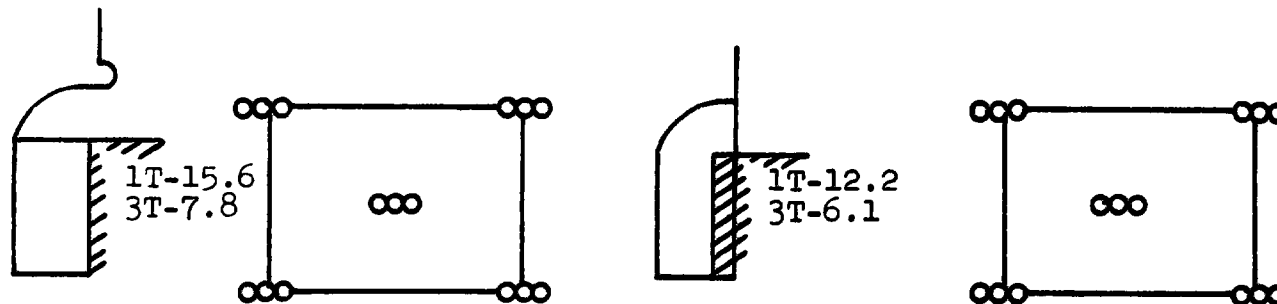


OBSERVATIONS

- SMALL ENTRANCE DEFINITELY DESTABILIZING
- SIGNIFICANT INCREASE IN 3T/1R FREQUENCIES IN 1/2 ENTRANCE TRACE
- INTERIM ENTRANCE SIZE SUGGESTED AS A BETTER COMPROMISE

FIGURE XI-15

TASK XIV - TEST RESULTS
COMPARISON OF STABLE CONFIGURATIONS



OBSERVATIONS

- EXAMINED FOR SIGNIFICANT DIFFERENCES DUE TO CONFIGURATION -
RESULT OF EVALUATION SHOW NO DIFFERENCE

FIGURE XI-16

Bell Aerospace Company

The F and T critical values at 5% were also calculated with the following results:

$$F_{\text{Critical @ 5\%}} = 2.48$$

$$T_{\text{Critical @ 5\%}} = 2.048$$

Since the F and T values must exceed the F and T critical values to indicate a significant difference between groups, it was concluded that there was no statistically significant difference in the chamber lip and full fin configurations.

D. Conclusions Resulting from Task XIV Testing

The result of these tests were considered quite informative in defining some areas affecting stability. Important to the damping is the chamber-to-injector overlap, open area, damper fin length and cavity entrance size and shape. While the program was quite successful in showing some of the interrelated damper design parameters, unfortunately all these variables could not be examined in depth to provide design data. To be more explicit the conclusions were as follows:

- Full damper fins are more stable
- Chamber injector overlap entrance is more stable
- Cavity entrance should not be restricted
- Open area required is a function of entrance configuration
- Fuel coolant film injected downstream of damper opening is more stable

Bell Aerospace Company

XII. TASK XV - OME - 8 INCH TRIPLET INJECTOR OPTIMIZATION

During the course of studies leading to the OME engine definition, designs had been considered at both the 8 and 10 inch diameters. The original Bell design used the 10 inch diameter triplet element injector as the least risk, most cost-effective approach to high performance. Other investigators elected smaller 8 inch diameters and required extended combustor lengths and/or pattern changes to achieve performance. In addition, some changes in performance were experienced with propellant temperature which did not appear with the triplet element design.

Because of this apparent success of the 10 inch triplet configuration, an 8 inch injector triplet element injector design was undertaken to see if the design was also applicable at the smaller diameter. The objective of this task was to design, fabricate, and test an 8 inch diameter injector in an attempt to approximate the success of the larger 10 inch diameter test injector.

Since the original triplet design was based on the best experience information available, the 8 inch diameter injector presented a challenge as to which design parameters should be maintained; so that the single item try at the smaller diameter would be sufficiently successful to be representative of what might be achieved in a development program. To this end, a small scale injector parameter trade-off study was conducted before the design release.

In addition to the performance design trade-off studies conducted, an additional requirement of the injector design was to fit the interface of the 8 inch chamber interface design supplied by NASA-JSC. The test evaluation included performance, heat flux, and stability data utilizing a combination of new and existing hardware. A new injector and acoustic cavity adapter/acoustic cavity ring was provided with cavity configuration adjustments similar to that used on the 10 inch diameter injector. To minimize the cost for test chamber hardware the 10 inch diameter water cooled nozzle was used, and a new 8 inch diameter steel bomb chamber fabricated.

A. Design Definition

1. Core Pattern

The design rationale for the 8 inch injector diameter was to retain, wherever possible, the design features of the highly successful 10 inch diameter injector. Various tradeoffs were completed to establish triplet element arrangement and quantity

Bell Aerospace Company

including pressure map comparisons. The major design parameters are summarized in Table 1 which also includes a comparison of 8 inch diameter injector designs with 7, 6 and 5 rows of triplet elements.

The primary concern with the smaller diameter injector was the injection element pattern compression since only 66% of the injection surface is available with the 8 inch diameter design. The natural tendency is to decrease the number of elements as the diameter decreases. It is most desirable, however to provide a large number of triplet elements to assure high performance and preferably the same number as used on the 10 inch diameter design. The design studies revealed a 7 row, 196 element injector was practical by designing narrower, but deeper propellant supply manifolds at the injector face. Tradeoffs were made between various triplet element configurations with the preference to retain the same type elements used on the 10 inch diameter injectors. Figure XII-1 shows a comparison of the narrower manifolds for a 7 and 6 row, 8 inch diameter configuration with the 10 inch diameter configuration of S/N 2 injector. Impingement distance, impingement angle, stream velocity, manifold propellant velocities, and orifice entrance location and conditions are the major design parameters critical to the injection element. The 10 inch diameter injection element has a 0.397 impingement distance with the fuel orifice inlets located in the center of the fuel manifold and an impingement half angle of 32°. OME type injector S/N 1, which has the same performance level as S/N 2 has an impingement angle of 28°. The 8 inch diameter, 7 row configuration shown in Figure XII-1 reveals the fuel orifice inlet location closer to the manifold wall.

To determine what influence, if any, the location of fuel orifice inlet to manifold wall had on flow characteristics, a flow model was designed, fabricated and evaluated. This flow model was a simple but effective device that simulated the inner fuel manifold configuration for the 8 inch diameter, 7 row injector design. Three types of element configurations with two elements each were provided in half of the flow model. The design provided for identical flow area and velocity and fuel orifice/manifold wall relationship anticipated on the final design. Figure XII-2 and Figure XII-3 identify the flow model and the element configuration. Flow tests revealed no flow discrepancies with the narrower but deeper manifolds and closer position of the fuel orifice inlet to the manifold wall.

A pressure map study was made of various element/row configurations for comparison with the 10 inch diameter injector pressure map.

TABLE 1

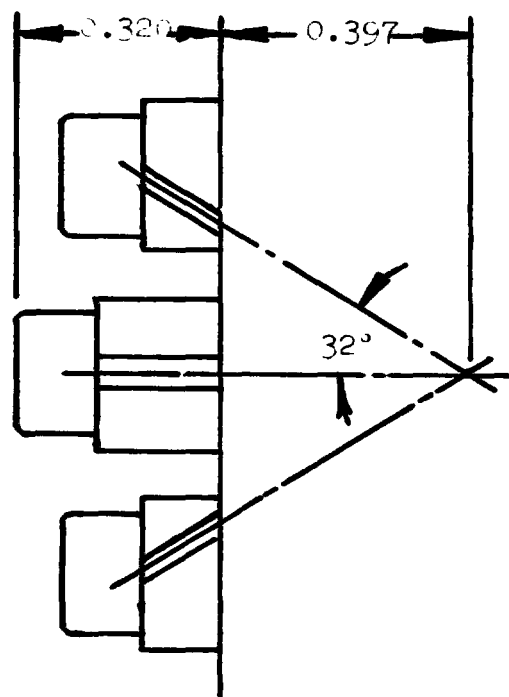
8 INCH DIAMETER INJECTOR DESIGN

INJECTOR CORE DESIGN COMPARISON

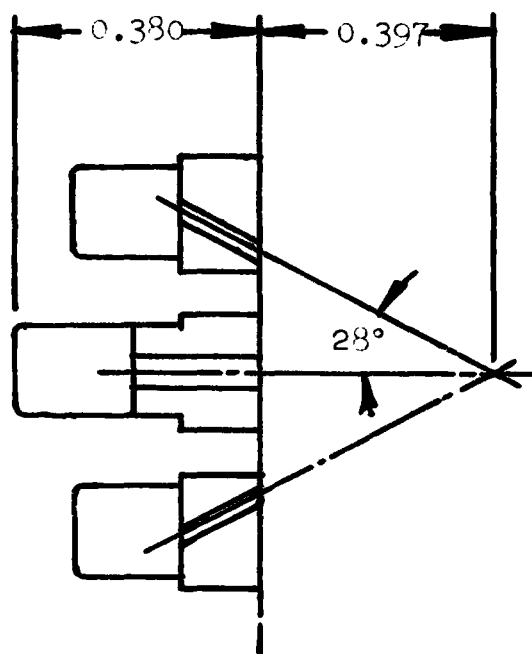
	<u>10 INCH DIAMETER (S/N 2)</u>	<u>8 INCH DIAMETER (7 ROW)</u>	<u>8 INCH DIAMETER (6 ROW)</u>	<u>8 INCH DIAMETER (5 ROW)</u>
DIAMETER (INCH)	10	8.2	8.2	8.2
THRUST (LBS)	6000	6000	6000	6000
ELEMENT TYPE	TRIPLET	TRIPLET	TRIPLET	TRIPLET
NUMBER OF ELEMENTS (PRIMARY)	196	196	156	144
THRUST/ELEMENT (LBS)	31	31	38.5	40.8
OX MANIFOLD VELOCITY (FT/SEC)	8	8	8	8
FUEL MANIFOLD VELOCITY (FT/SEC)	9.5	9.5	9.5	9.5
PROPELLANT FLOW/A _C (LBS/IN ²)	0.24	0.35	0.35	0.35
NUMBER OF ELEMENT ROWS	7	7	6	5
<u>ELEMENT CONFIGURATION</u>				
● IMPINGEMENT DISTANCE (INCH)	0.397	0.397	0.397	0.397
● IMPINGEMENT ANGLE (°)	32	28	32	32
● OX ORIFICE DIAMETER (INCH)	0.0492/0.0465	0.0492/0.0465	0.055	0.57
● FUEL ORIFICE DIA. (INCH)	0.0295/0.0276	0.0295/0.0276	0.033	0.34
● L/D OX	4.0	4.0	4.0	4.0
● L/D FUEL	5.0	5.0	5.0	5.0
● ΔP OX (PSI)	41	41	41	41
● ΔP FUEL (PSI) (2%)	43.5	43.5	43.5	43.5
● FACE RING WIDTH (INCH)	0.250	0.190	0.220	0.300

8 INCH DIAMETER INJECTOR ELEMENT COMPARISON

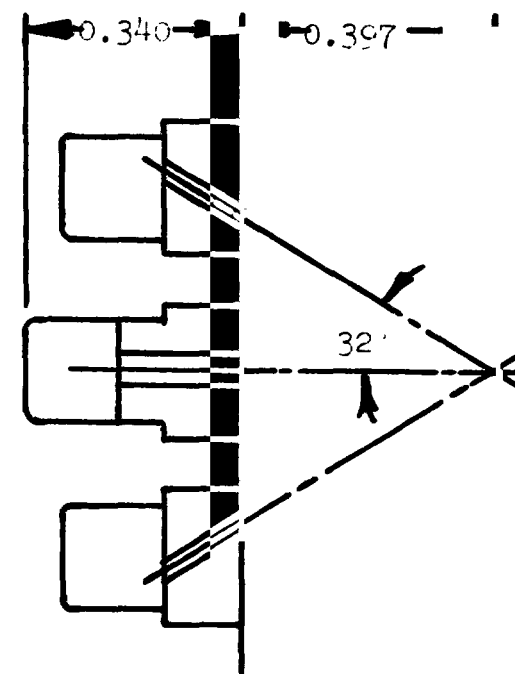
XII-4



10 INCH DIAMETER
7 ROW



8 INCH DIAMETER
7 ROW



8 INCH DIAMETER
6 ROW

FIGURE XII-1

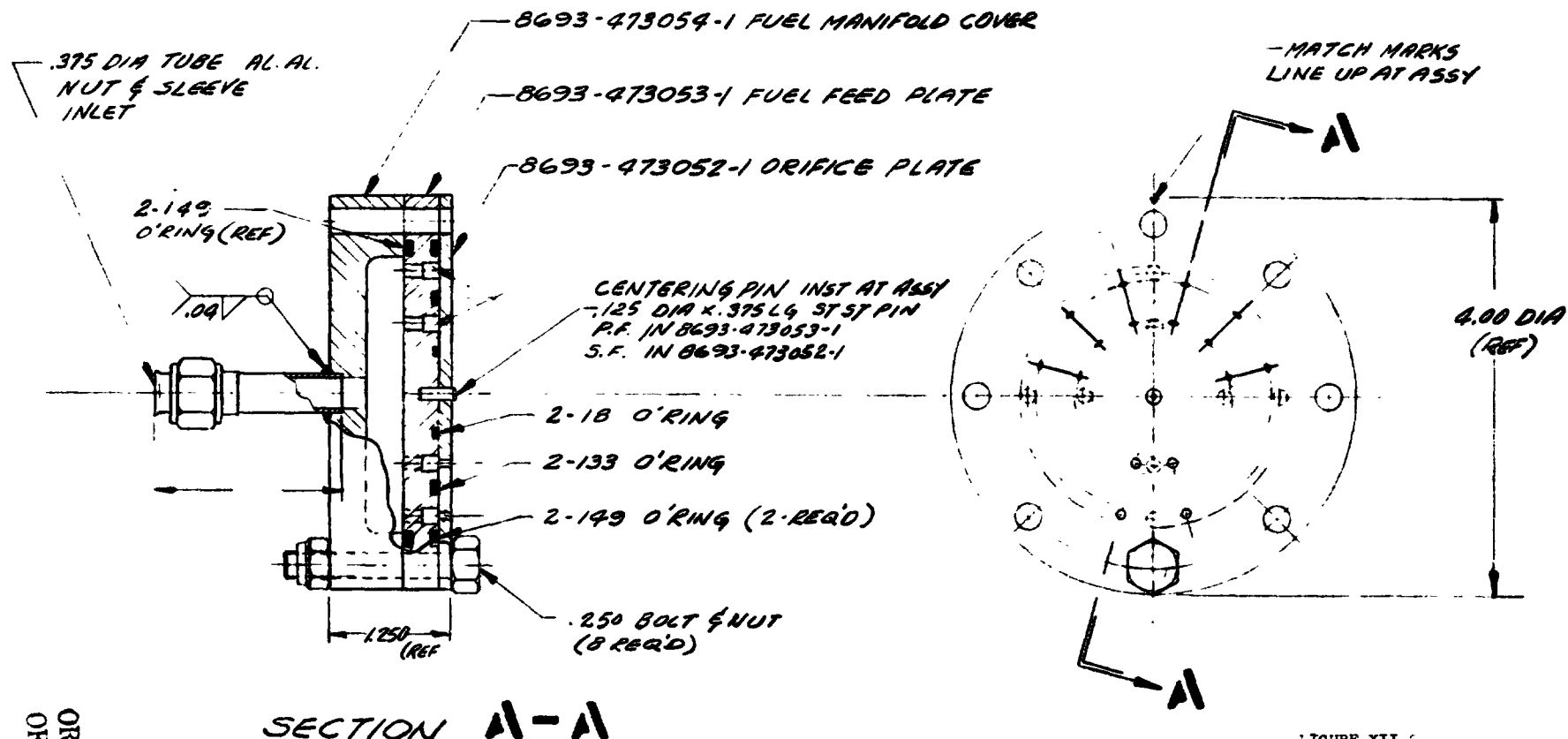
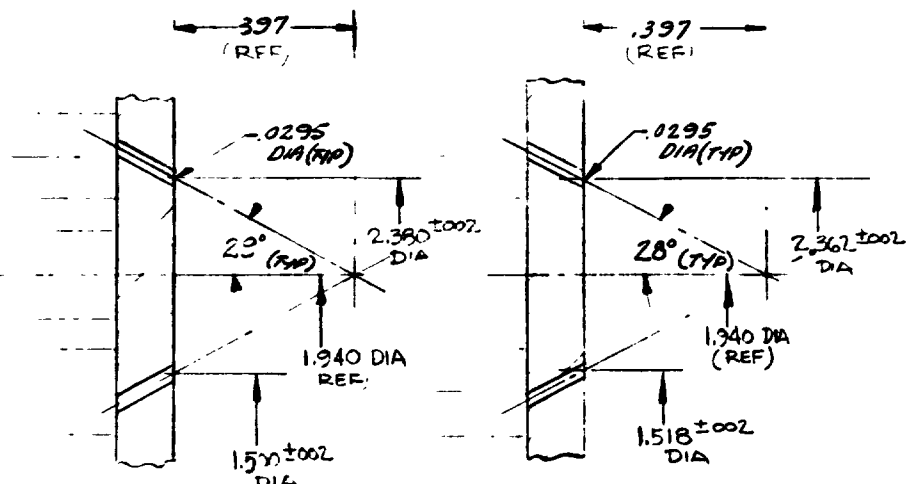
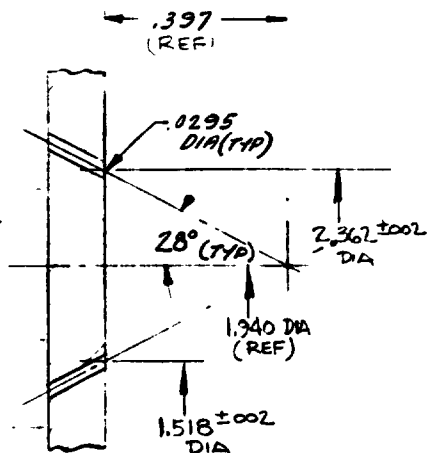


FIGURE XII-2

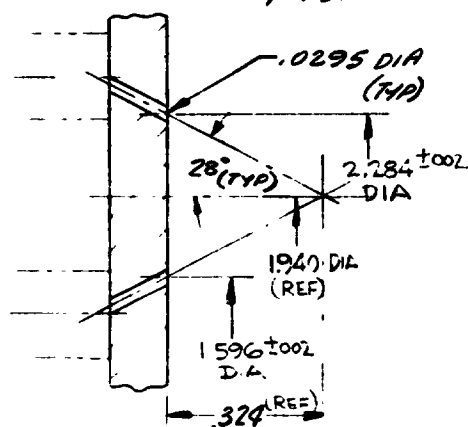
UNLESS OTHERWISE SPECIFIED DIMENSIONS ARE IN INCHES TOLERANCES ON DECIMALS		DESIGN <i>72-14200-1</i> GROUP <i>1</i> APVD <i>John W. 11/1/72</i>		BELL AEROSPACE COMPANY DIVISION OF TEXTRON INC. POST OFFICE BOX ONE BUFFALO, NEW YORK 14240	
X XX XX3 ANGLE ± .1 ± .03 ± .010 ± .0° 30		HOLE TOLERANCES EXCEPT AS SHOWN		WATER FLOW MODEL, ASSY/CM	
.040 TO .125 + .005, -.001 .130 TO .250 + .005, -.001 .261 TO .425 + .008, -.001 .430 TO .750 + .010, -.001 .750 TO .985 + .012, .001 985 AND LARGER ± .010		RISE UNLESS OTHERWISE SPECIFIED BREAK EDGES .015 MAX RAD OR CHAMFER		8" ONE FUEL ORIFICES	
MACHINED SURFACES <i>21</i> EXCEPT AS NOTED		SIZE CODE IDENT NO B 80070		8693-473051	
		SCALE <i>1/1</i>		DEVELOPMENT SH	



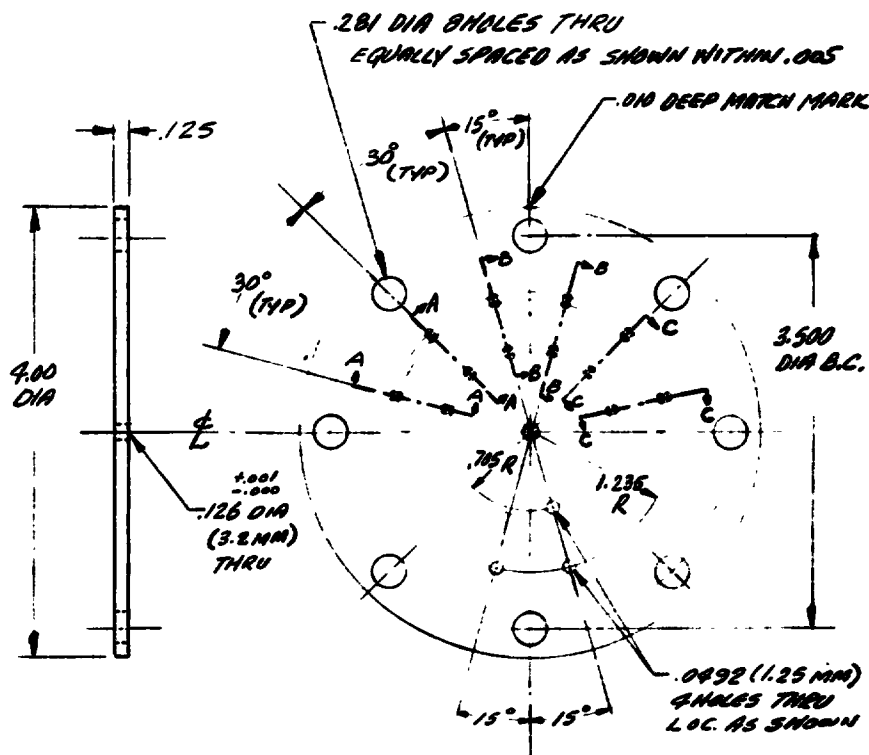
SECTION B-B
(2 PLACES)
4 x SIZE



SECTION A-A
(2 PLACES)
4 X SIZE



SECTION C-C
(2 PLACES) 4x SIZE



MATL: AL.AL.

FIGURE XII-3

UNLESS OTHERWISE SPECIFIED DIMENSIONS ARE IN INCHES. TOLERANCES ON DECIMALS		DESIGN <i>11/22/80</i> GROUP <i>1</i> APVD <i>[Signature]</i>		BELL AEROSPACE COMPANY DIVISION OF TEXTRON INC. POST OFFICE BOX ONE BUFFALO, NEW YORK 14240	
1 11 111 ANGLES ± 1 ± 02 ± 010 ± 0° 30'		HOLE TOLERANCES EXCEPT AS SHOWN		ORIFICE PLATE - WATER FLOW MODEL	
040 TO .125 + .005, -.001 .130 TO .250 + .005, -.001 .251 TO .488 + .005, -.001 .489 TO .735 + .010, -.001 .736 TO .989 + .012, -.001 .990 AND LARGER ± .005		RLSE UNLESS OTHERWISE SPECIFIED BREAK EDGES .015 MAX RAD OR CHAMFER MACHINED SURFACES EXCEPT AS NOTED		SIZE CODE IDENT NO B 80070 8693473052	
		SCALE <i>1/8" = 1"</i>		DEVELOPMENT SH	

Bell Aerospace Company

The similar and acceptable comparison between the two 7 row configurations with the same number of elements (196) is shown in Figure XII-4.

Based upon the tradeoff studies, flow model tests and pressure map comparisons, the 7 row, 196 element triplet pattern was selected for the 8 inch diameter injector design. To allow positioning of the fuel orifice inlet as close to the manifold center as possible and not exceed the impingement angle range of 28° to 32° used on the successful 10 inch diameter injectors S/N 1 and S/N 2, a 28° impingement angle was used. The same impingement distance and orifice diameters used on the 10 inch diameter injector were incorporated, (Table II and Figure XII-5).

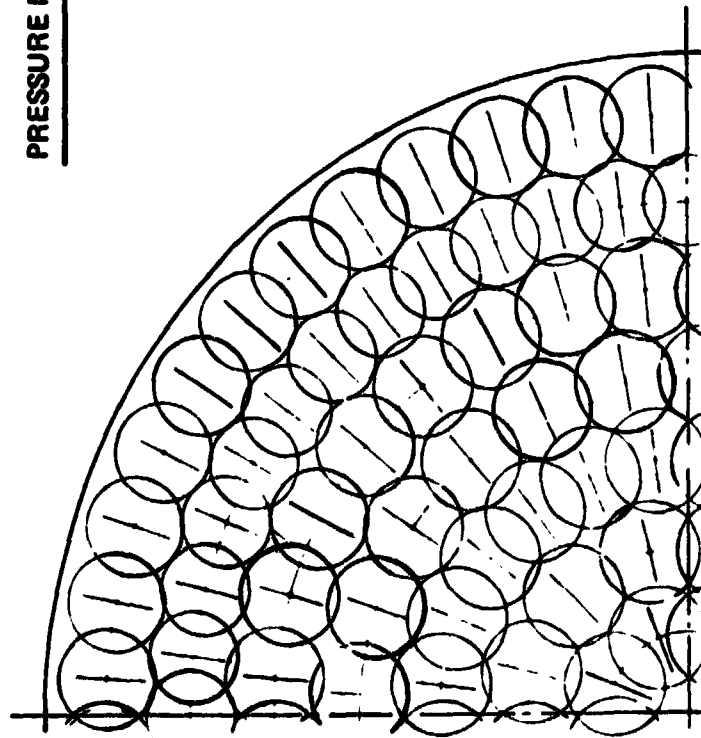
B. Film Coolant Orifices

The film coolant orifice configuration of the 10 inch was also used on the 8 inch diameter injector. A total of 48, .0197 inch diameter orifices equally spaced between the 48 outer triplet elements provide for a fuel flow of approximately 2% of the total propellants. This propellant is injected through the combustor at a 5° wall impingement angle.

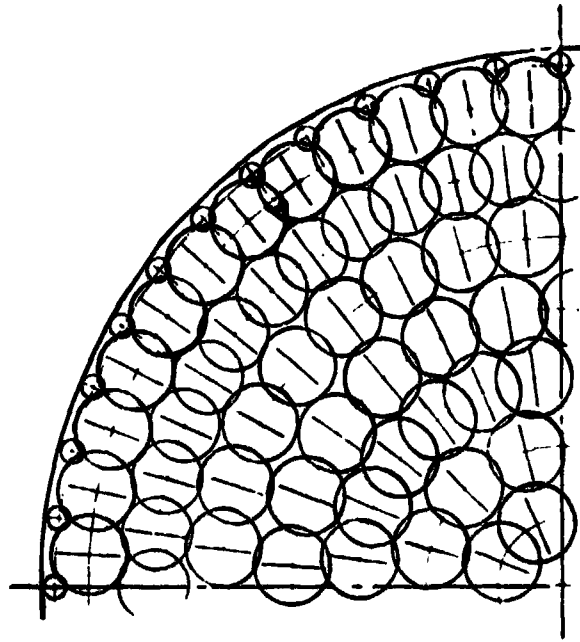
C. Acoustic Cavity

The acoustic cavity design for the 8 inch injector incorporated all the same options of the 10 inch injector with the added flexibility of an increased cavity depth. The cavity depth was increased to 2.5 inches to provide for a very substantial increase over that tested on the 10 inch diameter injector. The depth increase was required due to the uncertainty of the cavity temperature relation to the speed of sound (density and consequent damping as a $1/4$ wave tube). The depth of approximately 2 $1/2$ inches corresponded to a $1/4$ wave tube depth for temperatures recorded in the 10 inch diameter hardware. Although this feature was provided by design, subsequent testing never used a depth of more than 1.6 inches. The provision for this cavity depth did result in one other design characteristic, that being the very "thick" appearance of the injector with the long radial full inlet feed holes. This manifold arrangement was made to be compatible with the NASA-JSC 8 inch diameter regeneratively cooled chamber. The cavity width was selected as 0.5 inches based upon successful experience reported with the Rocketdyne 8 inch diameter injector. Acoustic cavity inlet variations were also provided by changing the insert (8693-943175-1) shown also in Figure XII-5. The resulting injector design is shown in Figure XII-5.

PRESSURE MAP COMPARISON



10 IN. OME
7 ROWS 196 ELEMENTS



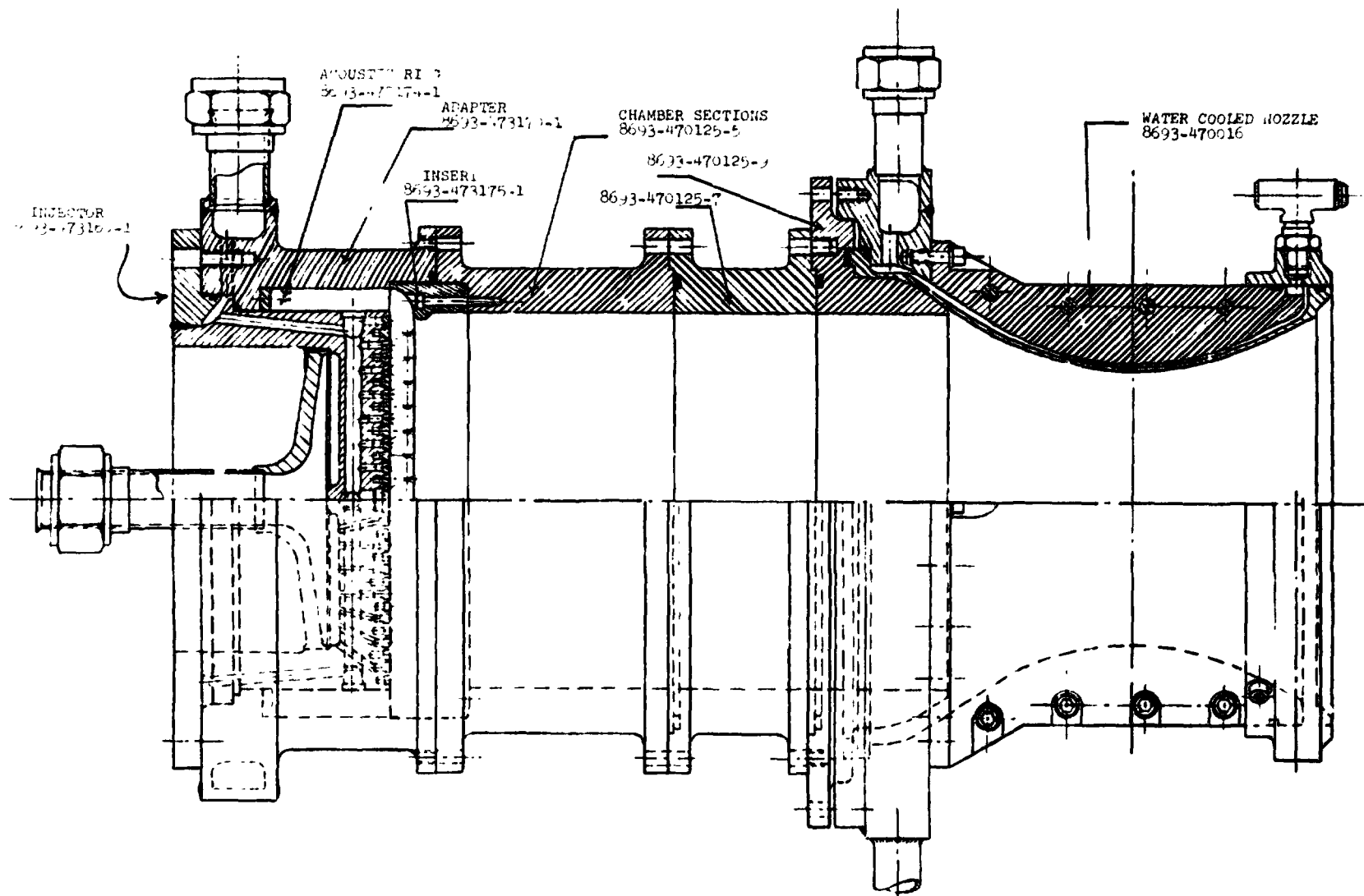
8 IN. DIA
7 ROWS 196 ELEMENTS

FIGURE XII-4

TABLE II
INJECTOR COMPARISON

	10" INJECTOR	8" INJECTOR
Total Number of Elements	196	140
Number of Element Rows	7	7
Impingement From Face	.397" (32°)	.397" (28°)
Nominal Face Ring Width	.250"	.220"
Pressure Drop Across Orifice (psi)	45 (Both Sides)	45 (Both Sides)
Primary Oxidizer Orifice	.0492" (148 Holes)	.0492" (148 Holes)
Primary Fuel Orifice	.0295" (296 Holes)	.0295" (296 Holes)
Fuel Film Coolant	.0197" (48 Holes)	.0197" (48 Holes)
Minimum Oxidizer Orifice L/D	3.96	3.96
Minimum Fuel Orifice L/D	5.1	5.1

XII-10



TEST HARDWARE ASSEMBLY
(1/2" DIAMETER INJECTOR)
FIGURE XII-9

Bell Aerospace Company

D. Test Chamber

A new steel chamber design was used that allowed the interface with the new 8 inch diameter injector and the available 10 inch diameter water cooled nozzle, as shown in Figure XII-5. This chamber incorporated the same bomb port/pressure transducer capability as used on the 10 inch diameter chamber. The nozzle was water cooled with individual outlet temperatures measuring longitudinal segments of heat rejection.

1. Test Results

In the interest of economy, tests were combined on the 8 inch injector evaluation program to produce stability, performance and heat rejection all in one group of tests. The initial question to be answered was the performance level, for without performance all the other recorded parameters were somewhat academic. Next, if performance was achieved, then stable operation at some reasonable heat rejection was considered. Since recent designs for competing 8 inch diameter chambers had been conducted in lengthened combustors, the initial tests of this series were conducted in such a chamber. The injector to throat length of this chamber was approximately 16 inch yielding a 31 L* combustor. The second series of tests was conducted with the 8693-470125-7 spacer removed. The result was testing in an approximately 13 inch chamber length with a 26 L* chamber. The test results in either case were extremely encouraging. The data obtained from the tests using the 8 inch injector are tabulated in Table VII.

2. Performance

The initial tests (Runs 460 through 4613) were conducted on the longer chamber. The test c* presented results from a chamber pressure measured in the acoustic cavity and corrected to the entrance to the nozzle. Unfortunately, the limited funding on the program did not allow the use of expanded nozzles for thrust measurements, therefore the performance assessment has been done using the combustion efficiency (c*).

Although the test sample is limited, the test results were reasonably consistent and indicated that the performance goal was actually exceeded. The original performance goal for this injector was unofficially considered to be approximately 97% with no real "guess" as to the effect of the short chamber. The performance noted was above 98% and only a few (15) feet per second decrease for the reduced length. These results more than justified the design care exercised in the injector. Comparable performance by selected runs are indicated in Table IV.

TABLE III
MODEL 8693 ONE - 8 INCH DIAMETER INJECTOR S/N 1 - STABILITY
TEST SUMMARY

Injector: 8693-43160-1 S/N 1 Chamber Sections -125-5, -7, -9 $A_t = 26,103 \text{ in}^2$; Bomb Size = 6.8 grain PETN; Adaptor - 170-1;
Acoustic Ring - 165-1; H₂O Cooled Nozzle 8693-470016-1 S/N 1; Test Conditions - Sea Level Ambient

Configuration	Test Date 1974	Test No. Cell Data	Dur. Sec.	Bomb Poz. (4)			Damp Time (3)			Avg. Max. Fr. Spiked Above P_c (1)			Data Pt	TcPc corr (2)	R _o /r	C*	Oilt °F	(6) Flt °F	Nozzle Heat Flux	Nozzle Q	Avg. Acoustic Temp °F	Kistler Frequency				
				1	2	3	1	2	3	1	2	3										Acoustic Cavity		Chamber Cavity		
																						K ₃	K ₄	K ₁	K ₂	K ₅
1* 38 (See ITP 83-T-1 for Basic Configuration)	1-13	4609	3.2	--- Check Firing ---									1.0	119.2	1.635	5199	48	52				Not Used No instability encountered duration tests of high frequency Low frequency OSC's noted on test 4617: See OSC				
	11-14	4610	5.9	X	X	X	4.2	4.0	4.4	186	124	195	*	126.6	1.671	5636	57	190	1.79	395.9	2227					
		4611	1.2	X	X _T		3.7	5.1		204	202		.9	154.3	1.878	5616	39	105								
		4612	7.0			X			3.9			171	*	152.5	1.917	5607	56	191	2.22	492.8	2252					
		4613	7.0	X	N	X	3.5		4.6	182		244	*	105.9	2.111	5551	53	182	1.68	371.5	2040					
1* 24	11-20	4614	7.0	X	X	X	4.2	5.2	3.6	177	208	272	*	127.5	1.693	5614	62	192	1.78	393.5	2184					
		4615	1.4	X	X _T		5.3	4.1		229	248		1.0	149.2	1.803	5617	56	155								
		4617	7.0			X			3.6			291	*	148.1	1.829	5598	61	200	2.22	493.0	2259					
		4618	5.9	X	X	X	4.6	2.8	4.0	142	157	290	*	91.8	1.814	5588	57	167	1.54	341.8	1952					
		4619	6.0	X	X _T		5.0	4.2		157	178		1.0	126.0	1.421	5586	45	123								
						X			3.6			258	*	123.3	1.463	5590	58	196	1.76	389.8	2597					

- TEST NOTES:
- (1) Average of 2 highest chamber Kistler Valves (K₁, K₂, K₅) above S.S. P_c
 - (2) Average of P_c's 4 and 5 (corr factor 0.955) also used for C* calculation.
*Performance data at 5.5 sec. data point for normal duration tests; as indicated on short duration tests
 - (3) Longest damp time from all K P_c's for bomb number indicated
 - (4) Bomb data legend: Y Bomb detonated
X Bomb caused instability
X_T Bomb detonated thermally
N Bomb did not detonate (bad bomb - did burn)
 - (5) Nozzle area used for q/A = 221.50 in.²
 - (6) Used Flt #1
 - (7) Average of all acoustic temperatures: Tests 4614-4619, All # 6 was N. G.

ORIGINAL PAGE IS
OF POOR QUALITY

Bell Aerospace Company

TABLE IV

Run No.	Chamber Diameter	Injector To Throat Length	P _c (Psia)	O/F (Mixture Ratio)	c*
4610	8.2	15.9	126.6	1.67	5636
4614	8.2	12.8	127.5	1.69	5614
4604	10	12.8	127	1.66	5589

The interesting data from these tests was the lack of performance decrease noted when the shorter chamber was used. Literature information using this chamber had indicated significant performance changes in going to the longer combustor. The conclusion, which must be preliminary in view of the small data base, was that the combustion process had adequate volume in the twelve inch length and longer chamber was not really required.

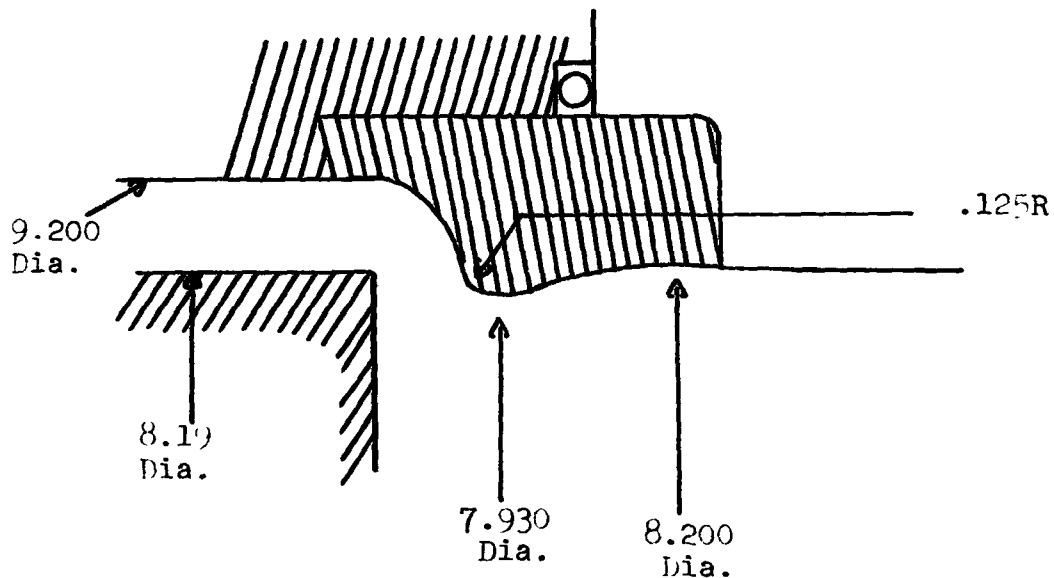
The further examination of the 10 inch injector c* should also be made. During the 4609-4619 test series, the injector tested was with fuel film cooling, but also some face damage was observed resulting from bomb shrapnel. The lower than expected performance may have been attributed to the film cooling but it is considered more likely to be a result of performance calibration de-emphasis for the bomb tests and/or orifice distortion due to the shrapnel effects. As a consequence, it is felt that the 5589 ft/sec is pessimistic for the design, and that the previously recorded value for this injector with vortex cooling is more accurate. In that case the 10 inch injector would have a c* near the 5650 ft/sec recorded at WSTF, and would have approximately the same performance recorded for the 8 inch injector.

3. Stability Results

The acoustic damper configuration tested on the 8 inch diameter injector was incorporated as a direct result of the 10 inch diameter testing conducted in Task XIV. The configuration tested was one of two stable configurations defined in Figure XIV-6. No attempt was made to optimize this damper as neither available time or funding was available for that activity.

The flush fin damper configuration was selected over the full fin configuration for simplicity considerations. In the 10 inch injector testing, substantial erosion of the uncooled fins occurred during testing while little if any erosion of the flush fins took place. For hardware stability and simplicity, the uncooled arrangement (Figure XII-6 was selected).

FIGURE XII-6
ACOUSTIC CAVITY TEST CONFIGURATION



The results of the bomb tests are also shown in the tabulated data of Table III. In addition, a diagrammatic depiction of the tests are shown in Figure XII-2.

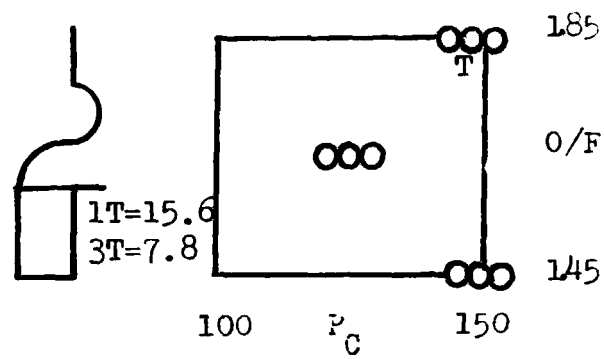
The tests conducted in both the long and short chamber were conducted at conditions found more sensitive at the 10 inch diameter. Since the 10 inch injector bomb sensitivity was found primarily at lean mixture ratios, most of the investigation was at those (oxidizer rich) operating conditions. No sensitivity was found on these bomb tests. All tests remained stable. Due to the limited testing conducted, the stabilizing area was not reduced to produce a limit. Unfortunately due to this lack of limits, no direct comparison could be made between the 8 inch and 10 inch instability.

The tests were also examined for low frequency instability and for "football" type starts. The "football" type start (with approximately 500 hz frequency), was noted on test 4517 where a chamber pressure of less than 100 psia occurred. These oscillations are typical of limiting combination of operating conditions such as lean (mixture ratio) operation and low chamber

Bell Aerospace Company

TASK XV

STABILITY TEST RESULTS



30L* CHAMBER

- Stable
- Unstable

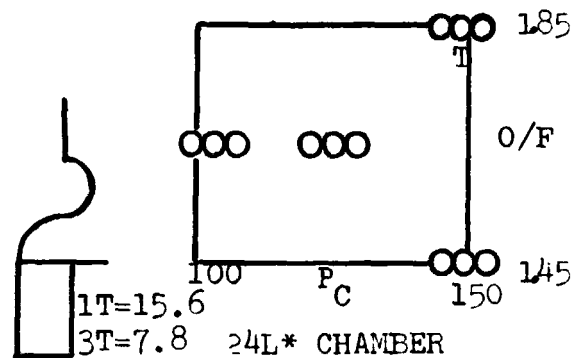


FIGURE XII-7

XII-10

Bell Aerospace Company

pressure. Both conditions produce a low fuel pressure drop which has previously been limited to about 23 psi. This test produced a fuel pressure drop of approximately 20 psi and the start oscillations resulted. The oscillations damped on this test and were not observed on other tests which maintained a higher fuel pressure drop.

The water cooled nozzle data for both the 10 inch and 8 inch diameter injectors were examined in order to ascertain the effects on the local heating rates. In order to compare the results the measured total heating rate was used to predict the heat flux at the throat station and this value was then corrected to the nominal chamber pressure and mixture ratio.

The ratio of the heat flux at the throat to the total heating rate was found using theoretical gas side heat transfer coefficients. The ratio was found to be 0.006308 (1/in²) for the 10 inch injector and 0.008044 (1/in²) for the 8 inch injector. In order to correct for chamber pressure and mixture ratio (which effects the percent barrier flow), a previously developed regression fit of test data was used. The equation is

$$Q \propto P_c^{.8} / \rho^{.186}$$

This equation was used to correct all the test data to the nominal chamber pressure of 125 psia and 2 percent barrier at a mixture ratio of 1.65. The following table presents the results of the testing.

Injector Diameter	Barrier	Chamber Length	Throat System Heat Flux-Average	Number Of Tests Averaged
10 in.	Vortex	12 in.	3.095 Btu/in sec	7
10	Axial	12	3.253	18
8	Axial	12	3.306	4
8	Axial	16	3.325	3

It is seen that for the axial injection of the barrier the heat flux was about 5 percent higher than the vortex barrier for the 10 inch diameter injector. The 8 inch injector showed slightly higher heat flux; about 2 percent more than for the 10 inch injector.

Bell Aerospace Company

RECOMMENDATIONS AND CONCLUSIONS

The testing and analysis performed on this contract was extensive and encompassed many elements of rocket engine technology. The successful demonstration of both computer techniques and operating designs indicated the design inputs for the study to be basically sound and the resulting hardware useful. On the basis of this program the following conclusions are made.

1. The computer techniques used to perform the original program studies were adequate although in many cases the "least" sophisticated techniques for the analysis were used. The extensive data accumulated for the original trade-off studies would have been impossible to accomplish without the logical simplification incorporated. However, the analytical program outputs agreed closely with the finally demonstrated hardware defending the methods and offering reduced cost techniques to performing extensive tradeoff studies.

2. The insulated columbium thrust chamber demonstration was adequate to prove useful operation, and the achievement of the original design goals. The vortex cooling used with the engine was considered to be superior in cooling capability to the commonly used axially injected "film" cooling. The program test results provide data for an engine which could be readily constructed to provide a performance of some 310 seconds I_{sp} in an CME application.

3. The triplet injector concept also provided the basis for a regeneratively cooled chamber operating at a level of 317 seconds I_{sp} . Limit stability testing of this injector with heated propellants indicated a substantial stability margin and a capability of operation under unusual conditions. The flat face design also incorporates a simplicity of both installation and fabrication in comparison to a stable baffled injector. The design information for this 6000 lb. thrust engine is readily available and could be used as required.

4. The preliminary testing conducted with the 8 inch diameter injector was sufficient to show a high level of performance achievement and stability. The testing performed confirmed the selection of injection parameters used and also indicated a very much lower sensitivity to chamber length than originally anticipated. The results of these tests were sufficiently encouraging to recommend further testing.

Bell Aerospace Company

RECOMMENDATIONS

On the basis of the eight inch injector tests conducted the following recommendations are made to provide complete information on this design.

1. Perform altitude performance tests at WSTF with the injector available, and in a NASA provided regeneratively cooled thrust chamber. This data confirmation would provide the "certainty" of performance to justify further testing.
2. Conduct "limit" combustion stability testing with the injector and a variety of acoustic cavity combinations. This information would provide a basis of final acoustic cavity sizing.
3. The final recommendation is to fabricate a stainless steel injector of the 8.2 inch design. Although the aluminum injector has performed in a completely satisfactory manner, long duration requirements dictate the final use of a stainless steel or an equivalent structural material. The construction of such an injector would complete the identification of the 8.2 inch injector for performance, stability and fabrication.

Bell Aerospace Company

REFERENCES

1. "Advanced Experimental Thrust Chamber Program", Report No. R-7281, Rocketdyne Division of North American Rockwell, 9 July 1971.
2. Leach, A. and Dietrich, Frank, "Advanced Thrust Chamber Designs", Contract NAS3-7068, NAS-CR-72006, Bell Aerospace Company, July 1971.
3. Senneff, John, "High Pressure Reverse Flow APS Engine", Report No. 8636-950004, Contract NAS3-14353, Bell Aerospace Company, CR-120881, November 1972.
4. McPherson, W. B., "High Pressure Hydrogen Effects on Metals", Materials Division, MSFC Proceedings of STS Propulsion Technology Conference, April 6 and 7, 1971.
5. Berman, K. and Andrysiak, S., "Barrier Film Cooling Study", Journal of Space Craft and Rockets, March 1972.
6. Hughes, T. A. and King, H. M., "High Temperature Insulation for Reradiative TPS", SAMPE, Space Shuttle Materials, October 1971, Volume 3.
7. Griffith, P., "The Correlation of Nucleate Boiling Burnout Data", ASME 57-HT-21 August 1957.
8. Eckert and Drake, "Heat and Mass Transfer", McGraw-Hill Company, 1950.
9. Robinson, Ernest L., and Taira, S., "Calculation of Thermal-Fatigue Life Based on Accumulated Creep Damage, NASA TN D5489, October 1969.
10. Manson, S. S., "Thermal Stress and Low-Cycle Fatigue", McGraw-Hill, 1966.
11. "Investigation of Light Hydrocarbon Fuels with Flox Mixtures as Liquid Rocket Propellants", NASA CR-5445, PWA FR-1443, 1 September 1965.
12. Private Communication, Simon, R. C. to Alverson, D. J., "Properties of 6061-T6 Aluminum, Battelle Memorial Institute, Defense Metals Information Center, September 6, 1967.
13. "(Hastelloy X) Comparative Properties of Haynes High Temperature Alloys", Cabot Stellite Division Data Sheet

Bell Aerospace Company

REFERENCES (Cont'd)

14. Rousar, D. C., "Heat Transfer Characteristics of Aerozine 50 at High Velocities and High Sub-Coolings", Aerojet General Report TCER-9648-003, November 1966.
15. Propellant Properties Manual - Volume 2 Fuels, Bell Aerospace Company.
16. Space Shuttle Orbit Maneuvering Engine Reusable Thrust Chamber Program Monthly Progress Reports Numbers 8693-933001 thru 8693-933023, August 18, 1972 - August 30, 1974, Bell Aerospace Company
17. Space Shuttle Orbit Maneuvering Engine Reusable Thrust Chamber Program - Parametric Engine Data Report, Report No. 8693-953006, Volumes I and II, November 1972